Analysis of the Domain Specific Function of the Wiskott Aldrich Syndrome Protein, in Vitro and in Vivo

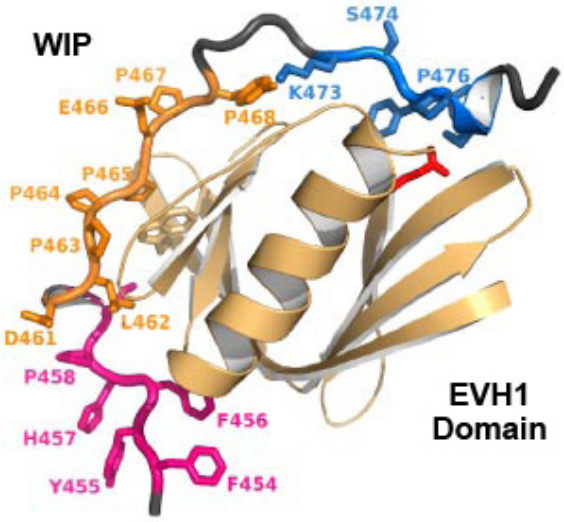

By
Austen Jonathan Jacob Worth

A thesis submitted for the degree of Doctor of Philosophy

2009

Abstract

Wiskott Aldrich Syndrome (WAS) is an X-linked immunodeficiency characterised by low numbers of low volume platelets, eczema, severe immunodeficiency and increased susceptibility to malignant and autoimmune diseases. Wiskott Aldrich Syndrome protein (WASp), the product of the gene mutated in WAS is a multidomain cytosolic protein which acts by integrating downstream signals from cell surface receptor signalling cascades and transduces these signals into remodelling of the actin cytoskeleton. WASp is involved in cellular processes as diverse as cell polarisation, migration, phagocytosis and T cell synapse formation. Dendritic cell function and migration is known to be impaired in WAS. Specifically, dendritic cells lacking WASp in both mice and humans show an impaired ability to form transient actin rich adhesive structures called podosomes.

In this thesis, I am presenting the characterisation of a panel of domain deletion WASp proteins and a series of point mutations which, in children give rise to a range of disease phenotypes. I have expressed these constructs as GST tagged proteins and developed a bead based in vitro assay to asses the protein activity. I have compared the ability of these mutants to bind key regulators of WASp function, WIP and Cdc42, using a variety of immunoprecipitation techniques. Finally I have expressed EGFP tagged WASp proteins in myeloid cell lines to assess expression and stability of these constructs and in WASp null murine dendritic cells to assess their ability reconstitute podosomes.

Point mutations which cause WAS have slightly increased actin polymerisation activity compared to wild type WASp (WT) and have a normal affinity for Cdc42. Although they have a reduced affinity for WIP compared to WT, there is still significant association of WIP to mutant WASp in cells. These mutants have reduced stability and different patterns of phosphorylation compared to WT, when expressed in myeloid cells lines. The EVH1, Polyproline and VCA domains of WASp are all essential for optimal actin polymerisation activity, whereas the Basic domain and the point mutation H246D (which inhibits Cdc42 binding) could be deleted with no loss of molecular activity. The EVH1 domain is essential for WIP binding and the Basic domain is essential for Cdc42 binding. Deletion of the EVH1 domain resulted in protein which had greater stability than WT WASp, suggesting that residues within the EVH1 domain are essential for the physiological degradation of WASp.

This work demonstrates that mutant WASp which causes WAS in patients has normal molecular activity, but the regulation of mutant WASp degradation is impaired in myeloid cells. Results from this project also suggest that Cdc42 is not essential for normal WASp functioning, but does appear to be essential for the phosphorylation of the Y291 residue, which is known to be critical for the regulation of WASp activity. Further work will aim to elucidate the functional (in vivo) significance of these findings.

Acknowledgements

I would like to thank all the members of the Molecular Immunology Unit at the Institute of Child Health for their help and patience during my three years work in the lab. In particular Gerben Bouma, Mike Blundell, Dale Moulding and Joao Metelo have been a constant source of advice, help, learning and encouragement, and Sue Ballard's continual practical assistance has been invaluable. I would like to thank my collaborators for their help and useful discussion of my results. This includes Gareth Jones, Yolanda Calle, David Adamovich, Scott Snapper and particularly Giles Cory, who gave me an invaluable grounding at the start of my project. I would also like to acknowledge several colleagues from other laboratories who have kindly provided me with reagents or protocols. These include Ines Anton, Marc Krishner, Narayanaswamy Ramesh, Ritu Garg and Anne Ridley.

I must give particular thanks to my supervisors Siobhan Burns and Adrian Thrasher, and to Christine Kinnon, head of the Molecular Immunology Unit, for their scientific, academic and professional help and advice. Siobhan in particular, has been a fantastic support, providing exemplary supervision to a difficult and single minded student.

Finally I would like to thank my family, particularly Perys Worth, for their love and support during a difficult time completing this project. My greatest thanks, however, must be reserved for my wife, Louise, and son, Jonathan, without whose unerring love and support none of this would have been possible.

Declaration

All the work presented in this thesis is entirely my own with the following exceptions; (1) The Y291E and I294T WASp constructs were generated by Giles Cory and were a gift to me. (2) Cell sorting of U937 cells into high and low expressing cells was performed by Joao Metalo. (3) The counting of podosomes for figure 9.1e was performed by Joao Metelo and Siobhan Burns. One of the two DC preparations for this data was performed by myself, the other by Joao Metelo.

Publications

Blundell,M.P., Bouma,G., Metelo,J., Worth,A., Calle,Y., Cowell,L.A., Westerberg,L.S., Moulding,D.A., Mirando,S., Kinnon,C., Cory,G.O., Jones,G.E., Snapper,S.B., Burns,S.O., and Thrasher,A.J. (2009). Phosphorylation of WASp is a key regulator of activity and stability in vivo. P**roc. Natl. Acad. Sci. U. S. A 106, 15738-15743.**

Adamovich,D.A., Nakamura,F., Worth,A., Burns,S., Thrasher,A.J., Hartwig,J.H., and Snapper,S.B. (2009). Activating mutations of N-WASP alter Shigella pathogenesis. **Biochem. Biophys. Res. Commun. *384*, 284-289.**

Ancliff,P.J., Blundell,M.P., Cory,G.O., Calle,Y., Worth,A., Kempski,H., Burns,S., Jones,G.E., Sinclair,J., Kinnon,C., Hann,I.M., Gale,R.E., Linch,D.C., and Thrasher,A.J. (2006). Two novel activating mutations in the Wiskott-Aldrich syndrome protein result in congenital neutropenia. **Blood *108*, 2182-2189.**

Chou,H.C., Anton,I.M., Holt,M.R., Curcio,C., Lanzardo,S., Worth,A., Burns,S., Thrasher,A.J., Jones,G.E., and Calle,Y. (2006). WIP regulates the stability and localization of WASP to podosomes in migrating dendritic cells. **Curr. Biol. *16*, 2337-2344.**

Frontpiece Acknowledgement

Image of the tertiary structure of the interaction between WIP and the EVH1 domain of NWASp. Reproduced with kind permision of the authors from Volkman et al., 2002

Contents

Detailed contents

Figures

Chapter 4

Chapter 5

Chapter 6

Chapter 7

Chapter 8

Chapter 9

Appendix

Tables

Abbreviations

A	Acidic region
Abi	Abl interactor
ACK	Activated Cdc-42 associated Kinase
ADF	Actin Depolymerising Factor
ADP	Adenosine Diphosphate
ALLM	Alanine-Leucine-Leucine-Methionine polypeptide
Amp_R	Ampicillin resistance
ANCOVA	Analysis of Covariance
APB	Actin Polymerisation Buffer
APC	Allophycocyanine
Arp 2	Actin Related Protein 2
Arp 2/3	Actin Related Protein 2/3 complex
Arp 3	Actin Related Protein 3
ARPC	Actin Related Protein Complex
ATP	Adenosine Triphosphate
B	Basic domain deleted WASp construct
Bacterial LB	Bacterial lysis buffer
BCA	Bicinchoninic Acid (assay)
BGH polyA	Bovine growth hormone polyadenylation signal sequence
$Blast_R$	Blastomycin Resistance Gene
BSA	Bovine Serum Albumin
Btk	Bruton's Tyrosine Kinase
C	Central (cofilin homology) domain
CCL19	Chemokine (C-C motif) Ligand 19
CD	Cluster of Differentiation
CD2AP	CD2 Adaptor Protein
Cdc-42	Cell Division Cycle protein 42
Cdc-42 12V	Constitutively active Cdc-42
Cdc-42 17N	Constitutively null Cdc-42
cDNA	Complementary DNA
CIAP	Calf Intestinal Alkaline Phsphatase
CIP4	Cdc42 interacting protein 4
CMV	Cytomegalovirus
CMV_P	Cytomegalovirus early Promoter
cPPT	Central Polyproline Tract
CRIB	Cdc42/Rac Interactive Binding domain
CSF1	Colony Stimulating Factor 1
CT	Cycle Threshold
C-Terminus	Carboxyl terminus
CTL	Cytotoxic T Lymphocyte (cell)
DAPI	4,6-Diamidino-2-Phenylindole
dBasic	Basic domain deleted WASp construct
DCs	Dendritic Cells
dEVH1	EVH1 domain deleted WASp construct
df	degrees of Freedom
DMEM	Dulbecco's Modified Eagle's Medium
DMSO	Dimethyl Sulphoxide
DNA	Deoxyribonucleic Acid
dNTP	Deoxynucleotide Triphosphate
dPolyP	Polyproline domain deleted WASp construct
DTT	Dithiothreitol
dVCA	VCA domain deleted WASp construct
dVCA bind	VCA binding site deleted WASp construct
ECCC	European Collection of Cell Cultures
ECL	Enhanced Chemiluminescence
EDTA	Ethylenediaminetetraacetic Acid
EGF	Epidermal Growth Factor
EGFP	Enhanced Green Flourescent Protein
EGFR	Epidermal Growth Factor Receptor
$EM7_P$	EM7 prokayotic promoter
ENA	Enabled (protein)
ERK	Extracellular signal Related Kinase
ERM	Ezrin, Radixin, Moesin family of

	proteins
EVH1	Ena Vasp Homology Domain 1
EVL	Ena / VASP like protein
F	F ratio
FACS	Flourescence Activated Cell Sorting
f-actin	Filamentous Actin
FBP17	Formin Binding Protein 17
FBS	Foetal Bovine Serum
FITC	Fluorescein-Isothiocyanate
fMLP	N-Formyl-Methionyl-Leucyl-Phenylalanine
FRET	Fluorescence Resonance Energy Transfer
g-actin	Globular Actin
GAP	GTPase Activating Protein
GAPDH	Glyceraldehyde 3-phosphate dehydrogenase
GBD	Guanosine Triphosphate Binding Domain
G-CSF	Granulocyte Colony Stimulating Factor
GDI	Guanine nucleotide Dissociation Inhibitor
GDP	Guanosine Diphosphate
GEF	Guanine nucleotide Exchange Factor
GFP	Green Flourescent Protein
GM-CSF	Granulocyte Macrophage Colony Stimulating Factor
GRAP2	Grb2 Related Adaptor Protein
Grb2	Growth factor Receptor Bound protein 2
GST	Glutathione Sepharose Transferase
GST EB	Glutathione Sepharose Transferase Elution Buffer
GTP	Guanosine Triphosphate
GTPase	Guanosine Triphosphatase
GTPγS	Guanosine 5′-[γ-thio]triphosphate
hEF1α	Human Elongation Factor 1α
HEPES	N-2-Hydroxyethylpiperazine-N'-2-Ethanesulphonic Acid
HIS	poly Histidine tag
HIV	Human Immunodeficiency Virus
HPLC	High Performance Liquid Chromatography
HPSF	High Purity Salt Free
HRP	Horseradish perioxidase
HSCP300	Haematopoietic stem cell protein 300
HSV TK polyA	Human Simplex Virus Thymidine Kinase polyadenylation signal sequence
ICAM-1	Intracellular Adhesion Molecule 1
Ig	Immunoglobulin
IL	Interleukin
IPTG	Isopropyl β-D-1-Thiogalactopyranoside
ITAM	Immunoreceptor Tyrosine-ased Activation Motif
$Kano_R$ / Neo_R	Kanomycin / Neomycin resistance gene
kDa	Kilo Dalton
KLH	Keyhole Limpet Haemocyanin
KS	Kolologorov-Smirnov (test or statistic)
LAT	Linker for Activation of T cells
LB	Cellular Lysis Buffer
LB broth	Luria-Bertani (broth)
Ln	Natural logarithm
LNT	Lentiviral (vector)
Log	Logarithm to base 10
LPS	Lipopolysaccharide
LTR	Long Terminal Repeat
MAP kinase	Mitogen Activated Protein kinase
MCP1	Monocyte Chemoattaractant Protein-1
MCS	Multiple Cloning Site
MFI	Mean Flourescence Intensity
MHC	Major Histocompatibility Complex
MIP1α	Macrophage Inflammatory Protein 1α
MMLV	Moloney Murine Leukemia Virus (reverse trasnscriptase)
MOI	Multiplicity Of Infection
MOPS	3-(n-Morpholino) Propanesulphonic Acid
mRNA	Messanger Ribonucleic Acid
mWASp	Murine WASp

MWCO	Molecular Weight Cut Off
NA	Not Applicable
Nap1	Nck-associated protein 1
Nck1	Non-Catalytic region of tyrosine Kinase adaptor protein 1
NF-AT	Nuclear Factor of Activated T cells
NF-κB	Nuclear Factor Kappa-light-chain-enhancer of activated B cells
NK	Natural Killer (cell)
NMR	Nuclear Magnetic Resonance
NOE	Nuclear Overhauser Effect
NWASp	Neural Wiskott Aldrich Syndrome Protein
OptiMEM	Reduced serum modification of Eagle's Minimal Essential Medium
PAGE	Polyacrylamide Gel Electrophoresis
PAK	p21 Activated Kinase
PAR6	Partitioning defective protein 6
PBS	Phosphate Buffered Solution
PBS-T	Phosphate Buffered Saline with Tween (0.1%)
PC	Polyclonal
PCH	Pombe Cdc-15 Homology (family)
PCR	Polymerase Chain Reaction
PE	Phycoerythrin
PEI	Polyethylenimine
PGK	Phosphoglycerate Kinase
PH	Plekstrin Homology (domain)
PHA	Phytohaemaglutanin
PI(3)P	Phosphatidylinositol 3-monophosphate
PI(3,4)P_2	Phosphatidylinositol 3,4-bisphosphate
PI(3,5)P_2	Phosphatidylinositol 3,5-bisphosphate
PI(4)P	Phosphatidylinositol 4-monophosphate
PI3K	Phosphatidylinositol 3-Kinase
PIP_2 [PI(4,5)P_2]	Phosphatidylinositol 4,5-bisphosphate
PIP_3	Phosphatidylinositol 3,4,5-Triphosphate
PIP5K1	Phosphatidylinositol-4-Phosphate 5-Kinase 1
PIR121	p53 inducible messenger RNA
PMA	Phorbol Myristate Acetate
PMSF	Phenylmethylsulphonyl Fluoride
PolyP	Polyproline region (proline rich region)
PPP assays	Purified Protein Actin Polymerisation assays
PS	Penicillin and Streptomycin
PSTPIP1	Proline-Serine-Threonine Phosphatase Interacting Protein 1
PTP-PEST	Protein Tyrosine Phosphatase - proline, glutamic acid, serine and threonine-rich family protein tyrosine
pUC ori	pUC origin of replication
PVDF	Polyvinylidene Fluoride
qPCR	Quantative Polymerase Chain Reaction
RNA	Ribonucleic Acid
RPMI	Roswell Park Memorial Institute (media)
rpm	Revolutions Per Minute
RRE	REV Responsive Element
RT	Room Temperature
RT PCR	Real Time Polymerase Chain Reaction
SB	Sample Buffer
SCAR	Suppressor of G-protein coupled Cyclic AMP Receptor
SDF1	Stromal Cell Derived Factor 1
SDS	Sodium Dodecyl Sulphate
SEB	Special Electroporation Buffer
SEW	SFFV- EGFP-WPRE (vector)
SEWW	SFFV- EGFP-WASp-WPRE (vector)
SFFV	Splenic Focus Forming Virus (promotor)
SH2	Src Homology (domain) 2
SH3	Src Homology (domain) 3
SHD	SCAR Homology Domain
Sig	Significance
SIN	Self Inactivating (virus)
SLAP	SLP76 Associated Protein

SLP76	SH2-containing Leucocyte Protein of 76 kDa
SNX9	Sorting Nexin 9
SOS	Son Of Sevenless (a GAP)
$SP6_P$	SP6 promoter
SS_M	Corrected total model of squares
SS_R	Error (residual) sum of squares
SS_T	Corrected total sum of squares
SV40 ori & $early_P$	Simian Vacuolating virus 40 origin of replication and early promoter
$T7_p$	T7 promoter
TAE	Tris-Actetate EDTA buffer
TBS-T	TRIS Buffered Saline with Tween (0.1%)
TCR	T Cell Receptor
TE	TRIS EDTA (buffer)
TEV site	Tobacco Etch Virus protease cleavage site
TIRF	Total Internal Reflection Microscopy
TOCA-1	Transducer of Cdc42 dependant actin assembly 1
TRIS	Tris(hydroxymethyl) aminomethane
TRITC	Tetraethylrhodamine-Isothiocyanate
UDG	Uracil DNA Glycosylase
UT	Untransfected / Untransduced
V	Verprolin homology domain
v/v	Volume per volume
VASP	Vasodilator-Stimulated Phosphoprotein
VCA	Combined casette of Verprolin homology, Central domain and Acidic region
VZV	Varicella Zoster Virus
WAS	Wiskott Aldrich Syndrome
WASp	Wiskott Aldrich Syndrome Protein
WAVE	WASp family verprolin-homologous protein
WdW	WIP with WASp binding domain deleted
WICH	WIP and CR16 Homologous protein
WIP	WASp Interacting Protein
WIRE	WIP Related protein
WPRE	Woodchuck Hepatitis Post-Transcriptional Regulatory Element
WT	Wild Type
XB	Purified protein pulldown buffer
XLN	X-Linked Neutropenia
XLT	X-linked Thrombocytopenia
YFP	Yellow Flourescent Protein
ZAP70	Zeta-chain (TCR) Associated protein Kinase of 70kDa

1 Introduction

Wiskott Aldrich Syndrome (WAS) is a rare X-linked recessive immunodeficiency syndrome characterised by microcytic thrombocytopenia, eczema, susceptibility to infections and an increased risk of developing both autoimmune diseases and malignancies. It was first described in two brothers with chronic bloody diarrhoea and infected eczema in 1937 (Wiskott, 1937), and the X-linked pattern of inheritance and platelet abnormalities were characterised in 1954 (Aldrich et al., 1954). The gene responsible for the disease was not cloned and sequenced until 1994 (Derry et al., 1994). The product of this gene was named the Wiskott Aldrich Syndrome protein or WASp, and is a regulator of actin polymerisation, playing a critical role in the remodelling of the actin cytoskeleton.

X-linked thrombocytopenia (XLT) is a less severe condition, associated with microcytic thrombocytopenia resulting in susceptibility to bruising and bleeding. In occasional patients thrombocytopenia is intermittent (Notarangelo et al., 2002), and some patients develop transient eczema, and but severe clinical manifestations are not associated with XLT. Mutations in the WASp gene were subsequently also found to be responsible for XLT (Derry et al., 1995; Zhu et al., 1995; Villa et al., 1995). More recently 3 patients with a markedly different clinical phenotype, X-linked neutropenia (XLN), have been described. Each have point mutations localised to a discrete area, adjacent to a structurally distinct region (GTPase binding domain) within exon 9 of the WASp gene (Ancliff et al., 2006; Devriendt et al., 2001).

1.1 Clinical syndromes

1.1.1 Wiskott Aldrich Syndrome

The incidence of WAS is estimated at between 1 in 10^5 and 1 in 10^6 cases per live birth (Stray-Pedersen et al., 2000; Ryser et al., 1988; Perry, III et al., 1980). In 2007, 220 new cases of WAS were registered on the European Society for Immunodeficiency disease registry, and WAS was responsible for approximately 3% of all congenital immunodeficiencies registered (including antibody deficiencies) (ESID 2008).

The most consistent finding at presentation is small volume thrombocytopenia, but the classical triad of small volume platelets, eczema and susceptibility to infection is only found in 30% of patients (Sullivan et al., 1994). Common presentations include one or more of significant bruising and petichiae, eczema (often infected), bloody diarrhoea, sino-pulmonary infections and otitis media. Presentation is

usually within the first six months of life. Immunodeficiency in WAS is highly varied, even among members of the same family, and patients with the same genetic mutation. B and T cell function are both usually affected, and additionally there are defects in the innate immune system. A clinical scoring system has been adopted to categorise the severity of WAS and XLT (Notarangelo et al., 2002) (figure 1.1).

1.1.1.1 Actin cytoskeleton in a normal immune response

The dynamic regulation of the actin cytoskeleton is central to the ability of all leukocytes to function normally. When not challenged by infection or tissue damage, each different type of leukocyte shows its own pattern of trafficking between tissues, lymphoid organs and the circulation. This steady state re-circulation is essential for immuno-surveillance of infection and malignancy, but also plays a vital role maintaining peripheral tolerance to self antigens and the viability of immune cells.

To re-circulate, leucocytes must be able leave the peripheral circulation. They do this via a complex, but stereotyped sequence of tethering, rolling and finally adhering to the vessel wall, before squeezing through the junctions between endothelial cells (diapedesis) (Springer, 1994). Once within tissues, cells migrate in response to interaction with both cells and the extracellular matrix, and to secreted paracrine mediators. All these functions require coordinated restructuring of the cytoskeleton to facilitate shape change, and to assemble and disassemble actin based structures adjacent to the cell membrane.

Once a cell has received a signal to migrate, it polarises and develops a leading edge at the “front” of the cell. The leading edge is characterized by dynamic, actin rich membrane protrusions, which are morphologically divided into broad ruffles (lamellipodia), spikes (filopodia) and podosomes. All three are thought to be critical in initiating cell locomotion. They are generated by actin polymerisation and are stabilized by cell membrane adhesion to the extra cellular matrix or to other cells (Ridley et al., 2003; Verkhovsky et al., 2003). Podosomes consist of an actin rich core surrounded by a ring of integrins and other structural proteins (Linder and Kopp, 2005; Marchisio et al., 1988; Marchisio et al., 1987; Tarone et al., 1985). Podosomes localise to the leading edge of polarised cells, and it has been postulated that they play a role in adhesion and in sensing the microenvironment at the earliest stage of cell movement.

Directional migration to soluble inflammatory mediators is called chemotaxis, and requires cells to detect differences in chemokine concentration around the cell

Score	Low platelets	Small Platelets	Eczema		Infections	Malignancy/ Autoimmunity
0.5	Intermittent	Yes	No		No	No
1	Yes	Yes	No		No	No
2	Yes	Yes	Mild	and/or	Mild	No
2.5	Yes	Yes	Mod	or	Mod	No
3	Yes	Yes	Mod	and	Mod	No
4	Yes	Yes	Severe	and/or	Severe	No
5	Yes	Yes	Mild to severe		Mild to severe	Yes

Intermittent X linked thrombocytopenia

X linked thrombocytopenia

Wiskott Aldrich Syndrome

Eczema

Mild Localised and responsive to treatment
Mod Persistent but responsive to therapy
Severe Requiring continuous treatments +/- systemic treaments

Infections

Mild Recurrent uncomplicated respiratory infections
Mod Recurrent infections severe enough to use prophylactic antibiotics or immunuglobulin
Severe Life treatening infections

Fig 1.1 Clinical scoring system for Wiskott Aldrich Syndrome - X linked thrombocytopenia
From (Jin et al., 2004; Ochs et al., 2007; Zhu et al., 1995)

surface, and respond to these differences by polarisation (Manes et al., 2005). Once at the site of insult, innate effector cells (such as macrophages and neutrophils) become specialised in phagocytosing microbes, damaged cells, tissue debris and apoptotic cells. This also requires rapid, complex and coordinated cytoskeletal rearrangement (Vicente-Manzanares and Sanchez-Madrid, 2004).

Dendritic cells (DCs) are professional antigen presenting cells, which both circulate and reside in peripheral tissues. They specialise in capturing both soluble and particulate antigen after which they migrate, via lymphatics, to T cell areas of lymphoid organs where they present this antigen to T cells (Randolph et al., 2005; Banchereau and Steinman, 1998). Both the long migration to lymphoid organs, and homing within lymphoid organs are highly specialised actin dependent functions. DCs play a crucial role in determining the outcome of this antigen presentation,

as the soluble and cell surface “second signals” they give to lymphocytes are determined by the inflammatory environment in which they took up the antigen, and the degree of DC activation (Banchereau and Steinman, 1998). In response to inflammation, dendritic cells increase their rate of lymph node recirculation and thereby initiate the acquired arm of the immune response.

The binding between peptide loaded MHC class II and antigen specific T cell receptors during the interaction between antigen presenting cells (DCs, macrophages or B cells) and CD4+ve T cells, results in the formation of a highly specialised structure called the T cell synapse (Vicente-Manzanares and Sanchez-Madrid, 2004). The generation, development and signalling through a T cell synapse is dependent on temporally and spatially regulated actin polymerisation. Similar interactions form between cytotoxic cell (CTLs, NK cells) and their targets.

The diversity and variability of the immunodeficiency and immune dysregulation seen in patients with WAS reflects the widespread involvement of coordinated actin polymerisation at every level of the immune response.

1.1.1.2 T cell defects

In WAS the absolute numbers of lymphocytes may be normal or low at birth, but they appear to progressively decrease throughout childhood (Park et al., 2004; Rawlings et al., 1999; Ochs et al., 1980). In humans, CD8+ve T cells are more frequently lower than CD4+ve T cells (Sullivan et al., 1994). T proliferative responses are impaired in many (but not all) patients across a wide range of T cell stimulants, including mitogens (Sullivan et al., 1994; Cooper et al., 1968), allogeneic cells (Sullivan et al., 1994; Ochs et al., 1980) and immobilised CD3 monoclonal antibody (Molina et al., 1993). The variability of T proliferative responses is illustrated by *Sullivan et al* who found that 26% of patients had absent T cell responses to three different mitogens, but 46% of patients had normal responses to all three. By contrast delayed type hypersensitivity skin tests were more reliably impaired (90%) in WAS patients (Sullivan et al., 1994).

The functional significance of these impaired T cell functions tests is demonstrated by an increased susceptibility to the opportunistic fungal pathogen *Pneumocystis jiriveci* (formally *P.carinii*) pneumonia, other disseminated fungal infections (candida, aspergillosis), disseminated herpes virus infections (varicella zoster, EBV and CMV) and severe complication from paramyxovirus infections (mumps, measles). Children with undetectable WASp levels have an approximately 25% risk per year of developing a severe fungal or viral infection (Imai et al., 2004).

At a cellular level, WAS T cells show abnormal morphology with reduced numbers of surface microvilli and a less structured submembranous actin cytoskeleton (Molina et al., 1992). They demonstrate reduced actin polymerisation at the site of antigen presenting cell engagement, impaired CD3 capping and impaired (but not absent) T cell synapse formation (Badour et al., 2003; Snapper et al., 1998; Gallego et al., 1997; Molina et al., 1993; Molina et al., 1992). Signalling through this synapse is also aberrant, resulting in reduced IL-2 secretion from T cells, which probably accounts for the abnormal T cell proliferative responses (Cannon and Burkhardt, 2004).

Defects in chemotaxis to the T cell lymphokines SDF1 and CCL19 have been described in WASp null cells for humans and mice (Gallego et al., 2006; Snapper et al., 2005; Haddad et al., 2001). Abrogated homing to T cell areas of lymph nodes has been seen in murine adoptive transfer experiments (Gallego et al., 2006). In WAS patients, lymph node histology shows a relative depletion of small lymphoytes in T cell areas (Snover et al., 1981).

Recently several reports have described defects in the suppressor function of T regulatory cells in humans and in mice, despite normal numbers of thymic emigrants (Marangoni et al., 2007; Humblet-Baron et al., 2007; Maillard et al., 2007; Adriani et al., 2007). It is likely that this contributes to the autoimmunity seen in WAS.

1.1.1.3 B cell defects

B cell numbers and absolute levels of serum immunoglobulins (Ig) are usually normal in WAS (Park et al., 2005), and although there is often a skewing of the normal Ig distribution. IgG levels are usually normal, whereas IgM is frequently reduced, and IgA and IgE levels are usually raised. WAS patients make poor specific responses to polysaccharide antibodies and other T dependent antigens. Isohaemaglutinin titres are characteristically low (Imai et al., 2004; Dupuis-Girod et al., 2003; Sullivan et al., 1994), and immunisation with the bacteriophage neoantigen phi X174 (a T dependent antigen) results in class switch but poor immunological memory (Ochs et al., 1980). By contrast responses to live viral vaccines are normal (Sullivan et al., 1994; Ochs et al., 1980).

The most common infectious complications of WAS bear the hallmarks of antibody deficiency (otitis media, pneumonia, sinusitis and sepis), illustrating the functional significance of the above laboratory observations. These clinical findings, however may just represent a lack of T cell help for the humoral response, and evidence from the WAS mouse model suggested that B cell activation is normal in the

absence of WASp (Snapper et al., 1998) (see section 1.1.1.10).

More recent evidence from humans and from the WAS mouse model suggest that intrinsic B cell defects are also present in WAS. B cells show impaired actin polymerisation and abnormalities of morphology and polarisation (Westerberg et al., 2005; Westerberg et al., 2001; Facchetti et al., 1998). Although B cell receptor signalling is normal, B cell receptor capping is impaired (Westerberg et al., 2003; Westerberg et al., 2001; Zhang et al., 1999). Abnormal architecture of B cell areas of lymphoid tissue has been demonstrated in both WAS patients and in WASp null mice. The presence of atypical plasma cells and a progressive loss of volume and definition of the marginal B cell zones, have suggested impairment of B cell - T cell interaction, which may be responsible for the poor T dependant antibody responses seen in WAS (Westerberg et al., 2008; Westerberg et al., 2005; Andreansky et al., 2005; Vermi et al., 1999; Snover et al., 1981).

1.1.1.4 Innate Immunity defects

WAS macrophages and their blood-borne precursors, monocytes, show defects in their ability to polarise, migrate and phagocytose. They are severely impaired in their ability to form podosomes (Linder et al., 2000a) and have abnormal morphology (Calle et al., 2004). WAS macrophages and monocytes show impaired chemotaxis *in vitro*, in response to colony-stimulating factor-1 (CSF1), N-formyl-methionyl-leucyl-phenylalanine (fMLP), monocyte chemoattaractant protein-1 (MCP1) and macrophage inflammatory protein-1 (MIP1α) (Badolato et al., 1998; Zicha et al., 1998). They are able to bind these chemokines at the cell surface normally, and induce an appropriate respiratory burst following binding, suggesting some signalling through the chemokine receptors remains normal. Similarly WAS macrophages are able to move at normal speeds, but their directional movement is impaired. WASp gene replacement in WAS macrophages restores normal chemotaxis (Jones et al., 2002).

WASp null macrophages show impaired FcγR mediated phagocytosis (Lorenzi et al., 2000), and impaired phagocytosis of apoptotic cells (Leverrier et al., 2001). Although binding apoptotic cells was not impaired, macrophages lacking WASp are incapable of forming the actin rich “phagocytic cup” necessary for phagocytosis (Tsuboi and Meerloo, 2007; Leverrier et al., 2001; Lorenzi et al., 2000). Pinocytosis and endocytosis, which do not require phagocytic cup formation, are normal in WASp null murine macrophages (Westerberg et al., 2003; Snapper et al., 1998).

Neutrophil function in WAS has not been studied as extensively as other myeloid cell lines. Defective phagocytosis has been demonstrated in murine WASp null

neutrophils (Zhang et al., 1999). Data concerning chemotaxis is contradictory. *In vitro* studies demonstrated no defect in chemotaxis towards fMLP or IL-8 (Zicha et al., 1998), but more recently abnormalities in transendothelial migration were detected using an *in vitro* system where neutrophils under physiological shear flow interacted with activated monolayers of endothelial cells overexpressing E-selectin and ICAM-1. This study also demonstrated abnormal β2-intergrin clustering, integrin mediated superoxide production, neutrophil adhesion, (all in WAS patient and murine WASp null neutrophils) and reduced perionteal neutrophil recruitment in response to intra-peritoneal thioglycolate (Zhang et al., 2006).

WAS patients have increased numbers of Natural Killer (NK) cells, but these cells have an impaired ability to kill target cells (Gismondi et al., 2004; Orange et al., 2002). In normal cells, WASp is recruited to the immune synapse formed between NK cells and target cells. Cytolytic granules are then released from the NK cell into the synaptic space, resulting in pore formation in the target cell plasma membrane. In WASp deficient cells there is reduced actin polymerisation at the immune synapse and resultant impaired cytotoxicity.

1.1.1.5 Dendritic cell defects

WAS dendritic cells show many of the same abnormalities seen in macrophages. They have abnormal cell morphology, impaired ability to polarise, impaired ability to form podosomes, abnormal chemotaxis, abnormal migration and trafficking, and impaired phagocytosis (Snapper et al., 2005; de et al., 2005; Linder and Kopp, 2005; Calle et al., 2004; Burns et al., 2001; Binks et al., 1998). Immature WAS DC characteristically form a long spindle shape on interaction with substratum, developing two or more poles, without a clear leading edge. In response to chemokine gradients these protrusions elongate and retract without coordinated, directional movement (Burns et al., 2001; Binks et al., 1998). Specifically WAS immature DCs show reduced chemotaxis toward CCL19 and CCL21 gradients, two chemokines crucial in homing to T cell areas within lymph nodes (von Andrian and Mempel, 2003). The functional importance of this is demonstrated by impaired *in vivo* DC migration to lymph nodes and failure of appropriate homing to T cell areas within lymph nodes in mouse models (Bouma et al., 2007; Snapper et al., 2005; de et al., 2005).

Migration defects have not been described in mature DCs (Burns et al., 2004). The functional specificity of DCs changes with their state of activation and maturity. Immature DC are specialized for antigen uptake, DC activated following uptake of antigen become specialised in migration and antigen processing, and mature DC optimally present antigen to T cells. WAS DC have an impaired ability to form

functional antigen presenting contacts with T cells (Pulecio et al., 2008), and therefore the mechanism by which WASp deficiency hinders immune function changes throughout the immune response.

Wiskott Aldrich syndrome is one of few genetic immunodeficiency with a primary dendritic cell abnormality. Although WAS demonstrates abnormalities in every arm of the immune system, it is very likely that abnormal dendritic cell function plays a major role in the immunodeficiency and immune dysregulation seen in Wiskott Aldrich syndrome.

1.1.1.6 Platelets

Low platelet count and low platelet volume is a consistent finding in WAS, and platelet volume is usually less than half the normal value for healthy controls (Ochs et al., 1980). The cause of these abnormalities remains unknown, however it is likely to be due to a combination of increased destruction of platelets and ineffective thrombocytopoesis. Following splenectomy WAS patient's platelet counts and volumes rise, but they remain significantly reduced compared to healthy controls.

Bleeding is major cause of morbidity and mortality for patients with 30% suffering a life threatening bleed prior to diagnosis (Sullivan et al., 1994). Intracranial haemorrhage has been observed in 2% of patients.

1.1.1.7 Eczema

Eczema is present in 80% of patients with WAS (Sullivan et al., 1994), although the severity of symptoms is highly variable. It has been postulated that eczema in WAS is caused by the defective migration of DCs and Langerhans cells, resulting in a breakdown in the normal peripheral tolerance mechanisms to self skin antigens (Thrasher et al., 1998), but in fact few studies of pathogenesis have been reported.

The relationship between WAS and atopy is less clear. Wiskott patients characteristically have an eosinophilia and a raised IgE level, and food specific IgE has been detected in symptomatic patients (Root and Speicher, 1963; Huntley and Dees, 1957). The lack of specificity of these tests and the multiple alternative gastrointestinal pathologies associated with WAS, make it difficult to characterise the association with atopy.

1.1.1.8 Autoimmunity

Autoimmunity, inflammatory conditions and vasculitis are common complication

of WAS and an incidence of 40% was described in the largest published cohort of patients (Sullivan et al., 1994). Autoimmune haemolytic anaemia is the most frequently observed complication, but autoimmune neutropenia, cerebral and other vasculitis, inflammatory bowel disease, renal disease and Henoch-Schonlein purpura are all reported. A high serum IgM level is predictive of morbidity from autoimmunity (Dupuis-Girod et al., 2003).

Interestingly, a large cohort of WAS / XLT patients from Japan reported a high incidence of IgA nephropathy in patients without other WAS associated clinical complications (Imai et al., 2004). This is further discussed in sections 1.1.2 and 1.2.1.

1.1.1.9 Malignancy

As with other immunodeficiencies, WAS predisposes to malignancy. The most frequent malignancy described is B cell lymphoma, often associated with Epstein Barr Virus positivity, which may partly relate to defective immune surveillance. The incidence of all malignancies in WAS is 13% with a median age of onset of 9.5 years (Sullivan et al., 1994), and historically these patients have had a poor prognosis.

1.1.1.10 Mouse model of Wiskott Aldrich Syndrome

Although some research elucidating the functional role of WASp has been performed on patient cells and tissues, a WAS mouse model (WASp knockout generated by gene targeted mutation) has been extensively used to address the systemic and cellular effects of WASp. The WAS murine model has many similarities, but also significant differences to the human clinical condition.

Like humans, WAS mice have peripheral lymphopenia and thrombocytopenia, although platelet size does not differ significantly from WT mice. Basic T and B cell subsets also appeared in normal proportions, and there was no specific loss of CD8 +ve T cells as seen in humans (Zhang et al., 1999; Snapper et al., 1998). T cell receptor signalling following CD3 stimulation and resultant T cell capping was abnormal, but stimulation using a combination of PMA and ionomycin was normal (Snapper et al., 1998). T cell signalling following CD28 mediated co-stimulation is also impaired (Zhang et al., 1999). In contrast with human studies, signalling through the B cell antigen receptor was normal, and WAS mice showed normal levels of immunoglobulins, and had the capacity to generate antibodies to T dependant and independent antigens (Snapper et al., 1998). WAS mice show no eczematous skin changes but a prominent clinical feature is the strain dependant development of a severe colitis in the majority mice by the age of four

months (Snapper et al., 1998).

The lymphopenia seen in the WAS mouse model may at least partly be explained by defects in T cell development. Transgenic dVCA WASp mice show a block in early T cell development, resulting in impaired production of surface αβTCR and a failure to progress to single positive T cells. *Zhang et al* argue that the fact this defect is not seen in WAS mice is due to redundancy between NWASp and WASp and that a functional defect is only detected when the dominant negative dVCA WASp protein is expressed (Zhang et al., 2002).

1.1.2 X-linked Thrombocytopenia

The true incidence of XLT is difficult to assess as many patients only have mild symptoms, mainly related to thrombocytopenia. It is likely that many cases of XLP will be diagnosed late or incidentally, and many other children with XLT have been misdiagnosed with idiopathic thrombocytopenia purpura (Canales and Mauer, 1967). Like WAS, XLT has a high correlation with low platelet volume.

Although by definition patients with XLT cannot have serious clinical manifestations, it is becoming increasingly apparent many patients do develop WAS like clinical disease, in an abrogated form. The continuum of disease spectrum between the mildest asymptomatic form of XLT and the most severe manifestation of WAS has been long recognised (De Saint-Basile et al., 1991; Donner et al., 1988).

Platelet numbers, size and morphology are indistinguishable between WAS and XLT. Both groups have a life long risk of bleeding diathesis. Immune function tests in XLT, are often not completely normal, but they are much closer to normal than those seen in WAS. T cell proliferative responses to mitogens are slightly reduced compared to WT, but are not abnormal enough to have any clinical significance. XLT patients make class switched antibody responses with memory to phi X174, but the response is not as large or as long lived as control patient responses (Ochs and Rosen, 2007).

Eczema in XLT is either absent, mild or intermittent (Notarangelo et al., 2002), but is rarely severe. Levels of atopy, asthma and food allergy are indistinguishable between WAS and XLT.

Classically, WAS was thought to have a much higher incidence of autoimmune diseases than XLT. This has recently been questioned by a Japanese cohort of 50 WAS and XLT patients, in which similar levels of autoimmunity were found (Imai et al., 2004). Patients with XLT seemed to be specifically susceptible to

developing an aggressive form of IgA nephropathy, which progressed to chronic renal failure in 2 out 5 patients by the age of 25. The authors postulated this discrepancy may arise from the impaired ability of WAS patients to generate the pathogenic class switched antigen.

The evidence for malignancy is clearer, with no published case series showing an increased incidence of malignancy with XLT. Despite this, a recent presented abstract of a multicentre long term follow up of 182 patients with XLT, suggested that XLT does predispose to malignancy, but there is much greater time lag before disease appearance. They demonstrated that 5% of XLT patients developed malignancy, producing a cumulative incidence of approximately 30% by 40 years (Albert et al., 2008). A similar pattern was seen with autoimmunity (prevalence 12%, cumulative incidence 40%). These figures are very similar to those for classical WAS (Sullivan et al., 1994).

1.1.3 X-linked Neutropenia

4 families have now been described with X-linked neutropenia secondary to missense mutation in or adjacent to the WASp GTPase binding domain (GBD) (Ochs, 2008; Ancliff et al., 2006; Devriendt et al., 2001). Each family has a unique mutation, resulting in a different amino acid substitution (L270P, S272P, I276S and I294T).

These children have a completely different clinical syndrome to WAS / XLT. They have all presented with severe congenital neutropenia ($<0.3x10^9$/L) or myelodysplasia. Additional findings have included a peripheral monocytopenia, normal platelet counts with slightly increased platelet volume. Where tested neutrophil phagocytosis and oxidative burst were impaired compared to normal controls. Two out of three patients have demonstrated intermittently low absolute lymphocyte counts with impaired proliferative responses to CD3 (but normal to PHA). NK cells were low and CD4:CD8 ratios were reversed in all patients. Analysis of bone marrow has revealed haematopoetic arrest at the promyelocyte / myelocyte stage, and one patient demonstrated trilineage dysplasia (myeloid, lymphoid and platelet). Cultured macrophages have, from one patient (I294T), demonstrated higher levels of cytoplasmic f-actin, impairment in cell polarisation and, although they do form structurally normal podosomes, they appear to be larger and cluster in ring formations (Ancliff et al., 2006).

Clinically all patients so far have remained relatively well on minimal and conservative treatment. One patient has made a good response to G-CSF. The definitive mechanism of neutropenia is as yet unconfirmed, but evidence of

impaired diakinesis following cell division, resulting in apoptosis of cells containing WASp I294T, has been demonstrated (Moulding et al., 2007).

1.2 Genetics of WAS

Positional cloning mapped the WASp gene to the Xp11.22-Xp11.3 locus (Kwan et al., 1991). The gene consists of 12 exons which give rise to a 502 amino acid protein, with a molecular mass of approximately 65 kDa (figure 1.2). The WASp protein consists of 5 functional domains and the positions of these relative to the exonic structure of WASp is demonstrated in figure1.2.

1.2.1 WASp gene mutations

Over 150 different mutations have now been described to cause either WAS or XLT. These are made up of approximately 35% missense mutations, 25% splice site mutations, 15% nonsense mutations and 25% frameshift mutations (insertions, deletions and complex mutations) (Lutskiy et al., 2005; Jin et al., 2004; Imai et al., 2004). The majority of the missense mutations are found in exons 1-4 (within the EVH1 domain of the protein), whereas the splice site mutations are usually found towards the carboxyl terminus (exons 6 - 10). Other mutations are evenly distributed throughout the gene.

6 mutational hotspots have been described, where common mutations account for disease in at least 7 unrelated families (Ochs and Thrasher, 2006; Jin et al., 2004). 168C>T (producing Tre45Met), 290C>N/291G>N (producing Arg86Cys/His/Gly) and IVS6+5g>a (disruption of a variant splice site, resulting in a protein truncation at 190aa and normal full length protein) invariably result in some WASp protein production within cells. 664C>T (producing a truncation with a stop at aa211), IVS8+1g>n (exon 8 deletion) and IVS8+1 to +6 del gtga (exon 8 deletion) all result in a WASp null phenotype. Between them these hotspots account for 25% of all WAS / XLT mutations. The mutation hot spots are illustrated in figure 1.2.

1.2.2 Genotype – Phenotype correlations

In view of the extensive clinical variability and large number of different causative mutations, for many years there was doubt as to whether a true genotype – phenotype link existed for WAS / XLT (Greer et al., 1996; Schindelhauer et al., 1996; Sullivan et al., 1994). Several large studies have now clearly demonstrated a correlation between disease severity and cellular levels of WASp protein (Lutskiy et al., 2005; Jin et al., 2004; Imai et al., 2004; Lemahieu et al., 1999; Zhu et al., 1997; Remold-O'Donnell et al., 1997). In light of this, a diagnostic assessment

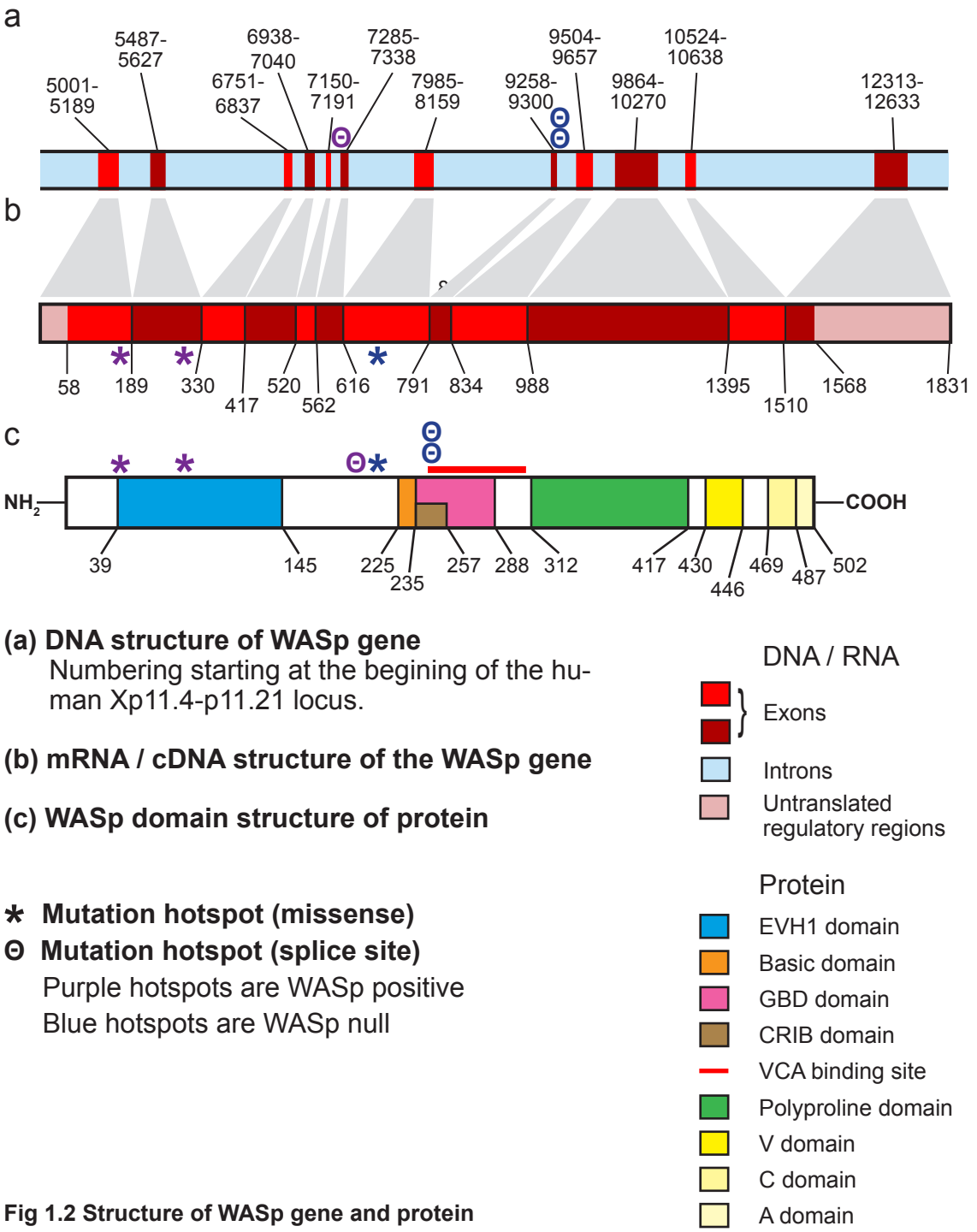

(a) DNA structure of WASp gene
Numbering starting at the begining of the human Xp11.4-p11.21 locus.

(b) mRNA / cDNA structure of the WASp gene

(c) WASp domain structure of protein

∗ Mutation hotspot (missense)
Θ Mutation hotspot (splice site)
Purple hotspots are WASp positive
Blue hotspots are WASp null

Fig 1.2 Structure of WASp gene and protein

of patients with WAS / XLT should include both sequencing the WASp gene for mutations in genomic or cDNA, and an assessment of lymphocyte WASp expression (using either a Western blot of lymphocyte lysate or flow cytometry of permeablized lymphocytes immunostained for WASp (Yamada et al., 1999)).

75% of patients with WASp mutations who express full length WASp protein have missense mutations, with the majority of the remainder having variant splice site mutations (usually IVS6+5g>a). Of these patients, 75% have reduced cellular

levels of WASp (usually under 20% normal levels (Lutskiy et al., 2005)), whereas in 25% the levels are normal (Jin et al., 2004; Imai et al., 2004). For patients with variant splice site mutations the protein expressed is normal full length WASp, but this only represents a fraction (usually about 30%) of the WASp gene's transcriptional output. *Lutskiy et al* described a patient with an IVS6(+5)g>a mutation in whom there was normal WASp expressed in T cells, but not B cells, suggesting that splicing patterns are cell specific (Lutskiy et al., 2005). Patients with missense mutations produce only mutant WASp protein.

The majority of patients with detectable cellular WASp levels have XLT. In one study 78% of WASp positive patients had no serious or recurrent infections and only mild, transient, or no eczema (clinical score 1 or 2). 22% of patients developed WAS (clinical score 3-5), but the majority of these attained a clinical score of 5 on the basis of developing autoimmunity (Imai et al., 2004). Interestingly patients with missense mutations in exon 4, seem to be more likely to have undetectable WASp levels and have a more severe clinical phenotype (Lutskiy et al., 2005; Zhu et al., 1997).

85% of patients with absent WASp expression (or expression of truncated WASp only) had frameshift mutation, nonsense mutation, or invariant splice site mutations. Approximately 90% of WASp null patients developed full blown WAS (clinical score 3-5). This figure may be falsely low as children may have undergone bone marrow transplant on the basis of lack of WASp expression, or a sibling's clinical phenotype, and prior to developing WAS qualifying symptoms. In some patients fully symptomatic WAS takes 2-3 years to develop (Jin et al., 2004).

The level of WASp mRNA in cells from patients with missense mutations is normal, suggesting that transcription of mutant WASp genes is not impaired and that low WASp levels are due to proteolysis (Lutskiy et al., 2005; Zhu et al., 1997). For nonsense and frameshift mutations, the WASp products are very likely to be incorrectly folded, as well as functionally inactive, and will therefore be efficiently ubiquitinised, explaining the undetectable protein levels seen in patients. This is less likely to explain the reduced levels of protein seen with patients with single amino acid changes.

With a better understanding of how the genotype and proteotype relate to clinical phenotype, Imai et al reanalysed the clinical consequence of thrombocytopenia in 50 patients based on their WASp expression. They found that there was a difference in the presenting symptom between the two groups, with WASp null patients most commonly presenting with petichiae, but WASp+ve patients

presenting with active bleeding. Both groups had similar rates of intracranial haemorrhage, but the outcome following this was much more favourable for the WASp+ve group. Similarly the WASp null group of patients were much more likely to develop serious bleeding of the gastrointestinal tract (Imai et al., 2004). Whether these patterns are borne out in larger case series, remains to be seen.

Although the relationship between clinical phenotype and WASp expression is clear, it is not absolute. Patients with the same mutation, and even within the same family, can have markedly different clinical courses, and express different levels of WASp protein. This suggests that the clinical phenotype of WASp mutations is highly influenced by other (genetic and environmental) factors, which also account for the heterogeneity and diversity of defects seen within the disease.

1.3 WASp family proteins

WASp was the first member described of a new family of proteins, which now contains five mammalian members. WASp is only expressed in haematopoeitic cell lineages (Derry et al., 1994), however neural WASp (N-WASp), identified in 1996 (Miki et al., 1996), is ubiquitously expressed. Since then 3 further mammalian proteins in the same family have been discovered and these are known by one of 2 acronyms - WAVE (WASp family verprolin-homologous protein) or SCAR (suppressor of G-protein coupled cyclic AMP receptor) (Suetsugu et al., 1999; Machesky and Insall, 1998; Miki et al., 1998b).The comparative structure of WASp family members is shown in figure 1.3.

The family is defined by a common module at the carboxyl terminal, which is made up of a verprolin (V) homology domain (also called WASp homology 2, WH2 domain), followed by a central (C) domain and a final an acidic (A) sequence. Together this will be referred to as the VCA domain and individual components will be referred to by their single letter abbreviation. The VCA domain is the “output” domain of WASp family proteins, and once bound to the Arp2/3 complex it mediates actin polymerisation. Other proteins containing verprolin homology domains include WIP and β thymosin (see sections 1.7 and 1.6.2). Additionally all proteins have a polyproline domain (P) of approximately 100 amino acids length adjacent to the VCA, and a short basic domain (B) towards the amino terminus.

WASp and N-WASp also have an amino terminal domain called the WASp homology domain 1 or the Ena/VASp homology domain 1 (EVH1), and a central GTPase binding domain (GBD). The WAVE proteins have a unique domain, called the SCAR homology domain (SHD) at their amino terminus.

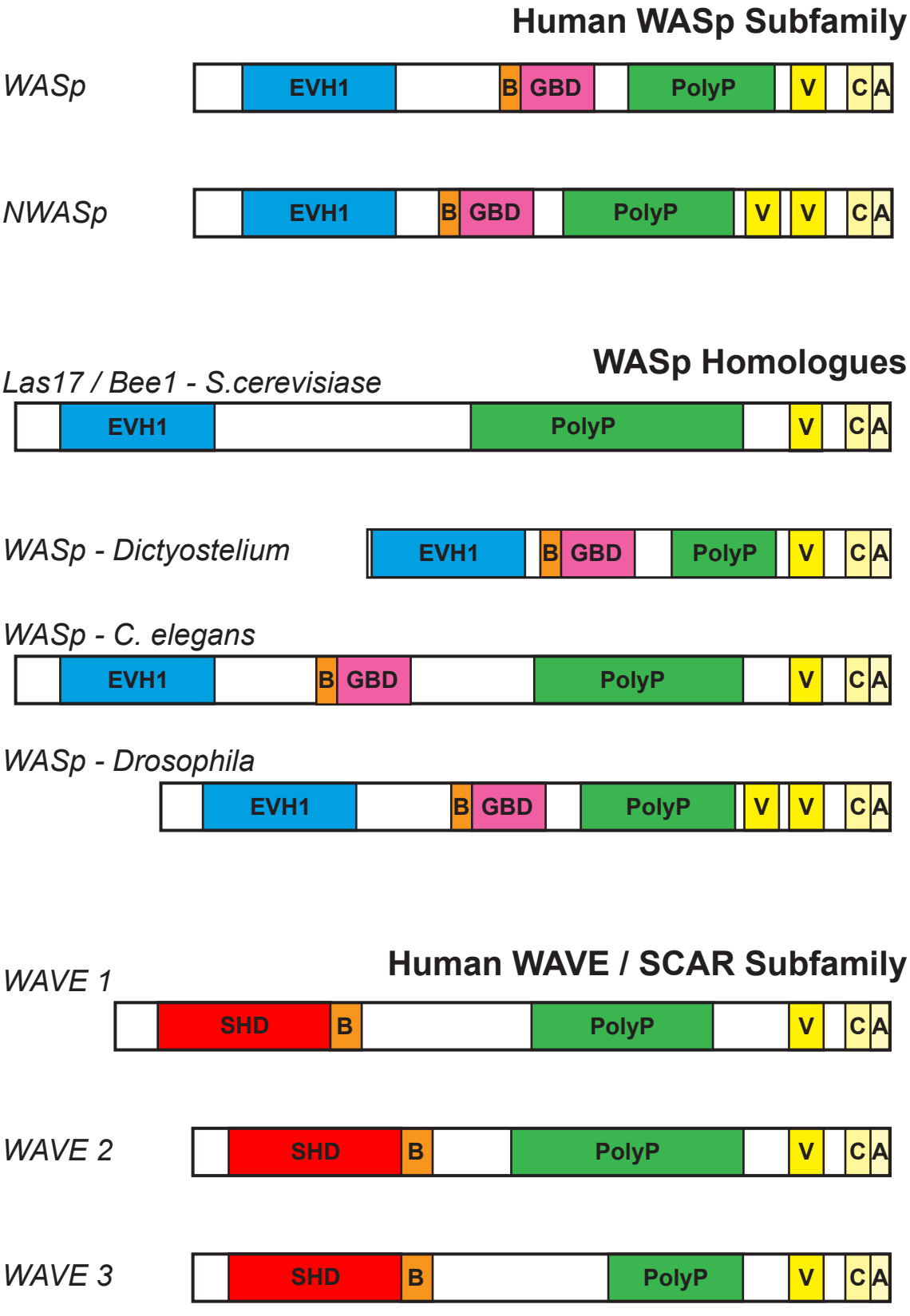

Fig 1.3 Domain structure of WASp family proteins
EVH1 - Ena / VASP Homology domains, B - Basic domain, GBD - GTPase binding domain
PolyP - Polyproline domain, V - Verprolin homolgy domain, C- Central region, A - Acidic region
SHD - SCAR homology domain

1.3.1 Evolution of WASp family proteins

WAVE proteins appear to have evolved more recently than WASp / NWASp and seem to have become critical once cells start to become motile. WAVE homologues are found in *Drosophila*, *C. elegans* and *Dictyostelium*, but not in yeasts. The WASp family protein in *Saccromyces. cerevisiae* (Las17/Bee1p) has features of both WASp and WAVE proteins, containing an EVH1 domain, but no GBD. In more primitive organisms WASp proteins primarily function for intracellular trafficking.

Work using knockout models in mice and *Drosophila* suggest that WASp / NWASp and WAVE proteins have discrete functions and that redundancy of function between them is at best partial.

1.3.2 NWASp

NWASp shows approximately 50% sequence homology to WASp (Fukuoka et al., 1997). Structurally it is unique in that it contains a second verprolin homology domain adjacent to the carboxyl terminal VCA, although the functional significance of this remains unknown. Otherwise its domain structure is very similar to WASp (figure 1.3).

Although NWASp expression is ubiquitous among mammalian cells, expression is greatest in brain tissue. NWASp mutations have never been detected in humans, and NWASp knockout mice are emybryonically lethal at day 11 (Snapper et al., 2001; Lommel et al., 2001). Early studies of NWASp function in cells had suggested that it acted by translating Cdc42 signals into actin polymerisation, resulting in filopodia formation. Cells from the embryonically lethal knockout mouse referenced above did not bear this out, and both studies were able to demonstrate Cdc42 induced filopodia formation in the absence of both NWASp and WASp. Motility of the intracellular pathogens *Shigella, vaccinia* virus and enteropathogenic *Escherichia coli*, (all of which are known to hijack the cellular Arp2/3 actin polymerisation machinery within cells to move), was however impaired in NWASp knockout cells. These results and others (Yamaguchi et al., 2005; Weaver et al,. 2002; Benesch et al., 2002), suggest a non-redundant role for NWASp in invadipodia and podosome formation, and in vesicular traficking within cell.

1.3.3 WAVE / SCAR proteins

WAVE proteins do not contain the autoinhibitory loop found in WASp and NWASp (see section 1.4.6) and as a result they exist in a relatively constitutively active

state, both *in vitro* and if overexpressed in cells (Machesky et al., 1999). WASp and NWASp are directly actived by the Rho type GTPase Cdc42, whereas WAVE proteins are actived downstream by Rac (another Rho type GTPase), despite lacking a GTPase binding domain (GBD). Within cells, WAVE1 and WAVE2 form a stable pentamic complex with PIR121 (p53 inducible messenger RNA), Nap1 (Nck-associated protein), Abi (Abl interactor), and HSPC300 (haematopoietic stem cell protein 300), with only Abi and HSPC300 interacting directly with WAVE (via the SCAR homology domain). The Arp 2/3 complex also contitutively associates with WAVE within this complex, but is not activated under resting conditions. WAVE activation of Arp2/3 occours following Rac or Nck binding to PIR121, which provides the mechanism of Rac regulation of WAVE function.

The exact mechanism of this signal transduction remains controversion, and it is likely that prolyproline domain binding proteins will also contribute to the regulation of WAVE activity. Like WASp, phosphorylation, degradation and spatial localisation of WAVE regulatory proteins provide further levels of complexity to the control of WAVE activity.

All three WAVE proteins show different tissue distributions, with WAVE 2 being most widely distributed and WAVE 1 showing highest expression in brain tissue. Functionally WAVE proteins are involved actin cytoskeletal rearrangements, and have been specifically implicated as downstream effectors of Rac induced lamelipodia formation (Miki et al., 1998b).

1.4 Molecular structure of WASp

WASp has no intrinsic catalytic or transcriptional activity of its own, it merely acts as a control hub, integrating downstream mediators of cell surfacing signalling cascades, and translating these signals into expansion of the dendritic actin cytoskeleton, via the protein complex Arp2/3. The activation of WASp imparts two signals - temporal and spatial actin remodelling.

WASp's structure reflects this complex function. Its highly modular domain structure facilitates the binding of several different proteins or phospholipids simultaneously to different protein regions (figure 1.4). Its flexible structure (lacking disulphide bonds) allows conformational changes in response to these interactions. A discrete Arp2/3 binding effector domain (VCA) remains hidden until WASp is activated by appropriate conformational changes, induced by the interaction of mediators with other domains. This provides the biological mechanism of signal integration.

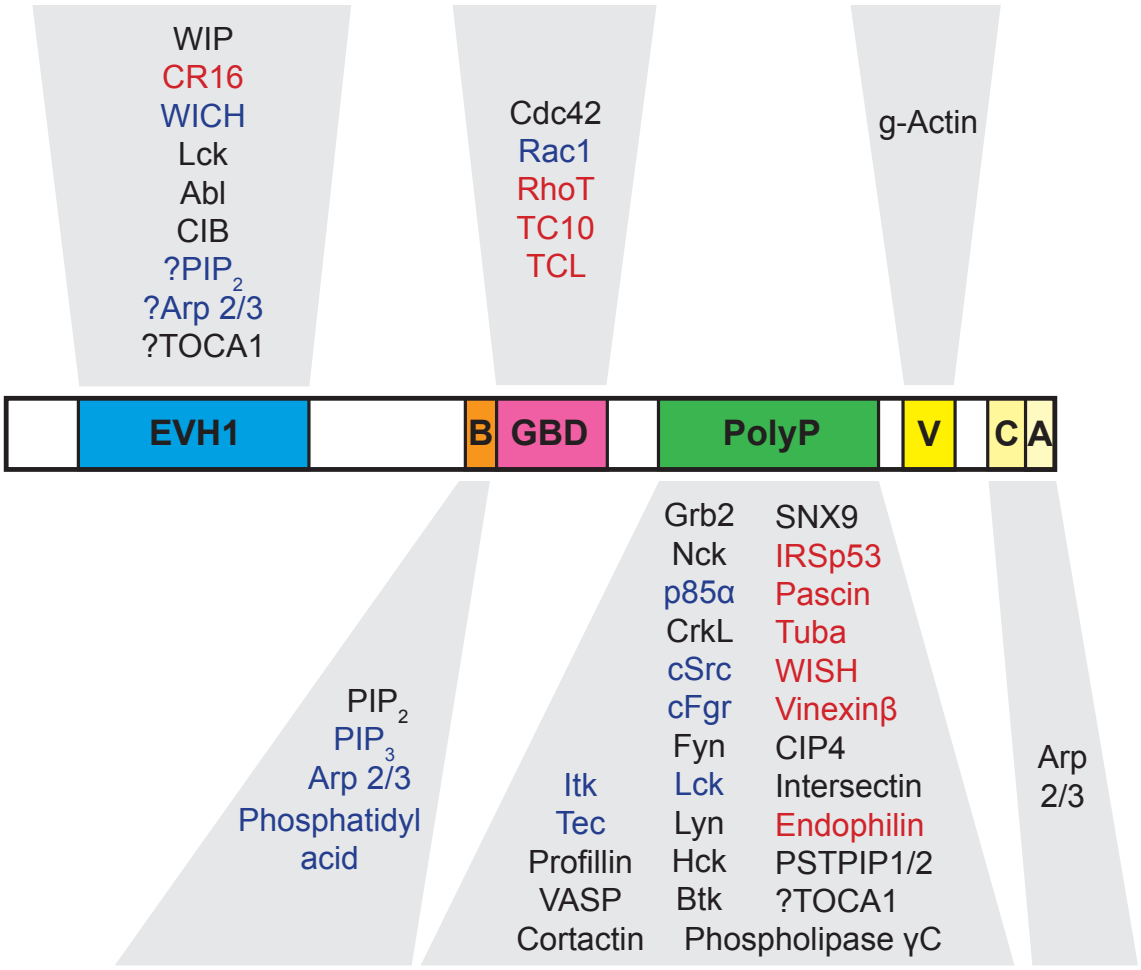

Fig 1.4 WASp binding partners
In vivo binding partners of WASp are shown in black, interactions only estabilished *in vitro* are shown in blue, and interactions only demonstrated with NWASp are shown in red

1.4.1 EVH1 domain

1.4.1.1 Proteins with homologous domains

The Ena-VASP homology domain 1 (EVH1) is a proline rich protein module of approximately 115 amino acids. It is found in actin scaffold proteins (Mena, VASP, Evl) and has been functionally implicated in the assembly and spatial localisation of multi-protein complexes involved in actin cytoskeletal remodelling. It binds the proline rich amino acid target sequence of L/FPPPP/E via a series of conserved aromatic amino acids. The structure of the Mena EVH1 domain bound to its polyproline target demonstrated a similarity in tertiary structure to the Plekstrin Homology (PH) domain, a PIP_2 binding domain involved in membrane localisation (Prehoda et al., 1999). As a results of these findings, and other experimental data, it has been postulated that the WASp EVH1 domain may be responsible for targeting WASp to the cell membrane, where it directly interact with membrane bound signalling complexes (Volkman et al., 2002).

1.4.1.2 Interaction with WIP and crystal structure

The best characterised binding partners of the WASp / NWASp EVH1 domains are the verprolin family proteins. Verprolin is a yeast protein involved in cell polarity, endocytosis and cytoskeletal organisation (Donnelly et al., 1993). Three mammalian verprolin family proteins have been identified and each are known to interact with the WASp EVH1 domain; WASp interacting Protein (WIP) (Ramesh et al., 1997), CR16 (Ho et al., 2001) and WIP and CR16 Homologous protein (WICH, also called WIRE – WIP related) (Kato et al., 2002; Aspenstrom, 2002). WIP is the mammalian homologue of verprolin, and WIP expression in verprolin deficient yeast reverses the defects of Verprolin deficiency (Vaduva et al., 1999). WIP is ubiquitously expressed, whereas CR16 expression is largely restricted to neural tissue. WICH has greatest expression in the brain but is significantly expressed in the lung and in the gastrointestinal tract. WICH only binds weakly to WASp, but binds strongly to NWASp. As neither WICH nor CR16 are expressed haematopoietic cells, WIP is the only physiological Verprolin binding partner of WASp.

The crystal structure of the NWASp EVH1 domain bound to the target WIP sequence was solved by *Volkman et al* in 2002 (Volkman et al., 2002). Firstly the authors demonstrated the minimal sequences of NWASp and WIP required for interaction. The entire NWASp EVH1 domain and a 25 amino acid sequence from the carboxyl terminus of WIP were required for binding. This suggested a much longer interaction sequence than expected, and the WIP binding sequence was over double the length of the minimal required sequence in other EVH1 domain target proteins. Like other EVH1 targets, this sequence contained a similar polyproline motif (DLPPPEP).

NMR spectroscopy was performed on a recombinant protein comprising of the NWASp EVH1 domain bound to the 25 amino acid WIP sequence via a short linker sequence. This demonstrated the WIP sequence wrapping circumferentially around the entire EVH1 domain, and therefore interacting with residues throughout the EVH1 domain (Volkman et al., 2002). Subsequent investigations have suggested the optimal interaction between NWASp and WIP is even longer, involving 34 WIP amino acids, and three distinct WIP motifs which anchor NWASp binding via hydrophobic contacts (Peterson et al., 2007; Zettl and Way, 2002). This offers a possible explanation for the distribution throughout the entire EVH1 domain of missense mutation causing WAS / XLT, and yet not throughout the rest of the protein (see section 1.7.4). The functional importance of WASp – WIP interaction is discussed more fully in section 1.7.

1.4.1.3 PIP_2 binding

The binding of PIP_2 to the amino terminal WASp (or N-WASp) has been demonstrated *in vitro* (Imai et al., 1999; Miki et al., 1996). The physiological importance of this finding has been questioned by the *Rohatgi et al* and others, who demonstrated that NWASp with the EVH1 domain deleted still responded to activation by PIP_2, and demonstrated that the basic domain was essential for PIP_2 responsivity (Volkman et al., 2002; Rohatgi et al., 2000; Prehoda et al., 2000). *Higgs and Pollard* found the opposite effect for EVH1 and basic domains of WASp in a series of similar *in vitro* experiments. They found that WASp fragments containing the basic domain were unable to bind or respond to PIP_2 containing vesicles (Higgs and Pollard, 2000). Whether or not PIP_2 binds to the WASp EVH1 domain *in vivo* remains controversial and unclear. These experiments and others raise the possibility of differences in the site of PIP_2 binding between WASp and NWASp, and also the possibility of multiple PIP_2 binding sites (Yarar et al., 2002).

1.4.1.4 Src family kinase binding

Src family protein kinases are membrane associated proteins which act in signal transduction pathways downstream from surface receptor ligation. Each kinase has three domains; a catalytic domain, an SH2 domain which binds phosphorylated tyrosine residues, and an SH3 domain which binds structural motifs in polyproline domains inducing activation of the catalytic domain. There are 8 Src family kinases, several of which have been implicated in binding to the WASp polyproline domain via their SH3 domains (see section 1.5.5).

Schulte et al demonstrated Src kinase Lck binding to a 10 amino acid sequence in the middle of the EVH1 domain of WASp (83-93 amino acids) (Schulte and Sefton, 2003). The WASp sequence bound to the catalytic domain of Lck and inhibited its kinase activity to other substrates, both *in vitro* and *in vivo* (using a protein overexpression system in Cos7 cells). This is a unique regulatory mechanism of Src kinase activity.

1.4.1.5 Arp 2/3 binding and EVH1 contribution to WASp activation

Suetsugu et al demonstrated weak Arp 2/3 binding to the EVH1 domain, and a cooperative contribution of the EVH1 domain to the interaction of Arp 2/3 to the VCA Central region. They also demonstrated that the EVH1 provides an intrinsic contribution to WASp activity, which they proposed was due to aligning the Arp 2/3 complex optimally for VCA binding and Arp 2/3 activation. This contribution is overridden in the presence of Cdc42 and PIP_2. Other results suggested a

Author	Year	Protein	Experimental system	Findings
Kato	1999	WASp	Actin clustering in Cos7 cells following overexpression of WASp	N terminal of EVH1 domain (aa 1-155) required for clustering
Zhang	1999	WASp	T cell development in knock-in mice (WASp dEVH1)	Normal thymic cellularity and subsets
Moreau	2000	NWASp	Vaccinia motility in HeLa cells	Increased cytoplasmic f actin Impaired recruitment to *Vaccinia* induced actin tails
Rohatgi	2000	NWASp	Purified protein pyrene assay	Increased actin polymerisation in the absense of Cdc42 or PIP_2
			Xenopus lysate actin polymerisation assay	Normal responses to PIP_2 and Cdc42
Suetsugu	2001	NWASp	Purified protein pyrene assay	Reduced actin polymerisation, but normal sensitivity to Cdc42 and PIP_2
			Bovine brain extract motility assay	Reduced, but not abolished motility
Cannon	2001	WASp	Localisation to T cell - APC contact	Normal recruitment and actin cytoskeletal rearrangement
Castellano	2001	WASp	Membrane protrusion after forced WASp recruitment to cell surface	Normal membrane protrusion
Yarar	2002	WASp	Purified protein pyrene assay	Reduced actin polymerisation
			Bead motility in *xenopus* lysate	Reduced bead motility
Benesch	2002	NWASp	Intracellular vesicle rocketting	Normal recruitment to vesicle but reduced vesicle motility

Fig 1.5 Published effects of EVH1 domain deletion on WASp / NWASp function
Impaired activity compared to WT shown in blue, enhanced activity in red and similar activity in green

contribution to WASp activity from EVH1 binding partners in addition to its intrinsic activity (Suetsugu et al., 2001a).

1.4.1.6 Deletion of the EVH1 domain

The biochemical and functional effects of deletion of the EVH1 domain have been assessed in several studies. These contradictory findings are summarised in figure 1.5. Generally they show that deletion of the EVH1 domain results in impaired actin polymerisation and actin based motility, although the impairment of *in vitro* activity can be overcome by Cdc42 and PIP_2. These results support an intrinsic role for the EVH1 domain in WASp activation. One study demonstrated impaired recruitment to *Vaccinia* induced actin tails with a dEVH1 NWASp construct (Moreau et al., 2000), whereas other studies have shown normal recruitment to T cell – APC contact sites (Cannon et al., 2001) and PIP_2 coated vesicles (Benesch et al., 2002). Whether the EVH1 domain is absolute required for WASp localisation to certain sites of active actin polymerisation, or whether this finding is a peculiarity of the *Vaccinia* system, remains to be determined.

1.4.2 Basic domain

The Basic domain consists of a sequence of 10 amino acids, 6 of which are lysine residues. A similar basic domain is found in all WASp group proteins, although the specific sequence is poorly conserved. The region was originally thought to play an important role in the binding of the VCA domain acidic region as part of WASp's autoinhibitory conformation (Miki et al., 1998a). It has subsequently been established that the basic domain is not essential for the formation of the autoinhibitory fold in either WASp or NWASp (Kim et al., 2000; Rohatgi et al., 2000). There is, however, evidence of a role for the basic domain stabilizing the autoinhibitory fold once it has formed (Leung and Rosen, 2005; Suetsugu et al., 2001b), through the (non-activating) binding of Arp2/3 (Suetsugu et al., 2001a; Prehoda et al., 2000) (see section 1.4.6 for further discussion).

1.4.2.1 Phospholipid binding

The Basic domain of NWASp has been shown to bind the acidic phopholipids $PI(4,5)P_2$, PIP_3, $PI(3,4)P_2$ and phosphatidic acid, all of which contribute to NWASp activation *in vitro* (Papayannopoulos et al., 2005; Otsuki et al., 2003; Rohatgi et al., 2000; Prehoda et al., 2000). Of these, $PI(4,5)P_2$ (PIP_2), both has the highest affinity for NWASp and greatest abundance in cell membranes. The binding of PIP_2 to the Basic domain can be eliminated by mutating four of the lysine residues within the domain to neutral amino acids, illustrating the importance of ionic attraction in this binding (Rohatgi et al., 2000). In contradiction to these

findings, Higgs and Pollard were unable to detect binding of a WASp fragment containing both Basic domain and GBD to PIP_2 containing vesicles (Higgs and Pollard, 2000).

The basic domain also plays an important role in attracting Cdc42 to WASp for binding to the GBD, and this is discussed more fully in section 1.5.1.3 (Hemsath et al., 2005).

1.4.2.2 Deletion of the Basic domain

Suetsugu et al compared the activity of NWASp constructs with the Basic domain deleted to a range of other NWASp constructs in a series of *in vitro* assays. They found that Basic domain deletion severely impaired Arp2/3 mediated motility of NWASp coated beads and bovine brain lysate actin polymerisation (assessed using a pyrene based assay). By contrast, the same Basic domain deleted construct appeared constitutively active in a purified protein pyrene assay, having greater activity in the absence of Cdc42 than WT NWASp had in the presence of Cdc42 (Suetsugu et al., 2001b). Although the authors conclude that these results can be explained by dysregulated activity of the dBasic domain construct, if this were true similar results would be expected from both pyrene based actin polymerisation assays. An alternative explanation is that the bovine brain lysate contains an inhibitory factor whose interaction with WASp is stabilised by the deletion of the basic domain, and this binding negates the constitutive activity of the purified NWASp protein.

Similar results (constitutive activity in a purified protein system, but impaired activity in a *Xenopus* egg lysate system) were demonstrated by Rohatgi et al (Rohatgi et al., 2000). They additionally showed a relative (but not absolute) insensitivity to PIP_2 induced NWASp mediated actin polymerisation. Impaired actin polymerisation with a Basic domain deleted NWASp construct has also been demonstrated in another *in vitro* lysate system, and in cellular actin comet formation assays (Papayannopoulos et al., 2005). Other studies with Basic domain deleted constructs have demonstrated no difference to WT in localisation to and motility induction of PIP_2 coated vesicles (Benesch et al., 2002) or induction of actin clustering in Cos7 cells (Kato et al., 1999).

1.4.3 GBD and CRIB

Cdc42 was the first identified binding partner of WASp (Symons et al., 1996; Kolluri et al., 1996; Aspenstrom et al., 1996). The GTPase binding domain (GBD) (235-288) in WASp is defined as the minimum sequence required to maintain high affinity binding to Cdc42 (Abdul-Manan et al., 1999; Rudolph et al., 1998).

Contained within this is the Cdc42/Rac interactive binding domain (CRIB), a sequence of 14 amino acids (238-251) which is highly conserved between all Rho type GTPase binding proteins (Kolluri et al., 1996; Burbelo et al., 1995; Manser et al., 1994; Manser et al., 1993). Interaction between WASp and Rho type GTPases other than Cdc42 has been demonstrated (Rac1, TC10), but the affinity with Cdc42 is always higher (see section 1.5.1.3).

1.4.3.1 Deletion of the GBD

Investigation of WASp / NWASp constructs with the GBD deleted has been less extensive than similar experiments for other domains. Such a deletion will effect both WASp autoinhibitory conformation and Cdc42 binding, making dissection of function difficult in these experiments. It is therefore surprising that, where tested, these constructs have demonstrated a relatively unimpaired phenotype. A GBD deleted WASp “knock-in” mouse model revealed that deletion of the GBD had no effect on T cell proliferative responses to anti-CD3 stimulation, or the actin polymerisation within T cells following activation (Badour et al., 2004). GBD deleted WASp overexpressed in Jurkat cells showed normal recruitment to the T cell synapse (Cannon et al., 2001), and CRIB deleted WASp proteins were still localised to and able to induce movement of PIP_2 coated vesicles in a cell lysate system (Benesch et al., 2002).

1.4.4 Polyproline domain

The polyproline domain is the largest functional domain in WASp, and is the binding site of the largest number of WASp regulatory proteins. It contains multiple SH3 domain binding motifs (PXXP), but it does not exclusively interact with SH3 containing proteins. Binding partners include kinases, proteins involved in cytoskeletal reorganisation and proteins implicated in targeting proteins to sites of cytoskeleton rearrangement. Polyproline domain binding proteins have been demonstrated to recruit proteins to the T cell synapse, podosomes, endosomes and the microtubule network. The functional significance of the best understood polyproline domain ligands, and their interaction with WASp and NWASp are summarised figure 1.6.

1.4.4.1 Deletion of the Polyproline domain

Deletion of the polyproline domain has generally been found to have a profound effect on WASp induced actin polymerisation and localisation. Impairment in actin polymerisation has been demonstrated in *in vitro* and *in vivo* systems (Yarar et al., 2002; Benesch et al., 2002; Castellano et al., 2001; Suetsugu et al., 2001b), and only one study has suggested normal actin polymerisation induced by a

Binding Partner	Protein Family	Effect on WASp	Reference
Grb2	SH3-SH2 adapter protein	Synergistically activates NWASp with Cdc42. Recruits WASp to activated EGFR	She 1997 Carlier 2000 Kempiak 2003
NcK		Synergistically activates NWASp with PIP2. Targets WASp to T cell synapse	Rivero-Lezcano 1995 Rohatgi 2001 Kempiak 2003
p85α		*In vitro* binding demonstrated	Banin 1996 Finan 1996
CrkL		Forms a complex with Syk in platelets	Oda 2001
Fyn	Src (a)	Essential for WASp tyrosine phosphorylation following TCR ligation	Banin 1996, 1999 Zhu 1997 Badour 2004 Suetsugu 2002
cSrc, cFgr		*In vitro* binding demonstrated	Banin 1996 Finan 1996 Bunnell 1996
Lck	Src (b)	Binds and tyrosine phosphorylates WASp *in vitro*	Zhu 1997 Torres 2006
Lyn		Increases tyrosine phosphorylation. Co-operative with Cdc42	Guinmard 1998
Hck		Increases tyrosine phosphorylation. Microspike formation. Cdc42 independent.	Cory 2002 Scott 2002
Btk	Tec	Binds and increases WASp tyrosine phosphorylation. Cooperative with Cdc42	Cory 1996 Baba 1999 Guinmard 1998
Itk, Tec		*In vitro* binding demonstrated	Cory 1996 Bunnell 1996
PSTPIP	PCH	Recruits phosphatase to WASp resulting in dephosphorylation, stabilising autoinhibbition. Recruits WASp to T cell synapse	Cote 2002 Bardour 2003, 2004
CIP4		Localises WASp to microtubules. Required for Microtubule organising centre polarity	Tian 2000 Linder 2000 Banerjee 2007
Intersetin 2		Localises WASp to endosomes. Induces WASp mediated TCR endocytosis after TCR engagement	McGavin 2001
Phospho-lipase γC		*In vitro* binding demonstrated	Cory 1996 Zhu 1997 Finnan 1996
VASP	ENA/ VASP family	Induces (and required for) actin polymerisation at leading edge and WASp coated bead motility. Co-localises with WASp to phagocytic cup	Castellano 2001 Yarrar 2002
Profilin		Activates WASp and Arp2/3. Required for WASp induced actin polymerisation. Stimulates NWASp induced microspike formation	Miki 1998 Suetsugu 1998 Yarrar 2002
SNX9	Sorting nexin family	Recruits WASp to complex which mediates clatherin pit induced endocytosis of Cd28 following TCR activation	Bardour 2007
Cortactin		Activates WASp and co-localises with it to the immune synapse	Martinez-Quiles 2004

Fig 1.6 Mediators known to bind to the WASp Polyproline domain

WASp construct with the polyproline domain deleted (Kato et al., 1999). Deletion of the WASp polyproline domain abolishes WASp recruitment to the immune synapse in T cells (Zeng et al., 2003; Badour et al., 2003; Cannon et al., 2001). By contrast, a dPolyP NWASp construct was normally recruited to PIP_2 coated vesicles (Benesch et al., 2002), and recruitment to *Vaccinia* induced actin tails appears to be independent of the polyproline domain (Moreau et al., 2000)

These results illustrate the combined function of the polyproline domain in WASp; contributing to efficient activation and participating in WASp localisation in certain circumstances.

1.4.5 VCA domain

The carboxyl terminal VCA module, defines the identity of WASp family proteins, and it provides the output through which these proteins signal. The verprolin homology domain is shared with several other actin regulatory proteins, and it acts as the monomeric actin (g-actin) binding site of WASp (Marchand et al., 2001; Hufner et al., 2001; Miki and Takenawa, 1998).

The central domain was originally thought to be a cofilin homology domain, but subsequently structural differences have suggested that any sequence similarity is coincidental (Marchand et al., 2001). The majority of this region contains predominantly basic residues, but the final three amino acids are acidic (over lapping with the terminal acidic domain). The C and A domains together are the minimal sequences required for autoinhibition, and for binding to both the GBD and Arp 2/3 following activation. These interactions are described in detail in sections 1.4.6.1 and 1.6.4.

The VCA domain is the minimal sequence required for actin polymerisation *in vitro* (Blanchoin et al., 2000a; Yarar et al., 1999; Rohatgi et al., 1999; Machesky et al., 1999), but due to its unregulated activity (both in term of activation and localisation), over-expression in cells leads to disruption of actin based structures and processes (Moreau et al., 2000; Machesky and Insall, 1998). Deletion of the WASp VCA domain inhibits induction of actin polymerisation (Yarar et al., 2002; Benesch et al., 2002; Suetsugu et al., 2001b), and leads to the dysregulation of many actin based structures (Kato et al., 1999; Machesky and Insall, 1998; Symons et al., 1996) and functions including phagocytosis (Tsuboi and Meerloo, 2007) and T cell development (Zhang et al., 2002). WASp localisation is unaffected by deletion of the VCA domain (Benesch et al., 2002; Cannon et al., 2001; Moreau et al., 2000).

1.4.6 Autoinhibition and Crystal structure

In the unbound state, WASp and NWASp adopt an autoinhibited conformation, where the VCA domain binds to the GBD, inhibiting any intrinsic activity of WASp (Kim et al., 2000). Evidence for this autoinhibition initially came from experiments demonstrating that the isolated VCA domain of WASp / NWASp could bind protein constructs containing the GBD, and this interaction inhibited the intrinsic actin polymerisation activity of the VCA fragment (Kim et al., 2000; Rohatgi et al., 1999; Miki et al., 1998b). If the EVH1, Basic and Polyproline domains are included in the GBD fragment, then the affinity for the VCA fragment is increased, and the minimal sequence required to suppress VCA induced actin polymerisation is the Basic domain and GBD sequence (Prehoda et al., 2000). Full length WASp or constructs containing the VCA domain did not bind isolated VCA fragments (Rohatgi et al., 2000; Prehoda et al., 2000).

1.4.6.1 VCA – GBD autoinhibitory pseudo-domain

Interaction between the VCA domain and the GBD involves two essential sequences within WASp. The first, (amino acids 482-492), spans part of the C and A domains within the VCA cassette, and the second (amino acids 242-310) spans the carboxyl end of the GBD and the adjacent sequence between the GBD and polyproline domains. The NMR structure of the WASp GBD bound to VCA was solved using a recombinant WASp polypeptide consisting of residues 242-310 linked to 461-492 by a short flexible linker sequence (Kim et al., 2000). In isolation the GBD exists in an unfolded state, forming no tertiary structural motifs, however in the presence of the VCA the sequence becomes highly structured and forms a hydrophobic core. The Central region of the VCA forms an amphipathic helix (α5) which packs down into the hydrophobic GBD surface formed by four other α helices (α1 – α4) and two β pleated sheets (Kim et al., 2000). The α1 helix is formed by residues which bind Cdc42, whereas residues within the α2, α3 and α4 helices do not directly interact with Cdc42 (Kim et al., 2000; Abdul-Manan et al., 1999).

The result of this binding and structural rearrangement is the cooperative formation of a pseudo-domain between the CA region and the GBD. The Arp2/3 binding site in the C domain is hidden in the middle of this hydrophobic core, and additionally it adopts a conformation unfavourable to Arp 2/3 binding. These mechanisms ensure that WASp is unable to bind and activate Arp 2/3 in its resting (autoinhibited) conformation (Panchal et al., 2003).

The hydrophobic fold within the GBD which forms upon binding of the Central

region, is sterically incompatible with the conformation seen when bound to Cdc42 (Kim et al., 2000; Abdul-Manan et al., 1999). The minimal sequence required for high affinity Cdc42 binding is residues 230-280 (Abdul-Manan et al., 1999; Rudolph et al., 1998), and therefore overlaps, but is not entirely included within the critical VCA interaction site.

1.4.6.2 Other autoinhibitory interaction

Although not required for the structural formation of the autoinhibitory pseudodomain, other WASp domains play a role in stabilising the autoinhibitory conformation. The basic domain binds Arp 2/3, and simultaneously maintains Arp 2/3 in an inactive conformation and stabilises NWASp's autoinhibited conformation (Leung and Rosen, 2005; Prehoda et al., 2000). This interaction alone is not sufficient to auto inhibit NWASp, but is additive to the effect of the autoinhibitory fold. In one study deletion of the terminal eight acidic residues in NWASp (484-502) resulted in constitutive activity *in vitro* (discussed further in section 1.4.1.5) suggesting a role for these residues in stabilising NWASp autoinhibition (Suetsugu et al., 2001a). This data, however, is difficult to rationalise with the essential role of the tryptophan 500 residue in Arp2/3 activation (Marchand et al., 2001). Together these results suggest that full WASp / NWASp autoinhibition requires the interaction of Arp 2/3, with both the basic region and the carboxyl terminus, in addition to the GBD - VCA binding (Prehoda et al., 2000).

Interestingly the interaction between GBD and VCA is specific for each WASp family member, and therefore the VCA domain from a WAVE protein does not bind to the WASp GBD.

1.4.6.3 Autoinhibitory conformation in vivo

The existence of WASp / NWASp in an autoinhibited conformation *in vivo* has been investigated using fluorescence resonance energy transfer (FRET) (Lorenz et al., 2004) and using a split yellow fluorescent protein (YFP) fluorescent probe (Lim et al., 2007). Both these techniques used fluorescent tags at the amino and carboxyl terminals of WASp / NWASp which emit a specific fluorescent signal only when the two probes are spatially adjacent to each other (i.e. in the autoinhibited conformation). These results have demonstrated the existence of WASp and NWASp in an autoinhibitory conformation in cells. NWASp showed loss of autoinhibition at the leading edge of carcinoma cells in response to EGF stimulation and at the base of invadopodia (Lorenz et al., 2004), whereas stabilisation of WASp autoinhibition was demonstrated by the co-expression of WIP and WIRE, and disrupted by TOCA1 and Nck1 (Lim et al., 2007).

1.4.6.4 XLN point mutations and WASp phosphorylation in GBD

XLN is caused by missense mutations within the WASp GBD. Each of these mutations occurs in residues which form part of the α1 or α3 helices of the autoinhibitory pseudo-domain (Ancliff et al., 2006; Devriendt et al., 2001). GBD sequences containing one of these mutations (L270P), showed much less structural stability than WT GBD when bound with VCA (Devriendt et al., 2001), and all XLN mutations are predicted to disrupt the autoinhibitory conformation (Ancliff et al., 2006; Leung and Rosen, 2005; Kim et al., 2000). The Tyr291 residue, which plays an important role in the regulation of WASp activity by phosphorylation (see section 1.5.5), is also found in α3 helix of the autoinhibitory fold, and the phosphorylation of this residue, and resultant introduction of a strongly ionic residue in the centre of the amphipathhic domain is predicted to destabilise the autoinhibitory conformation (Torres and Rosen, 2006; Kim et al., 2000). The conformational change induced in the GBD following Cdc42 binding (see section 1.5.3.3) normally exposes the Y291 residue, facilitating phosphorylation (Buck et al., 2001; Kim et al., 2000).

These findings provide a structural mechanism for both the constitutive activity of XLN point mutations and the regulation of WASp activity by Y291 phosphorylation.

1.5 WASp activation

1.5.1 Cdc42

Originally described as a protein essential for *Saccharomyces cerevisae* cell division, Cdc42 was the first protein identified to bind WASp both *in vitro* and *in vivo* (Symons et al., 1996; Kolluri et al., 1996; Aspenstrom et al., 1996). This interaction results in WASp activation and actin polymerisation via the Arp2/3 complex (Higgs and Pollard, 2000; Rohatgi et al., 1999; Ma et al., 1998b). Subsequent research has elucidated the complexity of the regulation of WASP activity and the involvement of many proteins and signalling cascades, nonetheless it is likely that Cdc42 remains a critical WASP activating protein *in vivo.*

1.5.1.1 Rho Family GTPases

Cdc42 is a monomeric GTPase, and a member of the Rho superfamily. These proteins are involved in translating cell surface signals to the cytoskeleton, and regulate a wide range of cellular processes including cell division, adhesion, cell morphogenesis, migration, vesicular transport, microtubule dynamics and gene expression (Heasman and Ridley, 2008; Jaffe and Hall, 2005; Nobes and Hall, 1995). An indication of the importance of monomeric G proteins and the

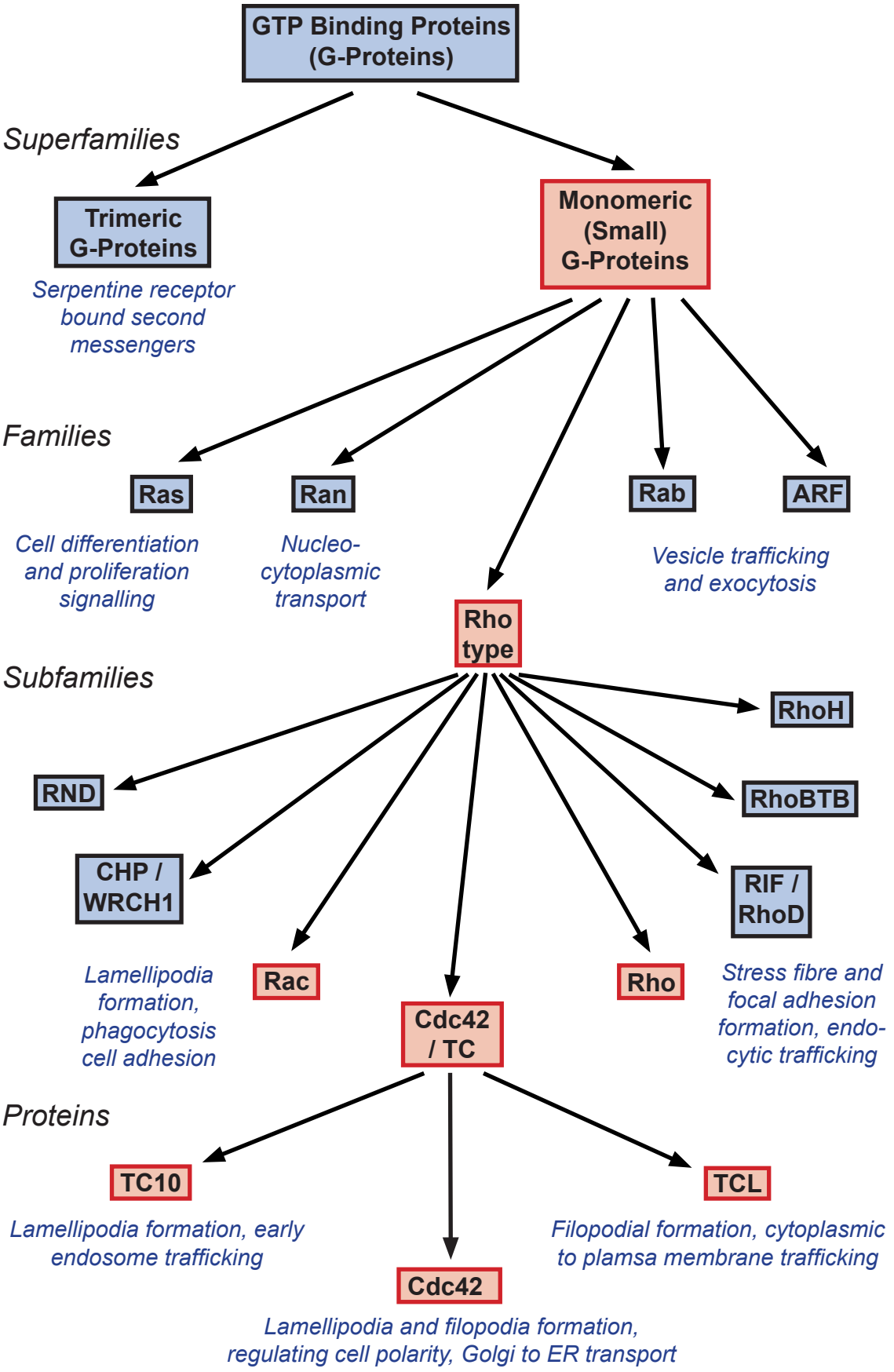

Fig 1.7 Family structure of G proteins
Boxes coloured red represent families or proteins which interact with WASp family proteins

regulation of their activity is provided by the fact that 2% of genes predicted by the sequencing of the human genome encode for these proteins or their regulators (Bernards, 2006). The Rho family has been divided into 8 subfamilies, of which the Rac, Rho and Cdc42 like subfamilies have been best studied (Fig 1.7). Cdc42, RhoA and Rac1 show the greatest sequence conservation between species of the Rho type GTPases. The other two GTPases in the Cdc42 subfamily are TC10 (RhoQ) and TCL (RhoJ).

Rho family GTPases, like other monomeric GTPases, function as molecular switches with a common basic mechanism (Nobes and Hall, 1994). In a GTP bound conformation they are active, but hydrolysis of the GTP to GDP results in a subtle conformational change at the nucleotide binding site. This causes the movement of one or more (conserved) “switch” α helices within the GTPase, which in turn induces conformational changes or positional realignment of the effector binding domains. Hydrolysis of the GTP nucleotide results in deactivation of the GTPase. Most monomeric GTPases are prenylated at their C terminus allowing lipid anchoring and resultant localisation to the intracellular surface of the cell membrane.

1.5.1.2 GEFs, GAPs and GDIs

The activity of monomeric G proteins is regulated by three groups of proteins (Fig 1.8). Guanine nucleotide exchange factors (GEFs) act by deforming the nucleotide binding site on the GTPase, inducing the release of GDP and stabilising the nucleotide free form of the GTPase. This allows the binding of GTP, (as the GTP concentration in the cell cytoplasm is much higher than that of GDP) and activation of the GTPase (Vetter and Wittinghofer, 2001).

GTPase activating proteins (GAPs) enhance the intrinsic GTPase activity of the protein and catalyse the transition of the GTPase to an inactive, GDP bound, state. Although some GTPase effector targets act as GAPs, not all do, and WASp appears to have no GAP activity on Cdc42 (Aspenstrom et al., 1996). GAPs and GEFs are themselves activated by a variety of mechanisms, including phosphorylation, binding of phospholipids and interaction with other secondary messengers such as cAMP and Ca^{2+} (Bos et al., 2007). Activation of GAPs and GEFs is important in localising GTPases to the cell surface and is frequently associated with activated receptor signalling complexes. Deactivation of GEF and GAP proteins is largely by ubiquitination and subsequent degradation.

The third group of regulatory proteins are the guanine nucleotide dissociation inhibitors (GDIs). These sequester GTPases in the cytoplasm in their GDP bound

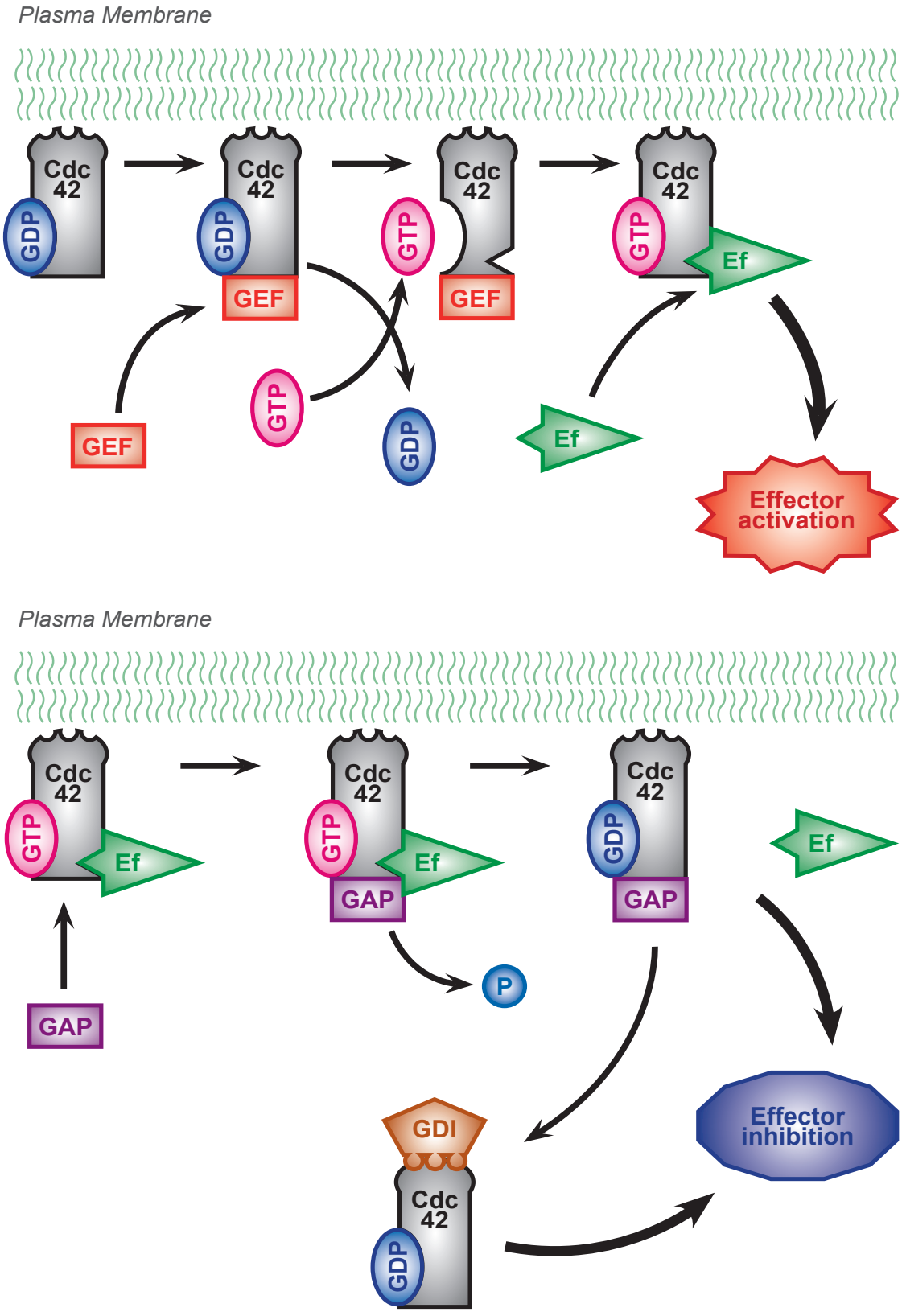

Fig 1.8 Mechanisms of how GEFs, GAPs and GDIs activate and inactivate Cdc42
Top panel demonstrates how guanine nucleotide exchange factors (GEFs) catalyse the exchange of GDP for GTP bound to Cdc42, increasing Cdc42 activity. The bottom panels demonstrates how GTPase activating proteins (GAPs) catalyse the hydrolysis of GTP to GDP, inactivating Cdc42. It also demostrates the role of guanine nucleotide dissociation inhibitors (GDIs) in sequesting Cdc42 away from the plasma membrane. *GDP - Guanosine Diphosphate, GTP - Guanosine Triphosphate, Ef - Cdc42 effector protein, P - Phosphate residue.*

form, by binding their prenylated carboxyl termini. This isolates them from potential effectors or activating proteins (Dransart et al., 2005).

A common theme of the regulation and signalling of Rho type GTPases is the crosstalk between signalling pathways and the promiscuity of interactions. Most Rho family GEFs and GAPs have activity on several different proteins (Bos et al., 2007), and many effectors are activated by several different GTPases. To further complicate these signalling networks, some monomeric G proteins activate other G proteins. For example, in Swiss 3TC fibroblast cells, Cdc42 activates Rac, which in turn activates Rho in the sequential formation of filopodia and lamelipodia (Nobes and Hall, 1995; Ridley and Hall, 1992). This complexity makes identifying the specific role of individual proteins extremely difficult. The biological relevance of *in vitro* interactions must always be questioned, and results interpreted in the context of *in vivo* animal knockout models.

1.5.1.3 Specificity of the Cdc42 – WASp interaction

Cdc42 is known to act on a range of target proteins including PAKs (Manser et al., 1994), ACKs (Manser et al., 1993), IQGAP (Erickson et al., 1997), PAR6 (Joberty et al., 2000; Qiu et al., 2000), and CIP4 (Aspenstrom, 1997), in addition to WASp. Furthermore, TC10, Rac1, TCL, and RhoT have all been described to interact with NWASp (Abe et al., 2003; Vignal et al., 2000; Neudauer et al., 1998; Aspenstrom et al., 1996). Interestingly, the kinetics of interaction demonstrate a much faster association rate for Cdc42 binding to WASp / NWASp than for any of the other GTPases. This results in an equilbrium dissociation constant for Cdc42 - WASp/ NWASp complexes at least 1000x lower than those for complexes formed with other Cdc42 binding proteins (Hemsath et al., 2005). This degree of specificity is unusual among small GTPases (ACK, and MRC kinase which also preferentially bind Cdc42 do not show this kinetic), and mechanistically appears to be related to the ionic attraction between the basic domain upstream of the Cdc42 binding site and two glutamic acid residues (Glu49 and Glu178) which are specific for Cdc42. The interacting interfaces between WASp and GTPase are very similar for Cdc42 and TC10. This “electrostatic steering mechanism” allows a very rapid turnover of signaling between Cdc42 and WASp.

In summary, WASp probably is capable of being activated *in vivo* by a range of specific Rho type GTPases, but its affinity and kinetics of interaction with Cdc42 are higher and faster. Cdc42 activates a wide range of different effector proteins involved in diverse cellular functions, and Cdc42 induced WASp activation itself is responsible for a range of different cellular functions.

1.5.2 PIP_2

1.5.2.1 Phosphatidylinositides in membrane dynamics

Phosphatidylinositol derivatives play a central and ubiquitous role in the cell biology of all organisms. There are seven functional phosphorylated derivatives (called phosphoinositides) and the generation of each is controlled by phosphoinositide kinases and phosphatases. Each phosphoinositide has a unique distribution among subcellular compartments and this is determined and maintained by the tight localised control of these generating enzymes.

$PI(4,5)P_2$ is the predominant phosphoinositide throughout the cell, but shows particular concentration in the plasma membrane. PI(4)P is concentrated in the golgi, PI(3)P in early endosomes and $PI(3,5)P_2$ in late endosomes. In the plasma membrane the interaction and balance between $PI(4,5)P_2$ and $PI(3,4,5)P_3$ is critical in the regulation of actin polymerisation. In resting cells, $PI(3,4,5)P_3$ exists in very low concentration in the plasma membrane, but stimulation of cells by growth factors, induces the enzyme phosphatidylinositol 3-kinase (PI3K), which generates $PI(3,4,5)P_3$ from $PI(4,5)P_2$.

Phosphoinositides are anchored in plasma membranes by their lipid tails, but the differentially phosphorylated ionsitol heads sit in the cytosol and bind proteins. Individual proteins show binding specificity towards individual phosphoinositides species, but individual interactions tend to be of low affinity. Protein sequences which bind phosphoinositides tend to be either unstructured clusters of basic residues (using electrostatic attraction for association), or folded phosphoinositide binding modules such as the pleckstrin homology domain (Lemmon, 2003; Yin and Janmey, 2003). Affinity is increased by the cooperative binding of multiple phosphoinositides or by protein co-receptors. This dual recognition is a powerful mechanism for defining organelle identity and provides the functional basis for protein and vesicle trafficking between cell compartments (Wenk and De, 2004).

1.5.2.2 Cooperation with monomeric GTPases

Phosphatidylinositides work in concert with small GTPases to recruit cytosolic proteins to specific membrane compartments. Several GAPs and GEFs, including those for Rho-type GTPases, have phosphoinositide binding modules and are recruited to membranes by phosphoinositides (Cantley, 2002). Additionally, several phosphoinositide kinases and phosphatases are the targets of GTPases, resulting in activation, and the subsequent synthesis or elimination of specific phosphoinositide species. Finally, GTPases and phosphoinositides act as co-receptors in many cellular functions, participating in co-operative binding and

recruitment. By having a specificity for both GTPase and phosphoinositide, proteins have an extensive potential repertoire of localisation signals (Behnia and Munro, 2005). These mechanisms inexorably link the activation and localisation functions of GTPases and phosphoinositides.

1.5.2.3 Phosphatidylinositide interaction with the cytoskeleton

PIP_2 binds and modulates the activity of most groups of actin binding proteins (reviewed in (Yin and Janmey, 2003)). Its role in stimulating the dendritic branching of actin networks can be summarised by four mechanisms. As discussed extensively below, it helps activate WASp family proteins to stimulate Arp 2/3 mediated actin nucleation. Secondly, PIP_2 facilitates actin filament elongation directly by binding capping proteins (gelsolin and CapZ) and destabilising their association with actin filament barbed ends. Thirdly, it promotes the dissociation of profilin and g-actin, increasing the concentration of g-actin at the actin filament barbed end, and therefore driving filament elongation. Finally, PIP_2 inhibits the severing action of cofilin / ADF and gelsolin, thereby reducing the number of available barbed ends and inhibiting the rate of network expansion (see section 1.6.2 for further discussion).

The main mechanism for increasing the local concentration of PIP_2, appears to be via recruitment of the enzyme phosphatidylinositol-4-phosphate 5-kinase 1 (PIP5K1). Both Rho and Rac GTPases bind and recruit PIP5K1 to the plasma membrane in a GTP independent manner.

PIP_3 has very similar actions to PIP_2 although it acts on a more discrete and distinct set of effect proteins. Among these, PIP_3 is responsible for the recruitment and activation of WAVE2 and resultant lamellipodia formation (Oikawa et al., 2004). Functionally, phosphatidylinositol 3-kinase (PI3K) and the generation of PIP_3 is pivotal for the generation of cell polarity and promotion of normal chemotaxis (Jones et al., 2003; Haugh and Meyer, 2002; Hannigan et al., 2002; Vanhaesebroeck et al., 1999).

1.5.2.4 PIP_2 binding to WASp

Although it is generally accepted that PIP_2 binds to the Basic domain in NWASp *in vitro* (Rohatgi et al., 2000; Prehoda et al., 2000), the site of binding in WASp remains unclear (Higgs and Pollard, 2000). Experimental evidence suggests binding sites within the EVH1 domain, the Basic domain and throughout the rest of WASp, and some data suggests multiple sites of bind (Yarar et al., 2002). The physiological relevance of these interactions also remains controversial and several groups have argued that upstream activation of Cdc42 (via GAP

activation) is more physiologically important (Ho et al., 2004; Ma et al., 1998a).

The *in vitro* affinity of PIP_2 for the NWASp Basic domain is highly dependant on the positive charge of the lysine residues within the domain. Binding is cooperative, with affinity for PIP_2 increasing as more phospholipids bind. This makes PIP_2 induced activation highly dependent on PIP_2 concentration in the local membrane, and results in sharp concentration threshold of activation (Papayannopoulos et al., 2005). The functional consequence of this is that *in vitro* NWASp responds to activation by PIP_2 as an “on - off switch” requiring a relative high concentration of membrane bound PIP_2 before it is activated. This enhances the specificity of NWASp signalling.

1.5.3 WASp activation by Cdc42, PIP_2 and TOCA

Cdc42 activates WASp by destabilising the autoinhibitory pseudo-domain formed between the VCA, and the GBD and surrounding residues (Kim et al., 2000). As described above (Hemsath et al., 2005), Cdc42 is attracted to WASp by the Basic domain, and is therefore able to “dock” adjacent to its target binding residues in the CRIB and GBD despite the binding of the VCA domain. Upon Cdc42 binding to the GBD, the VCA domain is released, exposing the actin and Arp 2/3 binding sites, and activating WASp (Panchal et al., 2003).

Although this basic mechanism is now widely accepted, many of the details and co-stimulations required for this process remain controversial, and much of the evidence is contradictory. This is partly due to differences in the experimental systems used to investigate WASp activation, but also due to the complexity and subtlety of WASp regulation.

1.5.3.1 Experimental systems

The elucidation of the mechanisms of WASp activation has come from several experimental modalities;

(1) Determination of binding affinities of WASp (or NWASp) fragments and domain deletion constructs, to each other, and to binding partners.

(2) The functional effects of these interactions have been assessed using purified component pyrene actin polymerisation assays (PPP assays) (Rohatgi et al., 2000; Prehoda et al., 2000; Higgs et al., 1999; Machesky et al., 1999).

(3) Actin polymerisation in a more physiological context has been measured using cell lysate pyrene assays (lysate assays) (Suetsugu et al., 2001b; Ma et al., 1998a; Ma et al., 1998b).

(4) Functional actin filament formation has been assessed by visualisation of actin comet formation or bead motility in cell lysates (Yarar et al., 2002; Suetsugu et al., 2001b; Higgs and Pollard, 2000; Ma et al., 1998b).

(5) I*n vivo* activity has been determined with the assessment of actin structures in cells following the microinjection of purified proteins or overexpression of protein constructs in cells (Machesky and Insall, 1998; Miki et al., 1998a; Miki et al., 1996; Nobes and Hall, 1995).

Pyrene based actin polymerisation assays use the fluorescence emitted by pyrene labelled actin which has been incorporated into actin filaments, to quantify the amount of f-actin formed. Pyrene labelled actin monomers are added to the purified protein reaction (containing actin, Arp 2/3 and ATP) or lysate, such that the pyrene labelled actin makes up 1-10% of the total actin content in the reaction. Fluorescence is measured following the addition of the construct under investigation and / or actin polymerisation initiator (e.g. Cdc42). The maximal rate of actin polymerisation and the maximal amount of f-actin formed are used as output measurements.

1.5.3.2 Evidence of Cdc42 induced activation

The first evidence for Cdc42 inducing WASp / NWASp activation came from cell lysate systems where the addition of GTP bound Cdc42 induced actin filament formation (Mullins and Pollard, 1999; Ma et al., 1998a; Zigmond et al., 1997). This was abolished with the immunodepletion of NWASp from the lysate (Rohatgi et al., 1999). Similar evidence came from cellular systems where inhibited or activated Cdc42 or WASp were microinjected or over expressed, and the subsequent formation of de novo actin structures required both active Cdc42 and WASp (Miki et al., 1998a; Symons et al., 1996). NWASp and WASp overexpression resulted in different patterns of actin remodelling in cells, with NWASp inducing filopodia (Miki et al., 1998a) and WASp producing discrete actin patches (Symons et al., 1996).

The structure of WASp GBD bound to Cdc42 demonstrated a specific interaction, resulting in conformational changes to both proteins (see section 1.5.2.4) (Abdul-Manan et al., 1999). In immunoprecipitation assays, GTP loaded Cdc42 was found to compete with the VCA domain for the binding of extended WASp / NWASp protein fragments containing both GBD and basic domains (Kim et al., 2000; Rohatgi et al., 2000; Prehoda et al., 2000; Miki et al., 1998a). Once released from GBD binding, the VCA domain was capable of binding Arp2/3 and instigating actin polymerisation.

Further biochemical studies demonstrated that Arp2/3 and the NWASp GBD compete for VCA binding. The presence of Cdc42 and PIP_2 in the precipitation reaction, however, reduces the VCA affinity for the GBD, and encourages VCA – Arp2/3 binding (Rohatgi et al., 2000). In all these experiments the binding of VCA to Arp2/3 correlated with the actin polymerisation induced in PPP assays.

1.5.3.3 Crystal structure of Cdc42 bound to WASp GBD

The NMR crystal structure of WASp GBD bound to Cdc42 was solved in 1999 (Abdul-Manan et al., 1999). It demonstrates that residues within the WASp CRIB domain form an extended binding sequence starting at the carboxyl end of the Cdc42 switch 1 motif (Cdc42 has two switch motifs - see section 1.5.1.1). An amphipathic WASp region downstream from the CRIB forms two anitparallel β sheets and an α helix upon binding Cdc42, which pack down into a hydrophobic region of Cdc42 adjacent to both switch 1 and switch 2 regions. Hydrogen bonds are formed by WASp residues Val250, Val247 / Ser248, Lys245 and His246 / His249 with their respective Cdc42 counterparts, and these are essential for stabilisation of the interaction. The NWASp equivalent of His246 (His208) has been mutated to Asp with resultant loss of Cdc42 affinity (Miki et al., 1998a), and a similar mutation of His246 has been used in this project to inhibit Cdc42 binding (see section 1.8).

This structure demonstrates that there is an extensive contact surface between Cdc42 and WASp, and that much of this contact is buried within a deep hydrophobic core. The involvement of both switch sequences in this interaction provides structural evidence of the necessity for Cdc42 to be GTP bound (and therefore activated) to facilitate WASp binding. The affinity of GDP – Cdc42 for WASp is 500 fold less than that of GTP – Cdc42 (Kolluri et al., 1996). Binding results in a conformational change in the GBD, destabilising the cooperative autoinhibitory domain formed with the VCA, and releasing the Arp2/3 binding site on the CA domain (Leung and Rosen, 2005; Buck et al., 2001; Kim et al., 2000).

Although this model is attractive, Cdc42 alone cannot fully explain the *in vivo* regulation of WASp activity. As described in section 1.4.6.2, other WASp domains, independent of the GBD, contribute to WASp's autoinhibition, and many other mediators activate WASp, many synergistically with Cdc42.

1.5.3.4 Activation of full length WASp

Assessment of the activity of full length WASp or NWASp in the absence of Cdc42 stimulation has resulted in heterogeneous results, ranging from constitutive maximal activity to no activity at all (Yarar et al., 2002; Suetsugu et al., 2001a;

Suetsugu et al., 2001b; Higgs and Pollard, 2000; Prehoda et al., 2000; Yarar et al., 1999; Rohatgi et al., 1999; Egile et al., 1999). The most accepted view is that WASp is fully autoinhibited in the absence of activators, and this is consistent with the findings of the only published study which assessed WASp purified from mammalian tissue (Higgs and Pollard, 2000). These findings fit with the structural models of WASp autoinhibition, and also with the cellular function of WASp, namely to initiate the formation of actin structures in a temporally and spatially controlled manner. Due to the relatively high concentration (10 μM) of WASp in haematopoietic cells (Higgs and Pollard, 2000), any constitutive WASp activity would lead to significant unregulated actin polymerisation. Generally, in the absence of activators, NWASp shows low grade actin polymerisation activity in PPP assays, suggesting predominant, but not absolute autoinhibition.

In contrast to full length WASp, the isolated VCA domain shows maximal constitutive activity in *in vitro* actin polymerisation assays. The full VCA domain is sufficient for initiating actin polymerisation, and its activity is unaffected by known regulators of WASp (Pantaloni et al., 2000; Blanchoin et al., 2000a; Rohatgi et al., 1999; Higgs et al., 1999). When over expressed in cells, it disrupts the formation of actin structures (Machesky and Insall, 1998), further emphasising the importance of regulated WASp activity for functionality.

1.5.3.5 Synergistic activation by Cdc42 and PIP_2

Addition of GTP loaded Cdc42 to WASp in PPP assays results in a small increase in actin polymerisation. The addition of PIP_2 instead of Cdc42 resulted in a much larger increase in activity, but maximal activity was only achieved by the addition of both Cdc42 and PIP_2 (Yarar et al., 2002; Higgs and Pollard, 2000). When these nucleation reactions were visualised, WASp supplemented with PIP_2 induced branching of actin filaments whereas WASp alone or supplemented with Cdc42 induced shorter unbranched filaments. Supplementation with both PIP_2 and Cdc42 resulted in the formation of actin rich halos around PIP_2 micelles (Higgs and Pollard, 2000).

Interestingly, NWASp appeared to be more sensitive to GTP-Cdc42 in PPP assays, with PIP_2 alone having a minimal effect on activity. A similar synergism between Cdc42 and PIP_2 exists (Papayannopoulos et al., 2005; Rohatgi et al., 2000; Prehoda et al., 2000; Rohatgi et al., 1999). Further work has demonstrated that the binding of Cdc42 and PIP_2 to NWASp is cooperative and that both are able to bind NWASp simultaneously (Prehoda et al., 2000). NWASp activity in cell lysate systems is more tightly inhibited than in purified protein systems, but activation appears to be induced with GTP loaded Cdc42 only. PIP_2 micelles were

absent from these assays as the lysate had been ultracentrifuged to remove all lipid vesicless (and f-actin) (Ho et al., 2004; Rohatgi et al., 1999).

1.5.3.6 TOCA1

The differences in activity and sensitivity to activators seen between purified protein and lysate systems suggested an additional activator is essential for NWASp activation *in vivo*. TOCA1 (transducer of Cdc42 activation) was identified and characterised in 2004 (Ho et al., 2004). It is required for both Cdc42 and PIP_2 induced NWASp meditated actin polymerisation in *Xenopus* lysate, and its presence negates the need for both other activators to be present simultaneously (Lim et al., 2007; Ho et al., 2004). It binds directly to NWASp via an SH3 domain and to Cdc42 via a novel GTPase bind motif, and binding to both of these is required for NWASp activation.

In cells, the majority of NWASp exists bound to WIP or CR16, which has an inhibitory effect on Arp 2/3 activation (Martinez-Quiles et al., 2001). NWASp complexed to WIP is resistant to activation by Cdc42, and requires the additional binding of TOCA1, to facilitate Arp 2/3 activation. This mechanism explains some of the differences in experimental systems described above.

The equivalent experiments on WASp have not been performed, although significant differences in results between PPP assays and more physiological systems have been detected (Yarar et al., 2002). TOCA1 is a member of the Pombe Cdc-15 homology (PCH) family, and WASp is known to bind two other proteins in this group, CIP4 (Tian et al., 2000) and formin binding protein 17 (FBP17) (Tsuboi et al., 2009). Both have been implicated in localising WASp to specialised actin structures. Interestingly TOCA1 has recently been implicated in localising NWASp to endocytic vesicles and filopodia (Bu et al., 2009), suggesting all these proteins may play a role in targeting as well as activating WASp proteins.

1.5.3.7 Prenylation of Cdc42

Several studies have demonstrated the need for Cdc42 to be prenylated to induce actin polymerisation in cell lysate systems (Ma et al., 1998b; Zigmond et al., 1997). Although several groups have reported GTP loaded Cdc42 purified from E.coli (not prenylated) activating both NWASp (Suetsugu et al., 2001b; Egile et al., 1999; Miki et al., 1998a) and WASp (Yarar et al., 2002), activation of purified bovine thymic WASp required Cdc42 to be prenylated for activation (Higgs and Pollard, 2000). Interestingly, the same group found, however, that un-prenylated Cdc42 was able to disrupt the autoinhibitory binding between recombinant WASp VCA and WAS p Basic – GBD fragment.

These conflicting data certainly suggest a role for Cdc42 prenylation in some aspect of WASp activation. Whether this is specific to WASp (and not NWASp), to the method of WASp synthesis and resultant post-translational modification, to the specialisation of cell (or lysate) WASp is functioning in, or to the specific species, remains unknown. One possibility is that prenylation of Cdc42 will bring it into much closer proximity to PIP_2 thereby facilitating the synergistic activation of WASp.

1.5.4 Cdc42 independent WASp activation

There is now excellent evidence for Cdc42 activating WASp and NWASp both *in vitro* and *in vivo*, however there is increasing evidence that Cdc42 is not essential for these processes. Depending on the specific cell or experimental system, and the subcellular actin structure being generated, the role of Cdc42 can be bypassed. The evidence for this is summarised below.

The use of dominant negative Cdc42 17N, and a specific Rho type GTPase inhibitor (*clostridium dificile* toxin) have revealed that Cdc42 is not required for *vaccinia* motility (Moreau et al., 2000), EGF induced actin polymerisation (Kempiak et al., 2003) or the Hck mediated tyrosine phosphorylation of WASp (Cory et al., 2002). In these systems and in *in vitro* systems other mediators (Nck, WISH, Hck, Grb2) have provided the necessary activation signals rendering Cdc42 redundant (Cory et al., 2002; Fukuoka et al., 2001; Rohatgi et al., 2001; Moreau et al., 2000) (see sections 1.5.5 and 1.5.6).

As described above (section 1.4.3.1) deletion of the GBD seems to have minimal impact on *in vivo* WASp or NWASp functioning. Localisation to APC – T cell contacts, T cell development, TCR induced T cell proliferation and actin polymerisation, and vesicle movement were all normally induced by GBD deleted WASp or NWASp constructs (Badour et al., 2004; Benesch et al., 2002; Cannon et al., 2001). Furthermore, similar results were found using a point mutation substituting a histidine residue for an aspartate residue at WASp 246 (NWASp 208) which abolishes Cdc42 binding (Kato et al., 1999; Miki et al., 1998a), but retains an autoinhibited conformation (Kato et al., 1999). Experiments using this mutant WASp / NWASp have demonstrated normal actin polymerisation *in vitro* (Fukuoka et al., 2001), normal vesicular motility (Benesch et al., 2002) and normal actin patch (WASp) or microspike (NWASp) formation *in vivo* (Fukuoka et al., 2001; Kato et al., 1999).

These results demonstrate that, although Cdc42 plays a central role in the translation of cell surfacing signalling to the cytoskeleton, there is sufficient

redundancy within these signalling networks that Cdc42 is not essential for WASp induced actin polymerisation.

1.5.5 Protein kinase binding and WASp phosphorylation

1.5.5.1 Tyrosine kinases

Non-receptor tyrosine kinases play a critical role in downstream signalling following ligation of several cell surface receptors. They can act at several functional levels of signalling cascades, as illustrated by their interaction with Rho type GTPases. They phosphorylate and activate GEFs initiating the activation of GTPases, but also directly phosphorylate GTPase targets (such as WASp) and can cooperatively modulate the activity of these targets with GTPases.

Two families of non-receptor tyrosine kinases have been identified to bind and phosphorylate WASp and NWASp. The structure of Src family kinases is described in section 1.4.1.4, and of these Fyn, cFgr, cSrc, Hck, Lck, Lyn have all been shown to bind WASp. Tec family kinases are related to Src kinases, but in addition to SH2, SH3 and kinase domains, they have an amino terminal pleckstrin homology domain, a Zn^{2+} binding Btk motif and a short polyproline sequence. Btk, Itk and Tec have all been linked to WASp function.

The SH2 domains from these proteins are able to bind phosphorylated tyrosine residues within specific short motifs, such as the immunoreceptor tyrosine-based activation motif (ITAM) found in the cytoplasmic tails of cell surface receptors (Cambier, 1995; Reth, 1989). Their activity is mediated by their interaction with other proteins and phospholidids, but also by phosphorylation, and many are capable of autophosphorylation. These kinases play an important role in amplifying the signalling response and in recruiting new proteins to cell surface signalling complexes. It is likely that each kinase family is important in recruiting a specific subset of downstream effectors, at a specific time point within the signalling cascade.

1.5.5.2 Phosphorylation of WASp

WASp is tyrosine phosphorylated *in vivo* in response to a range of cell stimuli including collagen stimulation of platelets (Oda et al., 1998), IgE activation of mast cells (Guinamard et al., 1998) and pre-B cell receptor cross linking (Baba et al., 1999). There are seven tyrosine residues in WASp, six in the EVH1 domain or the sequence between EVH1 and basic domains, and one in the GBD. By point mutation of each of these sites and by mass spectroscopy, Tyr291 was identified as the critical site of WASp tyrosine phosphorylation, both *in vitro* and *in vivo*. (Badour et al., 2004; Cory et al., 2002; Baba et al., 1999). Subsequently an

equivalent tyrosine phosphorylation site (Tyr256) has been identified in NWASp (Suetsugu et al., 2002).

The activity of tyrosine phosphorylated WASp / NWASp has been investigated by phosphorylating recombinant NWASp *in vitro* using recombinant kinases (Torres and Rosen, 2006; Torres and Rosen, 2003), and by generating the phosphomimicking WASp point mutation Y291E (Cory et al., 2002). In this construct the tyrosine residue is replaced by the negatively charged glutamate residue which mimics the charge produced by a phosphorylated tyrosine residue. Both approaches have demonstrated a modest increase in activity for the tyrosine phosphorylated protein over WT. Y291 sits deep in the centre of the GBD / VCA autoinhibitory fold. The increase in WASp activity upon phosphorylation is thought to be due to the destabilising effect of the highly charged phosphorylated tyrosine on the autoinhibitory conformation (Kim et al., 2000). Despite this destabilisation, the tyrosine phosphorylated NWASp is still able to adopt the autoinhibited conformation (Torres and Rosen, 2006), and without phosphorylation NWASp is still able to induce actin polymerisation (Suetsugu et al., 2002; Miki et al., 1996).

The functional significance of Y291 phosphorylation has been demonstrated in a number of systems. An increase in WASp induced macrophage filopodia was observed following cellular treatment with phosphatase inhibitors, which correlated with an increase in WASp tyrosine phosphorylation (Cory et al., 2002). WASp null mice, bone marrow reconstituted with Y291F “phosphodead” (unphosphorylatable) WASp, were used to demonstrate that Y291 phosphorylation was essential for immune synapse formation, actin polymerisation adjacent to the TCR following ligation and coupling of TCR engagement to NF-AT activation (Badour et al., 2004).

The relationship between tyrosine phosphorylation and Cdc42 induced WASp / NWASp activation has been extensively explored by *Torres and Rosen (2003, 2006)*. They used an *in vitro* purified protein system, testing amino terminally truncated and / or polyproline domain deleted NWASp constructs, generated in *E.coli*. They demonstrated that NWASp was 40x more easily phosphorylated following Cdc42 binding (and therefore disinhibited), and once phosphorylated, NWASp was 30x more sensitive to dephosphorylation in the presence of Cdc42, compared to when autoinhibited. They proposed that this difference related to changes in the surface accessibility of NWASp Y256 between the two conformations of NWASp, and that this mechanism accounts for the cooperativity they found between phosphorylation and Cdc42 binding. They also postulated that in the presence of transiently bound Cdc42, phosphorylation acts as a

molecular marker of previous NWASp activation (Torres and Rosen, 2006; Torres and Rosen, 2003).

There is some *in vivo* data to support these findings. Overexpression of constitutively active Cdc42, enhanced the WASp tyrosine phosphorylation produced by Lck and Btk protein kinases in mast cells (Guinamard et al., 1998). Data from other studies, however, does not support cooperation between Cdc42 and kinase activity. Cdc42 had no effect on the efficacy of Hck phosphorylation of WASp, when all three proteins were over-expressed in Cos7 cells (Cory et al., 2002), and similar results were found for NWASp phosphorylation with Fyn in PC12 (rat phaeochromocytoma) cells (Suetsugu et al., 2002). *In vitro* NWASp tyrosine phosphorylation by Fyn was significantly enhanced by PIP_2 but not by Grb2 or by Cdc42 (Suetsugu et al., 2002).

Tyrosine phosphorylation increases susceptibility of NWASp to degradation by the proteasome (Suetsugu et al., 2002), but there is no equivalent published data for WASp. Tyrosine phosphorylation has also been shown to reduce the affinity of WASp for the adaptor protein Grb2 following collagen stimulation of platelets (Oda et al., 1998). These examples suggest that WASp tyrosine phosphorylation may well have a more widespread regulatory role than simply reducing the threshold for WASp activation.

In addition to tyrosine phosphorylation, two sites of serine phosphorylation have been identified within the VCA domain of WASp. These have also resulted in increasing WASp actin polymerisation activity *in vitro* and the mechanism of this is enhanced Arp 2/3 binding. Unlike phosphorylation of Y291, S483 / S484 phosphorylation appears to be constitutive, and mediated by casein kinase 2 (Cory et al., 2003).

For phosphorylation to act as a regulatory signal there must be physiological antagonists to WASp kinases. LAR-PTP (*in vitro*) and PTP-PEST (*in vivo*) have been identified as WASp specific phosphatases (Torres and Rosen, 2003; Cote et al., 2002). The later cannot bind directly to WASp, but does so via the adapter protein PSPPIP as described in section 1.5.6.2.

1.5.5.3 Role in WASp activation

Although tyrosine kinases partially activate WASp through phosphorylation of Y291, there is *in vitro* evidence that they destabilise the WASp autoinhibitory conformation in addition to the effects of phosphorylation. This effect has been proposed to be through induced GBD conformational change following interaction

between the kinase SH2 domain and the WASp Y291 residue (Torres and Rosen, 2003). Src and Tec kinases have both SH3 and SH2 domains and are therefore capable of binding to both the polyproline domain and the GBD, and the presence of both domains is required for maximal activation of WASp by kinases (Torres and Rosen, 2003). Interestingly the affinity of WASp for Btk and Hck is unaffected by the phosphorylation status of Y291 suggesting that the primary binding site of tyrosine kinases is via SH3 domains to the WASp polyproline domain (Cory et al., 2002; Baba et al., 1999). WASp activation by protein tyrosine kinases, like the effects of other WASP activators, is cooperative with Cdc42 and with PIP_2 (Suetsugu et al., 2002).

1.5.6 SH3 domain containing proteins

1.5.6.1 SH3 – SH2 adaptor proteins

Src homology domain 3 (SH3) - SH2 adapter proteins are a small group of proteins with no intrinsic catalytic activity, which function by binding and co-localising at least two different effector proteins, facilitating their interaction. These proteins are able to bind both proline rich motifs (via SH3), which are generally found in regulators of the cytoskeleton, and phosphorylated tyrosine residues (SH2), usually associated with intermediates downstream of receptor tyrosine kinase signalling cascades. Structurally they have a single SH2 domain but multiple SH3 domains (Chen et al., 1998).

Nck and Grb2 are SH3 – SH2 adapter proteins and were among the first proteins identified to bind the WASp polyproline domain (She et al., 1997; Rivero-Lezcano et al., 1995). Both bind a diverse range of effector proteins and are involve in a variety of cellular functions. A well characterised example of this, is Grb2 recruitment to the cell surface by Epidermal Growth Factor Receptor (EGFR). Following activation, EGFR is tyrosine phosphorylated facilitating Grb2 binding via its SH2 domain. Grb2 constitutively binds SOS, a promiscuous GAP for Ras family GTPases, and through activation of Ras GTPases co-localised to EGFR, Grb2 links receptor tyrosine kinase signalling to activation of the MAK kinase / ERK pathway (Schlessinger, 1994; Pawson, 1994). Protein co-localisation, and coordinating the formation of multiprotein signalling complexes are central to SH3 – SH2 adapter protein function.

The binding of these adaptors to NWASp contributes to activation and release of autoinhibition. It was originally demonstrated that Grb2 and Cdc42 synergistically activated NWASp in a PPP assay, negating the need for PIP_2 for maximal activation (Carlier et al., 2000). By contrast Nck and PIP_2 synergistically activated NWASp, with Cdc42 activation redundant in the presence of Nck. Nck alone produced

a similar degree of activation as Cdc42, and was a more potent activator than Grb2. Maximal Nck activation of NWASp was achieved if all three SH3 domains bound the NWASp polyproline domain (Rohatgi et al., 2001).

No synergism was detected between Grb2 and Nck in the *in vitro* PPP assay, however more recently an *in vivo* EGF induced membrane protrusion model demonstrated a need for both Grb2 and Nck to activate NWASp. The resultant actin polymerisation and membrane protrusion was independent of both Cdc42 and phosphatidyl ionositol-3-kinase (and therefore PIP_2) (Kempiak et al., 2005; Kempiak et al., 2003). Further evidence of a concerted role for Nck and Grb2 in NWASp activation comes from the recruitment of both adaptors to lipid vesicles during NWASp mediated vesicle rocketing (Benesch et al., 2002). Nck is important in targeting WASp to the immune synapse following T cell receptor ligation, and this is more fully discussed below. In addition to WASp and NWASp, Nck also binds WIP and p21 activated kinase 1 (PAK1), illustrating its pivotal role in actin dynamics (Anton et al., 1998; Bokoch et al., 1996).

Two other SH3 – SH2 adaptor proteins have been identified, as playing a role in WASp / NWASp signalling although details of their physiological significance are limited. The p85 subunit of phosphatidylinositol 3-kinase (p85) has been shown to bind WASp *in vitro* (Banin et al., 1996), and recently has been identified as part of a complex with WASp, SNX9 and CD28, which mediates the endocytosis (and therefore internalisation) of CD28 following TCR activation (Badour et al., 2007). CrkL has been found to bind WIP when complexed to WASp, and may play a role in recruiting WASp – WIP complexes to ZAP-70 in lipid rafts adjacent to the immune synapse (Sasahara et al., 2002).

1.5.6.2 Other SH3 adaptor proteins

As shown in figures 1.4 and 1.6 there are a large number of SH3 domain containing protein which interact with WASp / NWASp. Several of these have demonstrated roles in localising WASp to specific cytoskeletal structures such as microtubules (CIP4) and endosomes (intersectin 2, SNX9), without having any additional catalytic activity.

Proline-Serine-Threonine phosphatase interacting protein 1 (PSTPIP1) is a member of the Pombe Cdc-15 homology (PCH) family, (like TOCA), whose interaction with the WASp polyproline domain results in impaired WASp activity. Following overexpression of WASp and PSTPIP1 in various cell lines, the two proteins immunoprecipitated together and WASp induced actin bundling was disrupted (Wu et al., 1998). PSTPIP1 also binds a PEST family protein tyrosine

phosphatase, PTP-PEST, and *in vivo* these two proteins are bound together in haematopoietic cell lines. PSTPIP1 act as a scaffold protein, simultaneously binding WASp and PTP-PEST, mediating the dephosphorylation of WASp at Tyr291, and reducing its actin polymerisation activity (Badour et al., 2004; Cote et al., 2002; Wu et al., 1998). This physiological antagonism to Tec family kinases has been best characterised for WASp activation in T cells. Following TCR engagement, Fyn binds to WASp and phosphorylates it at Tyr291, inducing the activation of Arp 2/3 mediated actin nucleation. Within minutes, WASp is recruited by PSTPIP1 to PTP-PEST and is dephosphorylated (Badour et al., 2004). As discussed below this interaction is also important in recruiting WASp to the immune synapse.

1.5.6.3 WASp localisation to the immune synapse

WASp is essential for the formation of the T cell synapse, as demonstrated by WASp null T cells having impaired synapse formation and impaired actin polymerisation adjacent to the synapse following TCR stimulation (Badour et al., 2003; Snapper et al., 1998; Gallego et al., 1997; Molina et al., 1993; Molina et al., 1992). Exactly how signal transduction, actin remodelling, protein compartmentalisation and endocytosis of surface receptors are coordinated, and what role WASp plays in these processes, is an active area of ongoing research.

At least two pathways for WASp recruitment to the T cell synapse have been described. Nck is rapidly recruited to the CD3ε chain following CD3-TCR engagement, and this appears to be critical for T cell synapse formation (Gil et al., 2002). Nck also binds the adapter protein SLP-76 via its SH2 domain, following SLP-76 phosphorylation (Wunderlich et al., 1999). SLP-76 is localised, and recruits WASp, to the synapse by an inducible interaction with the membrane bound adapter protein LAT, via the Grb2 related protein, GRAP2 (Liu et al., 1999). SLP-76 simultaneously binds Vav-1 (a Cdc42 GEF) and Cdc42, facilitating temporally and spatially appropriate WASp activation (Zeng et al., 2003). SLP-76 associated protein (SLAP) completes the multimeric complex (Krause et al., 2000). Thus Nck can recruit WASp to the synapse both directly via its SH3 domain, and indirectly via its association with SLP-76.

In the second described pathway, PSTPIP1 binds to both CD2 and CD2 adapter protein (CD2AP) following CD2 engagement. WASp is then recruited to this complex by PSTPIP2 (via polyproline - SH3 domain binding), and this recruitment is essential for synapse formation (Badour et al., 2003).

Whether these different recruitment mechanisms represent different time points after T cell stimulation, relate to different co-stimulatory signals or represent

differences in the antigen presenting cell or TCR stimulation conditions remains to be determined.

1.5.7 Profilin and VASP

The actin monomer binding protein profilin, plays a central role in the dynamics of actin polymerisation and depolymerisation as described below (section 1.6.2). It also has a significant effect upstream on the activation of WASp.

Profilin depletion from neutrophil lysate abolishes Cdc42 induced actin polymerisation, and its role in this process is dependent on binding the polyproline domain of WASp (Yang et al., 2000). This role in activation appears to be dependent on the presence of VASP (Yarar et al., 2002). It is likely that profilin catalyses nucleation by delivering actin monomers to Arp 2/3 at the point of nucleation, helping to overcoming the thermodynamic instability of initiating filament branching. However profilin's role in actin nucleation is complex as it also sequesters g-actin and enhances barbed end polymerisation. These actions reduce free g-actin concentration, which in turn limits the rate of Arp 2/3 nucleation. Additionally, there is evidence for profilin having an effect on activating WASp, by partially relieving WASp autoinhibition, in a manner similar to Grb2 (Yang et al., 2000).

Vasodilator-stimulated phosphoprotein (VASP) is an actin regulatory protein which plays a role in localising proteins to the actin cytoskeleton and regulating actin remodelling. It contains an EVH1 domain, and an f- and g-actin binding domain which facilitates VASP oligomerization (EVH2 domain) (Bachmann et al., 1999). Like profilin, VASP promotes actin polymerisation at several different levels. It binds WASp directly via the interaction of the VASP EVH1 domain with the WASP polyproline domain (Castellano et al., 2001). VASP and WASp cooperate in regulating actin polymerisation via multimeric signalling complexes formed in response to Fcγ receptor evoked phagocytosis (Coppolino et al., 2001) and TCR engagement (Krause et al., 2000).

In summary, profilin and VASP are important factors which act together to stimulate WASp induced Arp2/3 nucleation and function at several level in this process.

1.5.8 Model of WASp as signal transducer

The functional analysis of individual WASp domains and their interaction with multiple binding partners gives an insight into how WASp functions *in vivo*. It integrates inputs from several signalling cascades; balancing the activating signals (GTP bound Cdc42, PIP_2, TOCA, Nck, Grb2 binding and tyrosine phosphorylation)

against the inhibitory factors (intrinsic stability of autoinhibitory conformation, WIP binding). If the activating signals overcome the inhibitory factors, the autoinhibitory conformation of WASp is disrupted and the protein opens. Other binding partners act by localising WASp and Arp2/3 to specific sites of actin polymerisation, and by recruiting other regulatory proteins.

Several models have been proposed to explain these increasingly complex finding, and integrate them into a mechanisms of WASp regulation (Dong et al., 2007; Torres and Rosen, 2006; Leung and Rosen, 2005; Hemsath et al., 2005; Kempiak et al., 2005; Insall and Machesky, 2004; Ho et al., 2004; Martinez-Quiles et al., 2001; Higgs and Pollard, 2000; Prehoda et al., 2000). How relevant these models are to the *in vivo* situation remains largely unknown. It does appear, however, that WASp induced actin polymerisation is tightly controlled both temporally, by molecular release of autoinhibition, and spatially, by the targeting of WASp to specific locations and by the colocalisation of synergistic WASp activators.

1.6 Actin Polymerisation and Arp 2/3

1.6.1 Actin dynamics

Monomeric actin (g-actin) is a 43 kDa protein made up of 4 similar subdomains (numbered 1-4) which form a central cleft containing binding sites for an adenosine nucleotide (either ATP or ADP) and a magnesium ion. When bound, the central cleft closes around the nucleotide resulting in a structurally globular shape, but the protein remains functionally polarised. Purified actin will polymerise spontaneously when heated or exposed to high salt concentration (Straub, 1989). Polymerised actin forms a double stranded, right handed helix with a width of 5-9 nm and a complete helix turn length of 37nm, and is called filamentous actin (f actin) (Holmes et al., 1990). Actin filaments will spontaneously depolymerise on cooling or dilution of the solution. There is a time lag between increase in temperature / salt and instigation of polymerisation, which is avoided if small amounts of filamentous actin are added to the reaction. This is because the formation of a *de novo* filament from individual monomers, a process called nucleation, is inherently thermodynamically unfavourable (due to the instability of actin dimers and trimers). The longer a filament is, the more favourable actin monomer addition becomes (Pantaloni et al., 2001; Oosawa, 1975; Kasai et al., 1962).

Once a filament is established, ATP loaded actin monomers bind with different affinity to each end of the filament. As a result in the presence of an excess of actin one end will elongate faster (the barbed or positive end) than the other (the pointed or negative end). As the reaction continues and the concentration of free

actin monomers reduces, the filament stability at the pointed end changes to favour depolymerisation. Eventually equilibrium forms where the rate of polymerisation at the barbed end equals the rate of depolymerisation at the pointed end, and the filament “treadmills”, generating a propulsive force in the direction of the barbed end. Treadmilling occurs when the actin concentration within the reaction lies between the critical concentrations (the concentration at which actin is added to a filament) of each end (Hill and Kirschner, 1982; Kirschner, 1980; Wegner, 1976; Wegner, 1982).

The actin subunit, once bound to the filament will hydrolyse ATP to ADP (Carlier et al., 1994; Korn et al., 1987; Wegner, 1977). This “slow hydrolysis” occurs at some time point after binding to the filament (and therefore usually when the actin unit is in the middle of a filament). Hydrolysis and phosphate release induce a conformational change around the ATP binding cleft, which influences the stability of protein interactions with the actin unit (Otterbein et al., 2001; Maciver et al., 1991; Korn et al., 1987). Actin-ADP is less stable in the filamentous form, particularly at the pointed end of the filament, and therefore ATP hydrolysis encourages depolymerisation. This provides a temporal element to the stability of filamentous actin.

In biological systems, actin monomers and the filamentous actin network of the cell cytoskeleton exist in equilibrium together. In eukaryotic cells, actin is the most abundant protein and has a cytoplasmic concentration of the order of 100μM, although the vast majority of this filamentous actin. The critical concentration for actin at the ATP bound barbed end of a filament is approximately 10x that of the ADP bound pointed end. Monomeric actin concentration, although highly locally variable, is usually approximately the same as the critical concentration at the barbed end. This means a steady state of treadmilling is just maintained, but the rate limiting step for filament elongation is actin concentration, and therefore pointed end depolymerisation (Kirschner, 1980).

1.6.2 Actin cytoskeleton

The actin cytoskeleton is highly specialised to meet the functionality of specific cells. In this discussion I will be considering the generalised properties of cells with the capacity to migrate.

Upon detecting a signal to move, the cytoskeleton rapidly rearranges and polarises the cell. The cell develops a broad leading edge with an elongated trailing tail at the opposite pole. To sense the environment and as an initial step towards movement, the cell forms finger like projections, called filopodia, from the leading

edge. If appropriate attractant signals are received the filopodia stabilise, and then evolve into broader projections called lamellipodia or ruffles. These advance the cell membrane, and the concerted advancement of several lamellipodia results in movement of the leading edge of the cell. To counteract this fluidity, cells have focal adhesions which consist of bundles of actin filaments bound to membrane anchoring proteins, which in turn anchor the filament bundles (and therefore the cell) to the extracellular matrix. When the cell does move, these structures are simultaneous deconstructed, facilitating cell remodelling (Pantaloni et al., 2001).

To be able to rapidly remodel the actin cytoskeleton, the cell must be able harness, enhance and regulate (both spatially and temporally) the treadmilling of actin filaments. It does this through a series of actin binding proteins with differential functions. To aid the investigation of the regulation of actin networks a series of *in vitro* models of actin based motility have been developed. These include the visualisation of motility and actin comets formed by bacteria (Listeria or Shigella) or beads coated with proteins of interest (Wiesner et al., 2003; Suetsugu et al., 2001b; Yarar et al., 1999).

The rate of expansion of a branched actin network is determined by the number of free barbed ends and the elongation rate of these filaments. There are three main mechanisms the cell uses for regulating the number of free barbed ends. Capping proteins, such as gelsolin, capping protein (CapZ) and CapG bind to the barbed ends of filaments with high affinity, blocking elongation and therefore inhibiting network protrusion (Rogers et al., 2003; Schafer et al., 1996). Barbed end capping also encourages nucleation and filament branching, as a reduction in available barbed ends leads to an accumulation of ATP loaded actin monomers. Capping proteins and profilin (see below) act synergistically in increasing Arp 2/3 nucleation rates (Blanchoin et al., 2000a). They have been shown to be essential for efficient cell motility (Hug et al., 1995).

There are also capping proteins specific for filament pointed ends (such as Spectrin and Arp 2/3) (Mullins et al., 1998; Pinder et al., 1984), which providing the filament is in equilibrium, will block depolymerisation, resulting in longer (and older) filaments. Pointed end capping will also block the replenishment of free actin monomers and therefore reduce the rate of elongation at free barbed ends.

Severing of actin filaments generates new barbed and pointed ends, resulting in shorter filaments, and additional focuses of filament protrusion and depolymerisation. The Actin Depolymerising Factor (ADF) / cofilin family of proteins bind to the sides of ADP-actin subunits within filaments. Once bound they

induce depolymerisation from the pointed end (Carlier et al., 1997), encourage debranching of filaments (Blanchoin et al., 2000b) and destabilise the helical structure of the filament resulting in filament severing (Blanchoin and Pollard, 1999; Maciver et al., 1991). The net effect of ADF / cofilin is an enhancement of actin based motility (Carlier et al., 1997).

Finally, nucleation of actin monomers generates new filaments, and therefore new barbed ends. The most important nucleating protein complex is Arp 2/3, which in addition to initiating a new filament, also anchors it to an existing filament, resulting in 70° branch (Mullins et al., 1998; Svitkina et al., 1997). Arp 2/3 activation results in the generation of an orthogonal matrix with short actin filaments and a high density of free barbed ends, optimal for exerting a 2 dimensional distributed force on the cell membrane.

A second major group of actin nucleating proteins are the formins. These proteins are a large family of ubiquitously expressed and highly conserved proteins. Unlike Arp 2/3 (see sections 1.6.5 and 1.6.6) these protein nucleate filaments from the barbed end and remain bound as the filament elongates. They antagonise the binding of capping proteins and as a result, formin filament nucleation results in elongated actin filaments. Although formins play little role in generating an orthogonal actin network, they are essential for structures requiring discrete actin bundles, such as filopodia, stress fibres and the contractile ring formed during cytokinesis (Faix and Grosse, 2006).

The rate of filament elongation is largely determined by the concentration of capping proteins and the concentration of free ATP loaded actin monomers. As discussed above, free actin concentration is determined by local rates of depolymerisation, but various monomer binding proteins also influence the availability of actin to the barbed ends. Thymosin β4 is actin sequesting protein which reduces the available pool of actin monomers for polymerisation (Pantaloni and Carlier, 1993). A related protein, profilin plays an important role in enhancing actin network branching and extension, by catalysing the exchange of ADP for ATP in actin monomers, and then delivering the recycled actin to the barbed end of filaments (Loisel et al., 1999; Pantaloni and Carlier, 1993). This delivery stimulates barbed end polymerisation of actin filaments. The nucleotide exchange in monomeric actin, however, results in the release of cofilin (which preferentially binds to ADP – actin). Free cofilin is then able to bind to F-actin, stimulating pointed end filament depolymerisation. Although profilin is inhibitory towards actin nucleation, it is a more potent inhibitor of spontaneous nucleation than Arp 2/3 mediated nucleation, and as such promotes filament branching (Blanchoin et al.,

2000a; Machesky et al., 1999).

Other actin binding proteins are involved in packaging filaments into bundles, cross linking filaments, anchoring filaments to the plasma membrane and organising higher actin structures.

Filopodia and focal adhesions have long unbranched bundles of actin filaments in their cores, but lamellipodia, by contrast, consist of a high density dendritic array of branched actin filaments. The actin cytoskeleton is far more branched at the leading edge of cells, than within the main cell body, where actin filaments are less branched and are longer (Svitkina and Borisy, 1999; Small et al., 1995). Recently some groups have suggested two distinct actin networks underlying the leading edge, a lamellipod network and a “deeper” lamellum network (Le Clainche and Carlier, 2008; Iwasa and Mullins, 2007; Ponti et al., 2004). Although both appear capable of instigating cell membrane protrusion, they showed distinct architecture and a different composition of actin binding proteins. Arp 2/3 localises to lamellipodia and the leading edge (Svitkina and Borisy, 1999; Welch et al., 1997; Machesky et al., 1994), but is not found in the lamella (Iwasa and Mullins, 2007). Similarly there are much higher concentations of capping protein, APF / cofilin and free actin within the lamellipodia. These results demonstrate that the cell maintains the greatest dynamic potential adjacent to the cell membrane, particularly at the leading edge.

1.6.3 Arp 2/3 structure

The Arp (actin related protein) 2/3 complex was first isolated in 1994, from *Acanthamoeba* (Machesky et al., 1994) and its ability to initiate actin polymerisation *in vitro* was first demonstrated on the surface of *Listeria monocytogenes* in 1997 (Welch et al., 1997). Subsequently Arp 2/3 was shown to localise to areas of active actin polymerisation (Svitkina and Borisy, 1999; Machesky et al., 1994) and it is essential for actin based cellular functions such as phagocytosis, pinocytosis and establishment of cell polarity (Magdalena et al., 2003; Insall et al., 2001; May et al., 1999). Electron microscopy and kinetic studies of purified protein have suggest a role for Arp 2/3 as an actin nucleator, a branching agent and pointed end capping protein (Mullins et al., 1998).

Arp 2/3 is a stable complex of 240 kDa, made up of 7 different proteins each represented once within each complex. Arp 2 and Arp 3 are structurally homologous to actin, differing mainly at the pointed end. The other 5 proteins are structurally unique (Mullins et al., 1997) and are named ARPC (actin related protein complex component) 1-5, with molecular sizes of 42, 34, 21, 20 and 16 kDa respectively

(in humans).

Once the homology between Arp 2, Arp 3 and actin was recognised, it was hypothesised that Arp 2 and Arp 3 would form a pseudotrimer “nucleus” with an actin monomer bound to a nucleator activator (such as WASp/SCAR). This trimer would then initiate the formation of a new filament (Robinson et al., 2001; Kelleher et al., 1995). The WASp – Arp 2/3 complex would therefore stabilise the trimer formation, overcoming the thermodynamic opposition to nucleation. Extensive and ongoing work, particularly using structural biological and electron microscopy techniques, have explored this hypothesis.

The crystal structure of bovine Arp 2/3 with no nucleotide bound was solved in 2001 (Robinson et al., 2001). ARPC2 and ARPC4 form the backbone horseshoe of the complex, with Arp2 and Arp3 bound between the open jaws of the horseshoe. ARPC1 is structurally distinct from the other units being a seven-bladed WD40 β-propeller protein, and it interacts with Arp2, ARPC4 and ARPC5. By contrast the globular ARPC3 binds only Arp3. Arp2 and Arp 3 have minimal contact and are separated from each other by a cleft, which would require a significant conformational change in the complex to mimic the configuration of adjacent actin units within a filament (Lorenz et al., 1993). This structure is presumed to be an inactive form of Arp2/3, and the crystal structure of a fully activated Arp2/3 complex remains elusive.

Subsequent structural studies have assessed the impact of ATP binding to both Arp2 and Arp3, and have shown that although both subunits themselves change conformation (closing around the nucleotide), there was insufficient change in their juxtapositions to mimic an actin dimer, and further conformational change would be necessary to initiate nucleation (Kiselar et al., 2007; Nolen et al., 2004; Goley et al., 2004).

1.6.4 WASp activation of Arp 2/3

In isolation, Arp 2/3 alone is relatively ineffective at initiating actin nucleation (Mullins et al., 1998). In addition to monomeric actin and ATP, it requires activation (Higgs et al., 1999), and the minimal activating unit is the VCA domain from a WASp/SCAR family protein (Machesky et al., 1999). The presence of pre-existing actin filaments increases the speed and efficiency of actin polymerisation (Marchand et al., 2001; Machesky et al., 1999).

The binding of WASp to the Arp2/3 complex involves the interaction of Arp2, Arp3, ARPC1 and ARPC3 with the CA domains of WASp (Kreishman-Deitrick et

al., 2005; Beltzner and Pollard, 2004; Panchal et al., 2003). This binding can only occur following WASp activation as the Arp2/3 binding sites within the CA domain are hidden in the autoinhibited conformation (Panchal et al., 2003). Two critical anchor points within WASp appear to be the carboxyl terminal of both the C region (M474) and the A region (Trp500) (Kiselar et al., 2007; Kreishman-Deitrick et al., 2005). The exact interaction sites within Arp2/3 remain unclear. Truncation of the carboxyl terminal of NWASp to amino acid 484 severely impaired Arp 2/3 induced actin polymerisation *in vitro* (Suetsugu et al., 2001a). The V domain provides no additional affinity for Arp2/3 binding (Rohatgi et al., 2000).

Phosphorylation regulates the interaction between WASp and Arp 2/3. As described in section 1.5.5.2, two serine residues within the C domain of WASp (Ser283 and Ser484) are constitutively phosphorylated by casein kinase II, resulting in a higher affinity of WASp for Arp2/3, and an increase in resultant actin nucleation activity (Cory et al., 2003). Interestingly, recent data has demonstrated that phosphorylation of Arp2 is also essential for Arp2/3 mediated actin nucleation (at residues Thr237 and Thr238), but this effect is independent of WASp binding (LeClaire, III et al., 2008).

Interaction between Arp2/3 and WASp is more complex than just the binding of the VCA domain. Arp2/3 binding to the EVH1 and Basic domains has been demonstrated (Suetsugu et al., 2001a; Prehoda et al., 2000), and these interactions also effect the autoinhibition of WASp and the activity of Arp2/3 (see sections 1.4.1.5, 1.4.2.1, 1.4.6.2 and 1.5.8)

ATP bound monomeric actin binds to the V domain of WASp, although interaction with residues in the C domain further stabilise this binding (Marchand et al., 2001; Machesky and Insall, 1998). Actin binding to the V domain is essential for Arp 2/3 activity, and deletion of the V domain eliminates the actin polymerisation (Marchand et al., 2001; Miki and Takenawa, 1998). It is likely that profilin plays a role in delivering ATP loaded actin monomers to the V domain, via its interaction with the WASp polyproline domain.

Although there remains controversy over the exact nature of the interaction with the mother filament during Arp2/3 nucleation, it is certain that Arp2/3 binds “side on” to filamentous actin (Egile et al., 2005; Beltzner and Pollard, 2004; Volkmann et al., 2001; Gournier et al., 2001). As Arp2/3 shows much greater actin polymerization activity in the presence of existing f-actin, it is likely that the binding of Arp2/3 to the mother filament changes the alignment of the Arp2 and Arp3 subunits, resulting in complex activation.

The role Arp2/3 ATP hydrolysis during nucleation and branching is important, but the exact details remain controversial. The affinity of ATP for Arp2 and Arp3 is significantly lower than that for monomeric actin, and Arp2/3 is structurally stable with no ATP bound. WASp binding to Arp2/3 increases the affinity of the complex for ATP by 3-fold (Dayel et al., 2001; Le et al., 2001). *Dayel et al* suggest that ATP hydrolysis is necessary for actin nucleation, as Arp2/3 loaded with ADP or a non-hydrolysable ATP analogue were unable to nucleate actin (Dayel et al., 2001). Mutations in the ATP binding cleft of either Arp severely impairs actin polymerization (Martin et al., 2006; Goley et al., 2004). An alternative model has been proposed by *Le Clainche et al*. They demonstrated that the binding of ATP to Arp2 (following WASp binding) is the critical step to initiate actin nucleation. They suggested ATP hydrolysis occured after nucleation and led to instability between the daughter and mother filaments, encouraging debranching (Le et al., 2003; Le et al., 2001)

Several lines of evidence suggest that binding of WASp and initiation of actin nucleation are distinct steps. *Marchand et al* identified two point mutations in the NWASp V domain which decrease the ability of bound Arp 2/3 to instigate actin polymerisation by 10 fold, without influencing the affinity of NWASp for either monomeric actin or the Arp 2/3 complex (Marchand et al., 2001). Different WASp/SCAR family proteins have different capacities to activate Arp2/3, but this capacity does not correlate to their affinities for either Arp 2/3 or monomeric actin (Panchal et al., 2003; Zalevsky et al., 2001). Finally, demonstration that Arp2/3 with a WASp V domain fused to it in an appropriate position was unable to initiate actin polymerisation, suggests that the CA domain plays a distinct and active role in Arp 2/3 activation. (Goley et al., 2004).

Conformational change of Arp 2/3 upon binding of WASp CA domains was demonstrated by an increase in fluorescent resonance energy transfer (FRET) between fluorophore labelled ARPC3 and ARPC1, upon WASp VCA domain binding (Goley et al., 2004). Electron microscopy findings have corroborated this and suggest that ARPC2 instigates the closure of Arp2 / Arp3 cleft, with this conformational change stabilised by the WASp CA domain (Rodal et al., 2005). These results combined with the structural data on WASp - Arp2/3 binding suggest a model whereby the WASp V domain binds an actin monomer and the A domain anchors WASp to Arp2/3. The C domain interaction with Arp2/3 instigates a change in the relative positions of several Arp 2/3 components (either by a rotational or a sliding Arp2 model) and provides a platform for pulling together Arp2, Arp3 and the actin monomer (Goley and Welch, 2006; Aguda et al., 2005)

1.6.5 Actin nucleation

Although much of the mechanism and structural biology of Arp2/3 activation and actin filament branching has been worked out, the exact site of branching remains controversial. Two main models exist. In the dendritic nucleation model, Arp2/3 binds entirely on the side of the mother filament and Arp2, Arp3 and the WASp bound actin monomer form the first 3 actin units of the daughter filament. Nucleation is initiated on the side of the pre-existing filament (Amann and Pollard, 2001; Blanchoin et al., 2000a; Mullins et al., 1998). Evidence for this model came initially from real time observation of fluorescently labelled actin filament branching, and subsequently from cyro-electron microscopy.

Real time imaging of actin filaments revealed that mother and daughter filaments following branching were generally the same length, and it was unusual to find a capped actin filament nucleating downstream from the cap. These findings and kinetic modelling studies lead to the proposition of an alternative nucleation mechanism. In the barbed-end branching model, Arp2/3 binds to the barbed end of the filament and one of Arp2, Arp3 or the WASp bound actin monomer is incorporated into the mother filament, whereas the other two units form the initial units of the daughter filament. Filament elongation occurs synchronously from mother and daughter filaments (Falet et al., 2002; Pantaloni et al., 2000).

Although this debate has not resolved, it does not affect the principles of the regulation of the actin cytoskeleton.

1.6.6 Filament debranching

Following branch formation, WASp and other activators of Arp 2/3 (except cortactin) immediately dissociate from the actin filament (Martin et al., 2006; Egile et al., 2005; Uruno et al., 2003). Although not universally accepted, *Dayal et al* suggested that this dissociation is mediated by the hydrolysis of ATP to ADP by Arp2/3, which destabilises the Arp2/3-WASp binding, releasing Arp2/3 and the actin filament from WASp and the cell membrane (Dayel et al., 2001). By contrast the Arp2/3 complex remains at the junction point of the filaments (Svitkina and Borisy, 1999).

Branched filaments are inherently unstable and have a half life of only 500-800s, before dissociating from the mother filament (Le et al., 2003; Blanchoin et al., 2000b). The stability of branched filaments is determined by the hydrolysis of ATP bound to the individual subunits (Otterbein et al., 2001; Blanchoin et al., 2000b; Blanchoin and Pollard, 1999). The hydrolysis of ATP bound to Arp2/3 (see above)

may also encourage debranching of the daughter from the mother filaments (Le et al., 2003). Once the daughter filament has debranched, affinity between Arp2/3 and the filament pointed end is reduced by hydrolysis of ATP in either (or both) elements. This leads to Arp2/3 decapping from the filament pointed end, inducing depolymerisation (Blanchoin et al., 2000a). This process is enhanced by the ADF / cofilin.

1.7 WASp Interacting Protein (WIP)

WIP was first identified as a WASp binding protein by yeast 2-hybrid assays, and subsequent co-immunoprecipitation from cells lines lysates following over-expression both proteins (Ramesh et al., 1997). Subsequently constitutively formed complexes have been immunoprecipitated from cells (Martinez-Quiles et al., 2001), and in resting lymphocytes between 80 and 95% of WASp is constitutively complexed with WIP (de la Fuente et al., 2007; Sasahara et al., 2002). Although ubiquitously expressed, it is found in much higher concentrations in haematopoietic cells, mirroring the expression of WASp, but not NWASp (Ramesh et al., 1997). It also shows tissue specific alternative splicing, although the functional significance of this is not known (Vetterkind et al., 2002).

1.7.1 WIP Structure and binding partners

WIP is very rich in proline residues, which make up 28% of the protein's amino acids. Runs of consecutive proline residue motifs are prominent in each of the recognised functional domains of WIP, and this high proline content has been blamed for the difficulties experienced in generating recombinant WIP.

The domain structure of WIP is shown in figure 1.9. Two regions are conserved among all three family members (see section 1.4.1.2), a double Verprolin homology domain at the amino terminus, and a WASp / NWASp binding domain at the carboxyl terminus. WIP also contains three potential profilin binding sites (containing the motif XPPPPP), which are also capable of binding both monomeric and filamentous actin (Martinez-Quiles et al., 2001). WIP has also been shown to bind cortactin via a proline rich region at the carboxyl end of the double Verprolin domain (110 -170) (Kinley et al., 2003), and the SH3 – SH2 adaptor proteins Nck and CrkL via a polyproline domain (Sasahara et al., 2002; Anton et al., 1998). WIP also binds Hck, although the site of binding has not yet been identified (Scott et al., 2002).

WIP domain structure

V - Verprolin homology domain
CBS - Cortactin binding site
PolyP - Polyproline domain
WBS - WASp binding site

Profilin binding site
(Actin based motilitiy motif 2)

Fig 1.9 WIP domain structure

1.7.2 WIP function

1.7.2.1 WIP molecular function

The functions of WIP at a molecular level can divided into those mediated by its interaction with actin and profilin, cortactin and WASp.

WIP stabilises F-actin from depolymerisation and stabilises actin bundling *in vitro* (Anton and Jones, 2006; Martinez-Quiles et al., 2001). When over-expressed in cells WIP induces increased F-actin content, and conversely WIP null cells show a reduction in F-actin content (Anton et al., 2002; Ramesh et al., 1997).

Cortactin is an actin binding protein (both f- and g- actin), which localises to lamellipodia at cell leading edges in a Rac-dependent manner, following growth factor receptor activation (Weed and Parsons, 2001; Kaksonen et al., 2000; Weed et al., 1998). It appears to play an important role in initiating cell motility, via actin remodelling (Bryce et al., 2005). Cortactin binds and activates Arp 2/3, initiating actin filament branching, and also has a function in inhibiting actin filament debranching (Weaver et al., 2001; Weed et al., 2000). WIP stimulates cortactin induced Arp 2/3 activation and actin polymerisation in a concentration dependent manner, and co-expression of WIP and cortactin resulted in membrane protrusion (Kinley et al., 2003). The interaction of WIP with WASp / NWASp is discussed in section 1.7.3.

1.7.2.2 Cellular function of WIP

In resting fibroblasts, WIP is asymmetrically distributed in the perinuclear areas, with a pattern suggestive of a Golgi distribution (Vetterkind et al., 2002; Martinez-Quiles et al., 2001). WIP also localises to stress fibres in resting fibroblasts, perhaps reflecting its role in filament stabilisation (Vetterkind et al., 2002). Upon cell stimulation, WIP is recruited to sites of polarisation, such as the T cell synapse and the leading edge (Myers et al., 2006).

The role of WIP in actin dynamics and remodelling has been investigated by microinjection and over-expression experiments assessing cellular function. Over-expression of WIP in fibroblasts leads to the Cdc42 dependent induction of filopodia (Martinez-Quiles et al., 2001) and enhanced ruffle formation following PDGF stimulation (Anton et al., 2003). WIP over-expression slowed fibroblast spreading and adhesion, whereas WIP deficiency accelerated the rate of adhesion and the size of focal contacts (Lanzardo et al., 2007). In *Dictyostelium,* both WIPa (WIP homolog) over-expression and deletion impaired chemotaxis. When WIPa was in excess, migrating cells showed frequent changes of direction in response to a chemoattactant gradient, whereas deficiency resulted in delayed directional pseudopod extension (Myers et al., 2006). WIP is recruited to and is necessary for the intracellular motility of *Vaccinia* virus and PIP_2 induced vesicular rocketing (Benesch et al., 2002; Vetterkind et al., 2002; Moreau et al., 2000).

1.7.2.3 WIP knockout mouse model

WIP knockout mice survive to adulthood, but die prematurely of a multisystem auto-inflammatory disease, involving ulcerative colitis, hypersensitivity pneumonitis and glomerulonephritis. They have a granulocytosis and lymphopenia involving all lymphoid lineages, but have normal lymphopoeisis. T cells show abnormal proliferative responses and impaired IL-2 production in response to CD3 ligation. There is no increase in f-actin following TCR ligation, and T cells show poor spreading and filopodia formation. Interestingly T cell activation by PMA and ionomycin, protein tyrosine phosphorylation, NF-κB and NF-AT nuclear translocation and T cell capping following activation are all normal. By contrast, B cells have enhanced antigen induced proliferative responses, and make normal T independent antibody responses. T dependent antigen responses are absent (Curcio et al., 2007; Anton et al., 2002). T cells from WIP deficient mice showed impaired chemotaxis to SDF1α (a T cell chemokine), which was exacerbated in the double, WASp / WIP knockout mouse. T cell homing to lymphoid tissue was impaired as a result of this (Gallego et al., 2006). One caveat with analysis of the WIP mouse is that WASp is also deficient in haematopoietic cells (see section 1.7.3.4) and studies comparing WASp knockout with the double, WASp / WIP knockout mouse to delineate the specific role of WIP are awaited. WIP deficiency has not been recognised in humans as a disease entity.

1.7.3 The WASp – WIP complex

1.7.3.1 Effect on WASp activation

Unlike its effect on cortactin, WIP has been demonstrated to inhibit NWASp activation of Arp 2/3 in response to Cdc42 *in vitro*. WIP, however, had no effect on

VCA induced Arp 2/3 activation, and minimal effect on Cdc42 – PIP_2 costimulation. These results indicate that WIP's mode of suppression is by desensitising the autoinhibitory destabilising effect of Cdc42 on NWASp (Martinez-Quiles et al., 2001). Evidence of a similar role in stabilising the WASp autoinhibitory conformation *in vivo* has come from overexpression of a split YFP WASp construct in yeast cells. Co-expression of WIP led to an increase in YFP fluorescence, indicating an increase in the concentration of autoinhibited WASp (Lim et al., 2007).

Interestingly, WIP, WASp and Cdc42 have are capable of forming a stable trimeric complex *in vitro,* demonstrating that WIP and Cdc42 interactions with WASp are not mutually exclusive (Martinez-Quiles et al., 2001). This also suggests that Cdc42 binding does not destabilise the NWASp – WIP interaction, although there is no direct proof of this. Whether or not this trimeric complex exists *in vivo*, how activated it is and whether TOCA is able to bind this complex are important unanswered mechanistic questions. The inhibitory activity of WIP has not been demonstrated for WASp, or for NWASp *in vivo.*

1.7.3.2 The WASp – WIP complex and actin assembly

The NWASp and WIP complex is an important functional unit for the formation of filopodia in response to Cdc42 (in 3T3 cells) (Martinez-Quiles et al., 2001).

WASp – WIP complexes are required for establishing cellular polarity and migration in response to chemotactic gradient in haematopoietic cell lines and human monocytes, whereas WASp alone was sufficient for *in vivo* actin polymerisation (Tsuboi, 2006).

NWASp – WIP complex formation has been shown to be essential for the recruitment of NWASp to the surface of *Vaccinia* in infected cells, and the subsequent formation of actin tails (Moreau et al., 2000). This recruitment appears to be mediated through the interaction between WIP and Nck (Anton et al., 1998).

Co-transfection of NWASp and WIP in cell lines resulted in a change in the localisation of NWASp from the nucleus to the perinuclear area and membrane protrusions. This also provoked and the disassembly of stress fibres and the preferential formation of filopodia (Vetterkind et al., 2002).

1.7.3.3 Effect on WASp stability

The recognition that although most WAS / XLT patients with missense mutations express WASp, the cytosolic level of this protein is severely impaired, was critical to understanding the phenotype – genotype (proteotype) relationship in WASp

mutations (Lutskiy et al., 2005; Jin et al., 2004; Imai et al., 2004; Lemahieu et al., 1999; Zhu et al., 1997; Remold-O'Donnell et al., 1997). Several recent publications have demonstrated that WIP plays a crucial role in inhibiting the constitutive degradation of WASp, and as a consequence the cytosolic level of WIP determines the level of WASp (de la Fuente et al., 2007; Konno et al., 2007; Chou et al., 2006). A similar stabilising role for WIP has been demonstrated for the tyrosine kinase Syk in mast cells (Kettner et al., 2004).

It had been previously been shown that WASp but not NWASp is cleaved by the protease calpain both in intact platelets (following stimulation resulting in calcium influx) and in cell lysates (Shcherbina et al., 2001; Oda et al., 1998). Degradation of NWASp, by contrast, has been demonstrated via the ubiquitinsation pathway, following tyrosine phosphorylation by Src family kinases (Suetsugu et al., 2002). As yet there are no studies assessing the ubiquitination of WASp.

Calpains are a family of 14 mammalian intracellular cysteine proteases. Many are ubiquitously expressed and they play central roles in a wide range of cellular processes including the regulation of migration and chemotaxis. Initially they were described as being regulated by calcium concentration (Guroff 1964) and all contain EF hand calcium binding domains. It is now clear that activation is complex and multifactorial, but includes phospholipid binding, tyrosine phosphorylation and autolysis. Additional regulation of calpain activity is achieved by its endogenous antagonist, calpastain. Generally calpains cleave by limited proteolysis, and frequently their products are biologically active. They do not, however, cleave at predictable amino acid sequences, and although significant amino acid preferences exist around cleavage sites, calpain cleavage partly appears to be determined by protein secondary structure (Tompa et al., 2004).

Haematopoeitic cells from WIP knockout mice were found to have very low levels of WASp in addition to WIP, and the levels of WASp were restored with the transfection of WIP genes (de la Fuente et al., 2007; Chou et al., 2006). Similar results were seen using RNA interference in WIP expressing cell lines (Konno et al., 2007). Treatment of WIP null cells with protease inhibitors has revealed that in the absence of WIP, WASp is degraded by both calpain proteases and the proteasome (de la Fuente et al., 2007; Chou et al., 2006).The minimal WIP sequence required to inhibit this degradation was the carboxyl terminal 100 amino acid residues (410 – 503) (de la Fuente et al., 2007; Konno et al., 2007). Interestingly, in a purified protein system the minimal WASp binding sequence of WIP (461 – 485) did not prevent calpain cleavage, whereas the longer WIP fragment did. This suggests the effect of WIP is to hide the calpain recognition

site or inhibit calpain binding, rather than changing the sensitivity of WASp to calpain degradation through conformational change. Similarly, WIP does not inhibit calpain, as calpain was able to cleave CrkL in the presence of WIP (de la Fuente et al., 2007).

Increasing the cellular WASp level in the absence of WIP (either with protease inhibitors or overexpression of WIP carboxyl terminus) did not return cells to full functionality. Podosome formation in dendritic cells, and normal NF-AT signalling and IL2 production following T cell activation required expression of a WIP construct containing at least the polyproline and cortactin binding domains (de la Fuente et al., 2007; Konno et al., 2007; Chou et al., 2006).

The relative contribution of calpain and the proteasome to WASp degradation seems to vary according to cell type, experimental system and stage of differentiation of the cell. In adhesive WIP null dendritic cells, calpain inhibitors were able to rescue WASp levels to approximately 50% of normal cells, whereas proteasome inhibitors had no effect (Chou et al., 2006). By contrast, primary T cells from a patient with XLT had no response to calpain inhibitors, but increased WASp levels from 9% to 22% of normal control T cells with proteasome inhibitors (de la Fuente et al., 2007). In activated T cells and EBV transformed B cells calpain inhibitors and proteasome inhibitors both increased WASp levels to 25-30% control levels (de la Fuente et al., 2007).

An attractive hypothesis suggested by these results is that the proteosome is responsible for background turnover of WASp degradation, and that calpain is induced in response to activation and cell surface signalling. Although this hypothesis needs mechanistic investigation, some anecdotal evidence supports it. T cells activation results in calpain activation (Sato and Kawashima, 2001; Penna et al., 1999; Noguchi et al., 1997; Selliah et al., 1996; Sarin et al., 1993), and dendritic cell podosomes, which form following activating adhesive signals from the extracellular matrix, have reduced turnover in response to calpain inhibitors (Calle et al., 2006b).

1.7.4 EVH1 missense mutations and WIP

The impaired interaction between WIP and WASp containing clinical missense mutations was first demonstrated using yeast two hybrid assays (Luthi et al., 2003; Stewart et al., 1999). Both groups found a range in the degree of WIP binding demonstrated by clinical WASp mutants, and of the four missense mutations tested the order from highest to lowest WIP affinity appears to be Y107C > R86H = R138P > A134T.

As discussed in section 1.4.1.6 the crystal structure of NWASp EVH1 and WIP suggested that missense mutations over a wide range of residues may interfere with WIP binding (Peterson et al., 2007; Volkman et al., 2002). Based on this structure, the effect of specific WAS / XLT missense mutations on WIP interaction have been modelled, and 28 out of 35 disease causing mutations in the EVH1 domain were predicted to disrupt WASp-WIP interactions (Volkman et al., 2002; Rong and Vihinen, 2000). Residues on the EVH1 domain surface have been predicted to disrupt WIP interaction either directly, or by displacement of adjacent residues which form direct contacts with WIP (Kim et al., 2004; Volkman et al., 2002). Buried residues have been predicted to disrupt the conformation of the EVH1 domain and therefore impair WIP binding. It has been hypothesised that disruption of EVH1 conformation is more disruptive of WASp function than inhibiting WIP binding alone, and that these buried point mutations may result in more severe disease (Volkman et al., 2002). Larger analyses of genotype - phenotype correlation, however, have not corroborated this hypothesis. Interestingly neither of the EVH1 domain mutation hotspots (T45 or R86) are predicted to form direct nuclear Overhauser effect (NOE) contacts with WIP (Volkman et al., 2002).

There is some limited data on the functionality of WASp with clinical missense mutations. The cellular levels of WASp in lymphocytes from XLT patients with R86H and T45M point mutations can be modestly increased by incubation with both protease and calpain inhibitors (de la Fuente et al., 2007). Macrophages from patients with XLT have an impaired ability to form podosomes (Linder et al., 2003). Missense mutations made in NWASp equivalent to the WASp clinical mutations C43W, R86C and E133K, abolished the recruitment of NWASp to the surface of *Vaccinia* and thereby inhibited actin tail formation (Moreau et al., 2000). Prior to this study, however, no data on the *in vitro* activity of WASp containing disease causing missense mutations had been published.

1.8 Aims of project

Much of the experimentation on WASp has been done *in vitro,* often at a biochemical level, using recombinant proteins or protein fragments in cell free systems. There has been less work addressing the function of WASp or domain deficient WASp mutants in living systems, or haematopoietic cellular systems. In addition most studies of the role of WASp in cell biology have focused on WASp-deficiency or domain deletions and very little is known about the molecular or cellular function of disease causing mutants which preserve some (mutant) WASp expression. As this group of mutations accounts for the majority of patients affected by WAS, a better understanding of their effects on cellular function is clinically important.

The aims of my project were to;

1. Design and make a panel of WASp mutants covering domain deletions, and mutations found in patients with WAS, XLT or XLN.

2. Test their actin polymerising ability within a haematological cell lysate system, and to assess biological reagents which influence this activity.

3. Transfect these constructs into haematopoietic cell lines and WASp deficient primary dendritic cells and analyse protein expression and stability, WASp localisation and reconstitution of normal cell function.

The structures of the mutants created, and the abbreviations used for them in this thesis are shown in figure 3.1.

Four point mutations associated with WAS / XLT were chosen and two point mutation causing XLN. T45M and R86H were chosen because they were the two most commonly found “hotspot” mutation. Both generally give mild disease, and R86H has previously been shown to have impaired WIP binding (Stewart et al., 1999). A134T and R138P are both missense mutations contained within exon 4 and appear to have a more severe clinical phenotype than the hotspot missense mutations (Lutskiy et al., 2005; Zhu et al., 1997). Impaired WIP binding has also been demonstrated with both these mutations (Luthi et al., 2003; Stewart et al., 1999).

The sequence deleted for the dVCA bind mutant (VCA binding site deletion) was determined by the minimal sequence required for VCA-GBD binding as described by the NMR structure of the bound complex (242-310) (Kim et al., 2000), minus the minimum sequence required for high affinity binding of Cdc42 (230-288) (Abdul-Manan et al., 1999; Rudolph et al., 1998). The resulting construct has residues 289-310 deleted, which were predicted to disrupt VCA binding to the GBD, but still allow high affinity binding of Cdc42. The H208D point mutation in the CRIB of N-WASp has been demonstrated to disrupt Cdc42 binding to the GBD (Miki et al., 1998a). The equivalent residue in the WASp CRIB is H246, therefore a H246D point substitution was created to mimic a functional CRIB deletion, without impairing VCA autoinhibitory binding. Finally the Y291E phosphomimicking construct was investigated. This missense mutation replaces the critical phosphorylation site, tyrosine 291, with a glutamic acid residue which mimics the negative charge of phosphorylation. This substitution is thought to induce a similar conformational change in WASp as phosphorylation of tyrosine 291.

2 Materials and Methods

2.1 Materials

All chemicals and reagents were purchased from Sigma unless otherwise stated. Standard buffers used are shown in table 2.2, commercial kits used in table 2.4 and antibodies used in table 2.5. Unless otherwise stated all centrifugation steps were performed with a Heraeus Biofuge Fresco microcentrifuge.

2.2 Molecular cloning

2.2.1 Starting vectors

The vectors used as the sources of genetic material for further manipulation are shown in table 2.1 and figure 2.1.

2.2.2 Restriction digests

Restriction endonucleases were purchased from New England Biolabs or Promega and reactions were performed according to manufacturers' recommendations. 0.5-5 µg of plasmid DNA was incubated with an excess of one or two endonucleases, a compatible buffer and distilled, RNAase free water (Sigma) to make a total reaction volume of 20-60ul. Where two enzymes with incompatible buffers or incubation temperatures were used, reactions were carried out serially, with either correction of buffer conditions or removal of buffer salts using a DNA PCR clean up kit (Qiagen). Total amount of enzyme within any reaction never exceeded 10% (v/v) of the final reaction volume.

Where a blunt end was required following a restriction digest resulting in a 5' overhang, DNA Polymerase I Large (Klenow) fragment (New England Biolabs) was used to fill in the 5' overhang. 5 units of Klenow and 33µM of each dNTP was added to each 20µl of digest reaction, and the blunting reaction was incubated for 20 minutes at room temperature, before inactivation by heating to 75˚C for 20 minutes.

For reactions used to generate the backbone for a ligation reaction, following restriction digests and blunting reactions each was dephosphorylated with calf intestinal alkaline phosphatase (CIAP, Promega). 1 unit of CIAP was added to each reaction and incubated at 37˚C for 30 minutes.

2.2.3 Agarose Gel Electrophoresis

Following restriction and subsequent manipulation, DNA fragments were resolved

Table 2.1 Starting Vectors

Name	*Abbreviation*	*Expression*	*Promoter*	*Tag*	*Source*
FL3 WASp		Mammalian expression vector	T3	VSV epitope	Jonathan Derry, Howard Hughes Medical Institute
C1-EGFP	C1	Mammalian expression vector	CMV	EGFP	Clonotech
EF-Bos-GST		Mammalian expression vector	hEF1α	GST	Giles Cory
SIN-LNT-cPPT-SFFV-WPRE	Lenti (SIN lenti SW)	Mammalian expression vector	SFFV	EGFP	Molecular Immunology Unit
SIN-LNT-cPPT-SFFV-EGFP-WASp-WPRE	pHRsinc-SEWW	Mammalian expression vector	SFFV	EGFP	Molecular Immunology Unit
pcDNA3 EGFP-WIP	EGFP-WIP	Mammalian expression vector	CMV	EGFP	Narayanaswamy Ramesh, Harvard Medical School
pOS135 zzWIP-V5/HIS	zzWIP	Mammalian expression vector	SP6	zz domain of protein A HIS x6 V5	Narayanaswamy Ramesh, Harvard Medical School
pcDNA6 WIP-HIS/V5	WIP-HIS	Mammalian expression vector	CMV	HIS x6 V5	Narayanaswamy Ramesh, Harvard Medical School
pCS2+ TOCA	TOCA	Mammalian expression vector	CMV / Sp6	Myc	Marc Krischner, Harvard Medical School
pMDG.2 (VSV-G)	Envelope plasmid	Mammalian expression vector	CMV		
pCMVΔ8.74 (gag-pol)	Packaging plasmid	Mammalian expression vector	CMV		
pGEX-2T Cdc-42	Cdc-42	Bacterial expression vector	E.coli tac	GST	Anne Ridley, University College.

by electrophoresis through 0.8% agarose gels dissolved in TAE buffer. To prepare these gels, agarose (Invitrogen) was dissolved in 1 x TAE buffer with the assistance of microwave warming. After cooling, ethidium bromide (0.5 μg/ml) was added to the gel immediately prior to setting, to facilitate the visualisation of DNA with UV light. DNA samples were mixed with Orange G loading buffer (10 mM Tris pH 7.5, 50 mM EDTA, 10% Ficol 400, 0.4% Orange G) before loading onto agarose gels. A 1 kb DNA ladder (New England Biolabs) was loaded onto each gel to

Fig 2.1

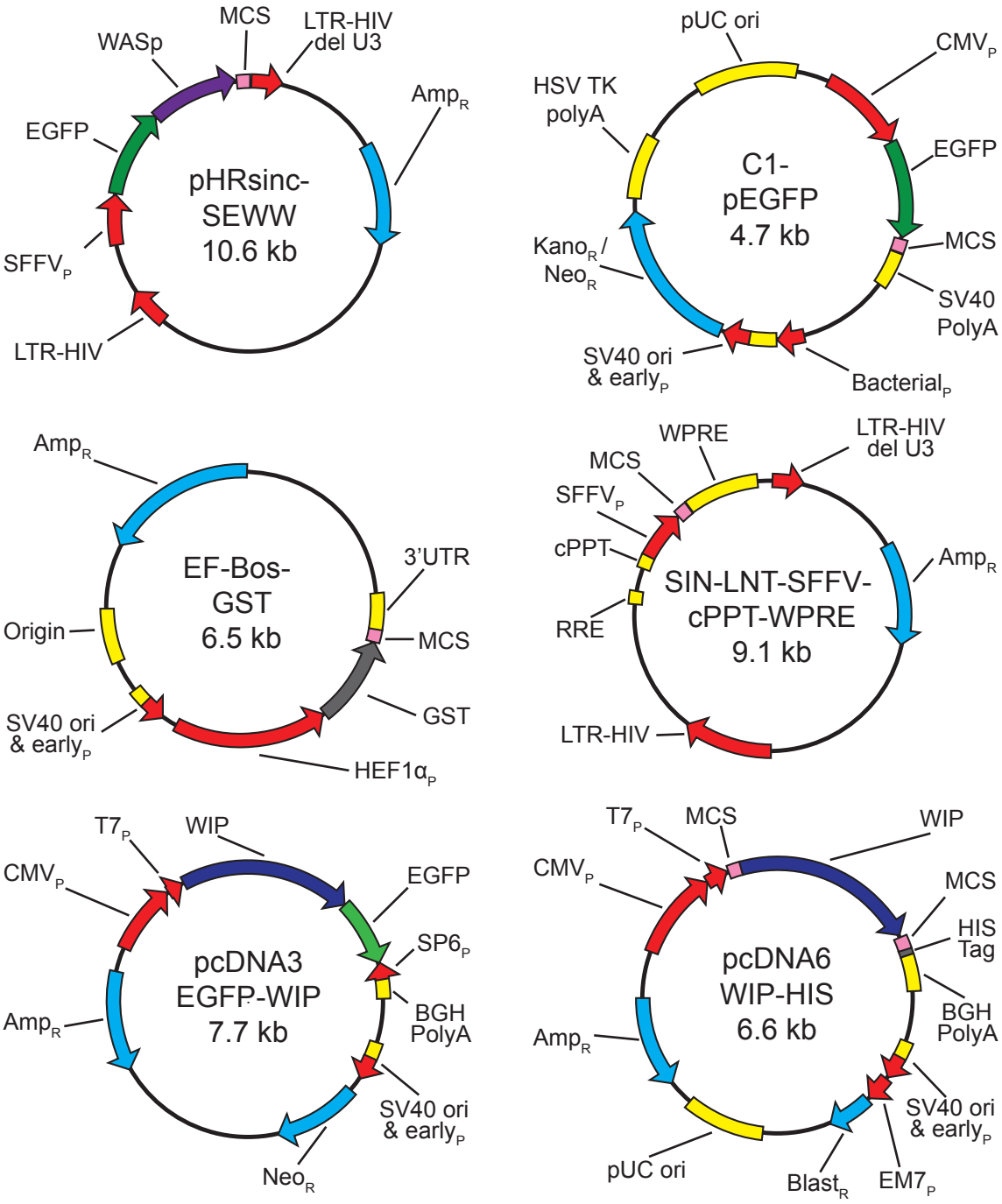

Figure 2.1 Structure of Starting Vectors
Abbreviations used; Amp$_R$ – ampicillin resistance, BGH polyA – Bovine growth hormone polyadenylation signal sequence, Blast$_R$ – Blastomycin resistance gene, CMV$_P$ – Cytomegalovirus early promoter, cPPT – central polyproline tract, EM7$_P$ – EM7 prokayotic promoter, HEF1α$_P$ – Human elongation factor α promoter, HSV TK polyA – Human Simplex Virus thymidine kinase polyadenylation signal sequence, Kano$_R$ / Neo$_R$ – Kanomycin / Neomycin resistance gene, LTR – Long terminal repeats, MCS – multiple cloning site, pUC ori – pUC origin of replication, RRE – REV responsive element, SFFV$_P$ – Splenic focus forming virus promoter, SP6$_P$ – SP6 promoter, SV40 ori & early$_P$ - simian vacuolating virus 40 origin of replication and early promoter, TEV site – Tobacco etch virus protease cleavage site, T7$_P$ – T7 promoter, WPRE – Woodchuck hepatitis virus post-transcriptional regulatory element

Table 2.2 Buffers

Name	***Abbrev-iation***	***Composition***	***Storage***
Cellular lysis buffer	LB	1% IGPAL CA-630, 130mM NaCl, 20mM Tris-HCl pH 8.0, 1mM EDTA, 10mM NaF, 2mM Na orthovanadate, 1% aprotinin, 10µg/ml leupeptin, 1µM pepstatin, 1mM PMSF	Base buffer stored at 4˚C for maximum of 2 months. Na orthovanadate, aprotinin, leupeptin and pepstatin were added within 2 hours of use. PMSF added immediately prior to use.
Tris-actetate EDTA buffer	TAE	40 mM Tris-acetate and 5 mM EDTA	10x solution stock (autoclaved).
Bead storage buffer		75% glycerol, 10mM Tris-Hcl pH 8.0, 1mM EDTA	Autoclaved and stored at RT
Actin polymerisation buffer	APB	1% IGPAL CA-630, 130mM NaCl, 20mM Tris-HCl pH 7.4, 2mM EDTA, 1% aprotinin, 10µg/ml leupeptin, 1µM pepstatin, 1mM PMSF	Base buffer stored at 4˚C for maximum of 2 months. Na orthovanadate, aprotinin, leupeptin and pepstatin were added within 2 hours of use. PMSF added immediately prior to use.
Purified protein pulldown buffer	XB	20mM HEPES, 150mM NaCl, 1mM DDT, 10% glycerol, 10mM $MgCl_2$, 1mM EDTA, 0.5mg/ml ovalbumin.	Base buffer stored at 4˚C for maximum of 2 months. Ovalbumin added prior to use.
Tris EDTA	TE	10 mM Tris·Cl, pH 8.0; 1 mM EDTA	RT Purchased from Qiagen.
Luria-Bertani broth	LB broth	10 g/L tryptone, 5 g/L of yeast extract, 10 g/L of NaCl	Made up fresh
Agar	Agar	10 g/L tryptone, 5 g/L of yeast extract, 10 g/L of NaCl, 15g/L Agar	Petri dishes stored at 4˚C
Bacterial lysis buffer	Bacterial LB	50mM Tris-HCl pH 7.5, 50mM NaCl, 5mM $MgCl_2$, 2mM PMSF, 1µM GTP	Made up fresh. PMSF and GDP added immediately prior to use.
Special electroporation buffer	SEB	120 mM KCl, 10 mM K_2PO_4/KH_2PO_4 pH 7.6, 2mM $MgCl_2$, 25 mM Hepes pH 7.6, 0.5% Ficoll 400	50ml aliquots stored at -20°C. Filtered before use.
Phosphate buffered solution	PBS	11.9mM Phosphates, 137mM NaCl, 2.7mM KCl.	10x stock purchased from Fischer Bioreagents. For tissue culture Gibco PBS was used.
Cellular fixing buffer	Fix buffer	4% Paraformaldehyde, 3% glucose in PBS	Made up fresh
NuPage® Lithium Dodecyl Sulphate sample buffer (x4)	SB	40% glycerol, 564mM Tris Base, 424mM Tris HCl, 8% Lithium Dodecyl Sulphate, 2mM EDTA, 0.88mM SERVA blue, 0.7mM phenol red	Purchased from Invitrogen. NuPage® antioxidant added immediately prior to use.

Table 2.2 Buffers *cont.*

Name	***Abbrev-iation***	***Composition***	***Storage***
NuPage® MOPS SDS running buffer	Running buffer	MOPS 50mM, Tris base 50mM, SDS 0.1%, EDTA 1mM	20x buffer purchased from Invitrogen
NuPage® Transfer buffer	Transfer buffer	Bicine 50mM, Bis-Tris 50mM, EDTA 2mM, Chlorobutanol 0.1mM, 10% Methanol.	10x buffer purchased from Invitrogen. Methonol added immediately prior to use.
BSA blocking buffer	Blocking buffer	PBS with 1-5% BSA (w/v), 0.1% Tween, 0.1% sodium azide	4°C for 2 months
Phosphate buffered saline - Tween	PBS-T	PBS with 0.1% Tween	10x stored at RT
GST elution buffer	GST EB	130mM NaCl, 50mM Tris pH 8.0,20mM reduced glutathione	Made up fresh
Thrombin buffer		50mM Tris-HCl pH 7.5, 2.5mM $CaCl_2$, 100mM NaCl,5mM $MgCl_2$, 1mM DDT, 1µM GDP.	Made up fresh. DDT added immediately prior to use.
Coupling Buffer		0.1M sodium phosphate buffer pH 7.4	Store at RT for 3 months.
Tris buffered saline - tween	TBS-T	150mM NaCl, 25mM Tris-HCl pH 7.6, 0.1% Tween	10x stored at RT
Fix Buffer		4% Paraformaldehyde, 3% glucose in PBS	Made up fresh.
FACS buffer		PBS with 0.5% BSA, 0.1% sodium azide.	Made up fresh
DNA lysis buffer		10mM Tris pH 8.0, 1mM EDTA, 0.5% NP40, 0.5% Tween 20, 1.25 mg/ml Proteinase K (Roche)	Made up fresh
Quenching buffer		1M Tris HCl, pH 7.4	Autoclaved and stored at RT.

enable size determination of DNA fragments. DNA fragments were visualized and images recorded using a UVIdoc gel documentation system (UVItec).

Where gel fragments were generated for ligation, DNA was excised from agarose gels using a scalpel blade under ultra-violet light (screening UV source to minimize DNA exposure to UV). The DNA was then extracted from the agarose using a QIAquick gel extraction kit (Qiagen) as per the manufacturer's instructions and DNA was quantified using a NanoDrop ND-1000 spectrophotometer.

2.2.4 Polymerase chain reaction

Primers for PCR (see appendix figure A.1) were generated with the assistance of the software package Bioedit, and were synthesized by the MWG, using HPSF (high purity salt free) liquid chromatography. PCR reactions were performed in 50µl using 25ng template DNA, forward and reverse primers at 340nM, dNTPs (Promega) at 250µM each, 2.5U of Pfu DNA polymerase (Stratagene) in the accompanying buffer (containing 2mM $MgCl_2$). A PCR cycle of 95˚C (denaturation) for 30s, 60.0˚C (annealing) for 60s, and 75.0˚C (elongation) for 6.5 minutes was used, and reactions were performed in an Eppendorf Mastercycler. 25 cycles were used, with the first being a “hot start” (95.0˚C for 30s only). Following PCR, DNA fragments were separated by agarose gel electrophoresis and visualised and purified as above.

2.2.5 DNA ligation

DNA ligations were set up with 3:1 molar ratios of purified insert and backbone DNA fragments, with 25ng of backbone DNA used in each reaction. Reactions were carried out in 20µl using 3 units of T4 ligase (Promega) and an appropriate volume of T4 ligase buffer diluted in RNAase free water. Ligation mixtures were incubated overnight at 14˚C, followed by 3 hours at room temperature, prior to transformation of supercompetent XL1-Blue E.coli. Negative control ligations containing all reagents except the insert DNA fragment were performed in parallel.

2.2.6 Growth and transformation of bacterial cells

Agar plates were made from 20g/L LB base and 15g/L bacto agar (Merck) dissolved in water prior to autoclaving, and appropriate antibiotic was added once the agar had cooled to below 60ºC, but was still liquid. The agar was then poured into sterile petri dishes and allowed to set. 250µl aliquots of supercompetent XL1-Blue E.coli cells (Stratagene) were thawed and kept on ice. 3.4µl of 1.42M β mercaptoethanol was added to each aliquot and was kept on ice for a further 10 minutes. 40µl of chemically sensitised cells were then added to 10ul of each DNA ligation reaction and the samples were mixed regularly throughout 30 minutes of incubation on ice. The DNA bacteria mix was then incubated at 42ºC for 45 seconds before returning to ice for 2 minutes. 360µl of pre-warmed antibiotic free Luria-Bertani broth (LB broth) (made up from LB base, Invitrogen) was then added to each sample and they were agitated in an orbital shaker at 37˚C for 30 minutes. Following this, cultures were centrifuged for 5 minutes at 1200g and bacterial pellets were resuspended in 100µl of fresh warmed LB, and then plated

out on agar plates. Plates were incubated overnight at 37˚C.

The following morning isolated single bacterial colonies were selected using a sterile P20 tip and used to inoculate 5ml of warmed LB containing the appropriate antibiotic (mini prep culture). Cultures were grown overnight at 37˚C in an orbital shaker (250 rpm), before 1.4ml of culture broth was harvested for DNA extraction and purification.

For generation of DNA stocks, 5µl of a miniprep culture was diluted with 100µl of warmed LB and then plated out on agar plates containing an appropriate antibiotic. After overnight culture a single bacterial colony was picked and a starter culture was initiated as above. After 4-8 hours of agitation 100µl of the starter culture was used to inoculate 100ml of warmed LB containing an appropriate antibiotic, and this maxiprep culture was incubated overnight at 37˚C in an orbital shaker (225 rpm). The following morning 700µl of this culture was mixed with 300 µl of 75% glycerol and frozen at -80˚C as a glycerol stock, and the remaining culture was used for DNA extraction.

2.2.7 DNA extraction from bacterial cultures

DNA extraction was performed using a modified alkaline lysis (Bimboim and Doly, 1979), using miniprep or maxiprep kits (Qiagen) according to manufacturer's protocols. For minipreps 1.4ml of bacterial culture broth was centrifuged at 15000g for 5 minutes in a microcentrifuge, and the pellet was used as the substrate for extraction. Purified DNA was eluted using TE buffer.

For maxipreps, 100ml of culture broth was centrifuged at 5000g for 30 minutes to generate a bacterial pellet. Eluted DNA was purified by isopropanol and then ethanol precipitation. The precipitate was then air dried and dissolved in 1ml of TE buffer. To remove any insoluble impurities, dissolved DNA samples were centrifuged at 15000g for 5 minutes and the supernatant was kept. The concentration of all DNA samples was determined using a NanoDrop ND-1000 spectrophotometer (absorbance at 260nm). Absorbance of light at a wavelength of 260nm (A_{260}) has a linear relationship to the concentration of double stranded DNA. Centrifugation steps during maxi preps were performed using either a Sorvall legend RT or a Sorvall Evolution RC.

Samples were stored at -20ºC, and concentration was rechecked before every use.

2.2.8 Checking of ligated plasmids

Following transformation of ligation reactions, at least 3 colonies from each agar plate were selected and miniprep DNA samples were generated. These minipreps were then restricted using two restriction enzymes, which would generate a restriction patterns upon electrophoresis which would allow identification of plasmids containing the correct insert in the correct orientation. Each DNA sample was tested with two different restriction enzyme combinations and the restriction pattern was compared to DNA containing positive and negative control DNA restricted in parallel. If none of the minipreps appeared to contain the correctly ligated insert, further colonies were selected and tested (upto a maximum of 20 minipreps).

For any plasmid subsequently used in experiments the sequence of the gene of interest was verified. Sequencing was performed by MWG using standard primers or specifically designed primers as shown in appendix 1.

2.2.9 Site directed mutagenesis

For the generation of point substitution in WASp, the Quikchange protocol (Stratagene) was used (see figure 2.2). Briefly, primers of approximately 20 nucleotides were designed with the altered nucleotide(s) required to generate the appropriate amino acid substitution in the middle. The reverse primer was the reverse complement of the forward primer sequence. The sequences of primers used for site directed mutagenesis are shown in the appendix (figure A.1). Primers were synthesized by MWG and were purified using HPLC (high pressure liquid chromatography, a higher level of purity than HPSF). C1-EGFP containing WT WASp was used as the template for site directed mutagenesis PCR reactions, unless otherwise stated. A PCR cycle with a “hot start” of 95°C for 30s, followed by 95°C for 30s (denaturation), 60°C for 60s (annealing) and 72°C for 390s (elongation) repeated 14x, under the same reaction conditions as described for PCR above, was used. The PCR products were then digested with Dpn1, a restriction enzyme which only cuts when its recognition site is methylated, and therefore “nicked” any residual template DNA (this is of bacterial origin, as stock DNA samples were purified from bacterial cultures). The complete reaction sample was used for transformation of supercompetent bacteria, and selected colonies were screened by check restriction as above.

To reduce the risk of accidental mutagenesis as a consequence of the long length of the PCR product (6.2 kB), clones which restricted correctly were subcloned back into the C1-EGFP WT WASp vector using the 800 bp Bgl II restriction fragment

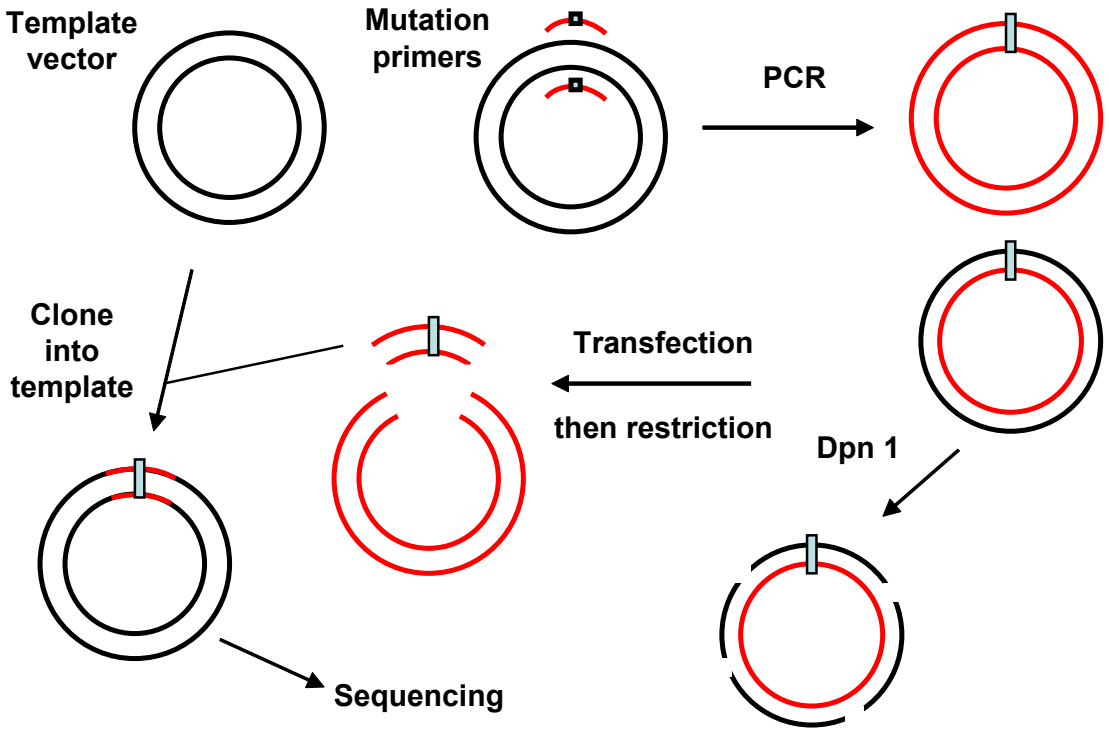

Figure 2.2 Site directed mutagenesis protocol
Schematic representation of the protocol used for site directed mutagenesis. Red strands represent DNA generated by PCR, black strands represent original (bacterial origin) DNA, and the blue box represents a point mutation.

(see figure 3.4e) which contains each individual point mutation. Following check restriction to ensure the correct orientation of the subcloned fragment, the C1 EGFP mutant WASp constructs were sequenced as above (MWG).

The Y291E WASp point mutation within the EF-Bos GST vector was a gift from Giles Cory at Bristol University.

2.3 Cell culture

All media and media supplements were supplied by Gibco (Invitrogen), except foetal bovine serum (FBS) which was supplied by Sigma. FBS was heat inactivated by heating to 60ºC for 2 hours prior to use. Details of the cell lines and primary cells used and their culture conditions are contained in table 2.3. All tissue culture centrifugation was performed with a Hettich Zentrifuge Rotofix 32 centrifuge.

2.3.1 Cell lines

Cos 7 cells were purchased from the European Collection of Cell Cultures (ECCC). The other cell lines were donated by other members of the Molecular Immunology Unit (Institute of Child Health), as frozen cell aliquots which were known to be of

Table 2.3 Cell lines

Name	*ECACC number*	*Species*	*Description*	*Medium grown in*
U937	85011440	Human	Histiocytic lymphoma cell line	RPMI 1640, 10% FBS, 1% PS
Cos 7	87021302	African Green Monkey	SV-40 transformed kidney fibroblast	DMEM, 10% FBS, 1% PS
THP 1	88081201	Human	Acute myeloid leaukaemia cells	RPMI 1640, 10% FBS, 1% PS, 10mM HEPES, 1.0 mM sodium pyruvate, 1.5g/L sodium bicarbonate
293T	04072121	Human	Embryonic kidney epithelial cells	DMEM, 10% FBS, 1% PS
Raw 264.7	85062803	Mouse	Abelson murine leukaemia virus transformed monocyte-macrophage	DMEM, 10% FBS, 1% PS
Primary dendritic cells	NA	Mouse	Bone marrow derived	RPMI 1640, 10% FBS, 1% PS, GM-CSF

RPMI – Roswell Park Memorial Institute media
DMEM - Dulbecco's modified eagle medium
FBS – Foetal bovine serum
PS – penicillin and streptomycin. 1% PS represents 100IU/ml penicillin and 100ug/ml streptomycin
GM-CSF – Recombinant murine granulocyte/macrophage colony stimulating factor at 20ng/ml

Table 2.4 Kits

Name	*Company*	*Cat. number*	*Use*
jet PEI	Polyplus transfection	101-10	Small scale Cos-7 transfection
Silver stain	Sigma	PROT-SIL1	Silver staining of polyacylamide gels
Qiagen mini prep	Qiagen	12125	Rapid DNA extraction from bacterial cultures for colony screening
Qiagen maxi prep	Qiagen	12163	Generation of stock DNA samples errom bacterial cultures (medium scale)
Qiagen Gel extraction	Qiagen	28706	Extraction of DNA bands from agarose gels
BCA protein estimation kit	Pierce	23225	Estimation of protein concentration
AminoLink plus immobilisation kit	Pierce	44894	Covalently linking antibodies to a sepharose resin

passage 15 or less. To change media, cells were centrifuged at 1500 rpm for 5 minutes and old media was aspirated off. The cell pellet was then resuspended in pre warmed fresh medium. Cell density and viability was estimated by diluting 20µl of cell culture with 20µl of 0.4% trypan blue (Sigma) and counting at least

100 cells using a haemocytometer.

All the cultures were maintained at 37°C with 5% CO_2. Cos 7 and 293T cells were detached, by initially washing adherent layers with phosphate buffered solution (PBS) and then incubating with trypsin-EDTA for 5-10 min prior to splitting. Cells were subcultured upon reaching 80-90% confluence (between every 3 and 5 days) and were split with a ratio of 1:4 to 1:8 (seeding at approximately 3000 cells/cm^2). RAW cells were detached by scraping and were split with a similar ratio.

U937 cells were subcultured every 2-4 days and were split to a confluence of 1-2x10^5 cells per ml. THP1 cells were subcultured every 3-5 days and were split to a confluence of 2-3x10^5 cells per ml. it was ensured that neither cell line reached a cell concentration of greater than 1x10^6 per ml.

For long term storage of cell lines, the equivalent of a 50% confluent 80 cm^2 tissue culture flask (adherent cells) or 5x10^6 cells (non adherent cells) were pelleted, washed, resuspended in 0.5ml of fresh medium and transferred to a 1.5ml cryovial. Pre-cooled (on ice) freezing mix (60% FBS, 20% DMSO, 20% medium) was then added to the cells, one drop at a time. Cells were frozen slowly overnight to -70°C in an isopropanol freezing bath and then transferred to liquid nitrogen.

For revival of frozen cell lines, cells were rapidly defrosted by incubation in a 37ºC water bath. The cell aliquot was then transferred to 10ml of warmed medium in a falcon tube to wash off the DMSO. The cells were then pelleted, resuspended in fresh medium and transferred to an 80 cm^2 tissue culture flask for ongoing culture.

All cell lines in stable culture were regularly screened for mycoplasma infection.

2.3.2 Primary Dendritic cells

Mice were culled using a Schedule 1 technique. Femurs and tibias were dissected out and were cleaned. Bone marrow was flushed out of the long bones with media using a syringe and 26G needle, and boney debris was excluded by passing the bone marrow through a cell strainer. Bone marrow from one limb was then transferred to a 80cm^2 flask and cultured in 10ml of RPMI supplemented with 20ng/ml recombinant murine GM-CSF (see table 2.3).

On days 3 and 5 of culture, 5ml of fresh GM-CSF supplemented media was added to the culture, without washing or removal of existing media. Cells were

harvested on day 6, by scraping, and therefore removing both adherent and non adherent cells from the culture. Cells were washed and counted prior to use.

2.4 Cell transfection

2.4.1 Electroporation of Cos7 cells

Electroporation of Cos 7 cells was based on a previously published protocol (Cory et al., 2002). Fully confluent 15cm tissue culture plate of Cos-7 cells were split (1 in 2) 24 hours prior to electroporation. The cells were washed with PBS and removed from the culture plates. 1.2 x 10^7 cells (for each construct) were then washed once with 5ml of special electroporation buffer (SEB), before being resuspended in 400µl of SEB and transferred to a pre-cooled 4mm electroporation cuvette containing 20µg of plasmid DNA. The cells and DNA were incubated together for 5 minutes on ice and then were electroporated using a Biorad Genepulser II at 250V and 975µF. Post electroporation the cuvette was incubated for a further 5-10 minutes on ice before the whole cuvette contents were seeded to a 15cm plate. Medium was changed once at 8-12 hours and cells were harvested at 24 to 36 hours.

2.4.2 Lipofectamine transfection

Cos 7 cell transfection using lipofectamine (Invitrogen) and “Peptide 6” had previously been optimised by Dr Michelle Writer within the Molecular Immunology Unit. 1x10^7 Cos 7 cells were seeded into 15cm plates 24 hours prior to transfection. 80µl of lipofectamine and 0.14mg of peptide 6 were mixed with 2.4ml of OptiMEM. 40 µg of DNA was diluted in 1ml of OptiMEM and added slowly to the lipid peptide mixture and then mixed thoroughly. The mixture was left at 4ºC for 30 minutes, before being diluted to 20 ml with OptiMEM, and then being added to 1 washed plate of Cos7 cells. The medium was changed for fresh DMEM 4 hours later and the cells were harvested at 48 hours.

2.4.3 Polyethylenimine (PEI) transfection

For generation of lentivirus, 293T cells were transfected using PEI, as described below. Cos 7 cells growing in 6 well plates were transfected using jetPEI (Polyplus transfection) for use in co-immunoprecipitation experiments. 2x10^5 cells per well were plated out the day before transfection. For each well 3µg of DNA was mixed with 100µl of 150mM sodium chloride, and 6µl of jetPEI was mixed with 100µl of 150mM sodium chloride. Both samples were vortexed before the jetPEI solution was added to the DNA. This mixture was also vortexed and left to stand for 30 minutes at room temperature. This mixture was then added drop by drop on one

well of a 6 well plate (without removing medium). The cells were harvested at 48 hours.

2.4.4 Lentivirus preparation

1.2 x 10^7 293T cells were seeded into 15cm tissue culture plates the day before transfection. For each plate lentiviral vector DNA (40 µg), packaging plasmid pCMVΔ8.74 (gag-pol) (30 µg) and envelope plasmid pMDG.2 (VSV-G) (10 µg) were added to 5ml of OptiMEM and filtered through a 0.2µm filter. 1µl of 10mM PEI stock was added to 5ml of OptiMEM (for each plate) and was similarly filtered, before mixing with the filtered DNA (1:1 v/v). The mixture was left to stand at room temperature for at least 20 minutes.

The resultant PEI / DNA complexes were added to plates of 293T cells (10ml per plate) previously washed with OptiMEM, and incubated for 4 hours at 37°C/5%CO_2. The media was then replaced with 14 ml DMEM, from which viral supernatant was harvested at 48, 72 and sometimes 96 hours post-transfection. Supernatant was centrifuged at 2000g for 10 minutes and filtered through a 0.22 µm filter (to remove cellular debris) prior to viral concentration by ultracentrifugation at 50,000 g for 2 hours at 4ºC, using a Sorvall *Discovery* SE ultracentrifuge. Lentiviral pellets were resuspended in 150µl of RPMI and stored at -80ºC in aliquots of 10-50µl.

2.4.5 Titration of lentivirus

Lentivirus concentration was titrated using an infectious method on 293T cells. 5x10^4 293T cells in 500µl of DMEM were plated into 24 well plates. 500µl of virus stocks diluted in DMEM at dilutions of 1/100 to 1/10^6 were then added the 24 well plates. A negative control using medium only was included for each construct. At 48 hours, cells in each well were scraped off, pelleted and washed with PBS, prior to fixing for FACS as described below. % EGFP positive cells were determined by FACS with a negative control gate of EGFP positivity set at 1%.

To calculate the infectious titre, % EGFP positivity for each dilution was corrected by subtracting the % of positive cells in the negative control, and the dilution with a % positivity of between 2.5% and 10% was identified. The formula below was used to calculate the titre of the viral stock, where the titre represents the number of infectious viral particles per ml.

$$\text{Titre} = \frac{N \times (\%\ EGFP_{2.5\text{-}10\%}/100) \times Dil_{2.5\text{-}10\%}}{V}$$

Where %EGFP is the % EGFP positivity at dilution (Dil) where the positivity falls between 2.5% and 10%. N equals the number of cells infected and V equals the volume in ml in which the infection was performed

Where no dilution gave a % positivity of between 2.5% and 10%, titres were calculated for the two dilutions adjacent to this range and an arithmetical mean was used as the titre.

2.4.6 Lentivirus transfection of dendritic cell

8 well chamber slides (Lab-Tek II, Nunc) were coated with fibronectin by washing each well with 75µl of PBS, aspirating, and then pipetting 75µl of 10µg/µl fibronectin (Sigma) into the centre of each well. The slides were then incubated at 37º for 2 hours, before aspiration and washing with 200µl of PBS.

Primary murine dendritic cells were generated as above. On day 6 of culture $2x10^4$ dendritic cells in 50µl of medium (50% fresh DMEM and 50% conditioned medium) were added to each fibronectin coated well of a chamber slide. The medium formed a discrete drop in the centre of the well. The appropriate volume of virus was calculated using the formula below and was then added directly to the drop of cells. After 2-4 hours of incubation at 37ºC, the wells were flooded with a further 200µl of media.

$$\text{Volume of virus } (\mu l) = \frac{N \times MOI \times 1000}{\text{Titre}}$$

N equals the number of cells to be infected and
MOI equals the multiplicity of infection required

Infected dendritic cells were cultured for a further 48-72 hours determined by cell morphology and expression of EGFP by fluorescence microscopy. They were then washed in PBS before incubation in fix buffer for 20 minutes, followed by 3 further PBS washes and storage in PBS with 0.1% sodium azide, awaiting staining.

Infection of dendritic cells for FACS analysis, was performed in fibronectin coated 48 well plates with $1x10^5$ dendritic cells per well. Cells were harvested by scraping, and were fixed and stained as for other cells (see below).

2.4.7 Lentivirus transfection of cell lines

$1x10^5$ U937s or THP1 cells were plated into 96 well plates at a cell density of $1x10^6$ cells/ml. Lentivirus was added directly to the cell culture at a volume calculated for MOIs of 1 and 5. 100µl of fresh medium was added at 4 hours post infection. Cultures were rapidly scaled up to larger volumes following infection.

2.5 Protein electrophoresis and Western blotting

2.5.1 Cell lysis and estimation of protein concentration

Non adherent cells were washed in PBS and then centrifuged to form a pellet. Upon aspiration of the supernatant, pellets were place on ice and pre-cooled cellular lysis buffer (LB), unless otherwise stated, was added. Cells were mixed by pipetting and then left on ice for 10 minutes. The lysate mix was then centrifuged at 15000g, at 4ºC for 10 minutes using a microcentrifuge, or a Sorvall Evolution RC for larger lysate volumes. Supernatants were immediately transferred to ice and pellets were discarded.

Estimation of protein concentration was done using a bicinchoninic acid (BCA) assay (Pierce), according to manufacture's instructions. Cu^{+1} ion concentration was quantified using a FLUOstar Optima plate-reader (BMG) reading absorbance at a wavelength of 560nm. Excel was used to generate a standard curve and linear regression was used to estimate protein concentration of unknown lysates.

2.5.2 Cytoskeletal and cytosolic fractionation of cell lysates

Stably growing U937 cells were split to a confluence of $5x10^5$ and reincubated in fresh medium 24 hours prior to harvest. 10^6 cells were washed with PBS, pelleted and then resuspended in 50µl of either standard LB, or LB with the 1% IGPAL replaced with 0.5% Triton X. Lysates were incubated on ice for 15 minutes before centrifugation at 13000 rpm at 4ºC on a bench top centrifuge. Supernatants were extracted and reduced in SB as below, in preparation for SDS-PAGE. The pellet from the Triton X lysed sample was then resuspended in 50µl of standard LB, incubated on ice for 15 minutes and then recentrifuged. The supernatant was then reduced as above. All three samples were separated by SDS-PAGE in adjacent lanes for comparison of WASp band intensity.

2.5.3 SDS-PAGE electrophoresis

One dimensional electrophoresis of protein samples was performed using the Invitrogen Novex NuPage® electrophoresis system. Cell lysate samples were denatured and reduced, by the addition of an appropriate volume of 4x NuPage® LDS sample buffer (SB) and 10x reducing agent (500 mM dithiothreitol (DTT)), and by heating to 70°C for 10 minutes. Samples were then centrifuged at 15000g for 5 minutes and stored at -20°C until electrophoresis was performed.

Following thawing, incubation at 70°C and centrifugation was repeated, and samples were then kept on ice prior to loading onto a gel. 4-12% Bis-Tris Novex pre-cast mini gels (10, 12 or 15 well) or midi gels (12, 20 or 26 well) were used in

XCell *SureLock* Mini-Cell (upto 2 gels) or XCell4 *SureLock* Midi-Cell (upto 4 gels) gel tanks. 10 µl of SeeBlue Plus2 pre-stained standard (Invitrogen) was loaded at one or both outer wells of the gel. NuPage® MOPS SDS running buffer (pre-chilled on ice) with NuPage® antioxidant (proprietary agent) was used as running buffer and the gels were run for 60-90 minutes at 200V, with the gel tank enclosed by ice.

2.5.4 Western blotting

Following electrophoresis, gels were removed from precast cassettes and were washed in NuPage® transfer buffer for 15 minutes on an orbital shaker. Resolved proteins were then Western blotted onto PVDF membranes (Millipore) using a Biorad semi dry blotter (with NuPage® transfer buffer) set at 18V for 20-50 minutes, depending on the surface area of gels to be transferred. Adequate transfer was assessed by observation of the pre stained markers.

2.5.5 Immunoblotting

Following transfer, membranes were incubated in 5% BSA blocking buffer for between 2 hours and overnight (at 4°C). For immunoblots known to have high background signals a commercial blocking agent was used (Starting block T20, Pierce). Where appropriate membranes were wrapped in Saran wrap and cut into strips for different antibody staining using a scapel blade.

Membranes (or strips) were incubated in primary antibody in 2% BSA blocking buffer for between 2 hours (on an orbital shaker at room temperature) and overnight (4°C). They were then washed 5 times with PBS-T, before incubation with an appropriate horseradish peroxidase (HRP) conjugated secondary antibody in 1% BSA blocking buffer for 45 minutes on an orbital shaker. Following 5 further PBS-T washes, membranes were developed with enhanced chemiluminescence (ECL) substrate (SuperSignal West Pico (Pierce)) for 5 minutes, before the ECL was drained off and the protein bands were visualised using a supercooled camera, the UVIchemi chemiluminescence gel documentation system (UVItec). Details of antibodies used and their concentration are shown in table 2.5.

For membranes due to be blotted with anti phospho antibodies, all washes and blocking steps were performed using TBS-T instead of PBS-T.

Membranes which required re-probing were stripped using *Re-Blot plus* Western re-cycling reagent (Chemicon), used according to manufacturer's instructions, and then re-blocked prior to primary antibody staining.

Table 2.5 Antibodies

Name / description	*Abbrev-iation*	*Raised against*	*Raised in*	*Isotype*	*Conju gation*	*Company*	*Identifi-cation number*	*Use*	*Dilution*
anti WASp	α WASp	Amino acids 1-250 of human WASp	Mouse	IgG2a	None	Santa Cruz	B9 sc-13139	WB, IP	1:1000
anti GST	α GST	GST protein encoded in the pGEX.3X recombinant vector	Mouse	IgG1	None	Santa Cruz	B-14 sc-138	WB	1:1000
Anti actin (α and β)	α Actin	C-terminal actin fragment	Rabbit	PC	None	Sigma	A2066	WB	1:600
Anti WASp (near C-terminus)	α WASp CT	Synthetic peptide near C terminus of human WASp conjugated to KLH	Rabbit	PC	None	Abcam	ab29046	WB	1:1000
Anti mouse IG		Anti mouse immunoglobulins	Rabbit	PC	HRP	Dako	P	WB	1:1000
Anti rabbit IG		Anti rabbit immunoglobulins	Goat	PC	HRP	Dako	P 0448	WB	1:1000
Anti goat IG		Anti goat immunoglobulins	Rabbit	PC	HRP	Dako	P 0449	WB	1:1000
anti ARPC2	α ARPC2	Amino acids 288-300 of human ARPC2 (p34 subunit of Ap 2/3 complex)	Goat	PC	None	Abcam	ab11798	WB	1:500
anti GAPDH	α GAPDH	Purified mouse GAPDH	Mouse	IgG1	None	Santa Cruz	6C5 sc-32233	WB	1:1000
anti WIP	α WIP	199 amino acids from the amino terminus of human WIP	Rabbit	PC	None	Anton lab[1]		WB	1:600
anti GFP	α EGFP	Amino acids 1-238 of GFP from *Aequorea victioria*	Rabbit	PC	None	Santa Cruz	FL sc-8334	WB	1:1000
anti N-WASp	α NWASp	Human NWASp peptide	Rabbit	PC	None	Santa Cruz	D-15 sc-10122	WB	1:1000
anti c-myc	α Myc	C terminus of human c-myc	Goat	PC	None	Santa Cruz	A-14 sc-789-G	WB, IP	

Table 2.5 Antibodies *cont.*

Name / description	*Abbrev-iation*	*Raised against*	*Raised in*	*Isotype*	*Conju gation*	*Company*	*Identifi-cation number*	*Use*	*Dilution*
Anti-Phospho-tyrosine	α pTYR	Phosphotyramine-KLH	Mouse	IgG2b κ	None	Upstate	clone 4G10 05-321	WB, IF	1:1000 1:100 IF
Phospho-Detect Anti-WASp pSER$^{483/484}$	α pSER$^{483/484}$	Synthetic phosphopeptide containing human WASp residues surrounding S483 and S483	Rabbit	PC	None	Calbiochem	ST1087	WB	1:1000
anti GFP		Amino acids 1-238 of GFP from *Aequorea victioria*	Mouse	IgG2a	None	Abcam	ab1218	IP	NA
QIAexpress anti HIS	α His	Penta-HIS tag	Mouse	IgG1	None	Qiagen	34660	WB	1:1000
anti TOCA	α TOCA	human TOCA 1	Rabbit	PC	None	Kirschner lab[2]		WB	1:500
anti Cdc-42	α Cdc-42	Peptide at C terminus of human Cdc-42	Rabbit	PC	None	Santa Cruz	P1 sc-87	WB	1:200
anti GFP		GFP purified directly from the jellyfish *Aequorea victoria*	Rabbit	PC	None	Molecular probes	A-6455	IF	1:1000
anti rabbit IG		Anti rabbit immunoglobulins	Goat	PC	Alexa 488	Molecular probes	A-11008	IF	1:100
anti Vinculin		Purified chicken vinculin	Mouse	IgG1	None	Sigma	clone VIN-11-5 V4505	IF	1:200
anti mouse IG		Anti mouse immunoglobulins	Goat	PC	Cy5	Jacksons immuno-research	115-175-003	IF	1:200
DAPI		NA	NA	NA	None	Molecular probes	D1306	IF	1:1000

Table 2.5 Antibodies *cont.*

Name / description	*Abbrev-iation*	*Raised against*	*Raised in*	*Isotype*	*Conju gation*	*Company*	*Identifi-cation number*	*Use*	*Dilution*
Rhodamin Phalloidin		NA	NA	NA	Rhod-amine	Molecular Probes	R415	IF	1:100
anti CD11c	α CD11c	C57BL/6 mouse intestinal intraepithelial lymphocytes	Armenian Hampster	IgG1	APC	BD Bioscience	Clone HL3 550261	FACS	1:25
anti CD86	α CD86	LPS-activated mouse B cells	Rat	IgG2a	FITC	BD Bioscience	Clone GL1 553691	FACS	1:50
anti MHC class II (I-A/I-E)	α MHCII	Activated C57BL/6 mouse spleen cells	Rat	IgG2b	PE	BD Bioscience	Clone M5/114.15.2 557000	FACS	1:100
anti rabbit IG		Anti rabbit immunoglobulins	Goat	PC	Alexa 405	Molecular probes	A-31556	IF	1:500
anti GFP		GST fusion protein to amino acids 1-238 of GFP from *Aequorea victioria*	Goat	PC	Biotin	Rockland	066-106-215	IF	1:1000

1. Gift from Dr Ines Anton, Centro de Biologia Molecular Severo Ochoa, Universidad Autonoma de Madrid, Spain.
2. Gift from Prof Marc Kirschner, Harvard Medical School

2.5.6 Silver staining and gel drying

Gels to be silver stained were removed from their cassettes as above, and were then incubated in 50% ethanol, 10% acetic acid overnight. Staining was performed using a *ProteoSilver™* silver staining kit (Sigma), according to manufacturer's instructions. Where increased sensitivity was required, gels were stained with Coomassie Brilliant blue, prior to silver staining.

Stained gels were washed three times in deionised water and were then incubated in *Gel-Dry* solution (Invitrogen) for 20 minutes. Gels were then mounted on gel dying frames between cellophane sheets saturated in *Gel-Dry* solution, and left to dry over 24-48 hours.

2.6 Calpain inhibition

2.6.1 Storage and stock solutions of specific protease inhibitor

Calpain inhibitors, ALLM and calpeptin, proteosome inhibitor MG132 and cysteine protease inhibitor, cathepsin, were all purchased from Calbiochem. All were made up as 500x stock solutions in ethanol (ALLM, MG132 and cathepsin inhibitor) or DMSO (Calpeptin), and stored at -20ºC. Starting functional concentrations were 20μM (Calpeptin and MG132) or 50μM (ALLM and Cathepsin), as suggested by published data (Nicola et al., 2005; Coers et al., 2004; Steinhilb et al., 2001; Ravid et al., 2000).

2.6.2 Effect of protease inhibitors on U937 cells transfected with EGFP WASp

U937 cells stably transfected with EGFP WT WASp and EGFP A134T WASp were seeded in 24 well plates at $1x10^6$ cell in 2ml. After 2 hours incubation at 37ºC, protease inhibitors (at specified concentrations) were added directly to the wells and cells were incubated for three hours. Cells were washed with PBS and 10% of cells were stained with Trypan Blue and viability was assessed using a haemocytometer as above. The remainder were lysed in ice cold LB (pH 7.4 with no protease inhibitors or phosphatase inhibitors) and lysates were clarified as above. An aliquot of lysate inhibited by ALLM was used to assess residual calpain activity. All samples were resolved by reducing PAGE and Western blotted for WASp.

2.6.3 Calpain activity assay

Residual calpain activity was measured using a *Calpain-Glo* Protease Assay (Promega). Breifly, 50μl of lysate was mixed with 50μl of Calpain-Glo reagent,

containing the synthetic calpain substrate succinyl-LLVY-aminolyciferin, luciferase and 2mM $CaCl_2$. Reactions were performed in 96 well plates. Upon cleavage by calpain, succinyl-LLVY-aminolyciferin is cleaved to release aminoluciferin which produces a luminescent signal in the presence of luciferase, Mg^{2+}, and ATP. The strength of the luminescence is proportional to the activity of the calpain in the sample. Luminescence was measured using a FLUOstar Optima plate-reader, 20 minutes into the reaction. Control reactions performed with lysis buffer only were used as negative controls, and the average background luminescence was subtracted from each sample reading.

2.7 Densitometry and analysis of quantification

2.7.1 Band quantification from western blots

Quantification of protein bands from Western blots was performed using the software package UviBand (UVItec) in conjunction with images taken with the UviChemi supercooled camera.

Images used for quantification, were obtained after first performing a test exposure, to ensure the final exposure time would utilise the full range of the camera's sensitivity without saturating the highest intensity band. This ensured a linear relationship between protein concentration and densitometry reading.

Densitometry bands were created according to the manufacturer's instructions, and background subtractions were performed manually for each band. Comparisons were only be made between protein bands run in the same gel, immunoblotted with the same antibodies, developed with the same ECL and imaged for the same exposure.

2.7.2 Analysis of densitometry for actin polymerisation assays

Densitometry readings were obtained for WASp bands (anti GST), actin bands and ARPC2 bands. Absolute quantities of WASp and Actin were calculated by standardising raw densitometry readings to those of known standards of WASp and actin run in an independent gel lane in each experiment. Data from all assays performed under the same experimental condition and were analysed together as a single dataset (three dataset – constitutively active constructs, standard panel and NWASp constructs). Raw densitometry data (relative values) and calculated absolute data (absolute values) were analysed in parallel to monitor the validity of the techniques used. As a result each dataset contained several constructs tested from several experiments, but each individual experiment contained a variable subset of constructs (see chapter 4.42 for further discussion).

Statistical support in the analysis of data from the actin polymerisation assays was provided by Prof Tim Cole (Professor of Medical Statistics at the Institute of Child Health). Guidance as to which approach to use and assistance with the setting up of the regression models used in the analysis was provided by Prof Cole, but the analysis itself and interpretation of the results was performed by the author.

Densitometry readings for actin and WASp were transformed to percent units by taking natural logs and multiplying by 100 (T.J.Cole, 2000). %Actin levels for each construct across experiments were then adjusted for %WASp using two-way analysis of covariance (i.e. two-way analysis of variance plus the covariate %WASp), and including adjustments for differences between experiments and between constructs. This allowed the significance of differences in %Actin between constructs to be tested for.

Further analysis showed that the %Actin-%WASp relationship varied from one experiment to another, and therefore the adjustment ought to include a %WASp by experiment interaction. Adding this to the model provided a different set of construct effects, which could be compared with those obtained from the simpler main effects analysis. The analyses of the basic model (main effects) and the model containing a WASp by experiment interaction compensation (interaction model) are shown for all analyses.

N-WASp input samples were found to have high levels of actin bound to purified protein, before assay incubation. For these experiments, the amount of actin bound to beads prior to incubation in U937 lysate was determined and this value was subtracted from the actin readings determined during the assay (see chapter 4.8).

For some experiments performed with the constitutively active constructs, high levels of background actin polymerisation were detected (as defined by high actin signals in the GST only lanes). For this series of experiments, actin readings were corrected for this background by subtracting the GST only readings from actin readings obtained in experimental lanes.

2.7.3 Analysis of densitometry for U937 lysates

Densitometry reading were obtained for EGFP-WASp, endogenous WASp, GAPDH, and where stated for WIP and WASp phosphoserine. Reading were standardised for loading by dividing the densitometry reading by the densitometry reading for GAPDH for the same construct. For EGFP-WASP, the corrected

densitometry reading was divided by the EGFP-WASp reading for WT-EGFP WASp transfected lysates to give an EGFP-WASp reading relative to WT. For each experiment these relative values were then averaged between values derived from anti WASp immunoblotting and anti EGFP immunoblotting.

In summary

$$\text{EGFP-WASp (x) relative to WT} = \left(\frac{{}^{W}EW_x / G_x}{{}^{W}EW_{wt} / G_w} + \frac{{}^{E}EW_x / G_x}{{}^{E}EW_{wt} / G_{wt}} \right) \Big/ 2$$

The concentration of construct x EGFP-WASp relative to wild type (wt), where
${}^{W}EW$ = EGFP-WASp densitometry reading determined using αWASp antibody
${}^{E}EW$ = EGFP-WASp densitometry reading determined using αEGFP antibody
G = GAPDH densitometry reading.

For endogenous WASp, loading corrected readings were divided by the endogenous WASp reading for untransfected cells, to give quantify endogenous WASp relative to untransfected U937 cells.

$$\text{Endogenous WASp (x) relative to UT} = \frac{{}^{w}eW_x / G_x}{{}^{w}eW_{ut} / G_{ut}}$$

The concentration of endogenous WASp in cells transfected with construct x EGFP-WASp relative to the concentration of endogenous WASp in untransfected cells (UT), where
${}^{w}eW$ = endogenous WASp densitometry reading determined using αWASp antibody, G = GAPDH densitometry reading.

2.7.4 Analysis of densitometry for estimation of phosphorylation

To determine the relative proportion of WASp phosphorylated at serine 483/484, loading corrected phosphoserine readings for mutant constructs were divided by their loading corrected WASp readings, and these values were then divided by the equivalent value for WT EGFP-WASp. As before the values derived from anti WASp blots were averaged with values derived from anti EGFP blots. This final figure gives a level of phosphorylation for each construct relative to WT, where the proportion of WT-WASp phosphorylated is 1.

For each of these values the final reading for each mutant construct is compared to a standard value of 1, and as a result a paired one sample test was used to analyse the significance of any differences from these standards.

For determination of EGFP-WASp / endogenous WASp ratios for each cell line,

the raw densitometry data from the anti WASp immunoblot could be used, as

$$\text{Proportion of serine}^{483/484}\text{ phosphorylated EGFP-WASp (x) relative to WT proportion phosphorylated} = \left[\frac{\left(\frac{^{PSER}EW_x / G_x}{^{w}EW_x / G_x} \right)}{\left(\frac{^{PSER}EW_{wt} / G_{wt}}{^{w}EW_{wt} / G_{wt}} \right)} + \frac{\left(\frac{^{PSER}EW_x / G_x}{^{E}EW_x / G_x} \right)}{\left(\frac{^{PSER}EW_{wt} / G_{wt}}{^{E}EW_{wt} / G_{wt}} \right)} \right] \Big/ 2$$

^{PSER}EW = EGFP-WASp densitometry reading determined using α phosphoserine $^{483/484}$ antibody
^{w}EW = EGFP-WASp densitometry reading determined using αWASp antibody
^{E}EW = EGFP-WASp densitometry reading determined using αEGFP antibody
G = GAPDH densitometry reading

reading for both proteins were derived from the same blot. As result there was no need to compare these ratios to a standard. Paired 2 sample t tests were used to compare these values to WT-WASp transfected lysate.

2.7.5 Analysis of densitometry for pulldown and immunoprecipitation assays

For the analysis of the relative strength of WASp – WIP affinity between constructs, a similar ANCOVA analysis to that used to analyse the actin polymerisation assays was used. Natural logarithms of WASp and WIP densitometry readings were used as these were normally distributed, and a regression model including an interaction term between experiment and Ln WASp concentration was used.

2.8 Recombinant protein purification

2.8.1 GST-WASp purification

Cos 7 cells were cultured and electroporated as described above. GST tagged WASp constructs were generated in batches such that proteins to be tested against each other in subsequent experiments (actin polymerisation assays, pulldown experiments), were all synthesised at the same time (thus further standardising results).

Each 15cm plate of Cos 7 cells was washed in PBB and then placed on ice. 800µl of pre-cooled cellular lysis buffer (LB) supplemented with 2µM latrunculin B (Sigma) and 2 µM cytochalasin D (Sigma) was then added. After 10 minutes of incubation in LB on ice, cells were detached with a cell scraper, and transferred to microtubes for centrifugation at 15000g for 15 minutes at 4°C. Supernatants were then added to 125 – 250µl glutathione Sepharose 4B beads (GE biosciences) (pre-

washed 2x with LB), either as neat supernatant or diluted with LB to a specified dilution. Lysates and beads were incubated for between 2 hours and overnight at 4°C on a rotator. Beads were then pelleted and washed 3x with lysis buffer, 2x with 0.5M lithium chloride, 20mM Tris pH 8.0, and once with 20mM Tris pH 8.0. Pelleted beads were then resuspended in 5 bead volumes of 75% glycerol, 10mM Tris pH 8.0, 1mM EDTA and stored at -80°C.

50µl of each bead sample (8.3µl of beads) was washed and pelleted, and then separated by reducing PAGE. Gels were Western blotted and immunoblotted for GST and densitometry was performed. These measurements were used to standardise the amount of WASp used in subsequent experiments (by volume adjustment).

For purification of WT WASp eluted from Sepharose beads, lysate was generated from the equivalent of six 15cm plates of electroporated Cos 7 cells, and 1ml of washed glutathione Sepharose beads were used. Protein was eluted from the beads, after washing, by the addition of GST elution buffer and incubation for 10 minutes with rotation. Beads were then pelleted and the supernatant was removed. Elution was repeated 3 further times, elutants were pooled and were then dialysed three times against 5mM Tris pH 8.0, 1mM EDTA with protease inhibitors at 4°C for 30 minutes, using a *Slide-a-Lyzer* 0.5-3ml cassette (10kDa molecular weight cut off (MWCO), Pierce). GST-WASp protein was then concentrated using Microcon spin concentrators (Millipore) with a MWCO of 10KDa. Aliquots were frozen at -80°C.

2.8.2 Cdc42 purification

E.coli stably transfected with Cdc42 under transcriptional control of the *lac* operon (WT, constitutively active mutant 12V, and dominant negative mutant 17N) were gifts from Prof Anne Ridley (University College, London).

100ml of LB broth with 100µg/ml ampicillin was inoculated with Cdc42 transformed E.coli, and incubated on an orbital shaker overnight at 37ºC. The following morning the culture was diluted into 1L of pre-warmed LB broth containing 50µg/ml ampicillin, and cultured with shaking for one further hour. Protein production was then induced by the addition of 0.1mM isopropyl β-D-1-thiogalactopyranoside (IPTG, Sigma) and further cultured for 4 hours. Bacteria were then pelleted by centrifugation (5000g for 30 minutes, Sorvall Evolution RC) prior to resuspension in 10ml bacterial ice cold lysis buffer (bacterial LB). Bacterial suspensions were then lysed by sonication (6x 10s cycles at 70% power and 30% cycle time) using a Bandalin Sonoplus HD2070 sonicator, with cooling on ice between each

burst. Lysate was then re-centrifuged, supernatant was removed and DTT to a concentration of 15mM was added.

Lysate was then dialysed against bacterial LB (with 0.1mM DTT added), three times over 2 hours, at 4ºC (using *Slide-a-Lyzer* 3-12ml, 10kDa MWCO). The lysate was then added to 1ml of washed glutathione Sepharose 4B beads and rotated for 2 hours at 4ºC. Following this the beads were pelleted and washed 3 times with bacterial LB, twice with with 0.5M lithium chloride, 50mM Tris pH 7.5, and once with 50mM Tris pH 7.5, each wash solution containing 0.1mM of DTT, but no PMSF.

GST tags were cleaved from the Cdc42, using a variety of protocols as described in Chapter 3.6.2 (figure 3.14). Where elution from the beads was performed, four elutions with 5ml of GST EB were performed as described for GST-WASp. Cleavage was performed in thrombin buffer, and bovine thrombin was purchased from Sigma, and human thrombin from GE healthcare. Following cleavage, GST was removed by a 30 minute incubation with 1ml of fresh glutathione Sepharose beads, and the thrombin was removed by a 30 minute incubation with p-aminobenzamidine-agarose gel, for 30 minutes (both at 4ºC). Beads or resin were removed by centrifugation (twice) and supernatants were carefully extracted.

The resultant solution was dialysed three times against 20mM K-HEPES pH7.5, 100mM KCl, 5 mM $MgCl_2$, 1mM DTT, 1µM GDP, and post dialysis samples were concentrated using Centriplus spin columns (Millipore). Samples were then aliquotted and snap frozen in liquid nitrogen, prior to storage at -80ºC.

2.8.3 Cdc42 loading with GTP

Recombinant Cdc42 was loaded with GTPγS (a non hydrolysable GTP analogue which imparts constitutive activity to Cdc42), based upon previously published protocols (Suetsugu et al., 1998; Ma et al., 1998a). 10µl of Cdc42 (WT or 12V) at a concentration of 50-75µM was added to GTP loading buffer to give final concentration of 50mM Tris pH 7.4, 10mM EDTA and 100µM GTPγS, in 50µl. This sample was incubated at 30ºC for 30 minutes and then the reaction was quenched and the EDTA chelation overcome, by the addition of $MgCl_2$ to a final concentration of 50mM. Loaded Cdc42 was then used immediately.

2.8.4 Assessment of purity and quantification of purified protein

Protein concentration of purified protein samples was quantified using the BCA assay as described in 2.5.1.

Concentration estimates were checked by running an aliquot of the protein sample on a NuPAGE gel with a series of protein standards of known concentration (typically actin and bovine serum albumin). The gel was then silver stained (as above) and concentration was estimated by comparing the size of protein bands to those of the standards. Purity of protein samples was also assessed using silver staining gels and compared to immunoblots for the protein and its tag.

2.9 Actin polymerisation assay

2.9.1 Assay

U937 cells were split to $5x10^5$ cells per ml and incubated over night in fresh medium. The following day, cells were counted and then washed once in PBS, prior to pelleting (1500 rpm for 5 minutes). PBS was aspirated off and cell pellets were resuspended in ice-cold actin polymerisation buffer (APB) at a concentration of $1\text{-}6x10^7$ cells/ml. Lysates were incubated on ice for 10 minutes. After centrifugation (15000g for 10 minutes at 4ºC), the lysate was supplemented with 5mM $MgCl_2$ (and if stated 1mM ATP), then incubated with a standardised volume of GST-WASp coated Sepharose beads. GST only coated beads and beads incubated with actin polymerisation inhibitor cytochalsin D were used as negative controls.

Beads and lysate were incubated for 1 hour at room temperature on a rotator, after which the beads were pelleted and washed twice with APB. Where stated $1/10^{th}$ of the beads were fixed (4% paraformaldehyde in PBS for 10 minutes) and then fluorescently stained for f-actin (1 in 100 Rhodamine phalloidin in PBS for 25 minutes in the dark, followed by washing in PBS) before mounting for fluorescence microscopy. The remaining sample was reduced in SB and resolved by PAGE and western blotting. PVDF membranes were divided transversely at approximately 52 and 38 kDa, with the top third being stained for GST (to detect GST-WASp), the middle third being stained for actin and the bottom third being stained for ARPC2 (and subsequently GST). The concentration of substrate lysate was determined using a BCA assay to ensure the lysate concentration was within the range of 1.5 – 2.5mg/ml.

This basic protocol was extensively manipulated as described in various results chapters.

2.9.2 Fluorescence imaging of beads

Beads were imaged using a Zeiss Axiovert 135 fluorescent microscope (10x/0.25 NA lens) and analysed using Volocity 4.0 software (Improvision). Phase and

fluorescence images were taken. For fluorescence images exposure time was determined by analysing positive and negative control beads, and then using a fixed exposure time for all subsequent samples.

Images were manipulated in Photoshop®, with identical manipulations performed to each equivalent image taken.

2.10 Immunoprecipitation and radioisotope labelling experiments

2.10.1 Pulldown experiments

Lysates were generated (as above) using cell type, concentration and lysis buffer as specified. Protease inhibitors and phosphatase inhibitors were added to the lysis buffers, and lysates were modified as specified. 250µl of lysate was added to GST-WASp coated Sepharose beads and incubated at room temperature for 2 hours with rotation. Beads were then pelleted and were washed twice with the lysis buffer used, before being resolved by reducing PAGE and immunoblotted as specified.

For pulldown of zzWIP constructs, IgG Sepharose Fast Flow (GE healthcare) was used. The zz tag contains the IgG binding domain of protein A and therefore binds Sepharose beads coated with IgG with high affinity. IgG Sepharose was activated by incubating in 0.5M acetic acid (pH 3.4), twice, with TBS-T washes between and after. Lysates were then added to the beads and samples were processed as for glutathione Sepharose beads.

2.10.2 Generation of resin immobilised antibody

Immobilisation of antibodies to resin to facilitate immunoprecipitations was done using the AminoLink Plus immobilisation kit (Pierce). The beaded resin is activated to contain aldehyde groups which can then react with primary amines present in proteins to form Schiff Bases. These are then stabilised by reductive amination (using sodium cyanoborohydride) to form stable secondary amine bonds.

Briefly, 1.25ml of resin (2.5ml of resin slurry) was washed three times with coupling buffer (centrifuging at 3000g for 1 minute and aspirating washes). 200µg of αEGFP antibody was diluted to 1.25ml with coupling buffer and added to the washed resin. 0.5M sodium cyanoborohydride was added to the mixture and the sample was rotated for 4 hours at room temperature. The beads were then pelleted and supernatant was carefully removed, before the beads were re-washed with first coupling buffer and then quenching buffer. The beads were then resuspended in

1.25ml of quenching buffer and 2M sodium cyanoborohydride, for further rotation for 30 minutes. Following this, beads were washed twice with coupling buffer and twice with PBS, prior to storage in 1.25ml PBS with 0.1% sodium azide (stored at 4ºC).

Control resin was made by either performing the same reaction with no antibody added (quenched resin), or by using an isotype control antibody (isotype control resin).

2.10.3 Immunoprecipitation

Immunoprecipitation reactions were performed based on the protocol for the *ProFound* Mammalian Co-Immunoprecipitation kit (Pierce) using *Handee* screw cap spin columns. Resin is maintained in the column by a bottom frit which allows buffer to flow through upon centrifugation, whilst trapping the resin on the frit.

50µl of antibody bound resin slurry (25µl of resin containing 4µg antibody) was pipetted into a *Handee* column and washed with the specified lysis buffer. Lysate was added to the columns and the columns were sealed prior to rotation for the specified time. Resin was washed 3 times with lysate buffer prior to elution with 50µl of *ImmunoPure* IgG elution buffer (proprietary, Pierce). 2-4 elutions were performed.

Beads were regenerated following a further prolonged incubation with an excess of elution buffer (400µl for 30 minutes), and washing 2 times with coupling buffer, prior to re-storage in PBS with azide.

2.10.4 Radioisotope labelling of cells

Methods for radiolabelling cellular proteins with 35S were adapted from various on line protocols (sources included Invitrogen, Springer lab – Harvard Medical School, Tansey lab – Cold Spring Harbour, Department of Biological Sciences Warwick University, Hu and Heikka (Hu and Heikka, 2000)).

Stably transfected U937 cells were split to $5x10^5$ cells per ml and incubated overnight in fresh medium. Cells were counted and then washed twice in pre-warmed PBS. Cells were then incubated at $1x10^6$ cells/ml in starvation medium (RPMI lacking cysteine and methionine, with 1% PS, 10% dialysed FBS) for 30 minutes at 37ºC. Cells were then pelleted and resuspended in labelling medium (starvation medium with a stated amount of *Redivue Promix* 35S (GE Healthcare) added) and incubated for a stated period of time at 37ºC with 5% CO_2. After the labelling period, cells were pelleted and washed with warm PBS before

resuspending in chase medium (RPMI 1640, 10% FBS, 1% PS, 2mM methionine, 2mM cysteine) at $5x10^5$ cells per ml for the stated chase period.

At harvest cells were pelleted and then washed twice in ice cold PBS, before being resuspended in ice cold APB. Immunoprecipitation using αEGFP resin was performed as above.

Following PAGE of reduced samples, gels were dried as above and then exposed to Imaging Screen K (Kodak) storage phosphor screens in a light tight cassette for upto 6 weeks. Radio-emission was detected by analysing phosphor screens on a Molecular Imager FX (Biorad), and images were analysed using Quantity One (Biorad) software.

2.10.5 Analysis of protein stability experiments

Images of radio-emissions were exported to and optimised in Photoshop. Densitometry was performed in Quantity One. Boxes were manually drawn around bands, and local background radiation levels were subtracted (average signal from the boundary each box was proportionally subtracted from the counts within each box). % WASp degradation at each chase time point was calculated by dividing radio-emission reading form the value obtained at the end of the pulse period, and multiplying by 100. A one way repeated measures ANOVA test was performed and mean percentage degradations were compared to WT-WASp using the Dunnett multiple comparisons test.

2.11 Fluorescence activated cell sorting

2.11.1 FACS of transfected cell lines

Cell lines were analysed by flow cytometry to assess the proportion of positively transfected cells in culture and the level of EGFP-WASP expression within the cells.

Cells were washed with PBS, transferred to FACS tubes and then resuspended in Fix buffer for 20 minutes at 4ºC in darkness. Following this cells were pelleted, supernatants discarded and cells were resuspended in 0.5ml of PBS with 1% paraformaldehyde and stored at 4ºC until they were analysed by FACS. Cells were analysed using a Beckman Coulter XL flow cytometer and Expo2 software.

2.11.2 FACS of transfected primary dendritic cells

Murine dendritic cells were analysed by flow cytometry to assess the degree of maturation induced following lentivirus infections.

Cells were washed and fixed as for cell lines. For immunostaining, cells were pelleted and washed with FACS buffer, before resuspending in 100µl of FACS buffer containing primary antibodies (αCD11c and α MHC class II) at the appropriate concentrations (see table 2.5), and 2% (10µg/ml) murine Fc block. Tubes were wrapped in foil, and incubated on ice for 30 minutes. Cells were subsequently washed twice with FACS buffer and then resuspended in 100µl of FACS buffer containing secondary antibodies at appropriate concentrations, and murine Fc block. Tubes were incubated as for primary staining, and then washed before resuspending in 0.5ml of FACS buffer. Cells were analysed within 24 hours on a CyAn ADP flow cytometry analyser and Summit version 4.1 software (DakoCytomation). CD11c was analysed via the APC channel, EGFP via the FITC channel and MHC class II via the PE channel. Control samples with no primary antibodies, and with each individual primary antibody left out were used to set positivity threshold and to compensate for bleed through between fluorophores. LPS treated dendritic cells were used as a positive control for activation.

2.11.3 Cell sorting

Transfected U937 cells and THP1 cells were sorted into EGFP high and low populations using a Beckman Coulter EPICS Altra Cell Sorter. Cell sorts were performed by Joao Metelo from the Molecular Immunology Unit at ICH. Post sorting cells were returned to tissue culture incubators for normal culturing. 2 weeks after sorting aliquots of cells were frozen down.

2.12 Real time PCR

2.12.1 Genomic DNA extraction

2.5 x 10^5 stably transfected U937 cells were washed in PBS and then pelleted by centrifugation at 15000g for 10 minutes. Cells were resuspended in 40µl DNA lysis buffer and incubated at 56ºC for 2 hours. Lysed cell pellets were pulsed at 15000g, incubated at 95ºC for 15 minutes and then pulsed again at 15000g. 180µl of distilled DNase-free water was added, followed by centrifugation at 13,000 rpm for 5 minutes. The supernatant containing the genomic DNA was then transferred to sterile microtubes and stored at -20ºC.

2.12.2 Determination of viral copy number per cell

Quantitative PCR was used to determine the number of integrated viral copies per cell in stably transfected U937 culture as has been described previously (Greg, 1999).

Two separate PCR reactions were run for each sample (in triplicate) using a fluorescently labelled probe (FAM) against the lentiviral vector (WPRE) primer binding site and against β actin. Primers and probes were purchased from Applied Biosystems (see appendix 1). 5µl of extracted genomic DNA (from above) was used as the template, and primers (0.9µM) and probes (0.2µM) were added to Platinum qPCR SuperMix-UDG with ROX (Invitrogen) as the additional reagents. The probes are fluorescently labelled on the 5' end and have a quencher on the 3' terminus. The endonuclease activity of *taq* releases the 5' fluorescent label from the FRET activity of the quencher thus increasing the fluorescence in the well with each cycle of the PCR. This fluorescence is detected, quantified and monitored throughout the reaction. Real time PCR reactions were performed using an ABI Prism 7000 Sequence Detection System, using the default cycling parameters (1 cycle of 50°C for 2 minutes, 1 cycle of 95°C for 10 minutes followed by 40 cycles of 95°C for 15 seconds and 60°C for 1 minute).

In parallel, PCR reactions for a dilution series of lentivirus and actin standards of known copy number (gift from Dr Mike Blundell, Molecular Immunology Unit, ICH) were run in triplicate. By determining the cycle threshold values, (an arbitrary value assigned at a point where all the samples are in log phase expansion and graphs of fluorescence emitted are parallel), for both standards and samples, standard curves could be plotted and the number of viral copies present and the number of cell genomes in the reaction could be determined. From this the number of copies of integrated virus per cell was calculated.

2.12.3 mRNA extraction

1 x 10^6 stably transfected U937 cells were washed in PBS and then pelleted by centrifugation at 15000g for 10 minutes in a micro-centrifuge. Cell pellets were frozen at -80ºC until RNA extraction could be performed.

Cell pellets were thawed and resuspended in Tri-reagent BD (Sigma) and 1/5^{th} total volume of chloroform (stabilised with amylenes) was added. This mixture was centrifuged at 15000g to separate the RNA (top clear aqueous layer), DNA (cloudy interphase) and protein (red organic layer). RNA layer was removed and an equal volume of isopropanol added. The samples were mixed and then incubated at -20ºC overnight before centrifugation at 13,000rpm to pellet the precipitated RNA. The RNA pellet was washed in 70% ethanol, spun at 13,000rpm for 5 minutes and air dried. The dry pellet was resuspended in 10-20ul of water and stored at -20ºC until needed.

2.12.4 Making cDNA from RNA

5ul of RNA was incubated with 0.5ul RNAse inhibitor, 1ul of an oligo dT and 1ul of 2.5mM each dNTPs (all Applied Biosystems), at 70°C for 10 minutes. The reaction was then placed on ice for 5 minutes, before 1ul of 25mM $MgCl_2$, 1ul of PCR buffer 2 (Applied Biosystems) and 0.5ul MMLV reverse transcriptase (Applied Biosystems) was added and the mixture incubated at 42°C for 1 hour. The resulting cDNA/mRNA hybrid samples were stored at -20ºC in preparation for quantitative PCR.

2.12.5 Quantification of EGFP-WASp and endogenous WASp mRNA

Expression of EGFP WASp and endogenous WASp in stably transfected U937 cell lines was determined by performing quantitive PCR on the cDNA/mRNA hybrid generated as above.

Three separate PCR reactions were performed in triplicate, with primers against WPRE (to detect EGFP-WASp introduced by lentivirus), against the untranslated region adjacent to endogenous Human WASp (to detect endogenous WASp expression) and against phosphoglycerate kinase (PGK – a housekeeping gene). Primers and probes were purchased from Applied Biosystems (Assays by design) (see appendix 1), and probes were labelled with the FAM reporter. PCR reactions were performed as for determination of copy number, using the 5µl of the cDNA/mRNA hybrid solution as the reaction template.

Cycle thresholds were determined as above. By directly comparing the cycle threshold (CT) values obtained from the WPRE and endogenous WASp PCRs relative to the PGK gene, the expression levels of EGFP WASp and endogenous WASp can be compared between samples, using one sample as the reference (WT for EGFP-WASp, untransfected cells for endogenous WASp) to which all others can be compared. The fold increase or decrease in expression levels are calculated using the formulae below;

$$\text{WASp Cycle Threshold} - \text{PGK Cycle Threshold} = \Delta\text{CT for each sample}$$

$$\Delta\text{CT sample} - \Delta\text{CT reference} = \Delta\Delta\text{CT}$$

$$2^{-\Delta\Delta CT} = \text{fold increase between samples}$$

2.13 Confocal microscopy

2.13.1 Dendritic cell preparation and immunostaining

Dendritic cells were permeabilised and stained in the 8 well chamber slides in

which they were grown. Following fixation, dendritic cells were washed three times and then permeabilised by incubation in 0.1% Triton X in PBS for 3 minutes. This was aspirated off and replaced with 1% BSA in PBS for 30 minutes to block non-specific binding sites.

Cells were then incubated in 100µl of PBS with 1% BSA containing anti vinculin and anti EGFP antibodies at appropriate concentrations (see table 2.5) for 45 minutes at room temperature in darkness. Cells were then washed three times in PBS, 1% BSA, prior to incubation with secondary antibodies and agents (goat anti mouse Cy5, goat anti rabbit Alexa 488, Rhodamine phalloidin and DAPI) at appropriate concentrations (Table 2.5) for 45 minutes. The cells were then washed 3 further times with PBS, 1% BSA, and once with deionised water, before mounting with *ProLong Gold antifade* mountant (Invitrogen), covering with a cover slip and sealing with nail varnish.

2.13.2 Microscopy

Images were recorded digitally using a Leica TCS-SP2 confocal microscope and Leica software. Images were taken in four channels (Cy5 – vinculin, FITC – EGFP WASp, TRITC – actin, and UV DAPI of WIP) and z stacks of 8-12 sections were taken to allow composite and overlay images to be generated. Images were subsequently analysed using Leica Lite and Photoshop software packages.

2.13.3 Image analysis

To determine podosome restoration random fields of view were captured using a 40X magnification lens, until at least 50 EGFP positive cells were captured. Images were labelled using a random number code and were analysed later, with blinding as to the nature of the sample. During image analysis, individual cells were scored as EGFP positive or negative, and whether or not they expressed any podosomes. Scoring was performed by two independent investigators and results for the percentage of transduced cells expressing podosomes were averaged. Differences between constructs were analysed using the chi squared test.

Although all the confocal images presented in this thesis are entirely my own work, one dendritic cell preparation used for the enumeration of podosomes, and the quantification of podosomes expressing cells (figure 9.1e) was performed other members of my laboratory (Siobhan Burns and Joao Metelo).

3 Molecular Cloning, Protein Expression and Purification

3.1 Introduction

In this chapter I describe the experiments performed to generate the raw materials and biological reagents used in the rest of this project. This work includes the molecular cloning of the WASp constructs, their expression and purification from mammalian cell lines, medium scale purification of GST-WASp for use as a protein standard, expression and detection of WIP constructs in transfected mammalian cell lines, expression of endogenous WASp and WIP in cell lines used as experimental substrates and the medium scale purification of Cdc42. Details of the experimental procedures followed are contained in chapter 2.2-2.5 and 2.8.

3.2 Molecular cloning

3.2.1 Starting materials

The structure and position of the WASp constructs investigated in this project are shown in figure 3.1. The reasons for choosing these constructs for investigation are discussed in chapter 1.10. All WASp constructs were generated from WT WASp, with the exception of Y291E point mutation, which was a gift from Giles Cory (University of Bristol). This was provided as GST tagged WASp within the EF-Bos vector. The starting vectors and their sources are shown in table 2.1 and figure 2.1. The primary source of the WASp gene was the FL3-WASp plasmid from Jonathan Derry (Howard Hughes Medical Institute) (see table 2.1). WASp had been previously cloned into a lentivirus vector by members of my host laboratory, and it was this vector (pHRsinc-SEWW) which I used as the initial source of WASp for further molecular cloning (see figure 2.1 and table 2.1 for further details).

The WIP and Cdc42 containing vectors were used as they were received as gifts (see table 2.1) and no further cloning was performed on them.

3.2.2 Generation of C1 EGFP-WT-WASp

All the mutant WASp constructs were generated using WT WASp in the cloning vector pEGFP-C1 (Clonotech) as a template. The strategy used for cloning WASp into pEGFP-C1 from pHRsincSEWW is demonstrated in figure 3.2. Figure 3.4a shows gels of the isolation of WT WASp from pHRsincSEWW and the linearization of pEGFP-C1. These fragments were excised and ligated to generate C1 EGFP-

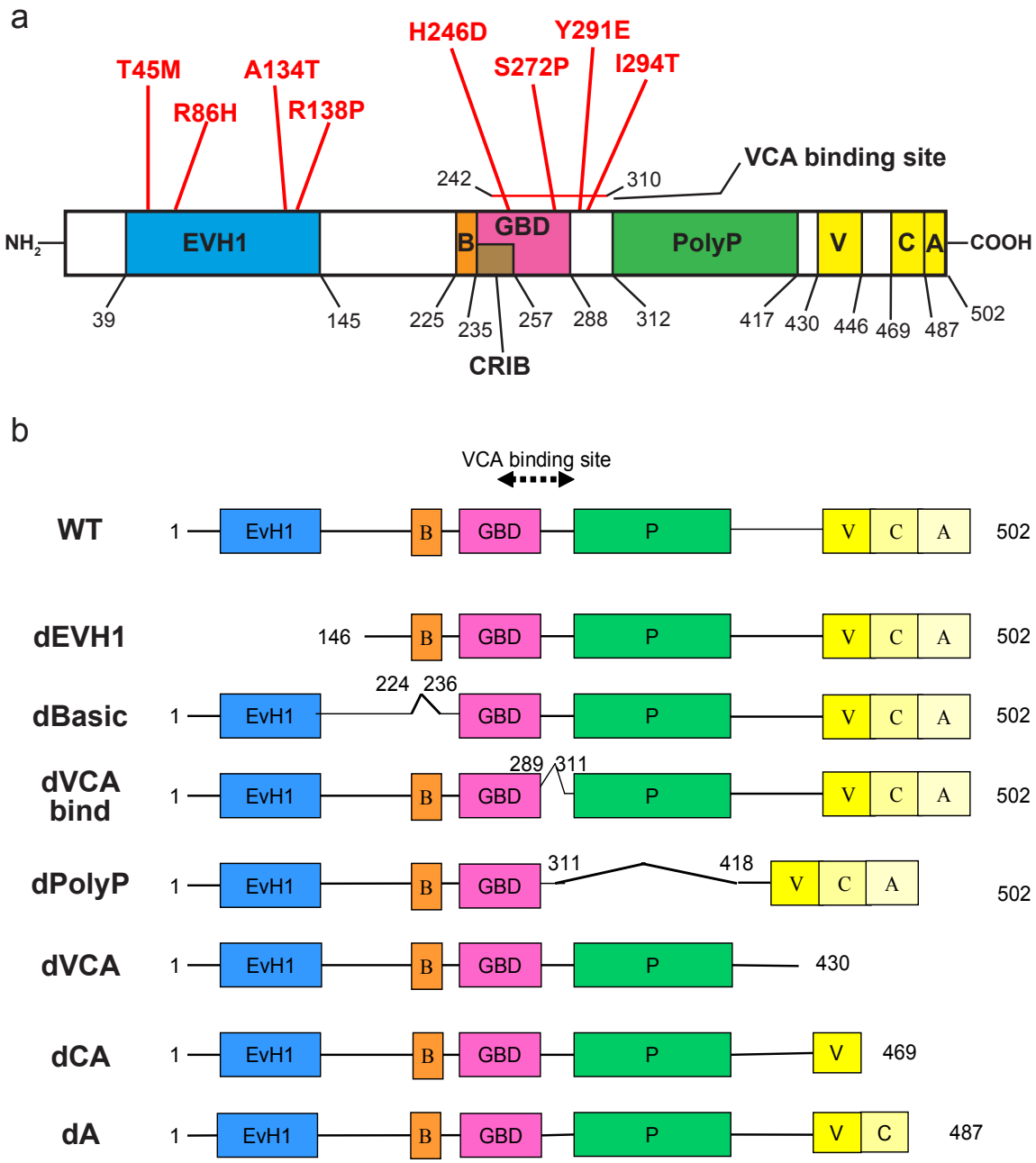

Abbreviations: EVH1 = Ena Vasp homology domain, B = Basic domain, GBD = GTP-ase binding

Fig 3.1 Structure of WASp constructs generated
(a) Sites of point mutations generated by site directed mutagenesis. **(b)** Domain structure of truncation and deletion constructs.

WT-WASp (C1-WT). Check restriction of six (correct) clones from this ligation are shown in figure 3.4b. The positions within the EGFP-WASP cassette of restriction sites used for check restrictions are shown in figure 3.4e.

3.2.3 Generation of deletion and truncation in C1-EGFP

The truncation and deletion constructs were generated using polymerase chain reaction (PCR) of WT WASp in C1-WT, as summarised in figure 3.2. Briefly, primers

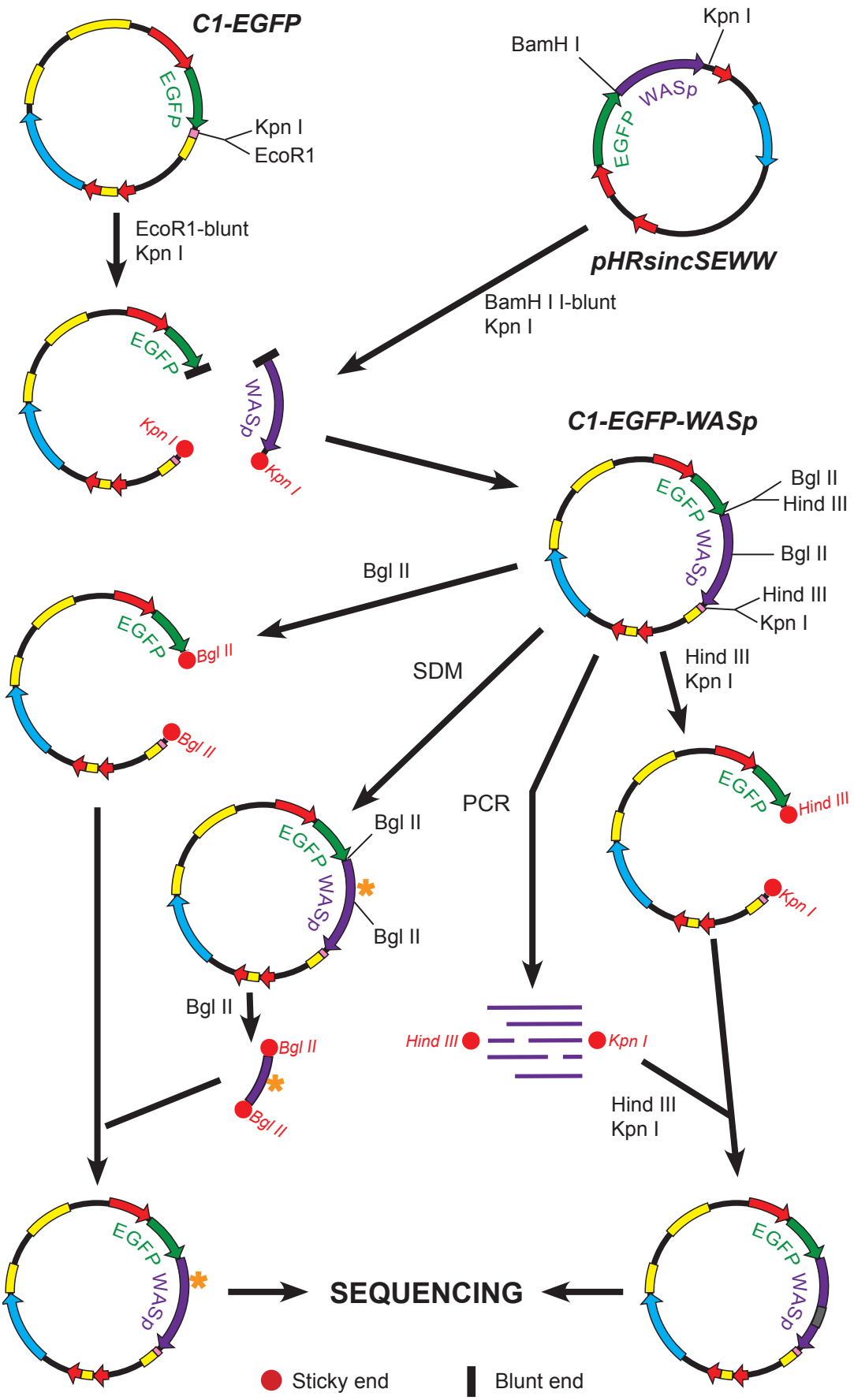

Fig 3.2 Cloning strategy for creating WASp mutant constructs in C1-EGFP

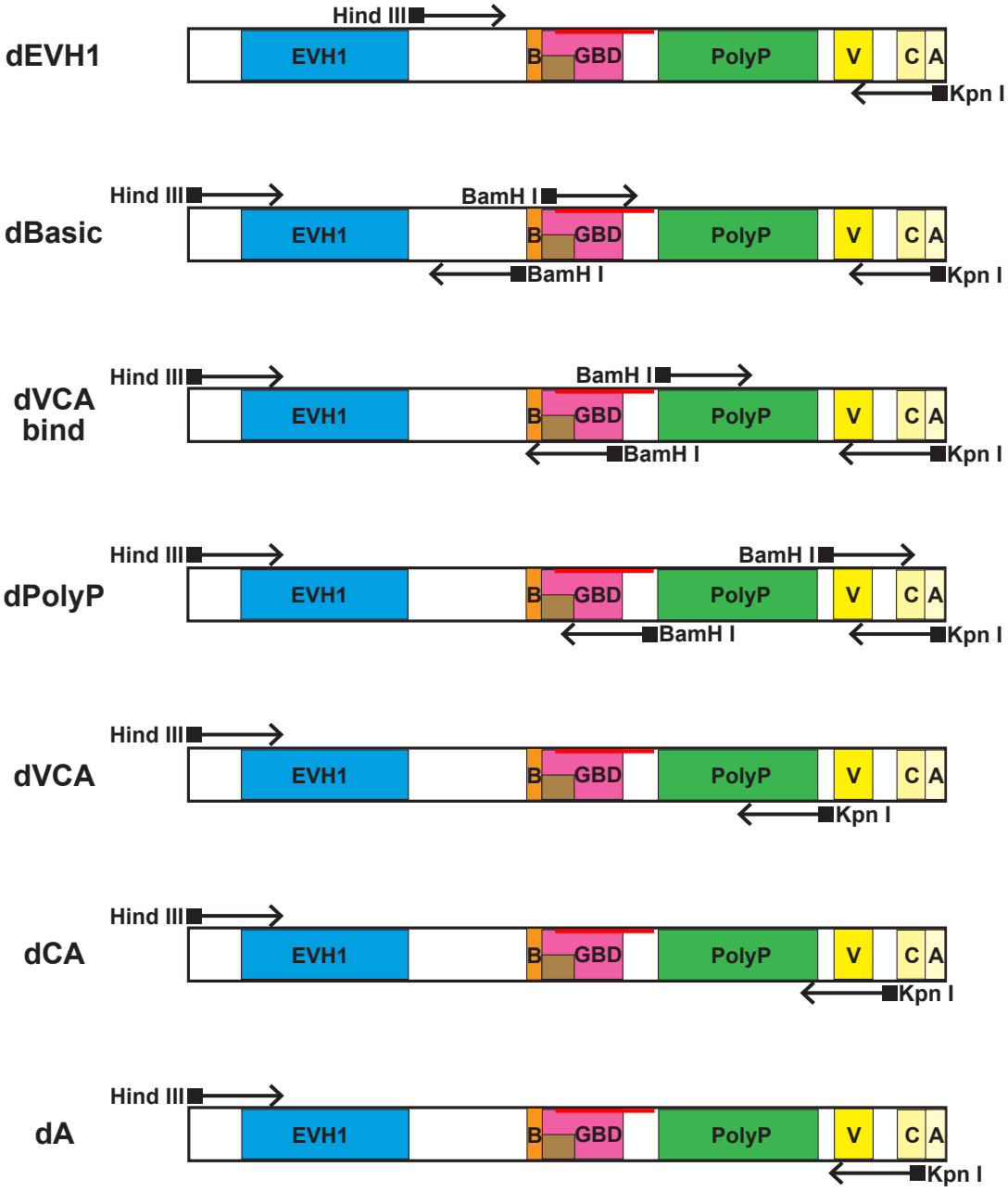

Fig 3.3 Primer sites used for generation of deletion and truncation WASp constructs
Deletion and truncation constructs were made by generating WASp fragments by PCR which excluded specific protein domains. These fragements were generated from primers which included a unique restriction site upstream from their DNA binding sequence (Hind III for forward primers, Kpn I for reverse primers), facilitating the insertion of these fragments into the C1-EGFP cloning vector. For constructs where the deleted domain is in the middle of the protein, two WASp fragments were generated, each with a BamH I site at the “internal” end of each fragment. These two fragments ligated to each other as well as to the C1-EGFP backbone during ligation.

The primer binding sites and conjugated restriction sites are shown in the above diagram. The sequences and labels given to each primer are shown in the appendix (fig A.1)

were designed to generate one or two WASp fragments resulting in the deletion of a functional protein domain. The primers contained a unique restriction site (HindIII at the amino terminus of the protein, BamHI in the middle of the protein and KpnI at the carboxyl terminus of the protein) to allow subcloning of the WASp fragment back into the C1-WT backbone. Figure 3.3 shows the binding sites, and incorporated restriction sites of the primers used to generate each construct. The sequence of the primers is shown in the appendix (figure A.1).

Following PCR the reactions were incubated with the appropriate restriction enzyme and the reactions were then run on agarose gels, as shown in figure 3.4c. This allowed visualisation of the WASp DNA fragments and purification by gel excision. The DNA fragments were then ligated into the HindIII and KpnI restricted C1-WT backbone. Constructs with deletions in the middle of WASp required a ligation reaction containing two WASp fragments and the vector backbone, and three “sticky-sticky end” ligation reactions. The exact position of the WASp insert is shown in the restriction map in figure 3.4e. Of note the constructs generated by PCR cloning are lacking the multiple cloning site (MCS) at the carboxyl end of WASp, which is retained in the C1 EGFP-WT-WASp construct (and therefore the site directed mutagenesis constructs – see below). Check restriction of clones selected following ligation of deletion and truncation WASp fragments is shown in figure 3.4d. Correctly and incorrectly inserted fragments are marked as appropriate. All deletion and truncation constructs were sequenced in C1-EGFP-WASp to determine the whether or not the predicted cloning had been successful and to check secondary mutations had not occurred during the PCR.

3.2.4 Generation of point mutations in C1-EGFP

Missense mutations in WASp were generated using the Stratagene Quikchange protocol as described in chapter 2.29 and figure 2.2. Following site directed mutagenesis the Bgl II WASp restriction fragment from each construct (see figure 3.4e) was sub-cloned back into C1-EGFP-WT-WASp (figure 3.2) to reduce the possibility of additional PCR induced mutations. Isolation of this fragment and the agarose gels from check restriction digests to determine the orientation of the Bgl II fragment are shown in figure 3.5a and b respectively. Because the point mutation constructs were all sub-cloned back into the C1-EGFP-WT-WASp vector each of these constructs retains the MCS at the carboxyl terminus of the WASp gene (see figure 3.4e).

Following this, all constructs were sequenced (by MWG), and the sequencing plots for all point mutation samples demonstrating the intended substitution is

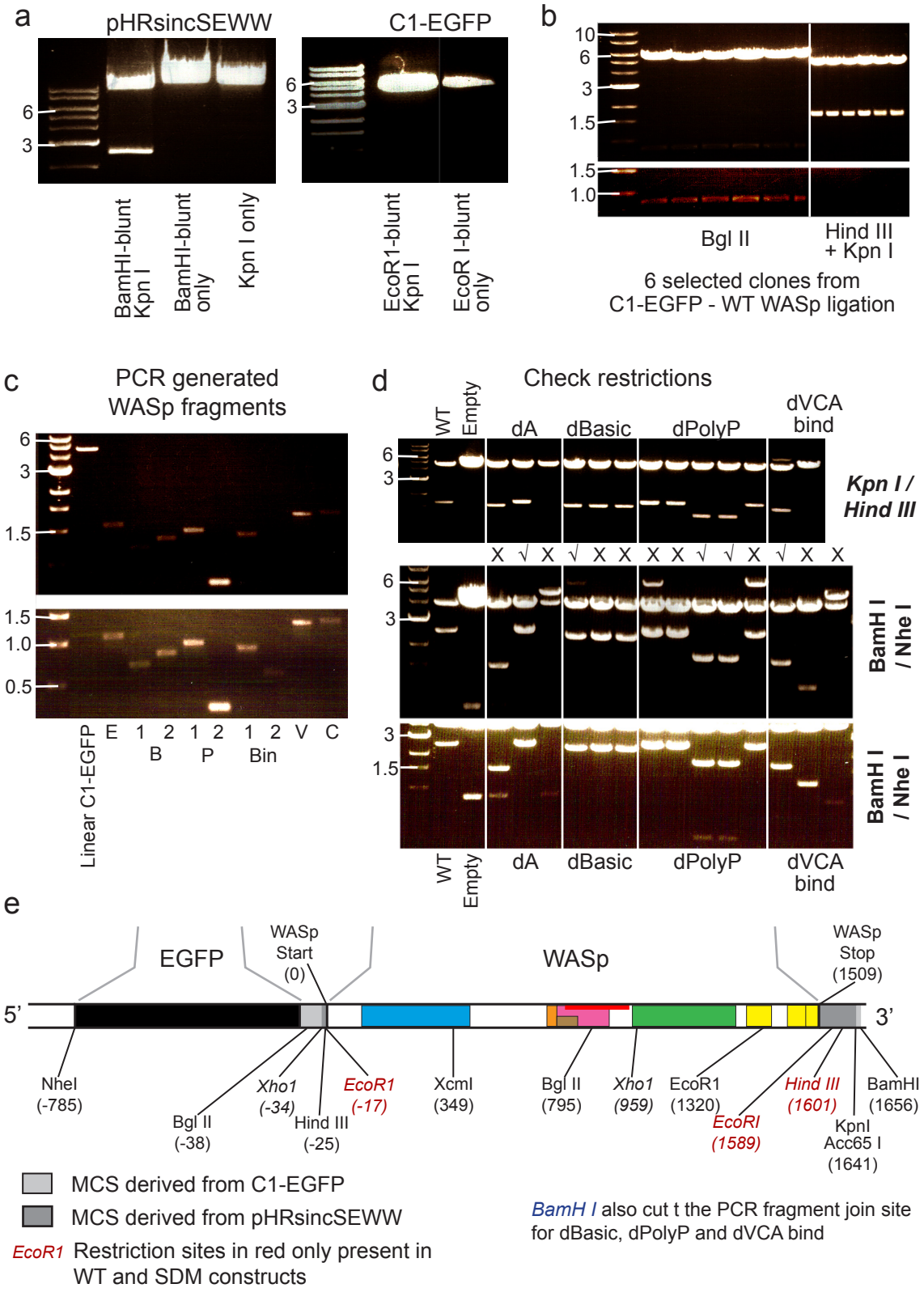

Fig 3.4 Generation of C1-EGFP-WT-WASp and deletion and truncation mutants
(a) Excision of WASp from pHRsincSEWW and linearisation of empty C1-EGFP. **(b)** Check restriction of 6 clones selected following ligation of WASp into C1-EGFP. All six show correct insertion of WASp. **(c)** Gel of WASp fragments generated by PCR and Hind III / Kpn I linearised empty C1-EGFP plasmid. Bottom panel is an overexposure of the top panel. **(d)** Check restriction of selected clones following ligation of WASp deletion fragments into C1-EGFP. Tick and crosses show correct and incorrect insertions. **(e)** Restrictions sites within EGFP-WASp (in C1) used for cloning and check ligation of WASp constructs.

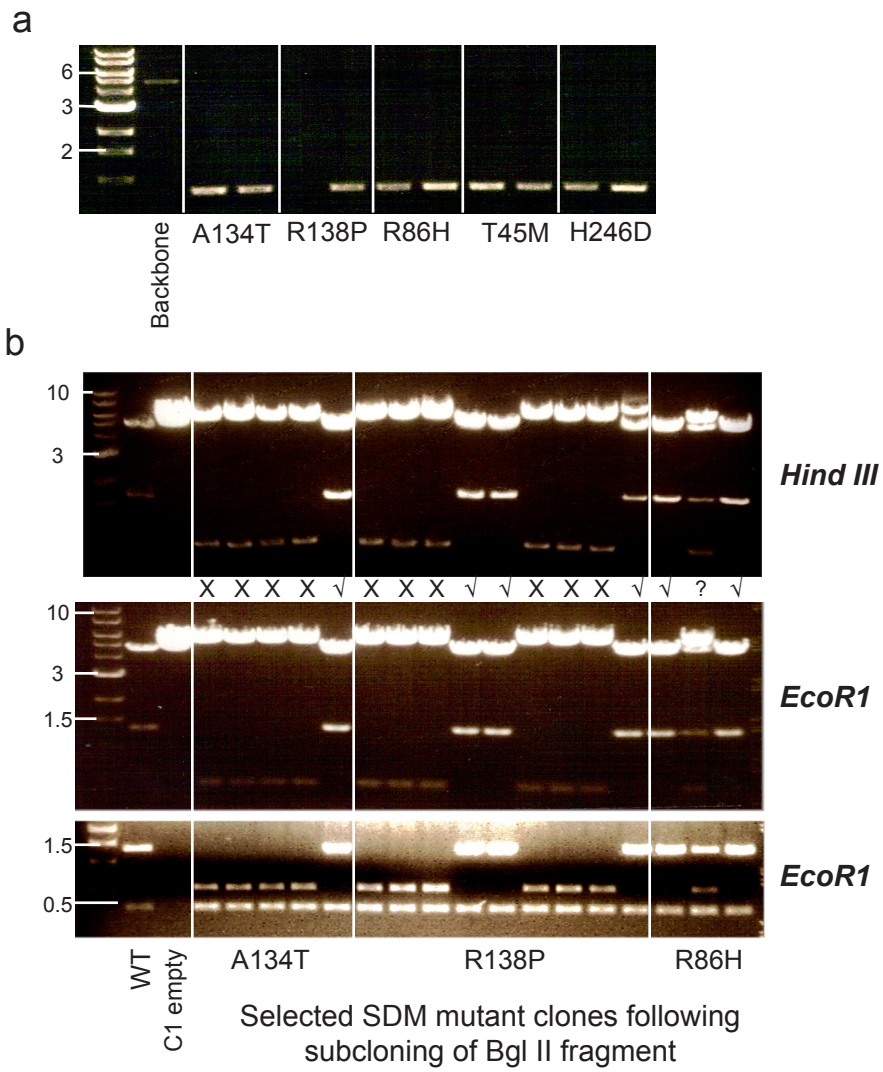

Fig 3.5 Subcloning of Bgl II restriction fragment back into C1-EGFP WT WASp following successful site directed mutagenesis
(a) Following site directed mutagenesis, selected clones were check restricted using Hind III and Bgl II (separate reactions). The fragment produced by the Bgl II restriction was cut out and sub-cloned back into C1-EGFP WT WASp (linearised using Bgl II). This gel shows the excised Bgl II fragments and cut C1 backbone prior to ligation. **(b)** Following ligation selected clones were restricted by Hind III and EcoR I to determine which clones had the Bgl II fragment inserted in the correct orientation. Correctly orientated clones produce a 1.6 and 1.3 kb WASp containing fragment respectively. All constructs contain the 0.3 kb EcoR1 frament from the carboxyl terminus of WASp (see figure 3.4e).

shown in figure 3.6.

3.2.5 Sub-cloning to EF-BOS plasmid

To allow generation of GST tagged WASp protein, the WASp constructs were cloned from C1-EGFP (without the EGFP tag) and inserted into the EF-BOS vector (figure 2.1). This resulted in WASp tagged with the GST at the amino terminus. The strategy for this cloning step is shown in figure 3.7. Briefly, this required a blunt ligation at the carboxyl terminus of WASp, and a partial Bgl II digestion at

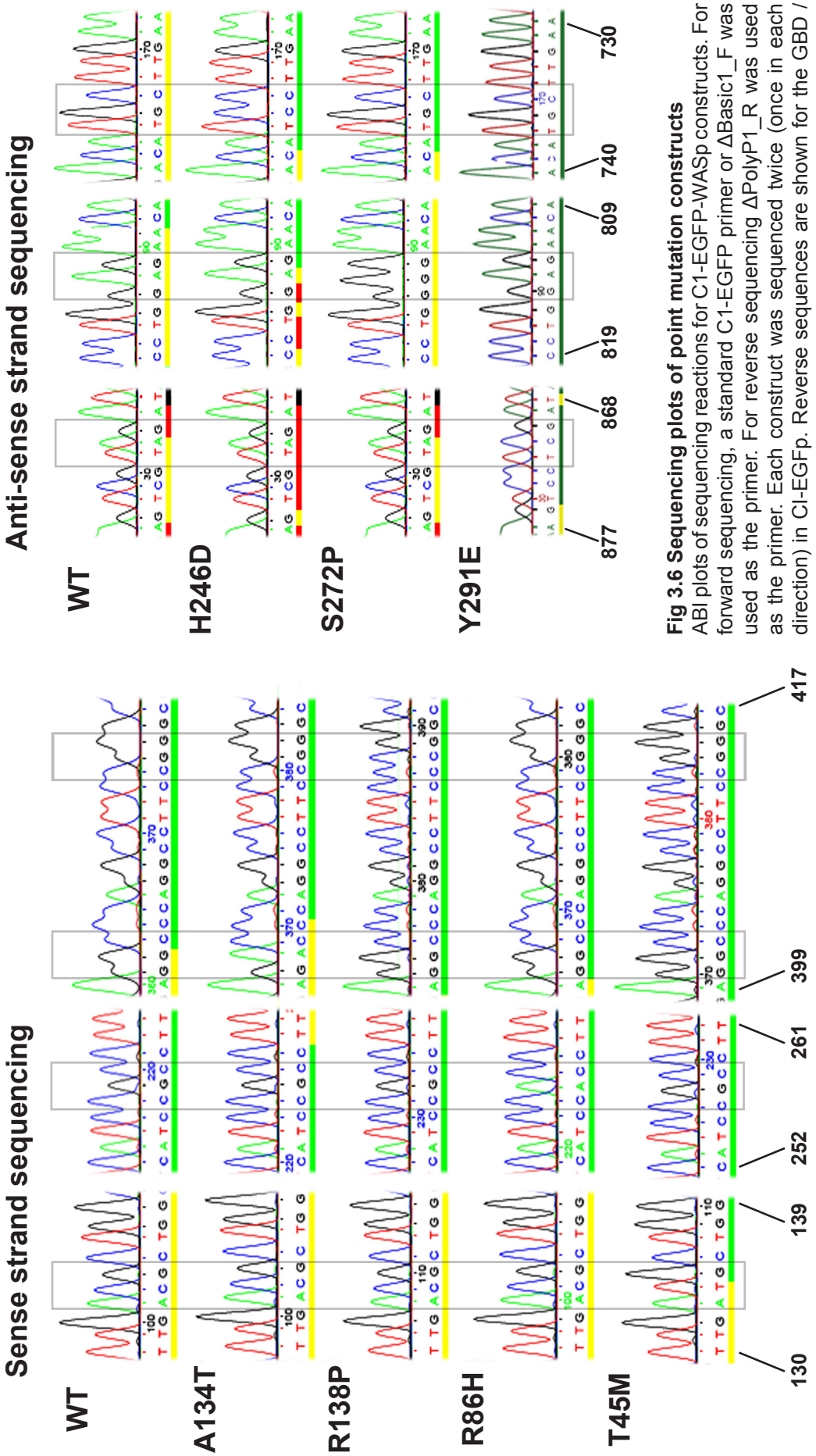

Fig 3.6 Sequencing plots of point mutation constructs
ABI plots of sequencing reactions for C1-EGFP-WASp constructs. For forward sequencing, a standard C1-EGFP primer or ΔBasic1_F was used as the primer. For reverse sequencing ΔPolyP1_R was used as the primer. Each construct was sequenced twice (once in each direction) in CI-EGFp. Reverse sequences are shown for the GBD / CRIB point mutations and therefore the sequences are the reverse complement of coding sequence. Primer sequences are shown in the appendix (figure A.1).

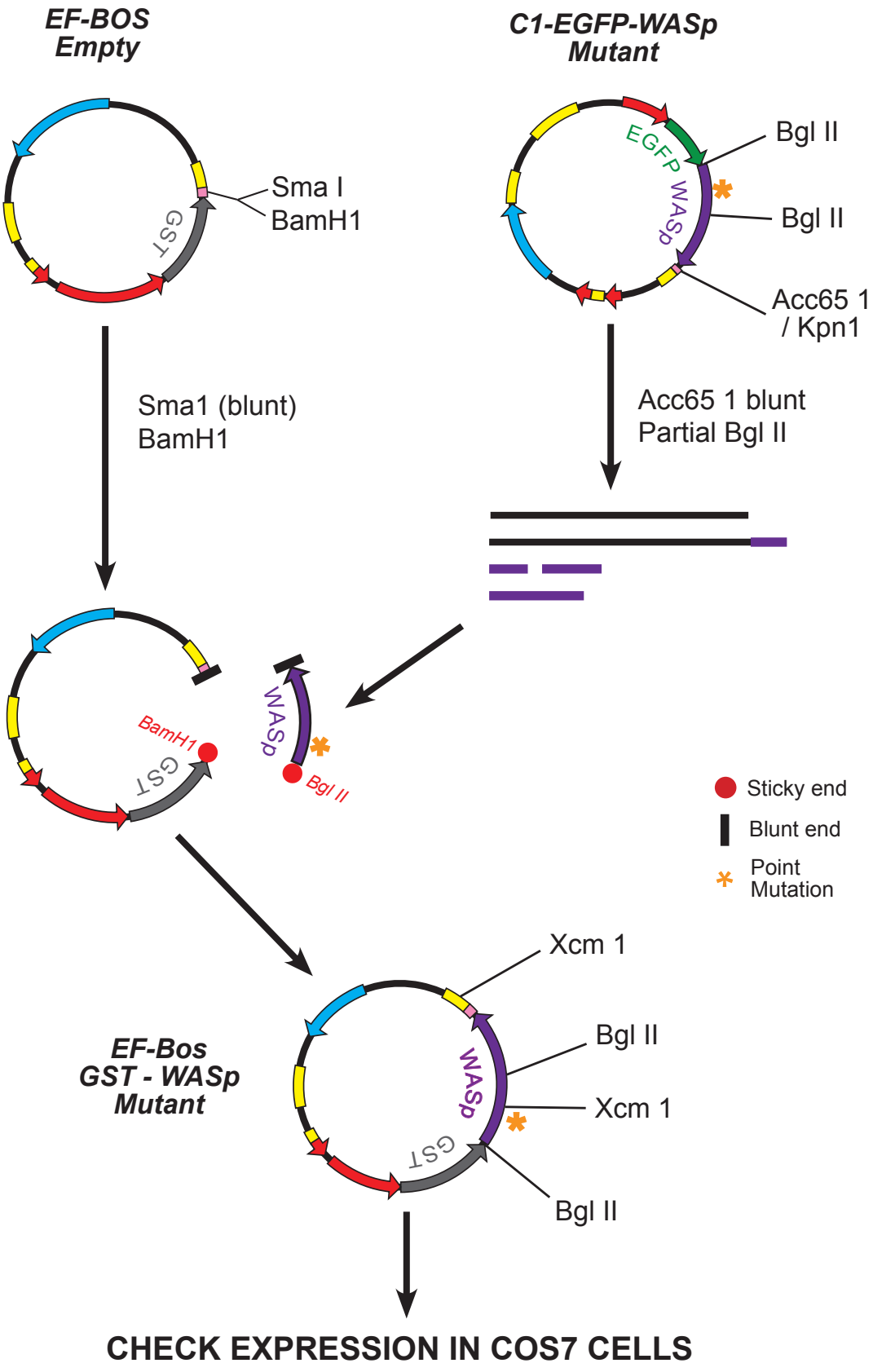

Fig 3.7 Cloning strategy for subcloning WASp constructs in to EF-GST-Bos
Cloning of WASp constructs generated in the C1-EGFP vector into EF-GST-BOS. Strategy shown for a WASp construct containing a missense mutation, although the same strategy was used for deletion and truncation mutations. The final EF-BOS vector map shows restriction enzyme sites used for check restrictions.

the amino terminus. Once full length WASp was separated and purified from the partial digestion reaction, it was ligated to the BamH I “sticky end” produced by linearising the EF-BOS empty vector. This took advantage of the homologous “sticky ends” generated by Bgl II and BamH I restriction. The Bgl II and Acc65 I sites used to excise WASp from the C1-EGFP vector are shown in figure 3.4e.

Figure 3.9a and b show examples of partial digestion reactions with complete digestion of C1-EGFP-WT-WASp and EF-BOS for comparison. 3.9a clearly shows two backbone bands and two WASp digestion bands for each construct subjected to a partial digestion. For WT-WASp (and each of the point mutations) the 0.8 kb band is made up by two fragments of approximately the same size (WASp base pairs -38 to 795 and 795 to 1641). 3.9b more clearly demonstrates the separation of these bands with the dEVH1 and dPolyP constructs (for these constructs one of the WASp fragments and is smaller than the other).

Figure 3.9c shows the purified WT-WASp fragments following gel extraction, and prior to ligation into the EF-BOS backbone. The dEVH1 and dPolyP fragments are only faintly seen. Figure 3.9d shows an example of check restrictions used to demonstrate correct insertion of the WASp constructs into EF-BOS. The positions of the restriction sites are shown in figure 3.7.

3.2.6 Sub-cloning to lentivector

For generation of lentivirus to allow stable transduction of primary cells and haematological cell lines, EGFP-WASp was cloned from C1-EGFP into the lentivector LNT-SIN-SFFV-cPPT-WPRE. The strategy for this cloning is shown in figure 3.8. Briefly, this step involved a “sticky end” ligation at the EGFP-WASp carboxyl terminus and a “blunt ligation” at the amino terminus. Figure 3.9e shows the check restriction digests for a selection of correctly inserted constructs. For the EcoR I digest, the deletion and truncation constructs have only two restriction sites and therefore produce a fragment of approximately 3 kb. By contrast, EcoR I sites are retained at the MCSs upstream and downstream of WASp for the constructs generated by site directed mutagenesis (see figure 3.4e), and therefore three fragments are generated. The dVCA construct has the only EcoR I site within the WASp sequence deleted, and therefore only linearises with EcoR I.

3.3 Protein expression in Cos 7 cells

3.3.1 Expression of constructs

To ensure that the generated WASp constructs expressed as GST tagged proteins, Cos 7 cells were electroporated with EF-BOS GST WASp and cell lysate was

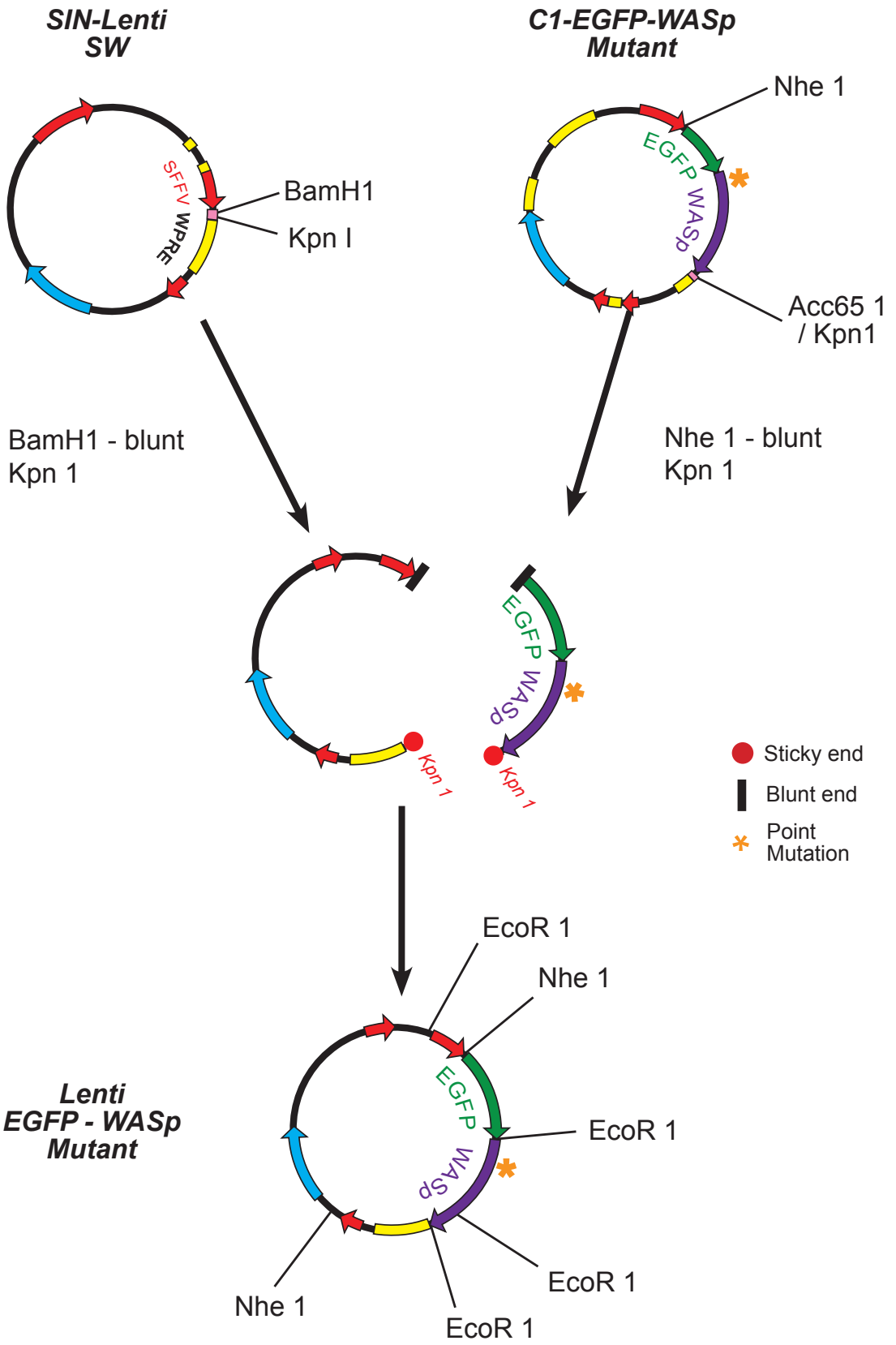

Fig 3.8 Cloning strategy for subcloning EGFP - WASp constructs in to lentivector
Cloning strategy shown for a WASp construct containing a missense mutation, although the same strategy was used for deletion and truncation mutations. The final lentivector map shows restriction enzyme sites used for check restrictions. *SIN-Lenti-SW = Self inactivating lentivector with SFFV and WPRE*.

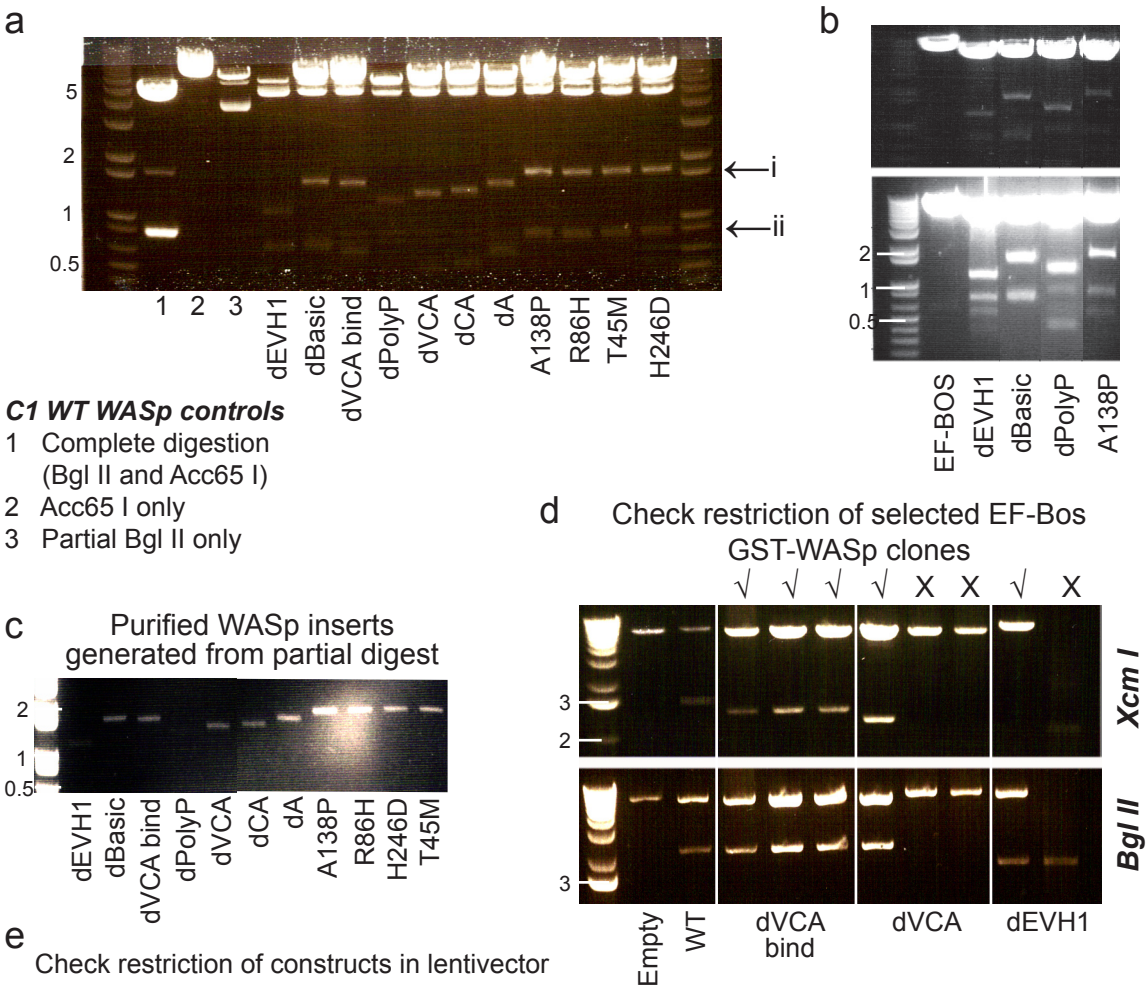

Fig 3.9 Subcloning of WASp constructs from C1-EGFP to EF-Bos and SIN-LNT

(a) WASp was excised from C1-EGFP by Acc65 I (blunt) followed by partial Bgl II restriction. The 1.5 kb (full lengh WASp) band was excised and purified. This gel shows the separation of these reactions for a range of constructs. C1-EGFP WT WASp individually and fully restricted by Bgl II and Acc65 I, is shown for comparison. *Band (i) complete 1.5 kb WASp fragment (excised and purified). Band (ii) 0.8 kb fragment generated by partial restriction at Bgl II 795.* **(b)** Further example of reaction described in (a) better demonstrating partial restriction degradation products. Linearisation of EF-Bos backbone with Sma I and BamH I also shown. **(c)** Gel of purified WASp fragments prior to ligation into EF-Bos backbone. **(d)** Check restrictions of clones selected post ligation. Correct insertions marked with a tick. As Xcm I site is within the EVH1 domain, the correctly inserted dEVH1 construct is only cut by Bgl II. **(e)** Restriction digests of selected clones following ligation of EGFP-WASp insert into the SIN-LNT lentivector backbone. The second EcoR I panel shows the cathode end of the same gel at higher exposure, demonstrating the 0.3 kb fragment generated by EcoR I digestion of point mutations. The dVCA construct is only linearised by EcoR I because the second site is found within the V domain. Some incomplete restriction is seen with Nhe I. All constructs show are correctly inserted.

formed from harvested cells at 48 hours (see chapter 2.4.1 and 2.5.1).

Figures 3.10a and b show examples of western blots of such transfected lysate, immunoblotted with anti-WASp or anti-GST antibodies. Firstly, these figures demonstrate that the molecular cloning of each of these constructs has resulted in expression of protein of the anticipated molecular weight, which is recognised by WASp specific antibody. Secondly, they demonstrate that the level of WASp expression for each mutant construct is approximately equal. Thirdly, they suggest the presence of WASp degradation products or alternatively spliced protein products within the transfected cell lysate, and that the pattern of these products is specific to individual mutant constructs. Specifically, several constructs showed a WASp protein 3-5 kDa smaller than full length WASp. The expression of the dPolyP construct results in the presence of several smaller proteins detected by anti-WASp antibody, some at equivalent levels of expression as the full length dPolyP construct.

Expression of EGFP-WASp from the C1 plasmid was tested in a similar manner with similar results (data not shown). EGFP-WASp expression from lentivector was assessed following generation of lentivirus and subsequent viral transduction of U937 cells. Results from such experiments are discussed in chapter 8.

3.3.2 Generation of WASp coated Sepharose beads

GST-WASp protein was purified from transfected Cos 7 cell lysate by generating GST-WASp coated Sepharose beads as described in chapter 2.8.1. Figure 3.10c shows transfected Cos 7 cell lysate before and after incubation with Sepharose beads. The continued detection of GST-WASp in lysate after Sepharose bead incubation suggests that within this purification process the Sepharose beads are saturated with GST-WASp. From this it can be assumed that the concentration of GST-WASp on the surface of Sepharose beads will be approximately the same between constructs, which is important for the standardisation of experiments using these beads.

Figures 3.10d and e show electrophoresis gels of equal volumes of purified sepharose beads for each WASp constructs. Figure 3.10d shows these beads immunoblotted with anti-GST, anti-actin and anti-ARPC2, and demonstrates that each set of beads is coated with a GST-WASp construct of an appropriate size. Although degradation products (or alternatively spliced protein) are detectible for some constructs, the full length protein is by far the predominant species for each construct. The lower two panels in figure 3.10d demonstrate that no or negligible actin or Arp2/3 is bound to the beads of any construct.

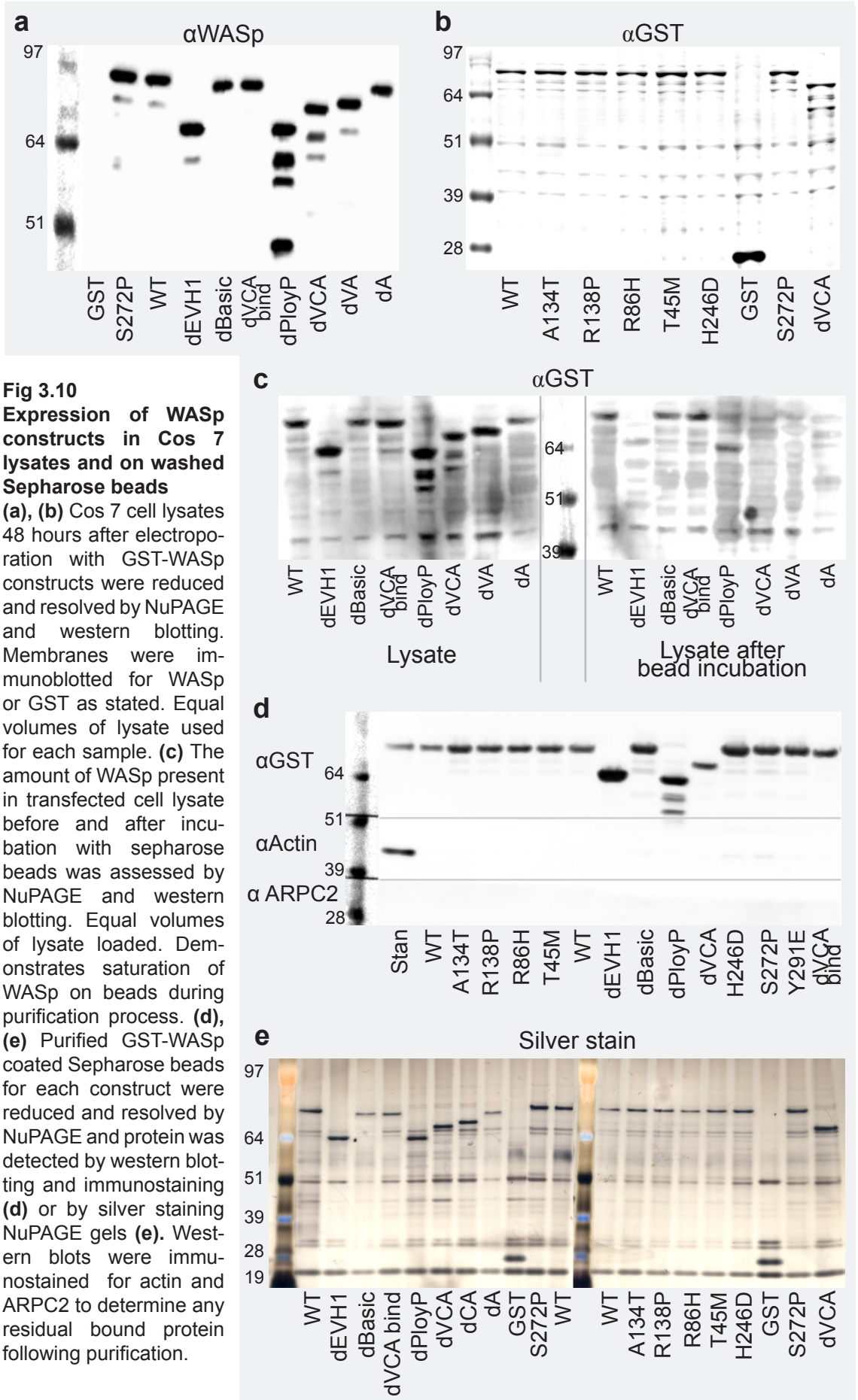

Fig 3.10
Expression of WASp constructs in Cos 7 lysates and on washed Sepharose beads
(a), (b) Cos 7 cell lysates 48 hours after electroporation with GST-WASp constructs were reduced and resolved by NuPAGE and western blotting. Membranes were immunoblotted for WASp or GST as stated. Equal volumes of lysate used for each sample. **(c)** The amount of WASp present in transfected cell lysate before and after incubation with sepharose beads was assessed by NuPAGE and western blotting. Equal volumes of lysate loaded. Demonstrates saturation of WASp on beads during purification process. **(d), (e)** Purified GST-WASp coated Sepharose beads for each construct were reduced and resolved by NuPAGE and protein was detected by western blotting and immunostaining **(d)** or by silver staining NuPAGE gels **(e).** Western blots were immunostained for actin and ARPC2 to determine any residual bound protein following purification.

Figure 3.10e shows a silver stain of the separated Sepharose bead bound proteins. The GST-WASp band is seen as the most prominent band on the gel, running at between 65 and 85 kDa according to the construct. Other significant bands are seen at 51, 20 and a double band at 30 kDa, for most constructs. These bands are also seen in the GST only lanes, suggesting these are either Sepharose associated proteins or non-specific binding protein. These bands are highly unlikely to account for any differences in the biological activity of the WASp coated beads between constructs.

3.3.3 Purification of GST-WASp

To standardise the amount of GST-WASp used between individual actin polymerisation assays, a quantification standard was required. This was run in a separate lane on the gel electrophoresis and western blot, adjacent to the experimental lanes in each assay. To generate this standard WT GST-WASp was generated from transfected Cos 7 cells as described in chapter 2.8.1.

The individual purification steps of this process are demonstrated by anti-WASp western blot and by silver stained gels in figure 3.11. From this it can be seen that the final product contains a single discrete band (85 kDa) on anti-WASp immunoblotting, making it suitable as a quantification standard. On the silver stained gel the same Sepharose associated proteins at 20, 30 and 50 kDa can be detected. Figure A.2 (in the appendix) shows gels used to quantify the purified GST-WASp standard.

3.4 Expression and detection of WIP constructs

The three WIP containing vectors used in this project were gifts from Narayanaswamy Ramesh (Harvard Medical School) (see table 2.1). WIP, and WIP with the WASp binding domain deleted (WdW) were cloned into EGFP tagged and HIS tagged mammalian expression vectors. Additionally WIP alone was tagged with both HIS and the zz domain of protein A in a mammalian expression vector (pOS135).

The expression of each of these constructs was tested prior to use in experimental assays, as shown in figure 3.12a. Immunoblotting with the anti-WIP antibody revealed that deletion of the WASp binding domain also eliminated the anti-WIP antibody binding site. Use of an anti-EGFP antibody clearly labelled the full length and truncated WIP constructs, but was associated with a number of non-specific bands (figure 3.12a right hand panel). The use of this antibody had been previously optimised in EGFP-WASP transfected U937 lines (data not shown). Immunoblotting with the laboratory standard anti-HIS antibody resulted in poor

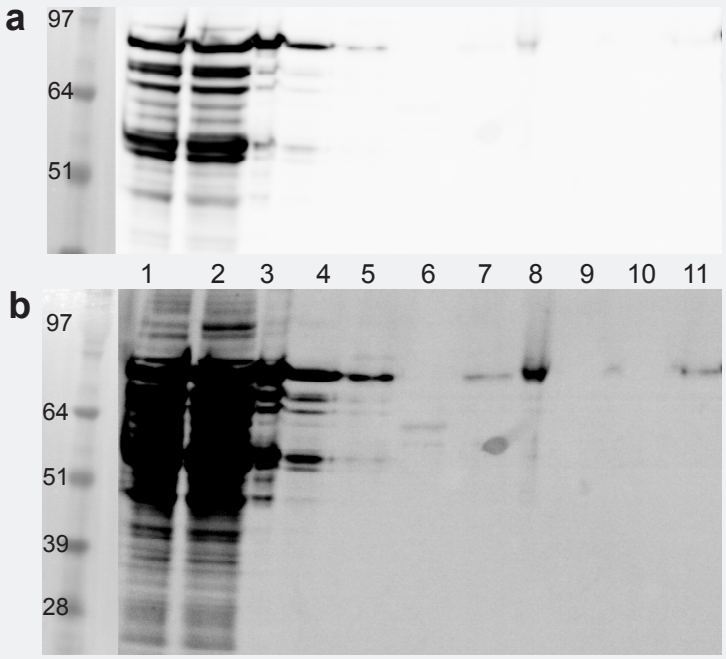

α WASp blot

Key for (a) and (b)

1 Lysate
2 Lysate post incubation
3 GST-WASp beads
4 Elutant 1
5 Elutant 2
6 Elutant 3
7 Elutant 4
8 Beads post elution
9 Elutants post dialysis
10 Spin through from column concentrator
11 Concentrated product

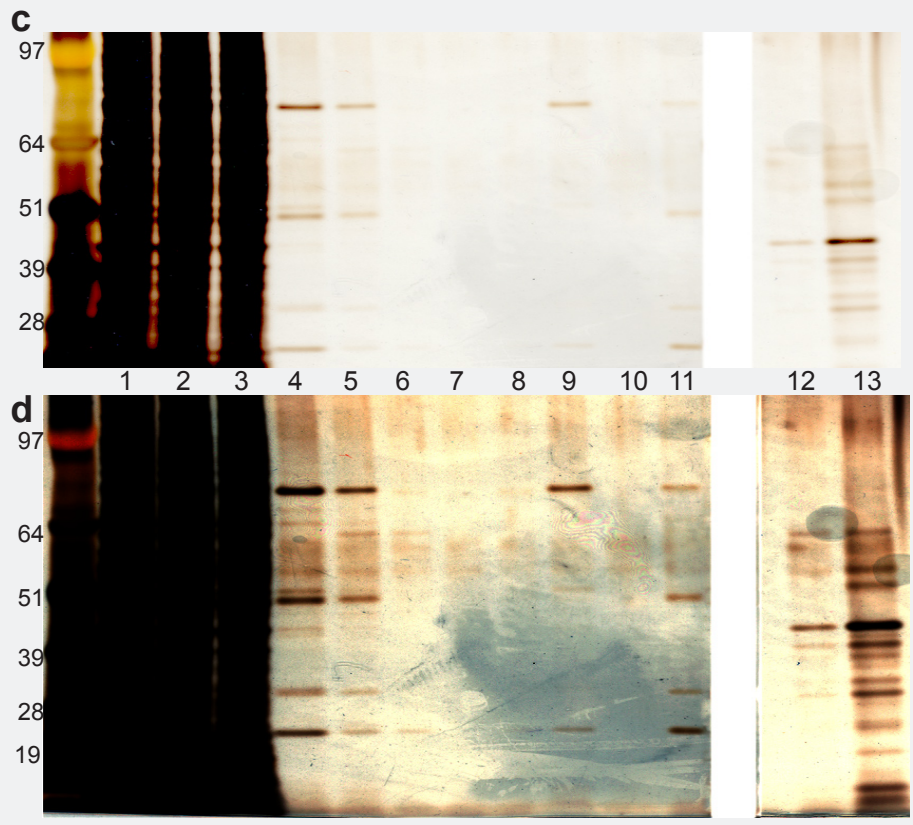

Silver stain

Key for (c) and (d)

1.	Lysate	10mcl/3ml
2.	Lysate post dialysis	10mcl/3ml
3.	Lysate post bead incubation	10mcl/3ml
4.	Beads post bead incubation	5mcl/1ml
5.	Elution 1	3.3mcl/1ml
6.	Elution 2	3.3mcl/1ml
7.	Elution 3	3.3mcl/1ml
8.	Elution 4	3.3mcl/1ml
9.	Beads post elutions	5mcl/1ml
10.	Spin through following spin purification	13mcl/4ml
11.	Concentrated product	1mcl/60mcl
12.	Actin 20ng	
13.	Actin 100ng	

Fig 3.11 Sequential purification of GST-WT WASp from transfected Cos7 lysate

See Chapter 2.8.1 for details of methodolgy. **(a) and (b)** show anti-WASp immunoblots (same blot at different exposures) and **(c) and (d)** show a silver stained gel following reduction and resolution by NuPAGE of samples from the purification intermediate steps (different exposures). *mcl - microlitre*

and variable detection of the HIS tagged WIP construct, with many additional non-specific bands (an example of this is shown in figure 3.12a middle panel). As a result a panel of anti-HIS antibodies were tested and optimised against HIS-WIP transfected cell lines. The result of this experiment is shown in figure 3.12b and as a result of this the anti-Penta HIS antibody at a dilution of 1:1000 was selected for use in further experiments. Details of all antibodies used in this project are shown in table 2.5.

3.5 WASP and WIP expression in cell lines

The WASp and WIP expression of cell lines used in experiments throughout this project was assessed. Figure 3.12c demonstrates that U937 cell and THP1 cells both express significant levels of WASp and WIP. Cos 7 cells by contrast express significantly less WASp and very little WIP, and neither protein was detectible in RAW cells. By contrast ARPC2 and Cdc42 levels are equivalent in all four cells lines. These results are of importance in the interpretation of several experiments throughout this project, and are discussed more extensively in later chapters.

3.6 Purification of Cdc42

3.6.1 Generation in E.coli

Recombinant Cdc42 has been used in several experiments in this project. As this protein is not commercially available and is unstable in storage, it was synthesised and purified as part of the project. The methodology of this process is described in chapter 2.8.2. Briefly, E.coli stably transfected with GST-Cdc42 under the control of the lac operon were induced to produce protein by IPTG. The bacteria were then lysed, and GST-Cdc42 was affinity purified using glutathione sepharose resin. The GST tag was then cleaved using thrombin, and the reaction purified.

Figure 3.13 shows anti-Cdc42 and silver stained gels for each intermediate step of the purification process. In this purification, a glutathione Sepharose column was used for affinity purification and thrombin cleavage was performed “on the column”. GST-Cdc42 is seen running at approximately 48 kDa, and Cdc42 is seen at 26 kDa. These blots demonstrate that the vast majority of Cdc42 was eluted from the column in the first wash following thrombin cleavage. They also demonstrate that approximately 50% of the purified Cdc42 was lost during the removal of thrombin using aminobenzamidine resin, and that the remaining Cdc42 was eluted from a desalting column in a single discrete elution. The yield of Cdc42 from “on column cleavage” was found to be very low, therefore an separate optimisation of the GST- tag cleavage was performed.

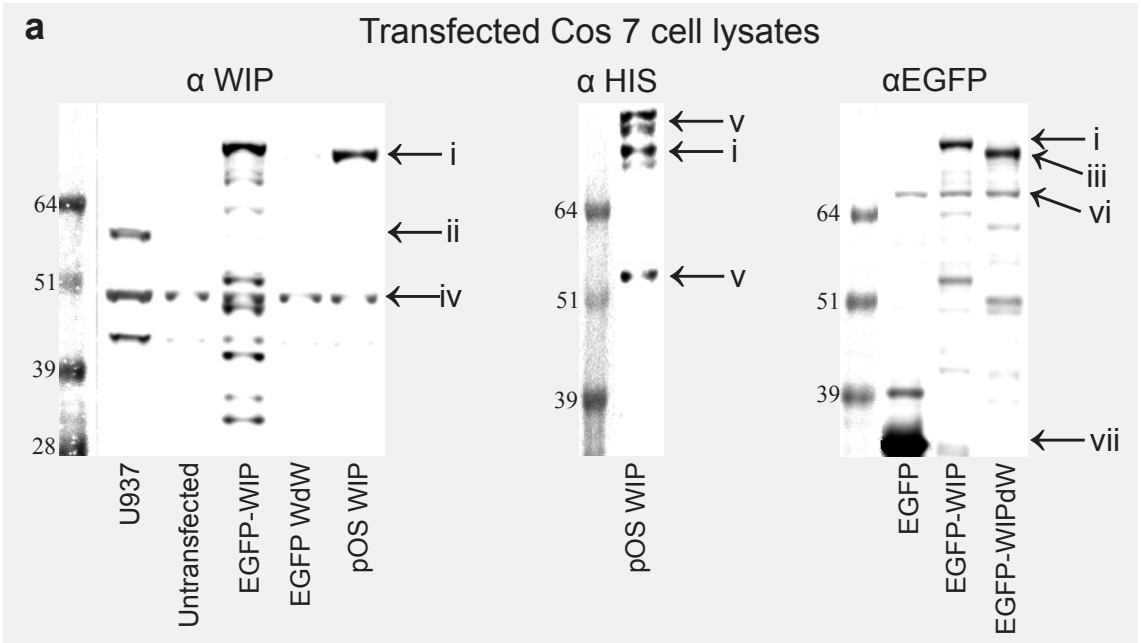

Bands
(i) EGFP-WIP or zzHIS-WIP
(ii) Endogenous WIP
(iii) EGFP-WIPdWASp binding site
(iv) Non-specific band with αWIP antibody
(v) Non-specific band with αHis antibody
(vi) Non-speicific band with αEGFP antibody
(vii) EGFP

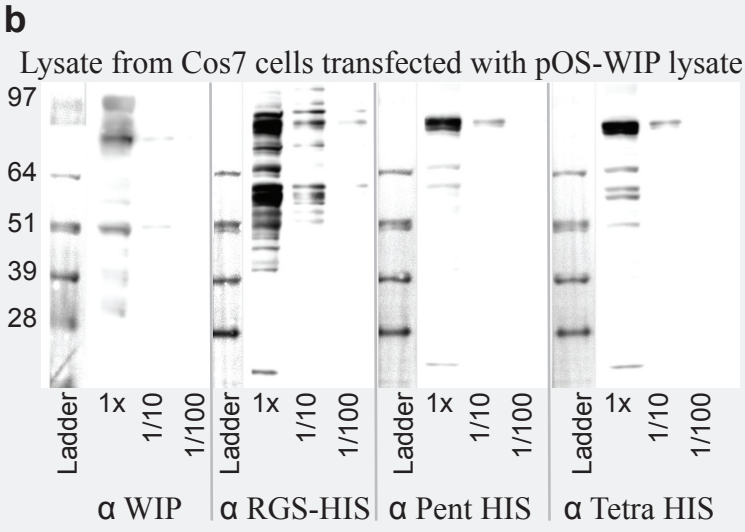

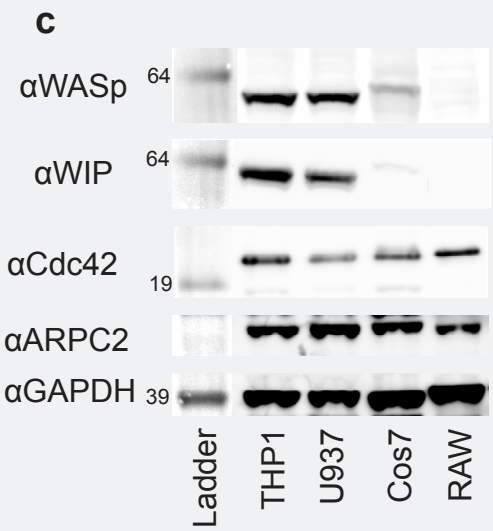

Fig 3.12 Expression of WIP constructs in Cos 7 lysates and WIP, WASp, Cdc42 and ARPC2 expression in untransfected cell line lysates
(a) Cos7 cells were transfected with the pOS-WIP (His tagged WIP bound to a protein A zz domain) EGFP-WIP and EGFP-WIPdW (WIP with the WASp binding domain deleted). Lysates from these cells were standardised by concentration, were reduced and resolved by NuPAGE and western blotting. The immunostaining of these lysates using an anti-WIP, anti-HIS and anti-EGFP antibodies is shown. **(b)** Optimisation of anti-HIS antibodies using pOS-WIP transfected Cos7 cell lysate. **(c)** Untransfected U937, THP1, RAW and Cos7 cell lysates were standardised by concentration and then reduced, resolved and immunoblotted for WASp, WIP, Cdc42 and ARPC2. GAPDH was used as a loading control.

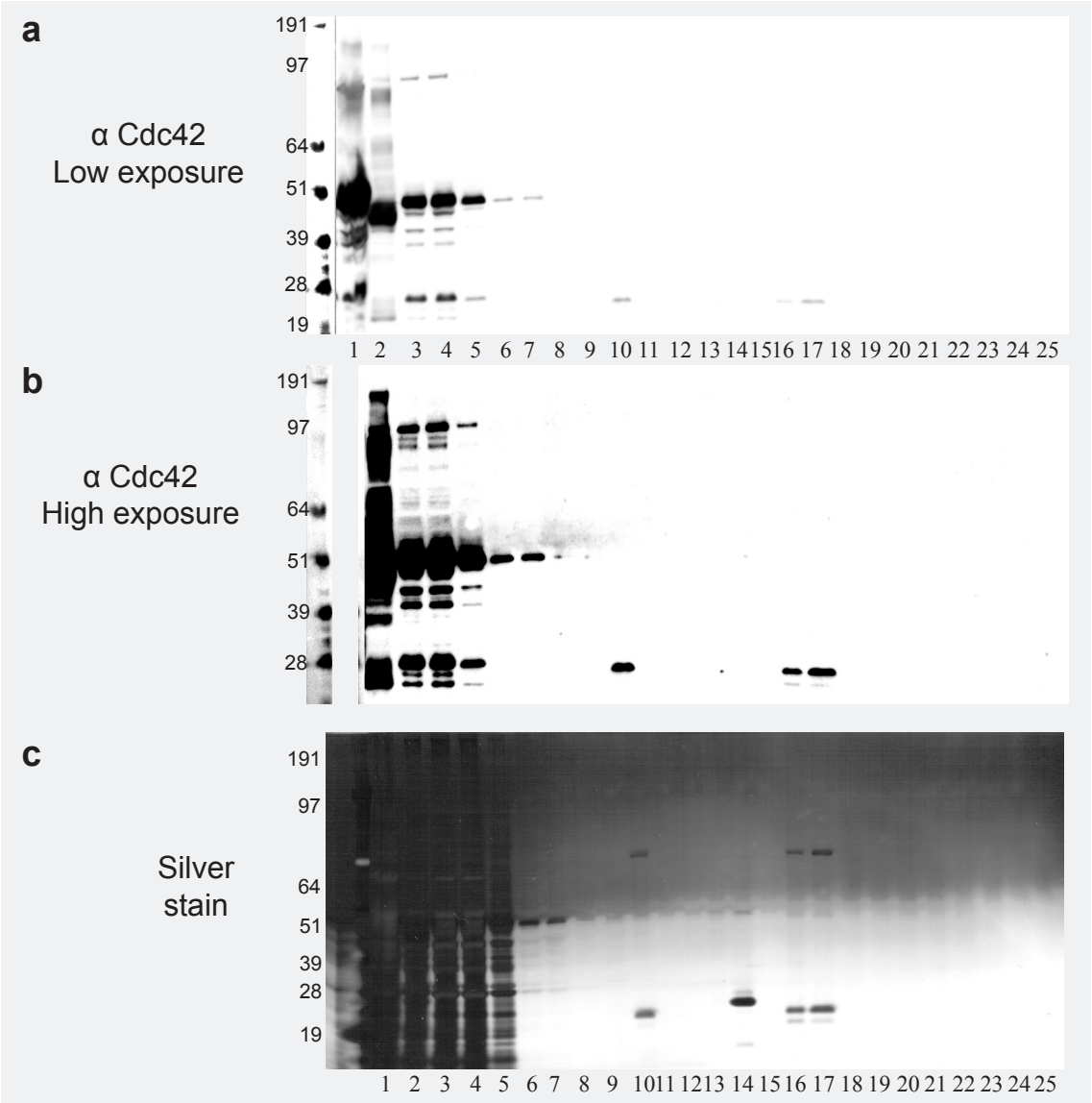

1 Bacteria post sonication
2 Lysate post sonication and filtration
3 Flow through following first column load
4 Flow through following second column load
5-9 4 serial washes of column
10-12 3 serial elutions of column following thrombin cleavage
13 High salt wash
14 Low glutathione wash
15 High glutathione wash
16 Aminobenzamidine agarose post incubation
17-19 First desalting fraction from elutions 1,2 and 3
20-22 Second desalting fraction from elutions 1,2 and 3
23-25 Third desalting fraction from elutions 1,2 and 3

Fig 3.13 Sequential purification of Cdc42
2L of broth containing exponentially growing E.coli, expressing Cdc42 WT, 12V and 17N mutants were harvested. The bacteria were lysed in PBS, 5mM PMSF, 15mM DTT and 1μM GDP, with sonification. Lysates were filtered and then loaded on 1ml glutathione Sepharose columns. The flow through was then reloaded onto the column. Columns were washed 4 x with PBS and then incubated with thrombin overnight. The columns were then eluted 3x with 1ml of PBS (each elution was processed separately), and the column was then washed with a high salt wash, a Low and high glutathione wash. Eluted samples were incubated with aminobenzamidine agarose to remove thrombin. 1/5000 of samples are loaded. Immunoblots **(a)** and **(b),** and silver stained gels **(c)** are shown from the reduced and resolved samples from intermediate stages of this purification.

3.6.2 Optimisation of GST tag cleavage

Two protocols for cleaving GST tags from recombinant protein were compared. The first (AR) used a low concentration of thrombin over a prolonged incubation period (22 hours), whereas the other (GE) used a high concentration of thrombin over a much shorter period (2-4 hours). The results of a time course optimisation for these two protocols are shown in figure 3.14. This demonstrates that protocol GE with a short incubation period (2 hours), resulted in efficient GST cleavage without extensive degradation. Longer incubation periods resulted greater non-specific degradation and reduced Cdc42 yields. This protocol was adopted for further generation of Cdc42.

Silver stained gels demonstrating the purity and quantification of Cdc42 are shown in the appendix (figure A.2).

3.7 Conclusions

The results presented in this chapter demonstrate the successful expression and purification of all the mutant WASp constructs under investigation.

Cos7 cells transfected with WASp constructs showed similar levels of expression between WT WASp and all other constructs. Specifically, the missense mutations which give rise to XLT and WT WASp have equivalent levels of expression. These results contrast with the findings in human lymphocytes from patients with XLT / WAS, and from the results seen in U937 cells (see chapter 8), where WASp containing EVH1 missense mutations has lower cellular concentrations than WT (Lutskiy et al., 2005; Jin et al., 2004; Imai et al., 2004; Zhu et al., 1997). The accepted model for this instability in patient's lymphocytes is the impaired ability of mutant WASp to bind WIP (de la Fuente et al., 2007; Konno et al., 2007; Chou et al., 2006). As demonstrated in figure 3.12c, Cos7 cells express very low levels of WIP and therefore this mechanism of WASp protection may not be important in Cos7 cells. Taken together, these results suggest that the control mechanisms of WASp degradation are cell type specific.

Another observation from these experiments is that individual WASp constructs have different patterns of degradation products. Although the clinical missense mutations and WT WASp have similar patterns, the dPolyP construct has a markedly different pattern. Experiments presented in chapters 5, 6 and 7 all demonstrate that the dPolyP construct is able to bind WASp regulatory proteins, suggesting this construct forms a correctly folded protein, and that the degradation products seen are not a consequence of the instability of abnormally folded protein.

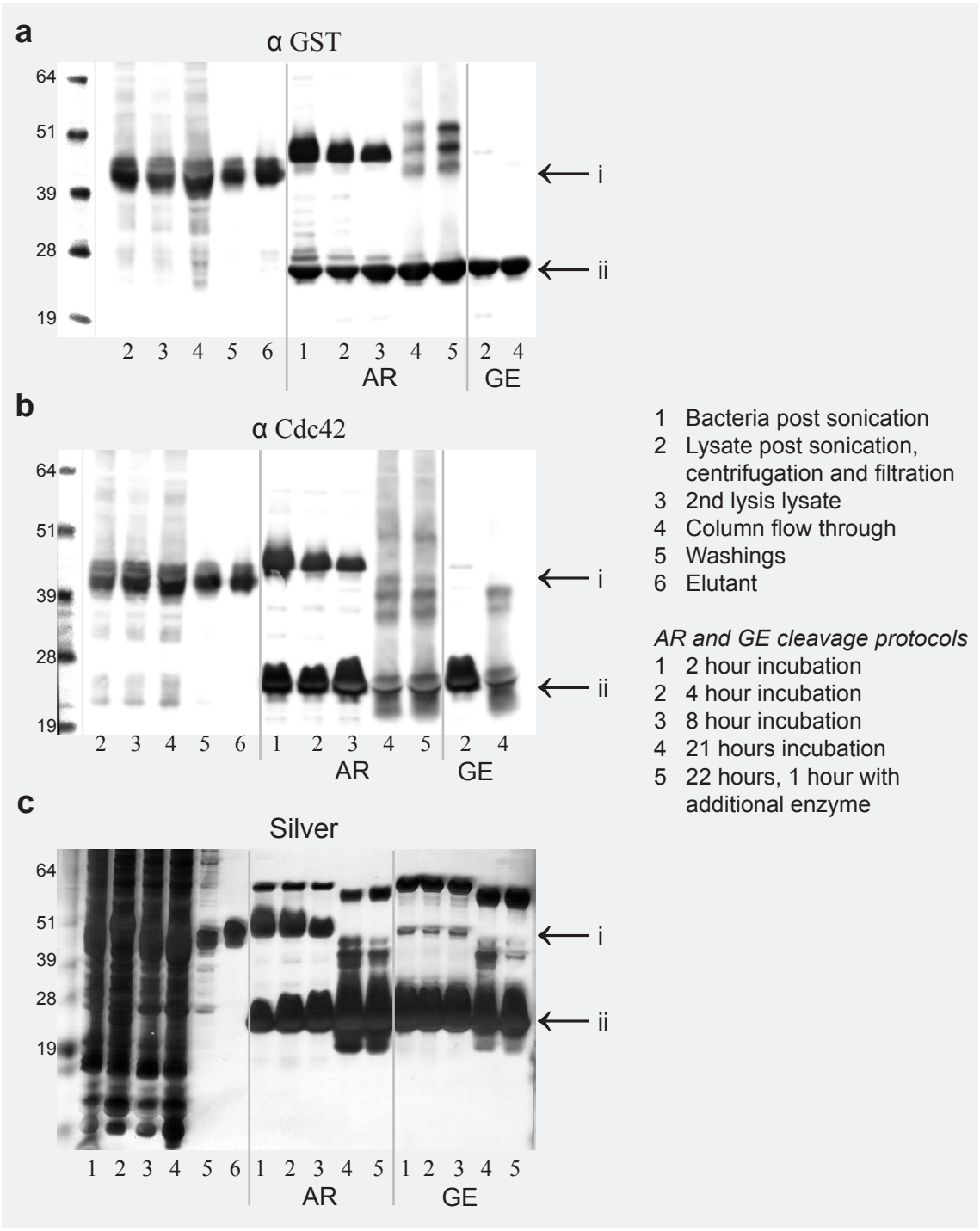

Fig 3.14 Optimisation of the cleavage of the GST tag from Cdc42
3L of E.coli broth expressing WT Cdc42 or 12V Cdc42 were used. Lysates were prepared as for figure 3.13 and two 1ml glutathione Sepharose columns were used (end on end) for affinity purification. GST-Cdc42 samples were then eluted from the columns using 3ml of GST EB buffer. Eluted samples were subjected to thrombin cleavage acocording to the following conditions; *AR cleavage:* 200µl of elutant was incubated with 0.66U of bovine thrombin and 0.16U of Human thrombin for 22 hours then a further 0.33U of bovine thrombin and 0.08U of Human thrombin for a further 1 hour. *GE cleavage* : 200µl of elutant was incubated with 5.3U of bovine thrombin alone. Samples were analysed at the time points stated, by NuPAGE and western blotting. *(i) GST-Cdc42 band (ii) Cdc42 and / or GST band.*

Alternatively, these results suggest that the Polyproline domain itself, or proteins which bind to it, have an important role in the regulation of WASp degradation. This is more fully discussed in chapter 8.

4 Optimisation of Actin Polymerisation Assay

4.1 Introduction

4.1.1 Assays of actin polymerisation

Several techniques have been described to investigate regulation of the initiation of actin polymerisation. Functional assays measuring the propulsion of plastic beads (Suetsugu et al., 2001b) (Yarar et al., 2002), visualising the formation of "actin comets" (Higgs and Pollard, 2000) or the recruitment of *Vaccinia* or S*higella* to actin tails (Moreau et al., 2000), all have the advantage of using cellular actin functions as an output. These experimental systems however are less suited to dissecting out the molecular interactions and signalling which lead to the initiation of these outcomes.

Pyrene based actin polymerisations assays (Ho et al., 2004; Yarar et al., 2002; Martinez-Quiles et al., 2001; Higgs and Pollard, 2000; Prehoda et al., 2000; Rohatgi et al., 1999; Ma et al., 1998a; Zigmond et al., 1997) measure the maximal rate of *de novo* actin filament formation by determining the fluorescence emitted by prenylated actin upon polymerisation. In *purified component* systems, recombinant proteins are mixed with prenylated actin and actin polymerisation is initiated with the addition of Cdc42, PIP_2 or equivalent (Yarar et al., 2002; Rohatgi et al., 2000; Higgs et al., 1999). In *High Speed Supernatant* systems, cell lysates (traditionally *xenopus egg extract* or bovine brain extract) (Suetsugu et al., 2001a; Ma et al., 1998a) have filamentous actin removed by centrifugation and then new actin filament formation is assessed following addition of Cdc42 or $PIP_{2.}$ The effects of selective deletion of lysate components or addition of excess recombinant components can then be assessed.

For this project I decided to use a bead based pulldown assay of actin polymerisation (Cory et al., 2002; Fradelizi et al., 2001). Recombinant protein is coated on sepharose beads which are then incubated in lysate from a myeloid cell line. The amount of filamentous actin produced is then quantified by SDS-PAGE and western blotting of washed beads and by immunofluorescence of phalloidin stained beads. There are several advantages of this assay. Firstly it allows assessment of actin polymerisation within a myeloid cell lysate, which is a more relevant substrate for the investigation of dendritic cell cell biology. Unlike the High Speed Supernatant pyrene assay, the bead based assay only measures filamentous actin induced directly by the bead bound protein of interest. Unlike

the purified components system, it uses cell lysate as a substrate which is more physiological, and does not rely on the artificial initiation of polymerisation by addition of an excess of Cdc42. An additional advantage of the bead based assay is that it facilitates the detection and quantification of other bound components involved in the initiation of actin polymerisation.

The bead based assay does not, however, have the same temporal sensitivity as pyrene based assays and is more dependent on measuring the amount of filamentous actin associated with the beads at the equilibrium point between polymerisation and depolymerisation. As a result the outputs of these two assays are measuring subtly different activities.

In this chapter I present results demonstrating optimisation and characterisation of the bead based actin polymerisation assay. This background information allows for a more insightful interpretation of the subsequent results of the panel of WASp constructs used in this project.

4.1.2 Detection of constitutively active but not wild type activity

Initially the bead based actin polymerisation assay was performed as most recently published (Cory et al., 2002) using U937 cell lysate generated with 10^7 cell per ml of lysis buffer. Following centrifugation at 20,000g for 10 minutes, the lysate was supplemented with 5mM $MgCl_2$ before incubation with GST-WASp coated sepharose beads for 1 hour. As WT WASp exists in an autoinhibited conformation at rest (Kim et al., 2000; Rohatgi et al., 1999; Miki et al., 1998b), WT protein was compared to the constitutively active WASp mutant I294T (Ancliff et al., 2006). As predicted the I294T mutant shows strongly active actin polymerisation. There is a dose response between the WASp input (concentration of WASp on a fixed volume of beads) and actin pulled down, demonstrating a sustained excess of actin in the lysate, and no saturation of activity (figure 4.1a and b). By contrast the WT WASp shows low levels of activity and a weak relationship between actin pulled down and WASP input. This suggests the filamentous actin bound to WT WASp is due to low grade non-specific polymerisation and little is caused by the activation of the WT WASp.

Two controls are shown with this experiment. Three concentrations of beads coated with GST alone show very low levels of actin pulldown and no correlation between dose and response. This demonstrates that the GST tag does not initiate actin polymerisation. The second control shows the I294T construct tested in the presence of cytochalasin D, a fungal toxin which binds to the barbed end of actin filaments, inhibiting elongation of the filament and encouraging depolymerisation

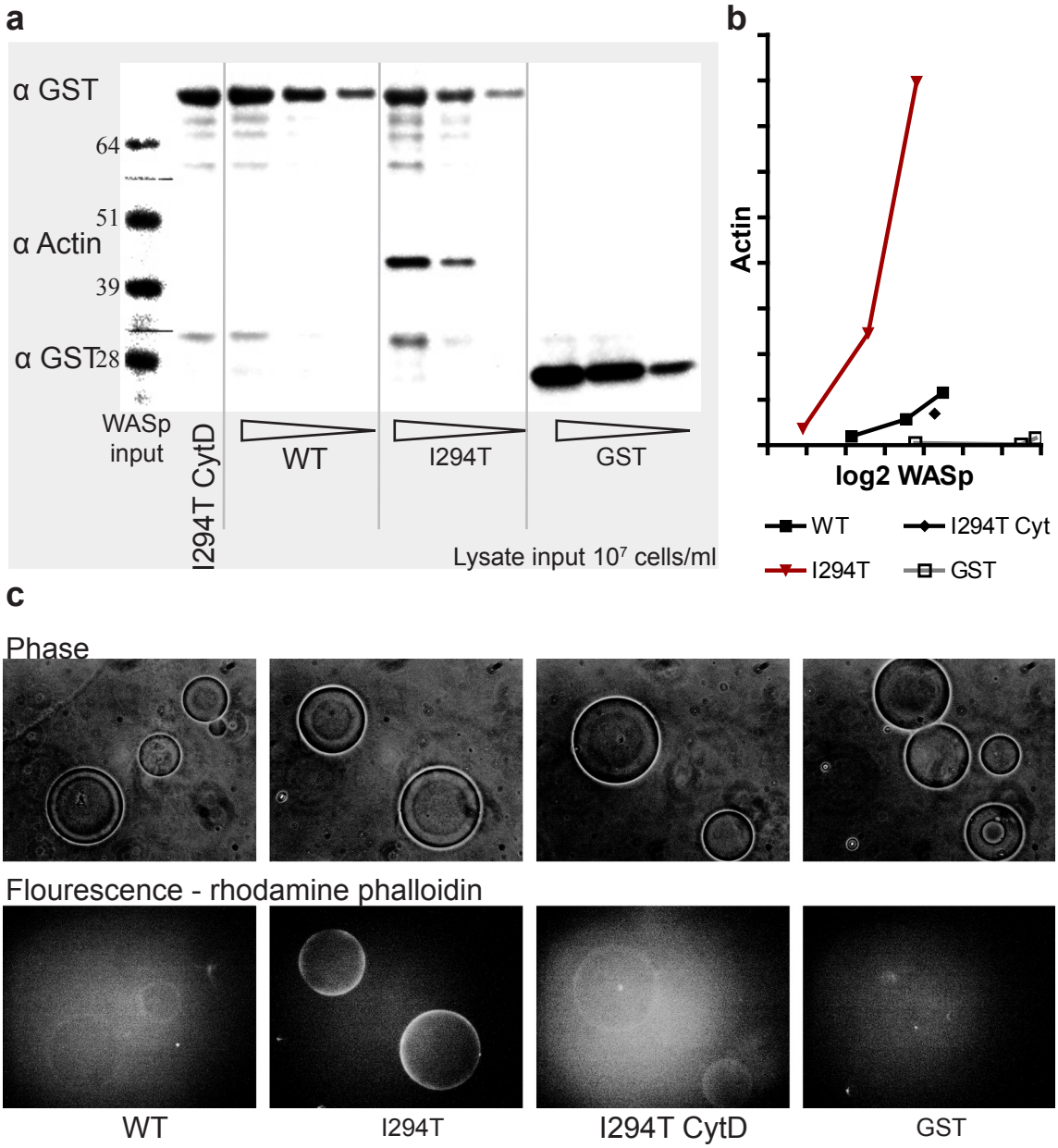

Fig 4.1 Unsupplemented actin polymerisation assay with wild type and I294T mutant U937 cell lysate was generated at 10^7 cells/ml. After centrifugation the lysate was supplemented with 5mM MgCl and then incubated with 50µl of GST-WASp coated Sepharose beads (3 WASp concentrations for each construct). One I294T sample was incubated with lysate containing 5µM cytochalasin D. After 1 hour of rotation, the beads were washed and a 1/10 of each sample was stained with rhodamine phalloidin and mounted for flourescent microscopy. The remaining sample was reduced in sample buffer and resolved by SDS-PAGE and western blotting. **(a)** Western blot of resolved beads. Top and bottom thirds of membrane immunoblotted simultaneously with anti GST antibody, middle thirds blotted with anti actin antibody. **(b)** Densitometry of bands from blot in (a). Units are arbitary densitometry units. **(c)** Phase and flourescent microscopy of rhodamine phalloidin labelled beads.

(Krucker et al., 2000; Dubinsky et al., 1999; Cooper, 1987). The fact that the activity of the I294T mutant is inhibited by cytochalasin D suggests that the actin detected by western blot in the assay is polymerised f-actin rather than sequested g-actin. The complete abolition of actin polymerisation with cytochalasin D with the WASp I294T mutant, suggests that the inhibitor may act by competitively inhibiting the binding of g-actin to WASp, in addition to inhibiting polymerisation downstream.

Although a WASp construct with the functional VCA domain deleted was not used as a negative control in these optimisation experiments, it was used as part of the panel of constructs which was fully tested (see chapter 5).

4.1.3 Detection of beads associated actin by immunoflourescence

Beads from the above experiment were stained with rhodamine phalloidin (a red fluorescent dye which binds to filamentous actin) and were imaged by fluorescence microscopy (see chapter 2.9.2). The images were optimised using Photoshop@ with identical processing used for each image. Figure 4.1 demonstrates strong fluorescence associated with the I294T beads, much weaker fluorescence associated with the WT and cytochalasin inhibited beads and no fluorescence above background on the GST beads. This confirms the findings on SDS-PAGE and western blotting and further demonstrates that the actin associated with the beads is f-actin.

This protocol appears robust in detecting constitutively active WASp constructs. However, because of the low level of WT activity, it is of limited use in assessing constructs whose activity is reduced compared to WT. The remainder of this chapter describes the optimisation of this assay, resulting in increased sensitivity of the assay and a shift in its dynamic range to span the activities of GST alone to activities just greater than WT WASp.

4.2 Optimising WT activity

4.2.1 WASp concentration on beads and bead volume

One possible explanation for the relative insensitivity of the assay to WT WASp was insufficient recombinant WASp in each experiment. To investigate this, the concentration of WASp bound to each sepharose bead and the total number of beads used in each individual assay was varied.

I have previously demonstrated that WASp coated beads made under standard procedures are saturated with recombinant protein, as GST-WASp transfected

lysate after incubation with sepharose beads still contains significant amounts of GST-WASp (see 3.2.3 and figure 3.10c). To try to generate beads with a higher concentration of WASp 15cm plates of transfected Cos7 cells were lysed in smaller volumes of lysis buffer (500µl compared to the standard 800µl) and incubated with smaller volumes of sepharose beads (50µl and 75µl compared to 100µl). Figure 4.2a shows that beads generated in this manner had similar concentrations of WASp on their surface and actin polymerisation assays gave very similar results.

Increasing the volume of beads used did increase the actin signal, and in several experiments a larger volume of beads with a lower WASp protein concentration produced greater activity per unit WASp than a smaller volume of more concentrated beads (figure 4.2b and data not shown). These findings suggest that as the proportion of final reaction volume made up by sepharose beads increases, the rate of new actin filament formation increases. A hypothetical explanation for this phenomenon is that increased breakage of elongating actin filament as a result of greater numbers of bead collisions, resulting in larger numbers of barbed ends being available for actin polymerisation. This increased WT WASp actin signal was still not as large as that seen with the constitutively active mutant S272P, which remained highly active even at low concentration. This strategy for sensitising the assay was abandoned for three reasons. Firstly this concentration affect appeared to be inconsistent between mutant constructs (figure 4.2 S272P columns and data not shown) and therefore may have given rise to misleading results. Secondly in some optimisation experiments large bead volumes gave rise to unacceptably high levels of background activity (GST samples in figure 4.4e).

Thirdly the volume of beads and transfected lysate required to make enough beads of sufficient sensitivity, made this strategy impractical. Nonetheless these experiments emphasised the importance of using equal WASp concentrations and equal numbers of beads between constructs in experiments when comparing WASp activities.

4.2.2 Magnesium concentration

Magnesium ions are required for the hydrolysis of ATP bound to monomeric actin to ADP, providing the energy required for the monomeric actin to bind to the barbed end of an actin filament. Magnesium chloride is added to U937 lysate in the actin polymerisation assay to overcome the chelating effect of EDTA in the lysis buffer. To asses whether the assay could be sensitised by adding additional magnesium

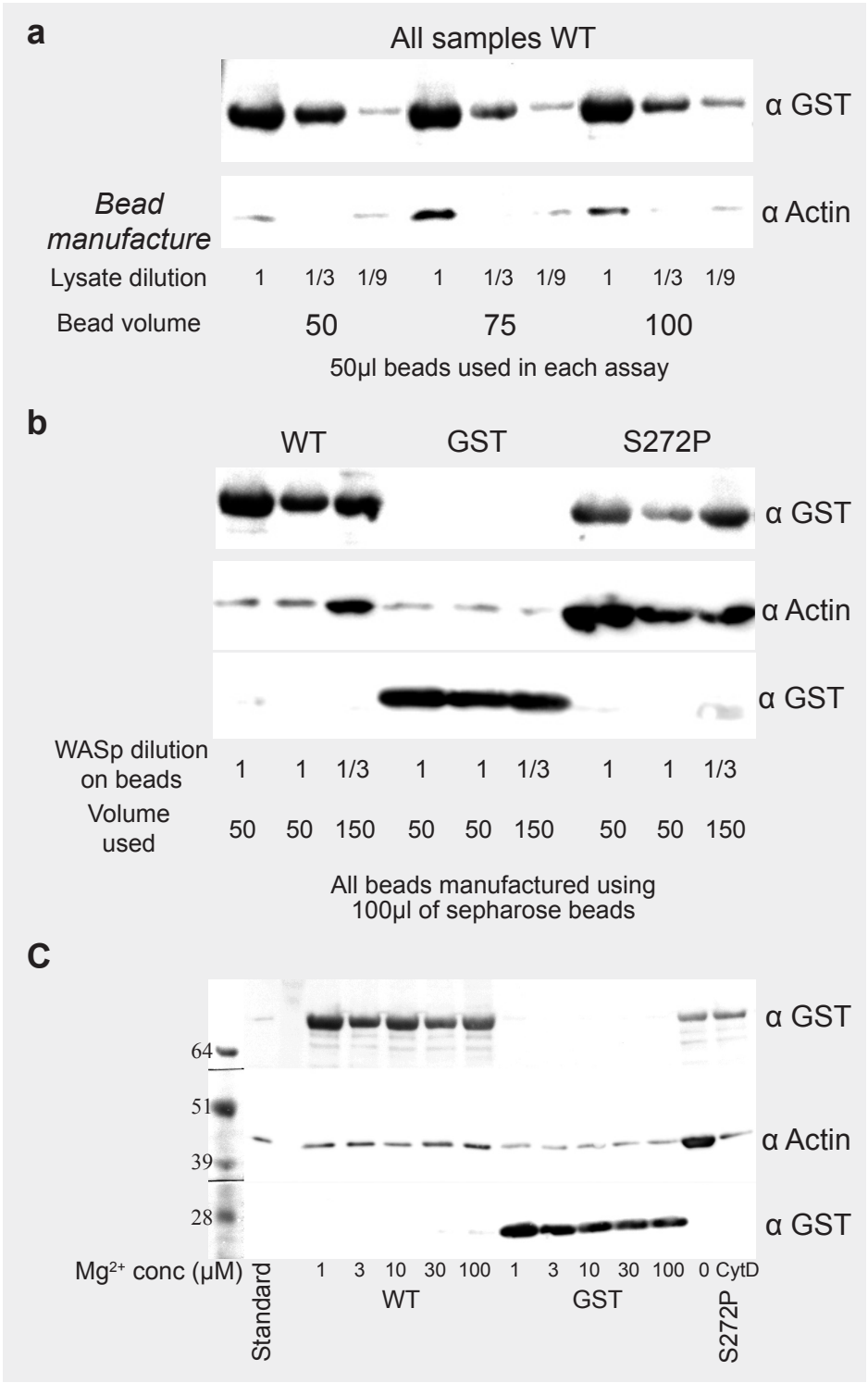

Fig 4.2 Effect of bead volume, beads WASp concentration and magnesium on actin polymerisation assay

(a) Actin polymerisation assay performed on WT GST-WASp coated beads generated by incubating transfected Cos7 lysate of 3 dilutions (lysate dilution) with 3 different volumes of beads (bead volume). **(b)** Actin polymerisation on WT, GST and S272P WASp beads comparing beads generated with full strength transfected lysate to 3 times the volume of beads generated with 1/3 strength lysate. Blots (a) and (b) were blotted simultaneously and therefore band intensities are comparable between both blots. U937 lysate concentration for both experiments was 2.4 mg/ml. **(c)** Actin polymerisation assay on WT, GST and S272P constructs with varying Mg^{2+} concentrations. Lysate concentration 1.7 mg/ml.

chloride, the assay was performed over a range of magnesium concentrations. Figure 4.2c demonstrates magnesium ion concentration had no effect on either WT activity within the assay or on background actin polymerisation.

4.2.3 ATP supplementation

As ATP is required for binding of monomeric actin to filamentous actin and for optimal Arp2/3 activity, I hypothesised that ATP may increase the amplitude of the actin signal in the assay, by acting down stream of WASp activation. Theoretically, ATP could amplify the signal from low levels of WASp mediated actin filament nucleation and therefore facilitate the differentiation of more subtle differences in WASp activity.

Figure 4.3a and b show the effect of increasing ATP supplementation of U937 lysate for WT and S272P constructs and for WT with cytochalasin D. Addition of 1mM ATP to the reaction brings the actin signal of the WT WASp to a similar level of the S272P mutant with no ATP supplementation. By contrast the S272P mutant even with no ATP is approaching saturation activity and therefore addition of ATP to the assay results in only minimal increase in actin pulldown. By contrast, increasing ATP has no effect on the activity of the WT construct in the presence of cytochalasin D. This strongly suggests the ATP is acting at the actin filament elongation stage of the reaction. ATP concentrations higher than 1mM were also tried, but they resulted in protein precipitation during the reaction making SDS-PAGE impossible (data not shown).

1mM ATP supplemented U937 lysate was then used to assess the WASp activity over a titration of WASP bead concentrations. Figure 4.3d demonstrates that addition of 1mM ATP to the assay gives WT WASp a dynamic dose – response relationship, allowing for more sensitive assessment of activity over a range of WASp concentrations. This experiment also demonstrates the lack of such a response for GST alone, and a widening in the activity gap between GST and WT with the addition of ATP. Other experiments have demonstrated no increase in actin polymerisation with increasing ATP supplementation for GST coated beads (data not shown).

4.2.4 Lysate concentration

Within cells, the equilibrium between polymerisation and depolymerisation is largely controlled by the relative concentrations of monomeric actin and filamentous barbed ends. A simple way of increasing the concentration of monomeric actin in an *in vitro* polymerisation assay is to increase the concentration of cell lysate

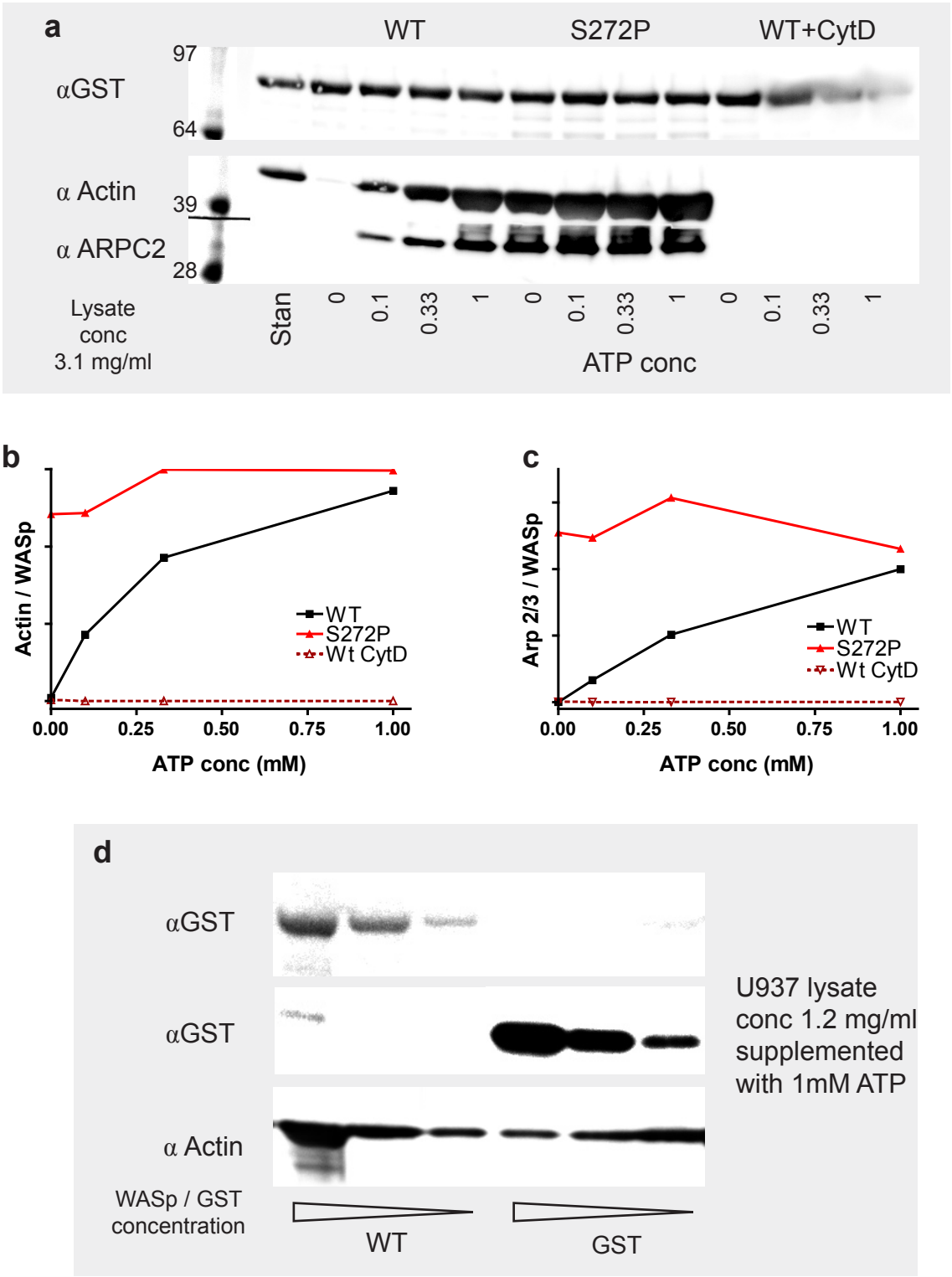

Fig 4.3 Effect of ATP on actin polymerisation assay
(a) Actin polymerisation assay on WT, S272P and WT with cytochalasin D added, with a range of ATP concentrations added to the U937 lysate immediately prior to bead incubation.
(b) & (c) Graphs of densitometry performed on blots from experiment in Fig 4.3a. Densitometry was performed on WASp, actin and Arp 2/3 bands and then expressed as actin / WASp and Arp2/3 / WASp ratios. **(d)** Actin polymerisation using the optimised ATP concentration of 1mM on beads coated with a titration of WT WASp and GST concentration.

used. This will also have the effect of increasing the interaction rate between the bead bound WASp protein and other regulatory proteins which may mediate its activation (such as Cdc42).

An initial experiment was performed comparing assay activity using U937 cell lysate at $1x10^7$ cells/ml with $2x10^7$ cells/ml (without supplementation of ATP). Figure 4.4a demonstrates that WT WASp activity is significantly increased by the more concentrated lysate, but the activity associated with GST alone and WT with cytochalasin D is also increased. A more comprehensive assessment of this effect is shown in figure 4.4b. In this experiment all lysate was supplemented with 1mM of ATP, and lysates were generated using between $1x10^7$ cells/ml and $6x10^7$ cells/ml, which yielded protein concentration of between 1.6 mg/ml and 4.9 mg/ml (as determined by BCA assay). WT WASp activity increases linearly with increasing lysate concentration (figure 4.4c). S272P WASp also shows increased activity with increasing lysate concentration, but the gap in activity between WT and S272P narrows as the concentration g-actin and WASp activators in the lysate increases (figure 4.4c and d).

Beads coated with both GST and dEVH1 WASp show an increase in actin polymerisation from $4x10^7$ cell/ml lysate. As suggested by figures 4.4a and 4.4b, increased lysate concentration increases non specific actin polymerisation as well as potentiating the activity of WT WASp. This experiment is representative of three similar experiments investigating the effect of lysate concentration. As a result of these experiments $2x10^7$ U937 cells/ml was felt to be the best lysate concentration for comparing the activity of WASp constructs to WT WASp.

Figure 4.4e shows the effect of freezing U937 lysate prior to using it in the actin polymerisation assay. Even the activity of the constitutively active WASp is impaired with the previously frozen lysate, (although this experiment was performed without ATP supplementation), and therefore fresh lysate only was used for further experiments.

4.2.5 Time course

The kinetics of the bead based actin polymerisation assay were investigated, both to provide information about the kinetics of WASp activity and to determine the optimal time point to use for assessing relative activity of WASp mutants.

Figure 4.5a shows an actin polymerisation assay without ATP supplementation, where WASp coated beads were rotated with lysate for up to 24 hours (at 4˚C), to determine whether WT WASp activity required a longer incubation period to

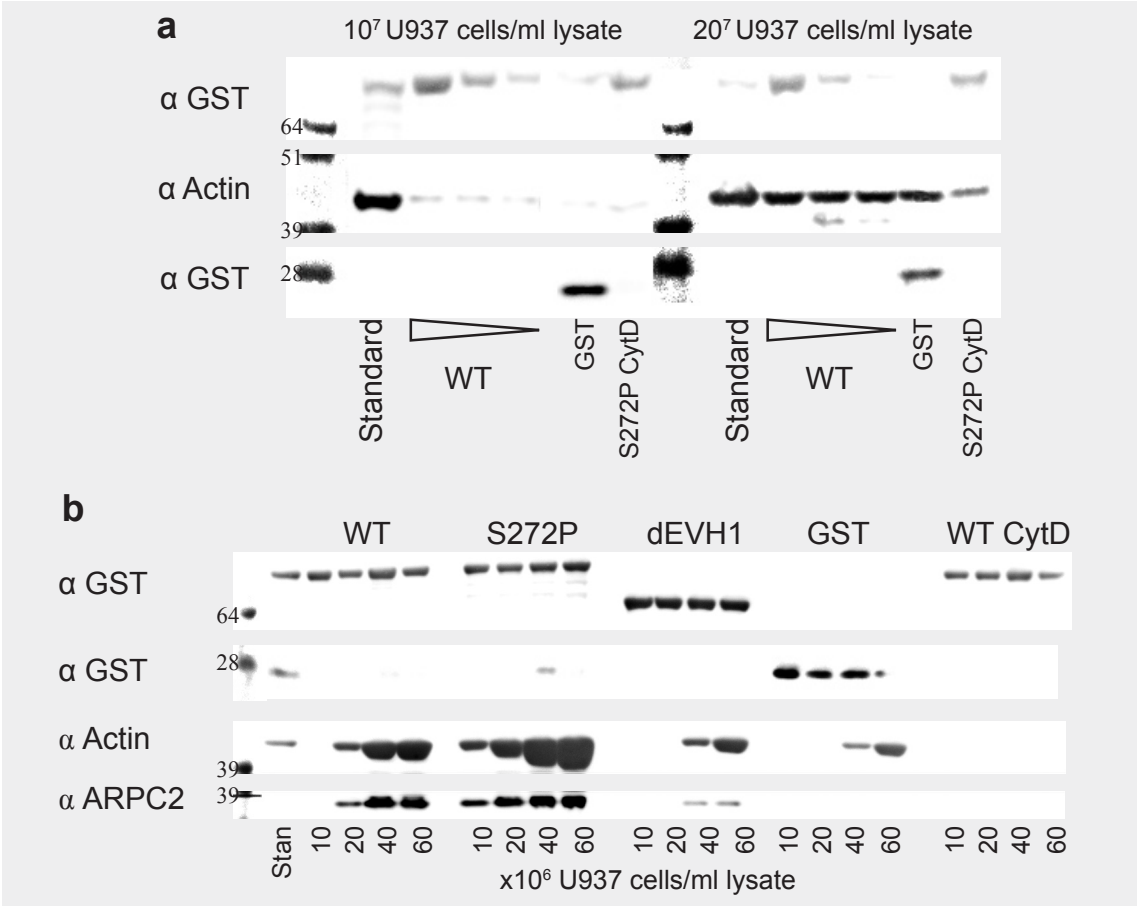

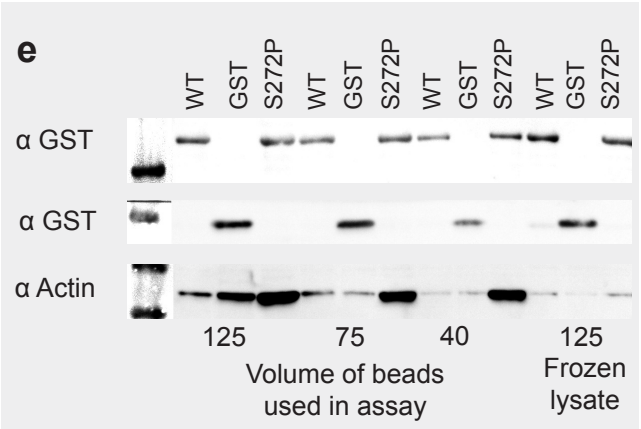

Fig 4.4 Effect of U937 lysate concentration on actin polymerisation assay

(a) Actin polymerisation assay with WT WASp and GST coated beads incubated with U937 lysate generated from 10^7 and 20^7 cells per ml of lysis buffer. **(b)** Actin polymerisation assay with U937 lysate generated from 10^7 ,$2x10^7$,$4x10^7$ and $6x10^7$ cells per ml. Resolved beads blotted for GST, Actin and p34 of ARP 2/3 complex. Protein concentrations of lysates were 1.6, 2.4, 4.3 and 4.9 mg/ml respectively. **(c) & (d)** Actin / WASp and Arp2/3 / WASp ratios were generated from densitometry on the bands from fig 4.4b and were plotted against lysate concnetration. **(e)** Actin polymerisation assay comparing previously frozen lysate with freshly prepared lysate. Also demonstrates higher levels of background actin pulldown with high volumes of GST only beads.

be detected. The results show that both WT and GST samples showed a small increase in actin binding over longer incubation periods, which is likely to be non specific polymerisation. Interestingly S272P shows maximal activity at 1 hour and the actin polymerised on the surface of the beads appears to depolymerise over time (figure 4.5b).

Figures 4.5c-e compare the activity of S272P, GST and WT WASp with and without ATP supplementation, over the first hour of bead incubation. The S272P WASp shows a maximal rate of actin polymerisation within the first 15 minutes of incubation, and its activity appears to have plateaued by 30 minutes. As shown before, WT WASp without ATP shows very little detectible activity. WT WASp with ATP supplementation by contrast shows its greatest rate of polymerisation after 30 minutes and continues to generate more polymerised actin beyond 1 hour.

4.2.6 Standard conditions

On the basis of these experiments I decided to use a 1 hour incubation period, with U937 lysate of $2x10^7$ cell/ml and 1mM ATP supplementation as the standard for comparing activity of mutant WASp construct to WT. Although the WT WASp in many such experiments may not yet have reached the equilibrium point where polymerisation equal depolymerisation rates, the one hour “snapshot” gives the opportunity for detecting constructs which are both more active (approaching or at equilibrium) or less active than WT. These conditions result in WT WASp activity being within the dynamic range of the assay. For experiments assessing the activity of constitutively active WASp constructs and NWASp constructs I have used the same conditions without ATP supplementation as the standard protocol.

4.3 Arp 2/3 complex binding during the assay

In addition to measuring the amount of actin bound to WASp coated beads after incubation with lysate, I also analysed the association of WASp binding proteins known to be involved in WASp activation. Although I have never consistently detected Cdc42 bound to beads, the presence of the p34 (ARPC2) subunit of the Arp2/3 complex correlates well with the quantity of actin polymerised (figure 4.3a, 4.3c, 4.4b, 4.4d and 4.5c). There is some inconsistency of p34 detection (compare the p34 detected in figure 4.5c, with the equivalent band detected in figure 4.4b (WT20) and figure 4.3a), however this is likely to represent a technical problem with the p34 detection figure 4.5c.

In fact, the quantity of Arp 2/3 bound appears to be a more specific marker of

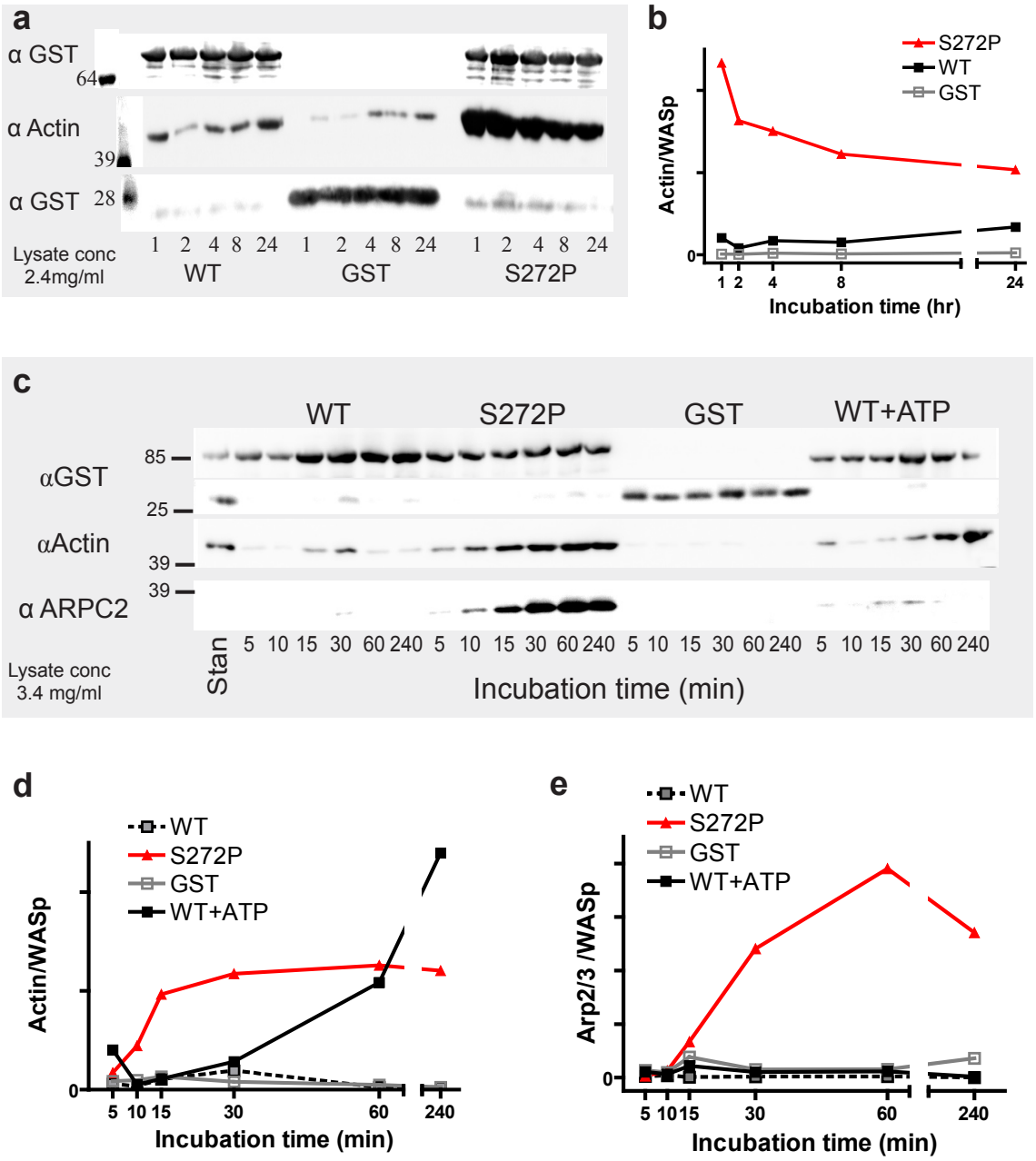

Fig 4.5 Kinetics of actin polymerisation assay and optimisation of incubation time
(a) Actin polymerisation assay using 10^7 U937s/ml (lysate concentration 2.4 mg/ml) and no ATP supplementation. Bead incubation time varied between 1 hour and 24 hours. **(b)** Densitometry was performed on Fig 4.5a and used to generate actin / WASp ratios for each sample. These were plotted against incubation time. **(c)** Actin polymerisation assay using $2x10^7$ U937s/ml (lysate concentration 3.41mg/ml) comparing kinetics of WT, S272P and GST without ATP with WT with 1mM ATP. Incubation time varied from 5 minutes to 4 hours. **(d) and (e)** Densitometry was performed on Fig 4.5c, and used to generate Actin / WASp and Arp2/3 / WASp ratios which were plotted against incubation time. These results are representative of four independent experiments.

WASp activation than actin, as the negative control experiments show no p34 binding even if low grade actin polymerisation is present (figure 4.3a, 4.4b, 4.5c). Interestingly WT WASp actin polymerisation assays without ATP lysate supplementation also have absent p34 binding (figure 4.3a, 4.5c, 4.12b and 4.13b). This raises the possibility that some low grade actin polymerisation is occurring via an Arp2/3 independent mechanism. Further evidence of two distinct pathways to actin polymerisation is suggested by the lysate concentration titration experiment (figure 4.4b). Both GST and dEVH1 constructs polymerised actin at the highest lysate concentrations, but whereas the dEVH1 domain mutant simultaneously bound p34 Arp2/3, the GST coated beads did not.

It is unknown whether in this assay the Arp 2/3 complex detected remains bound to an active GST-WASp, or whether it has dissociated from WASp and is bound to the branch points within the actin network. Each p34 subunit detected could represent one active WASp protein or it could represent a historical record of WASp mediated nucleation events, and therefore be proportional to the rate with which WASp cycles between an active and inactive state. Alternatively the p34 binding could be independent of bead bound WASp and be as a result the action of other mediators in the lysate acting on the dense actin network generated by the WASp on the surface of the bead. These hypotheses could be further explored using imaging techniques such as electron microscopy with gold labelled antibodies, but have been beyond the scope of this project.

4.4 Quantification and variability of the assay

4.4.1 Densitometry

In order to quantify the results of actin polymerisation assays, I have performed densitometry on immunoblots generated during the assay. As described in chapter 2.5, Western blots were developed using chemoilluminescence of HRP conjugated secondary antibodies, detected by a supercooled camera (Uvichemi). A strict protocol (chapter 2.7.1) was used for determining exposure time, background subtraction and band definition, which yielded reproducible results. Nonetheless, it was important to check the relationship between densitometry readings and protein concentration for the reagents and actin concentrations used in the actin polymerisation assay, to validate the assumption of a linear relationship.

Commercially purchased actin was reduced and resolved by SDS-PAGE, and the Western blot was immunoblotted for actin, using identical antibodies and techniques as used for the actin polymerisation assay. The results of two of four similar experiments are shown in figure 4.6. Figure 4.6a assesses low actin

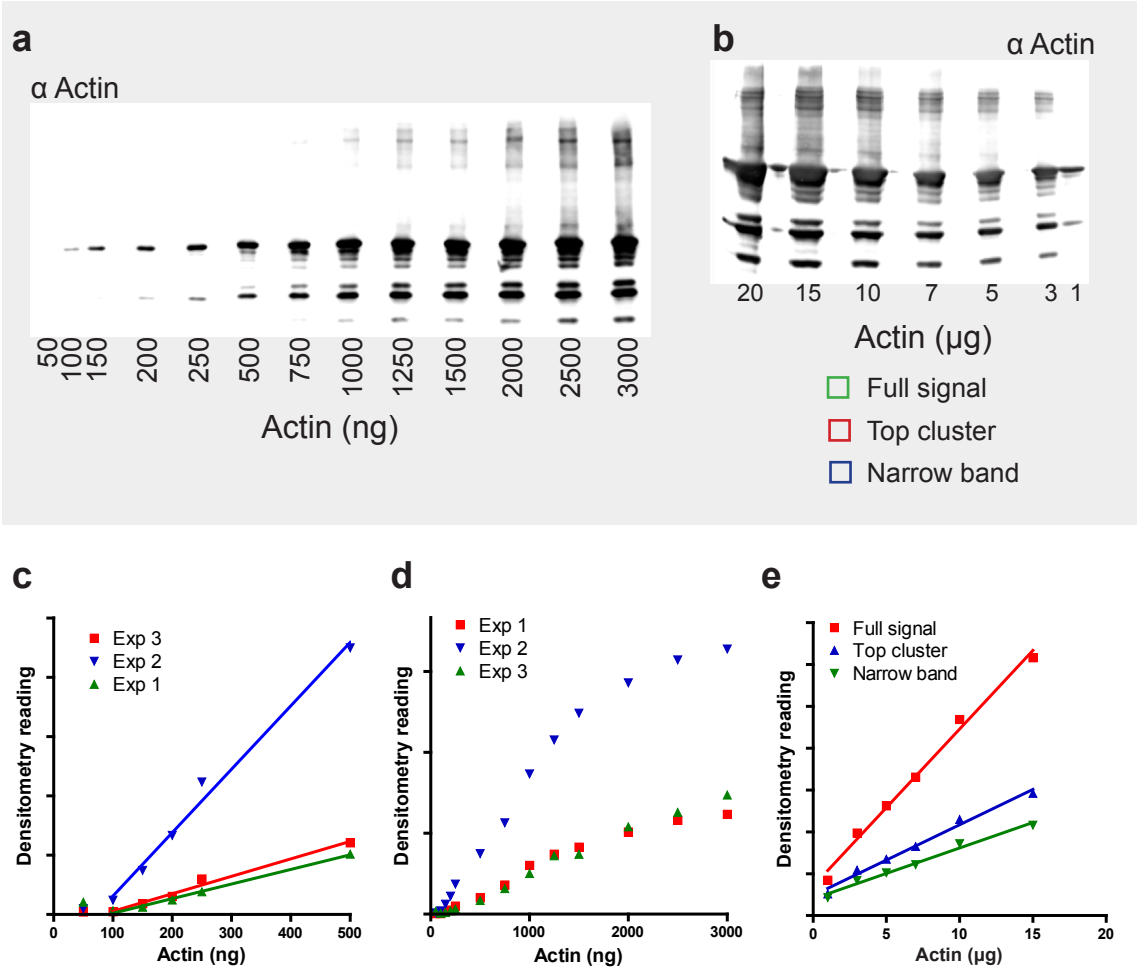

Fig 4.6 Assessment of linearity of densitometry of actin band resolved by SDS-PAGE and western blotting

(a) & (b) Known amounts of commercially purchased actin were reduced in sample buffer and resolved by SDS-PAGE and western blotting. The blots were developed on three separate occasions using different exposures (Exp1, 2 and 3). Densitometry was performed on the blots using 3 different band widths to define the actin band - narrow band (most selective), top cluster and full signal (most broad). **(c), (d) and (e)** Absolute densitometry readings were plotted against actual actin quantities and analysed by linear regression. Fig 4.6c and 4.6d relate to Fig 4.6a, and Fig 4.6e relates to Fig 4.6b. Regression lines plotted exclude the values for 20ng actin in Fig 4.6e. Data is representative of four independent experiments.

concentrations and figure 4.6b assesses densitometry for very high actin levels (comparable to positive signals in the actin polymerisation assay). For each, the blots were developed on three occasions (two optimised for exposure of the largest band and one optimised until the weakest band was just visible on the image prior to manipulation). Three definitions of “the actin band” were used (figure 4.6b) and densitometry readings were compared for all three at each of the exposures.

Both blots show a primary actin band and a series of degradation products below. In the actin polymerisation assay only full length actin will be bound to the beads and therefore these degradation products are not seen in these experiments. It was important to quantify the degradation products with the primary actin band in

order to accurately measure the total protein loaded.

Figures 4.6 c-e show examples of densitometry readings generated from these experiments. It can be seen that the densitometry signal varies linearly with actin concentration for a wide range of actin concentrations. In figure 4.6a there is linearity between 1µg and 15µg and in figure 4.6b between 100ng and 2000ng (or greater). Within each experiment there is linearity over a 20 fold increase in actin concentration, and with the correct exposure this linearity can be generated at any of the absolute actin concentrations tested.

Linearity of densitometry signals were also tested less formally for other proteins including WASp and similar correlations were found (data not shown). These results validate the use of densitometry for quantifying actin polymerisation assays.

4.4.2 Variability of individual experiments

From the results already presented in this chapter it is obvious that the bead based assay generates very significant variability in actin polymerisation responses between individual experiments. Similarly, there is inconsistency in the amount of WASp input both between constructs and between the same construct used for different reactions within a single experiment. As a result, presentation of the results from this assay using standard deviation or standard error to visualise variability would be misleading.

This variability is illustrated by figure 4.7 which shows scatterplots of the standardised densitometry values for actin and WASp for all experiments, grouped into each construct. Despite each construct being tested at three discrete WASp concentrations, WASp values appear as a continuum for every construct. Additionally, the actin responses for similar WASp concentrations of the same construct are markedly different between experiments. This is further illustrated by same dataset separated into individual experiments (appendix figure A.3).

The exact condition of the U937 lysate used for these experiments cannot be standardised. Although lysate was generated at a standard cellular concentration, this did not accurately correlate with a subsequently determined protein concentration. It was possible to quantify the lysate protein concentration before adding it to the beads, however this would have resulted in lysate being incubated on ice for at least 1 hour prior to be used in the assay. This would have introduced further variability (such as rate of endogenous ATP decay, changes in lysate actin dynamics), and there are limitations of the accuracy of rapid protein

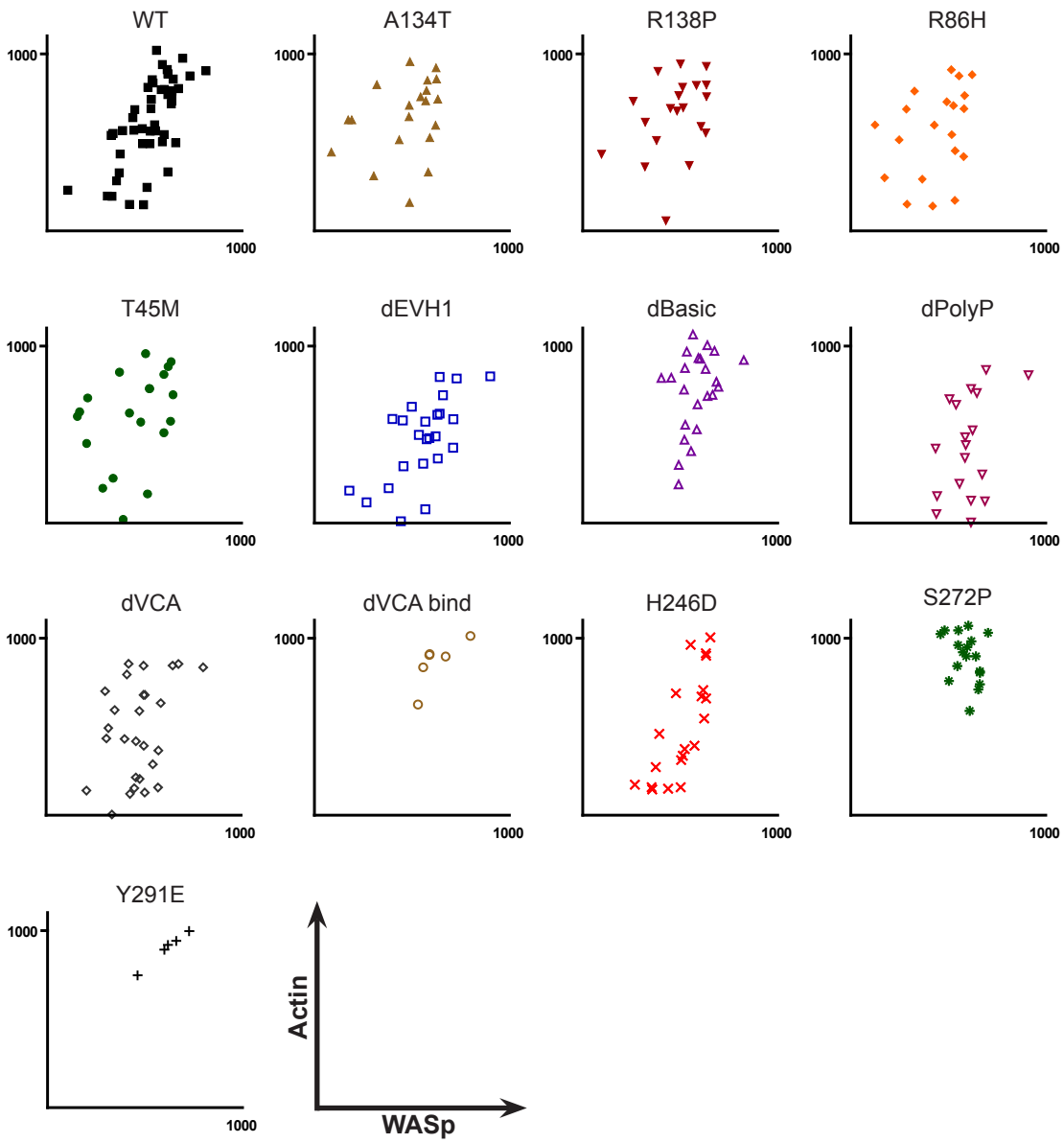

Fig 4.7 Actin - WASp scatterplots for individual constructs
Scatterplots of absolute densitometry values for actin and WASp, combined from all experments. Data sub-divided by construct.

estimation assays. I therefore elected to use the lysate fresh. Even if total protein concentration could be standardised the “quality” of the lysate will vary between experiments. This will be affected by the rate of division of the cells at the point of harvest and how healthy the cells are, among other factors.

Similarly, the exact delay between cell lysis and addition to WASp coated beads is likely to affect the potency of the actin response. Although, this delay was minimised and lysate was always kept on ice, there was inevitable variation between experiments and because of the short half life of mediators such as endogenous ATP and GTP, any variability may have a profound effect on the sensitivity of the assay. The bead incubation occurred at room temperature, which

will also have varied between individual experiments.

Sepharose beads are known to form clumps on storage, and as a result even when thoroughly mixed there will be significant heterogeneity in the number of beads present in equal volumes of reagent. This effect was minimised by storing the beads in a diluted buffer (1 in 5 v/v) and by ensuring the beads were well mixed (by flicking and pipetting) before being dispensed. During bead production (see chapter 3.3.2 and figure 3.10), there is variability in the amount of WASp generated for each construct and each bead batch, and this will inevitably result in differences in WASp concentration between sets of beads. WASp bead concentrations were determined, as described in chapter 3, and volumes loaded for each batch were adjusted to try to standardise the amount of WASp used in each experimental sample.

The detection of protein bands by Western blotting is also a source of variation between experiments. Efficiency of antibody binding, efficiency of blocking buffers, activity of ECL, evenness of ECL distribution of blot membranes and smudging or flare of high intensity signals all lead to inaccuracies in determining protein concentration within reactions. To minimise these effects each actin polymerisation gel was run with one well containing a standard of known actin and WASp amount. Densitometry readings were only compared within a single gel with a single exposure.

Despite the above variations between experiments, comparisons between constructs within experiments will remain valid. By using a multiple linear regression model to assess the relationship between actin and WASp, with experiment and construct as categorical factors, this variability can be compensated for. To further increase the accuracy of the results, most experiments were performed with a range of WASp concentration (at least 3) for each construct. This maximised the likelihood of detecting an actin response within the dynamic range of the assay for all construct, and could be used in a linear regression model.

4.5 Statistical analysis

4.5.1 Grouping of experiments for analysis

For analysis, data from experiments have been grouped into three datasets ; those assessing constitutively active constructs (S272P, I294T, Y291E and dVCA bind - without ATP supplementation), the standard panel (dEVH1, dBasic, dPolyP, dVCA, H246D, A134T, R138P, R86H and T45M - with ATP supplementation) and the NWASp constructs (S229P, S232P, murine WT WASp and murine WASp

S272P – without ATP supplementation). Data from every experiment performed under standard conditions (see chapter 4.26) was pooled into these groups and analysed together. Some of these experiments contained several WASp concentrations for each construct, others contained a single concentration. As described in chapter 2.72, raw densitometry readings (referred to as *relative* data) and standardised, quantitative readings (referred to as *absolute* data) were analysed in parallel.

In this chapter I explore and validate the statistical approach to analysing the actin polymerisation assays. To illustrate this I have used the largest data set available (the standard panel of constructs), and included all constructs tested in parallel including all negative controls. Similar results were obtained for the constitutively active and NWASp data sets and the descriptive statistics, frequency distributions and detailed statistical analyses of these data sets are shown in the appendix (figure A.4 - A.8 and A.10).

A summary of the statistical terminology used in the analysis of the actin polymerisation is shown in figure 4.8.

4.5.2 Statistical approach and terminology used

Details of the processing of densitometry data and further details of the statistical approach to analysis of this data are found in chapter 2.7.2. When analysing the actin polymerisation experiments, I was interested in differences between constructs in the amount of actin polymerised per unit WASp. Two null hypotheses were assessed for each construct – (i) the actin polymerisation activity of the construct is the same as WT WASp (or NWASp) activity, and (ii) the actin polymerisation activity of the construct is the same as a cytochalsin D inhibited assay activity.

An ANCOVA (two way analysis of covariance of actin with WASp) was performed, using linear regression corrections for differences between “experiment” and “construct”. This technique allowed a parametric analysis of the data, and a quantitative assessment of differences in actin values (standardised to WASp amount) between constructs. As described in chapter 2.7.2, two models were analysed – a *main effects model* analysis and an *interaction model* analysis. To be able to use this technique, actin and WASp values must be approximately normally distributed, and to compare differences between constructs the variances of the actin data should be approximately equal between constructs.

4.5.3 Data distribution and assessment of normality

To normalise the data, % natural logs were calculated for both actin and WASp

Table 4.8 Definitions of statistical terms

Term	Meaning
% Ln actin / WASp	Natural logarithm of actin (WASp) reading multiplied by 100
Absolute data	Densitometry readings standardised to absolute mass of protein using reading of known standards
ANCOVA	Analysis of Covariance. In this thesis this refers to the two analysis of the variance of % Ln Actin with the covariance of % Ln WASp
Corrected model of squares (SS_M)	Measure of total variation of % Ln actin values with % Ln WASp values
Corrected total sum of squares (SS_T)	Measure of variation of % Ln actin with % Ln WASp accounted for by the regression model
df	Degrees of freedom
Error (residual) sum of squares (SS_R)	Measure of variation of % Ln actin with % Ln WASp not accounted for by the model (unsystematic or random variation)
F ratio	Proportion of variation of % Ln actin values with % Ln WASp values accounted for by the model (or factor within the model) compared to unsystematic (random) variation
Interaction model	Regression model including an adjustment for the interaction between % Ln WASp and experiment
Kurtosis	Measure of the degree of clusters within the tails of a frequency distribution
Main effects model	Regression model of % Ln Actin with % Ln WASp including adjustments for differences between individual constructs and experiments
Marginal Mean	Estimate of the mean % Ln Actin value for an individual construct for fixed value of % Ln WASp (covariant)
R squared value (R_2)	Proportion of variability of % Ln Actin accounted for by % Ln WASp. A perfect correlation would give a value of 1.0
Relative data	Raw unstandardised densitometry readings
Skewness	Measure of the degree of asymmetry of a frequency distribution
z score	Number of standard deviations an individual value differs from the mean of the population

Fig 4.8 Summary of statistical terms used in this thesis

values (chapter 2.7.2). Scattergraphs, histograms and descriptive statistics for transformed and untransformed data is shown in Figure 4.9 for the absolute data and in 4.10 for the relative data. Untransformed data for actin and WASp have disparate mean and median values for both relative and absolute readings, demonstrating a lack of normality. Natural log transformation however produces a data set with very similar means and medians (figure 4.9h and 4.10h). Scatterplots show a positive correlation between WASp and actin with no obvious non-linear relationship.

Histograms of actin and WASp distributions (figure 4.9c-f and 4.10c-f) show that the log transformed distributions are approximately normally distributed. Statistics for skewness and kurtosis (for % Ln Actin / WASp) are between 2 and 3 standard deviations (z scores) from the normal mean (zero) (figures 4.9h and 4.10h), suggesting that, for the complete dataset both % Ln WASp and % Ln Actin show significant deviation from normality. Similarly more formal tests of normality, such as the Kolomogorov-Smirnov statistic, performed on the entire dataset demonstrate significant deviation form normality for both absolute and relative data of % Ln WASp and % Ln actin (analysis not shown). However, if each individual construct is tested as a sub population (as they will be subsequently analysed) almost every individual construct has a normal distribution for both % Ln actin and % Ln WASp. Figure 4.11a shows the Kolomogorov-Smirnov statistics for each individual construct's data subset. A p value of greater than 0.05 predicts a 95% chance that the distribution is normal, and these subsets are marked with an asterix.

Although these tests state whether or not a distribution is statistically normal, they do not describe whether deviation from normality within a data set is important enough to invalidate future analysis. The ANCOVA is a robust technique, particularly with a large dataset (267 data points in the standard panel), and can tolerate significant deviations from normality. Because of how these experiments were performed (with several different WASp input concentrations), actin and WASp distributions should not be normally distributed. The above analysis, however, demonstrates that they do show enough normality to allow the valid use of an ANCOVA analysis.

4.5.4 Assessment of equality or variances

Levene's test was used to assess the equality of actin variances between constructs within the whole dataset. This test assesses the null hypothesis that the variance of the dependant variable (% Ln actin) is equal for each construct.

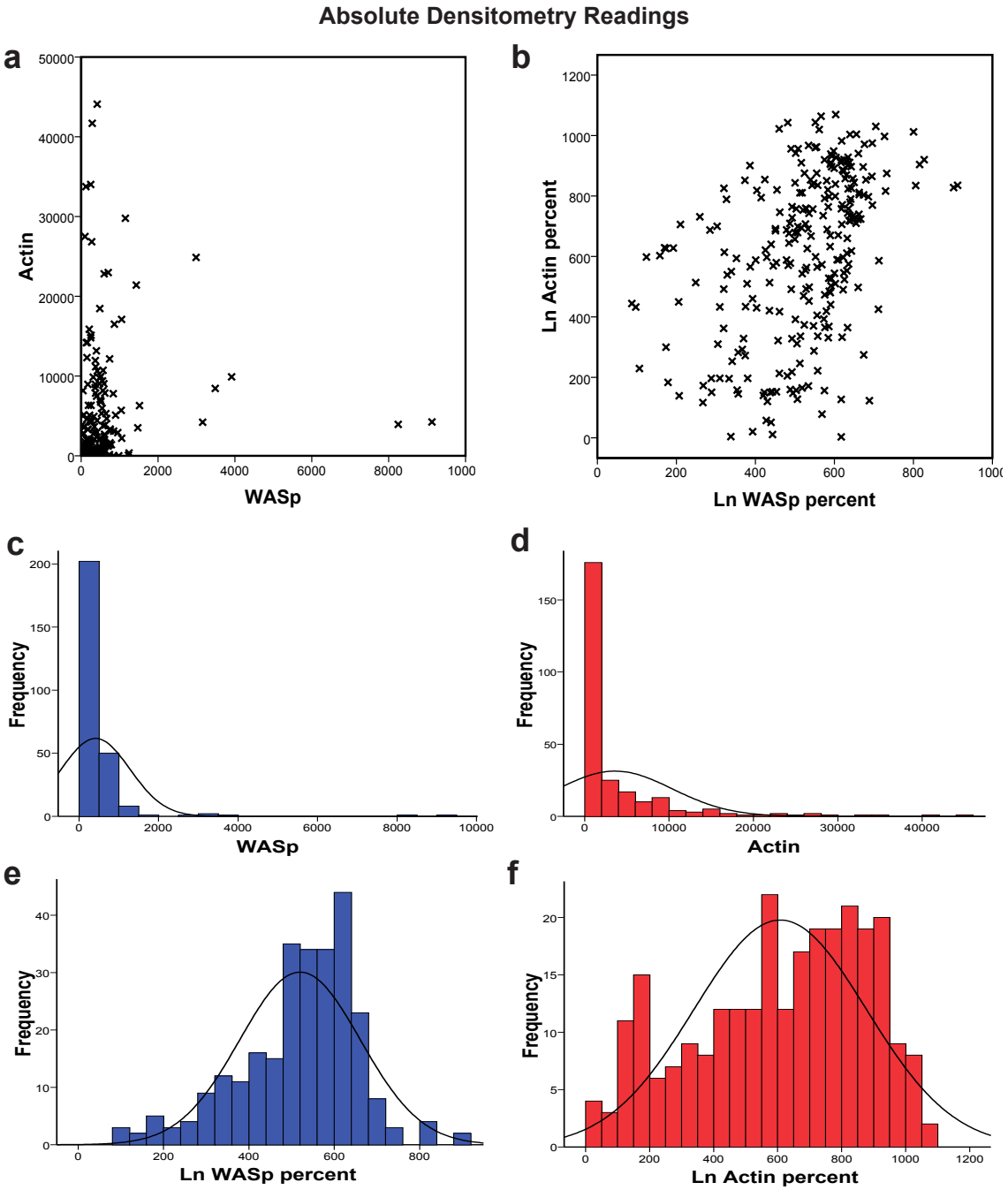

h **Descriptive Statistics - Absolute Values**

	WASp	Actin	% Ln WASp	% Ln Actin
N	267	267	267	267
Mean	417.0	3601.9	519.9	608.1
Median	223.2	715.0	540.8	657.2
Std. Deviation	862.8	6799.6	141.6	269.3
Skewness	7.386	3.210	-0.668	-0.441
SE of Skewness	0.149	0.149	0.149	0.149
Kurtosis	65.399	12.078	0.749	-0.816
SE of Kurtosis	0.297	0.297	0.297	0.297

Fig 4.9 Distribution and descriptive statistics of absolute densitometry readings
Absolute readings were generated by standardising densitometry readings to those of known WASp and actin standards. **(a) & (b)** Scatterplots of raw or transformed WASp and actin densitometry readings. Transformation was performed by taking natural logs and multiplying by 100 (to produce % Ln readings). **(c) - (f)** Frequency distributions of raw and transformed data.
(h) Descriptive statistics of raw and transformed data. *Ln - Natural log, SE - Standard error*

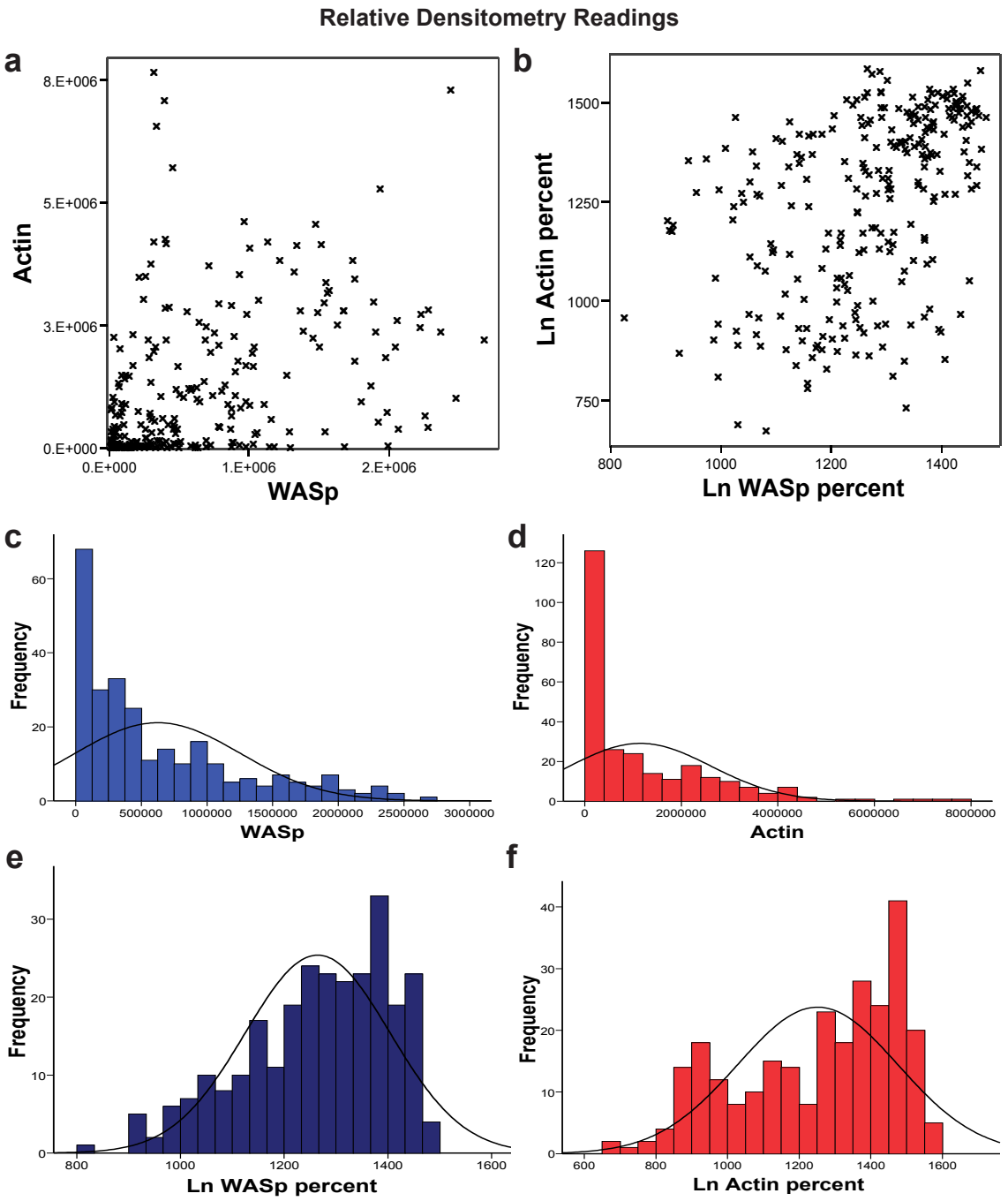

h **Descriptive Statistics - Relative Values**

	WASp	Actin	% Ln WASp	% Ln Actin
N	267	267	267	267
Mean	624393	1151125	1252	1265
Median	395627	480664	1308	1289
Std. Deviation	630857	1464507	224	140
Skewness	1.222	1.725	-0.574	-0.666
SE of Skewness	0.149	0.149	0.149	0.149
Kurtosis	0.652	3.328	-0.864	-0.204
SE of Kurtosis	0.297	0.297	0.297	0.297

Fig 4.10 Distribution and descriptive statistics of relative densitometry readings
Relative readings are the unstandardised densitometry readings generated from the UviChemi supercooled camera. **(a) & (b)** Scatterplots of raw or transformed WASp and actin densitometry readings. Transformation was performed by taking natural logs and multiplying by 100 (to produce % Ln readings). **(c) - (f)** Frequency distributions of raw and transformed data. **(h)** Descriptive statistics of raw and transformed data. *Ln - Natural log, SE - Standard error*

a Kolomogorov-Smirnov tests of Normality for individual constructs

		Absolute values				*Relative values*			
		KS Statistic	df	Sig.	P>0.05	KS Statistic	df	Sig.	P>0.05
% Ln WASp	WT	0.110	46	0.200	*	0.138	46	0.028	
	A134T	0.233	20	0.006		0.155	20	0.200	*
	R138P	0.138	20	0.200	*	0.120	20	0.200	*
	R86H	0.206	20	0.025		0.155	20	0.200	*
	T45M	0.149	20	0.200	*	0.103	20	0.200	*
	dEVH1	0.128	24	0.200	*	0.168	24	0.078	*
	dBasic	0.093	23	0.200	*	0.117	23	0.200	*
	dPolyP	0.141	18	0.200	*	0.131	18	0.200	*
	dVCA	0.137	27	0.200	*	0.082	27	0.200	*
	dVCA bind	0.297	6	0.106	*	0.190	6	0.200	*
	H246D	0.151	20	0.200	*	0.124	20	0.200	*
	S272P	0.106	18	0.200	*	0.166	18	0.200	*
	Y291E	0.243	5	0.200	*	0.257	5	0.200	*
% Ln Actin	WT	0.107	46	0.200	*	0.123	46	0.077	*
	A134T	0.116	20	0.200	*	0.208	20	0.024	
	R138P	0.144	20	0.200	*	0.213	20	0.018	
	R86H	0.145	20	0.200	*	0.159	20	0.200	*
	T45M	0.157	20	0.200	*	0.176	20	0.105	*
	dEVH1	0.123	24	0.200	*	0.122	24	0.200	*
	dBasic	0.150	23	0.196	*	0.181	23	0.048	
	dPolyP	0.133	18	0.200	*	0.169	18	0.188	*
	dVCA	0.126	27	0.200	*	0.172	27	0.040	
	dVCA bind	0.264	6	0.200	*	0.222	6	0.200	*
	H246D	0.140	20	0.200	*	0.206	20	0.026	
	S272P	0.124	18	0.200	*	0.115	18	0.200	*
	Y291E	0.270	5	0.200	*	0.207	5	0.200	*

b Levene's Test of Equality of Error Variances

Dependent Variable % Ln Actin

LS	df1	df2	Sig.
0.959	134	132	0.5961

Tests the Null hypothesis that the error variance of the dependent variable is equal across groups

c Analysis of Covariance (ANCOVA)

Dependent Variable % Ln Actin, Co-variable % Ln WASp, Fixed factors Experiment and Construct, Interaction term of Experiment with % Ln WASp (Experiment * %Ln WASp)

	Absolute values						**Relative Values**					
	Main Effects Model			*Interaction Model*			*Main Effects Model*			*Interaction Model*		
	df	F	Sig.	df	F	Sig.	df	F	Sig.	df	F	Sig.
Corrected Model	33	31.89	.000	53	26.25	.000	33	19.93	.000	53	16.95	.000
Intercept	1	17.89	.000	1	1.12	.292	1	4.15	.043	1	.36	.548
Experiment	20	27.38	.000	20	6.85	.000	20	11.74	.000	12	4.54	.000
Construct	12	15.99	.000	12	17.30	.000	12	15.99	.000	20	17.31	.000
% Ln WASp	1	127.51	.000	1	4.71	.031	1	127.51	.000	1	4.71	.031
Experiment * % LN WASp				20	3.89	.000				20	3.89	.000
Adjusted R Squared			.793			.834			.701			.761

Fig 4.11 Statistical analyses of normality, homogeneity of variance and comparison of different regression models used to perform ANCOVAs

(a) Assessment of normality. An insignificant KS statistic (p>0.05) suggests normally distributed data. **(b)** Assessment of homogeneity of variance **(c)** Comparison of ANCOVAs performed on absolute and relative densitometry data, and using *main effects* only and *interaction* multiple regression models. *df - degrees of freedom, LS - Levene's statistic, Ln - natural log, F - F ratio*

Figure 4.11b demonstrates that there is no significant difference in the variances between constructs.

4.5.5 Analysis of Covariance of % Ln actin with % Ln WASp (ANCOVA)

The ANCOVA assesses the regression model of Ln % actin with Ln % WASp, quantifies any variation from this model seen in the data, and categorises the source of this variation as due to differences between constructs, experiments or variation which cannot be accounted for by the model (unsystematic variation or error).

ANCOVA of Standard panel, absolute data, main effects model

Dependent Variable:% Ln Actin

Source	Type III Sum of Squares	df	Mean Square	F	Sig.
Corrected Model	15796195.384(a)	33	478672.587	31.894	.000
Intercept	268549.708	1	268549.708	17.893	.000
Experiment	8218579.651	20	410928.983	27.380	.000
Construct	2880357.713	12	240029.809	15.993	.000
% LN WASp	1913760.971	1	1913760.971	127.514	.000
Error	3496920.450	233	15008.242		
Total	118031332.477	267			
Corrected Total	19293115.835	266			

a R Squared = .819 (Adjusted R Squared = .793)
df = degrees of freedom, F = F ratio, sig = significance (p value)

Table 4.1 Full ANCOVA table following analysis of actin polymerisation assays performed on the standard panel of constructs, using absolute densitometry readings and a main effects only model

The total amount of variation in the data is represented by the corrected total Sum of Squares (SS_T), and the amount accounted for by the model is the corrected model sum of squares (SS_M). The residual (unsystematic) variation, unexplained by the model is the error sum of squares (SS_R). The sum of squares values are then adjusted by their degrees of freedom to give mean squares. The F ratio is the mean square value for the model (or any factor within the model) divided by the mean square of the error term. This represents the amount of variation attributable to the model (or a factor within the model), divided by the amount of residual variation. Therefore for the analysis above, it can be seen that the regression model accounts for 31.9x the amount of variation of % Ln actin, compared to unexplained variation. Unsurprisingly, the model is a significantly accurate representation of the data, with a p value of < 0.0005.

The construct F ratio represents the ratio of variation attributable to differences

between constructs, compared to the residual variation. This value is 15.99 and is highly statistically significant, suggesting that there are significant differences between the constructs in their ability to polymerise actin. The R squared value represents the regression coefficient of the correlation between % actin and % WASp. The higher this value, the stronger the linear relationship between % Ln actin and % Ln WASp.

By comparing F ratios and R_2 coefficient between absolute and relative data, and between the main effect analyses and the interaction analyses, it can be determined which data set is most strongly represented by which model, and proportionately how much variation is due to differences between constructs. Figure 4.11c compares the F ratios between these various combinations. The F ratios for all four analyses are very high and are all highly statistically significant. This suggests that compensations for experiment and construct explain the vast majority of the variation between % Ln Actin and % Ln WASp. Both the F ratios and the R_2 coefficients for the models using the absolute data are higher than those using the relative data. This validates the use of a densitometry standard in these experiments, and this technique has been accurate enough to significantly reduce the variation between experiments.

Comparisons between the main effects analysis and the interaction analysis (figure 4.11c), show that the interaction model has a slightly reduced F ratio, but the interaction term itself is significant (F ratio 4.71, $p<0.05$). Additionally the F ratio for the construct factor is increased in the interaction model (17.3 compared to 15.99, figure 4.11c), and the strength of the correlation between % Ln Actin and % Ln WASp (R_2) is higher. These results suggest that, as predicted from the experimental practicality (chapter 4.42), there is a significant interaction between % WASp and experiment, and therefore this should be included in the analysis. Although the proportion of variation accounted for by the interaction model is less, the relative contribution of differences between the constructs is greater.

To conclude, the absolute data is a more accurate representation of the actin polymerisation assay results. In subsequent chapters results and analysis of absolute data only will be shown. The ANCOVA model compensating for an interaction between % WASp and experiment is a more true representation of the data, but the main effects only model accounts for a greater proportion of the variability seen. As a result, both sets of analysis will be presented in subsequent chapters.

Although all experimental data (under the same experimental conditions) has

been included to assess the ANCOVA process, datasets analysed in chapter 5 have tailored to the more accurately answer the specific questions being addressed. For example, when addressing the differences between constructs within the standard panel and WT activity, experiments involving cytochalasin D inhibition and those using constitutively active constructs have been omitted from the analysis, as they are not relevant to this question.

4.5.6 Estimated means and pairwise comparisons

The ANCOVA analysis, assesses whether or not there are significant differences between the constructs within a dataset, but does give information about which individual constructs are responsible for these differences. “Marginal means” can be estimated for each construct, which act as a quantification of the average amount of actin polymerised per unit WASp. These values are estimates of % Ln actin at a fixed covariant (% Ln WASp) value, and are calculated using regression analysis. The significance of differences between these marginal means can be assessed using a t test.

In assessing the actin polymerisation activity of WASp constructs, I am only interested in comparing activity to WT (or cytochalasin D inhibited) activity. As the absolute marginal means of % actin are meaningless, I have expressed the activity of individual constructs in terms of their differences to WT (or cytochalasin D inhibited) activity, measured as multiples of the standard deviation of the WT marginal mean (a z score). In such representation, WT (or cytochalasin D inhibited) activity is expressed as 0, and individual constructs and their 95% confidence intervals have positive values if their activity is greater than WT and negative values if their activity is less than WT. An example of the graphical representation of such results is shown for NWASp constructs in figure 4.13d-f.

The expression of 95% confidence intervals and z scores is particularly helpful as they are identical for the log transformed and untransformed data, and give a realistic quantification for “relative ability to polymerise actin”, for which any absolute measure would be meaningless. Because I am assessing the difference between each construct and a predefined control (WT or cytochalasin D inhibited) only, I have used the least significant difference (LSD) pairwise comparison of marginal means to assess differences. Results of this analysis for individual constructs are shown in chapter 5.

4.6 Use of other haematopoeitic cell lines as assay substrates

U937 cells were chosen as a substrate for the actin polymerisation assay because they are of myeloid lineage and because they had been used in the previously published method for this assay. It was possible that other cell lysates may make the assay more sensitive, and it was important to validate the assay in other myeloid lysates. THP-1 cells (a human acute monocytic leukaemia cell line which can be differentiated into dendritic cell like cells in culture) and RAW 132 cells (a murine macrophage cell line) were compared to U937s as lysate substrate. The concentration of lysate produced by $2x10^7$ cells/ml had been previously determined and was used to calculate the number of cells of each cell line required to generate lysate of the same concentration as $2x10^7$ cells/ml U937s. These lysates were supplemented with 1mM ATP and tested with a range of WASp constructs.

Figure 4.12a demonstrates that although the assay does work using all three cell lines, it is most sensitive with U937 cells and least sensitive with RAW cells.

4.7 Optimisation of Cos 7 lysate as assay substrate

The actin polymerisation assay can be modified to investigate the effect of WASp binding partners on *in vitro* WASp activation. The most direct way of doing this is to add purified recombinant protein to the lysate prior to bead incubation. This strategy was suitable for investigating the effects of Cdc42, which can be generated and purified from bacterial cell lysates, but for larger more complex proteins such as WIP which need to be generated in mammalian cells, the quantity of WIP required made this approach impractical.

An alternative strategy of using lysate of cells overexpressing the protein of interest was investigated. U937 cells are difficult to transfect with high efficiency, but I have optimised transfection of Cos7 cells by electroporation, which results in greater than 90% transfection efficiency of viable cells at 48 hours post electroporation. To demonstrate an effect of a second protein on actin polymerisation it is essential to have the control experiment (WT-WASp without addition of second protein) reliably producing an actin response within the dynamic range of the assay. This will allow detection of both suppression and enhancement of activity.

Figure 4.12b shows an actin polymerisation assay using Cos7 lysates testing WT, S272P and dEVH1 WASp constructs with a range of lysate and ATP concentrations. This and other experiments have demonstrated that Cos7 lysate is very effective

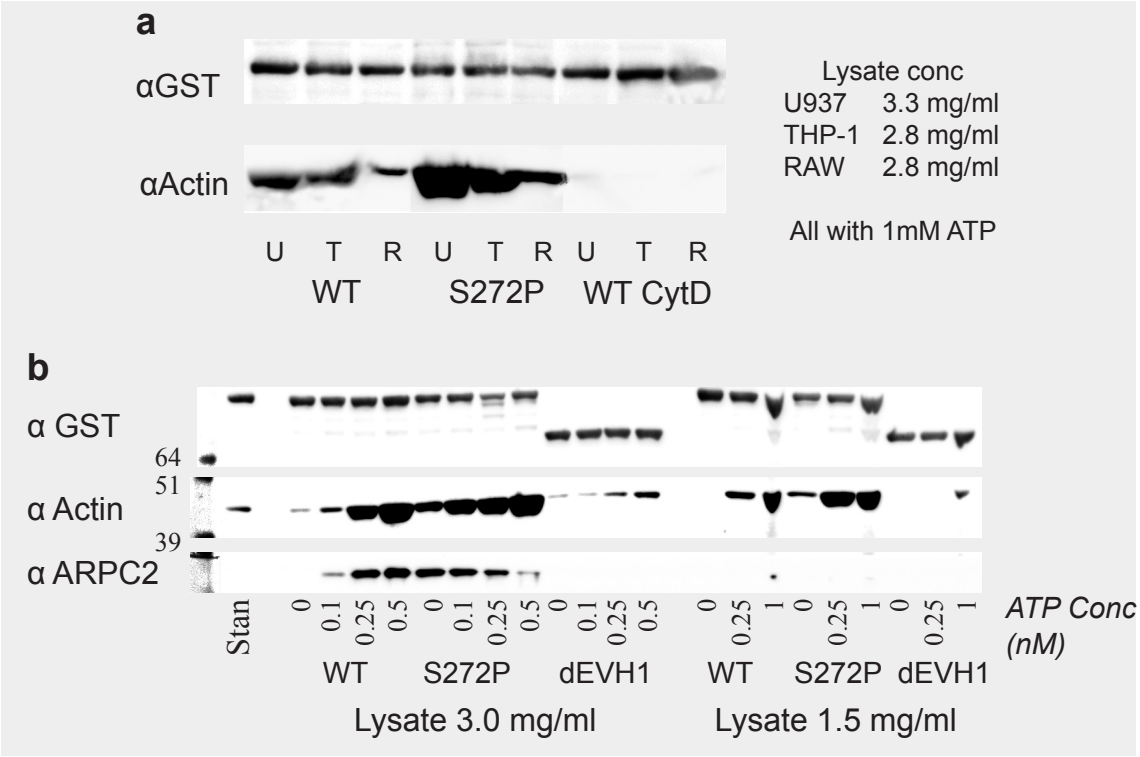

Fig 4.12 Other cell lines as substrate lysate for the actin polymerisation assay
(a) U937 (U), THP-1 (T) and RAW (R) cell lysates were generated at the equivalent of $2x10^7$ U937 cells (based on previous data). Lysates were supplemented with ATP and incubated with beads coated with WT, S272P and WT WASp with Cytochalasin D. **(b)** Actin polymerisation assays were performed using Cos7 cell lysate. Lysate was prepared exactly as for U937 cells. 3 constructs were tested (WT, S272P and dEVH1), at a range of ATP supplementation concentrations and at 2 lysate concentrations.

as a substrate for actin polymerisation. With no ATP supplementation there appears to be less low grade actin polymerisation than with U937 lysate, but saturation of actin signal is achieved with lower concentration of ATP.

4.8 Testing of murine N-WASp in assay

As part of a collaboration with another group (Adamovich et al., 2009), I was asked to use this assay to assess the activity of two N-WASp constructs (L229P and L232P) with point mutations which are predicted to result in constitutive activity. This has provided an opportunity to validate the assay for other initiators of actin polymerisation and to compare the relative activities of WASp and N-WASp in this assay. In addition I was asked to use murine WASp (WT and constitutively active L272P) as control.

Generation of N-WASp coated beads (from transfected Cos7 cell lysates), using the same protocol used for WASp bead generation, resulted in residual actin binding after bead washing (figure 4.13a). The murine WASp and GST beads made during the same preparation did not contain actin. This finding was

consistent over three separate bead preparations. The amount of actin bound to each batch of beads was quantified and actin readings from the assays were corrected accordingly for all samples within these experiments (as described in chapter 2.7.2).

An example of an NWASp actin polymerisation assay is shown in figure 4.13b, and the corrected densitometry from this experiment is plotted in figure 4.13c. This experiment is representative of 4 similar experiments, and the descriptive statistics and frequency distributions of the actin and NWASp / mWASp data are shown in the appendix (figure A.6 and A.7). An ANCOVA analysis was performed as described above and the full results of this analysis can also be found in the appendix (figure A.10). The differences in mean activities between L229P and L232P NWASP mutants and WT NWASp are shown in figures 4.13d and e (for main effects only and interaction models respectively). These demonstrate that both constructs are significantly constitutively active, showing an activity approximately 3x the standard deviation of WT NWASp activity.

I also compared the activity of NWASp constructs to their equivalent WASp samples, and found that WT NWASp was significantly more active than WT WASp (figure 4.13f). Interestingly the two constitutively active NWASp constructs showed slightly less activity than the equivalent murine WASp constitutively active point mutation (L272P), although this difference did not reach significance.

4.9 Conclusion

The experiments in this chapter demonstrate that the bead based actin polymerisation assay is a valid and versatile tool in assessing the activity of activators of actin filament nucleators, such as WASp family proteins.

In interpreting the results of this assay it is important to consider exactly what is being measured and what mechanisms may be responsible for this. The assay measures the total amount of filamentous actin bound to WASp coated sepharose beads. To produce f-actin, WASp must first be activated exposing the Arp 2/3 binding site within in the WASp VCA domain (Panchal et al., 2003). Arp 2/3 and ATP loaded monomeric actin (delivered by profilin) must then be recruited to form a nucleating complex (Marchand et al., 2001). This complex must then bind an existing actin filament from the lysate, activating Arp 2/3 and initiating nucleation. Following nucleation a daughter branch actin filament will form resulting in a new barbed end, which will spontaneously elongate, polymerising actin monomers into f actin. The Arp 2/3 complex will remain anchored to the branch site on the filament network (Svitkina and Borisy, 1999), however following nucleation WASp

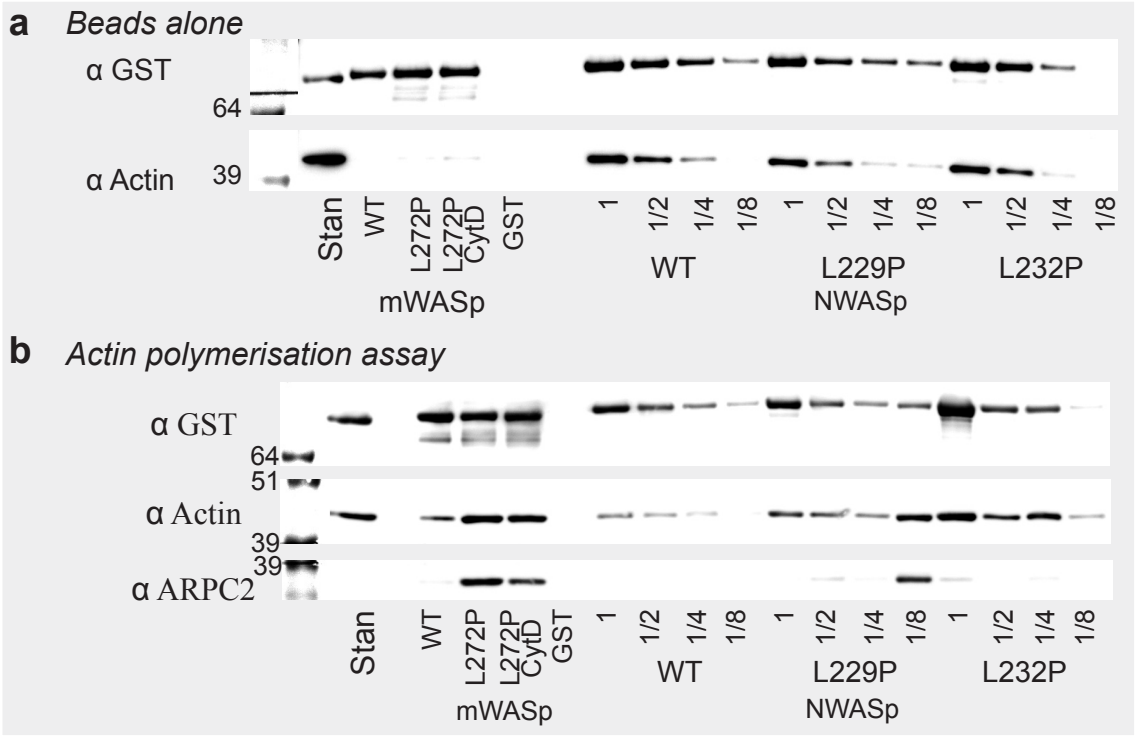

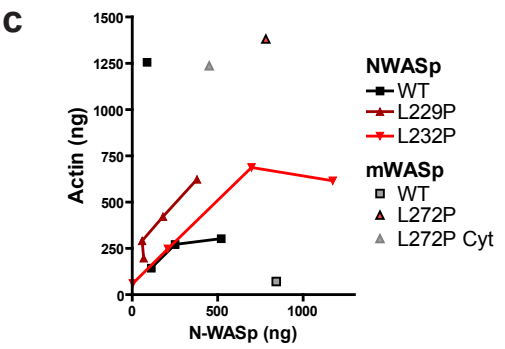

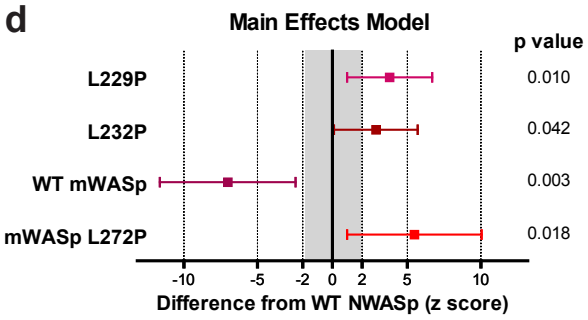

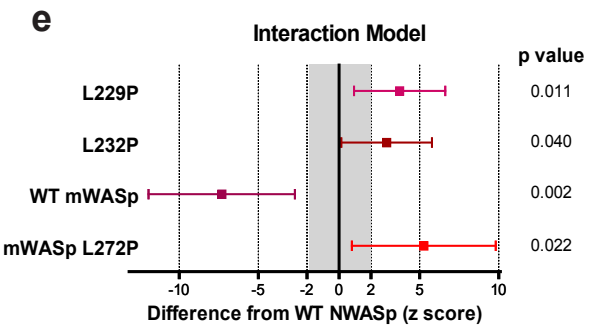

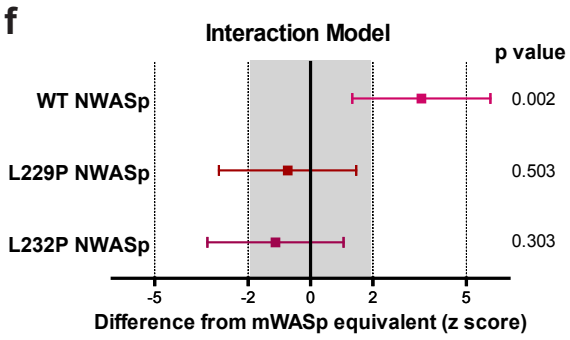

Fig 4.13 N-WASp and murine WASp in actin polymerisation assay
(a) Sepharose beads coated with GST N-WASp protein (WT, S229P and S232P) resolved by SDS-PAGE and western blotting. N-WASp constructs were associated with higher levels of actin following purification than mWASp constructs. Fractions above the labels of the NWASp constructs represent the dilution of lysate used to manufacture the beads. **(b)** Actin polymerisation assay with N-WASp and murine WASp (mWASp) constructs. U937 lysate prepared from $2x10^7$ cells/ml with no ATP supplementation was used. **(c)** Densitometry plots of actin against N-WASp/mWASp for fig 4.8b **(d),(e)** Estimated marginal means of activity for each construct were calculated from the ANCOVA analysis and were expressed in terms of numbers of standard deviations from WT activity (z scores). Means and their 95% confidence intervals are plotted on the graphs and the 95% confidence interval (z score 2) for WT is shaded in grey. **(f)** Comparison of mean activities of WT mWASp to WT NWASp, and between L229P/L232P NWASp and L272P WASp.

will dissociate from the actin filament (Martin et al., 2006; Egile et al., 2005).

In the presence of adequate concentrations of Arp2/3, the rate of actin polymerisation will be determined by the number of f-actin barbed ends and the concentration of ATP loaded actin monomers. Cell lysate formation results in an approximately 10 fold drop in the actin concentration in solution compared to the physiological concentration in the cell's cytosol. As the cellular monomeric actin concentration is maintained to allow a steady state of treadmilling of the actin cytoskeleton, this drop in actin concentration will encourage depolymerisation (in the absence of an activator of nucleation). This will be exacerbated by the reduction in ATP levels (due to inherent instability in aqueous solution) upon lysate formation. Depolymerisation will increase the concentration of monomeric actin in the lysate, but paradoxically will ultimately decrease the number of barbed ends present to allow filament elongation. Therefore the actin structures which will facilitate maximal actin polymerisation are highly branched networks of short filaments, with a high barbed end to total f-actin ratio.

Many other proteins will influence the dynamics of f-actin within the assay, such as capping proteins, actin sequestering proteins, severing proteins and profilin (Faix and Grosse, 2006; Rogers et al., 2003; Blanchoin et al., 2000a; Loisel et al., 1999; Carlier et al., 1997; Schafer et al., 1996; Pantaloni and Carlier, 1993). These should remain constant within the assay and will be the same for each individual sample tested within each experiment. Potentially they form an additional source of variation between experiments performed on different batches of lysate. Similarly as WASp is known to detach from f-actin following nucleation (Martin et al., 2006; Egile et al., 2005; Uruno et al., 2003), and is not thought to influence the stability of f-actin, the rate of actin depolymerisation should be constant between experiments performed with different WASp constructs.

It is apparent from the above discussion that the simplistic concept of each bead bound WASp protein initiating a single actin filament which elongates away from the bead, resulting in polymerised actin which is detected in the assay, is incorrect. The concerted activation of WASp proteins over the surface of the bead will result in the generation of a complex and dynamic orthogonal network of actin filaments. Each WASp activation will generate a new barbed end, inducing polymerisation, but also releasing the filament from the surface of the bead. As the barbed ends of daughter filaments elongate, so the branch sites becomes destabilised and pointed end depolymerisation accelerates. This results in the translocation of the new filament away from the bead, but also delivers new actin monomers and Arp2/3 complexes to the proximity of the bead surface and therefore the

immobilised WASp proteins.

Following initiation of the reaction there is a net polymerisation of actin. After a period of time an equilibrium point will form where all the short filaments and smaller actin networks have become incorporated into a single actin network surrounding the bead, in which the overall polymerisation rate will equal the depolymerisation rate. This network will be highly branched and interlinked (with a high concentration of immobilised actin nucleators at the centre), such that the decay of individual filaments will not lead to detachment from the main network. Attachment of the network to the bead itself may be due to the transient binding of activated WASp proteins, or due to the three dimensional shape of the network surrounding the bead.

Because the amount of actin polymerised on the surface of the bead will be determined by the ratio of barbed ends to total f-actin, the greater the activity of the WASp constructs (and therefore the greater the branching within the actin network), the larger amount of f-actin bound to a bead at the equilibrium point of the assay. The activity of an individual WASp construct determines the complexity, and therefore the size, of the actin network.

This model explains the different kinetics seen with the bead based assay compared to the pyrene actin polymerisation assay. The pyrene based assay measures the total polymerisation in the whole reaction, under conditions primed for polymerisation (such as excess actin and ATP). It follows the chain reaction of actin polymerisation throughout the experimental solution following an initiation stimulus. The activity of the nucleation activator is measured by the speed with which this chain reaction is instigated. The bead based assay is assessing the polymerised actin which remains localised to the surface of beads coated with nucleation activators. It provides a snap shot of a series of actin networks in a steady state of equilibrium, which is maintained by the ongoing nucleation activity of the WASp protein on the beads. The activity of the nucleation activator is measured as the amount of f-actin maintained in the network surrounding each bead.

The concentration of ARPC2 bound to the beads appears to correlate well with the amount of f-actin pulled down (figure 4.3a, 4.4b, 4.5c, 4.13b, 5.4a, 5.5b, 5.8a). In fact, subjectively it appears to be a more specific measure of true WASp activity, and does not appear to be pulled down in association with background polymerised actin. Arp 2/3 incorporation into the bead associated actin network should be a better indicator of WASp activity as it provides a historical record of

the nucleation events (within the stability window of the daughter filament).

The above model also explains the ARPC2 results seen with the cytochalasin D inhibited reactions. As cytochalasin D inhibits actin polymerisation downstream of Arp2/3 activation (Cooper, 1987) it will not affect the binding and activation of Arp2/3 by WASp. However, as WASp detaches from the actin filament following nucleation, the Arp2/3 bound actin will no longer be fixed to the bead. As it is unable to elongate, multiple branch point will not form, and a complex actin network will not be generated. The resultant short sections of nucleated actin filaments will become dissociated from the bead and Arp2/3 will not be detected by the assay. This is demonstrated in figures 4.3a and 4.4b.

The use of ATP to sensitise the assay is, I believe, both appropriate and physiological. ATP is highly unstable in aqueous solution and a combination of lysis and centrifugation will cause the lysate to be significantly depleted of ATP. Free availability of ATP mimics the intracellular environment, and ATP supplementation of *Xenopus* egg lysate and bovine brain lysate has been used in pyrene based actin polymerisation assays (Suetsugu et al., 2001a; Ma et al., 1998a).

ATP appears to have at least two distinct effects on the assay. In figure 4.3a and figure 4.12b, ATP causes an increase in Arp 2/3 recruitment as well as an increase in actin polymerisation, for WT WASp coated beads. By contrast the WASp containing the GBD missense mutation S272P (which has caused XLN in a patient), shows a reduction of Arp 2/3 recruitment with increased ATP concentration, whilst maintaining an increase in actin pulldown (figure 4.12b). These results suggest that ATP acts, either directly or indirectly, to reduce the threshold for WASp induced Arp 2/3 activation, in addition to amplifying the rate of actin polymerisation post filament nucleation. Although ATP does not directly bind WASp, it is known to be essential for several steps in the actin polymerisation cycle. Monomeric actin must be ATP bound to allow binding to the WASp V domain. ATP binding to Arp2 and probably Arp3 is also essential for Arp2/3 activation and increases their affinity for WASp (Martin et al., 2006; Goley and Welch, 2006; Dayel and Mullins, 2004; Le et al., 2003; Dayel et al., 2001; Le et al., 2001), and therefore increasing ATP concentrations will reduce the threshold at which WASp is able to activate Arp 2/3. Finally ATP bound monomeric actin has a much greater ability to polymerise at the barbed end of established actin filaments than ADP bound actin.

The fact that Arp2/3 recruitment is increased with increasing ATP concentration suggests that the rate limiting step for actin polymerisation within this assay is

likely to be either actin binding to WASp, or ATP binding to Arp2/Arp3. As Arp2 and Arp3 have significantly lower affinities for ATP than monomeric actin, it is logical to assume that the primary site of ATP augmentation in this assay is Arp2 and / or Arp3 activation. This mechanism could be dissected further by performing experiments where the availability of g-actin to WASp is decreased, such as immunodepleted profillin from the U937 lysate or overexpression thymosinβ4 (to sequest g-actin) in the U937 lysate. This would isolate the effect of ATP directly on Arp2 and Arp3.

The decrease in ARPC2 recruitment by S272P coated beads with increasing ATP concentration suggests that the S272P WASp is so active that it overcomes the rate limitation of ATP binding to Arp2 / Arp3. If this is the case, then the primary effect of ATP will be downstream of Arp2/3 (i.e. filament elongation), and so more actin will be polymerised for each nucleation event, and the equilibrium point of the assay will be reached with less Arp2/3 bound.

From the kinetic data presented in figure 4.5 (and other data not shown) I decided to use 1 hour as a pragmatic cut off for the end of reaction. It is clear that different WASp constructs and individual experiments will take different amounts of time to reach the equilibrium point. From the data presented and also from other experiments performed, it still remains unclear whether the equilibrium point of the assay has been reached in experiments where there is a low (but significant) activity (for example figure 4.3a WT samples with less than 1mM ATP, 4.5c WT samples with ATP). It is however clear that less active constructs (or conditions) have less f-actin bound at the equilibrium point, as well as having slower kinetic and therefore the 1 hour cut-off is a valid surrogate measure of activity.

ATP depletion may be an important factor in determining the equilibrium point of the assay. The gradual decrease in actin signal seen with the S272P construct over time (figure 4.5b and d) is likely to be caused by the reduction in ATP concentration following a sustained period of active actin polymerisation and depolymerisation. As ATP levels fall, so the amount of f-actin sustained within the bead associated actin networks will fall, reducing the assay actin signal.

I have also demonstrated that this assay can be successfully used to assess the activity of NWASp constructs. NWASp construct with point mutations within the GBD showed similar levels of constitutive activity to XLN causing WASp missense mutations (Adamovich et al., 2009; Ancliff et al., 2006; Devriendt et al., 2001). This work also suggested some subtle difference in the activity and regulation between WASp and NWASp. Further work is required to determine whether or

not these differences are significant, and what the mechanism

In summary, from the experiments described in this chapter I have determined two sets of conditions for assessing *in vitro* WASp activity and the assays described in the following chapters, unless stated, have been performed under these conditions. The *standard conditions* (for assessing activity compared to WT WASp) use U937 lysate at $2x10^7$ cells/ml, supplemented with 1mM ATP with an incubation period of 1 hour. The *constitutively active conditions* (for detecting unregulated actin polymerisation activity) use U937 lysate at $1x10^7$ cells/ml, with no ATP and an incubation period of 1 hour. I have demonstrated that this assay offers a versatile tool for assessing WASp induced actin polymerisation within myeloid cell lysate. This experimental system potentially mimics the role of WASp in generating a physiological dendritic branched actin network, mimicking the cortical lamellipod network of haematopoietic cells (Iwasa and Mullins, 2007).

5 In vitro Actin Polymerisation Activity

5.1 Introduction

In this chapter I present the results of bead based actin polymerisation assays performed on all the WASp constructs generated during this project. As described in chapter 4.5.1 the constructs were grouped as constitutively active or standard panel constructs, and activities were compared within these two groups.

For the statistical analysis of data presented in this chapter I have shown results from ANCOVAs using two linear regression models – a main effects only model (labelled *"main effects"*) and a model including compensation for interaction between WASp concentration and experiment (*"interaction model"*) (fully explained in chapter 4.5). I have shown both because the similarity of the patterns of the results between each approach demonstrates the robustness of the statistical analysis. The interaction model offers a more accurate representation of the data, as discussed in chapter 4.5.

5.2 Constitutively active WASp mutants

The activity of a series of WASp constructs predicted to have constitutive actin polymerisation activity was tested against WT WASp and constitutively active WASp inhibited by cytochalasin D. Two of these constructs contained point mutations found in patients with X-linked neutropenia (I294T and S272P) (Ancliff et al., 2006). Y291E WASp mimics the phosphorylation of the 291 tyrosine residue, which is predicted to destabilize the autoinhibitory conformation of WASp and result in constitutive activity (Torres and Rosen, 2006; Torres and Rosen, 2003; Cory et al., 2002; Kim et al., 2000). The VCA bind deletion mutant (∆288-310) has the critical autoinhibitory binding site for the VCA domain deleted and is therefore predicted to be incapable of forming the WASp autoinhibited conformation. This deletion does not impinge on the Cdc42 binding site (see figure 3.1 and chapter 1.4.6 and 1.5.3).

As demonstrated in chapter 4, the standard actin polymerization assay without ATP supplementation is a good discriminator between constitutively active WASp constructs and those (such as WT WASp) which need activation to induce actin polymerization. This assay has been used to determine the relative activity of these constitutively active mutants.

5.2.1 Equilibrium activity

Figure 5.1 shows the results of an illustrative actin polymerization assay performed without ATP supplementation (chapter 2.7). Figures 5.1a and b show the immunoblots and Coomassie stained gels respectively and figure 5.1c shows a graph of the densitometry for actin and WASp performed on this experiment. They demonstrate that Y291E, S272P and I294T WASp mutants show a dose response between WASp input and actin output, and all appear to induce more actin polymerization than WT WASp. The VCA bind construct also appears to be constitutively active although only one WASp concentration was tested in this experiment.

The Coomassie stain detects all proteins bound to the beads at the end of the experiment, and several protein bands, other than WASp and actin can be easily seen. The prominent bands at 50 kDa *(iv)* and 24 kDa *(vi)* and the faint band at 32 kDa *(v)* appear to be related to non-specific binding to the beads, as their concentration is constant regardless of WASp or actin concentrations. The prominent band at 24 kDa may well be endogenous GST from the U937 lysate, as the GST tag used in the EF-Bos construct is known to run slightly larger than endogenous GST (see GST only lane). The band at 51 kDa *(vii)* appears to be either a WASp breakdown product or a WASp binding proteins which is independent of WASp activation, as its concentration correlates with that of WASp rather than actin protein concentration. It has also been seen on Western blots of beads alone (Chapter 3.2).

From the Coomassie stain it can be seen that in this experiment the amount of actin pulled down was significantly less than the total amount of WASp protein loaded on the beads. This suggests that a relatively small proportion of individual WASp proteins are activating Arp2/3 complexes and initiating actin nucleation. It also more clearly illustrates the difference in amount of actin polymerized between the constitutively active constructs and WT WASp. There are no obvious protein bands which correspond to WIP (migrates at approximately 60 kDa), TOCA (62 kDa) or Cdc42 (25 kDa, although this may be obscured by the putative endogenous GST band). Proteins of the Arp 2/3 complex are also difficult to identify (band viii may represent p34), demonstrating that the concentration of the Arp 2/3 complex proteins is significantly less than that of either WASp or actin. This supports the hypothesis that only a small proportion of the WASp proteins are activating Arp2/3 complexes.

Figure 5.1d demonstrates rhodamine phalloidin staining of the sepharose beads. Beads coated with I294T and S272P WASp show significantly greater fluorescence

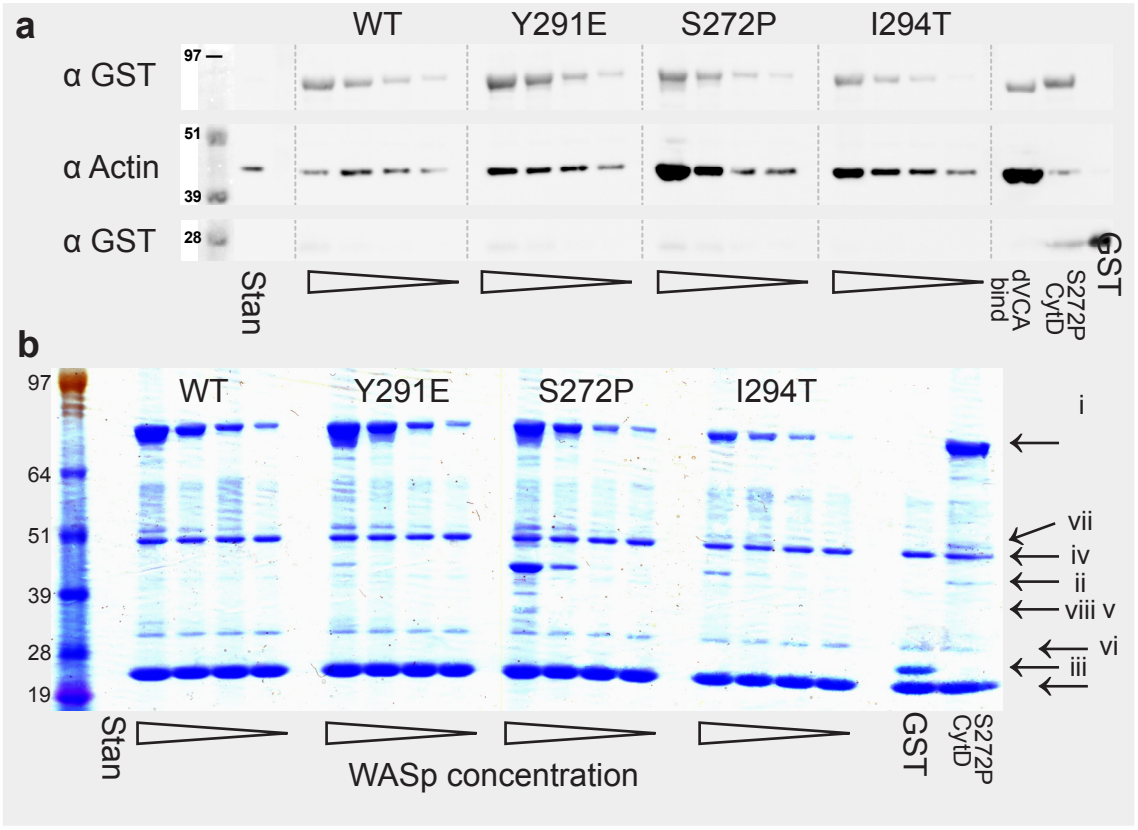

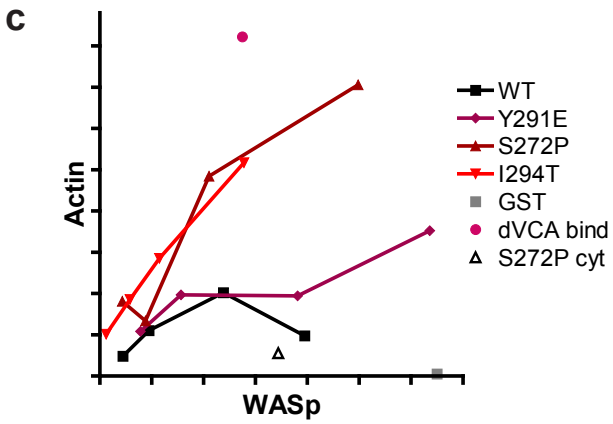

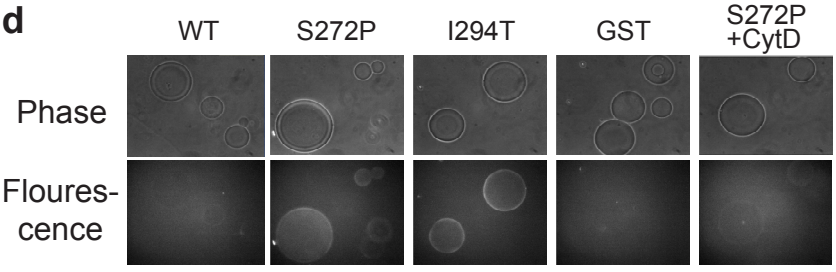

Fig 5.1 Actin polymerisation activity of constitutively active WASp point mutation constructs in the absence of ATP
A standardised volume of GST-WASp coated Sepharose beads were incubated with U937 lysate ($2x10^7$ cells/ml lysed in APB with 1% aprotinin, 1mM PMSF, 10µg/ml leupeptin, then clarified by centrifugation) supplemented with 5mM $MgCl_2$ only for 1 hour. Beads were then pelleted and washed twice with APB. 10% of the beads were fixed with 4% paraformaldehyde and stained with rhodamine phalloidin. The remainder were reduced in SB and resolved by NuPAGE and western blotting. 4 concentrations of WASp were tested for each construct (highest on the left, lowest on the right) with a constant bead volume of 8.3µl. **(a)** Immunblot showing bands of GST-WASp (78kDa), actin (42 kDa) and GST alone (25 kDa). **(b)** Coumassie stain from same experiment. *Band label (i) GST-WASp (ii) Actin (iii) GST (iv)-(vi) Non specific bead associated bands (iv 50kDa, v 32 kDa, vi 24kDa) (vii) 51 kDa (viii) 34 kDa.* **(c)** Densitometry plots from the above experiment, arbitary densitometry units. **(d)** Phase and flourescence microscopy of beads from the above experiment stained with rhodamine phalloidin (to stain f-actin). *CytD* cytochalsin D inhibited assay, *Stan* purified protein standard of 100ng GST-WASp and 50ng actin.

than WT WASp coated beads, which have show a similar level of fluorescence to the negative control beads. This result confirms the findings of the immunoblot, and demonstrates that the actin pulled down on the beads is f-actin.

5.2.2 Statistical analysis

Ten independent actin polymerization experiments involving some or all of these constitutively active WASp constructs were performed under similar conditions. Densitometry was performed on actin and WASp bands for these experiments and this data was processed and analyzed as described in Chapters 2.7.2, 4.4 and 4.5. The descriptive statistics and frequency distributions of this data are shown in the appendix (figures A.4 and A.5). A summary of the statistical terms used to describe the data processing and ANCOVA analysis can be found in figure 4.8.

Analysis of Covariance (ANCOVA) table
Dependent Variable % Ln Actin
Co-variable % Ln WASp
Experiment and Construct as fixed factors

	Excluding Cytochalsin D Controls						**Including Cytochalsin D Controls**					
	Main Effects Model			*Interaction Model*			*Main Effects Model*			*Interaction Model*		
	df	F	Sig.	df	F	Sig.	df	F	Sig.	df	F	Sig.
Corrected Model	14	23.90	.000	23	18.67	.000	15	22.34	.000	24	18.21	.000
Intercept	1	70.96	.000	1	17.72	.000	1	66.33	.000	1	14.15	.000
Experiment	9	24.71	.000	9	5.85	.000	9	24.73	.000	9	6.47	.000
Construct	4	28.28	.000	4	34.09	.000	5	23.79	.000	5	29.70	.000
% Ln WASp	1	38.91	.000	1	58.70	.000	1	40.01	.000	1	62.46	.000
Experiment * % Ln WASp				9	3.13	.003				9	3.44	.001
Adjusted R Squared			.745			.787			.729			.776

Fig 5.2 Statistical analysis of actin polymerisation assays performed on constitutively active mutants using lysate not supplemented with ATP
Data from 10 separate experiments, each with up-to 4 WASp concentrations per experiment was analysed. Data was separately analysed excluding cytochalasin controls (to asses differences between contructs and WT WASp) and including cytochalasin control (to assess differences between constructs and background signal). Analysis for a main effects only regression model and a model including an interaction term between experiment and WASp signal are shown. *df* = degrees of freedom, *F* = F ratio, *sig* = significance of contribution to overall variations (p value), *Ln* = natural logarithm. *R* = regresion cooefficient of correlation between Ln WASp and Ln Actin.

Figure 5.2 shows a summary of the analysis of covariance of actin concentration with WASp concentration, using the two linear regression models described in chapter 4. The full analysis can be found in the appendix (figure A.8). Both the main effects model and the interaction model account for the vast majority of

the variability within the data (F ratios of 23.9 and 18.7 respectively for the data excluding the cytochalasin D controls and similar values for the inclusive data). The high levels of significance ($p<0.001$) associated with each entire model and every factor within each model, demonstrates the strength of the relationship between WASp and actin concentrations, and the validity of the analysis. The high F ratios attributed to the construct adjustment (especially within the interaction model) indicates that the major deviation from a pure linear relationship between the natural logarithm of WASp concentration and the natural logarithm of actin concentration within this data set is due to the differences in activity between the WASp constructs. These findings are very similar to those seen with the complete standard panel dataset, presented in chapter 4.5.

Figure 5.3 graphically represents the differences in construct activity between each construct and WT WASp (Fig 5.3a and b) and cytochalsin D inhibited reactions (Fig 5.3c and d). S272P and I294T show a large and highly significant increase in activity compared to both WT WASp and the cytochalasin inhibited reaction. Both show an ability to polymerize actin approximately 10 times higher than the standard deviation of WT WASp activity. The dVCA bind construct appears to have even greater activity than either of the XLN point mutations, although this construct was only directly tested against both S272P and I294T in two independent experiments (hence the larger 95% confidence intervals). This finding was corroborated by other experiments assessing the dVCA bind construct as part of the standard panel of WASp constructs, which used the S272P construct as a positive control (figure 5.5a, data not included in this analysis).

The Y291E mutant is also significantly more active than WT ($p<0.1$), but the level of increased activity is much less than that for the S272P and I294T mutants. In fact, the phosphomimicking mutant is significantly less active than the S272P, I294T and dVCA bind mutants ($p<0.0005$ for all three constructs). The Y291E construct showed no difference in activity compared to the cytochalasin D inhibited reaction. This is likely to be because the cytochalasin D control was always performed with the S272P construct (so that a true inhibition could be detected). This construct has such a high level of constitutive activity, that some actin polymerization is detected despite the inhibition of actin filament elongation. This background activity in the inhibited control is illustrated in Figure 5.1a and 5.5a. This also explains why the WT WASp construct shows (insignificantly) less activity than the cytochalasin D inhibited control.

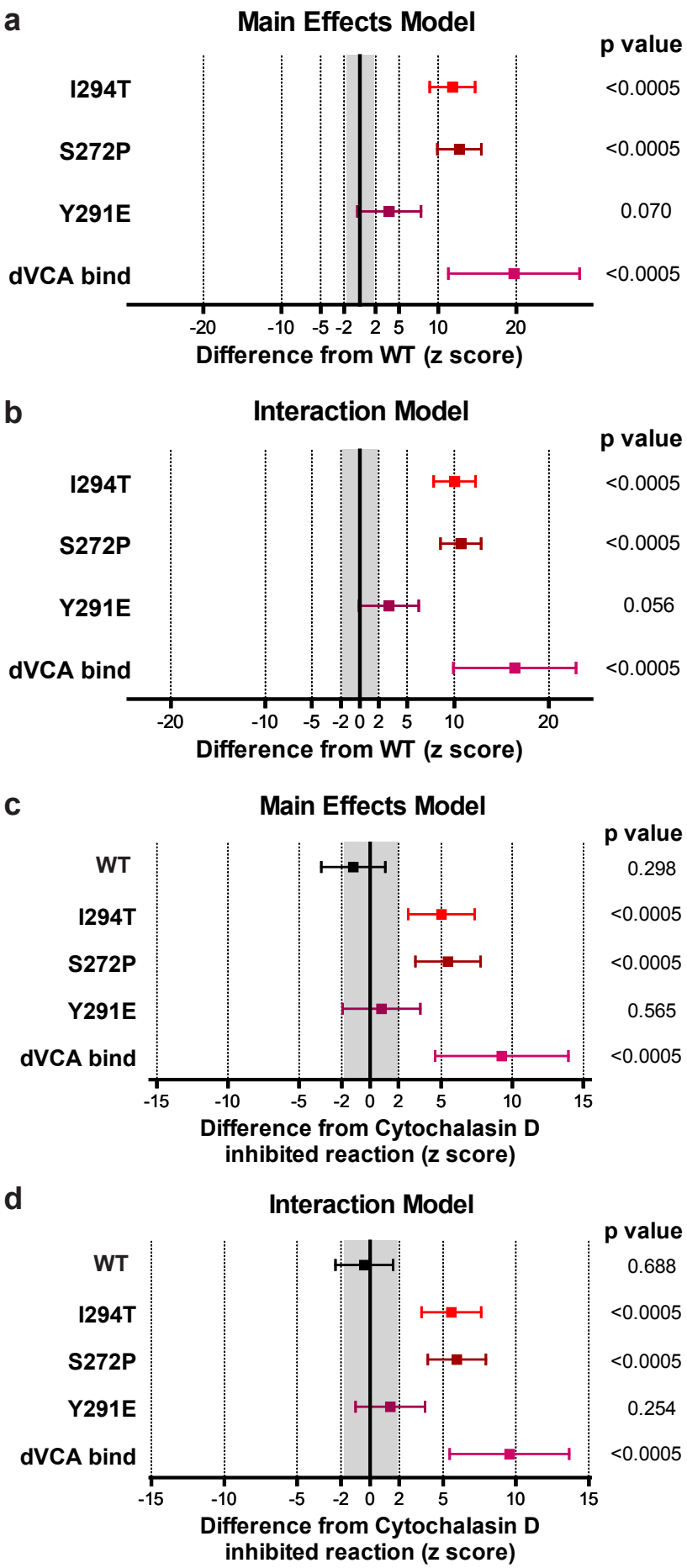

Fig 5.3 Actin polymerisation activity of constitutively active WASp constructs compared to WT WASp and Cytochalasin D inhibited reactions

Estimated marginal means of activity for each construct were calculated from the ANCOVA analysis and were expressed in terms of numbers of standard deviations from WT (or Cytochalsin D (CytD) inhibited) activity (z scores). Means and their 95% confidence intervals are plotted on the graphs and the 95% confidence interval (z score 2) for WT (or CytD) is shaded in grey for comparison. The significance of the differences of these means from WT or cytochalsin D inhibited activity was analysed using a least significant differences (LSD) pairwise comparison.

(a) and **(b)** show comparison of activity to WT WASp and **(c)** and **(d)** show comparisons to CytD activity. For both comparisons results from analyses using the main effects and interaction model are shown.

5.2.3 Activity in ATP supplemented lysate

As described in chapter 4 the ATP supplemented actin polymerisation assay was optimised to produce a large actin signal with WT-WASp to allow assessment of constructs less active than WT WASp. Figure 5.4 shows a series of experiments performed on the constitutively active WASp constructs using U937 lysate supplemented with 1mM ATP. Figure 5.4a illustrates that in the presence of ATP the S272P, Y291E and dVCA bind constructs all continue to polymerise more actin than WT WASp. Additionally they pull down more ARPC2 (p34) than WT WASp, suggesting that ATP potentiates Arp 2/3 activation and that a larger proportion of these WASp constructs are activated than WT WASp at the equilibrium point of the reaction.

Figure 5.4b shows a silver stained gel of an actin polymerisation assay directly comparing WT and constitutively active constructs with and without ATP supplementation. The addition of ATP increases the amount of actin pulled down by all constructs by several fold, resulting in an actin band much larger than the WASp input band. The similar actin band sizes for WT and the constitutively active mutants in the presence of ATP, suggests that WT WASp is approaching the maximum activity for the assay. Due to this “saturation” of the assay with ATP, there is less discrimination in activity between WT and the constitutively active WASp constructs.

Figures 5.4c and d show graphical representations of all these experiments combined. The results generally show a similar pattern to the experiments with the unsupplemented assay. S272P still shows a highly significant and large increase in activity compared to WT WASp, whereas the increase in activity seen with dVCA bind does not reach significance. In addition to the effect of assay saturation, the larger p values and wider confidence intervals seen in these experiments compared to the unsupplemented lysate experiments is partly because of relatively small numbers of experiments performed (n = 18 [S272P], n= 5 [Y291E], n = 6 [dVCA bind])

5.2.4 Kinetic activity

Figures 5.4e and f show a time course experiment for WT and S272P WASp using ATP supplemented lysate. This clearly demonstrates that although WT and S272P WASp coated beads polymerise similar amounts of actin at 60 minutes, the S272P construct has faster kinetics. This experiment can be compared to similar experiments using unsupplemented lysate in figure 4.5.

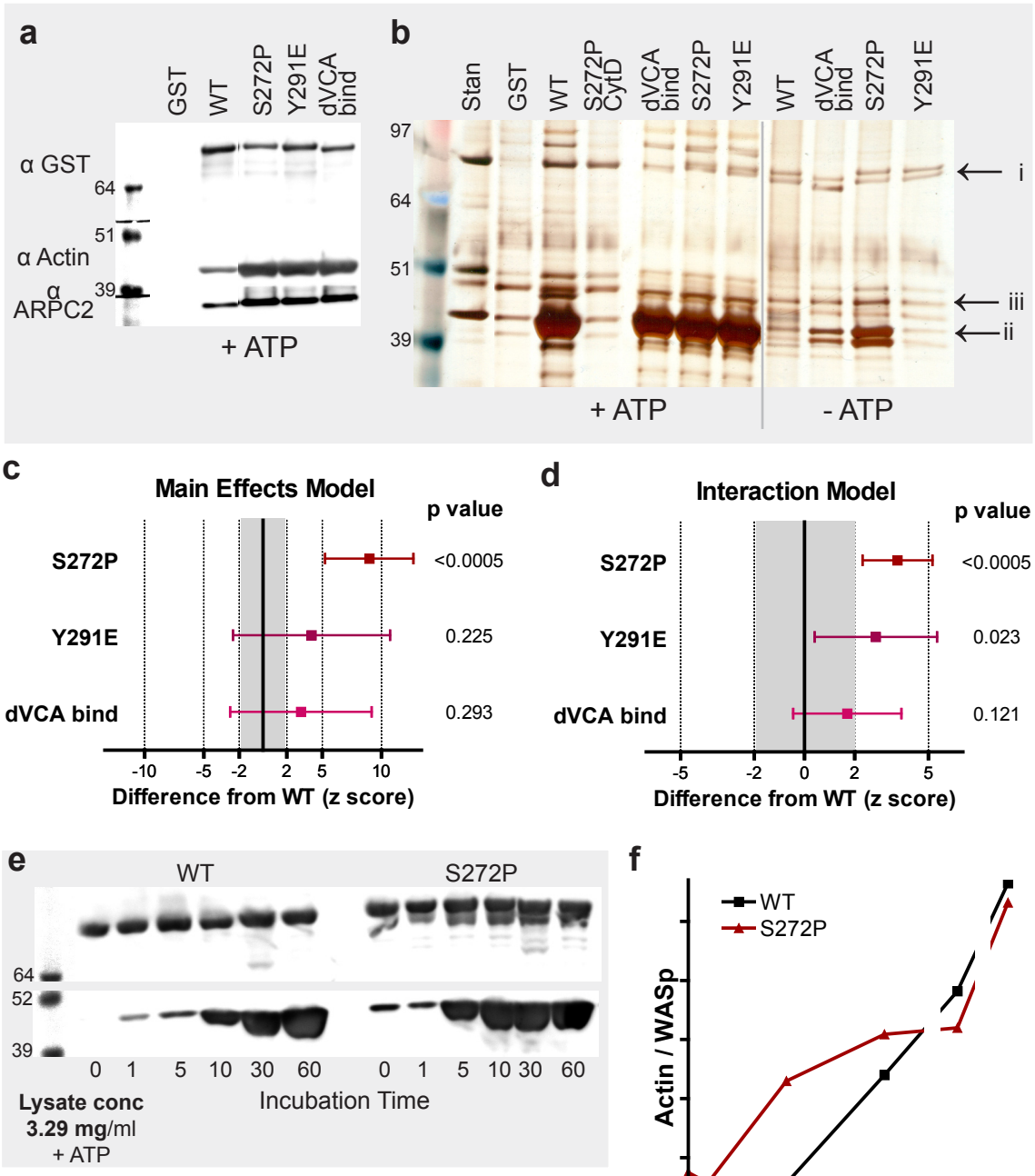

Fig 5.4 Actin polymerisation activity of constitutively active WASp mutants in the presence of ATP

A standardised volume of GST-WASp (WT or constitutively active mutants as labelled) coated Sepharose beads were incubated for 1 hour with U937 lysate ($2x10^7$ cells/ml lysed in APB with protease inhibitors, then clarified by centrifugation) supplemented with 5mM $MgCl_2$ +/- 1mM ATP. Beads were then pelleted and washed twice with APB, prior to reduction in SB and resolution by NuPAGE and western blotting. A single WASp concentration was tested. **(a)** shows an immunoblot of the experiment, whereas **(b)** shows a silver stained gel of the same experiment. *Band i - GST-WASp; band ii - actin; band iii - non specific / WASp degradation band.* **(c)** and **(d)** Estimated marginal mean activity compared to WT for constitutively active mutants, in the presence of ATP. These results are from the ANOVA analysis shown in chapter 4.5.5 and fig 4.11c. Methodology is described in chapter 4.5.5 and 4.5.6 and is identical to that used in figures 5.3 and 4.13. **(e)** Time course of actin polymerisation assay in the presence of ATP for WT and S272P constructs. 6 identical actin polymerisation assays were performed for each construct using the same experimental protocol as described in **(a)** and **(b)**. Reactions were stopped by washing beads at variuous durations of incubation. **(f)** Densitometry plot from experiment in (e). Actin / WASp units are a ratio of arbitary densitometry units.

5.3 Clinical point mutations and domain deletion constructs

The “standard panel” of WASp constructs was made up of four point mutations in the EVH1 domain which in humans cause either WAS or XLT (clinical mutants), as well as deletions of the EVH1 domain, the basic domain, the polyproline domain, the VCA domain and a point mutation which inhibits Cdc42 binding (H246D) (see figure 3.1). The activity of each of these constructs was compared to that of WT WASp, GST coated beads and WT WASp in the presence of cytochalasin D (as negative controls) and S272P WASp (as a positive control).

For the description of these results the constructs will be discussed in two groups – the clinical mutants and the dEVH1 domain construct, and the remaining domain deletion constructs and the H246D mutant.

5.3.1 Activity in the absence of ATP

Figure 5.5a shows the activity of each of the constructs in U937 lysate without ATP supplementation. It clearly shows that all WASp constructs in the standard panel and WT WASp show minimal actin polymerisation above background levels. The VCA bind construct, by contrast, shows strong actin polymerisation activity and even the cytochalasin D inhibited S272P construct shows more activity than any of the standard panel constructs.

5.3.2 Equilibrium activity in the presence of ATP

The above experiment repeated with ATP supplemented lysate is shown in figures 5.5b (immunoblot) and 5.5c (silver stained gel). A sample experiment showing each construct tested over a range of WASp concentrations is shown in figure 5.5d and the densitometry from this experiment is shown in figure 5.5e. Although each experimental sample was performed synchronously with the same lysate, the samples had to be split between two gels (due to lack of well space), with the standard wells used to compare results between gels.

The clinical mutants show at least as much activity as WT WASp, whereas the dEVH1 construct shows impaired (but some) actin polymerisation activity. Of the domain deletion constructs the dBasic and H246D mutants show similar or slightly increased activity compared to WT WASp, whereas the dPolyP construct shows less activity than WT. Like the dEVH1 construct, the dPolyP construct does appear to polymerise more actin than the negative control samples. The dVCA construct shows the least activity of all WASp constructs tested, and in the experiments shown in figures 5.5b and c shows no increase in activity above the

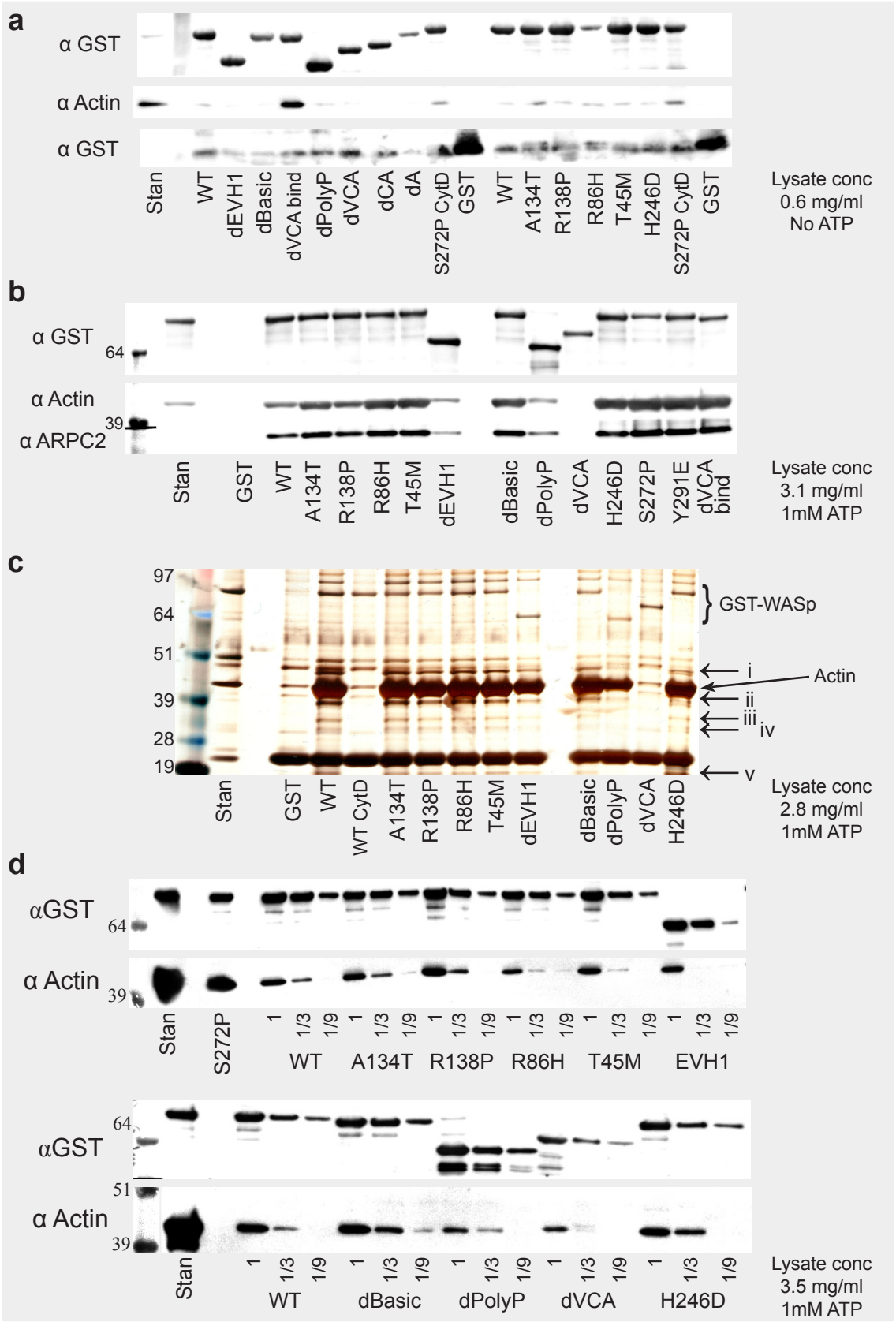

Fig 5.5 Western blots of actin polymerisation assays for standard panel of constructs
(a) Assay using U937 lysate without ATP. Top αGST panel shows GST-WASp, bottom panel shows GST. **(b)** Assay using U937 lysate supplemented with ATP. **(c)** Assay using U937 lysate supplemented with ATP (silver stain). *Bands (i) - (v) are activation associated bands.* (Experiments **a, b** and **c** are using single WASp concentration per construct). **(d)** Sample assay using U937 lysate supplemented with ATP, three WASp protein concentrations for each construct.

negative control.

Figure 5.5c demonstrates that with ATP supplemented U937 lysate, for each active constructs the actin band pulled down is significantly larger than the bead bound WASp band. Differences in protein bands visible on the silver stained gel between the experimental columns and the GST only or standard (purified WASp and actin protein) columns, may give clues about other regulatory proteins involved in WASp activation or actin polymerisation. Once again there is no prominent band around 60kDa in any column which may represent either WIP or TOCA. Bands at 39kDa *(ii)*, 34kDa *(iii)*, and 17kDa *(v)* all appear to be pulled down only when there is active actin polymerisation. These may well correspond to components of the Arp2/3 complex (p41, p34 and p16 respectively). A 30kDa band *(iv)* and the lower of a double band at approximately 46kDa *(i)* are also associated with active actin polymerisation, but do not have the appropriate sizes for Arp2/3 components. Each of these activation associated bands is best appreciated by comparing the WT column with the GST and cytochalasin inhibited columns.

As with the constitutively active constructs, fluorescence microscopy of rhodamine phalloidin stained Sepharose beads confirmed the results seen by western blotting and immunoblotting (data not shown).

5.3.3 Statistical analysis

The activity of the standard panel constructs was assessed over 21 independent experiments, and quantification and analysis was performed as above. Figure 5.7 shows a summary of the results table from the ANCOVA analysis performed on this data. The full statistical analysis can be found in the appendix (figure A.9), and further details of interpretation of this analysis are discussed in chapter 4.5. Once again the high F ratios for the corrected models demonstrate that the vast majority of variation seen within the data can be accounted for by the model, and the significance of the models show that once correction for experiment and construct are accounted for there is a tight correlation between (the natural logarithms of) WASp and actin concentrations.

Figure 5.6 shows a graphical representation of the estimated differences in mean activity of each construct compared to WT WASp (figures 5.6a and b) and the cytochalasin D inhibited reaction (background activity)(figures 5.6c and d).

Three of the four clinical mutants show significantly greater activity than WT WASp ($p<0.05$), whereas the increased activity of R86H does not reach significance. All four mutants show significantly greater activity above background actin

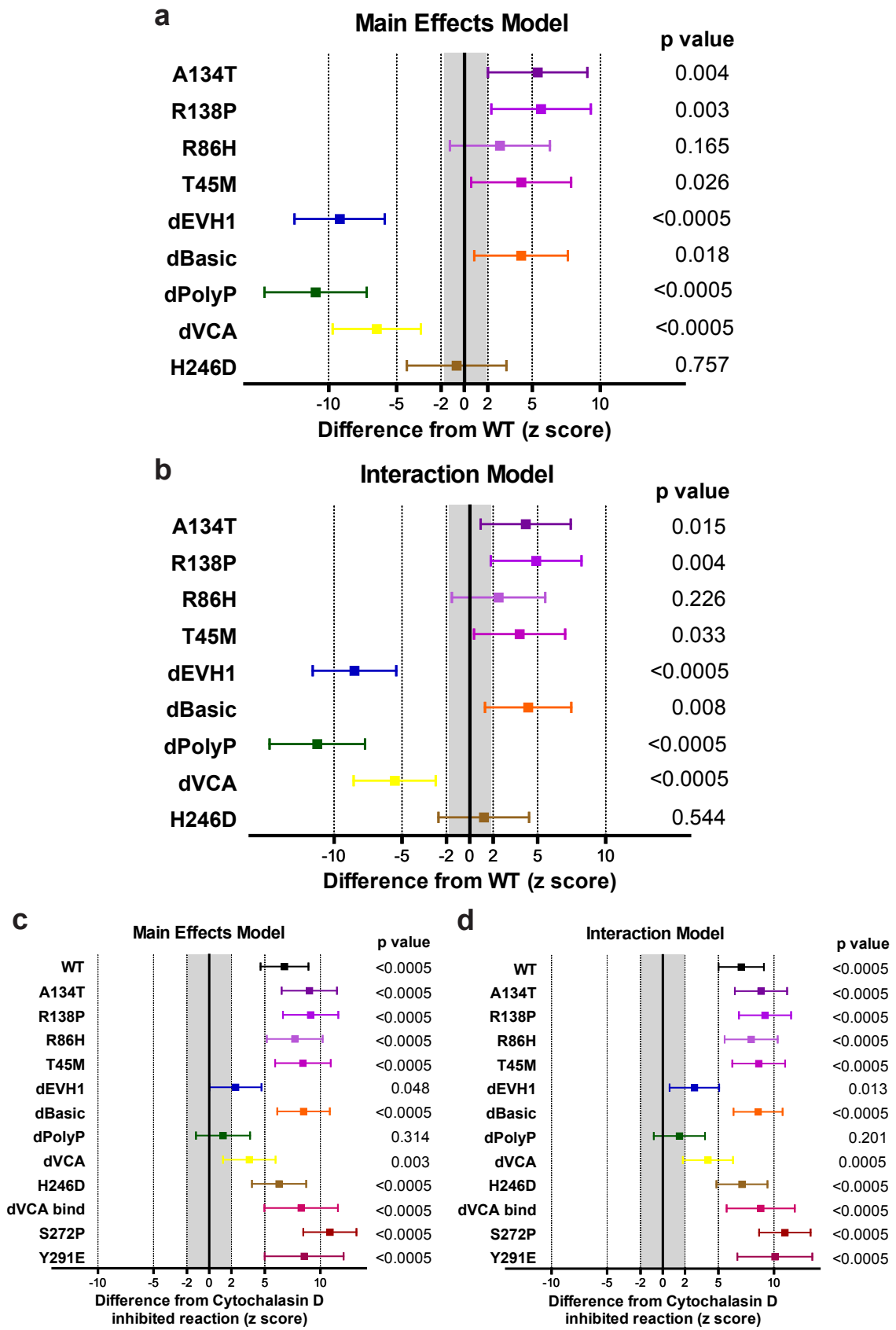

Fig 5.6 Actin polymerisation activity, with ATP supplementation, of standard panel of WASp constructs compared to WT WASp and Cytochalasin D inhibited reactions
Graphs were generated as described in Fig 5.3, and the ANCOVA table is shown in Fig 5.6. **(a), (b)** show comparison of activity to WT WASp. **(c)**,**(d)** show comparisons to CytD activity. For both comparisons results from analyses using the main effects and interaction model are shown.

Analysis of Covariance (ANCOVA) for the Standard panel of constructs
Dependent Variable % Ln Actin
Co-variable % Ln WASp
Experiment and Construct as fixed factors

	Excluding Cytochalsin D Controls						Including Cytochalsin D Controls					
	Main Effects Model			*Interaction Model*			*Main Effects Model*			*Interaction Model*		
	df	F	Sig.	df	F	Sig.	df	F	Sig.	df	F	Sig.
Corrected Model	30	26.97	.000	49	22.68	.000	34	29.52	.000	54	24.50	.000
Intercept	1	11.83	.001	1	0.29	.591	1	13.23	.000	1	1.89	.171
Experiment	20	24.63	.000	19	6.94	.000	20	25.97	.000	20	6.72	.000
Construct	9	15.55	.000	9	16.75	.000	13	17.65	.000	13	18.89	.000
% Ln WASp	1	115.02	.000	1	25.69	.000	1	120.17	.000	1	39.82	.000
Experiment * % LN WASp				19	4.03	.000				20	3.92	.001
Adjusted R Squared			.767			.818			.729			.776

Fig 5.7 Statistical analysis of actin polymerisation assays performed on standard construct panel using ATP supplemented lysate
Data from 21 separate experiments. Data was separately analysed excluding cytochalasin controls (to asses differences between contructs and WT WASp) and including cytochalasin control (to assess differences between constructs and background signal). Analysis for a main effects only regression model and a model including an interaction term between experiment and WASp signal are shown. *df* = degrees of freedom, *F* = F ratio, *sig* = significance of contribution to overall variations (p value), *Ln* = natural logarithm. *R* = regresion cooefficient of correlation between Ln WASp and Ln Actin.

polymerisation. The level of increased activity of these mutants was less than that of the two XLN mutants, but similar to that of the phosphomimicing mutant (3 standard deviations higher than WT activity). The dEVH1 construct shows significantly less activity than WT WASp ($p<0.0005$), but does show greater activity than background ($p<0.05$). It appears to have approximately 8 standard deviations less activity than WT WASp, but two standard deviation greater activity than the cytochalasin D inhibited reaction.

The dBasic construct has a similar activity to the clinical mutants with significantly greater activity than WT WASp. The H246D mutant has very similar activity to WT WASp with no significant difference between the two. The dPolyP and dVCA deletion constructs both have very significantly less activity than WT WASp, and the dPolyP construct shows no significant increase in activity above the cytochalasin D inhibited assays. The dVCA domain construct shows greater activity than would have been expected. An observation from several experiments was that the dVCA construct seemed to have disproportionate actin polymerisation activity at low concentrations, whilst no activity was detected when the highest concentration of dVCA was used. When an ANVOCA analysis is repeated using data only from beads coated with the highest WASp concentrations, the dVCA construct has

less activity than both the dEVH1 and dPolyP constructs and has no significant difference in activity from the inhibited control reactions (data not shown).

5.3.4 Kinetic activity

Figure 5.8 shows time course data for each standard panel construct, for assays performed with ATP supplemented lysate. These results show that the clinical mutants and WT WASp show a similar kinetic of actin polymerisation, with maximal rate of actin polymerisation being achieved between 30 and 60 minutes incubation. This is slower than the kinetic seen for the constitutively active construct S272P (figure 5.8c). The dBasic construct shows an intermediate kinetic between WT and S272P, and surprisingly the H246D show a rapid onset of actin polymerisation, similar to that of S272P. This data must be treated with caution, as it represents only a single experiment. Nonetheless, with the exception of the H246D construct, the activity of constructs at one hour correlate to the speed of actin polymerisation in the kinetic experiments. All constructs show a markedly slower kinetic than that seen with pyrene based actin polymerisation assays, as discussed in chapter 4.9.

5.4 Conclusion

The results presented in this chapter demonstrate that the bead based actin polymerisation assay is a robust tool in assessing differences in activity between different WASp constructs. Using unsupplemented U937 lysate it clearly differentiates constitutively active and inactive WASp constructs, and with ATP lysate supplementation, relative differences in susceptibility to activation of natively autoinhibited constructs are detected. The addition of ATP to lysate appears to lower the threshold for the detection of WT WASp activation in the absence of an excess of exogenous WASp activators such as Cdc42 and $PIP_{2.}$ The use of an ANCOVA statistical analysis overcomes the problems associated with variable activity between assays and differences in amount of WASp input for different constructs in the same assay. The activity differences detected between experimental WASp constructs and WT show high levels of statistical significance and corroborate the subjective observation of Western blots from individual experiment.

5.4.1 Constitutively active constructs

The first conclusion from these experiments is that the activation of WT WASp is significantly regulates in physiological lysate compared to the constitutively active WASp constructs. This is presumably because its constitutive conformation is autoinhibited. In the unsupplemented assay, WT WASp showed no significant

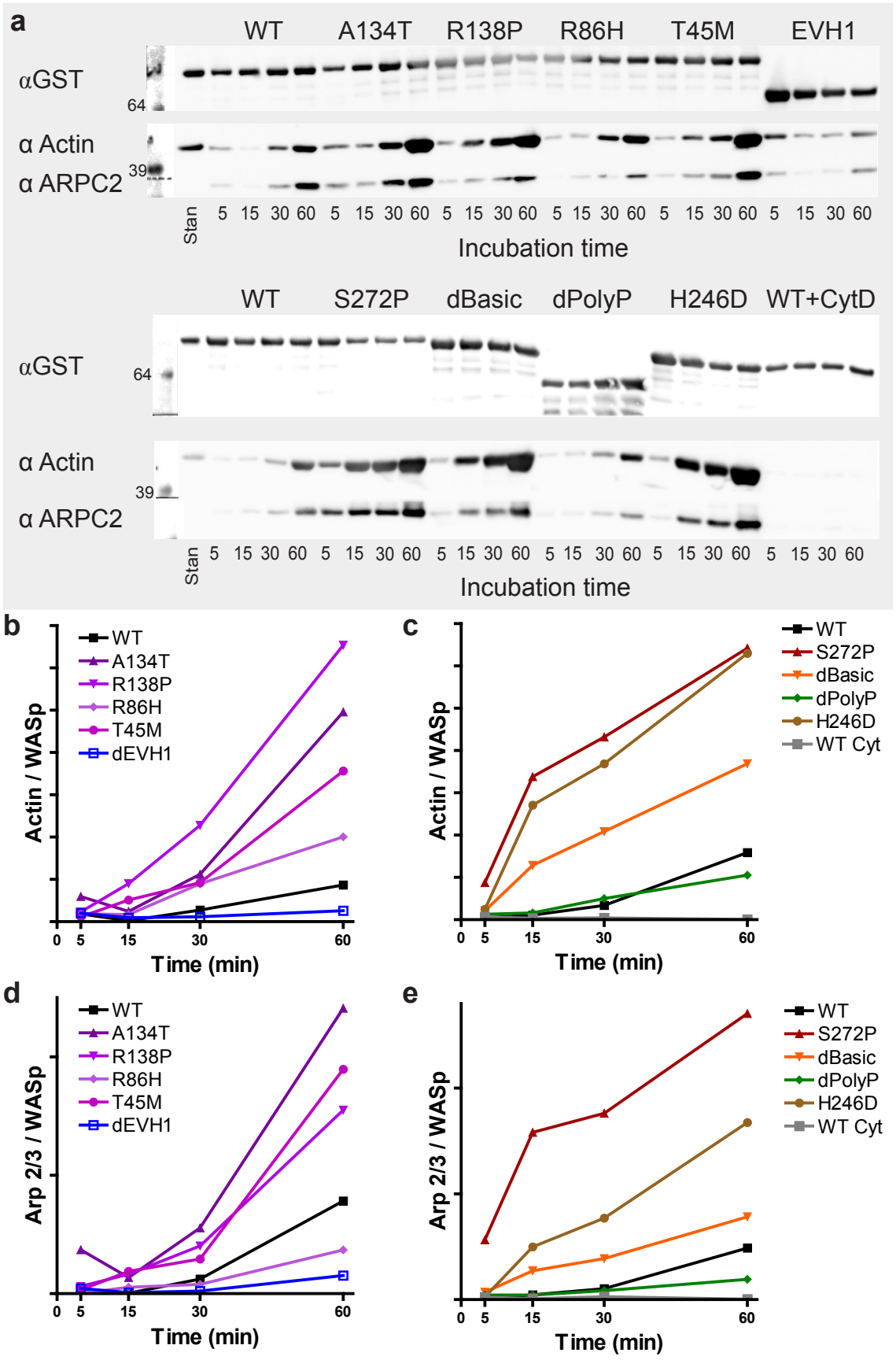

Fig 5.8 Kinetics of ATP supplemented actin polymerisation assay
(a) Immunoblots of time course experiments for the standard panel of WASp constructs (2 separate experiments). **(b) - (e)** Time courses for Actin / WASp and Arp2/3 / WASp ratios derived from densitometry performed on experiments shown in (a)

activity greater than that of a cytochalasin D inhibited reaction (figure 5.3c,d). By contrast, WASp constructs predicted to have an unstable autoinhibitory conformation show very significant activity under these conditions. Prior to the commencement of this project, results from two WASp constructs demonstrating constitutive activity had been published. *Devriendt et al* demonstrated constitutive activity and reduced structural stability of the first identified missense mutation causing XLN (L270P) (Devriendt et al., 2001). Predictions from the tertiary structure of the WASP GBD bound to the VCA, suggest that L270 would form part of the α1 helix of the autoinhibitory pseudodomain, and mutation of this residue to a bulky proline residue would disrupt this structure (Kim et al., 2000).

Tyrosine phosphorylation of the Y291 residue has also been demonstrated to destabilise the WASp autoinhibitory conformation (Torres and Rosen, 2006; Torres and Rosen, 2003; Cory et al., 2002). This residue is found within the α3 helix of the autoinhibitory pseudodomain, and phosphorylation of this residue will introduce a highly ionic charge into an amphipathic tertiary structure, inducing structural instability. Substitution of the tyrosine residue for a glutamic acid residue mimics this ionic change, and the resultant Y291E WASp mutant shows constitutive activity both *in vitro* and *in vivo* (Cory et al., 2002).

The results presented here demonstrate constitutive activity of two further missense mutations (S272P and I294T) which cause XLN in patients. These mutations are predicted to disrupt the α1 and α3 helices respectively, and are predicted to have an unstable autoinhibitory conformation (Ancliff et al., 2006; Kim et al., 2000). The activity of these two mutants was compared to that of the Y291E phosphomimicking mutant and a novel construct in which the WASp sequences essential for Cdc42 binding are preserved, but those uniquely involved in VCA (autoinhibitory) binding are deleted. Interestingly the XLN missense mutants showed greater activity than the Y291E residue, but less than the dVCA bind construct. These constructs therefore form a continuum of constitutive activity, suggesting that the autoinhibition of WASp does not function as an “on – off switch”, but rather as a “rheostat” grading the susceptibility of WASp to activation.

These conclusions provide functional evidence in a physiological system to support kinetic and stability studies performed on purified WASp protein which suggested a similar model of activation (Torres and Rosen, 2006; Torres and Rosen, 2003). This has important implications in understanding the role of tyrosine phosphorylation in regulating WASp activity. Phosphorylation induces a partial destabilisation of the autoinhibitory conformation, reducing the threshold for WASp activation, but not rendering it uncontrollably active. This suggests that

tyrosine phosphorylated WASp can exist in both open and closed conformations, and still be potentially activated by Cdc42, SH2-SH3 adapter proteins, PIP_2 and other WASp regulatory proteins. The interaction of Cdc42, protein kinases and WASp phosphorylation is further discussed below and in chapter 7.6.

5.4.2 The H246D construct and the role of Cdc42

The H246D WASp mutant has indistinguishable activity from WT WASp in these experiments. This construct is unable to bind Cdc42 as demonstrated in figure 7.1 and as has been previously published (Kato et al., 1999). These results suggest that the WASp induced actin polymerisation assessed by the bead based actin polymerisation assay is Cdc42 independent. Several previous studies have demonstrated similar Cdc42 independent WASp or NWASp activation in a variety of experimental systems (Badour et al., 2004; Kempiak et al., 2003; Benesch et al., 2002; Cory et al., 2002; Fukuoka et al., 2001; Cannon et al., 2001; Rohatgi et al., 2000; Moreau et al., 2000; Kato et al., 1999). As discussed above, WT WASp and the majority of experimental WASp constructs do not behave in a constitutively active manner and can therefore be assumed to be autoinhibited, requiring activation by mediators in the U937 lysate. PIP_2, Nck, Grb2, Hck and Lck have all been shown to activate or destabilise the autoinhibition of WASp or NWASp, independently of Cdc42 (Torres and Rosen, 2006; Kempiak et al., 2005; Benesch et al., 2002; Cory et al., 2002; Rohatgi et al., 2001; Rohatgi et al., 2000; Higgs and Pollard, 2000). PIP_2 and Nck cooperatively activated NWASp in a purified protein system, resulting in maximal activation and rendering Cdc42 redundant (Rohatgi et al., 2001). Similar cooperativity inducing maximal NWASp activation has been demonstrated for Nck and Grb2 (Kempiak et al., 2005; Benesch et al., 2002).

PIP_2, SH2 – SH3 adapter proteins and protein kinases are all potential activators of WASp in this experimental system. The U937 lysate used was not subjected to a prolonged high speed ultracentrifugation step, as *Xenopus* and bovine brain lysates have been in previously described lysate actin polymerisation assays (Suetsugu et al., 2001b; Ma et al., 1998a), and therefore is likely to contain some endogenous lipid vesicles containing PIP_2. The role of PIP_2 in this assay could be explored in a number of ways. Firstly, the activity of WT, dBasic and H246D WASp constructs could be compared in lysate prepared with and without high speed ultracentrifugation. Secondly, PIP_2 vesicles could be synthesised using standard protocols and these could be added at increasing concentrations to U937 lysate prior to incubation with WASp coated beads. PIP_2 binding could be assessed simultaneously using a cosedimentation lipid vesicle binding assays

(Prehoda et al., 2000).

The silver stained gels of figure 5.3b and 5.5c may give some clue as to the identity of possible WASp activators. Two bands were identified which were only pulled down by WASp when actin was polymerised, and were the wrong size for components of the Arp 2/3 complex (in figure 5.5c band labelled *(iv)* and the lower of the double band labelled *(i)*). The sizes of these bands are approximately equal to the molecular weights of Nck (44kDa) and Grb2 (28kDa), and are completely absent from the dPolyproline construct lane. This hypothesis could be investigated by performing the assay using lysate pre-treated by immunoprecipitation with anti-Nck, anti-Grb2, both or isotype control antibodies.

5.4.3 Clinical missense mutations and the EVH1 domain

All four missense mutation which lead to WAS / XLT (clinical mutations) showed a small but significant (in three out of four constructs) increase in actin polymerisation activity compared to WT WASp. Prior to this study the *in vitro* activity of clinical WASp mutants had not been assessed. There are several possible explanations for these findings.

The best established effect of EVH1 missense mutations on WASp function is to reduce its affinity for WIP (de la Fuente et al., 2007; Kim et al., 2004; Luthi et al., 2003; Volkman et al., 2002; Rong and Vihinen, 2000; Stewart et al., 1999). WIP stabilises the autoinhibitory conformation of WASP *in vitro* and *in vivo* (Lim et al., 2007; Martinez-Quiles et al., 2001) and inhibits WASp induced actin polymerisation *in vitro* (Martinez-Quiles et al., 2001). Therefore missense mutations which inhibit WIP binding might be expected to show greater activity than WT WASp. Against this hypothesis, it has been impossible to detect WIP binding to WT WASp within the bead based actin polymerisation assay using U937 lysate, despite its abundant presence in the lysate (see chapter 6.1, 6.4 and figures 6.1 and 2.12c). Nonetheless, impaired WASp – WIP association in clinical mutants could still be responsible for the increased actin polymerisation activity they show. It is possible that the association between WASp and WIP in the assay is of low affinity and that binding is disrupted during the bead washing steps prior to SDS-PAGE resolution. Published experiments demonstrating WASp – WIP interaction suggest that the interaction is strong and not disrupted by simple wash steps (de la Fuente et al., 2007; Sasahara et al., 2002; Martinez-Quiles et al., 2001; Ramesh et al., 1997), and experiments I have performed minimising wash steps have not elucidated WIP binding (data not shown).

A second possibility is that transient WIP association with WT WASp could be

involved in recruitment of a third (unknown) WASp inhibitory factor. This factor could then bind to WASp and stabilise its autoinhibition, without the ongoing binding of WIP. In the clinical mutants, impaired WIP binding would result in reduced recruitment of this inhibitory factor. This hypothesis is possible, but at present there is little or no supporting evidence for it. One group of candidate inhibitors are the ERM family of proteins which have been described as binding to the WASp EVH1 domain and inhibiting WASp activation (Manchanda et al., 2005). Testing the relative affinity of ERM proteins for WT and clinical mutant WASp would be possible within this experimental system.

An alternative hypothesis is that the missense mutations in the EVH1 domain induce a conformational change in WASp which slightly destabilises the autoinhibitory conformation and therefore reduces the threshold for WASp activation. I feel this possibility is unlikely as the EVH1 domain missense mutations are separated from the GBD by at least 100 amino acids, however as we have no data on the tertiary structure of a WASp construct containing both an EVH1 domain and a GBD, this is impossible to rule out. Several lines of evidence have suggested an intrinsic role for the EVH1 domain in WASp activation (Yarar et al., 2002; Benesch et al., 2002; Suetsugu et al., 2001a; Kato et al., 1999). It has been proposed that the mechanism underlying this is that the EVH1 domain acts by correctly aligning the Arp 2/3 complex, facilitating its binding and activation by the WASp CA domain (Suetsugu et al., 2001a). Perhaps a more plausible explanation for the increased activity of EVH1 missense mutations is that they enhance the association of WASp with the Arp 2/3 complex, lowering its threshold for activation.

A fourth possible explanation of these results is that the increased activity of the clinical mutant WASp relates to dysregulation of WASp phosphorylation. The EVH1 domain is known to bind to and inhibit the activity of Src family tyrosine kinases (Schulte and Sefton, 2003). EVH1 missense mutations could conceivably impair their inhibition, whilst maintaining their recruitment to WASp, resulting in increased tyrosine phosphorylation and WASp activation. Interestingly, preliminary data suggests that clinical mutant WASp has increased S483/484 phosphorylation when expressed in U937 cells (figure 8.7a), suggesting another mechanism of enhanced activity. Both these mechanisms are more fully discussed in chapter 8.7.4.

The results presented in this chapter clearly show that, in contrast to the clinical missense mutations, deletion of the entire EVH1 domains significantly decreased activity compared to WT. Similar findings have been demonstrated in some (Yarar et al., 2002; Benesch et al., 2002; Suetsugu et al., 2001a; Moreau et al., 2000; Kato

et al., 1999), but not all (Cannon et al., 2001; Castellano et al., 2001; Rohatgi et al., 2000; Zhang et al., 1999) studies assessing the functionality of dEVH1 constructs (see figure 1.5). As described above, a mechanistic model has proposed a direct role for the EVH1 domain in WASp activation (Suetsugu et al., 2001a). Two of these studies demonstrate that sensitivity to the cooperative activation of NWASp by Cdc42 and PIP_2 is normal in dEVH1 constructs, suggesting that these two mediators render redundant any intrinsic activation activity of the EVH1 domain (Suetsugu et al., 2001a; Rohatgi et al., 2000).

Taken together this data suggests that the EVH1 domain has a significant, but not essential role in WASp activation, and that this can be overcome by PIP_2 and Cdc42. As the bead based actin polymerisation assay appears to be a Cdc42 independent system (see chapter 5.4.2 and 7.6), defects in activity with dEVH1 constructs are detected. The variability in activity seen with dEVH1 constructs both between individual experiments within this study and between different experimental systems, may reflect difference in the presence of $PIP_{2,}$ which can be practically difficult to exclude and quantify in lysate systems. As WIP appears to inhibit NWASp activation (Martinez-Quiles et al., 2001), and enhanced actin polymerisation associated with WIP appears to be due to regulated localisation (Tsuboi, 2006; Vetterkind et al., 2002; Moreau et al., 2000), I feel it is unlikely that the impaired activity of the dEVH1 construct in this assay is due to its abolished WIP binding. The difference in activity between the dEVH1 contruct and the clinical missense constructs also supports this proposal.

5.4.4 Deletion of Basic, Polyproline and VCA domains

In contrast to deletion of the EVH1 domain, deletion of the basic domain results in a significantly enhanced ability of WASp to polymerise actin. This increased activity was approximately equal to that of the most active clinical missense mutation constructs. Previously published data on dBasic domain WASp and NWASp constructs has yielded mixed results. Some systems have demonstrated increased activity in purified protein actin polymerisation assays but impaired activity in whole lysates systems (Suetsugu et al., 2001b; Rohatgi et al., 2000). Other experiments have demonstrated no effect on activity with basic domain deletion (Benesch et al., 2002; Kato et al., 1999).

Three discrete roles for the basic domain in WASp activation have been proposed. Firstly it binds PIP_2 (demonstrated in NWASp, but not in WASp) resulting in activation (Papayannopoulos et al., 2005; Otsuki et al., 2003; Rohatgi et al., 2000; Prehoda et al., 2000). Secondly it intrinsically inhibits WASp activation by

stabilising the GBD – VCA autoinhibitory fold (Leung and Rosen, 2005; Suetsugu et al., 2001b; Prehoda et al., 1999). Finally it has a critical role in recruiting Cdc42 to WASp to allow Cdc42 binding to the GBD, resulting in activation (Hemsath et al., 2005). The impaired activity of basic domain deleted NWASp constructs has always been demonstrated following PIP_2 initiated polymerisation in lysate systems. Enhanced activity has only been seen in purified protein systems with spontaneously initiated actin polymerisation, without the addition of Cdc42 or PIP_2. Taken together, this suggests that in isolation the dBasic constructs have reduced autoinhibition, but in lysate systems inhibitory factors (such as WIP binding to the EVH1 domain) are present which then require PIP_2 and / or Cdc42 to allow NWASp activation. Deletion of the basic domain impairs the recruitment of these activators, preventing the displacement of the inhibitory factors and therefore increasing the threshold for NWASp activation.

If PIP_2 were an important activator in the bead based actin polymerisation assay, I would have expected the dBasic domain construct to be less active than WT. From the discussion above it is clear that the bead based assay is independent of Cdc42, and the dBasic domain results suggest that activation is also PIP_2 independent. This also helps to explain the impaired activity of the dEVH1 domain construct, as previously published data suggests that PIP_2 can overcome the inhibitory effects of deleting the EVH1 domain. It is more difficult to explain why the U937 lysate does not impart an inhibitory effect on the dBasic construct in the assay. Although WIP is present in U937 lysate, it does not appear to bind to WASp (figure 6.1), and this may explain why the dBasic construct remains active. Alternatively there may be another as yet unidentified inhibitory mediator which is present in the *Xenopus* and bovine brain lysate systems but not U937 lysate, whose binding to WASp is disrupted through interaction of PIP_2 or Cdc42 with the basic domain.

Finally, all of the previously published work on dBasic domain constructs has been performed on NWASp, and it is very plausible that the regulation of WASp differs from that of NWASp. The proposed mechanistic models for role of the basic domain in NWASp regulation may not be directly transferable to WASp, and therefore may not be valid for interpreting the results of the bead based actin polymerisation assay.

Deletion of the polyproline and VCA domains led to profound impairment of WASp activation. The polyproline domain is the binding site for a large number of mediators known to modulate WASp function (see figures 1.4 and 1.6), and it is important in both activation mechanisms and localisation of WASp. Previous

studies using polyproline domain deleted construct have demonstrated impaired or abolished function (Yarar et al., 2002; Benesch et al., 2002; Cannon et al., 2001; Castellano et al., 2001; Suetsugu et al., 2001b). The VCA domain is the effector output of WASp family proteins and the binding site for the Arp 2/3 complex (Panchal et al., 2003). Several studies have demonstrated its essential role in WASp activation (Yarar et al., 2002; Benesch et al., 2002; Suetsugu et al., 2001b; Machesky and Insall, 1998; Symons et al., 1996).

5.4.5 Summary

The results in this chapter demonstrate that WT WASp appears autoinhibited in unsupplemented U937 lysate and that point mutations that cause XLN are more active. WASp containing XLT / WAS missense mutations polymerise actin in a regulated manner and have a significantly reduced threshold for activation compared to WT WASp. The EVH1 domain, Polyproline domain and VCA domain all make an intrinsic contribution to WASp activation, and their deletion significantly reduces the ability of WASp to initiate actin polymerisation. The Basic domain plays a small but significant role in reducing WASp activity in this experimental system, possibly through stabilising the autoinhibition of WASp.

These results also suggest that the WASp induced actin polymerisation assessed by the bead based actin polymerisation assay is independent of both Cdc42 and PIP_2 induced activation. This concept is further explored in the following two chapters.

6 Effect of WIP on WASp function *in vitro*

6.1 Introduction

The NMR structure of the complex formed between the NWASp EVH1 domain and WIP has revealed an extended contact sequence, involving up to 34 amino acids and three distinct binding motifs (Peterson et al., 2007; Volkman et al., 2002; Zettl and Way, 2002). The WIP sequence wraps circumferentially around the EVH1 domain, interacting with EVH1 amino acid residues throughout the entire domain. This structure has provided a mechanistic explanation for why missense mutations causing WAS / XLT cluster within the EVH1 domain, but are still distributed throughout the domain.

Modelling of XLT / WAS missense mutations based on the above crystal structure, suggested that approximately two thirds of clinical mutations may result in disruption of WASp – WIP binding (Kim et al., 2004; Volkmann et al., 2001; Rong and Vihinen, 2000). This has been demonstrated with four missense mutations by yeast 2 hybrid assays and by purified protein pulldown assays (Luthi et al., 2003; Stewart et al., 1999). These studies have also suggested that different mutant WASps can bind WIP with different affinities. One study has suggested that WASp – WIP interaction may be disrupted by phosphorylation of WIP at residue S488 following WASp activation, and that this initiates complex dissociation (Sasahara et al., 2002), however more recent work has disputed the physiological relevance of this (Dong et al., 2007).

The interaction of WIP with WASp almost certainly has several distinct functionalities. It has a role in protecting WASp from degradation (Tsuboi, 2007; de la Fuente et al., 2007; Konno et al., 2007; Chou et al., 2006), and this is explored further in chapter 8. It appears to be central in localising WASp to sites of active actin remodelling within cells, such as the leading edge of migrating cells, filopodia, podosomes and the T cells synapse (Myers et al., 2006; Chou et al., 2006; Anton et al., 2003; Moreau et al., 2003; Benesch et al., 2002; Sasahara et al., 2002; Vetterkind et al., 2002; Martinez-Quiles et al., 2001; Moreau et al., 2000). WIP also plays a significant role in regulating actin polymerisation, and this is the focus of this chapter.

In vitro experiments have demonstrated that WIP inhibits the activation of NWASp, as demonstrated by purified protein pyrene actin polymerisation assay (Martinez-Quiles et al., 2001). *Ho et al* assessed the sensitivity of native NWASp

– WIP complexes in the same pyrene assay, and found (as before) that these complexes were relatively insensitive to Cdc42 induced activation compared to NWASp alone. They also found that with WIP bound, NWASp was activated by Cdc42 combined with TOCA1, suggesting that *in vivo* relief of WIP induced WASp inhibition may require the formation of a multimeric complex involving NWASp, Cdc42, TOCA1 and WIP (Insall and Machesky, 2004; Ho et al., 2004). There is no published data on the effect of WIP on WASp / NWASp activation in a lysate (and therefore more physiological) *in vitro* assay.

In contradiction to these *in vitro* results, over expression or microinjection experiments of WIP generally promote *in vivo* actin polymerisation (Anton et al., 2002; Martinez-Quiles et al., 2001; Ramesh et al., 1997). WIP, however, has other functions independent of WASp, including stabilising F-actin (Anton and Jones, 2006; Martinez-Quiles et al., 2001) and activating cortactin resulting in Arp 2/3 activation (Kinley et al., 2003). Both these roles induce de novo actin polymerisation. The integration of these opposing roles of WIP in the *in vitro* setting remains poorly understood.

In addition to binding WIP, purified protein *in vitro* experiments have suggested that the EVH1 domain may have intrinsic effects on inducing WASp activation, and may play a cooperative role in the binding and activation of Arp 2/3 (Suetsugu et al., 2001a). The role of WIP binding in such a mechanism, and its relevance in more physiologically systems remain unknown.

In this chapter I have presented data assessing the affinity for WIP of the WASp clinical mutants, domain deletion mutants and constitutively active mutants. I have then assessed the effect of WIP on the activity of these constructs using the bead based actin polymerisation assay. The aim of these experiments was; (1) to assess the differential WIP binding capacities of the four clinical mutants (2) to determine the impact of other WASp domains on WIP binding or function, (3) to determine whether constitutively active WASp constructs, with their autoinhibitory conformation destabilised, have a reduced affinity for WIP and (4) to determine the effect on WIP on WASP activation in a lysate actin polymerisation assay.

6.2 WASp – WIP affinity

In order to assess differences in affinity of WASp for WIP, between WT and mutant WASp constructs, it was necessary to establish a robust and reproducible experimental system in which good levels of WASp – WIP binding could be detected. This proved to be difficult and this chapter describes the strategies I employed to try to establish this system and the results these experiments

yielded.

I have used a variety of pulldown, immunoprecipitation and co-immunoprecipitation techniques. These have been used to either detect binding between immobilised, purified WASp and WIP from cell lysates or to detect WASp-WIP complexes generated within cells in which one or both of these proteins are overexpressed. These two experiments are measuring subtly different outputs. The first strategy is a better measure of biochemical affinity of the two proteins, but is likely to be influenced by the experimental conditions in which the pulldown is performed. The immunoprecipitation of WASp-WIP complexes generated in cells, is more representative of functional affinity of these proteins within cells, but pure differences in biochemical affinity may be masked by cellular processes favouring or attenuating WASp-WIP complex formation. The former approach measures the association of WASp with WIP whereas the later measures (the inverse) the dissociation of WASp and WIP complexes.

6.2.1 WASp WIP binding during actin polymerisation assay

Initially, the affinity of WASp for WIP during the *in vitro* actin polymerisation assay was assessed. A standard actin polymerisation assay was performed with U937 lysate supplemented with 1mM ATP. The resultant membrane was immunoblotted for WIP in addition to WASp, Actin and ARPC2. Figure 6.1 demonstrates that no WIP was bound to beads loaded with GST-WASp at the end of the assay for any construct tested. The size of endogenous WIP is shown in the far right hand column (U937 lysate), and none of the experimental lanes have a significant band present at this size. A silver stain of a similar experiment also demonstrated no significant, discrete band at 65 kDa, the molecular weight at which WIP migrates during SDS_PAGE (Anton and Jones, 2006; Martinez-Quiles et al., 2001) (figure 5.5c). Similar results were seen in at least 3 actin polymerisation assays.

6.2.2 WIP pulldown from U937 lysate by immobilised GST-WASp

Several hypotheses were considered as to why WIP is not pulled down by WASp during the actin polymerisation assay. Firstly, the majority of WIP in U937 lysates is likely to be bound to other proteins (including endogenous WASp) (de la Fuente et al., 2007; Sasahara et al., 2002) and therefore the level of free WIP may be very low. Secondly, as WIP may inhibit actin polymerisation in this assay (Martinez-Quiles et al., 2001) it may have a lower affinity for WASp following its activation. Thirdly, the concentration of WIP in the cell lysate of the assay may not have been high enough to induce WASp –WIP interaction. Although I was easily able to detect WIP within U937 lysates (at considerably greater concentration

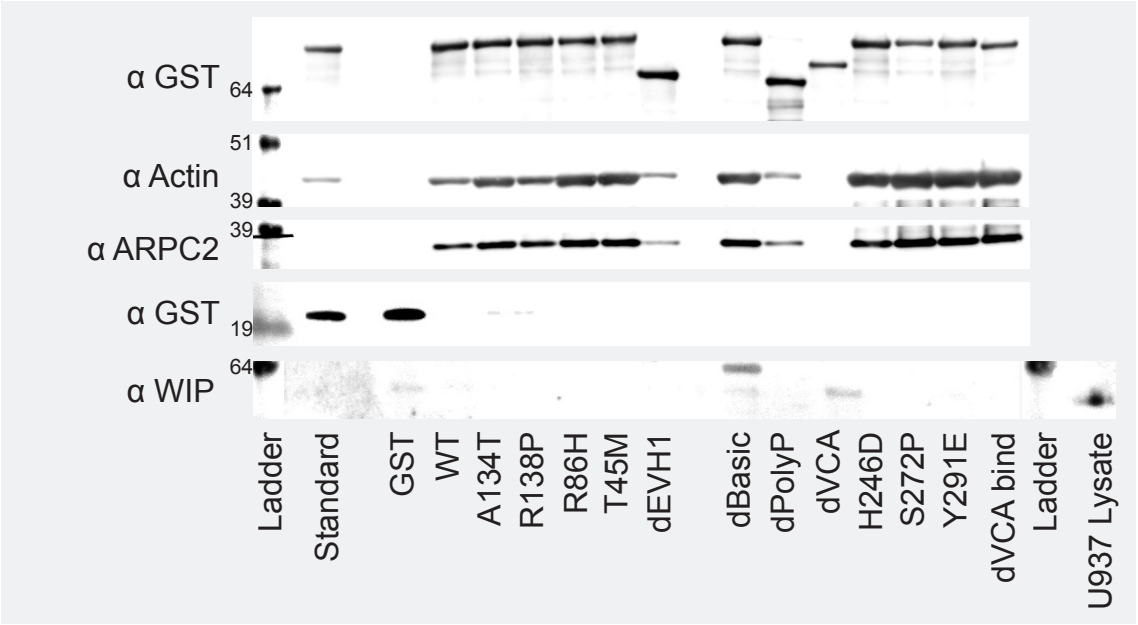

Fig 6.1 WIP does not bind to WASp during the actin polymerisation assay
Standard actin polymerisation assay supplemented with 1mM ATP. Reduced samples were divided into two, and two gels were run. The first was blotted for GST, Actin and ARPC2, the second was blotted for WIP. An aliquot of U937 lysate was run with the WIP samples as a positive control.

than was present in either Cos7 or RAW cells, see figure 3.12c), relatively low concentration of WIP in U937 cells has previously been reported (Tsuboi, 2006).

6.2.2.1 Optimisation

A strategy was explored to disrupt the binding of WIP to endogenous WASp in U937 lysate, prior to incubation with bead bound WASp constructs. Some published evidence suggested that WIP binds to autoinhibited WASp, and that on WASp activation, WIP and WASp dissociate as a result of WIP tyrosine phosphorylation (Sasahara et al., 2002).

Investigating this hypothesis, U937 lysate was treated with magnesium chloride, ATP and constitutively active Cdc42 to encourage WASp activation, actin polymerisation and therefore the proposed dissociation of endogenous WASp from endogenous WIP. After 30 minutes of incubation, these conditions were quenched with an excess of EDTA, actin polymerisation inhibitors and GDP (to deactivate Rho type GTPases such as Cdc42), generating lysate conditions which would be inhibitory for actin polymerisation. Upon quenching, the lysate was immediately transferred to the bead bound GST-WASp and incubated for 2 hours, to facilitate WIP-WASp binding. U937 lysate was generated using $6x10^7$ cell/ml lysis buffer, three times the concentration used in the standard actin polymerisation assay, to increase WIP concentration.

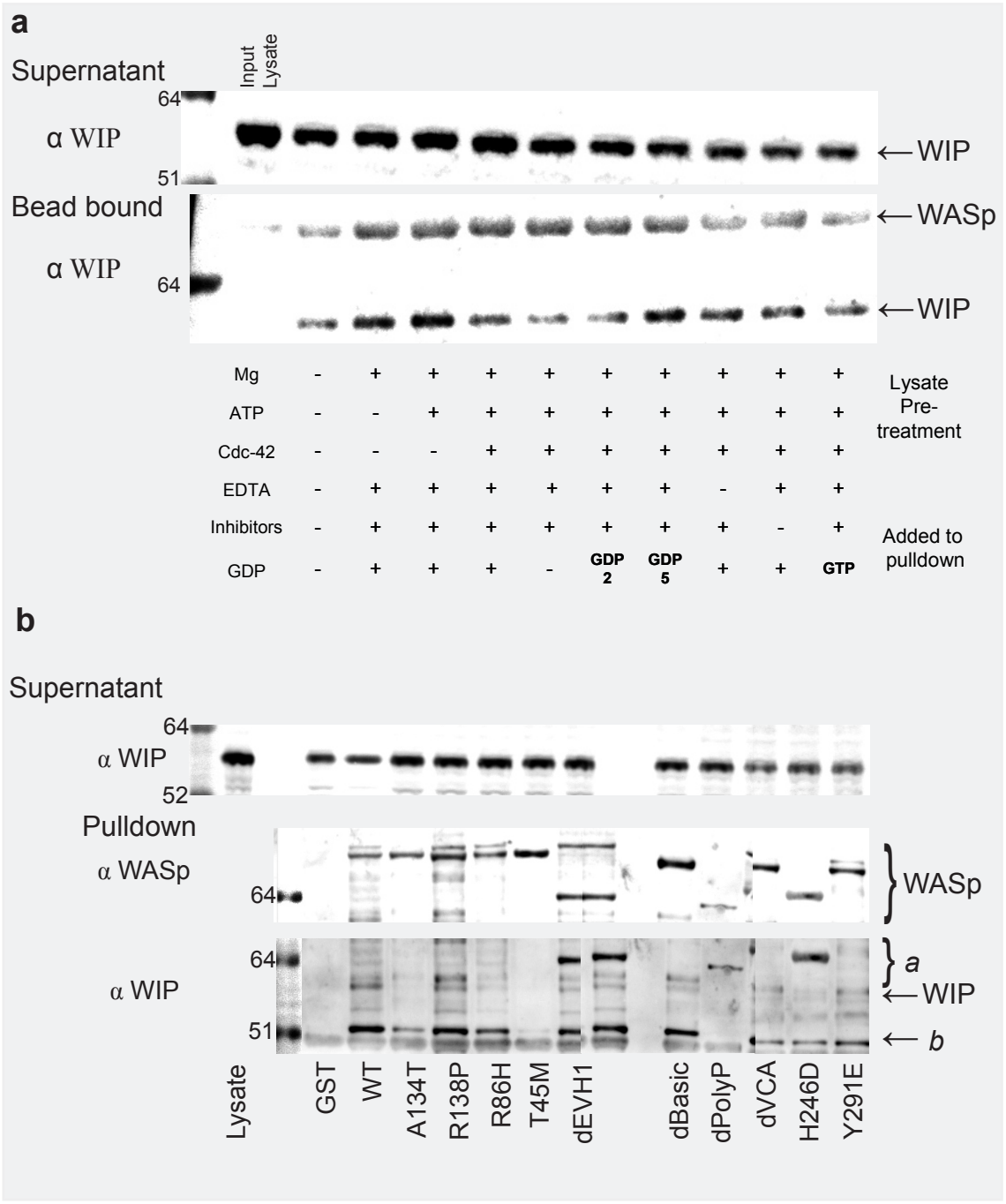

Fig 6.2 Pulldown of endogenous WIP from U937 lysate by bead bound GST WASp
(a) Untransfected U937 cells were lysed at a concentration of $6x10^7$ cells/ml in a modified lysis buffer (50% glycerol, 1% tritonX, 20mM HEPES pH 7.6, 150mM NaCl, 1mM EDTA, 2mM Na orthovanadate, 10mM NaF, 1% aprotinin, 10µg/ml leupeptin, 1mM PMSF). After centrifugation lysate was supplemented with all or some of 5mM MgCl, 1mM ATP and 500nM GTPγS loaded Cdc42 V12, according to the annotation in the figure, and "preincubated" for 30 minutes on a roller at room temperature. After this, a second addition of some or all of 10mM EDTA, 1mM GDP (labelled as +), 2 or 5 mM GDP, 1mM GTP, 5mM latrunculin B and cytochalasin D (given together and labelled as inhibitors). The lysate was then added to 75µl of WT GST-WASp coated sepharose beads, and incubated at room temperature for 2 hours. The beads (after washing) and supernatant were then resolved by SDS-PAGE and immunoblotting. **(b)** The above experiment was repeated with preincubation of lysate with 1mM ATP and 5mM MgCl, followed by a final addition of 5mM GDP. Lysate was incubated with a range of GST-WASp construct coated beads. Supernatants were immunoblotted for WIP and the beads were immunblotted for WASp and WIP. *(a) WASp bands and WASp degradation products (b) Non specific band*

The results of an experiment optimising the various aspects of this protocol using WT GST-WASp is shown in figure 6.2a. Assessing the effect of lysate pre-treatment, it can be seen that most WIP is pulled down when the lysate is incubated with magnesium chloride and ATP but not Cdc42. The critical component of the quenching conditions appears to GDP, with most WIP pulled down when the highest concentration of GDP (5mM) was used. EDTA and polymerisation inhibitors appeared to have little additional effect. From this experiment, it was concluded that maximal WASp-WIP interaction could be achieved with preincubation of lysate with magnesium chloride and ATP, and quenching with 5mM GDP.

6.2.2.2 Results and reproducibility

WIP pull down from U937 lysate was repeated using the optimised conditions for a panel of mutant WASp constructs. A typical experiment is shown in figure 6.2(b). Although a WIP band can be discerned (the lower of a double band running at approximately 58kDa, most clearly seen in the WT lane), there is much background and non specific staining, making interpretation of results very difficult. This experiment was performed a total of three times and no occasion was convincing WIP pull down demonstrated. There was no consistency between experiments as to which constructs demonstrated even the weakest of WIP binding.

Because of lack of reproducibility of results, this strategy for assessing WASp-WIP interactions was abandoned. Although I am unable to demonstrate the reasons for this inconsistency, a number of possibilities have been suggested by subsequent experiments. Firstly, the antibody used to detect (untagged) WIP (Anton et al., 2003), showed significant cross reactivity with several proteins (including WASp), and it has frequently been difficult to distinguish a WIP band on Western blots using this antibody unless there is a high protein concentration in the band. Several different blocking buffers and wash strategies were tried to improve the specificity of antibody binding, but none were successful. Subsequently a commercial WIP antibody has become available (Santa Cruz), which shows greater sensitivity and specificity than the Anton WIP antibody. Although not all of the above experiment have been repeated with this antibody, WIP binding to WASp coated beads could still not be detected following the actin polymerisation assay.

Secondly in all of these experiments a triton X based lysis buffer was used to generate the U937 lysate. Later experiments demonstrated problems detecting WASp-WIP complexes in triton X based lysis buffer (see figure 6.5(d) and 6.2.5.1 for further discussion).

6.2.3 Overexpressed zzWIP in Cos 7 cell pulldown by immobilised GST-WASp

An alternative approach was to incubate GST-WASp coated sepharose beads with Cos7 lysate transfected with the zzWIP construct (WIP carboxyl terminally tagged with the zz domain of protein A, a 6x His tag and the V5 epitope). This has two advantages over using U937 lysate. Firstly Cos7 cells are easily transfected and therefore high levels of WIP can be generated in cell lysates. Secondly, because Cos7 cells express low levels of WASp, very little if any of the WIP in the lysate will be complexed with WASp (see figure 3.12c).

Figure 6.3 shows such a pull down experiment. 5mM GDP and 5mM EDTA were added to the lysis buffer to enhance the WASp-WIP interaction. Unfortunately, as previously described, the anti WIP antibody shows significant cross reactivity with WASp. The WIP band can be distinguished, running at a slightly higher relative molecular weight than WASp (the size of the WASP band varies with the specific contruct tested). In this experiment there is a high level of background WIP pulldown (note GST and dEVH1 lanes), however there does appear to be more WIP pulled down by WT-WASp than with any of the four clinical mutants. The other domain deletion and the constitutively active point mutations mutants appear to bind a similar amount of WIP as WT.

The WASp and WIP bands could have been definitively separated using 2D gel electrophoresis, but in light of the high levels of background WIP binding and the cross-reactivity of the anti WIP antibody, this experimental approach was not repeated. Subsequent detection of the zzWIP construct used an anti His tag antibody, whose use was only optimised later on during the project (see figure 3.12b).

6.2.4 Co-immunoprecipitation of EGFP-WASp/zzWIP contructs from Cos7 cell overexpressing both constructs

To assess the ability of WASp mutants to bind WIP in cells, the GST-WASp construct and the zzWIP construct were co transfected into Cos7 cells and complexes were pulled down using glutathione sepharose (GST binding) beads and IgG sepharose (zz binding) beads.

Figure 6.4(a) shows zzWIP co-immunoprecipitated using GST WASp as bait and figure 6.4(b) shows GST-WASp co-immunoprecipitated using zzWIP as bait. It is apparent from these blots that there was little consistency of expression of bait protein between experimental samples (top layer in each figure). In particular the R138P construct and the constitutively active constructs (S272P, Y291E and VCA

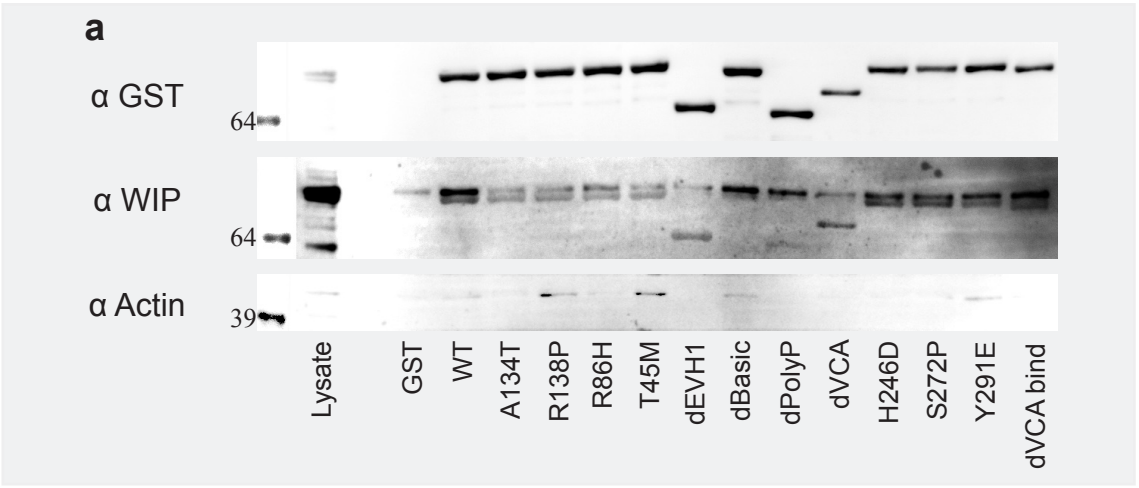

Fig 6.3 zzWIP pulldown by bead bound GST-WASp from Cos-7 cells transfected with the pOS-zzWIP construct

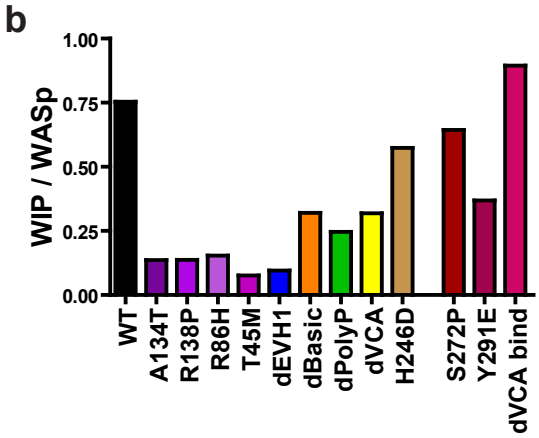

Cos7 cells were electroporated with the pOS-zzWIP construct. Plates of cells were harvested 48 hours later, were washed and snap frozen, and stored at -80°C. On defrosting the cells were lysed in a modified lysis buffer (10% glycerol, 1% tritonX, 20mM HEPES pH 7.6, 150mM NaCl, 5mM EDTA, 5mM GDP, 2mM Na orthovanadate, 10mM NaF, 1% aprotinin, 10µg/ml leupeptin, 1mM PMSF). Following centrifugation lysate was incubated with standardised volumes of a panel GST-WASp coated beads. The beads were incubated for 2 hours, then washed and resolved by SDS-PAGE and western blotting. Input lysate was run as a control (labelled lysate). **(a)** Shows immunoblots for GST (WASp), WIP and actin and **(b)** shows a graph of the WIP / WASp ratio of densitometry readings from this blot.

bind) showed very low levels of expression. I have previously demonstrated that GST-WASp expression in Cos7 cells can be comparable between the constructs under investigation (Figure 3.10a and b). The differences seen may be as a result of transfecting small numbers of cell (6 well plates compared to 15cm plates), because of using a different transfection mechanism (PEI compared to electroporation), or because of difference in levels of “DNA saturation” caused by the two transfection techniques. The low levels of protein detected with the constitutively active mutants, may be caused by WASp toxicity inducing cell death (this is discussed in detail in chapter 8). This experiment was repeated but similar inconsistencies in protein expression made interpretation of the results difficult.

The WIP binding capacity of each WASp mutant was quantified using band densitometry and the quantity of WIP or WASp bound per unit bait protein was determined. These values were expressed as a fraction of the equivalent value for WT WASp binding, and are expressed graphically in figure 6.4c and d. Only experimental samples whose bait protein quantification was at least 10% of

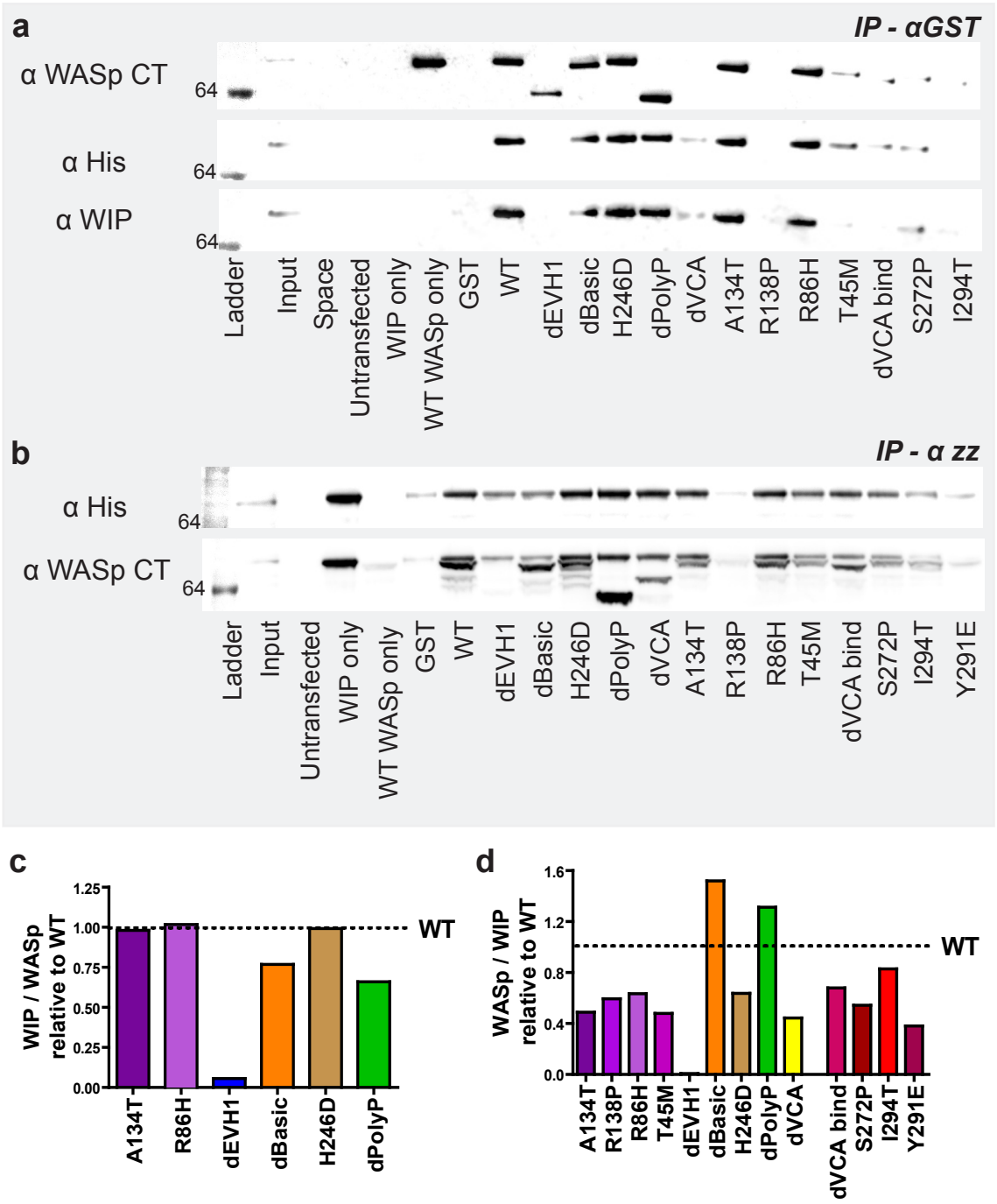

Fig 6.4 WASp and WIP co-immunoprecipitation from co-transfected Cos7 cells
Cos 7 cells were transfected with an equal amount of GST-WASp and zzWIP DNA, using the transfection agent JET-PEI™, according to manufacturer's instruction. Cells were harvested at 48 hours, washed and then lysed in a modified RIPA buffer (1% triton X, 0.1% SDS, 1% Na deoxycholate, 150mM NaCl, 20mM HEPES pH 7.6, 1mM EDTA, 5mM GDP, 2mM Na orthovanadate, 10mM NaF, 1% aprotinin, 10µg/ml leupeptin, 1µM pepstatin, 1mM PMSF), before clarification by centrifugation. Lysates were then incubated with 10µl of GST sepharose (figure **(a)**) or activated IgG sepharose beads (figure **(b)**) on a rotator at 4°C overnight. The beads were then washed 3x in RIPA buffer, prior to reduction in laemelli buffer and resolution by SDS-PAGE and western blotting. Reduced lysate was run on two gels for each experiment - one was blotted for the bait protein and the other for the prey protein. **(c)** and **(d)** Densitometry was perfomed on the above gels and prey / bait ratios were calculated. For each experiment these ratios were divided by the ratio for WT, to give a WIP / WASp ratio (c) or WASp / WIP ratio (d) standardised to WT. Only experiments where the bait protein densitometry reading was over 10% of that for WT were included in the analysis.

WT were analyses. Despite the limitations of these results, these experiments show that all WASp constructs except the dEVH1 (which has the WIP binding site deleted) are capable of forming WASp - WIP complexes within cells, if both proteins are over expressed.

6.2.5 Co-immunoprecipitation of EGFP-WASp / endogenous WIP complexes from stably transfected U937 lines

Cos7 cells have been a useful experimental tool for investigating WASp - WIP interaction, because of their ease of transfection and ability to synthesis large amounts of cytosolic protein with minimal toxicity. U937, however, are a more biologically relevant tool for investigating WASp molecular cell biology. I have therefore also assessed the ability of EGFP-WASp mutants to form WASp - WIP complexes (with endogenous WIP) in stably transfected U937 cells. To do this I have immunoprecipitated EGFP-WASp using an anti EGFP antibody, as described in chapter 2.

6.2.5.1 Optimisation

Figure 6.5a shows the WASp and WIP immunoprecipitated from U937 lysate transfected with EGFP-WT-WASp, under various experimental conditions (lysate concentration, incubation time for immunoprecipitation, volume of antibody resin used and transfection MOI of U937 cells used for lysate, were all varied). Non-specific binding was assessed using resin immobilised isotype control antibody and quenched resin with no antibody bound. It was found that a lysate concentration of at least 1.0 mg/ml was required to detect immunoprecipitation, and that overnight incubation reduced the strength of the immunoprecipitated WIP band. Complexes could be immunoprecipitated from cells transfected with MOIs of both 1 and 5, but more WIP was detected using lysate from MOI 5 cells. 25µl of resin was sufficient to immunoprecipitate a strongly detectible WIP band.

Fig 6.5b and c demonstrate that one wash is probably sufficient to eliminate non specific binding to the beads, as no WIP was detected in the post wash supernatant following the second and third washes. Similarly almost all of the WASp-WIP complexes were eluted from the beads on the first three elutions (WIP was only detected in the first elution, but EGFP WASp was still detected by silver stain in the third elution).

Figure 6.5d shows the effect of using different detergents in the lysis buffer on immunoprecipitation. Triton X based lysis buffers and RIPA buffer (containing SDS, Triton X and sodium deoxycholate) prevented WIP immunoprecipitation. APB (an IGPAL based buffer) resulted in the highest levels of WIP immunoprecipitation.

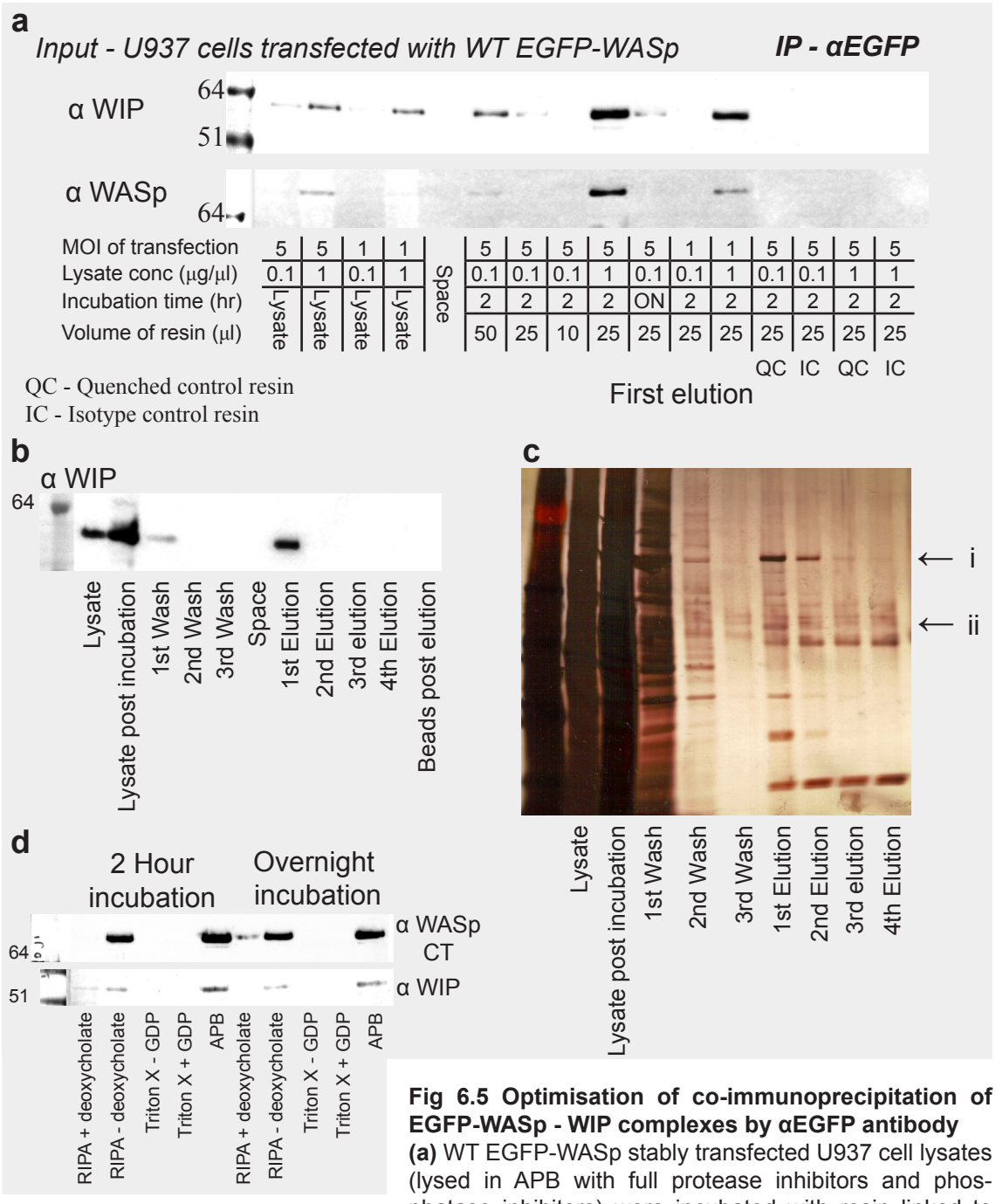

Fig 6.5 Optimisation of co-immunoprecipitation of EGFP-WASp - WIP complexes by αEGFP antibody
(a) WT EGFP-WASp stably transfected U937 cell lysates (lysed in APB with full protease inhibitors and phosphatase inhibitors) were incubated with resin linked to αEGFP antibody (250ng antibody / μl resin). Lysate concentration, incubation time, resin volume and MOI used to transfect U937 cells with EGFP-WASp, were varied to detemine optimal conditions for WIP immunoprecipitation. Resin bound with an unrelated isotype control antibody, and quenched resin with no antibody bound were used as controls. **(b)** Processing steps of the immunoprecipitation for the experiment with lysate of MOI 5 cell line, 1mg/ml concentration, 2 hour incubation and 25 μl of beads. **(c)** Silver stain of experiment (b). *Band labels (i) EGFP-WASp (ii) WIP.* **(d)** Effect of different detergents in the lysis buffer on immunoprecipitation. Immunoprecipitation perfomed as above using 25μl of resin, U937 cells transfected with WT EGFP-WASp and lysate generated using $1.2x10^6$ cells/ml in 5 different lysis buffers; RIPA +/- sodium deoxycholate (1% Triton X, 0.1% SDS, 150mM NaCl, 50mM TRIS pH 7.4, 1mM EDTA), Triton X lysis buffer +/- GDP 5mM (10% glycerol, 1% triton X, 20mM HEPES pH 7.6, 150mM NaCl, 5mM EDTA) and APB (1% IGPAL, 130mM NaCl, 50mM TRIS pH 7.6, 1mM EDTA). All lysis buffers contained full protease inhibitors and phosphatase inhibitors (2mM Na orthovanadate, 10mM NaF, 1% aprotinin, 10μg/ml leupeptin, 1μM pepstatin, 1mM PMSF).

Interestingly the removal of sodium deoxycholate from RIPA buffer partially restored immunoprecipitation. This experiment also confirms the finding that 2 hours incubation for the immunoprecipitation is more efficient than overnight incubation.

Sodium deoxycholate (weak) and SDS (strong) are both anionic detergents, which can denature of the tertiary structure of proteins, although antibodies are usually resistant to this (Neugebauer, 1990). There is some suggestion from the overnight incubation experiment that the addition of sodium deoxycholate additionally interferes with WIP – WASp interaction, rather than anti EGFP – EGFP-WASp interaction. This is perhaps not surprising as WIP is a highly ionic protein with a predicted isoelectric point of pH 11.99 and therefore may be more susceptible to denaturing by anionic detergents. Triton X and IGPAL are both non ionic detergents. Triton X selectively solublises cytosolic, but not cytoskeletal proteins (although this effect is usually seen using a lower concentration of Triton X than was used in this experiment). This however may be the explanation for the lack of efficacy of immunoprecipitation of EGFP-WASp using Triton X based lysis buffer. This effect is further explored in Chapter 8.4.

As these experiments were optimisation experiments they were only performed on a single occasion and were not repeated. On the basis of these experiments and those shown in figure 6.2a optimal experimental conditions were finalised (as described in legend to figure 6.6a) and these conditions were used in all subsequent immunoprecipitation experiments.

6.2.5.2 Results

Figure 6.6a shows the co-immunoprecipitation of WIP by a selection of EGFP-WASp constructs. It can be seen that the dEVH1 mutant shows no WIP binding, whereas the dBasic construct and the H246D mutant both show normal levels of WIP binding. There is less EGFP-WASp immunoprecipitated for the clinical mutants than for WT (as would be expected from the results presented in chapter 8). Despite this there appears to be disproportionately less WIP pulled down for the clinical mutants than for WT WASp. Similar results were produced when the experiment was repeated using lysate with concentration adjusted to standardise the concentration of EGFP-WASp in lysate for each construct.

Figure 6.6b shows a summary of the results of densitometry performed on the above experiments. Results are expressed as the amount of WIP immunoprecipitated per unit WASp, relative to WT-WASp (WT WASp = 1). This suggests there is a reduction in affinity of WIP for clinical mutant WASp compared to WT, but that

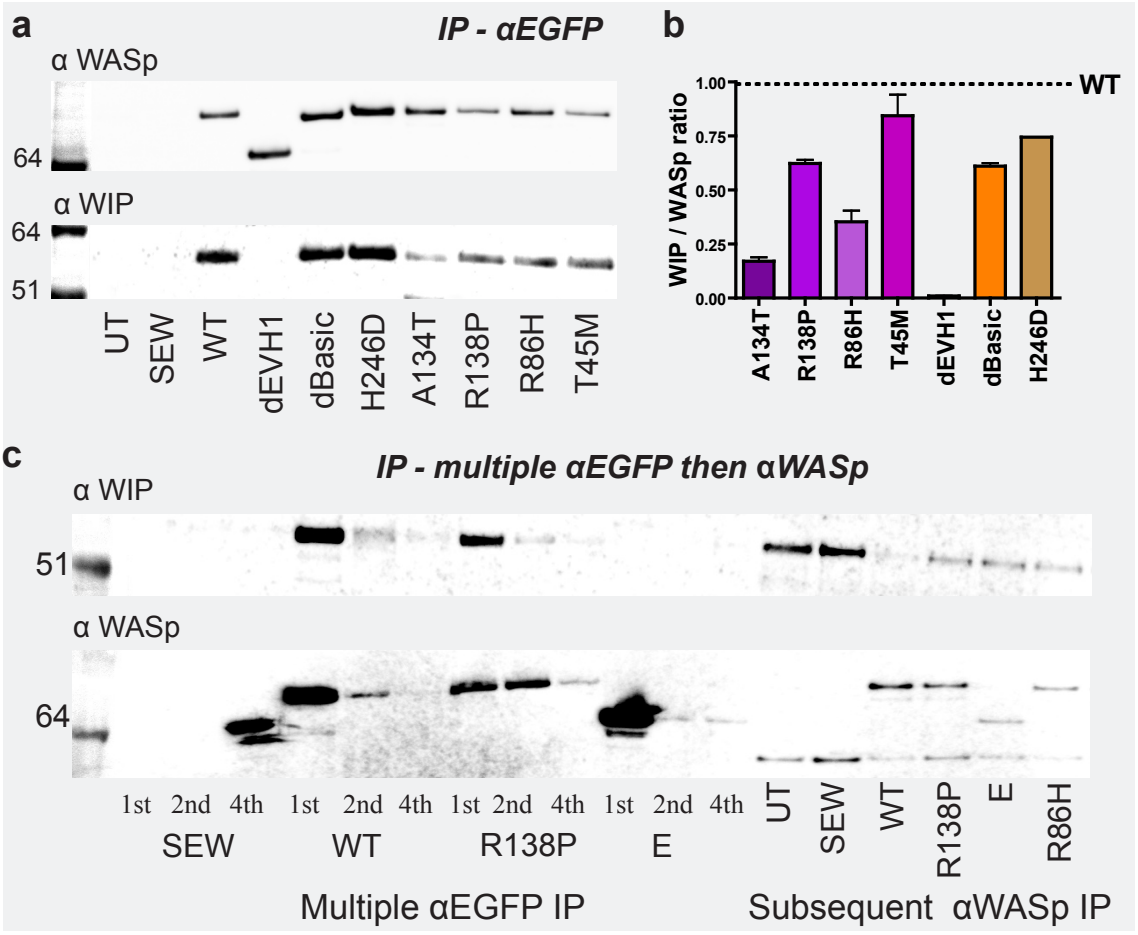

Fig 6.6 Co-immunoprecipitation of EGFP-WASp - WIP complexes by αEGFP antibody from transfected U937 cells

(a) 2.5x10^6 U937 cells stably transfected with a range of EGFP-WASp contructs were lysed in 100µl of APB supplemented with 10% glycerol, 0.1mM DTT and 5mM GDP. Lysates were clarified by centrifugation and incubated with 25µl of αEGFP resin (6.25µg antibody) for 2 hours. The resin was then washed 3x and eluted with 3 resin volumes of elution buffer. Samples were reduced and resolved by SDS-PAGE and immunoblotted for WASp and WIP. Blots shown are representative of 3 repeat experiments. **(b)** Densitometry was performed on the bands from 2 experiments as described in (a). Ratios of WIP / WASp were calculated and standardised to WT within each experiment. Average ratios are plotted (WIP / WASp for WT = 1). As data from only 2 experiments is shown, no statistics were performed. **(c)** 5x10^6 U937 cells were lysed in 200µl of supplemented APB and immmunoprecipitations were performd as above. Following immunoprecipitation, the lysate was subjected to 3 further αEGFP immunoprecipitations using fresh resin. Finally the lysate was incubated with 10µg of anti WASp antibody (B9) for 2 hours, before addition of protein G Sepharose and further incubation of 1 hour. The protein G Sepharose was then washed and reduced in laemelli buffer and resolved by SDS-PAGE (with the reduced elutants from the primary immunoprecipitation).

some WIP-WASp complexes do form within cells. This reduction is quite variable between constructs. By contrast the dEVH1 construct shows absent WIP binding. The constitutively active mutants were not tested with this assay.

6.2.5.3 Relative affinity of WIP for endogenous and mutant WASp

To investigate the relative proportion of endogenous WIP bound to EGFP-WASp and to endogenous WASp within U937s, a multiple immunoprecipitation experiment was performed. Lysate from each construct tested was serially

immunoprecipitated until all EGFP-WASp had been depleted from the lysates. The resultant lysates then underwent immunoprecipitation using anti WASp antibody to determine the amount of WIP bound to endogenous WASp. For each immunoprecipitation bound proteins were eluted off and resolved together by electrophoresis and immunoblotted for WIP.

Figure 6.6c demonstrates no WIP immunoprecipitated by anti EGFP from the SEW and dEVH1 expressing lysate as would be expected. The WT and R138P samples show reducing WIP pulldown with serial anti EGFP immunoprecipitation. The anti WASp immunoprecipitations demonstrate that the SEW transfected and untransfected cell lines have high levels of WIP bound to endogenous WASp. The dEVH1, R138P and R86H construct transfected lysates have lower but detectable levels of WIP bound to endogenous WASp. By contrast the WT transfected cells have very low levels of WIP bound to endogenous WASp.

This experiment demonstrates that in EGFP WT WASp transfected U937 cells, where there is a great excess of EGFP WASp over endogenous WASp, almost all of the cellular WIP is bound to the EGFP-WASp. For cells transfected with the clinical mutant WASp, there is still an excess EGFP-WASp over endogenous WASp, but a significant proportion of the cellular WIP is bound to endogenous WASp. Interestingly the majority of cellular WIP still appears to be bound to mutant EGFP-WASp, suggesting the affinity of clinical mutant WASp for WIP is biologically significant, if less than that for WT WASp.

6.2.6 Summary of WASp-WIP affinity experiments

Densitometry was performed on all successful experiments used to assess the affinity of WASp and WIP by immunoprecipitation or pulldown (as described in 6.22-6.25). 8 valid experiments were identified and their results were pooled and analysed together. Experimental samples were only included in the analysis if the amount of input (or bait) protein was at least 10% that of WT within that experiment. These results were analysed using an ANOVA with identical methodology to that employed for assessing the actin polymerisation assays. Absolute densitometry readings for WASp and WIP showed a skewed frequency distribution, but once log transformed they showed an approximately normal distribution (see appendix figure A.11).

Although pooling results from experiments using different methodologies is not ideal, each of the experiments I have used in this analysis is assessing the same biochemical interaction. I feel these results do provide a useful summary of the WASp-WIP interaction experiments presented in this chapter, although replication

a **ANCOVA of Ln WIP with Ln WASp - Ln WIP dependant variable**

	Sum of Squares	df	Mean Square	F	Sig.
Corrected Model	134.16	27	4.97	15.28	.000
Intercept	0.76	1	0.77	2.36	.133
Experiment	32.12	7	2.68	2.75	.020
Construct	6.25	12	0.89	8.23	.000
Ln WASp	9.61	1	9.61	29.56	.000
Experiment * Ln WASp	6.43	7	0.92	2.82	.018
Error	12.68	39	0.33		
Totals	10602	67			
Corrected total	146.8	66			
Adjusted R Squared					.854

b

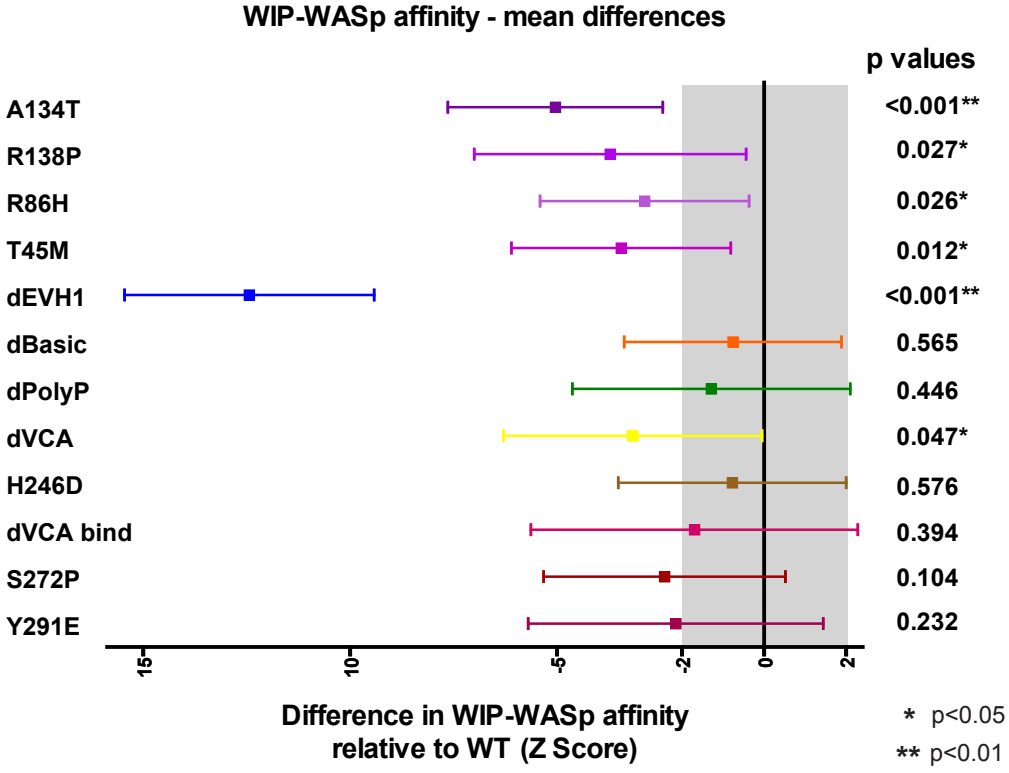

Fig 6.7 Summary of WASp - WIP affinity experiments
(a) Densitometry readings for WASp and WIP from all WASp - WIP binding affinity experiments were combined. The natural logs of these values were normally distributed (see appendix, figure A.11) and therefore used for parametric statistical analysis. An analysis of co-variance of Ln WIP with Ln WASP was performed using a main effects regression model and including an interaction term between experiment and Ln WASp concentration. The results of this model are summarised in the table. **(b)** Estimated marginal means of the affinity of WIP for WASp for each construct were calculated from the ANCOVA analysis and were expressed in terms of numbers of standard deviations from WT affinity (z scores). Means and their 95% confidence intervals are plotted on the graph and the 95% confidence interval (z score 2) for WT WASp is shaded in grey for comparison. The significance of the differences of these means from WT was analysed using a least significant differences (LSD) pairwise comparison, and p values are stated.

of specific experiments would increase the statistical certainty of the findings.

Figure 6.7 demonstrates that construct type is responsible for a significant proportion of the variation seen in these results. Comparing affinity to WT WASp, deletion of the Polyproline and Basic domains, and disruption of Cdc42 binding have no significant effect on WIP affinity, although each of these samples showed on average lower affinity for WIP than WT WASp. Similarly the constitutively active mutants have no significant difference in WIP binding capacity from WT, but on average show slightly reduced affinity. The clinical point mutations do however show a significant reduction in WIP affinity, with the A134T mutant having the least affinity for WIP. This data is in line with previously published results (de la Fuente et al., 2007; Tsuboi, 2006; Kim et al., 2004; Luthi et al., 2003; Volkman et al., 2002; Stewart et al., 1999).

6.3 Effect of WIP on actin polymerisation

6.3.1 Effect of WIP on WT WASp activity

To assess the effect of WIP on WASp mediated actin polymerisation *in vitro,* zzWIP transfected Cos7 cells were used as a substrate for the actin polymerisation assay. To ensure both an inhibitory or excitatory effect could be detected, the assay was performed using a range of WIP concentrations by mixing transfected and untransfected Cos7 lysates, and performing the assay with and without ATP supplementation. In addition to WT WASp, the S272P construct was also tested to determine whether WIP influenced WASp activity upstream of downstream of destabilisation of the WASp autoinhibitory conformation.

Figure 6.8b shows the concentration of WIP, actin and ARPC2 in the four lysates used in the assay, and compares them to the U937 lysate used in the standard actin polymerisation assay. The concentration of WIP in the lysates used varies from none to a greater concentration than that in U937 cells. By contrast the concentrations of actin and ARPC2 are approximately the same in all four lysates. Figures 6.8a,c and d demonstrate no significant effect of WIP on actin polymerisation activity in any of the conditions tested. Despite showing no effect on actin polymerisation the bead bound WASp was able to bind WIP, as shown in the anti WIP immunoblot of the beads.

6.3.2 Effect of GDP on actin polymerisation

It was been proposed that WIP binding to WASp may be destabilised by Cdc42 induced WASp activation (Sasahara et al., 2002). To investigate this, actin polymerisation assays were performed using WIP transfected Cos7 lysate in the

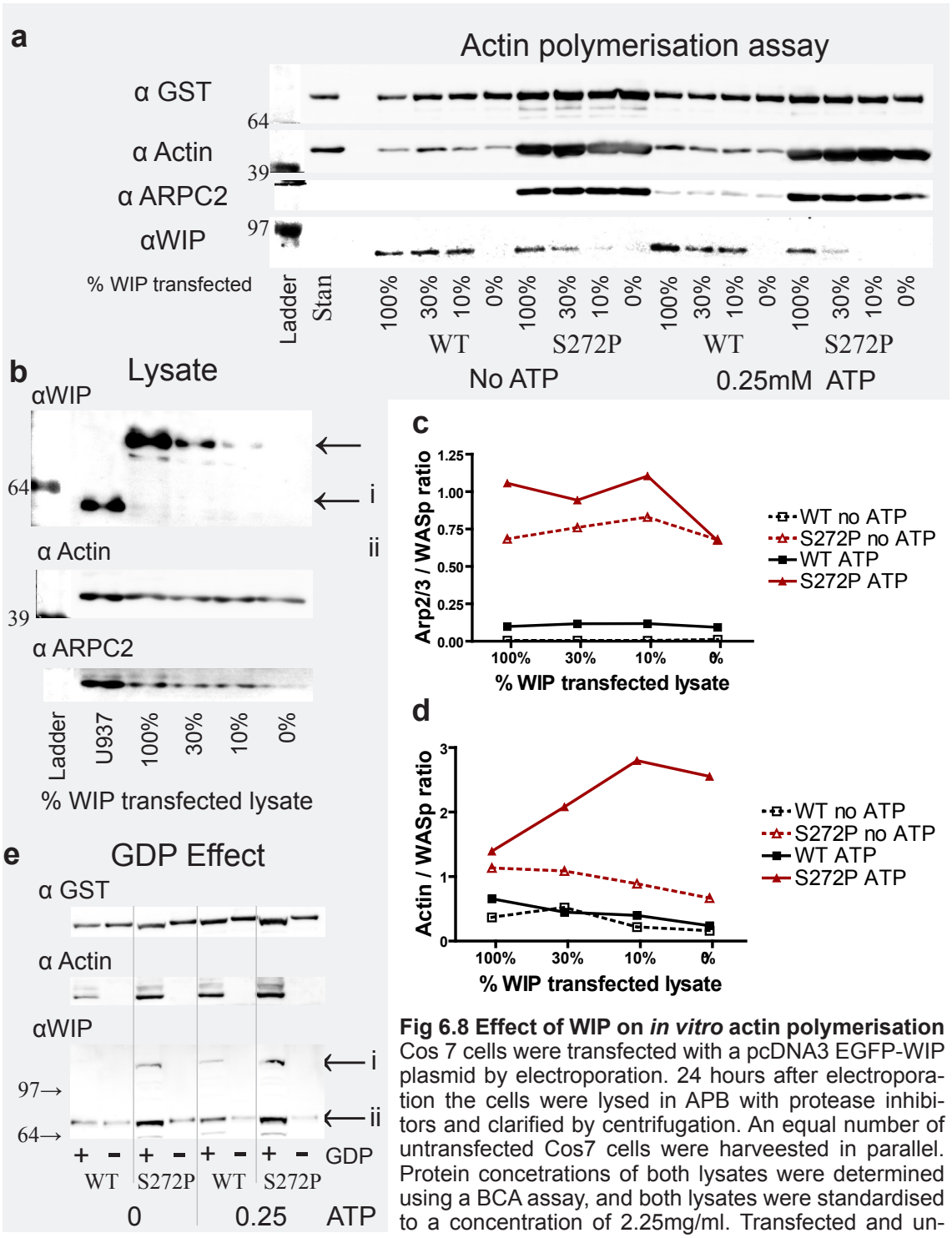

Fig 6.8 Effect of WIP on *in vitro* actin polymerisation
Cos 7 cells were transfected with a pcDNA3 EGFP-WIP plasmid by electroporation. 24 hours after electroporation the cells were lysed in APB with protease inhibitors and clarified by centrifugation. An equal number of untransfected Cos7 cells were harveested in parallel. Protein concetrations of both lysates were determined using a BCA assay, and both lysates were standardised to a concentration of 2.25mg/ml. Transfected and untransfected lysates were then mixed to give 4 different EGFP-WIP concentrations (100%, 30%, 10% and 0% transfected lysate). 250µl of lysate was then incubated with a standardised volume of WT or S272P WASp coated sepharose beads for each reaction condition. Assays were performed with and without ATP supplementation (0.25mM) of the lysate, but all lysates were supplemented with 5mM $MgCl_2$ prior to incubation. After 1 hours incubation, the beads were washed once with APB, prior to reduction in SB and resolution by NuPAGE and western blotting. **(a)** Immunoblots for GST, actin ARPC2 and WIP (using anti-WIP antibody) are demonstrated. *Stan* referes to a standard of 500ng of actin and 100ng of GST-WASp. **(b)** Immunoblots of lysate used in the assay, and U937 lysate used as a positive control. *(i) EGFP-WIP (ii) Endogenous WIP*. **(c)** and **(d)** Densitometry of bands from immunoblot shown in (a) were used to calculate Arp2/3 / WASp and actin / WASp ratios, which were then plotted against WIP concentration. (e) In parallel with experiment (a), an assay was performed to assess the effect of GDP (5mM) on actin polymerisation. 100% WIP transfected lysate was used for each sample. *(i) 130kDa band ?EGFP-WiP dimer. (ii) EGFP-WIP.*

presence and absence of an excess of GDP, and figure 6.8e shows the result.

This experiment suggests that an excess of GDP is associated with both increased actin polymerisation and increased WIP binding to WASp. Two other interesting results are demonstrated in this experiment. GDP also appears to induce the pulldown of a second band at approximately 150kDa which reacts to the anti WIP antibody. This could be a non specific band, but it is the correct molecular weight for a dimerised WIP complex, and the size of the band in each lane is proportional to the size of the WIP band. As the gel was run under denatured conditions (heated to 70°C for 10 minutes in NuPAGE Lithium Dodecyl Sulphate sample buffer with propriatory reducing agent), it would be unlikely that a dimer would remain following electrophoresis. This could be resolved by repeating the experiment using a range of denaturation conditions, or by identifying the band by mass spectropscopy. These experiments were beyond the scope of this project. Secondly, the addition of GDP appears to cause a motility shift in the WASp construct, and this effect appears to be proportional to the amount of WIP bound to the beads. A similar motility shift is seen when WASp is phophorylated at the Y291 residue (Cory et al., 2002).

These findings require further work to be validated and to explore the mechanisms behind them, but this work is beyond the timeframe of this project. Nonetheless, they do potentially challenge the hypothesis that WIP stabilises the autoinhibitory conformation of WASp.

6.3.3 Effect of WIP on other WASp constructs

Actin polymerisation assays were performed using Cos7 cells transfected with EGFP, EGFP-WIP and EGFP-WIPdWASp as lysate and a range of WASp constructs as the substrate. Figure 6.9a shows the composition of the lysate used in the experiment, and figure 6.9b shows the results. There appears to be no consistent difference in the results between any of the lysates for any of the constructs tested. Similar experiments have been performed on a total of four occasions using a range of different conditions and cell lysates, and on no occasion was a difference between lysate with a high or low WIP concentration detected in any construct.

These results demonstrate that WIP has no effect on WASp induced actin polymerisation in this bead based cell lysate *in vitro* system.

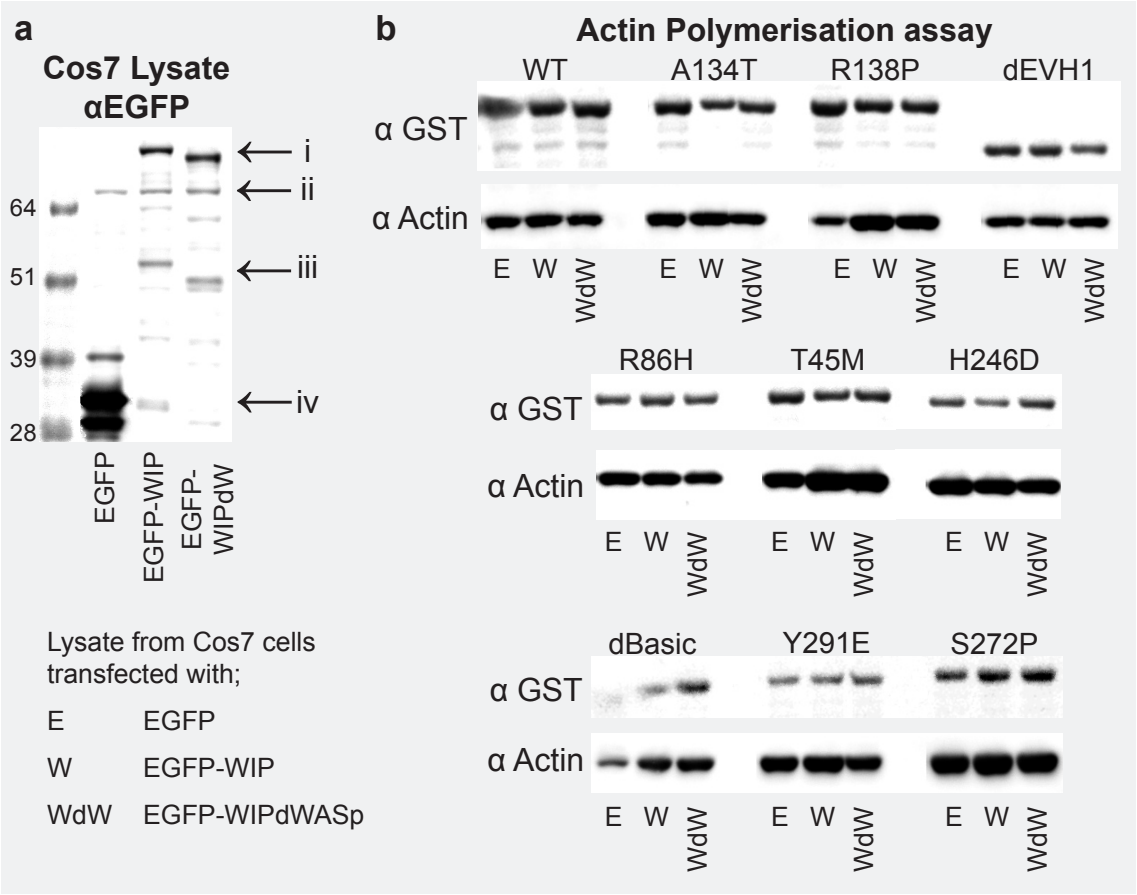

Fig 6.9 Effect of WIP on *in vitro* actin polymerisation (experimental WASp constructs)
Cos 7 cells transfected with EGFP, WIP-EGFP or WIPdWASp-EGFP (WIP with the WASp binding site deleted) were lysed in APB. Lysates were standardised to a concentration of 1mg/ml (determined by BCA assay) were and supplemented with 0.25mM ATP and 5mM Mg^{2+}. A standard actin polymerisation assay was then performed using a selection of WASp constructs purified on sepharose beads. **(a)** Immunoblots of lysates used. *(i) EGFP-WIP (ii) non specific band (iii) EGFP-WIP degradation band (iv) EGFP.* **(b)** Blots from actin polymerisation assay using all three lysates.

6.4 Conclusion

The key findings from the experiments presented in this chapter are;

(1) Missense WASp mutations which give rise to XLT / WAS in patients showed significantly reduced WIP affinity compared to WT WASp, whereas those giving rise to XLN have equivalent WIP affinity.

(2) WIP did not associate with bead bound WASp during the U937 lysate actin polymerisation assay.

(3) Over-expression of WIP in lysates had no effect on *in vitro* actin polymerisation.

6.4.1 Affinity determinants for WIP binding

The experiments presented in this chapter illustrate some the technical problems I encountered in reliably eliciting WASp – WIP binding. There is not a precedent for this in the literature, and WASp - WIP complexes have been co-immunoprecipitated from cells over-expressing protein, from native cell lysates and from purified protein interaction experiments (Tsuboi, 2007; de la Fuente et al., 2007; Dong et al., 2007; Tsuboi and Meerloo, 2007; Tsuboi, 2006; Sasahara et al., 2002; Martinez-Quiles et al., 2001; Moreau et al., 2000; Stewart et al., 1999; Ramesh et al., 1997). The cell lines used in this project (U937 and Cos7) have not been published as tools for investigating the formation of WASp – WIP complexes, although one study commented on low levels of both WASp and WIP in U937 cells compared to THP1 cells (Tsuboi, 2006). In my experience (as shown in figure 3.12c) and that demonstrated in other publications (Cory et al., 2003), U937 cells expressed equivalent levels of WASp and WIP to THP1 cells. Following transduction, U937 cells expressed higher levels of EGFP-WASp than transduced THP1 cells (data not shown). These differences may represent the well documented heterogeneity associated with U937 cell lines.

My difficulties in forming WASp – WIP complexes using bead bound recombinant WASp and endogenous WIP from U937 cells may well result from the vast majority of WIP being bound to endogenous WASp. I tried to address this by inducing the dissociation of endogenous WASp and WIP by WASp activation, based on published evidence in T cell signalling (Sasahara et al., 2002). Since my experiments were performed, other data has questioned whether WASp activation does induce WASp – WIP dissociation (Dong et al., 2007). Currently, the question as to whether WASp activation destabilises WASp – WIP complex stability remains unanswered, and my experiments provide no supportive evidence for this hypothesis.

The finding that the affinity of WAS / XLT WASp for WIP is reduced compared to WT is in keeping with previously published data from yeast two hybrid and pulldown experiments (Luthi et al., 2003; Stewart et al., 1999), as well as predicted binding affinities from structural modelling (Kim et al., 2004; Volkmann et al., 2001; Rong and Vihinen, 2000). Among the four clinical mutants I tested, I found that the order from least to greatest affinity was; A134T < R138P = T45M < R86H, which extends but is in keeping with previously published results: T45M had never been tested before and the other three constructs had not been tested simultaneously. R86H showed significantly greater affinity for WIP than A134T ($p=0.071$) and T45M ($p=0.038$), whereas there were no other significant differences between the

constructs (ANCOVA using a Bonferroni correction for comparing mean affinities – analysis not shown).

The finding that the constitutively active mutants bind WIP with similar affinity to WT is not previously published. These constructs were not tested in the most robust of the four techniques used (co-immunoprecipitation from stably transfected U937 cells), because these constructs did not allow the formation of stably transfected cells (see chapter 8). As a result they were tested in fewer assays and the results show wide confidence intervals. Nonetheless, the S272P construct was tested in 5 independent experiments and no significant difference from WT was detected. This is significant because point mutations causing XLN have been demonstrated to destabilise the WASp autoinhibitory conformation, based on structural modelling (Devriendt et al., 2001). If WASp is able to remain bound to WIP in the disinhibited conformation, WASp may exist *in vivo* simultaneously active (and Arp 2/3 bound) and WIP bound. This has implications for the role of WIP in localising WASp and for inhibiting its activation (Dong et al., 2007; Benesch et al., 2002; Sasahara et al., 2002; Martinez-Quiles et al., 2001), and also for the function of the WASp – WIP complex.

Deletion of the Basic domain and Polyproline domain appeared to have no significant effect on WIP binding. This provides us with useful information about the molecular mechanisms underlying WASp - WIP complex formation. Firstly it suggests that formation of the WIP-WASp complex does not require interaction with mediators which bind either of these two domains (such as kinases, SH3 – SH2 adaptors, profilin, other SH3 proteins, PIP_2 binding to the basic domain). Secondly, it suggests that deletion of these domains does not impair the folding and conformation of the EVH1 domain, and suggests that functionally the EVH1 domain is intact in these constructs. Thirdly it suggests that neither of these domains make a direct contribution to the WASp – WIP binding affinity. The fact that the H246D mutant does not have greater affinity for WIP than WT WASp is supportive of the hypothesis that WIP binding is not disrupted by (Cdc42 induced) WASp activation. Further support for this comes from the fact that addition of GTPγS to the co-immunoprecipitation reaction from transfected Cos7 cells has no effect on WASp – WIP affinity (see appendix figure A.12).

The dVCA domain mutant appears to have significantly reduced affinity for WIP. This has not been previously described in the literature, but could be compatible with one model of WASp-WIP interaction proposed by *Dong et al* in which the NH2-terminus of WIP interacts with the WASp VCA domain in a complex with actin and profilin (Dong et al., 2007).

6.4.2 WIP effect on actin polymerisation

It has been previously clearly demonstrated that *in vitro*, in a purified protein system, WIP inhibits the actin polymerisation activity of NWASp (Ho et al., 2004; Martinez-Quiles et al., 2001). By contrast, several lines of evidence suggest that over-expression of WIP *in vivo* leads to increased cellular actin polymerisation (Lanzardo et al., 2007; Anton et al., 2003; Benesch et al., 2002; Anton et al., 2002; Vetterkind et al., 2002; Martinez-Quiles et al., 2001; Moreau et al., 2000). In this project, I have assessed the role of WIP in an *in vitro* lysate system, and have found no impact on activity

When the assay was performed using U937 lysate, containing endogenous WIP and WASp, I was unable to demonstrate WIP binding to bead bound exogenous GST WASp. As suggested above, because of the stability of endogenous WASp – WIP complexes, the amount of free WIP in these assays may have been very low (de la Fuente et al., 2007). As a result, assays performed with U937 lysate, may have effectively been a “WIP free” experiment. In support of this, WIP did bind to WASp, during actin polymerisation assays performed with lysate from Cos7 cells transfected with WIP, which contained physiological levels of tagged WIP, but no endogenous WASp (or WIP). This hypothesis could be investigated by serially immunoprecipitating U937 lysate with anti-WASp antibody and measuring the amount of free WIP in the post precipitation lysate. An alternative hypothesis is that there is a mediator in U937 lysate which inhibits WIP binding to GST WASp. In support of this, when actin polymerisation assays were performed using U937 lysate mixed with WIP transfected Cos7 lysate, no WIP binding was detected (data not shown). The lack of WASp – WIP interaction detected during the actin polymerisation assay, and the activity of the WAS / XLT mutant WASp constructs is discussed in greater detail in chapter 5.4.3.

I was unable to detect any effect (either positive or negative) of WIP on *in vitro* lysate based actin polymerisation, despite five well controlled experiments. These experiments used lysates from different cell lines, combinations of mixed transfected and untransfected cell lysates, use of full length and truncated WIP and varying concentrations of ATP to try to detect any difference WIP may be producing. Assays were performed at both the “active” and the “largely inactive” spectrum ends to ensure an effect was not missed due to saturation or lack of sensitivity for a signal. This surprising result contradicts previously published data, but the effect of WIP in lysate based actin polymerisation assay has not been previously assessed.

It is possible that in Cos7 cells the levels of, or affinity for WASp of CR16 or WICH

/ WIRE is much higher than that of WIP. If this were the case, then it is possible that the WASp EVH1 domains would all become saturated with CR16 or WICH / WIRE, and therefore the effect of WIP overexpression in these cells would be negligible. Although I was unable to assess the levels of these other verprolin family proteins, I feel it is unlikely that they would be expressed in high enough concentration to completely saturate the effect of WIP. As WIP is the physiological binding partner for WASp it is unlikely that the affinity of WASp for CR16 or WICH / WIRE would be significantly stronger than that for WIP.

Alternatively, it is possible that WIP is only bound to a small subset of the bead bound WASp, and therefore inhibition of this subset does not result in a detectible difference in the measured activity in the assay. Again I feel this is unlikely, as although I did not formally quantify the amount of WIP generated in Cos7 cells following transfection, EGFP WIP transfected cells were robustly green under the fluorescent microscope prior to harvesting, and WIP was detected easily on Western blots of lysate used in the assays.

A further possible explanation is that WIP may have several effects on WASp which balance each other out. For example it has been postulated that WIP is required for TOCA1 binding, and that TOCA1 is essential for NWASp activation *in vivo* (Ho et al., 2004). Therefore any inhibitory effect of WIP, through WASp autoinhibitory stabilisation would be negated by the subsequent enhanced binding of TOCA1. In the absence of WIP, TOCA1 recruitment may be slower or alternative activation pathways (involving Nck or Grb2) may be required, and the net result would be similar levels of activity in the presence and absence of WIP. Although this hypothesis is attractive, I feel it is unlikely to explain the lack of WIP activity in the bead based assay, because TOCA acts in concert with Cdc42 to activate WASp but Cdc42 activation does not appear to be important in this assay.

Another alternative explanation for this discrepancy, is that WIP's role in stabilising the WASp autoinhibitiory conformation is an artefact of the purified protein system. In more physiologically systems, it has been suggested that WASp may polymerise actin as part of a multimeric complex (Insall and Machesky, 2004), where the effects of several mediators are balanced to determine final activity. In such a model, WASp would not exist in an autoinhibited conformation, but rather its conformation and activity would be governed almost exclusively by which mediators were bound to it. WIP may not have the same inhibitory activity on WASp as part of a complex containing TOCA1, Grb2, Nck and VASP, and in this context its role in localisation may be more critical. In the context

of WASp integrating activating signals from many different mediators, WIP may play a critical role in inhibiting Cdc42 mediated activation, but this effect may be bypassed by other activating signals (eg Grb2, Nck). In light of the other results presented in this study and breadth of published literature reviewed, I feel this is the most likely explanation for these findings.

A final hypothesis is that the post translational modification of WASp (or WIP) when over-expressed and manufactured in Cos7 cells, makes these proteins insensitive to one another. For example, it has been suggested that phosphorylation of specific tyrosine residues within WIP can lead to a reduced affinity for and dissociation from WASp. Non-physiological post-translational modification could lead to continued WASp – WIP association, but loss of autoinhibitory stabilisation. Evidence for enhanced and atypical tyrosine phosphorylation of WASp synthesised in Cos7 cells is discussed in chapter 7.5.3.

Unfortunately further investigation of the mechanisms underlying these results was beyond the time scale of this project. Experiments such as quantifying the amount of WIP, CR16 and WIRE in assay lysates, use of purified protein systems involving different proteins, and testing WASp constructs or WIP lysates which have been pre-treated with alkaline phosphatase to eliminate phosphorylation, would help clarify the mechanisms underlying these findings.

7 Effect of Cdc42 and assessment of phosphorylation on WASp activation *in vitro*

7.1 Introduction

The results described in chapter 5 suggest that the bead based actin polymerisation assay assesses *de novo* actin polymerisation independent of Cdc42 induced WASp activation (discussed in chapter 5.4). In this chapter I have explored this further by assessing the direct effect of Cdc42 on WASp activation and its affinity for various WASp constructs. It has been previously demonstrated that *in vitro* Cdc42 induced WASp activation reduces the threshold for WASp phosphorylation by 40 fold (Torres and Rosen, 2006), and a functional link between Cdc42 and WASp tyrosine phosphorylation has been proposed. To explore this hypothesis within the bead based actin polymerisation system, I have assessed the effect of the actin polymerisation assay on WASp phosphorylation.

In this chapter I present results of experiments which manipulate the activity of Cdc42 either by loading with an excess the non hydrolysable guanine nucleotide (GTPγS) or by using constitutively active or dominant negative Cdc42 mutants. The activity and the ability of Cdc42 to bind WASp are absolutely dependent on it being bound to GTP. As discussed in chapter 1.5.1, Cdc42 has an intrinsic GTPase activity which limits its duration of activation, and this is regulated by opposing actions of GAP and GEF proteins. As a result, activity of Cdc42 is tightly regulated, and the molecular basis of this regulation is the phosphorylation state of the guanine nucleotide bound to the Cdc42 switch region.

Guanosine 5′-[γ-thio]triphosphate (GTPγS) is a non hydrolysable analogue of GTP which once bound to a small GTPase maintains it in an active state for much longer than GTP. As a consequence, once loaded with GTPγS Cdc42 becomes constitutively active and loses its regulation by GAP and GEF proteins. The Cdc42 G12V (12V) missense mutant is GTPase deficient, and as a result once GTP has bound Cdc42 12V, it remains unhydrolysed, keeping Cdc42 in an active conformation. As a consequence, like GTPγS loaded WT Cdc42, Cdc42 12V is constitutively active, and resistant to regulation. By contrast, the T17N Cdc42 mutation (17N) has a much higher affinity for GDP than WT Cdc42. As a result the rate of nucleotide exchange from GDP to GTP in 17N Cdc42 is much slower than that of WT Cdc42, maintaining the 17N mutant in an inactive conformation. Cdc42 17N acts as a dominant negative mutant because it is still able to bind

Cdc42 activating proteins, such as GEFs, and therefore reduces the activation signals available to WT Cdc42. These mutants are well established tools in the investigation of Cdc42 function both *in vitro* and *in vivo* (Symons et al., 1996; Kozma et al., 1995).

7.2 WASp - Cdc42 affinity

7.2.1 Pulldown of exogenous Cdc42 by immobilised GST-WASp in presence of GTPγS

7.2.1.1 Purified protein system

The interaction of Cdc42 and WASp was initially investigated in a purified protein system based on previously published protocols (Suetsugu et al., 1998; Ma et al., 1998a). Bead bound GST-WASp was incubated with GTP or GDP loaded Cdc42 in XB buffer for 1 hour with rotation. Unfortunately no Cdc42 binding was detected on the washed beads (Appendix figure A.13) for any samples, and therefore this approach was abandoned.

7.2.1.2 Supplementation of U937 lysate

An alternative approach was explored where excess Cdc42 was incubated with bead bound WASp in the presence of physiological cell lysate. GTPγS loaded Cdc42 12V was added to U937 lysate and this was then incubated with GST-WASp coated beads, and the Cdc42 pulled down by WASp was assessed. Excess GTPγS was used because Cdc42 12V requires GTP binding to be constitutively active, and by preloading the Cdc42 with GTPγS, the potential confounding requirement of endogenous GTP (which is unstable in aqueous solution) is removed. This experiment is essentially the same as an actin polymerisation assay with Cdc42 supplementation replacing ATP supplementation. The Cdc42 binding in this experiment is shown in figure 7.1a, and the full actin polymerisation assay is shown in figure 7.2c.

Figure 7.1a demonstrates WASp binding to Cdc42, when excess exogenous Cdc42 12V is present, but no binding of endogenous Cdc42 from un-supplemented lysate. The H246D and dBasic domain WASp constructs show no Cdc42 binding, but the remaining domain deletion constructs, the clinical mutations and the constitutively active constructs all show good Cdc42 pulldown. The importance of GTP binding to Cdc42 in its interaction with WASp is demonstrated by the experiments with the S272P construct, where 12V Cdc42 binds WASp, but 17N Cdc42 does not. Unfortunately the equivalent WT WASp experiments were lost due to technical problems with the electrophoresis and Western blotting.

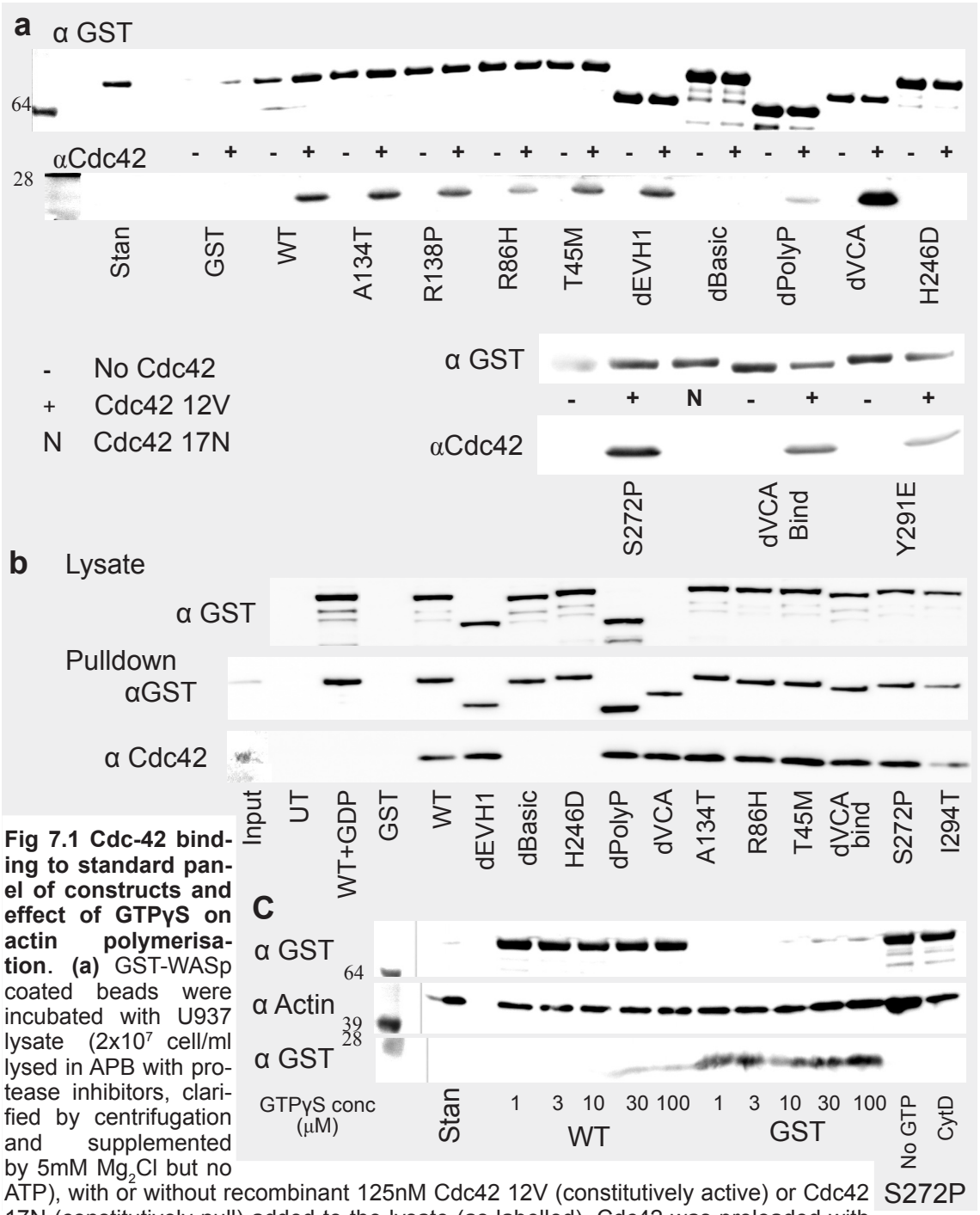

Fig 7.1 Cdc-42 binding to standard panel of constructs and effect of GTPγS on actin polymerisation. (a) GST-WASp coated beads were incubated with U937 lysate ($2x10^7$ cell/ml lysed in APB with protease inhibitors, clarified by centrifugation and supplemented by 5mM Mg_2Cl but no ATP), with or without recombinant 125nM Cdc42 12V (constitutively active) or Cdc42 17N (constitutively null) added to the lysate (as labelled). Cdc42 was preloaded with GTPγS for 1 hour (see 2.8.3 for details). Beads were incubated for 1 hour, then washed once with APB prior to being reduced and resolved by NuPAGE and western blotting. Blots were immunostained for GST (WASp) and Cdc42. **(b)** Cos 7 cells were transfected (using JET-PEI) in 6 well plates with GST-WASp constructs. At 72 hours, 200μM of GTPλS or GDP was added to the culture medium for 30 minutes. Cells were then washed and lysed in 250μl of ice cold LB containing protease and phosphatase inhibitors and clarified by centrifugation. Supernatants were incubated overnight with 10μl of sepharose beads, and then the following morning they were washed 3 times in lysis buffer. The resultant beads were reduced and resolved by SDS-PAGE and blotted for GST and Cdc-42. Immunoblots of lysate prior to bead incubation, and beads themselves are shown. *UT* - untransfected lysate. **(C)** A standardised volume of GST-WASp or GST coated Sepharose beads were incubated for 1 hour with U937 lysate ($2x10^7$ cells/ml lysed in APB with protease inhibitors, then clarified by centrifugation) supplemented with 5mM $MgCl_2$, no ATP, but with the stated concentration of GTPγS prior to bead incubation . Beads were then pelleted and washed twice with APB, prior to reduction in SB and resolution by NuPAGE and western blotting.

7.2.2 Co-immunoprecipitation of GST-WASp / Cdc42 complexes from transfected Cos 7 cells

The experiment described in 7.2.1.2 assesses the formation of WASp – Cdc42 complexes *in vitro* on the surface of sepharose beads. By transfecting Cos7 cells (using PEI) with GST WASp, and then treating the cells with GTPγS prior to lysis, the formation of *in vivo* cellular WASp – Cdc42 complexes was assessed. After GTPγS treatment Cos7 cells were washed and lysed, and GST-WASp was pulled down using glutathione sepharose beads. The beads were then washed, resolved by NuPAGE, Western blotted and immunoblotted for Cdc42.

Figure 7.1b again demonstrates good Cdc42 binding for all constructs except for H246D and the dBasic deletion constructs. This experiment again illustrates that this interaction is dependent on GTP binding to Cdc42, as treating the cells with GDP rather than GTPγS inhibited the WT WASp – Cdc42 binding.

These two experimental approaches demonstrate a similar pattern of Cdc42 binding among the experimental WASp constructs. Although this data is preliminary and requires further confirmatory experiments, it is supportive of previously published results (Hemsath et al., 2005; Kato et al., 1999). Other than the dBasic domain and H246D constructs the majority of the other WASp constructs tested appear to have a similar affinity to WT WASp for Cdc42. Both experiments suggest the dVCA domain construct has a higher affinity. In Figure 7.1 the Cdc42 band pulled down by the dVCA construct is larger than that for the other constructs, and in figure 7.1b the Cdc42 bands appear to be of similar size, but the input WASp band for the dVCA construct is significantly reduced. The first experiment suggests that the dPolyP construct may have a reduced Cdc42 affinity, but this is not borne out in the second experiment.

7.3 Effect of guanosine nucleosides on WASp activity

An initial approach I used to explore the effect of Cdc42 on the activity of different WASp constructs was to supplement the U937 lysate used in the actin polymerisation assay with GTPγS. Such a strategy should render all endogenous Cdc42 in the U937 lysate constitutively active, and therefore increase the level of Cdc42 dependent actin polymerisation. This approach has the advantage of being simple to implement, and maintains physiological proportions of Cdc42 and other mediators in the lysate. The major disadvantage to this approach is that GTPγS will indiscriminately activate all small GTPases, and therefore the actin polymerisation measured may reflect the activity of several small GTPases, acting on different aspects of actin dynamics.

Figure 7.1c demonstrates no effect of GTPγS on the activity of WT WASp in the absence of ATP. The level of actin polymerisation seen with WT in U937 lysate supplemented with 100μM GTPγS, was equivalent to the activity seen with cytochalsin D inhibition and with GST alone. This figure is representative of two experiments, with a total of six different constructs tested for GTPγS sensitivity (including constitutively active and constructs with reduced actin polymerisation activity). None showed any change in activity with addition of GTPγS.

A possible explanation for the lack of response to GTPγS is that the assay was not supplemented with ATP. I feel this is unlikely as the constitutively active constructs are able to polymerise actin in the absence of ATP, and binding of Cdc42 to WASp is thought to render WASp uninhibited and therefore active. A second possibility is that any increase in WASp activity is negated by a GTPγS induced inhibitory action on actin polymerisation upstream of WASp, mediated by other Rho type GTPases. In light of the other data presented in this chapter and in chapter 5, I feel it is more likely that these results represent insensitivity to Cdc42 in the bead based actin polymerisation assay.

7.4 Effect of exogenous Cdc42 on WASp activity

7.4.1 Optimisation

To investigate the direct effect of Cdc42 on the activity of WASp in the bead based actin polymerisation assay, it was necessary to supplement actin polymerisation reactions with exogenous Cdc42. Cdc42 was purified from transformed E.coli and preloaded with guanosine nucleotides prior to addition to U937 lysate, as described in chapters 2.8 and 3.6 and figure 3.13.

Figures 7.2a and b show the effect of increasing concentrations of exogenous Cdc42 on WASp activity. Fig 7.2a shows an actin polymerisation assay performed with lysate supplemented with 0.5mM ATP. GTPγS loaded Cdc42 (WT, dominant negative or constitutively active as stated) was then added to the lysate prior to incubation with WT WASp coated beads. Despite an increase in Cdc42 binding to WASp, increased Cdc42 concentration did not produce a corresponding increase in actin polymerised on the bead surface. Additionally there was no difference in activity between assays performed in the presence of WT or 12V, and no dominant negative effect on activity seen with 17N Cdc42.

One possible explanation for the lack of effect of Cdc42 in this assay, was that the addition of 0.5mM ATP had maximally enhanced the WASp activity induced by endogenous WASp activators, and therefore the effect of Cdc42 was not

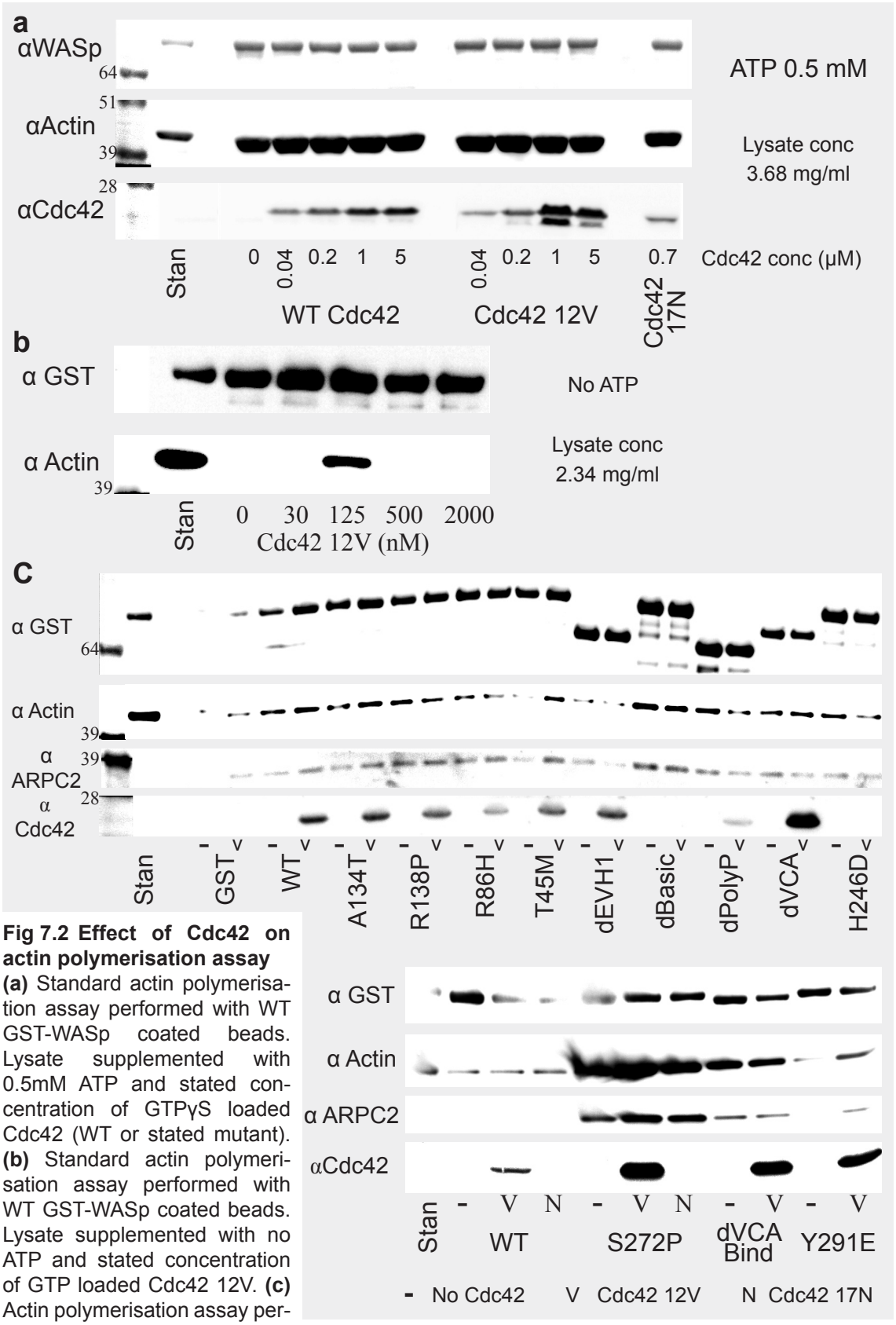

Fig 7.2 Effect of Cdc42 on actin polymerisation assay
(a) Standard actin polymerisation assay performed with WT GST-WASp coated beads. Lysate supplemented with 0.5mM ATP and stated concentration of GTPγS loaded Cdc42 (WT or stated mutant). **(b)** Standard actin polymerisation assay performed with WT GST-WASp coated beads. Lysate supplemented with no ATP and stated concentration of GTP loaded Cdc42 12V. **(c)** Actin polymerisation assay performed on standard and constitutively active panels of WASp constructs. Lysate was supplemented with 125nM GTPγS loaded Cdc42 12V (or Cdc42 17N) or an equal volume of GTPγS loading solution without Cdc42**.** No ATP added to the lysate. For all three experiments reactions were stopped at 1 hour and the beads were washed in APS. Beads were then reduced and resolved by NuPAGE and western blotting. Membranes were immunoblotted for WASp, GST, Actin, ARPC2 and Cdc42 as stated.

detected due to saturation of the assay. To investigate this, a similar experiment was repeated using U937 lysate without ATP supplementation, but with increasing concentrations of GTPγS loaded Cdc42 12V. Figure 7.2b suggests that at a concentration of 125nM Cdc42 12V does enhance actin polymerisation, but that at higher concentrations this effect is lost. It is important to emphasis that the image of the actin blot in figure 7.2b is significant overexposed compared to that in figure 7.2a, as demonstrated by the relative sizes of the actin standards. Therefore the activity of WASp in the presence of 125nM Cdc42 12V alone is still significantly less than that of WT in the presence of 0.5mM ATP. In light of the results of the other experiments presented in this chapter it is likely that this result is a technical artefact, as it is the only experiment which has demonstrated any effect of Cdc42 on the actin polymerisation assay. As it was performed as an optimisation experiment to determine the most appropriate concentration of Cdc42 to use in subsequent experiments, it was not repeated, and a concentration of 125nM Cdc42 was used in subsequent experiments.

7.4.2 Results

Figure 7.2c shows the effect of 125nM Cdc42 12V on the actin polymerisation activity of the full panel of experimental WASp constructs. The conditions used were the same as for figure 7.2b, with each construct's activity compared in Cdc42 supplemented U937 lysate to sham supplemented lysate. The results from this experiment were unable to reproduce the enhanced actin polymerisation with Cdc42 by WT WASp seen in figure 7.2b. None of the constructs tested showed any appreciable difference in actin polymerisation between the Cdc42 supplemented experiment and the un-supplemented experiment. Together, these results suggest that Cdc42 at most has a minimal effect on the activity of WASp constructs in the bead based actin polymerisation assay.

7.5 Tyrosine and serine phosphorylation of WASp during actin polymerisation assay

It has been proposed that phosphorylation of tyrosine 291 in WASp occours following destabilisation of the WASp autoinhibitory conformation (Torres and Rosen, 2006; Torres and Rosen, 2003; Cory et al, 2002). As this destabilisation must also occour for WASp activation, this hypothesis would suggest that tyrosine phosphorylation of WASp would increase during the actin polymerisation assay. To determine whether changes in WASp phosphorylation occur during the actin polymerisation assay, the degree of tyrosine and serine483/484 phosphorylation of bead bound WASp was compared before and after incubation with U937 lysate in the actin polymerisation assay. Figure 7.3 shows a series of immunoblots from

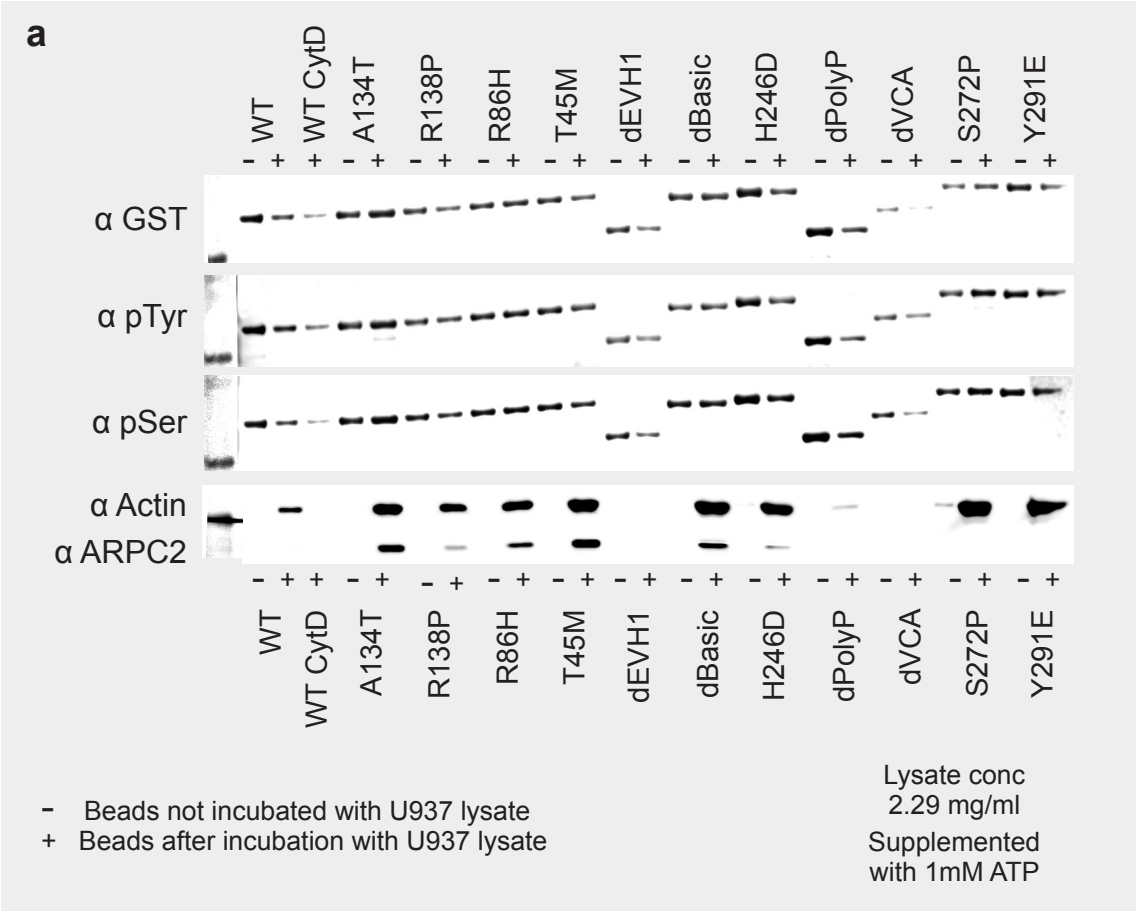

Fig 7.3 Serine and Tyrosine phosphorylation during actin polymerisation assay
(a) A standard actin polymerisation assay (with 1mM ATP) was performed and the resultant beads were washed, reduced and resolved next to equivalent beads which had not been incubated with U937 lysate. Following NuPAGE and Western blotting, membranes were first blotted for phosphotyrosine, and subsequently stripped and reblotted for phosphoserine. Finally the membrane was stripped and reblotted with anti GST antibody. Blots were developed following stripping to ensure no residual signal remained on the membrane. The secton of the membrane containing proteins smaller than 50 kDa was blotted for actin and ARPC2.

a standard actin polymerisation assay (ATP supplemented) comparing several WASp constructs from the standard and constitutively active panels of constructs. For each construct the first column shows purified bead bound WASp, and the second column shows the same volume of beads following incubation with U937 lysate as an actin polymerisation assay. The beads were immunoblotted for GST, phosphotyrosine and phosphserine483/484, as well as for actin and ARPC2 to demonstrate activity.

For all constructs, the purified WASp protein showed some tyrosine and serine phosphorylation, and the levels of phosphorylation appeared to be equivalent between each construct. There did not appear to be any change in phosphorylation status following the actin polymerisation assay, for any construct. Previous studies have demonstrated a subtle motility shift associated with tyrosine phosphorylation of WASp at Y291 (Cory et al., 2002). No difference in migration,

suggestive of phosphorylation, between the pre and post assay WASp samples is seen in figure 7.3, or in a similar experiment where the gel was run for much longer allowing greater separation of WASp bands (data not shown). This data is representative of two experiments, and a similar lack of correlation between actin polymerisation activity and WASp phosphorylation was seen when immunoblots from the ATP titration and time course experiments (figures 4.3a, 4.5c and 5.8a) were stripped and reblotted with anti phosphotyrosine antibody (appendix figure A.14). The results from these experiments would have been stronger if reliable positive and negative control samples had been run along side the experimental samples. Such controls could be generated by pretreating WT WASp beads with purified phosphatases and kinases, and this experiment will be repeated in future work. Nonetheless, these results suggest there is no net change in tyrosine or serine$^{483/484}$ phosphorylation of WASp during the bead based actin polymerisation assay.

7.6 Conclusions

The data in this chapter provides further information to that already published on the complex role of Cdc42 in the regulation of WASp activity. The key finding from these experiments, and those in chapter 5, is that Cdc42 has no effect on WASp activity in the bead based actin polymerisation assay, despite binding to WASp appropriately. I will discuss this surprising result in the context of previously published data.

7.6.1 WASp – Cdc42 binding

Binding of Cdc42 to WT WASp was demonstrated under conditions where the Cdc42 was constitutively active (either as mutant 12V Cdc42, or bound to GTPγS). Interestingly endogenous Cdc42 was not pulled down by WASp in physiological lysate (figures 7.1a and A.13). This may be because of the inherent instability of GTP in aqueous cell lysate, or it may represent the transient binding of GTP bound Cdc42 to WASp.

Both experimental approaches shown in figures 7.1a and b demonstrated that substitution of the WASp 246 histidine residue for an aspartate residue abolished Cdc42 binding. Both this missense mutation (Kato et al., 1999) and the equivalent point mutation in NWASp (H208D) (Miki et al., 1998a) had been previously shown to prevent Cdc42 binding. This histidine residue is highly conserved among the CRIB domains of Cdc42 binding proteins (Symons et al., 1996), and the large ionic change induced by substituting a basic amino acid for an acidic amino acid is sufficient to abolish Cdc42 binding.

Deletion of the basic domain similarly prevented Cdc42 binding. Although the Basic domain does not contain a direct binding site for Cdc42, *Hemsath et al* proposed a model in which the positive charge of the basic domain electrostatically attracts Cdc42. Association between the negatively charged Glu49 and Glu175 Cdc42 residues and the WASp Basic domain facilitate docking of Cdc42, which initiates destabilisation of the autoinhibitory conformation, and reveals the Cdc42 binding sites in the GBD (Hemsath et al., 2005). They demonstrated that substituting the WASp basic amino acids within the Basic domain for neutral amino acids reduced the affinity for Cdc42 by 93 fold, and this correlated with an equivalent reduction in WASp activity in a purified protein pyrene actin polymerisation assay. The results from this study support this hypothesis.

Alternative explanations for the dBasic domain mutant's impaired Cdc42 association should be considered. It is possible that the basic domain binds a third protein which is essential in recruiting Cdc42 to WASp. An obvious candidate for such a protein is TOCA1 (Ho et al., 2004), but against this, TOCA1 interacts with NWASp via its SH3 domain, and therefore almost certainly binds the polyproline domain. Alternatively the basic domain may play a role in the change in tertiary structure brought about in the GBD on transition from the autoinhibitory conformation to the Cdc42 bound conformation. As the tertiary structure has only been elucidated for Cdc42 bound to an isolated WASp GBD (Abdul-Manan et al., 1999), the basic domain may be critical for the stability of the Cdc42 – GBD complex, in the context of full length WASp.

Both H246D WASp and the dBasic construct are able to induce actin polymerisation at similar or greater levels compared to WT WASp. This functionality strongly suggests that the gross tertiary structure and folding of these constructs is similar to WT WASp. This cannot therefore account for their inability to bind Cdc42.

Both the missense mutations responsible for WAS / XLT, and the constitutively active WASp constructs showed normal affinity for Cdc42. Normal Cdc42 binding to R86H and R86C WASp has been previously demonstrated (Kolluri et al., 1996), but there is no published data on the Cdc42 affinity of XLN missense mutations or other constitutively active WASp constructs. These results support the conclusions from chapter 5, that the key activation mechanisms of WASp containing WAS or XLT point mutations is normal, and the clinical phenotype seen in these conditions is not due to an inability of the WASp protein to nucleate actin effectively and appropriately. The similar affinity of Cdc42 for WT-WASp and constitutively active WASp suggests that Cdc42 binds both the autoinhibited and open conformations of WASp.

WASp binding to Cdc42 was demonstrated in a cellular and a cell lysate system, but was not detected in a purified protein system. Cdc42 may require a further factor to optimally bind WASp, which is present in U937 lysate, but is not present in the purified protein experiments. Again TOCA-1, which is essential for Cdc42 mediated actin polymerisation in a pyrene based actin polymerisation assay (Ho et al., 2004), is a candidate protein. Direct binding of Cdc42 to WASp in purified protein systems has, however, been previously published by several groups (Hemsath et al., 2005; Torres and Rosen, 2003; Symons et al., 1996; Kolluri et al., 1996; Aspenstrom et al., 1996). I feel it is more likely, therefore, that my results represent a technical failure and that further optimisation work may have elucidated a similar interaction to that detected in the cell lysate system.

7.6.2 Cdc42 activation of WASp in bead based assay

Several lines of evidence suggest that Cdc42 has no effect on WASp activation in the bead based actin polymerisation assay;

1. WASP H246D and dBasic constructs show normal (or increased) actin polymerisation activity despite an inability to bind Cdc42.

2. The dEVH1 construct shows reduced actin polymerisation activity compared to WT, despite previously published data suggesting that in the presence of Cdc42 the EVH1 domain contribution to activation is redundant (Suetsugu et al., 2001a; Rohatgi et al., 2000).

3. Supplementation of U937 lysate with increasing concentrations of GTPγS has no effect on WASp activity.

4. Addition of recombinant Cdc42 to U937 lysate has no effect on WASp activity, and no difference is detected between WT and H246D WASp in the presence of Cdc42.

5. Supplementation of U937 lysate with constitutively active and dominant negative Cdc42 results in identical levels of WASp activity

6. Tyrosine phosphorylation of WASp is thought to be facilitated following Cdc42 binding (Torres and Rosen, 2003), but no change is seen in WASp tyrosine phosphorylation during the actin polymerisation assay.

Although some of this data represents experiments which need further repetition, taken together this strongly suggests Cdc42 insensitivity in the bead based actin polymerisation assay. Two questions arise from this observation; (1) why

does Cdc42 have no effect on WASp activity in this assay and (2) how is WASp activated when Cdc42 is having no effect?

One possible explanation for the lack of effect seen with Cdc42 is the fact that the exogenous Cdc42 was made in E coli and therefore would not be prenylated. Previous studies have found that Cdc42 synthesised using a Baculovirus transduction system (with Cdc42 synthesis in eukaryotic cells), but not by a prokaryotic synthesis system, has induced actin polymerisation in *in vitro* experiments (Higgs and Pollard, 2000; Ma et al., 1998b; Zigmond et al., 1997). Other groups, however, have demonstrated WASp or NWASp activation with unprenylated Cdc42 (Yarar et al., 2002; Suetsugu et al., 2001b; Egile et al., 1999; Miki et al., 1998a), and lack of prenylation cannot explain the similar activity of WT and H246D constructs, or the insensitivity of GTPγS supplementation of lysate.

As stated above, TOCA1 is also required for Cdc42 mediated WASp activation. A more plausible explanation for Cdc42 insensitivity is that U937 lysate is either lacking in TOCA1 or contains an excess of a TOCA1 inhibitor. I did obtain (gift from Marc Krischner, Harvard Medical School) a small aliquot of an anti TOCA1 antibody, which I used to try to determine the presence and relative concentration of TOCA1 in U937 lysate. Unfortunately I was unable to get clear signals in positive and negative control cell lines and therefore the results in U937 cells were meaningless. This hypothesis could be tested by performing the bead based actin polymerisation assay using *xenopus egg* lysate (the substrate from which TOCA1 was identified and purified) and testing WT and H246D WASp constructs. By mixing U937 and *xenopus egg* lysates it would be possible to differentiate between a TOCA1 deficiency and the presence of an inhibitor in U937 cells.

How WASp is activated independently of Cdc42 is discussed in chapter 5.4.2.

7.6.3 WASp phosphorylation in the actin polymerisation assay

Phosphorylation of WASp at Y291 (Torres and Rosen, 2003; Cory et al., 2002) is thought to occur following WASp activation and is associated with an increase in WASp activity. Phosphorylation of Y291 is markedly facilitated following Cdc42 binding *in vitro,* and it has been proposed that Cdc42 acts synergistically with tyrosine kinases to activate WASp via phosphorylation (Torres and Rosen, 2006; Torres and Rosen, 2003). In this model the release of WASp autoinhibition makes the Y291 residue sterically more accessible to kinases, which provides the molecular mechanism of this synergism. The authors demonstrate that tyrosine phosphorylated WASp is able to return to the autoinhibited conformation, but that

phosphorylation acts as a molecular marker of previous activation. This synergism, however, has not always been demonstrated in *in vivo* systems (Suetsugu et al., 2002; Cory et al., 2002).

Phosphorylation of WASp at S483 / S484 is thought to be constitutive in cells and has also been associated with an increase in WASp activity (Cory et al., 2003). Although casein kinase 2 has been shown to mediate this phosphorylation, the mechanisms and regulatory importance of this modification is less well understood.

Figure 7.3 suggests there is no change in WASp phosphorylation at either tyrosine or serine residues during the actin polymerisation assay. This finding is surprising, considering the model proposed for f-actin production in the bead based actin polymerisation assay, relies on multiple activation events for each bead bound WASp protein (Chapter 4.9). Each WASp construct appears to shows significant phosphorylation prior to incubation with U937 lysate, raising the possibility that the WASp may already be maximally phosphorylated. Although phosphorylation at S483 / S484 might be expected following purification from Cos7 cells, tyrosine phosphorylation would not be expected. WASp produced at physiological concentrations in haematopoietic cells is likely, however, to have a different phosphorylation pattern to WASp purified form a malignant monkey kidney fibroblast cell line.

Unfortunately no positive control lane for tyrosine phosphorylation was included in this experiment. It is possible that the tyrosine phosphorylation detected is unrelated to WASp activation and does not involve Y291. Although WASp has six other tyrosine residues, it has been published that tyrosine phosphorylation only occurs at Y291 (Badour et al., 2004; Baba et al., 1999). These experiments were all performed in haematopoietic cells, which may show more specific and tighter control of tyrosine phosphorylation than Cos7 cells. Other unpublished data suggests WASp is tyrosine phosphorylated at residues other than Y291 (Giles Cory personal communication).

Two other results are anecdotally supportive of this hypothesis. Firstly, as discussed above (chapters 7.6.2 and 5.4.2) the actin polymerisation assay is independent of Cdc42 induced WASp activation. It has been proposed that Y291 phosphorylation is specifically associated with Cdc42 activation. This is supported by the impaired *in vivo* tyrosine phosphorylation of H246D and dBasic WASp constructs expressed in U937 cells (figure 8.7 and chapters 8.3 and 8.7.4). The lack of change in tyrosine phosphorylation state during the actin polymerisation

assay, therefore, may reflect no Cdc42 induced WASp activation in this assay. Secondly, the Y291E WASp construct has an equal tyrosine phosphorylation signal to WT WASp, despite having no tyrosine residue at Y291. Furthermore if WASp were maximally phosphorylated at Y291 prior incubation with U937 lysate, then no difference in activity would be expected between WT WASp and Y291E. Figure 5.3, and previously published data (Cory et al., 2002) demonstrate a small but definite difference between these constructs. Together this data supports the hypothesis that the tyrosine phosphorylation detected on bead bound GST-WASp is neither at Y291 or related to WASp activation, and that no Y291 phosphorylation occurs during the bead based actin polymerisation assay.

8 EGFP-WASp expression in U937 cells

8.1 Introduction

8.1.1 Determinant of WASp expression

Genotype – phenotype studies in Wiskott Aldrich Syndrome and X-linked thrombocytopenia have demonstrated a correlation between levels of WASp expression in lymphocytes and severity of disease (Lutskiy et al., 2005; Jin et al., 2004; Imai et al., 2004; Lemahieu et al., 1999; Zhu et al., 1997; Remold-O'Donnell et al., 1997). Generally children with XLT have missense mutations within the EVH1 domain, although some of these children develop the more severe WAS phenotype, frequently with autoimmune complications. Exon 4 mutations, in particular, have been associated with worse clinical disease (Lutskiy et al., 2005; Zhu et al., 1997). Understanding the mechanisms which determine the level of mutant WASp protein in lymphocytes, and the effect this mutant protein has on cell survival and function, is important for understanding the pathogenesis of autoimmunity and immunodeficiency in these conditions.

WIP has been shown to be essential in maintaining cellular WASp levels (de la Fuente et al., 2007; Konno et al., 2007; Chou et al., 2006). In resting cells the vast majority of WASp is bound to WIP (de la Fuente et al., 2007; Sasahara et al., 2002), and in addition to preventing WASp degradation it also inhibits WASp activation (Martinez-Quiles et al., 2001) and probably directs WASp to sites of active actin remodelling (Myers et al., 2006; Vetterkind et al., 2002; Martinez-Quiles et al., 2001; Moreau et al., 2000). Both calpain and the proteasome have been implicated in WASp degradation (de la Fuente et al., 2007; Chou et al., 2006; Suetsugu et al., 2002) but the regulation of this degradation and how it relates to WASp function remains poorly understood.

Mutations in the WASp gene lead to cytopenias in several haematopoietic lineages, but classically WAS patients develop lymphopenia and patients with XLN develop neutropenia. The reasons for this are poorly understood, but toxicity of mutant WASp protein in blood cell precursors has been suggested as a possible aetiology (Moulding et al., 2007).

In this chapter I present experiments which assess the expression, stability and toxicity of EGFP-WASp when overexpressed in U937 cells following stable transduction with lentivirus. I have elected to use U937 cells for this purpose for several reasons. Firstly, they are a myeloid cell line and therefore representative

of cells which are effected in WAS / XLT. Secondly, they express high levels of both WASp and WIP, which facilitates a comparison of the expression of mutant EGFP-WASp with endogenous WASp. Finally they are a robust and rapidly dividing cell line, which allowed a high throughput of experiments in a realistic time frame.

8.1.2 Lentivirus as a tool for transduction

In this research project I have utilised modified (second generation) lentivirus as a tool for transducing primary cells and haematopoietic cell lines (U937 and THP1 cells), both of which are extremely resistant to transfect using non-viral methods (Zhong et al., 1999; Arthur et al., 1997). Lentiviral transduction of cell lines reliably yields very high efficiencies of gene transfer (>80%) and the genes are subsequently stably expressed for many months. Both of these attributes were essential for many of the experiments I have performed in haematopoietic cells lines.

For bone marrow derived primary dendritic cells, lentivirus transduction allows gene transfer at reasonable efficiency and low toxicity. Other viral vectors have been used successfully, but dendritic cells are resistant to transduction by gamma-retroviruses once terminally differentiated (and therefore not dividing) (Ardeshna et al., 2000; Gruber et al., 2000; Gasperi et al., 1999; Lewis and Emerman, 1994), and are therefore not suitable for transforming bone marrow derived dendritic cells. Other viral vectors which have been used to successfully transduce dendritic cells (Herpes simplex virus, Vaccinia virus and Influenza virus) have demonstrated significant dendritic cell cytopathic effects, and reduced viability (Jenne et al., 2001). Adenoviral vectors have lower transduction efficiencies than lentivirus, with similar low levels of toxicity (Esslinger et al., 2002).

Lentiviruses are members of the retroviridae family of viruses. These are RNA viruses characterised by an ability to reverse transcribe their RNA to DNA following host cell infection, and integrate the resultant proviral DNA into the host cell's genome. Following reverse transcription, a U3, R, U5 unit is generated at each end of the proviral genome, which is called the long terminal repeat (LTRs). These sequences are essential for the insertion of the proviral DNA into the host genome and also act as promoters for transcription of the viral DNA.

Lentiviruses (in particular HIV-1) have been manipulated to create a safe gene transfer system which has minimal toxicity to the target cell. Manipulations included in the second generation lentivirus include breaking the "infecting" viral genome into three plasmids (Naldini et al., 1996), removal of viral accessory

and regulatory genes which are not absolutely necessary for virus synthesis, and selective mutation of the U3 region of the LTR. This makes the virus self inactivating (SIN) and replication incompetent (Zufferey et al., 1998).

The three plasmids are a transfer vector, containing the gene of interest with an internal promoter contained within the LTRs, a packaging vector, containing *gag, pol* and other essential HIV-1 accessory factors under a CMV promoter, and an envelope vector containing a VZV-G envelope protein under a CMV promoter. These are co-transfected into a packaging cell line, which generates replication deficient virus containing only the RNA encoded within the LTRs of the transfer vector. The VZV-G envelope protein provides the virus with broader trophism than the HIV-1 envelope protein and therefore increases the efficiency of transduction of both DCs and U937 cells. The transfer vector also contains a Woodchuck hepatitis post translational regulatory element (WPRE) and a central polyproline tract (cPPT) both of which act to enhance the nuclear transport of the viral genome and increase the efficiency of transduction (Follenzi et al., 2000; Schambach et al., 2000; Zufferey et al., 1999).

8.2 Expression of EGFP tagged clinical and domain deletion mutants

U937 cells were infected with lentivirus encoding a panel of EGFP-WASP constructs (EGFP alone (SEW), WT, 4 EVH1 missense mutations, dEVH1, dBasic, dPolyP, dVCA, and the H246D point mutation) at MOIs of 5 and 1. These cells were then cultured for one month during which time expression of the EGFP-WASp was monitored by FACS, and by SDS-PAGE and western blotting of cell lysates. After 31 days of culture the MOI 5 stably transfected cell lines were sorted into high and low expression populations (with negative cells discarded), and these purer populations were then cultured for a further 2 months with monitoring of EGFP-WASp expression. Data from the “MOI 5” cell lines (figures 8.1) and the “high expression” lines (figures 8.2 – 8.4) are shown here, as these results were clearer, but the results from cell lines with lower expression of EGFP-WASp constructs are described in the text where relevant (data not shown). Examples of the gating used for sorting and the EGFP expression in the sorted populations are shown in figures 8.1b-i.

A second series of experiments was performed on a panel of constitutively active WASp constructs (WT, S272P, I294T, Y291E, dVCA binding domain). Previous evidence suggested that these constitutively active constructs are not stable in long term culture and lead to cell division defects and apoptosis in EGFP-WASp

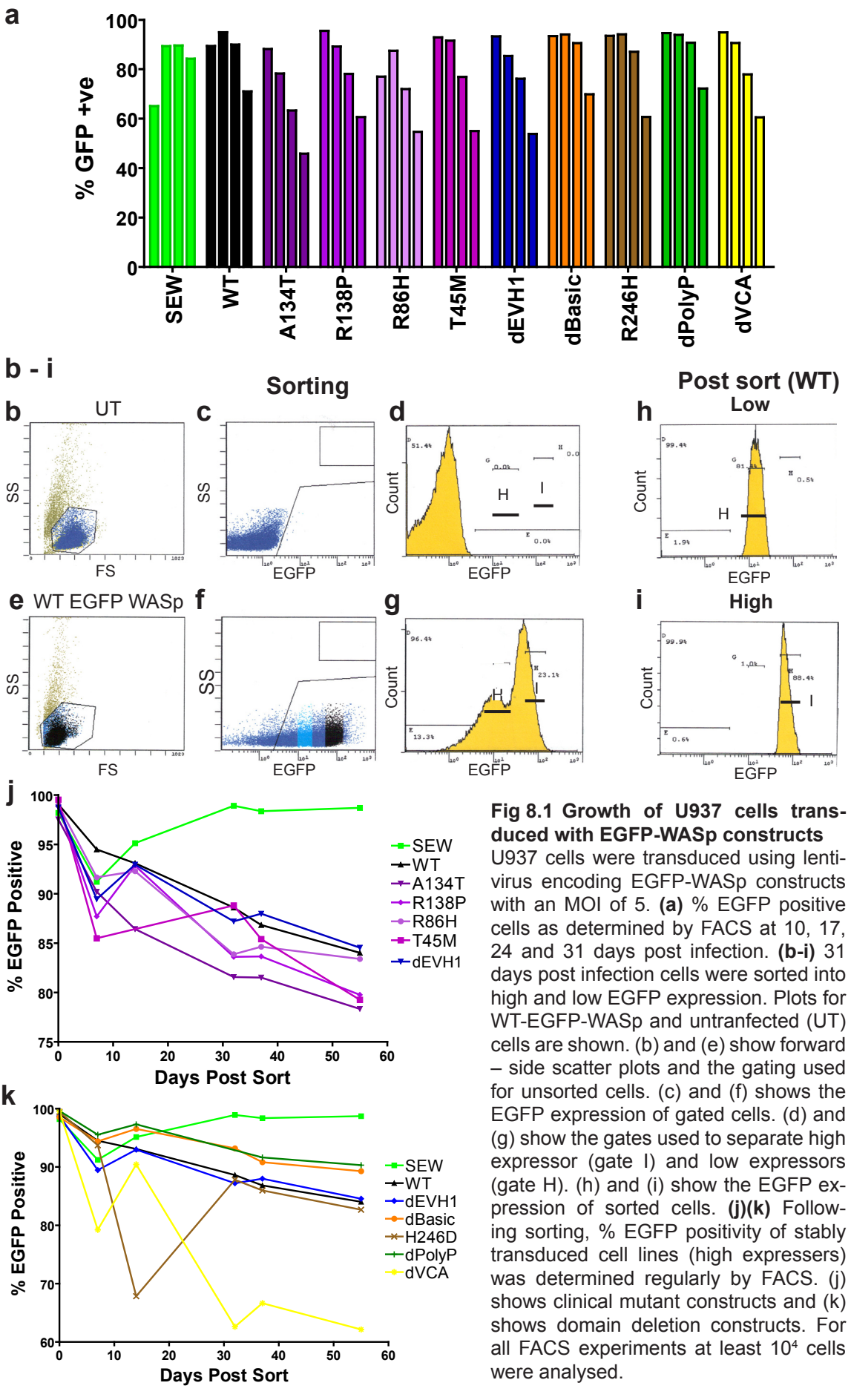

Fig 8.1 Growth of U937 cells transduced with EGFP-WASp constructs
U937 cells were transduced using lentivirus encoding EGFP-WASp constructs with an MOI of 5. **(a)** % EGFP positive cells as determined by FACS at 10, 17, 24 and 31 days post infection. **(b-i)** 31 days post infection cells were sorted into high and low EGFP expression. Plots for WT-EGFP-WASp and untranfected (UT) cells are shown. (b) and (e) show forward – side scatter plots and the gating used for unsorted cells. (c) and (f) shows the EGFP expression of gated cells. (d) and (g) show the gates used to separate high expressor (gate I) and low expressors (gate H). (h) and (i) show the EGFP expression of sorted cells. **(j)(k)** Following sorting, % EGFP positivity of stably transduced cell lines (high expressers) was determined regularly by FACS. (j) shows clinical mutant constructs and (k) shows domain deletion constructs. For all FACS experiments at least 10^4 cells were analysed.

positive cells ((Moulding et al., 2007) and personal communication Dale Moulding). As a result, these cell lines were established using an MOI of 5, and expression was checked using FACS at day 3 and 9. At day 9 cells were completely harvested for SDS-PAGE and western blotting (see figure 8.3).

8.2.1 Stability of EGFP-WASp expression

The percentage of EGFP-WASp positive cells within each transfected culture, gives a surrogate marker of the impact of over expression of each WASp construct on the cell's growth, division and survival. Any cell culture containing EGFP positive cells will also contain untransfected cells, and therefore any impairment of growth induced by transfection will result in a rising percentage of EGFP negative cells.

Figure 8.1a shows the percentage EGFP positivity for each construct during the 31 days following transfection and figures 8.1j and k show similar data for the 55 days following cell sorting. All the WASp constructs show a fall in expression by 31 day post transfection compared to the SEW transfected cells. The greatest loss of EGFP expression is seen with the 4 clinical, dEVH1, H246D and dVCA domain constructs.

Following sorting, EGFP positivity drops from 100% to between 85 and 95% for all constructs within the first 10 days (figure 8.1j and k). After this, however, EGFP expression remains stable at between 80 and 90% for all constructs except dVCA (figure 8.3a). The dBasic and dPolyP constructs retain higher levels of EGFP positivity than WT, whereas the H246D and dEVH1 constructs show a similar pattern to WT WASp. The clinical mutants have a small but consistent impairment of EGFP expression compared to WT WASp, with expression running at approximately 5% lower than WT. The dVCA construct showed a much faster fall in EGFP expression and once stabilised, this expression was approximately 20% lower than that of WT WASp.

The fall in EGFP WASp expression seen in lentivirus transduced cells could be due to toxicity of the virus itself or due to toxicity of the encoded protein. In the experiments shown a high multiplicity of infection was used (5) to transduce the U937 cells, with the aim of maximising the detection of any differences between the constructs. As a result some viral and / or transgene toxicity is very likely, and a high proportion of EGFP positive cells will contain more than one copy of the EGFP WASp gene. If it is assumed that cell death due to lentiviral toxicity is equal between each WASp construct, then differences in EGFP WASp expression are likely to reflect differences in toxicity of mutant WASp protein. The effect of viral toxicity was further minimised in these experiments by sorting the cells several

weeks after lentiviral infection, and following EGFP expression for a further 2 months following sorting.

In summary, these results demonstrate that the dVCA construct shows a significant fall in expression over time, and this fall continued throughout the 3 months of monitoring expression. The clinical mutants showed a small reduction in EGFP expression compared to WT, although this difference appeared to stabilise at approximately 5% less than WT WASp expression. The rate of decrease in EGFP-WASp positivity was similar between the clinical mutant and WT. The remaining truncation and deletion constructs showed a similar temporal pattern of EGFP-WASp expression to WT.

8.2.2 Level of EGFP WASp expression by FACS

Figure 8.2 shows the EGFP fluorescence profile, by FACS, of the stably transfected U937 cell lines 55 days following sorting and this information is shown graphically in figures 8.3a and 8.3b. These plots illustrate that although each of these cell lines may have similar levels of EGFP positivity, the amount of fluorescence within each cell varies between different cell lines. The SEW transfected cell lines show levels of fluorescence 20x higher than the next “brightest” cell line and the dVCA transfected cells showed a significantly lower mean fluorescence intensity (MFI) than the other WASp transduced cell lines.

The clinical mutants all show lower levels of fluorescence than WT. Although this difference appears quite small in figure 8.3b, it is more convincing when the individual FACS plots are assessed (figure 8.2). This difference in MFI between WT and the clinical mutants was repeatedly seen on a total of 10 FACS analysis taken at time points before and after the cell lines were sorted for expression. The MFI recorded is that of EGFP positive cells only, so this difference cannot be accounted for by small differences in the % positivity within each culture. The dEVH1 transfected cell line consistently showed higher levels of fluorescence than WT transfected cell line (figure 8.2 and 8.3b).

8.2.3 FACS data for constitutively active constructs

Figures 8.3c and 8.3d show the % EGFP positivity and median fluorescence intensity of U937 cells, 3 and 9 day following lentivirus transfection with various constitutively active EGFP-WASp constructs. All the constitutively active constructs tested dropped both the number of cells expressing EGFP-WASp and the intensity of expression much faster than WT WASp. For the constructs I294T, Y291E and dVCA binding, this fall in expression was noticeably more rapid than

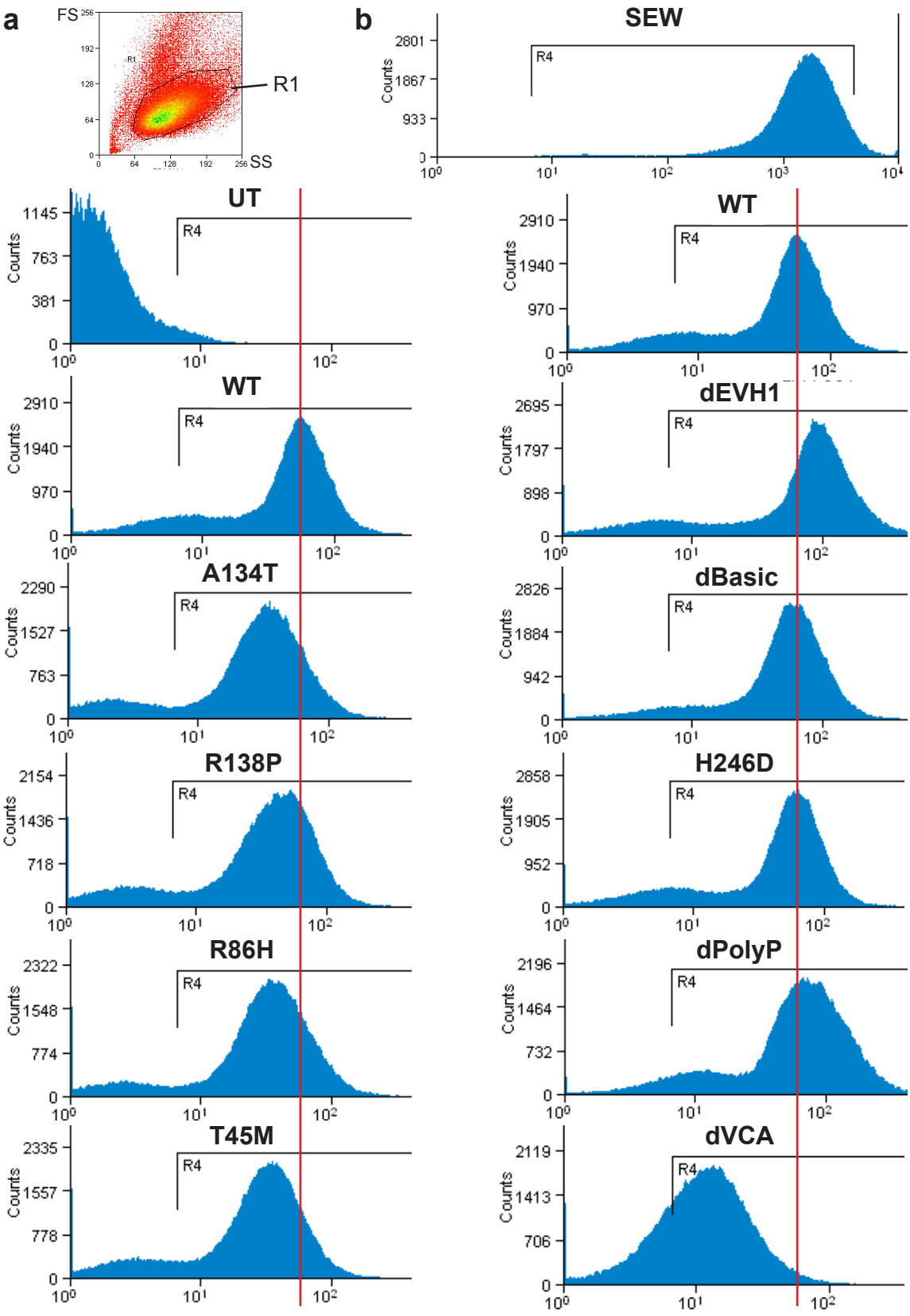

Fig 8.2 FACS plots of EGFP-WASp transduced U937 cells
U937 cells stably transduced with EGFP-WASp and sorted for high expression. These plots were generated 55 days after sorting. 10^5 cells were acquired with at least 80% within the viable cell gate (R1). **(a)** Forward - side scatter plot of untransduced cells showing gated cells analysed. **(b)** Frequency histograms showing EGFP fluorescence intensity plots for full panel of constructs. Red line illustrates the mean flourescence intensitiy for WT-WASp.

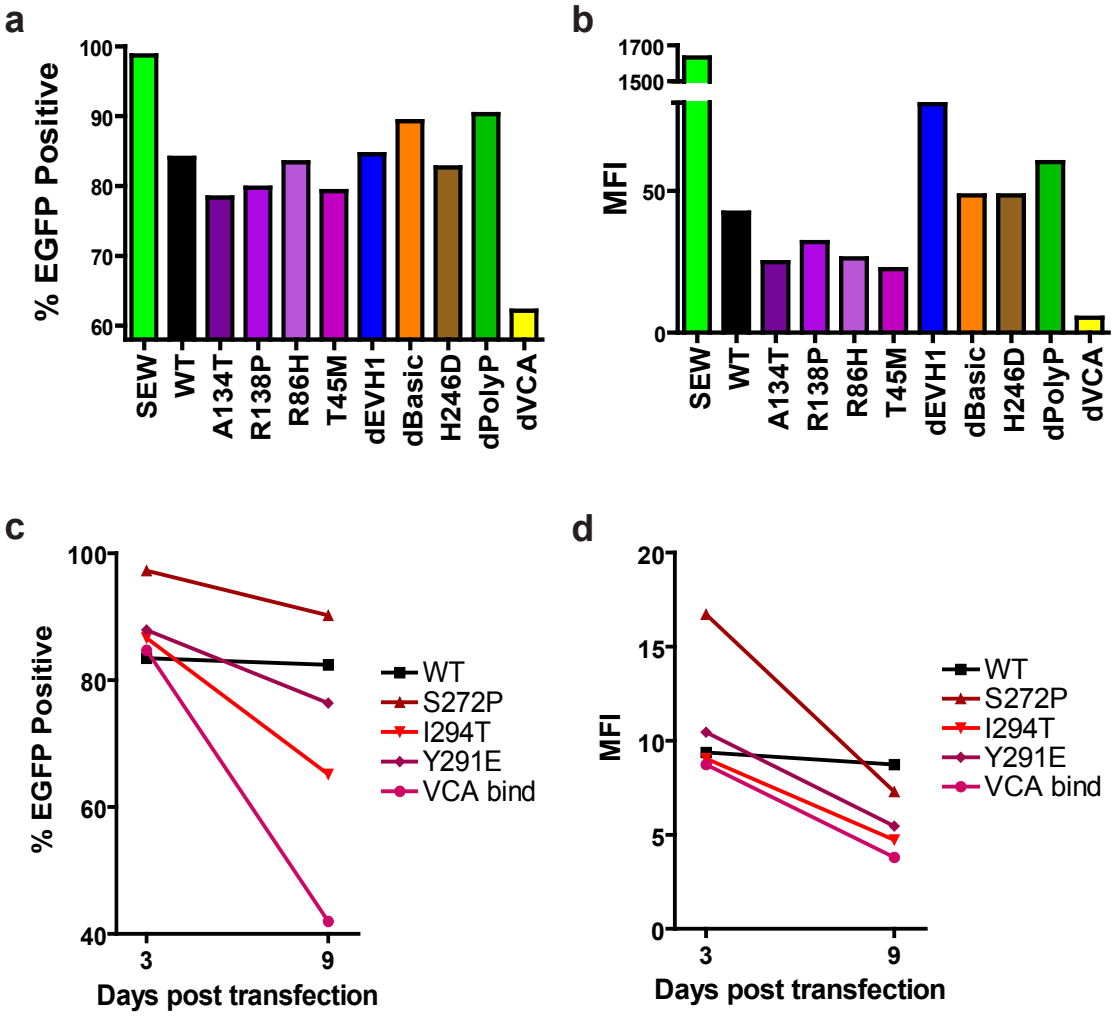

Fig 8.3 % EGFP positivity and mean fluorescence intensity of U937 cells transduced with EGFP-WASp constructs
(a) and **(b)** show % EGFP positivity and median fluorescence intensity for U937 cells after 55 days of culture following cell sorting for high expression. **(c)** and **(d)** show % EGFP positivity and mean fluorescence intensity for the constitutively active mutant panel of constructs, 3 and 9 days following lentivirus infection with an MOI of 5.

that seen with all the other constructs tested in the standard panel (compare % positivity at 9 days post infection in figure 8.3c, to 10 days in figure 8.1a). A fall in MFI of the remaining positive cells also supports this, suggesting cells with lower levels of WASp expression have a survival advantage over those with higher expression levels. Interestingly the rate of fall in expression (figure 8.3c) appears proportional to the level of constitutive activity (figure 5.3).

Transfection with the S272P construct led to very high levels of toxicity within the cell culture. In fact, at day 9 post infection only 15% of cell analysed fell into the viable cell gate as determined by side and forward scatter, compared to at least 55% for all other constructs. It is very likely that this high level of cell death will have impacted on the growth of untransfected as well as transfected cells in

culture, resulting in a falsely high % positivity reading. The cell culture growth of the S272P transfected cells was insufficient to allow any further experiments on this construct in U937 cells.

8.2.4 Expression by Western blotting

SDS-PAGE and western blots were performed on standardised cell lysates from post sorted stably transfected U937 cells lines. Blots were performed to analyse the expression of EGFP-WASp constructs within the U937 cells and also to assess the impact of over expression of mutant EGFP-WASp constructs on endogenous WASp expression. Because these cell lines stably express EGFP-WASp with similar levels of positivity (except for the dVCA construct) it is valid to directly compare lysates from these stable cell lines. The results from dVCA transduced lysate should be treated with more caution, as this cell line showed approximately 70% of the EGFP positivity of WT cell lines.

Figure 8.4a shows an example series of blots and figures 8.4b – d show the combined analysis of densitometry performed on blots from 3 separate batches of transfected U937 cell lysates. The methodology used to standardise the densitometry readings is described in detail in chapter 2.7.3

These results demonstrate that the clinical mutants have lower levels of EGFP-WASp expression than WT. Although this difference is small (25-50% protein levels of WT WASp), it is reproducible and significant. Of note a similar difference was also found in U937 cells lysates following initial transfection, but before sorting, and in THP-1 cells transfected with EGFP-WASp constructs (data not shown). The dEVH1, dBasic and dPolyP transduced cell lines all show higher levels of expression than WT, (although these differences never reached significance), and the H246D construct showed similar expression to WT. The dVCA construct expressed at significantly lower levels than WT, and this level (approximately 1/25th that of WT WASp) could not be explained by the differences see in % EGFP positive cells. All these results corroborate the MFI data from FACS analysis.

A more striking difference is seen in the effect of EGFP-WASp expression on endogenous WASp expression. The WT, dBasic and Polyproline constructs all markedly suppress endogenous WASp expression, whereas all the other constructs (including the dEVH1 construct) do not reduce endogenous WASp expression. The H246D construct shows a similar pattern of endogenous WASp suppression to WT WASp, but this suppression does not reach significance. Figure 8.4d demonstrates that the clinical mutants (and dVCA) have more endogenous WASp than EGFP-WASp, whereas WT EGFP-WASp and the remaining domain

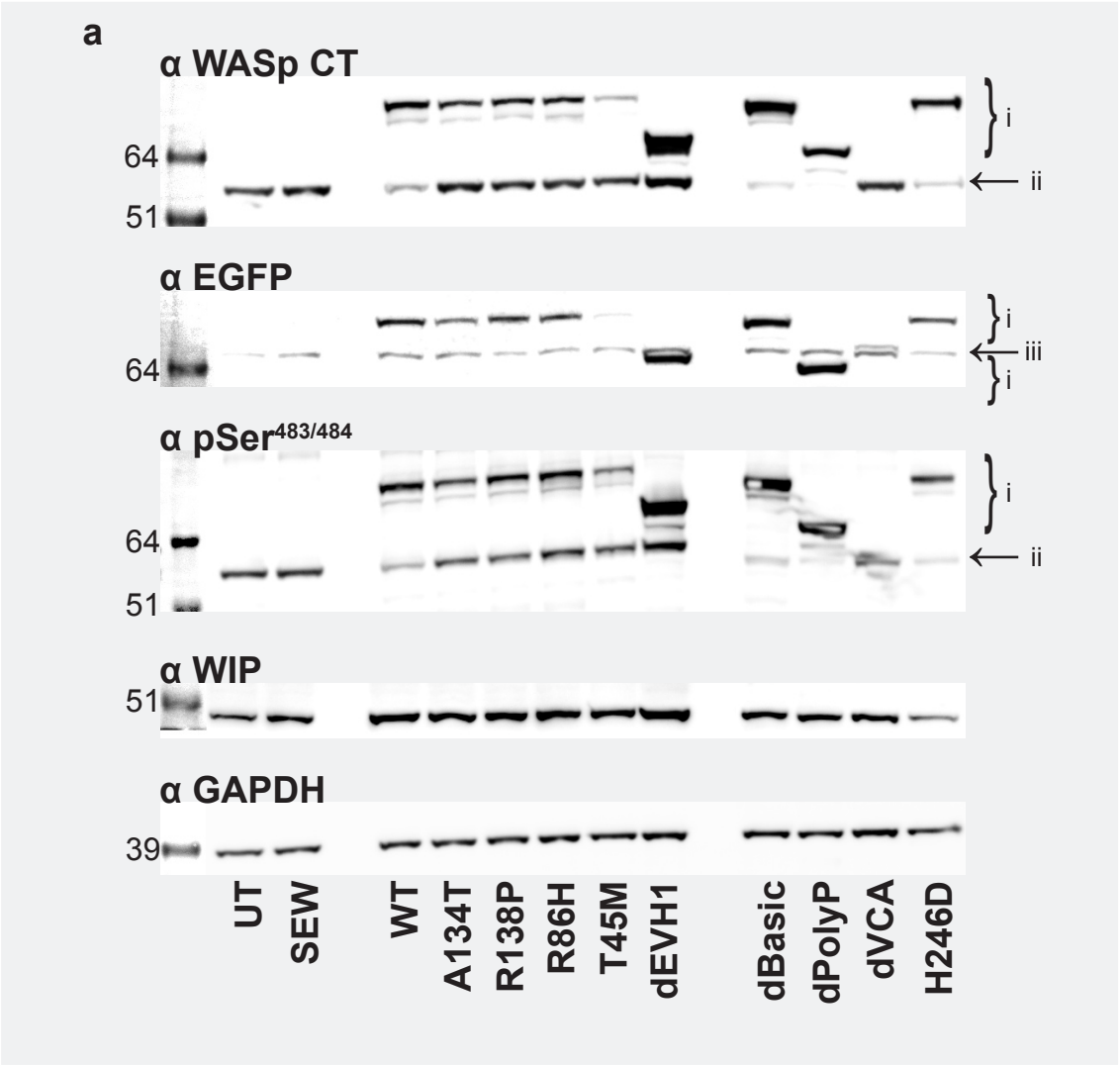

Fig 8.4 Western blots of lysates of U937 cells stably transduced with EGFP-WASp constructs (standard panel)

(a) 2x10^6 U937 cells stably transduced with EGFP-WASp constructs and sorted for high expression were lysed in 100µl of lysis buffer. Lysate was clarified by centrifugation and the concentration of supernatants was determined by BCA assay. Lysate concentration was standardised between constructs and then reduced in sample buffer, before resolution by SDS-PAGE. Each immunoblot shown represents a separate electrophoresis gel. *Band labels (i) EGFP-WASp (ii) endogenous WASp (iii) Non specific band cross reacting with anti EGFP antibody.*

(b) to (d) The above experiment was repeated with 3 separate batches of U937 cell lysate, from the same stably transfected U937 lines. Densitometry was performed on EGFP-WASp, endogenous WASp and GAPDH bands. From these readings, standardised values for EGFP-WASp (relative to U937 cells tranfected with WT-EGFP-WASp) and endogenous WASp (relative to levels in untranfected U937s) were determined for each experiment and the mean and standard error for this data are shown in (b) and (c). For ease of viewing the y axis of these graphs has been logged to base 2 and as a result the standardised values (WT in (b) and UT in (c)) appear as 0. (d) shows the mean and standard error of the EGFP WASp / endogenous WASp ratio for each construct. For graphs (b) and (c) paired one sample t tests were used to compare deviation of the means from a standard of 1, and for (d) paired two sample t tests were used to assess deviation of each sample from the WT mean. See materials and methods for further details of data processing and analysis.

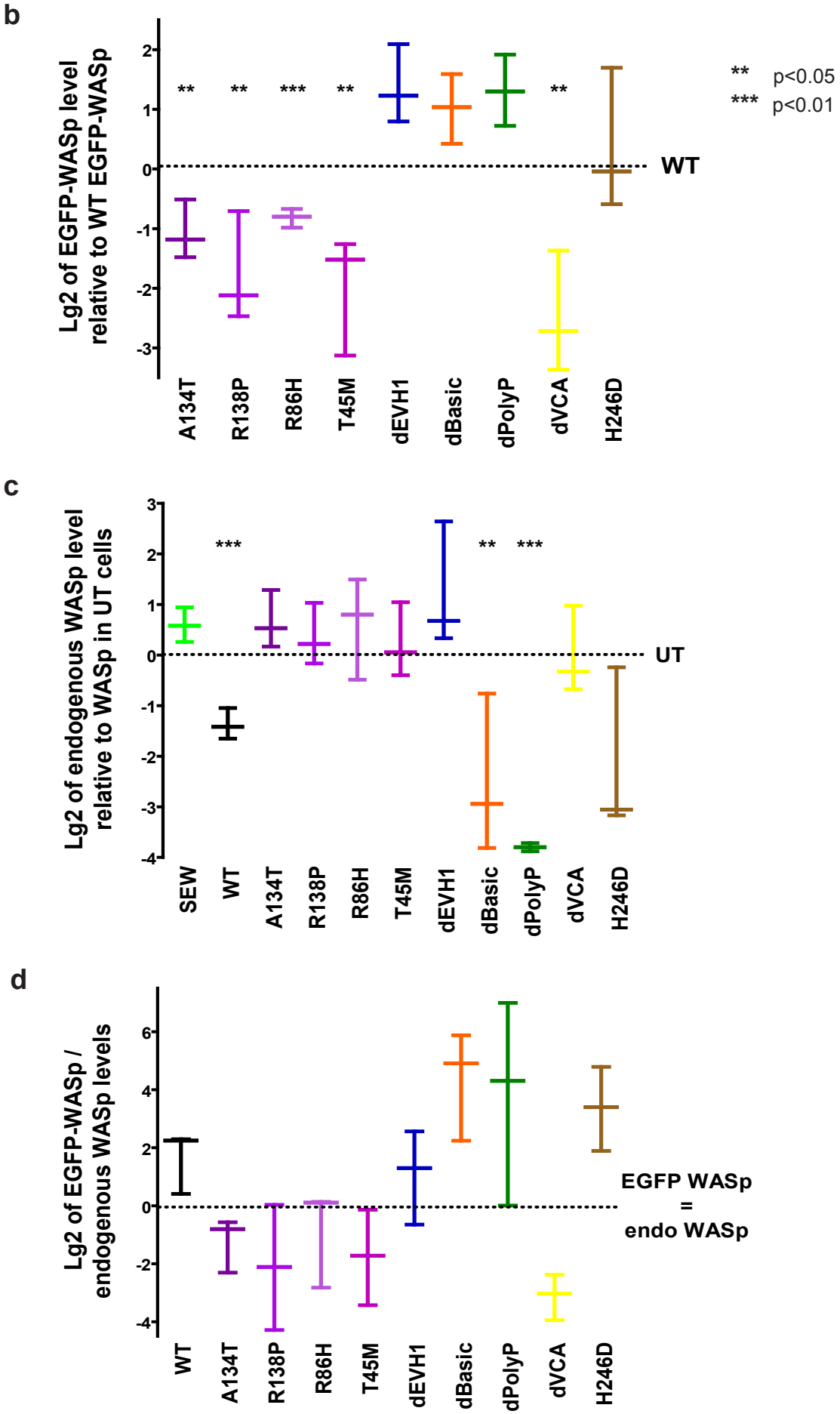
b
Lg2 of EGFP-WASp level relative to WT EGFP-WASp
2
1
0
-1
-2
-3
**
**
***
**
**
WT
** p<0.05
*** p<0.01
A134T
R138P
R86H
T45M
dEVH1
dBasic
dPolyP
dVCA
H246D
c
Lg2 of endogenous WASp level relative to WASp in UT cells
3
2
1
0
-1
-2
-3
-4
***
**
***
UT
SEW
WT
A134T
R138P
R86H
T45M
dEVH1
dBasic
dPolyP
dVCA
H246D
d
Lg2 of EGFP-WASp / endogenous WASp levels
6
4
2
0
-2
-4
EGFP WASp
=
endo WASp
WT
A134T
R138P
R86H
T45M
dEVH1
dBasic
dPolyP
dVCA
H246D

deletion constructs have a great excess of EGFP-WASp compared to endogenous WASp. All four clinical mutants show a weakly significant ($0.05 < p < 0.1$) reduction in the EGFP-WASp / endogenous WASp ratio compared to WT. Of importance the level of WIP in all these cell lines appears comparable (figure 8.4a). The serine phosphorylation results are discussed in chapter 8.3.

Figure 8.5 shows the equivalent results for U937 cells transduced with the constitutively active panel of constructs, with cells harvested 9 days post transfection. It can be seen that cells transduced with I294T, Y291E and dVCA bind EGFP-WASp show similar levels of EGFP-WASp expression as WT. Similarly all three constitutively active constructs induced marked suppression of endogenous WASp (figure 8.5c). Figure 8.5d demonstrates that within these transduced cell lines the vast majority of WASp is the exogenous EGFP-WASp.

8.2.5 Copy number of exogenous WASp genes

To assess whether the differences in intracellular protein concentration could be accounted for by differences in efficiency of cell transfection by different EGFP-WASp constructs, I assessed the copy number of exogenous EGFP-WASp genes within the cell lines being assessed. As U937 cells were harvested for lysate preparation in one of the experiments shown in figure 8.4, cells were simultaneously harvested for DNA and RNA preparation. Copy number of transfected genes was determined using real time PCR to a sequence within the WPRE, and was quantified by standardisation to actin (chapter 2.12). Unfortunately data from the A134T construct was uninterpretable and is therefore not shown.

Fig 8.6a shows that all the stable U937 cell lines had an average copy number within a factor of 2 of WT, (with the exception of R138P which had a copy number approximately 4x greater than WT). Of importance all the constructs with lower levels of protein expression showed higher copy numbers than WT. Therefore reduced transfection efficiency cannot account for the differences in protein expression seen.

8.2.6 mRNA transcription of EGFP-WASp and endogenous WASp

RNA isolated as above was converted to cDNA by reverse transcriptase and then real time PCR was performed on the cDNA to determine the levels of EGFP-WASP and exogenous WASp mRNA transcripts in each stably transfected cell line. The level of expression was standardised to the housekeeping gene PGK1, and transcript expression was calculated as a ratio of the expression seen in WT EGFP-WASp (for EGFP-WASp) or in untransfected cells (endogenous WASp).

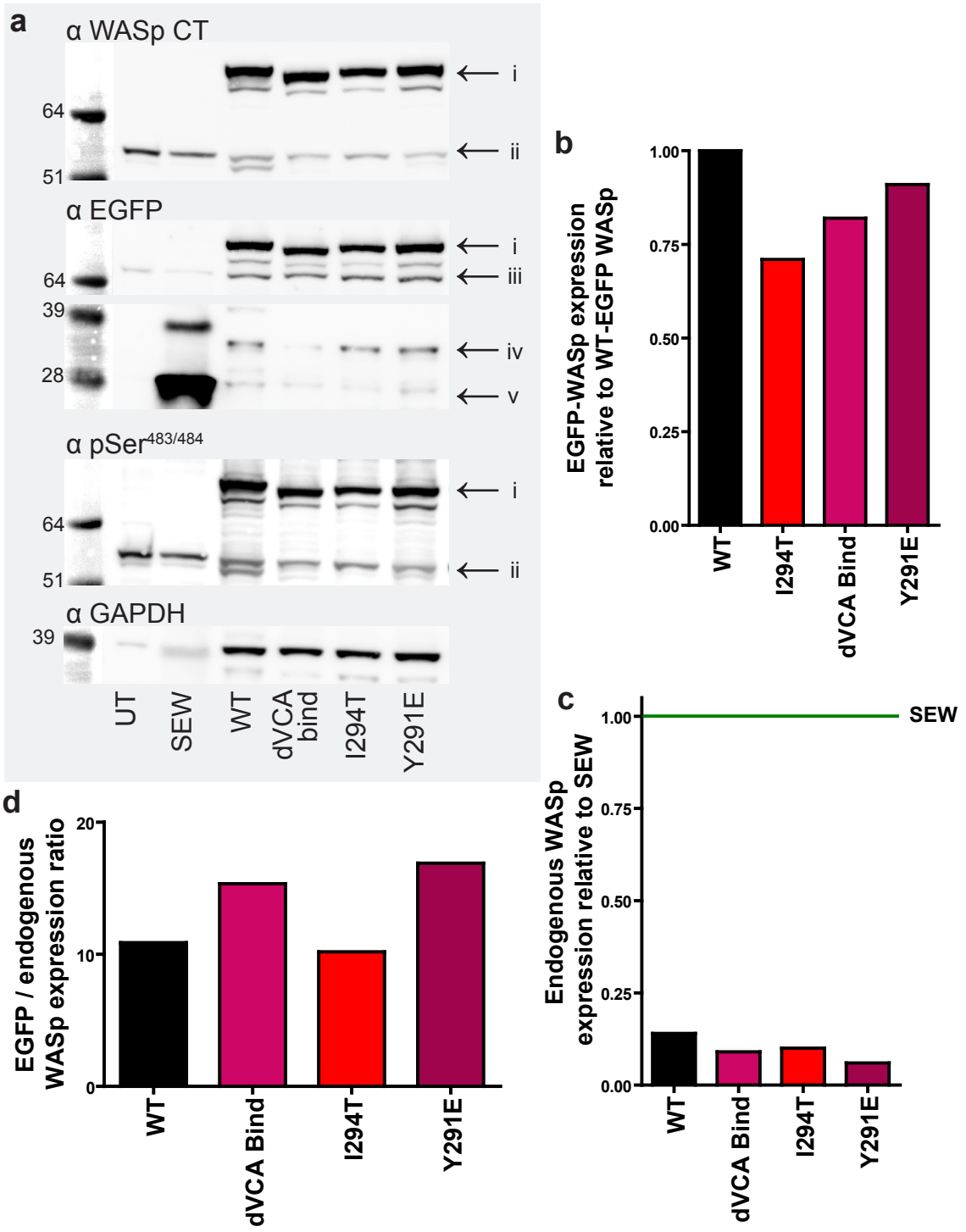

Fig 8.5 Western blots of lysates of U937 cells stably transduced with EGFP-WASp constructs (constitutively active panel)
(a) U937 cells transfected with EGFP-WASp by lentivirus were harvested on day 9 after infection. Lysate from $2x10^6$ cells lysed in 100µl of lysis buffer, was clarified by centrifugation and the concentration of supernatants was determined by BCA assay. Lysate concentration was standardised between constructs and then reduced in sample buffer, before resolution by NuPAGE. For each immunoblot a separate electrophoresis gel was run (using the same lysate). *Band labels (i) EGFP-WASp (ii) endogenous WASp (iii) Non specific band cross reacting with anti EGFP antibody (iv) 35kDa degradation band (v) EGFP.* **(b)** to **(d)** densitometry and analysis was performed as for fig 8.4, except western blots were only performed on a single batch of lysate.

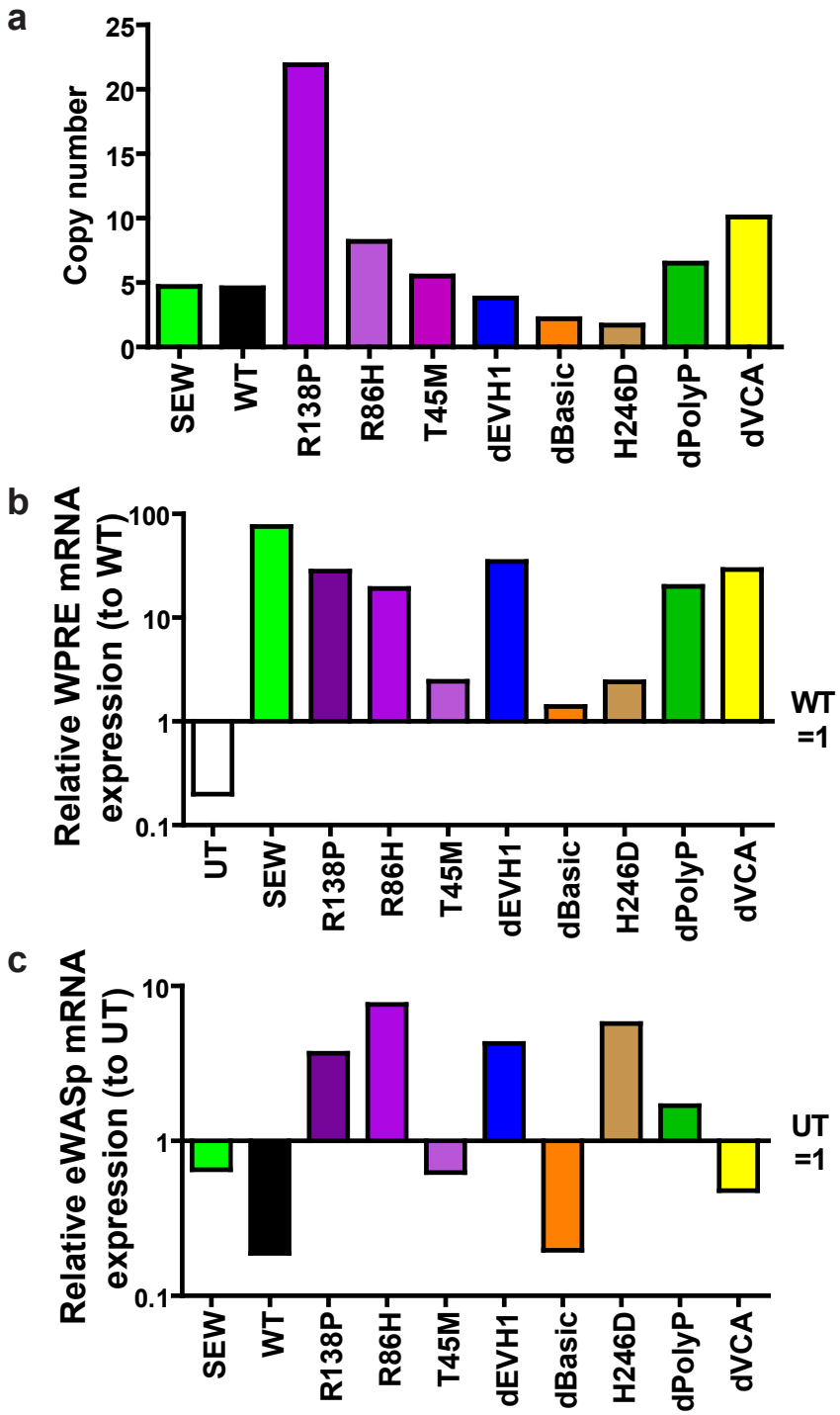

Fig 8.6 Copy number and expression of transduced EGFP-WASp genes in U937 cells
DNA and RNA was extracted from cell pellets of stably transduced U937 cells as described in chapter 2.12.1 and 2.12.3. **(a)** Copy number was determined by RT-PCR as described in chapter 2.12.2. The data presented is representative of two experiments, each performed in triplicate. **(b),(c)** mRNA expression was determined by reverse transcriptase RT-PCR as described in chapter 2.12.4 and 2.12.5. Expression of exogenous EGFP-WASp was determined by amplification of a sequence within the WPRE (Woodchuck Posttranscriptional Regulatory Element), which was contained within the lentivirally encoded transcript. This, and expression of endogenous WASp, were standardised to the expression of the housekeeping gene, phosphoglycerate kinase (PGK), and standardised expression was calculated relative to either WT-EGFP-WT (WT) trasnduced cells or untransduced cells (UT). Results are representative of two experiments each perofmred in triplicate. For each experiment the samples on the A134T construct were lost for technical reasons.

The technique and analysis are described in more detail in Chapter 2.12.

Figures 8.6b shows that the T45M, dBasic and H246D showed similar levels of transcription to WT, whereas the remaining constructs showed substantially greater levels of transcription. No construct tested had lower levels of mRNA detected than WT. Interestingly the WT and dBasic constructs also show suppression of endogenous WASp transcription compared to untransfected cells, whereas the majority of the other constructs show increased endogenous WASp transcription.

Together these results strongly suggest that the mechanism underlying the differential levels of cellular EGFP-WASp protein between constructs lies downstream of transagene copy number and expression. There is some suggestion that over expression of EGFP-WASP constructs with the greatest functionality (WT, dBasic, H246D), may lead to suppression of endogenous WASp (and even EGFP-WASp) gene transcription. Conversely constructs resulting in the lowest levels of functional WASp in cells have upregulation of endogenous WASp gene transcription. Unfortunately there were technical problems with repeats of the above experiments which would have strengthened this data. Further work could clarify this potentially interesting finding, but this was beyond the scope of this project.

8.3 Phosphorylation of EGFP-WASp

Phosphorylation is thought to play an important role in the regulation of WASp activity. Phosphorylation of residues ser242 (Yokoyama et al., 2005), ser483 and ser484 (Cory et al., 2003), and tyr291 (Torres and Rosen, 2006; Torres and Rosen, 2003; Cory et al., 2002) have been shown to increase actin polymerisation activity, and it has been demonstrated that this phosphorylation is required for normal WASp activity (Badour et al., 2004; Suetsugu et al., 2002).

To assess whether the mutant WASp constructs under investigation are phosphorylated normally in U937 cells, the levels of tyrosine and serine phosphorylation were compared between WT and mutant EGFP-WASp in cell lysates. An antibody specific to WASp phosphorylated at ser483 or ser484 is commercially available, therefore this was used to directly immunoblot cell lysates. To assess tyrosine phosphorylation, EGFP-WASp was immunoprecipitated using an anti EGFP antibody, and the immunoprecipitated was then immunoblotted with an anti phosphotyrosine antibody. For both experiments phosphorylation was expressed as a proportion of EGFP-WASp phosphorylated relative the proportion of WT EGFP-WASp phosphorylated (see chapter 2.7.4 and figure 8.7 legend).

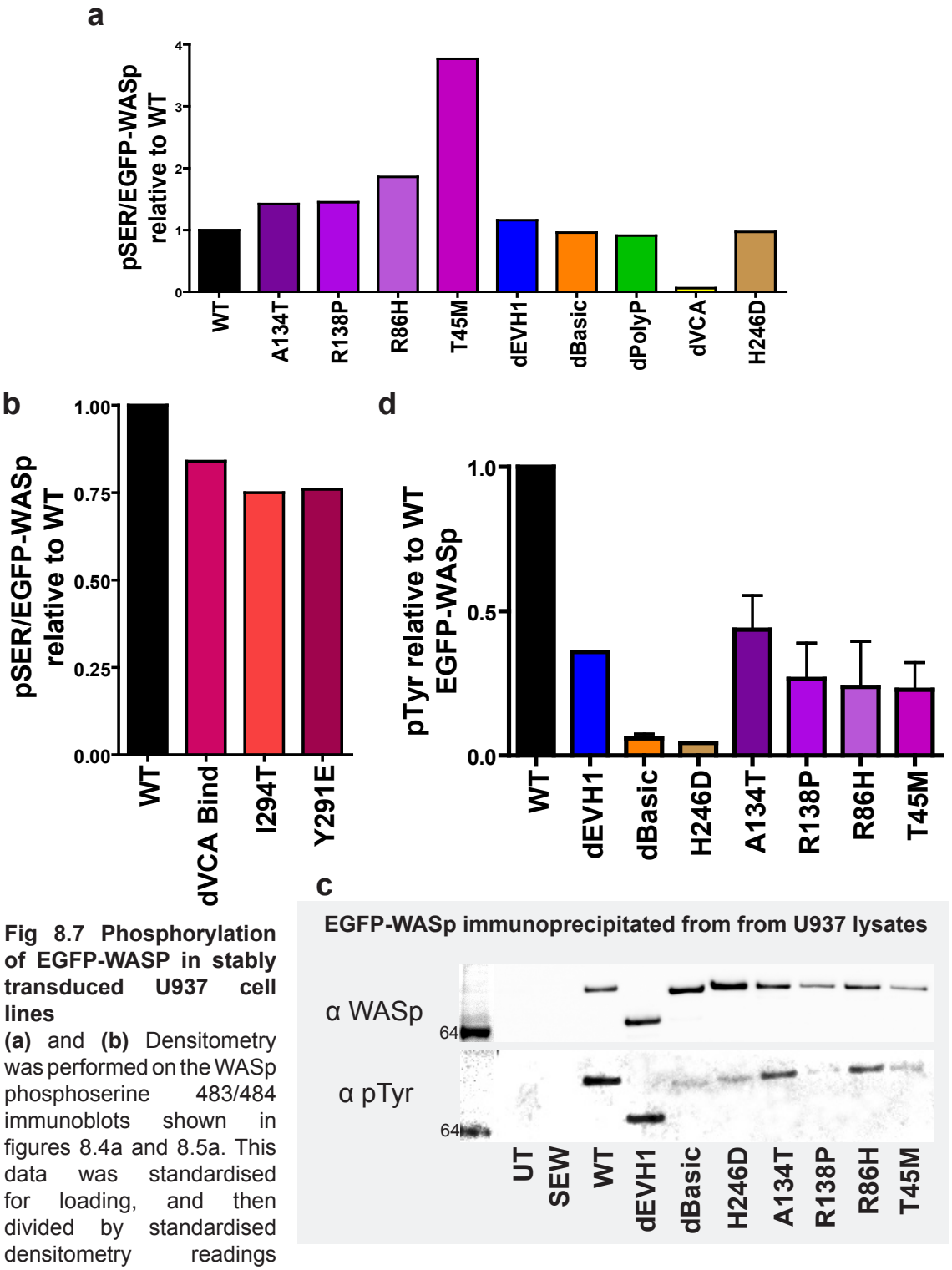

Fig 8.7 Phosphorylation of EGFP-WASP in stably transduced U937 cell lines

(a) and **(b)** Densitometry was performed on the WASp phosphoserine 483/484 immunoblots shown in figures 8.4a and 8.5a. This data was standardised for loading, and then divided by standardised densitometry readings for EGFP-WASp. This ratio was then standardised to WT EGFP-WASp to give a proportional serine phosphorylation relative to WT (see chapter 2.7.4 for more details and formulae used). The fraction of serine phosphorylated WASp in the WT EGFP-WASp cell line is standardised to a value of 1. **(c)** Tyrosine phosphorylation of EGFP-WASp immunoprecipitated from U937 lysates. $2.5x10^6$ transfected U937 cells were lysed in APB supplemented with 1mM DDT, 10% glycerol and 5mM GDP and clarified by centrifugation. Supernatants were incubated with 25µl of anti EGFP antibody immobilised on resin containing 6.25µg of antibody, overnight at 4˚C. The resin was then washed 3x with APB before elution with IP elution buffer. The elutant was then reduced in sample buffer and resolved by SDS-PAGE prior to immunoblotting for WASp and anti phosphotyrosine. **(d)** Densitometry was performed on WASp and phosphpotyrosine bands and was analysed as above.

The phosphoserine immunoblots of whole cell lysates shown as part of figure 8.4a and 8.5a, and the remaining data are in figure 8.7.

Figure 8.7a shows that the clinical mutants show proportionally more serine phosphorylation than WT, whereas the other constructs show very similar phosphorylation levels to WT. The low level of phosphorylation seen with the dVCA is expected because the ser483 and ser484 residues are deleted in this construct.

By contrast, the clinical mutants and the dEVH1 mutant showed reduced tyrosine phosphorylation compared to WT. Interestingly the dBasic and H246D constructs showed almost absent tyrosine phosphorylation. The two constructs were unable to bind Cdc42 (figure 7.1), and therefore emphasise the importance of Cdc42 binding to WASp for tyrosine 291 phosphorylation. These results are representative of two experiments.

8.4 Sensitivity to protease inhibition

Results presented earlier in this chapter demonstrated that intracellular levels of clinical mutant WASp are lower than WT WASp when over expressed in U937 cells. One explanation for this finding is that clinical mutant EGFP-WASp is degraded by cellular proteases faster than WT EGFP-WASp. Previous studies have suggested a specific role for calpain in both the degradation of WASp, and also in the normal turnover of WASp mediated actin based structures (Calle et al., 2006b; Shcherbina et al., 2001). Other groups have suggested that degradation by the proteosome is more important (de la Fuente et al., 2007). To test these hypotheses and to assess the role of specific proteolytic pathways in the degradation of mutant WASp, stably transfected U937 cells were treated with a range of protease inhibitors. For calpain inhibitition, ALLM and calpeptin were used, for proteosome inhibitition, MG132 was used and for cysteine protease inhibition, Cathepsin inhibitor 1 was used.

Figure 8.8a shows a western blot of lysates of A134T and WT EGFP-WASp transduced U937 cells treated for 3 hours with a range of protease concentrations. Selected data only is shown in figure 8.8a; the WT transduced cell line was tested with all four inhibitors but as the results were identical, the blots from only two inhibitors are shown. There appears to be no significant effect on the levels of either EGFP-WASp or endogenous WASp in response to any of these protease inhibitors (graphs of densitometry for this experiment are shown in figures 8.8d and e). There is a suggestion that treatment of the A134T cell lines with calpain inhibitors may cause a rise in both endogenous and EGFP-WASp levels (figure

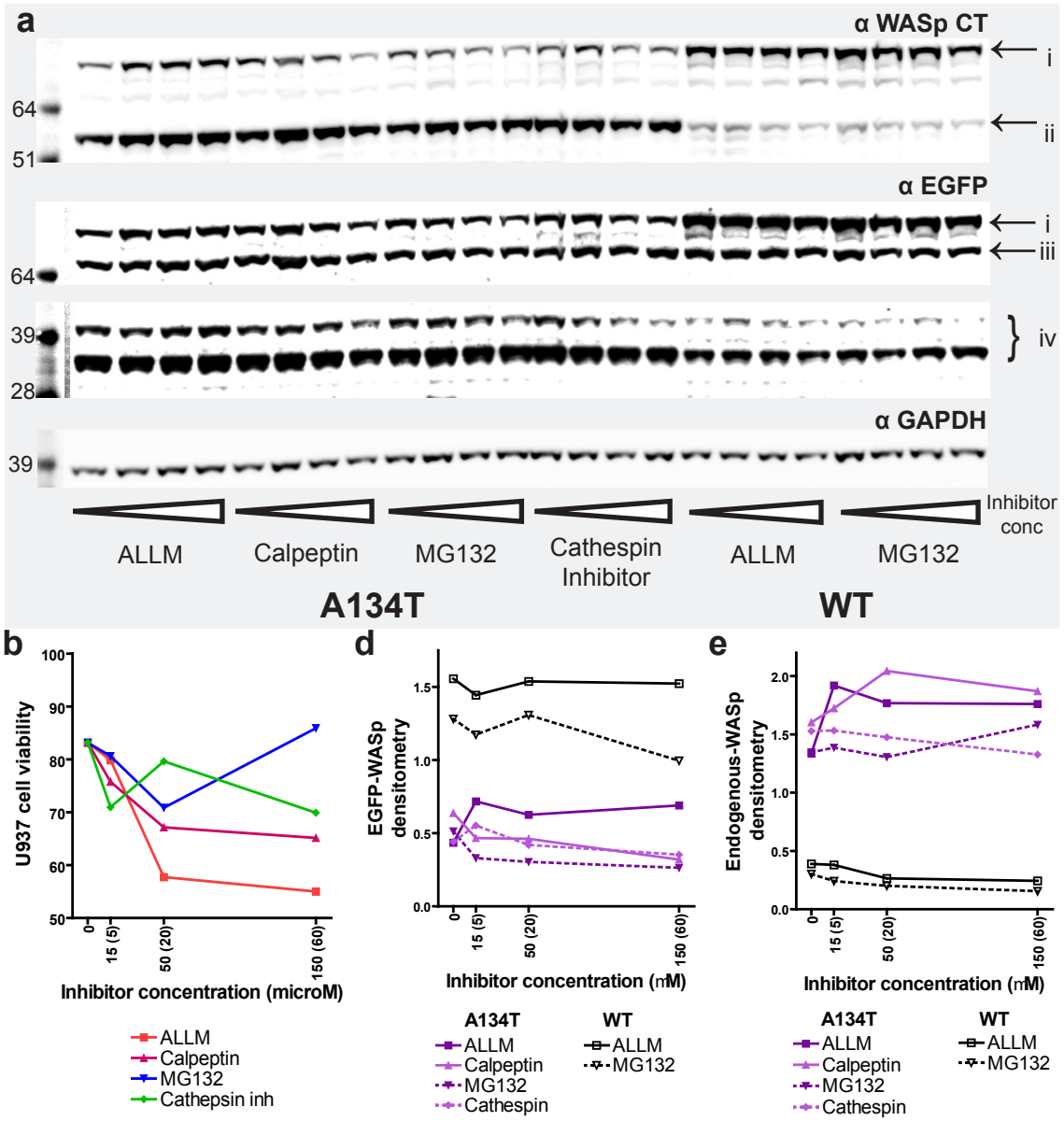

Fig 8.8 Effect of protease inhibitors on EGFP-WASp levels in U937 cells

WT and A134T EGFP-WASp transduced U937 cells were seeded in 24 well plates at 0.5x10^6/ml. The following day each construct was treated for 3 hours with 3 concentrations of 4 protease inhibitors (ALLM and Cathepsin inhibitor at 0mM, 15mM, 50mM and 150mM and Calpeptin and MG132 at 0mM, 5mM, 20mM and 60mM. Following this 20% of cells in each well were stained with tryphan blue and counted for viability, and the remaining cells were washed and then lysed in LB, reduced in SB and resolved by reducing NuPAGE and western blotting. Additional wells were treated with ALLM, and these were used to assay the effect of ALLM on calpain activity in cell lysates using the Calpain-Glo™ protease assay (Promega). Lysates were incubated with a proluminescent calpain substrate, which releases luciferase on cleavage by calpain. Luciferase activity was measured using a luminometer at 15 minutes. Background subtracted light emission is proportional to calpain activity. **(a)** Immunoblots of lysates of A134T transfected cells treated with all 4 inhibitors and WT transfected cells treated with ALLM and MG132. **(b)** Viability of inhibitor treated cells. **(c)** Effect of ALLM on inhibition of calpain activity as determined by Calpain-Glo™ assay. **(d)** and **(e)** Densitometry plots of EGFP-WASp and endogenous WASp from fig 8.8a

8.8d and e). As this effect is small, is based on a single low protein concentration for cells incubated with no inhibitors, and there is no correlation between increase in WASp concentration and inhibitor concentration, I think this observation is artefactual.

One possible explanation for this insensitivity is that even at the highest calpain inhibitor concentration used only 30% of normal calpain activity was blocked (figure 8.8c). Despite this the toxicity seen with these inhibitors was significant (45% death with 150mM of ALLM and 35% death with calpeptin, compared to 15% death with no inhibitors) (figure 8.8b). MG132 and cathepsin inhibitor 1 showed less toxicity, but the inhibition of functional activity in lysates was not tested. Although the protease inhibitor concentrations used spanned the published range of effective usage (Nicola et al., 2005; Steinhilb et al., 2001; Ravid et al., 2000; Melloni et al., 1998), it is possible that higher concentrations of inhibitors were required to see an effect in U937 cells. Similarly, generally the effects of protease inhibitors on protein levels are seen within one hour of treatment (Calle et al., 2006b) (and personal communication Y. Calle), but it is possible that U937 are particularly resistant to protease inhibition (being a malignant cell line) and require longer incubation. Repeat experiments using higher concentrations of protease inhibitors for longer periods of time would help clarify these issues.

8.5 Relative stability of EGFP-WASp constructs

Analysis of the levels of EGFP-WASp in U937 cell lysates suggest that WASp protein containing EVH1 missense mutations is less stable than WT WASp. These experiments, however, only measure the cellular protein levels at a single time point, and as such give a “snap shot” of the cellular processes involve in WASp metabolism. By radiolabelling WASp using ^{35}S at a set time point and following the persistence of this labelled population of WASp proteins over a period of time more accurate information can be obtained about the relative dynamics of the WASp proteins under investigation.

A full description of methodology used is given in the chapter 2.10. Briefly, U937 cells, were pulsed with ^{35}S labelled cyteine and methionine (pulse period), followed by incubation with RPMI medium supplemented with excess cyteine and methionine (chase period). Cell lysates were generated at various time-point into the chase period and EGFP-WASp was immunoprecipitated from these lysates using anti-EGFP antibody coated beads as previously described. Following elution form the beads the EGFP-WASp samples were then resolved by SDS-PAGE and the radioactive emission was measured from the dried gels using

amplifying phospholuminescence screens and a phosphoimager.

8.5.1 Optimisation

Initially two ^{35}S loading protocols were compared and a chase period of up to 48 hours was assessed (see chapter 2.10.4 and figure 8.9 legend). Figure 8.9a and b show the radioactive emission of immunoprecipitant from these experiments, and figure 8.9c shows a graph of the specific emission of the WASp band for each lane (background subtracted). These figures demonstrate that both strategies gave good levels of WASp labelling, and therefore the 6 hour load protocol was adopted as it used less radioisotope. Although there appears to be some difference in the WASp levels by 4 hours chase, the difference is much clearer by 48 hours. Based on these results a standard chase period of 24 hours was subsequently used.

To investigate the relative effects of proteosome mediated and calpain mediated degradation on WASp stability, protease inhibitors (ALLM and MG132) were added to the chase medium. Figures 8.9d and e, show that rather than decreasing degradation as had been hypothesised, addition of either protease inhibitor results in a markedly reduced EGFP-WASp signal post chase. The most likely explanation for this is that incubation with protease inhibitors for 24 hours has caused significant cell toxicity, and as a result fewer cells are viable, and therefore less WASp protein survived to be immunoprecipitated.

8.5.2 Results

Figure 8.10 summarises the results of pulse chase experiments performed on cells transfected with the clinical mutants and selected domain deletion mutants. Due to technical problems with the immunoprecipitation of the 0 hours chase dBasic sample no results are available for this construct. Figure 8.10b clearly shows that the amount of EGFP-WASp protein labelled at the end of the chase period is less for the clinical mutants than for WT. Additionally it can be seen that very little dVCA mutant protein was immunoprecipitated even at the end of the pulse period.

All four clinical mutant proteins show less stability than WT and for three of these proteins that difference was significant (figure 8.10c). By contrast the dEVH1 and SEW proteins are more resistant to degradation and appear to accumulate within the cell (the labelled dEVH1 protein level actually increases during the experiment, suggesting almost absent degradation). A higher proportion of the dPolyP and H246D WASp proteins are degraded by 24 hours than WT, but these

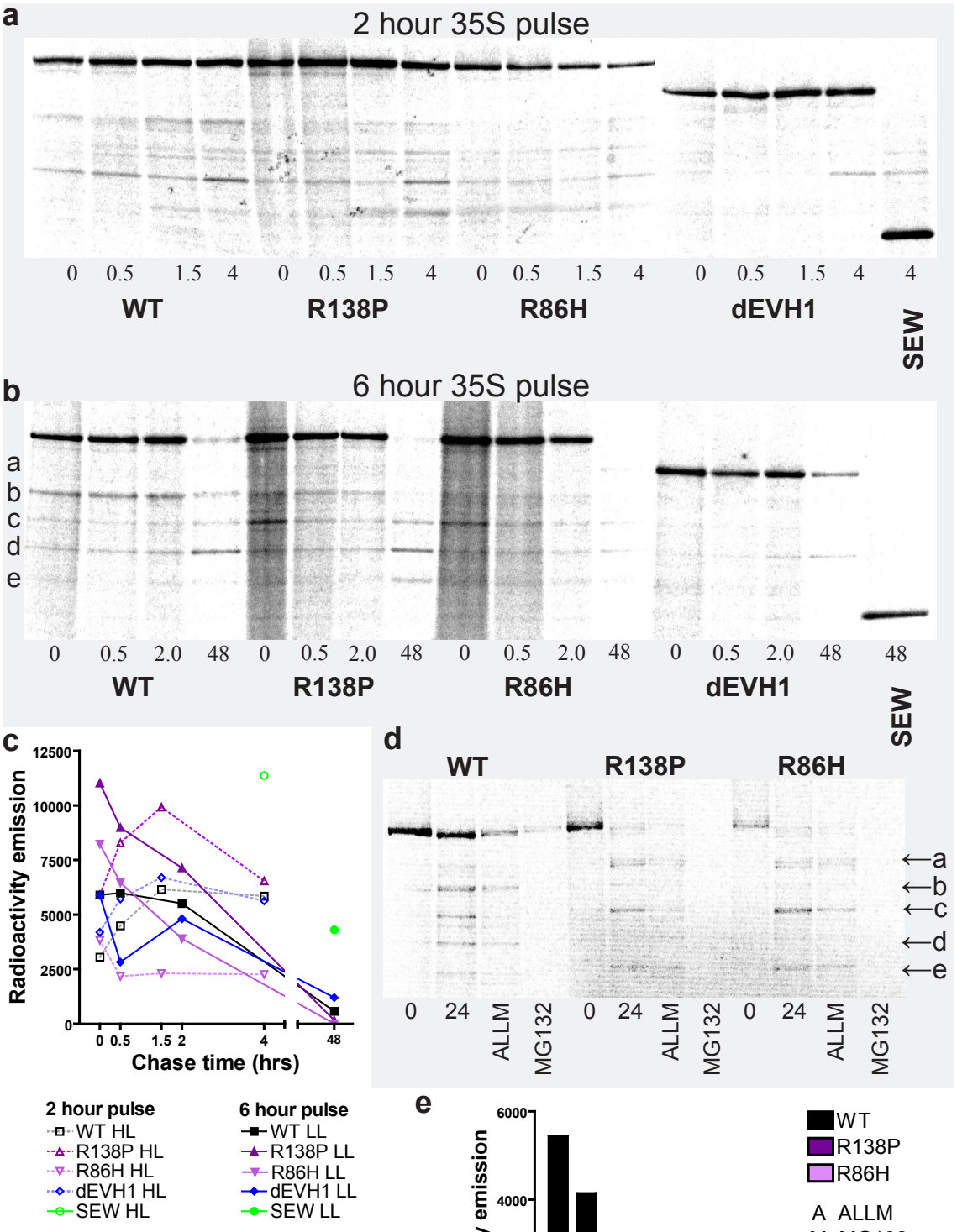

Fig 8.9 Optimisation of ^{35}S labelling of U937 cells and assessment of WASp stability

(a) and **(b)** U937 cells stably transduced with WT, R138P, R86H and dEVH1 EGFP-WASp and SEW, were labelled with ^{35}S cysteine and ^{35}S methionine (Redivue PRO-MIX L-[^{35}S]^{TM}) using two loading strategies. For the 2 hour load, 2x10^6 cells were incubated with 80µCi of PRO-MIX in 400µl of loading medium (cysteine/methionine free RPMI medium, 5% dialysed FCS, 5mM glutamine, penicillin and streptomycin). For the 6 hour load 2x10^6 cells were

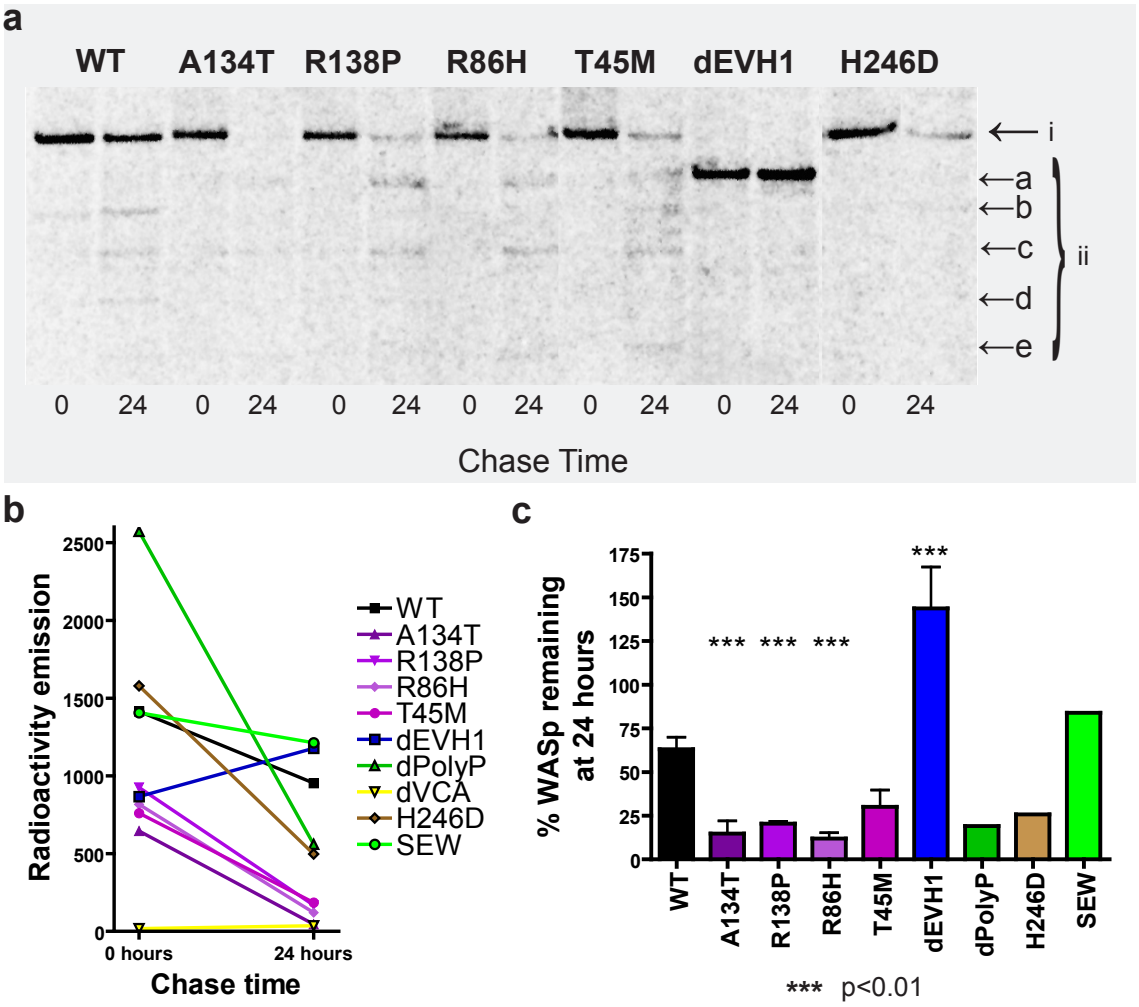

Fig 8.10 Stability of EGFP-WASp constructs expressed in U937 cells using intracellular ^{35}S protein labelling

U937 cells stably transduced with various EGFP-WASp constructs were labelled with ^{35}S using the 6 hour load, and EGFP-WASP protein was immunoprecipitated as described in figure 8.10. A chase period of 24 hours was used to assess relative stability of constructs. Experiments were performed in triplicate for WT, A134T, R138P, R86H, T45M and dEVH1 and singly for remaining constructs. (a) Radioactivity counts from the gel of one experiment. *Band labels (i) EGFP-WASp (ii) Degradation products - (a) 68kDa, (b) 62kDa, (c) 55kDa, (d) 48kDa, (e) 35kDa.* (b) Graph of mean absolute densitometry readings. (c) Mean and standard error for percentage of labelled EGFP-WASp degraded at 24 hours. A one way repeated measures ANOVA test suggested significant differences in the mean values for % degradation (p value of < 0.0001). The Dunnett multiple comparisons test was used to assess which constructs were significantly different from WT, and significance of these differences are marked by stars.

Fig 8.9 cont.

incubated with 50µCi of PRO-MIX in 1ml of loading medium, supplemented with 25mM ALLM and 10mM MG132. Following the load period, cells were washed and reincubated in chase medium (RPMI supplemented with 2mM cyteine and 2mM methionine), and harvested at 0, 0.5, 1.5, 2, 4 or 48 hours of chase incubation. Harvested cells were lysed in APB (containing protease and phosphatase inhibitors), and following centrifugation supernatants were incubated with anti-EGFP resin for immunoprecipitation as previously described. Immunoprecipitates were reduced in SB and resolved by reducing NuPAGE. Gels were dried and then exposed to a phosphor storage screen for 1 month before reading using a Biorad Molecular Imager FX. **(c)** Densitometry readings from experiments (a) and (b). **(d)** U937 cells were loaded as for the 6 hour incubation protocol described in (b). The effects of a 24 hour chase period with 25mM ALLM or 10mM MG132 added to the chase medium was assessed. **(e)** Densitometry from experiment (d). *Degradation bands (a) 68kDa, (b) 62kDa, (c) 55kDa, (d) 48kDa, (e) 35kDa.*

two constructs were only tested in a single experiment and therefore repeats are required to confirm these findings.

Figure 8.10a also demonstrates that the clinical mutants appear to give a different pattern of degradation compared to WT and H246D protein (no degradation bands are visible for the dEVH1 construct). Specifically the clinical mutants appear to have unique bands at 68 and 35 kDa, whereas the WT and H246D lanes have prominent bands at 62 and 48 kDa which are weaker in the clinical mutant transduced cells. All constructs have a band at 55 kDa. The sizes of these bands are all very approximate because of difficulty in determining band size from a radio-emission image.

These results categorically demonstrate a higher rate of turnover of clinical mutant EGFP-WASp protein in stably transfected U937 cell compared to WT WASp. They also show that the dEVH1 WASp mutant appears particularly resistant to degradation, and yet does not appear to be toxic to the cells. By contrast the dVCA construct appears extremely unstable. Importantly these results also demonstrate that the half life for WASp in U937 cells is in the region of 12 to 48 hours, relatively long for a dynamic cytosolic protein. Further experiments to assess whether this stability is reduced if U937 cells are induced to make *de novo* actin structure (for example by activation to become adherent), would provide interesting information.

8.6 Conclusions

In this chapter I have investigated the effect of over expressing EGFP-WASp in a human leukaemia cell line, on WASp homeostasis and modification, and host cell survival. The key findings from this work are the following;

1. EVH1 missense mutations (clinical mutations) have significantly lower levels of cellular expression than WT WASp, despite similar or greater levels of transgene transcription. I have demonstrated that this is due to an increased susceptibility to degradation, although it is possible that the clinical mutants also have a small increase in toxicity compared to WT WASp when over expressed.

2. Deletion of the entire EVH1 domain inhibits degradation, resulting in a WASp protein with a long half life and high levels of cellular expression. This construct does not show increased cellular toxicity compared to WT WASp.

3. The dVCA WASp construct shows greater toxicity and less stability than WT WASp and the clinical mutants, whereas the other domain deletion constructs show similar levels of toxicity, expression and stability to WT WASp.

4. The constitutively active WASp constructs showed the greatest toxicity of all constructs tested, making assessment of protein stability very difficult.

5. If EGFP-WASp was stably expressed at high levels within the cell, the instability of endogenous WASp was increased. The exception for this finding was dEVH1 WASp which had no impact of cellular levels of endogenous WASp.

8.6.1 Assessing WASp expression, stability and toxicity

In this project I have used four parameters to assess the cellular WASp levels in stably transduced U937 cells; (a) percentage EGFP positivity in cell line cultures, (b) mean fluorescence intensity of EGFP positive cells within these cultures, (c) densitometry from western blots of unsorted cell lysates of cultured cells and (d) a radio-isotope labelling degradation assay. Each of these parameters measures a subtly different output and gives information about a combination of WASp synthesis, WASp degradation and toxicity of over expressed WASp. It is important when interpreting the results of all of these assays, to try to dissociate which of these factors account for the behaviour of each WASp construct.

Interpretation of the EGFP positivity experiments is the most complex (figures 8.1 and 8.3a and c). Cell toxicity associated with viral transduction and cell sorting should be seen in the week immediately following this intervention. Interestingly, following cell sorting each transduced cell line (including SEW) has impaired cell division compared to untransduced cells. This suggests that even weeks following lentiviral transduction, the presence of lentivirally inserted genes increases cell toxicity (i.e. cell death or slowed cell division) induced by a stressful event such as cell sorting. If an EGFP-WASP construct exhibited toxicity at the sorted level of expression, then it would be expected that % EGFP positivity within the culture would progressively and rapidly drop to very low levels. This pattern was seen with the constitutively active constructs, but this simple explanation does not account for the stable but lower levels of EGFP positivity compared to WT, seen in the clinical mutants and dVCA transduced cell lines.

One explanatory hypothesis (“toxicity threshold model”) is that these constructs lower the toxicity threshold of U937 cells to an expression level with in the sorting

window. Therefore with WT WASp transduced cells, sorting by high expression will select cells with an evenly distributed range of EGFP-WASp expression within the sorting window. U937 cell cultures transduced with clinical mutants will have lost the higher expressing transduced cells due to toxicity. Sorting will therefore select only cells with the lowest expression within the (same) sorting gate. During long term culture, all cells have a slow attenuation of transgene expression, and as the clinical mutants have a higher proportion of cells with EGFP-WASp expression levels close to the positive / negative threshold, these cell cultures will exhibit lower EGFP positivity.

An alternative explanation ("degradation model") is that the clinical mutants / dVCA protein is less stable, and therefore any individual cell will have a lower MFI for a given transgene copy number. During sorting on identical MFI gates, the unstable WASP constructs will have cells with higher copy numbers selected compared to WT WASp. Greater numbers of lentiviral insertion events are likely to be more disruptive to the host cell genome, and therefore lead to higher levels of toxicity and lower stable levels of EGFP positivity. In support of this model, the copy number of transgenes present in the clinical mutant and dVCA transduced cell cultures was higher than that of WT WASp, despite exhibiting lower % EGFP positive cells in stably transduced culture.

The MFI data (figures 8.2 and 8.3b and d) shows that cell lines with lower stable % EGFP positivities have lower levels of EGFP-WASp expression within individual cells, and is therefore supportive of both the above hypotheses. Interpretation of MFI data assumes that the degradation rate of functional tagged WASp is equal to that of functional EGFP, and that EGFP fluorescence doesn't persist beyond the degradation of WASp. This assumption is also central to the "degradation model". Figure 8.10c suggests that EGFP has a similar half life to WT WASp (assessed at 24 hours only), but this is significantly longer than that of clinical mutant WASp.

The western blot data avoids this problem in that only full length EGFP-WASp is measured, although as discussed above (chapter 8.2.4), differences in % EGFP positivities between different cell lines may bias interpretation of results. The ^{35}S labelling experiments offer a complete dissociation between toxicity and protein stability, and are therefore the clearest to interpret. Even these experiments assume that the rates of degradation of EGFP-WASp are comparable when EGFP-WASp is present at different concentrations within the cell.

8.6.2 Toxicity

Reviewing the results in this chapter in the context of the above discussion, it is clear that the constitutively active constructs are markedly toxic to U937 cells. The rapid fall in EGFP positivity following transduction suggests a significant growth advantage to untransduced cells. This fall is proportionally greater than that seen in MFI, suggesting that toxicity rather than protein instability is the primary explanation for these findings. This is in keeping with previously published data (Moulding et al., 2007), which suggests that constitutively active WASp constructs induce cell division defects and apoptosis in U937 cells.

With results for the dVCA construct, it is difficult to definitively dissociate protein instability from cytotoxic effects of the protein. The ongoing fall in EGFP expression and the fluorescence profile in figure 8.2 suggest that an effect similar to the toxicity threshold hypothesis is occurring and that toxicity of the construct is the most important effect. Additional, no prominent degradation bands were found in western blots of dVCA cell line lysates. In the absence of results from the ^{35}S stability assay, however, and the presence of a high copy number and mRNA expression (figure 8.6) in the remaining cells it is difficult to exclude a major role for protein instability in these findings. Previously published data has demonstrated severe functional defects following over expression of dVCA WASp construct in cells (Tsuboi and Meerloo, 2007; Yarar et al., 2002; Zhang et al., 2002; Suetsugu et al., 2001b; Kato et al., 1999; Machesky and Insall, 1998; Symons et al., 1996), and from these findings a cytotoxic effect of this construct would be expected.

Although the clinical mutant cell lines show a reduced EGFP positivity in long term cell culture, I feel these results are entirely in keeping with the reduced stability of these proteins demonstrated in the ^{35}S stability assay. The reduced positivity can be entirely explained by the “degradation model” described above. Furthermore these clinical mutations are expressed in patients with XLT, who do not show signs of significant cytopenia in any haematopoietic lineage (except platelets).

8.6.3 WASp degradation and suppression of endogenous WASp

8.6.3.1 Clinical mutant WASp

Each of the WASp constructs containing an EVH1 missense point mutation clearly shows less stability than WT WASp, as demonstrated in all of the experimental approaches used to assess this. This is the first direct demonstration of reduced stability of WASp clinical mutants in haematopoietic cell lines and supports previously published experimental (de la Fuente et al., 2007) and clinical observational data (Lutskiy et al., 2005; Jin et al., 2004; Imai et al., 2004;

Lemahieu et al., 1999; Zhu et al., 1997; Remold-O'Donnell et al., 1997). This data combined with the demonstration that these constructs have a reduced affinity for WIP (chapter 6 and figure 6.7) is supportive of the hypothesis that WIP protects WASp from endogenous degradation (de la Fuente et al., 2007; Konno et al., 2007; Chou et al., 2006).

Figure 8.4 demonstrates that overexpression of WT EGFP-WASp in U937 cells leads to suppression of the levels of endogenous WASp, whereas expression clinical mutant EGFP-WASP has little impact on endogenous WASP levels. Expression of EGFP-WASp constructs in U937 cells in the presence of limited WIP, results in competition between endogenous and exogenous WASp for WIP binding. As WT EGFP-WASp is expressed in excess of endogenous WASp, but these two proteins have the same affinity for WIP, the vast majority of the cellular WIP will bind to EGFP-WASp, leaving the endogenous WASp susceptible to degradation. With clinical mutant EGFP-WASp transduced cells, the majority of the cellular WIP will be bound to endogenous WASp as it has a greater affinity for WIP than mutant EGFP-WASp, despite the higher rate of protein synthesis for EGFP-WASp. As a consequence the clinical mutant EGFP-WASP is degraded preferentially and the endogenous WASp is protected. The sequential immunoprecipitation experiment in figure 6.6c demonstrates this mechanism, and together this data is strongly supportive of the above hypothesis.

Unfortunately I was unable to detect any rise in WASp concentration following incubation of transduced cell lines with a range of protease inhibitors (figure 8.8 and 8.9d and e). Possible technical explanations for this are discussed above (chapter 8.5), and further optimisation of this experiment within the current system may yield useful mechanistic data. A further possibility is that the mechanism of WASp degradation is dependent on the cell type and / or level of cell activation / differentiation. Increases in cellular WASp concentration following incubation with protease inhibitors have been detected in cultured splenic derived dendritic cells (Chou et al., 2006) and in lymphocytes (de la Fuente et al., 2007). Interestingly, subtle differences in protease susceptibility were found between patient derived peripheral blood T cells, PHA / IL-2 propagated T cells and EBV-transformed B cells (de la Fuente et al., 2007), supporting an activation / differentiation dependent WASp degradation pathway. As discussed in chapter 1.7.3.3, there is some evidence for a link between WASp activation and degradation, and calpain is known to regulate the activity of other proteins by proteolysis (Calle et al., 2006b; Suetsugu et al., 2002; Sato and Kawashima, 2001; Penna et al., 1999; Noguchi et al., 1997; Selliah et al., 1996; Sarin et al., 1993).

Such a mechanism could be investigated using transduced U937 cell lines by activating U937 cells using PMA (causing them to adhere and spread), and determining the effect on cellular WASp levels and susceptibility to protease inhibitors. Unfortunately this experiment was beyond the time frame of this project. Some information on the relationship between WASp activation and degradation can be gained from the analysis of the results of the domain deletion constructs. The constitutively active WASp constructs showed similar levels of cellular WASp to WT, suggesting that disruption of autoinhibition during WASp activation does not appear to enhance WASp degradation within U937 cells. Because of the high levels of toxicity these constructs exhibited, the lysate of constitutively active construct transduced U937s was made from transiently transduced cell cultures. This data must therefore be treated with some caution. The fact that endogenous WASp was suppressed by the expression of constitutively active WASp suggests that the protective mechanism of WIP is maintained for WASp constructs in the activated conformation.

Other studies have suggested that tyrosine phosphorylation of NWASp is important in predisposing NWASp to degradation (Suetsugu et al., 2002). Both the dBasic and H246D constructs are unable to bind Cdc42 which is essential for *in vivo* phosphorylation at tyrosine 291 (figures 7.1 and 8.7). Neither construct showed any significant increase in cellular EGFP-WASP level compared to WT, by either FACS or by western blot. Testing the constitutively active, dBasic and H246D constructs in the ^{35}S labelled stability assay will provide useful data on the relationship between WASp activation and degradation.

8.6.3.2 dEVH1 WASp

Unlike the clinical mutant constructs, dEVH1 WASp showed a reduced rate of degradation compared to WT WASp (figure 8.10), resulting in accumulation of protein in U937 cells (figure 8.2). This result is surprising considering the WASp dEVH1 construct shows a significantly lower affinity for WIP than the clinical constructs (figure 6.7).

The most logical hypothesis to explain this result is that the critical binding or cleavage site for the protease responsible for initiating WASp degradation is also found within the EVH1 domain. Studies using WIP fragments to block WASp degradation suggested that the critical site for WASp degradation was not identical to the WASp binding site, and that WIP inhibited degradation by sterically inhibiting the binding of a critical protease (Konno et al., 2007). The EVH1 domain does not contain any classical protease recognition sequences, but calpain binds and cleaves at sites predicted by three dimensional conformation

rather than amino acid sequence, and therefore cleavage sites are difficult to predict (Tompa et al., 2004). Calpain most frequently cleaves at proline rich regions and at the boundaries of structural domains. The carboxyl terminus of the EVH1 domain (between the EVH1 and Basic domains) fulfils both of these criteria and is therefore the most likely calpain cleavage site. This could be investigated by generating missense mutations of the proline residues in this area, combining them with clinical missense mutations, and seeing the effect these mutations have on WASp stability.

The dPolyP WASp construct produces a unique pattern of degradation fragments, most obviously demonstrated in transfected Cos7 cells (figure 3.10), but also apparent in U937 cells. FACS and western blot data suggest that the levels of dPolyP WASp in U937 cells is equivalent or higher than that of WT WASp, yet unlike the dEVH1 construct, there is no impaired degradation and endogenous WASp is predictably suppressed. This data suggests the polyproline domain, or one of its many binding partners is also important for the regulation of WASp degradation.

8.6.4 Phosphorylation

In figure 8.7 I have presented some preliminary data assessing the phosphorylation state of EGFP-WASp constructs when expressed in unstimulated U937 cells. As expected, the dVCA construct showed no S483/484 phosphorylation (as the residues are contained within the deleted VCA domain), and provides a clean negative control for assessing serine phosphorylation. Similarly the H246D and the dBasic domain constructs showed low levels of tyrosine phosphorylation. This was expected as these constructs are unable to bind Cdc42, a step essential for Y291 phosphorylation (figures 7.1 and 8.7).

The clinical WASp mutants demonstrated enhanced levels of S483/484 but reduced levels of Y291 phosphorylation. As phosphorylation at both sites activates WASp, these events would be expected to have opposite effects on WASp activity. As Y291 phosphorylation is known to be induced by Cdc42 mediated WASp activation, and actin polymerisation in the bead based actin polymerisation assay is Cdc42 independent, it is tempting to speculate that the enhanced actin polymerisation seen with the clinical mutants is mediated by enhanced phosphorylation at S483/484. Against this hypothesis, WT WASp and the clinical mutants showed similar levels of S483/484 phosphorylation throughout the actin polymerisation assay (figure 7.3). This could be further explored by performing the actin polymerisation on beads pre-treated with phosphatases, or in the presence

of serine kinase inhibitors.

The relationship between tyrosine phosphorylation and EVH1 domain deletion and missense mutations also justifies further investigation. It has been previously demonstrated that Src family kinases bind to the EVH1 domain of WASp, resulting in an inhibition of kinase activity (Schulte and Sefton, 2003). }. Clarifying whether this interaction is dysregulated in the WASp clinical mutants or whether it influences the activity of these constructs would enhance the understanding of WASp activation. Finally the observation that the constitutively active constructs show less serine phosphorylation than WT raises several interesting mechanistic questions. This may reflect a greater activity of casein kinase 2 on WASp in the autoinhibited conformation, or it may suggest increased dephosphorylation at this site by active WASp proteins. Either mechanism may play an important role in the regulation of WASp activity.

8.6.5 Summary

In this chapter I have presented direct evidence of the increased rate of degradation of EVH1 missense mutation WASp. This data provides excellent support for the hypothesis that WIP protects WASp from degradation, and that this is the mechanism underlying the reduced levels of WASp seen in the cells of patients with XLT. The resistance to degradation of the dEVH1 WASp mutant provides important clues as to the mechanisms of WASp degradation, and this is an area which requires further work to elucidate more detailed mechanisms. I have also demonstrated cell toxicity with the overexpression of constitutively active and VCA domain deleted WASp. This and other data presented is additive to our understanding of the importance and the regulation of WASp activation in cells.

9 Discussion

9.1 Bead based actin polymerisation assay

In this project I have explored, optimised and enhanced the understanding of a previously published *in vitro* actin polymerisation assay (Cory et al., 2002; Fradelizi et al., 2001). Several different assay of WASp induced actin polymerisation have been published, ranging from purified component pyrene assays (Rohatgi et al., 2000; Prehoda et al., 2000; Higgs et al., 1999; Machesky et al., 1999), which measure the biochemical initiation of actin filament nucleation, to assays assessing complex actin based cellular functions such as vesicle rocketing or bead propulsion (Yarar et al., 2002; Benesch et al., 2002; Suetsugu et al., 2001b). The bead based actin polymerisation assay assesses the generation of branched actin networks within physiological lysates, and mimics the dynamics of the cortical dendritic branched actin networks within cells. The assay simultaneously maintains a (diluted) cytosollic protein composition, with the ability to assess the specific protein associations of WASp during activation. A practical advantage of this assay is that it only requires small scale WASp protein generation and purification. This makes the practicalities of experimentally assessing the details of WASp activation more feasible.

I have demonstrated the reliability of this assay and also its versatility in detecting differences in WASp activity under a range of experimental conditions. The actin polymerisation initiated in the assay appears to be both Cdc42 and PIP_2 independent, but requires an excess of ATP. Optimisation of the assay has suggested that the primary rate limiting step in WASp mediated actin polymerisation is activation of WASp itself. Following this, recruitment of ATP loaded g-actin to the V domain of WASp and the ATP loading of Arp2 and Arp3 determine the rate of actin polymerisation.

In this project I have not compared the results of the bead based actin polymerisation assay to those derived from other actin polymerisation assays. Such a comparison is likely to demonstrate differences in the relative activities of specific WASp constructs between assays. These differences may provide useful insights into WASp activation mechanisms and the dynamics of actin networks, reflecting the different biochemical activities being assessed. Disagreements between different experimental systems do not undermine the results from any specific assay, however as the bead based assay utilises a physiological lysate it is likely to be representative of the *in vivo* environment. The reproducibility of the bead based assay is impaired by the reliance on band quantification from

western blots and the variability of the activity of the cell lysate used as the assay substrate. This variability has been compensated for by adequately repeating experiments, and by using a statistical approach which allowed comparison to an invariable standard activity (WT) and compensation for inter-experimental variability.

Further work would provide a greater understanding of the assay and role WASp plays within it. Pre-treating U937 lysate by immunoprecipitation using anti-SH3 or specific WASp binding adapter proteins (such as Nck and Grb2), and performing the assay in the presence of kinase inhibitors would further define the crucial WASP activating proteins in this system. Generating WASp in cells treated with kinase inhibitors and phosphatase inhibitors will allow assessment of maximally phosphorylated and entirely dephosphorylated WASp. Testing these samples in the assay and this would enhance our understanding of the role of phosphorylation within this assay. The use of other cell lysates would assess how cell specific these activation mechanisms are. Finally, examination by electron microscopy, of the actin networks formed on the bead surface of various constructs, would confirm the branched structure of actin networks surrounding the beads and illustrate the position of Arp 2/3 complexes within the network.

9.2 Mechanisms of WASp activation

9.2.1 Cdc42 independent activation

Data presented in this study provides further insight into the understanding of the mechanisms of WASp activation in cellular systems. Actin polymerisation within lysate of resting myeloid leukaemia cells was assessed using an *in vitro* bead based assay. The results demonstrate that within this system, WASp initiated actin polymerisation was entirely Cdc42 independent and indirect evidence suggested it was also PIP_2 independent. A strength of this experimental system, is that unlike much of the *in vitro* work investigating WASp / NWASp activation, it assesses WASp (not NWASp) activation in human haematopoietic lysate. This is much more relevant for investigating the pathophysiology of WAS / XLT, than *xenopus* or bovine brain lysates. Further work is required to clarify the significance of these findings, and to facilitate interpretation of these results in the context of previously published data. In particular, it is necessary to assess the sensitivity of actin polymerisation to prenylated Cdc42, to compare the Cdc42 sensitivities of WASp and NWASp, and to directly determine the effect of PIP_2 on actin polymerisation.

Cdc42 induced WASp / NWASp activation has been extensively investigated in a variety of *in vitro* and cellular experimental systems. An increasing body

of evidence, however, has demonstrated Cdc42 independent WASp activation, suggesting redundancy among WASp activation pathways. Most strikingly, a WASp null mouse containing a transgenic WASp construct incapable of binding Cdc42, demonstrated normal T cell development, TCR induced T cell proliferation and cellular actin polymerisation (Badour et al., 2004).

The presence of parallel WASp activation pathways has several hypothetical functional implications. Firstly different WASp activation mechanisms may be employed by the same cell at different stages of activation or differentiation. For example, resting U937 cells may require Nck / Grb2 WASp activation. Once they are activated, however, and U937 cells become adherent and require actin cytoskeleton remodelling, Cdc42 induced WASp activation may become more important.

A second possibility is that the mechanism of activation is governed by the subcellular site of WASp activation. At a crude level, cytosolic WASp may require a different activation mechanism to that at both the plasma membrane and on the surface of vesicles. Alternatively, WASp activation mechanisms may be specific to the actin substructures being remodelled. For example, the proteins essential for WASp activation may be different at the immune synapse, at podosomes and at the surface of phagosomes. In support of this hypothesis, several proteins have been implicated in localising WASp to specific subcellular structures (Badour et al., 2007; Banerjee et al., 2007; Badour et al., 2004; Badour et al., 2003; McGavin et al., 2001; Tian et al., 2000; Linder et al., 2000b), and the composition of WASp containing multimeric complexes at specific structures appears to be different (Dong et al., 2007; Badour et al., 2007; Sasahara et al., 2002; Moreau et al., 2000). The synergism demonstrated by several WASp activating proteins or phospholipids, and the co-localisation of these activators may represent the molecular mechanism of this specificity of activation. Such a mechanism could explain how WASp activation is tightly regulated despite playing an essential role in many intracellular processes, spatially dispersed throughout a range of cellular compartments.

9.2.2 Constitutively active WASp constructs

The results presented on the XLN constitutively active WASp constructs support and extend previously published findings (Ancliff et al., 2006; Leung and Rosen, 2005; Devriendt et al., 2001). This work suggests that the change in WASp conformation from autoinhibited to open does not signal like a binary switch, but rather, that there is a continuum of conformations between the two extremes.

Phosphorylation of Y291 (if the Y291E is an accurate representation of 291 phosphorylation), does induce a less autoinhibited conformation in WASp, but it is significantly less active (open) than the XLN point mutations. A novel finding from this study is that the XLN missense mutant WASp constructs are able to bind both Cdc42 and WIP. This important finding suggests WASp doesn't dissociate from these binding partners in response to activation, which has been a controversial debate in recent literature (Dong et al., 2007; Sasahara et al., 2002). Important ongoing work includes an assessment of the tyrosine phosphorylation of the XLN constructs both *in vitro* and in cellular systems. This will provide a better understanding of the relationship between tyrosine phosphorylation, release of autoinhibition and the binding of Cdc42.

9.2.3 Tyrosine phosphorylation and WASp activation

Torres et al proposed an allosteric model of how Cdc42 and tyrosine kinases synergistically bind to, and regulate the activity of WASp by phosphorylation (Torres and Rosen, 2006; Leung and Rosen, 2005; Torres and Rosen, 2003). They propose that following Cdc42 induced disruption of the WASp autoinhibitory conformation, the Y291 residue is more accessible to tyrosine kinases.

Several experiments in this project have demonstrated a direct link between Cdc42 binding and Y291 phosphorylation, which is supportive of this model. Furthermore, the results presented on the Y291E WASp construct strongly suggest this construct (and therefore 291 phosphorylated WT WASp) exist in a partially autoinhibited conformation, which also supports this model. The model, however, does not address Cdc42 independent WASp activation, which also induces an open WASp conformation, and would therefore expose the Y291 residue, leaving it susceptible to phosphorylation. The preliminary results presented here, however, demonstrate no increase in Y291 phosphorylation during bead based actin polymerisation, however WASp purified from Cos7 cells demonstrated significant levels of tyrosine phopshorylation, prior to incubation with U937 lysate. Further experiments using the biological reagents generated in this project could clarify this mechanism and establish regulatory differences between Cdc42 dependent and independent WASp activation pathways.

9.2.4 WIP and WASp activation

The lack of an inhibitory effect of WIP in the bead based actin polymerisation assay was surprising in light of previously published data (Lim et al., 2007; Martinez-Quiles et al., 2001). A criticism of these experiments is that within the WIP enhanced assay lysate, no WIP mediated biological activity was demonstrated, and no

positive control for functional WIP was possible. The reproduction of previously published WASp inhibition using the WIP reagents used in this study, would confirm a real difference in WIP activity between the experimental systems. The purification of WIP and the optimisation of a purified protein actin polymerisation assay were beyond the time constraints of this project.

Several possible explanations for this result are discussed in chapter 6.4.2, however the most plausible explanation is that Cdc42 independent WASp activation bypasses the WIP inhibitory mechanism. Understanding the relative contribution of WIP to the localisation of WASp – WIP complexes to sites of actin remodelling, and to the regulation of WASp activity is a critical area for understanding the control of WASp function.

9.2.5 Two step WASp activation model

Many of the results presented in this thesis are difficult to explain using current models of WASp activation. As a result I have proposed a hypothetical activation model (figure 9.1) which will provide a useful framework for further investigation in this area. I will breifly discuss some of these key results which have suggested this model.

Firstly, the deletion mutant which most profoundly effected the ability of WASp to polymerise actin is the Polyproline domain deletion, despite have a normal ability to bind Cdc42 and WIP, and have similar levels of tyrosine 291 phosphorylation. Furthermore this protein is stable in haematopoeitic cell lines suggesting that it does not have aberant protein folding. This strong suggests the primacy of the polyproline domain in WASp activation.

Secondly, the Y291E construct shows increased activity compared to WT WASp, but decreased activity compared to XLN WASp constructs. Interestingly, once U937 lysate was supplemented with ATP the difference in activity between WT and Y291E WASp becames less significant. This suggests a WASp conformation with intermediate activity between maximal WASp activity and autoinhibited WASp activity. The importance of tyrosine phosphorylation for WASp activity has been demonstrated by the Y291F (“phosphodead”) transgenic mouse, which has completely non-functional WASp (Blundell et al., 2009), suggesting that this step is non-redundant. Although I have demonstrated a clear link between Cdc42 binding to WASp and 291 phosphorylation, the fact that the H246D WASp protein generated in Cos7 cells is tyrosine phoshorylaterd when purified, strongly suggests that tryosine phosphorylation can be mediated independently of Cdc42.

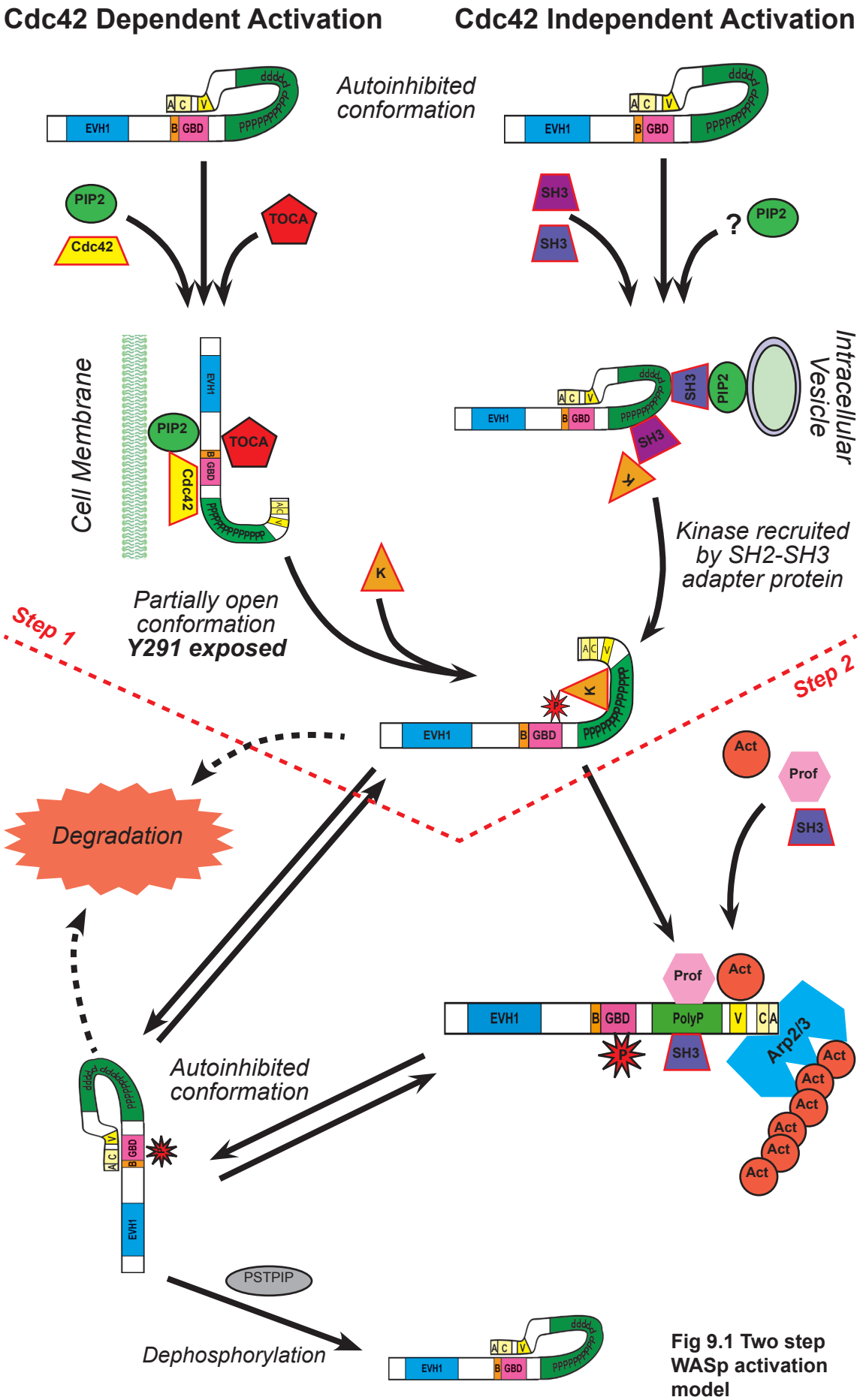

Fig 9.1 Two step WASp activation model

Fig 9.1 Two step WASp activation model
The results of the experiments performed for this thesis suggest a modification of current models of WASp activation is required. I propose a two step model of WASp activation. For maximal WASp activation, the autoinhibitory conformation must first be disrupted, resulting in a partially open WASp conformation. This step can be achieved in a Cdc42 dependent pathway, resulting in the cooperative binding of Cdc42 and PIP_2, and the Cdc42 induced conformational change in the WASp GBD. This results in exposure of the tyrosine 291 residue, facilitating phosphorylation. This WASp state can also be achieved in a Cdc42 independent manner. Polyproline domain binding mediators such as the SH2-SH3 adapter proteins, possibly with cooperative binding of PIP_2, bind to the polyproline domain. These are then able to recruit tyrosine kinases (Src and Tec family kinases) which also bind to the polyproline domain and phosphorylate tyrosine 291. Both pathways result in a tyrsoine phosphorylated WASp with a partially open conformation, which has some Arp2/3 activating activity, but is not maximally active. A second activation step, stabiising a fully open WASp conformation is then mediated by polyproline domain binding proteins such as profillin and VASP. This step is ATP dependent and facilitates the recruitment of actin to the V domain of WASp and to the Arp2/3 complex. Other SH3 containing adaptor proteins play a role in coordinating this complex and ensuring that full WASp activity is spatially and temporally regulated. Following activation, WASp can revert to its less active conformation and it exists in an equilibrium between each of its conformations, regulated by its binding partners. Similarly, phosphatases such as PSTPIP bind to the polyproline domain and dephosphorylate tyrosine 291, stabilising a more autoinhibited conformation. A final level of regulatation of WASp activity is achieved through WASp degradation, either by ubiquitination and subsequent degradation via the proteasome, or by calpain. The suseptibility of WASp to degradation is increased by phosphorylation of tyrosine 291.

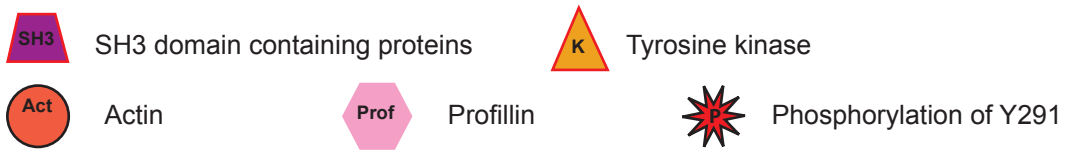

Thirdly, the two step model, can account for the essential role for ATP in actin polymerisation in the bead based assay. Although I have not provided any evidence for a mechanism of the role of ATP, the central role of profillin and VASP (both actin binding proteins) in WASp activation has been demosntrated by others (Yarar et al., 2002). By constrast Cdc42 activity is not influence by ATP.

Finally, this model also provides a possible explanation for why WIP had no supressive effect in this assay. WIP may be important in stabilising the autoinhibitory conformation of WASp prior to tyrosine phosphorylation, but have no effect once WASp conformation has been changed by phosphorylation of 291. In terms of the model, WIP in inhibititory for step one of WASP activation, but not for step two. Whether or not WIP is inhibitory for both Cdc42 dependent and independent step one pathways is an interesting question which should be addressed.

Two other concepts are important for this model. The first is that WASp is continually in a state of conformational flux between autoinhibited and activate states. Secondly this model presumes that WASp activity is regulated by a large complex of several proteins, which is itself in a continual state of flux. This regulatory mechanism, draws parallels with our understanding of how WAVE proteins are regulated.

9.3 Pathogenicity of WASp mutations

Although many immunological and cellular characteristics of patients with WASp mutations have been described, very little work has been published on the functional activity of (clinical) mutant WASp protein (Kolluri et al., 1996). The impaired binding of WIP to WASp containing specific EVH1 missense mutation had been previously demonstrated experimentally, and predicted from structural modelling studies (Kim et al., 2004; Luthi et al., 2003; Volkman et al., 2002; Rong and Vihinen, 2000; Stewart et al., 1999).

In this study I have demonstrated that four WASp mutants with missense mutations in the EVH1 domain bind Cdc42 normally and have a normal ability to polymerise actin *in vitro*. I have also demonstrated that each of these has a reduced but not absent affinity for WIP compared to WT WASp. Despite this impaired binding, mutant WASp – WIP complexes could be immunoprecipitated from lysate of U937 cells over-expressing mutant WASp. I have directly demonstrated that EVH1 missense mutant WASp is degraded more rapidly than WT WASp, but that these mutants are minimally more toxic than WT when over-expressed in U937 cells.

These results, and other contemporaneously published data, have suggested a model whereby WIP acts as a chaperone for WASp, protecting it from degradation (de la Fuente et al., 2007; Konno et al., 2007; Chou et al., 2006). WASp with EVH1 missense mutations has a lower affinity for WIP, and therefore has a higher rate of degradation, resulting in the reduced cytosolic concentration seen in the lymphocytes of patients with these mutations (de la Fuente et al., 2007). In patients the cellular level of WASp is proportional to the severity of the clinical phenotype (Lutskiy et al., 2005; Jin et al., 2004; Imai et al., 2003).

The majority of patients with missense mutations in the EVH1 domain have the mild clinical phenotype of XLT, without clinically relevant abnormalities of the cells of the myeloid or lymphoid lineages. This is despite having a fraction of a normal individual's cellular WASp concentration in these cells. This observation suggests that immune cells can function relatively normally with low levels of WASp, and even lower levels of WASp – WIP complexes. This may be due to functional redundancy between WASp and NWASp in these cells, as has been proposed to explain the normal T cell development of WASp null mice (Zhang et al., 2002). Alternatively these cells only require very low levels of WASp, which functions transiently prior to degradation, to maintain normal function.

The fact that immune cells are able to function effectively despite an impaired ability to form WASp – WIP complexes, raises several questions about the

functional significance of these complexes. In addition to protecting WASp from degradation, it has been proposed that WIP regulates WASp activity and localises WASp to sites of actin remodelling. If these latter two functions are important, then other WASp binding proteins must compensate for WIP to allow for normal, or near-normal functionality. Despite the relatively benign clinical course of XLT, functional defects do occur in these patients (e.g. low platelet volume, autoimmune disease), and understanding why problems arise in these specific situations will provide a better understanding of the function of WIP.

WASp containing point mutations which cause X-linked neutropenia were highly toxic when over-expressed in U937 cells. Investigating the mechanism of this toxicity would have been a diversion from the primary aims of this project, however other published work has suggested that unregulated actin polymerisation disrupts the cytokinesis of dividing cells (Moulding et al., 2007). There was no evidence of direct cellular toxicity of constitutively active WASp. As discussed below, investigation of the degradation of constitutively active WASp constructs would enhance the understanding of both the pathogenicity of XLN and the regulation of WASp.

9.4 Mechanisms of WASp degradation

Although increased susceptibility to degradation has now been established as the mechanism underlying the low cellular levels of WASp in XLT / WAS patient cells, the regulation, mechanism and functional significance of WASp degradation remains poorly understood. The results from this study provide some important, novel insights into this area.

What limited data exists about the protease pathways responsible for WASp degradation is largely contradictory. Calpain and the proteasome have been implicated as prime candidates, however the relative importance of these systems appears vary according the cell type or experimental system under investigation (de la Fuente et al., 2007; Chou et al., 2006; Suetsugu et al., 2002; Shcherbina et al., 2001; Oda et al., 1998). Tyrosine phosphorylation has been shown to increase the susceptibility of NWASp to degradation via ubiquitination (Suetsugu et al., 2002), which suggests a hypothesis whereby the more active a WASp protein is, the more rapidly it is degraded.

I was unable to demonstrate any enhanced WASp stability in U937 cells, with a range of protease inhibitors (including calpain and proteasome inhibitors). Further optimisation of the use of these and other protease inhibitors, and the use of alternative cell lines to assess the susceptibility of different WASp constructs to

specific proteases, could provide valuable data in this area.

The difference in susceptibility to degradation between the EVH1 missense WASp mutants and the dEVH1 WASp, emphasises the central role of this region in determining WASp stability. As discussed in chapter 8.7.3.2, these results suggest that binding site of the critical WASp protease resides within the EVH1 domain. Furthermore, the difference in sizes and lysate concentration of WASp degradation fragments between the EVH1 missense mutants and the dPolyP construct, and WT WASp, raises the possibility that these constructs are degraded by different pathways. The comparable expression levels of the H246D construct (which cannot be tyrosine phosphorylated) to WT WASp, suggests phosphorylation of WASp does not target WASp for degradation. Unfortunately the radio-isotope degradation assay was not performed on the Y291E and other constitutively active WASp constructs due to their toxicity, but this experiment would more adequately address this question.

The results relating to WASp degradation presented in this project are significant, but preliminary. They raise many important questions and hypotheses about the regulation of WASp activity and cellular control of protein levels. The key experiments required to expand and clarify these preliminary findings are outlined below;

1. Definitive testing of the remaining domain deletion and constitutively active WASp constructs with the radio-isotope protein stability assay. The constitutively active constructs would have to be tested in cell lines transduced using a low MOI and the assay performed rapidly following transduction, to avoid the effects of toxicity.

2. Further optimisation of the effects of protease inhibitors on WASp transduced cell lines as outlined above.

3. Purification of WASp degradation products from WT WASp, EVH1 missense mutants and dPolyP WASp transduced cell lines. Characterisation of these constructs by mass spectroscopy.

4. Generation of point mutations within potential calpain and proteasome cleavage or binding sites within the WASp EVH1 domain. Testing the stability of WASp containing these mutations.

5. Assessment of the ubiquitination of selected WASp constructs, when stably expressed in U937 cells, and assessing any differences in ubiquinisation

following cell activation.

9.5 Functional and WASp localisation experiments

In this thesis I have not yet presented any data demonstrating the ability of individual WASp constructs to reconstitute cellular functions lost from WASp null cells. This next stage of investigation is critical, and will allow the assessment of domain function or missense mutation, from molecular characterisation, through cellular expression, to cellular function. The WASp null mouse (Zhang et al., 1999; Snapper et al., 1998) and cells from WASp null patients have both been used successfully for demonstrating the reconstitution of aberrant cellular functions following lentiviral transduction of WT WASp (Dewey et al., 2006; Martin et al., 2005; Dupre et al., 2004; Strom et al., 2003; Jones et al., 2002; Burns et al., 2001).

The impaired ability of dendritic cells and macrophages to form podosomes on adhesion to fibronectin is a consistent finding in WAS and XLT patient cells and in the WAS mouse model (Calle et al., 2004; Linder et al., 2003; Jones et al., 2002; Burns et al., 2001; Linder et al., 2000a; Binks et al., 1998). In human WAS dendritic cells, podosomes are usually absent, whereas in murine dendritic cells a residual 5% of cells express podosomes (Calle et al., 2006a). Although controversy exists over the function and *in vivo* relevance of podosomes in haematopoietic cells, it is now generally thought that these structures are important for adhesion to and focal degradation of the extracellular matrix, and for sensing the microenvironment to facilitate cell polarisation in response to external stimuli (Gimona et al., 2008; Calle et al., 2006a). Structurally, podosomes consist of a core of actin filaments extending from the cell membrane, surrounded by structural and adhesion proteins such as paxillin, talin, vinculin and integrins (Linder and Kopp, 2005; Marchisio et al., 1988; Marchisio et al., 1987). Actin nucleators (such as Arp2/3 and formins) and polymerisation activators (WASp, cortactin and WIP) are all found in the core of the podosomes, immediately adjacent to the cell membrane (Calle et al., 2006a). Visualisation of the reconstitution of podosomes in WASp null murine dendritic cells therefore assesses both the formation of a functionally important cellular structure and the localisation of WASp to a dynamic site of actin polymerisation.

Figures 9.2 and 9.3 show some preliminary data from podosomes reconstitution experiments in dendritic cells. DCs were cultured from the bone marrow of WAS and Black 6 mice (a wild type strain), and were transduced with EGFP-WASp by lentiviral infection (as described in chapters 2.3.2 and 2.4.6). Cells

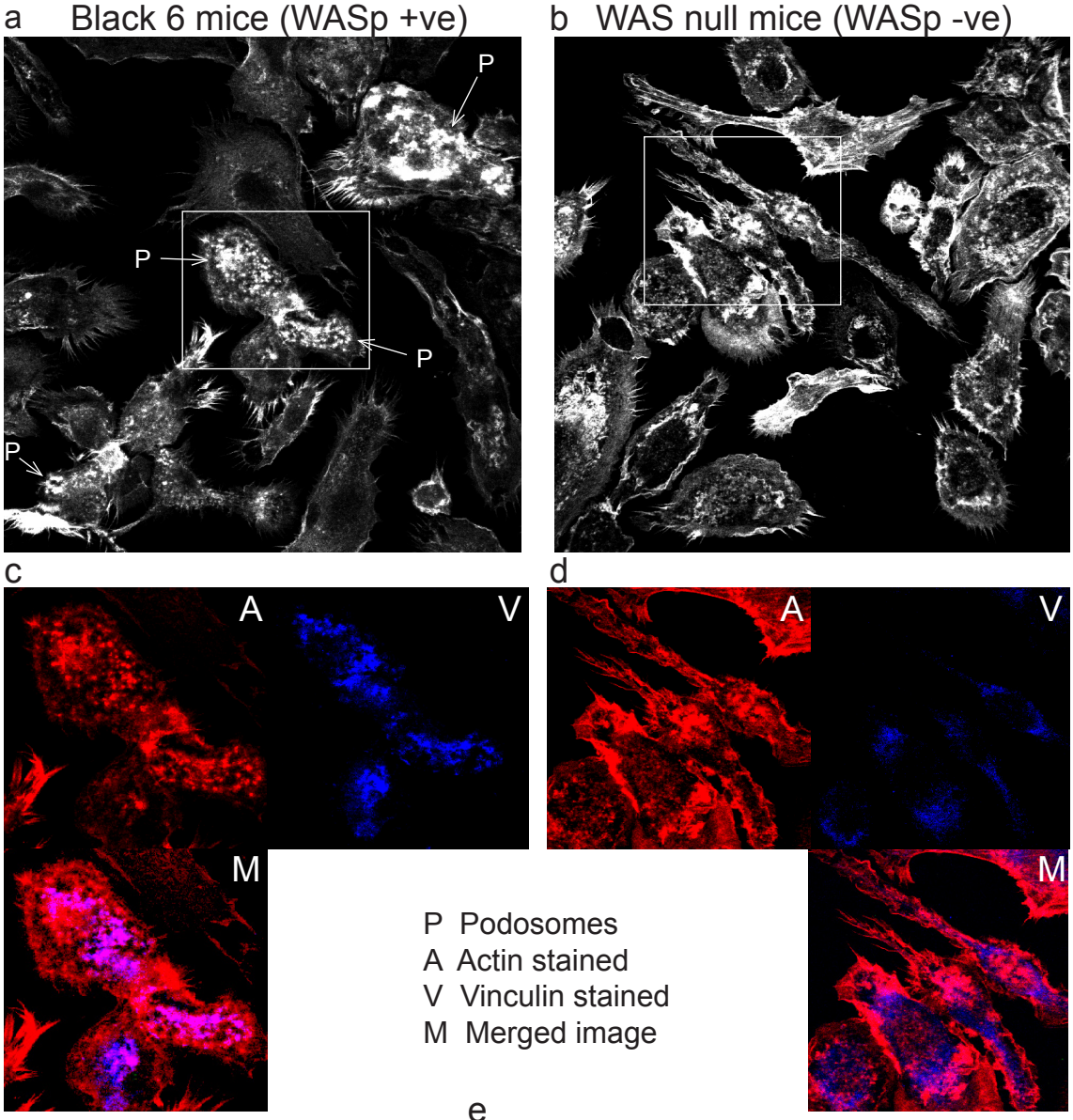

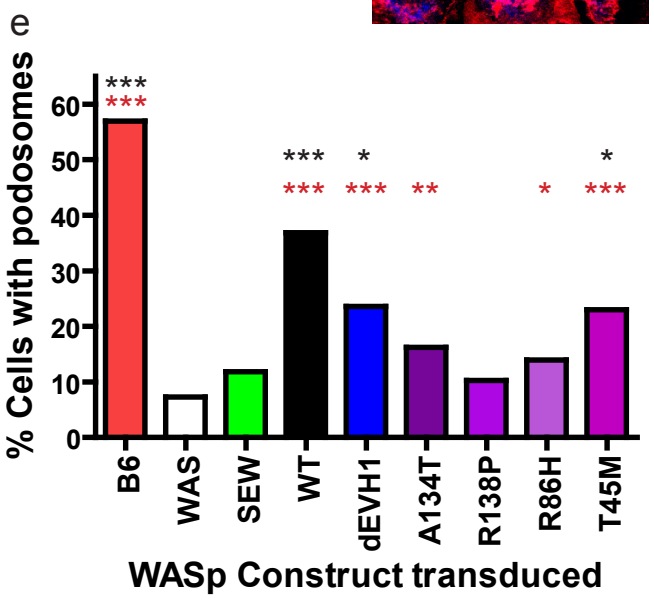

Fig 9.2 Podosome reconstitution of WASp null dendritic cells following transduction with EGFP-WASp
(**a)(b)** Actin staining of Black 6 (WT stain) and WAS murine bone marrow derived DCs. Clusters of podosomes marked with *P* and arrows. **(c)(d)** Actin (A), Vinculin (V) and merged (M) confocal micrographs of the areas marked with a box in (a) and (b). Black 6 cells demonstrate co-localisation of actin and vinculin at podosomes, whereas WAS DCs lack co-localisation. **(e)** WAS bone marrow derived DCs were infected with EGFP-WASp encoding lentivirus at a MOI of 30, on day 6 of culture. Cells were fixed and immunostained at 48-72 hours post infection. % of DCs with podosomes for each construct is shown (two experiments). Differences between contructs and untransduced (WAS) DCs (red stars) and SEW transduced DCs (black stars) were assessed by Chi squared analysis. * *p<0.05, ** p<0.01, *** p<0.001. WAS - WAS DCs, B6 - Black 6 DCs.*

were then cultured for 48-72 hours on fibronectin coated slides before fixing and immunostaining for FACS and for confocal microscopy (chapter 2.11.2 and 2.13). The expression of DC activation markers (MHC class II and CD86) by FACS revealed that the majority of dendritic cells were of an immature phenotype and that expression of activation markers was similar between all WASp (and SEW) constructs assessed (data not shown). The podosome reconstitution data is the summary from two separate experiments using a lentiviral MOI of 30, whereas the confocal micrographs are representative images from three independent experiments each transducing cells with an MOI of 100.

Figures 9.2a-d illustrate the differences in morphology and podosomes formation between murine WAS and Black 6 dendritic cells. Black 6 DCs show clear co-localisation of actin and vinculin “hotspots”, illustrated by the discrete purple spots seen in the merge images (figure 9.2c). By contrast, the WAS cells show the typical spindle shaped morphology of WAS dendritic cell, and a lack of discrete actin – vinculin co-localisation within actin rich structures (figure 9.2d). Figure 9.1e demonstrates, as previously published, that transduction of WAS null DCs with WT WASp leads to a significant repopulation of podosomes positive cells, although the level seen in Black 6 cells was not attained. Transduction of DCs with the EGFP only lentivirus (SEW) results in a small and insignificant rise in podosomes formation. The dEVH1 WASp construct and one of the clinical mutant constructs (T45M) show a significant rise in cells expressing podosomes ($p<0.05$ when compared to SEW transduced cells). Although the remaining clinical constructs show a greater number of podosomes expressing cells compared to untransduced WAS DCs, there is no significant rise compared to SEW transduced cells.

Figure 9.3 shows a higher resolution view of the podosomes formed in dendritic cells transduced by each construct. Interestingly like WT WASp, the three EVH1 missense mutant WASp constructs localise to the cores of podosomes. By contrast the SEW construct shows no localisation to any actin structures. The podosomes formed by the dEVH1 WASp transduced dendritic cell are very atypical, being larger in size, irregular in shape and forming ring like structures. This appearance was typical of the podosomes-like structures formed by dEVH1 WASp transduced cells. In the illustrated cell there is little colocalisation of WASp to these structure, but in other cells more localisation was apparent (data not shown), although it was never as pronounced as for WT WASp.

It is unclear from this data whether or not WASp containing EVH1 missense mutations are able to reconstitute podosomes. There is some evidence that

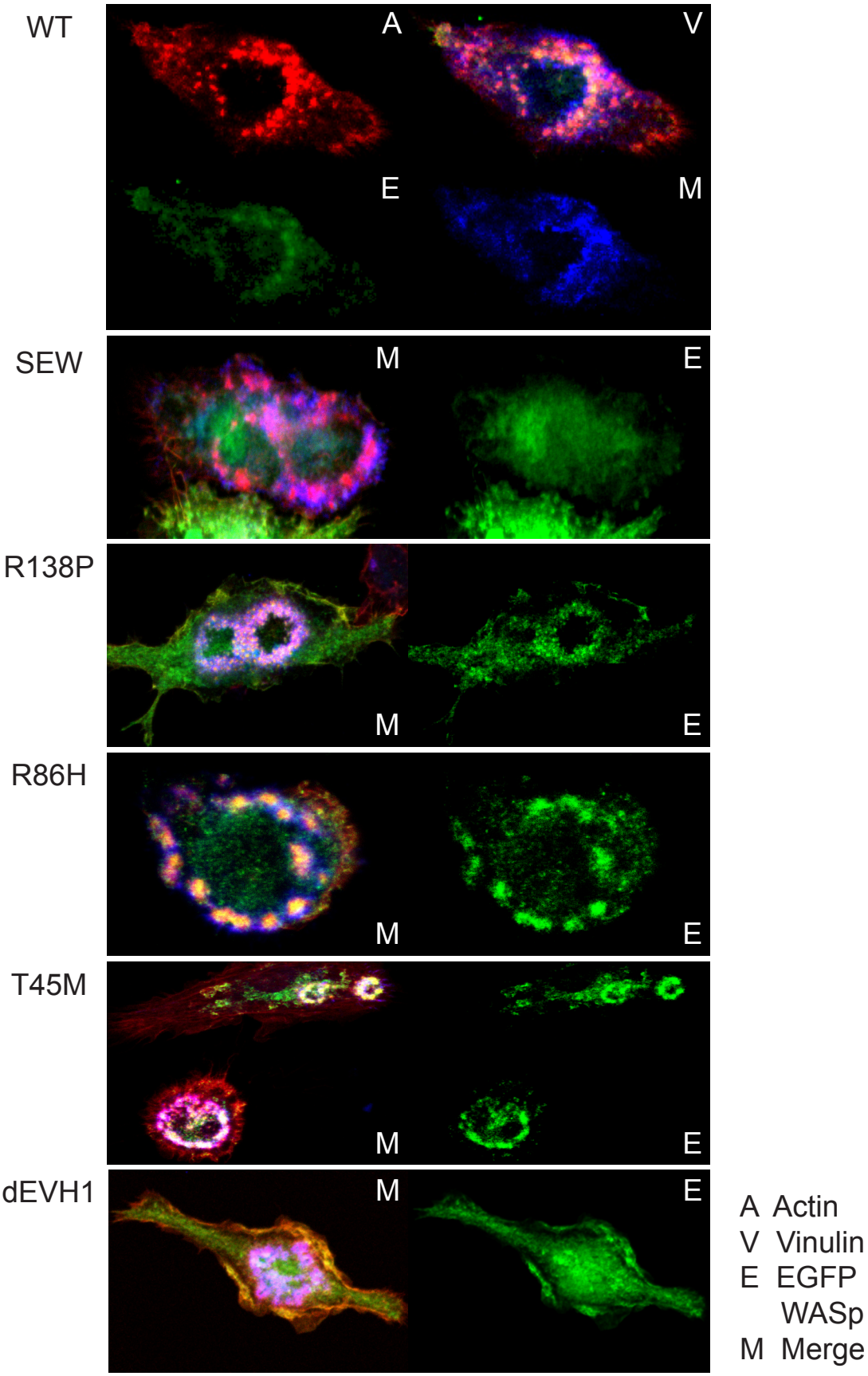

Fig 9.3 Localisation of EGFP-WASp to podosomes in transduced WASp null DCs
High magnification confocal micrographs of podosomes from WASp null dendritic cells transduced with EGFP-WASp constructs (MOI 100). EGFP-WASp panels demonstrate the co-localisation of EGFP-WASp constructs to podosomes.

these constructs do partially reconstitute podosomes, but further experiments are required to detect a significant difference from SEW alone transduced cells. It is apparent that these constructs do not reconstitute podosomes as efficiently as WT WASp, however the fact that these constructs are able to polymerise actin normally and localise to podosomes supports a role in podosomes formation.

It is possible that, due to their greater instability, these WASp constructs may require higher MOIs than WT WASp, or the presence of protease inhibitors, to allow sufficient cytosolic WASp concentration to reconstitute podosomes. Evaluation of results using a range of MOIs to compare different WASp constructs requires caution, because the high MOIs required to induce podosomes in some constructs (e.g. clinical mutants) may result in toxicity and reduced podosome formation in other constructs (WT). Studies in patient cells bearing these mutations would be complimentary and would avoid the problems of toxicity due to vector over-expression. Alternatively, DCs transduced with EVH1 missense mutation WASp may induce podosome formation, but the stability of these podosomes may be significantly reduced, resulting in less podosomes positive cells at any one time point. Other studies have suggested a role for WASp-WIP complexes in determining the stability, rather than the formation of podosomes (Chou et al., 2006).

The results in figures 9.2 and 9.3 raise interesting questions about the role of WIP in podosomes formation and in localising WASp to podosomes. The fact that the dEVH1 construct is able to form significantly more podosome-like structures than SEW transduced cells, suggests that WIP is not essential for podosomes formation. It is unclear, however, whether the structures demonstrated in figure 9.3 are true podosomes or aberrant actin based structures, which might be due to an excess of the dEVH1 construct or specific functional defects associated with this mutation. More detailed imaging, using techniques such as total internal reflection fluorescence (TIRF) microscopy, should resolve this issue. This technique selectively assesses the cell-substratum contacts of adherent cells and allows real time imaging, and would therefore also assess the dynamic turnover of podosomes in transduced living dendritic cells.

The localisation of EVH1 missense mutant WASp to podosomes does not exclude a role for WIP in WASp localisation, as these results may reflect the residual WIP binding to these constructs demonstrated in figure 6.7. To definitively answer this question we are in the process of generating a WIP construct linked to the flourophore mCherry, which when co-expressed with EGFP-WASp would allow the assessment of WASp-WIP colocalisation by fluorescence resonance energy

transfer (FRET).

Although the *in vivo* results presented here are only preliminary data, they illustrate the some important mechanistic questions about the *in vivo* function of WASp and its role in podosome biology, which can be answered by this experimental system. Such reconstitution and localisation experiments can be extended to assess the function of WASp in phagocytosis, T cell synapse formation, chemokine induced migration and cytotoxic granule release. Assessment of the clinical WASp mutants and the dEVH1 construct in these systems will provide important information about the pathophysiology of WAS, XLT and XLN, and the biological importance of WASp-WIP complexes. The assessment of the domain deletion constructs in these experiments will help tease out the *in vivo* mechanisms of WASp activation and localisation at different sites of actin polymerisation. Furthermore, the H246D construct provides an invaluable tool in assessing the hypothesis that Cdc42 dependent and independent activation mechanisms are important in the formation of different cellular structures.

Much of the continuation work suggested in this thesis will be addressed as part of an ongoing program of research into Wiskott Aldrich Syndrome at the Institute of Child Health, London. This work will advance our understanding of the role of WASp in the healthy and dysregulated immune system, and help elucidate some of the mechanisms of the cell biology which underpins immunology.

Appendices

PCR Primers

Sequence of primers used for PCR reactions are shown below. (F) are forward primers and (R) are reverse primers.

ΔEVH1_F	GACAAGCTTCTCAAAAAAGGAATCAGAGGCAAAG
ΔEVH1_R	GTCGGTACCTCAGTCATCCCATTCATCATC
ΔBasic1_F	GACAAGCTTCTATGAGTGGGGGCCCAATG
ΔBasic1_R	CTCGGATCCATCAGCTGGGCTAGGTCC
ΔBasic2_F	GAGGGATCCGCTGATATTGGTGCACCC
ΔBasic2_R	GTCGGTACCTCAGTCATCCCATTCATCATC
ΔPolyP1_F	GACAAGCTTCTATGAGTGGGGGCCCAATG
ΔPolyP1_R	CTCGGATCCCTCCTGGCGCCTCATCTC
ΔPolyP2_F	GAGGGATCCGCTCTGGTGCCTGCCG
ΔPolyP2_R	GTCGGTACCTCAGTCATCCCATTCATCATC
ΔVCABind1_F	GACAAGCTTCTATGAGTGGGGGCCCAATG
ΔVCABind1_R	CTCGGATCCTTTAGAGGTCTCGGCGTCG
ΔVCABind2_F	GAGGGATCCGAGCCACTTCCGCCGC
ΔVCABind2_R	GTCGGTACCTCAGTCATCCCATTCATCATC
ΔVCA F	GACAAGCTTCTATGAGTGGGGGCCCAATG
ΔVCA R	GTCGGTACCTCACCCACCAGGGGCCAGG
ΔCA F	GACAAGCTTCTATGAGTGGGGGCCCAATG
ΔCA R	GTCGGTACCTCACTTGTTCAGCTGAATTCCCTG
ΔA F	GACAAGCTTCTATGAGTGGGGGCCCAATG
ΔA R	GTCGGTACCTCACCCTTCGTCGGAGGAGTG
A134T_F	CAGACGAGGACGAGACCCAGGCCTTCCG
A134T_R	CGGAAGGCCTGGGTCTCGTCCTCGTCTG
R138P_F	GCCCAGGCCTTCCCGGCCCTCGTGCAG
R138P_R	CTGCACGAGGGCCGGGAAGGCCTGGGC
R86H_F	GAAGTCCTACTTCATCCACCTTTACGGCCTTCAGG
R86H_R	CCTGAAGGCCGTAAAGGTGGATGAAGTAGGACTTC
T45M_F	GCTTGGACGAAAATGCTTGATGCTGGCCACTGCAGTTGTTC
T45M_R	GAACAACTGCAGTGGCCAGCATCAAGCATTTTCGTCCAAGC
H246D_F	CCCAGTGGATTCAAGGATGTCAGCCACGTGGGG
H246D_R	CCCCACGTGGCTGACATCCTTGAATCCACTGGG
Y291F_F	CTCTAAACTTATCTTCGACTTCATTGAGGACCAGGG
Y291F_R	CCCTGGTCCTCAATGAAGTCGAAGATAAGTTTAGAG
Y291E_F	GACCTCTAAACTTATCGAGGACTTCATTGAGGACCAGG
Y291E_R	CCTGGTCCTCAATGAAGTCCTCGATAAGTTTAGAGGTC
S272P_F	GCGGAGTCTGTTCCCCAGGGCAGGAATC
S272P_B	GATTCCTGCCCTGGgGAACAGACTCCGC

Fig A.1 Sequences of the PCR primers used to generate WASp missense mutation and domain deletion / truncation constructs

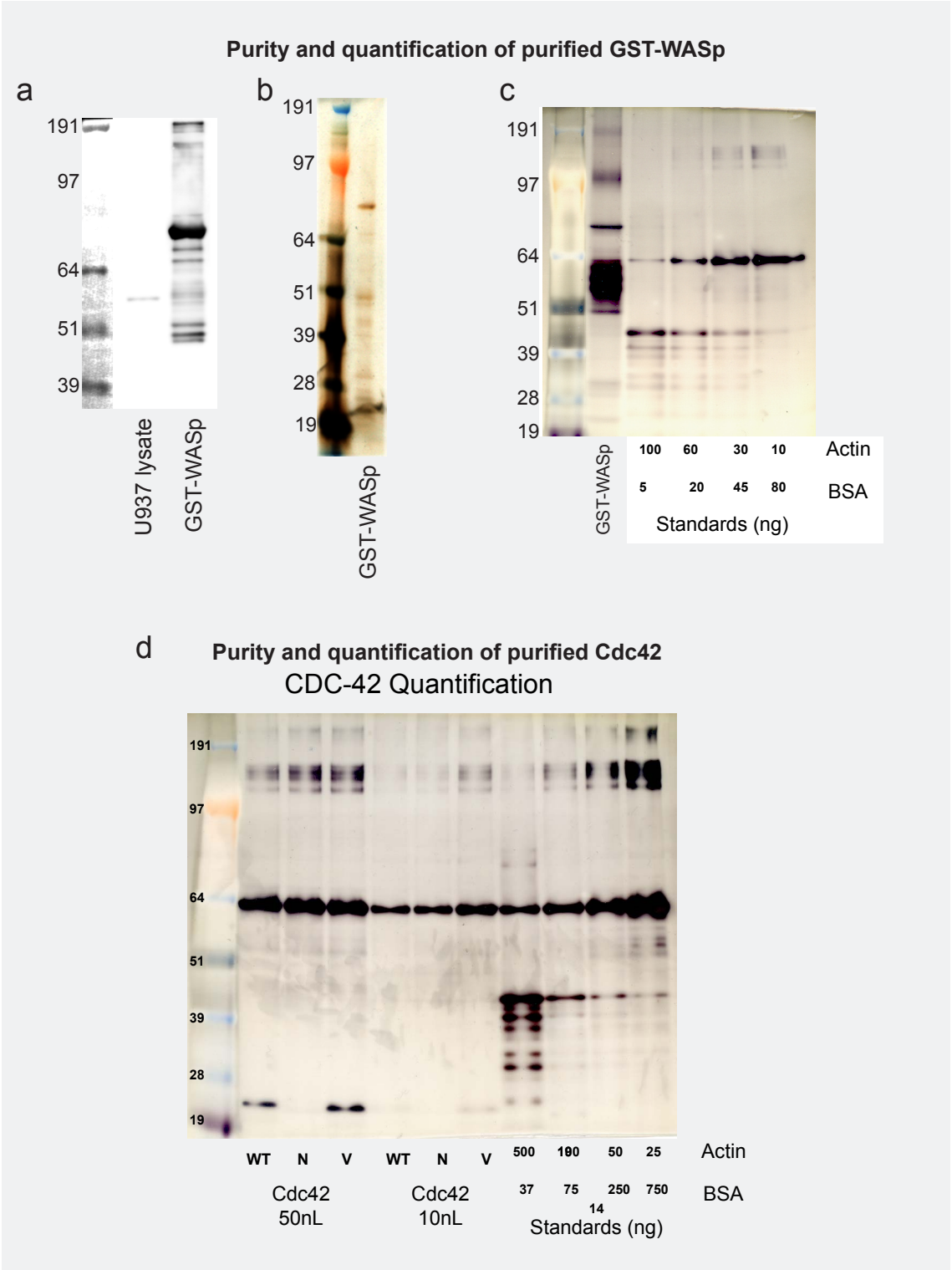

Fig A.2 Assessment of purity and quantification of purified GST-WT-WASp and Cdc42
(a) Purity of GST-WASp standard assessed by anti-WASp immunoblot. Comparison to 20µg of U937 lysate **(b)** Purity of GST-WASp standard as assesed by silver stain **(c)** Quantification of GST-WASp standard by comparison of intensity of silver staining to that of known commercial purchased standards *(BSA - Bovine serum albumin, and actin)*. **(d)** Purity and quantification of Cdc42 proteins by silver stain. *N - 17N mutant, V - 12V mutant.*

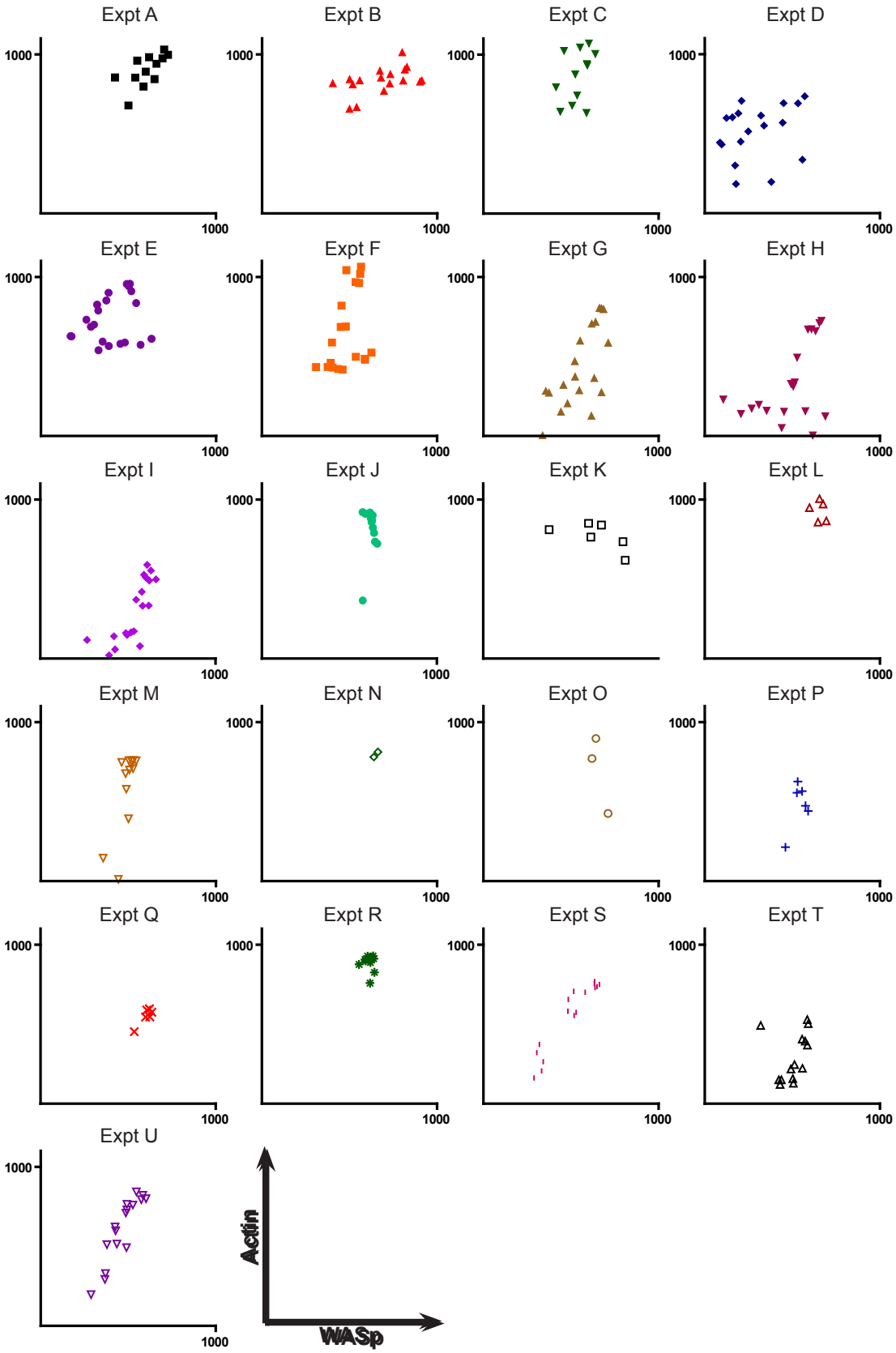

Fig A.3 Actin - WASp scatterplots for individual experiments
Scatterplots of absolute values for Actin and Wasp, demonstrating variablity in response between individual experiments.

Distribution and Descriptive Statistics of Constitutively Active Construct experiments - Absolute readings

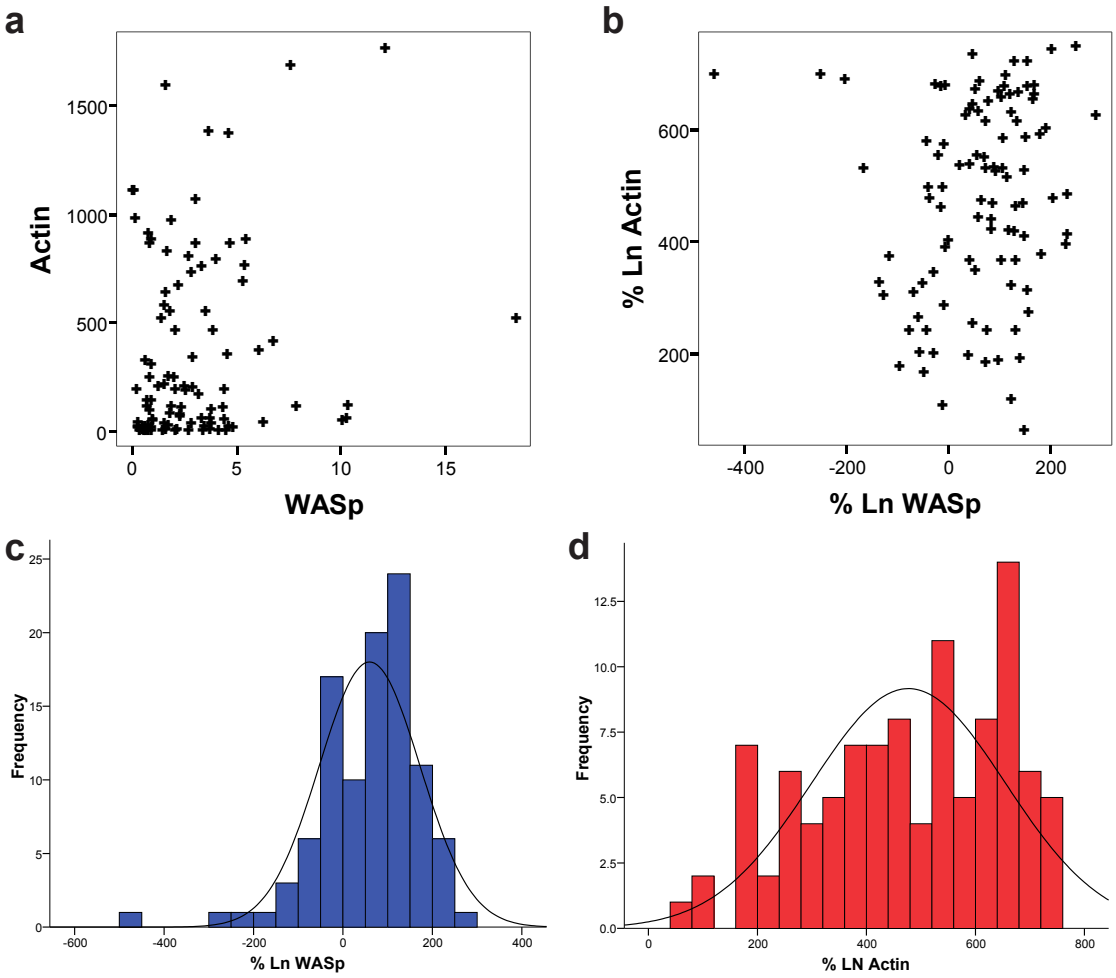

e

	Relative				*Absolute*			
	WASp	Actin	% LN WASp	% LN Actin	WASp	Actin	% LN WASp	% LN Actin
N Valid	120	120	120	120	102	102	102	102
N Missing	0	0	0	0	18	18	18	18
Mean	163662	508759	1008	1195	2.900	350	477.1	59.63
Median	25697	209964	1015	1225	2.120	144	497.1	75.12
Std. Deviation	385446	676038	228	183	2.842	426.1	177.6	113.0
Skewness	4.870	1.901	-.407	-.280	2.498	1.428	-.391	-1.270
Kurtosis	31.292	3.621	.288	-1.117	9.114	1.433	-.910	3.773

Fig A.4 Distribution and descriptive statistics of absolute densitometry readings for constitutively active constructs

Actin polymerisation assays were performed under conditions described in chapters 2.7 and 4.2.6. Absolute readings were generated by standardising densitometry readings to those of known WASp and actin standards. **(a) & (b)** Scatterplots of raw or Ln transformed WASp and Actin densitometry readings. **(c)(d)** Frequency distributions of transformed data. **(e)** Descriptive statistics of raw and transformed data, for absolute and relative data. *Ln - Natural log, SE - Standard error*

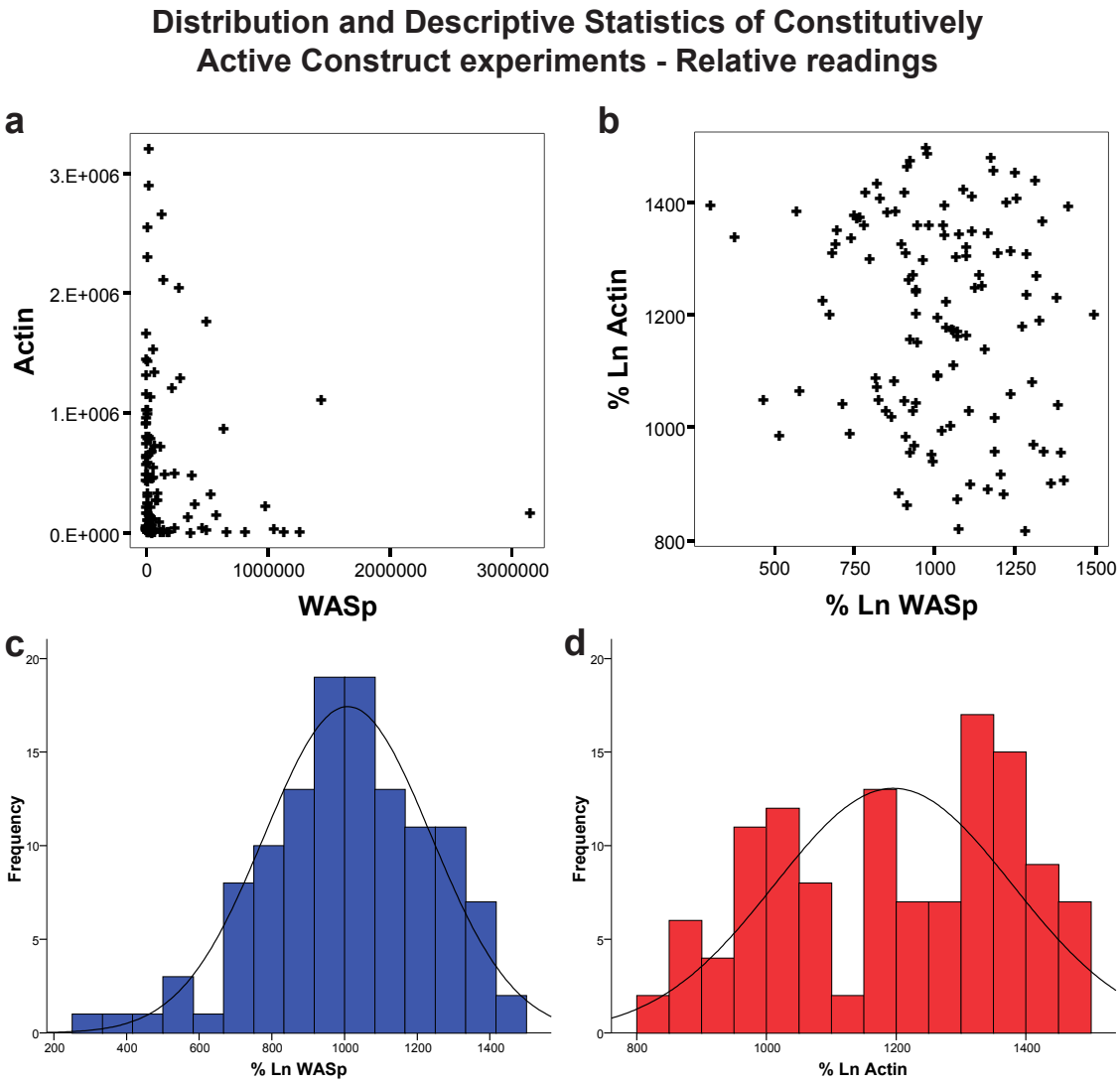

Fig A.5 Distribution and descriptive statistics of absolute densitometry readings for constitutively active constructs

Actin polymerisation assays were performed under conditions described in chapters 2.7 and 4.2.6. Relative readings are the unstandardised densitometry readings generated from the Uvi-Chemi supercooled camera. **(a) & (b)** Scatterplots of raw or natural log (Ln) transformed WASp and actin densitometry readings. **(c)(d)** Frequency distributions of transformed data.

Distribution and Descriptive Statistics of NWASp experiments - Absolute readings

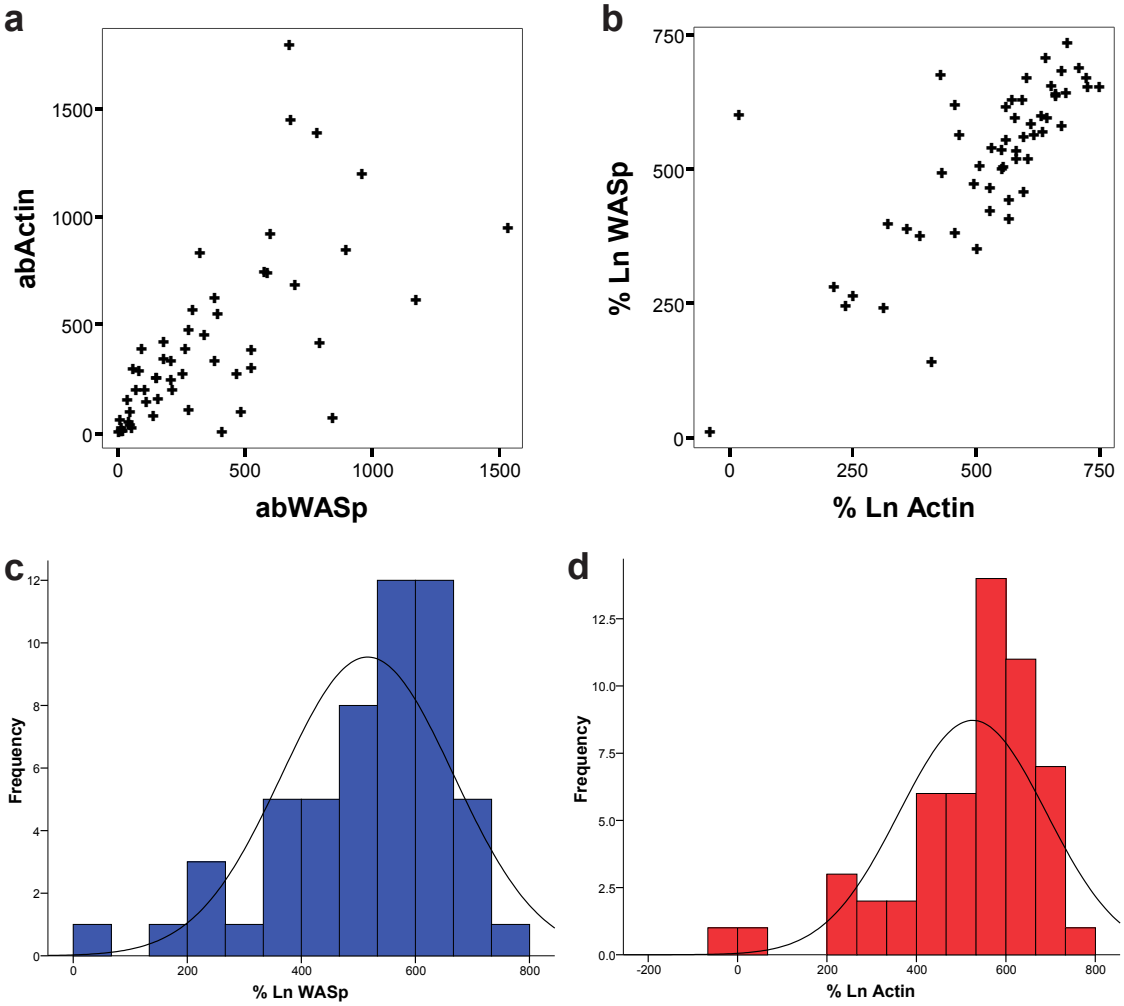

e

		Relative				*Absolute*			
		WASp	Actin	% LN WASp	% LN Actin	WASp	Actin	% LN WASp	% LN Actin
N	Valid	54	54	54	54	54	54	54	54
N	Missing	0	0	0	0	0	0	0	0
Mean		739152	558781	1263	1255	516	526	347	402
Median		431832	452483	1298	1302	556	567	259	290
Std. Deviation		779353	531340	177	157	150	165	333	399
Skewness		1.45	1.52	-1.17	-1.58	-1.23	-1.55	1.36	1.57
Kurtosis		2.09	2.35	1.15	2.95	1.60	2.77	2.03	2.52

Fig A.6 Distribution and descriptive statistics of absolute densitometry readings for NWASp and mWASp experiments

Actin polymerisation assays were performed under conditions described in chapters 2.7 and 4.2.6. Absolute readings were generated by standardising densitometry readings to those of known WASp and actin standards. **(a) & (b)** Scatterplots of raw or Ln transformed NWASp/ mWASp and Actin densitometry readings. **(c)(d)** Frequency distributions of transformed data. **(e)** Descriptive statistics of raw and transformed data, for absolute and relative data. *Ln - Natural log, SE - Standard error*

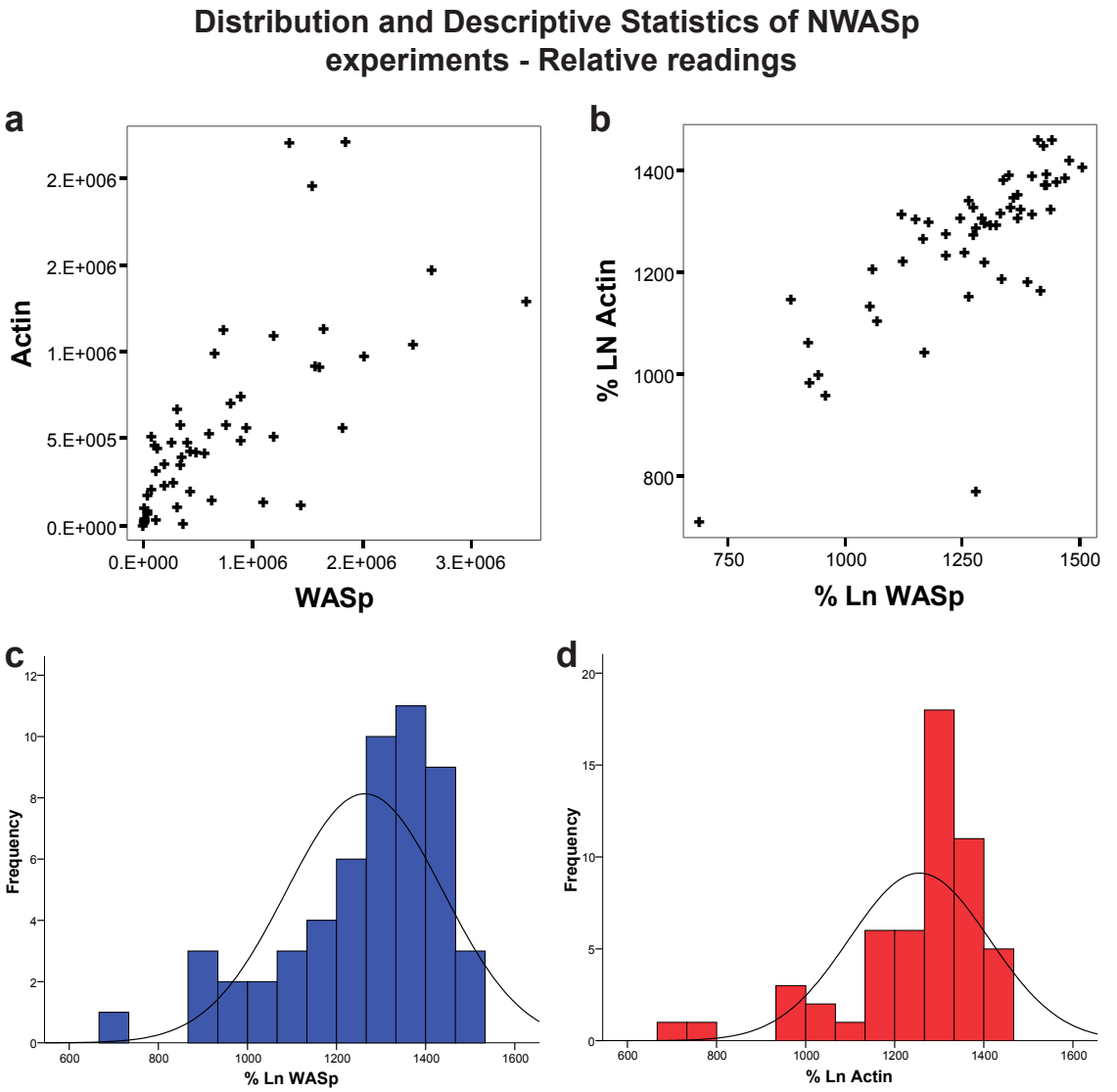

Fig A.7 Distribution and descriptive statistics of absolute densitometry readings for NWASp and mWASp experiments

Actin polymerisation assays were performed under conditions described in chapters 2.7 and 4.2.6. Relative readings are the unstandardised densitometry readings generated from the Uvi-Chemi supercooled camera. **(a) & (b)** Scatterplots of raw or natural log (Ln) transformed NWASp/ mWASp and actin densitometry readings. **(c)(d)** Frequency distributions of transformed data.

Main Effects model excluding Cytochalasin D controls

Source	Type III Sum of Squares	df	Mean Square	F	Sig.
Corrected Model	3023606.965[a]	14	215971.926	23.895	.000
Intercept	641346.914	1	641346.914	70.960	.000
Experiment	2009607.221	9	223289.691	24.705	.000
Construct_Code	1022334.725	4	255583.681	28.278	.000
WASp_percent	351667.576	1	351667.576	38.909	.000
Error	867665.741	96	9038.185		
Total	163412542.4	111			
Corrected Total	3891272.706	110			

a. R Squared = .777 (Adjusted R Squared = .745)

WASp*Experiment interaction model excluding Cytochalasin D controls

Source	Type III Sum of Squares	df	Mean Square	F	Sig.
Corrected Model	13951367.958[a]	49	284721.795	22.679	.000
Intercept	3635.667	1	3635.667	.290	.591
Experiment	1655206.318	19	87116.122	6.939	.000
Construct_Code	1892997.471	9	210333.052	16.754	.000
WASp_percent	322548.172	1	322548.172	25.692	.000
Experiment * WASp_percent	962376.040	19	50651.371	4.035	.000
Error	2360203.105	188	12554.272		
Total	94737282.715	238			
Corrected Total	16311571.063	237			

a. R Squared = .855 (Adjusted R Squared = .818)

Main Effects model including Cytochalasin D controls

Source	Type III Sum of Squares	df	Mean Square	F	Sig.
Corrected Model	16413060.578[a]	34	482737.076	29.518	.000
Intercept	216351.047	1	216351.047	13.229	.000
Experiment	8493473.417	20	424673.671	25.968	.000
Construct_Code	3752469.513	13	288651.501	17.650	.000
WASp_percent	1965263.222	1	1965263.222	120.172	.000
Error	3973969.374	243	16353.783		
Total	120993799.1	278			
Corrected Total	20387029.952	277			

a. R Squared = .805 (Adjusted R Squared = .778)

WASp*Experiment interaction model including Cytochalasin D controls

Source	Type III Sum of Squares	df	Mean Square	F	Sig.
Corrected Model	17446815.856[a]	54	323089.183	24.505	.000
Intercept	24888.570	1	24888.570	1.888	.171
Experiment	1771584.482	20	88579.224	6.718	.000
Construct_Code	3236962.409	13	248997.108	18.885	.000
WASp_percent	524993.669	1	524993.669	39.818	.000
Experiment * WASp_percent	1033755.278	20	51687.764	3.920	.000
Error	2940214.096	223	13184.817		
Total	120993799.1	278			
Corrected Total	20387029.952	277			

a. R Squared = .856 (Adjusted R Squared = .821)

Fig A.8 Complete ANCOVA statistics for each constitutively active construct analysis
df - degrees of freedom, F - F ratio, Sig. - significance

Main Effects model excluding Cytochalasin D controls

Source	Type III Sum of Squares	df	Mean Square	F	Sig.
Corrected Model	12988991.918[a]	30	432966.397	26.974	.000
Intercept	189894.398	1	189894.398	11.831	.001
Experiment	7907065.899	20	395353.295	24.631	.000
Construct_Code	2231072.404	9	247896.934	15.444	.000
WASp_percent	1846192.437	1	1846192.437	115.020	.000
Error	3322579.146	207	16051.107		
Total	94737282.715	238			
Corrected Total	16311571.063	237			

a. R Squared = .796 (Adjusted R Squared = .767)

WASp*Experiment interaction model excluding Cytochalasin D controls

Source	Type III Sum of Squares	df	Mean Square	F	Sig.
Corrected Model	13951367.958[a]	49	284721.795	22.679	.000
Intercept	3635.667	1	3635.667	.290	.591
Experiment	1655206.318	19	87116.122	6.939	.000
Construct_Code	1892997.471	9	210333.052	16.754	.000
WASp_percent	322548.172	1	322548.172	25.692	.000
Experiment * WASp_percent	962376.040	19	50651.371	4.035	.000
Error	2360203.105	188	12554.272		
Total	94737282.715	238			
Corrected Total	16311571.063	237			

a. R Squared = .855 (Adjusted R Squared = .818)

Main Effects model including Cytochalasin D controls

Source	Type III Sum of Squares	df	Mean Square	F	Sig.
Corrected Model	16413060.578[a]	34	482737.076	29.518	.000
Intercept	216351.047	1	216351.047	13.229	.000
Experiment	8493473.417	20	424673.671	25.968	.000
Construct_Code	3752469.513	13	288651.501	17.650	.000
WASp_percent	1965263.222	1	1965263.222	120.172	.000
Error	3973969.374	243	16353.783		
Total	120993799.1	278			
Corrected Total	20387029.952	277			

a. R Squared = .805 (Adjusted R Squared = .778)

WASp*Experiment interaction model including Cytochalasin D controls

Source	Type III Sum of Squares	df	Mean Square	F	Sig.
Corrected Model	17446815.856[a]	54	323089.183	24.505	.000
Intercept	24888.570	1	24888.570	1.888	.171
Experiment	1771584.482	20	88579.224	6.718	.000
Construct_Code	3236962.409	13	248997.108	18.885	.000
WASp_percent	524993.669	1	524993.669	39.818	.000
Experiment * WASp_percent	1033755.278	20	51687.764	3.920	.000
Error	2940214.096	223	13184.817		
Total	120993799.1	278			
Corrected Total	20387029.952	277			

a. R Squared = .856 (Adjusted R Squared = .821)

Fig A.9 Complete ANCOVA statistics for each standard panel construct analysis
df - degrees of freedom, F - F ratio, Sig. - significance

Main Effects model

Source	Type III Sum of Squares	df	Mean Square	F	Sig.
Corrected Model	1132180.564[a]	8	141522.570	20.885	.000
Intercept	40296.384	1	40296.384	5.947	.019
Experiment	102592.677	3	34197.559	5.047	.004
Construct_Code	215379.212	4	53844.803	7.946	.000
abWASp_percent	373824.390	1	373824.390	55.166	.000
Error	304937.349	45	6776.386		
Total	16368726.453	54			
Corrected Total	1437117.913	53			

a. R Squared = .788 (Adjusted R Squared = .750)

WASp*Experiment interaction model

Source	Type III Sum of Squares	df	Mean Square	F	Sig.
Corrected Model	1163605.889[a]	11	105782.354	16.244	.000
Intercept	19837.773	1	19837.773	3.046	.088
Experiment	58649.774	3	19549.925	3.002	.041
Construct_Code	218893.217	4	54723.304	8.403	.000
abWASp_percent	285518.730	1	285518.730	43.844	.000
Experiment * abWASp_percent	31425.326	3	10475.109	1.609	.202
Error	273512.024	42	6512.191		
Total	16368726.453	54			
Corrected Total	1437117.913	53			

a. R Squared = .810 (Adjusted R Squared = .760)

Fig A.10 Complete ANCOVA statistics for each NWASp/mWASp construct analysis
df - degrees of freedom, F - F ratio, Sig. - significance

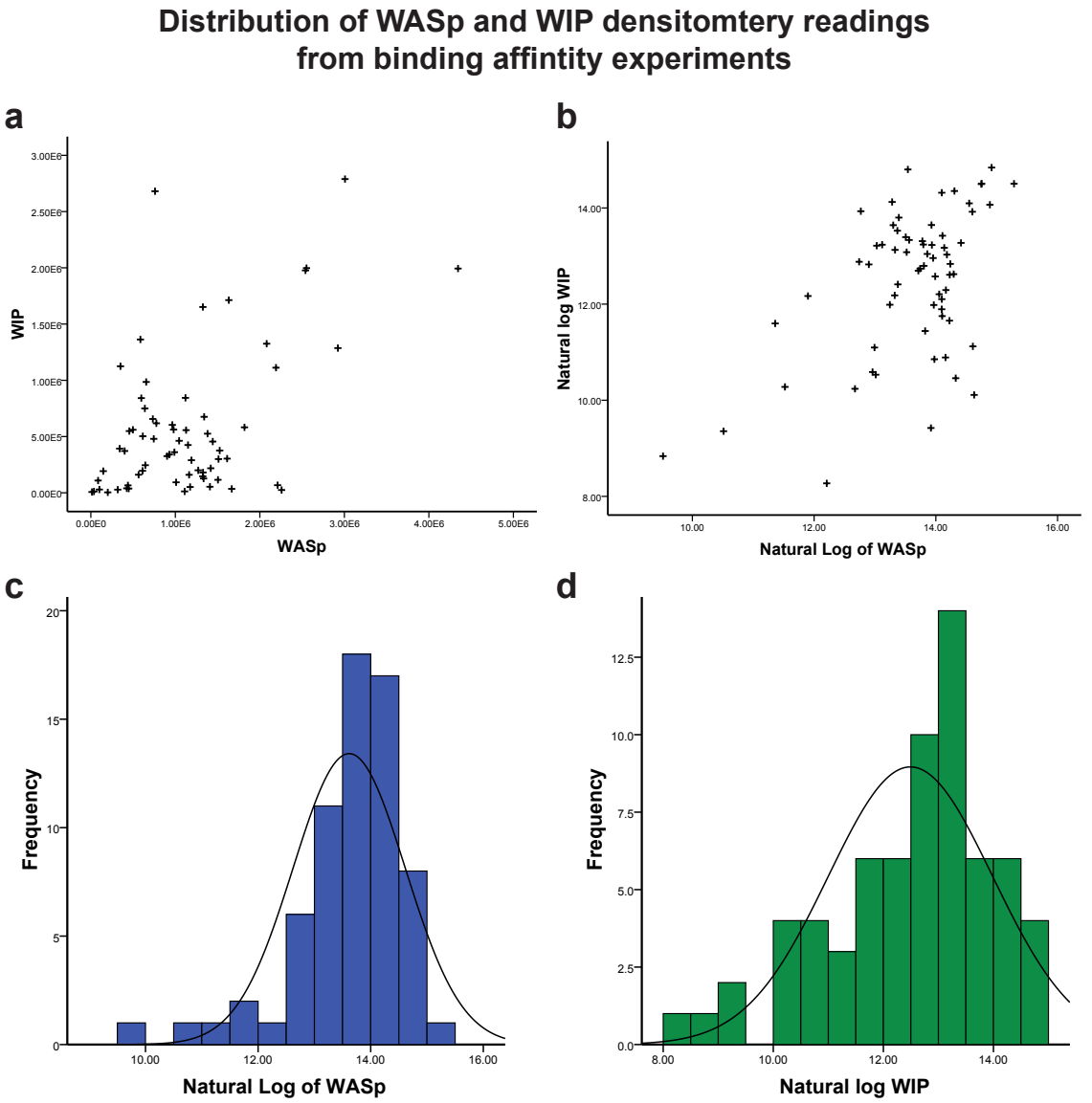

Fig A.11 Distribution and descriptive statistics of densitometry readings for WASp and WIP from affinity experiments

Experimental proceedures and methodology for data selection are described in chapter 2.10.1, 2.10.3 and 6.2.6. **(a) & (b)** Scatterplots of raw or natural log (Ln) transformed WASp and WIP densitometry readings. **(c)(d)** Frequency distributions of transformed data, demonstrating approximate normality.

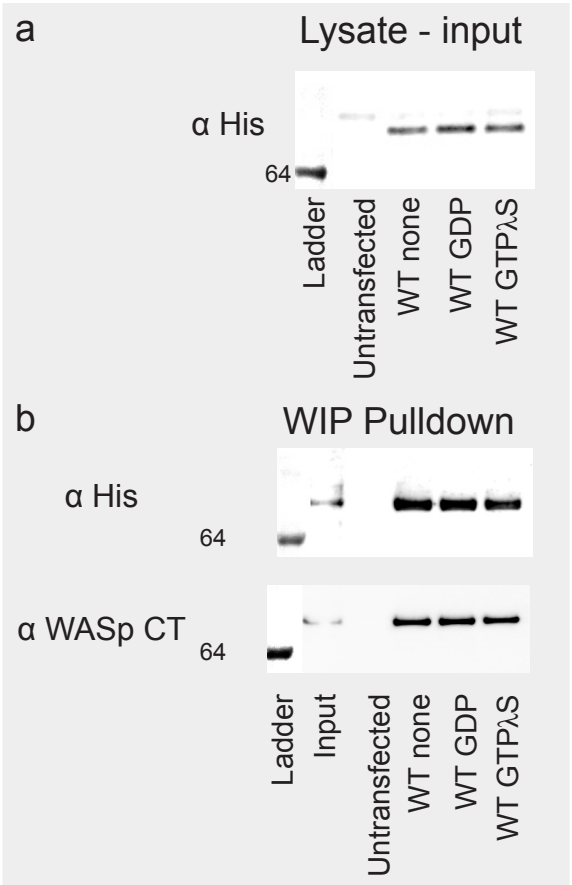

Fig A.12 No effect of guanine nucleotides on WASp - WIP affinity
Cos 7 cells were transfected with an equal amount of WT GST-WASp and zzWIP DNA, using the transfection agent JET-PEI™, according to manufacturer's instruction. At 72 hours cells were treated with 200μM of GTPλS, GDP or water for 30 minutes. Cells were then washed and lysed in 250μl of ice cold LB containing protease and phosphatase inhibitors. Supernatants were incubated overnight with 10μl of activated IgG Sepharose beads, and then washed 3 times in lysis buffer. The resultant beads were reduced and resolved by SDS-PAGE and blotted for His (WIP) and WASp. **(a)** WIP expression in lysate prior to incubation with IgG Sepharose beads **(b)** Immunoblot of pulldown.

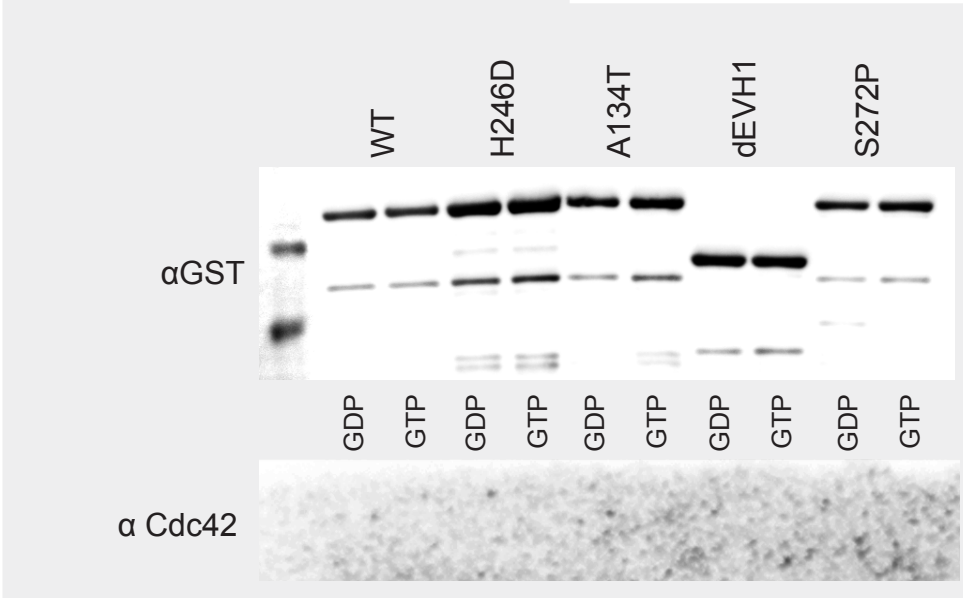

Fig A.13 Cdc42 pulldown by GST-WASp using purified proteins
WT Cdc42 was preloaded with either GDP or GTP as described for GTPγS in chapter 2.8.3. GST-WASp beads were washed in XB and then resuspended with XB and Cdc42 to a total volume of 300μL and a Cdc42 concentration of 1μM. Samples were rotated at room temperature for 1 hour. These beads were then washed 3x with XB before reduction and resolution by NuPAGE and western blotting. Membranes were divided and proteins larger than 50kDa were blotted for WASp using anti GST antibody, and proteins smaller than 50kDa were blotted with anti Cdc42.

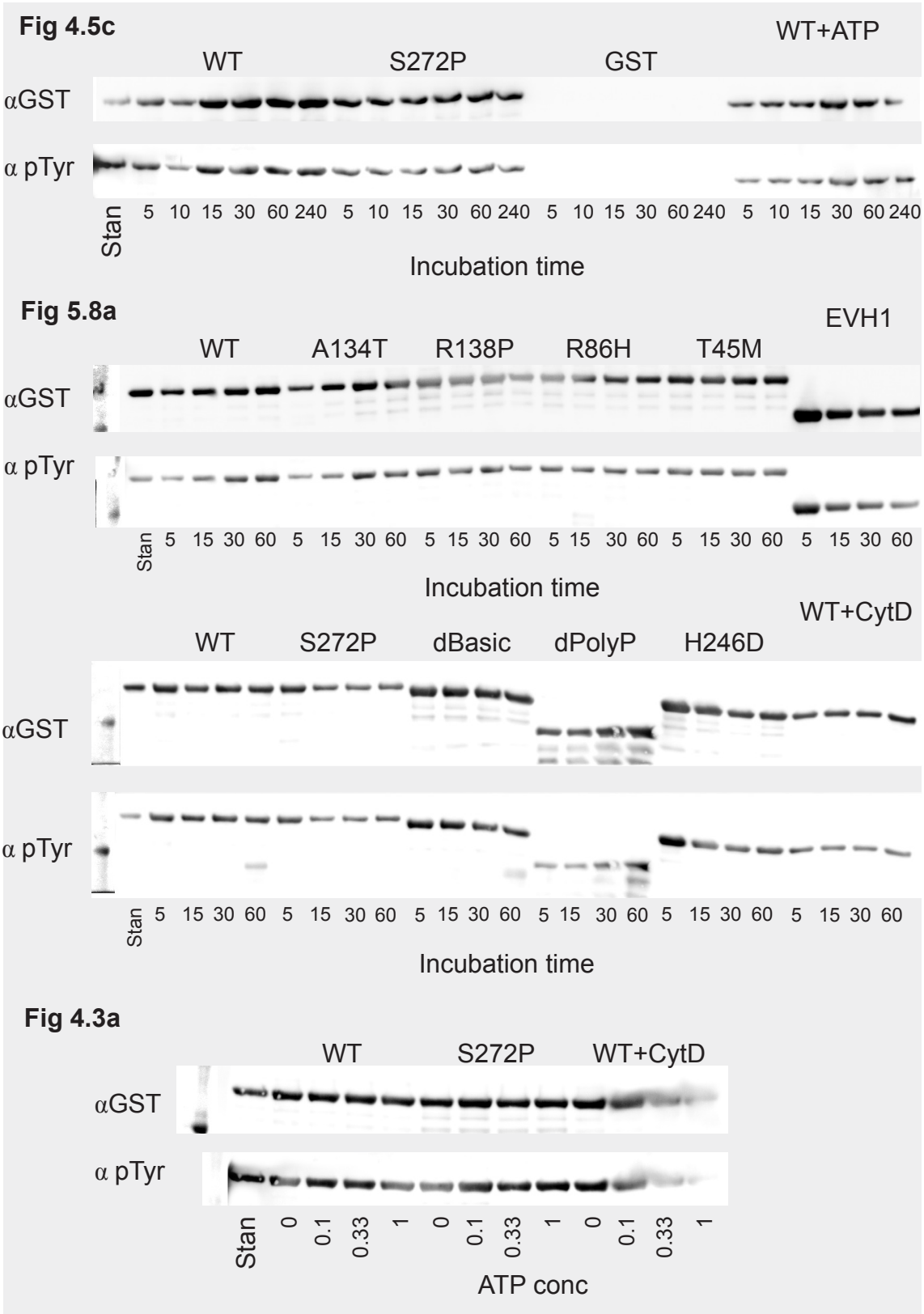

Fig A.14 Tyrosine phosphorylation of WASp during optimisation actin polymerisation assays

Immunoblots from the stated experiments were stripped following probing with anti-GST antibody and then re-probed with anti-phosphotyrosine antibody. Membranes were test exposed following stripping to ensure no residual signal was left on the membranes. Figure 4.5c and 5.8a were time course experiments, whereas figure 4.3a was an ATP cocentration titration experiment.

References

European Society for Immunodeficiency congenital immunodeficiency registry. (data as of 15-9-2008).

Abdul-Manan,N., Aghazadeh,B., Liu,G.A., Majumdar,A., Ouerfelli,O., Siminovitch,K.A., and Rosen,M.K. (1999). Structure of Cdc42 in complex with the GTPase-binding domain of the 'Wiskott-Aldrich syndrome' protein. Nature *399*, 379-383.

Abe,T., Kato,M., Miki,H., Takenawa,T., and Endo,T. (2003). Small GTPase Tc10 and its homologue RhoT induce N-WASP-mediated long process formation and neurite outgrowth. J Cell Sci. *116*, 155-168.

Adamovich,D.A., Nakamura,F., Worth,A., Burns,S., Thrasher,A.J., Hartwig,J.H., and Snapper,S.B. (2009). Activating mutations of N-WASP alter Shigella pathogenesis. Biochem. Biophys. Res. Commun. *384*, 284-289.

Adriani,M., Aoki,J., Horai,R., Thornton,A.M., Konno,A., Kirby,M., Anderson,S.M., Siegel,R.M., Candotti,F., and Schwartzberg,P.L. (2007). Impaired in vitro regulatory T cell function associated with Wiskott-Aldrich syndrome. Clinical Immunology *124*, 41-48.

Aguda,A.H., Burtnick,L.D., and Robinson,R.C. (2005). The state of the filament. EMBO Rep. *6*, 220-226.

Albert, M. H., Bittner, T., Nonoyama, S., Notarangelo, L., Burns, S. O., Pellier, I., Strauss, G., Morio, T., Imai, K., Espanol, T., Bathmann, B., Honig, M., Noordzij, J. G., Nathrath, M., Meindl, A., Wintergerst, U., Fischer, A., Thrasher, A. J., Och, H. D., and Belohradsky, B. H. Clinical phenotype and long term outcome in a large cohort of X-linked thrombocytopenia (XLT)/mild Wiskott-Aldrich sundrome patients. Clin.Exp.Immunol. 154 (suppl. 1), 122-123. 2008.
Ref Type: Generic

Aldrich,R.A., Steinberg,A.G., and Campbell,D.C. (1954). Pedigree demonstrating a sex-linked recessive condition characterized by draining ears, eczematoid dermatitis and bloody diarrhea. Pediatrics *13*, 133-139.

Amann,K.J. and Pollard,T.D. (2001). The Arp2/3 complex nucleates actin filament branches from the sides of pre-existing filaments. Nat. Cell Biol. *3*, 306-310.

Ancliff,P.J., Blundell,M.P., Cory,G.O., Calle,Y., Worth,A., Kempski,H., Burns,S., Jones,G.E., Sinclair,J., Kinnon,C., Hann,I.M., Gale,R.E., Linch,D.C., and Thrasher,A.J. (2006). Two novel activating mutations in the Wiskott-Aldrich syndrome protein result in congenital neutropenia. Blood *108*, 2182-2189.

Andreansky,S., Liu,H., Turner,S., McCullers,J.A., Lang,R., Rutschman,R., Doherty,P.C., Murray,P.J., Nienhuis,A.W., and Strom,T.S. (2005). WASP-mice exhibit defective immune responses to influenze A virus, *Streptococcus*

pneumoniae, and *Mycobacterium bovis*. Exp. Hematol. *33*, 443-451.

Anton,I.M., de la Fuente,M.A., Sims,T.N., Freeman,S., Ramesh,N., Hartwig,J.H., Dustin,M.L., and Geha,R.S. (2002). WIP deficiency reveals a differential role for WIP and the actin cytoskeleton in T and B cell activation. Immunity. *16*, 193-204.

Anton,I.M. and Jones,G.E. (2006). WIP: a multifunctional protein involved in actin cytoskeleton regulation. Eur. J. Cell Biol. *85*, 295-304.

Anton,I.M., Lu,W., Mayer,B.J., Ramesh,N., and Geha,R.S. (1998). The Wiskott-Aldrich syndrome protein-interacting protein (WIP) binds to the adaptor protein Nck. J. Biol. Chem. *273*, 20992-20995.

Anton,I.M., Saville,S.P., Byrne,M.J., Curcio,C., Ramesh,N., Hartwig,J.H., and Geha,R.S. (2003). WIP participates in actin reorganization and ruffle formation induced by PDGF. J. Cell Sci. *116*, 2443-2451.

Ardeshna,K.M., Pizzey,A.R., Thomas,N.S., Orr,S., Linch,D.C., and Devereux,S. (2000). Monocyte-derived dendritic cells do not proliferate and are not susceptible to retroviral transduction. Br. J Haematol. *108*, 817-824.

Arthur,J.F., Butterfield,L.H., Roth,M.D., Bui,L.A., Kiertscher,S.M., Lau,R., Dubinett,S., Glaspy,J., McBride,W.H., and Economou,J.S. (1997). A comparison of gene transfer methods in human dendritic cells. Cancer Gene Ther. *4*, 17-25.

Aspenstrom,P. (1997). A Cdc42 target protein with homology to the non-kinase domain of FER has a potential role in regulating the actin cytoskeleton. Curr. Biol. *7*, 479-487.

Aspenstrom,P. (2002). The WASP-binding protein WIRE has a role in the regulation of the actin filament system downstream of the platelet-derived growth factor receptor. Exp. Cell Res. *279*, 21-33.

Aspenstrom,P., Lindberg,U., and Hall,A. (1996). Two GTPases, Cdc42 and Rac, bind directly to a protein implicated in the immunodeficiency disorder Wiskott-Aldrich syndrome. Curr. Biol. *6*, 70-75.

Baba,Y., Nonoyama,S., Matsushita,M., Yamadori,T., Hashimoto,S., Imai,K., Arai,S., Kunikata,T., Kurimoto,M., Kurosaki,T., Ochs,H.D., Yata,J., Kishimoto,T., and Tsukada,S. (1999). Involvement of wiskott-aldrich syndrome protein in B-cell cytoplasmic tyrosine kinase pathway. Blood *93*, 2003-2012.

Bachmann,C., Fischer,L., Walter,U., and Reinhard,M. (1999). The EVH2 domain of the vasodilator-stimulated phosphoprotein mediates tetramerization, F-actin binding, and actin bundle formation. J. Biol. Chem. *274*, 23549-23557.

Badolato,R., Sozzani,S., Malacarne,F., Bresciani,S., Fiorini,M., Borsatti,A., Albertini,A., Mantovani,A., Ugazio,A.G., and Notarangelo,L.D. (1998). Monocytes from Wiskott-Aldrich patients display reduced chemotaxis and lack of cell polarization in response to monocyte chemoattractant protein-1 and

formyl-methionyl-leucyl-phenylalanine. J. Immunol. *161*, 1026-1033.

Badour,K., McGavin,M.K., Zhang,J., Freeman,S., Vieira,C., Filipp,D., Julius,M., Mills,G.B., and Siminovitch,K.A. (2007). Interaction of the Wiskott-Aldrich syndrome protein with sorting nexin 9 is required for CD28 endocytosis and cosignaling in T cells. Proc. Natl. Acad. Sci. U. S. A *104*, 1593-1598.

Badour,K., Zhang,J., Shi,F., Leng,Y., Collins,M., and Siminovitch,K.A. (2004). Fyn and PTP-PEST-mediated Regulation of Wiskott-Aldrich Syndrome Protein (WASp) Tyrosine Phosphorylation Is Required for Coupling T Cell Antigen Receptor Engagement to WASp Effector Function and T Cell Activation. J. Exp. Med. *199*, 99-112.

Badour,K., Zhang,J., Shi,F., McGavin,M.K.H., Rampersad,V., Hardy,L.A., Field,D., and Siminovitch,K.A. (2003). The Wiskott-Aldrich Syndrome Protein Acts Downstream of CD2 and the CD2AP and PSTPIP1 Adaptors to Promote Formation of the Immunological Synapse. Immunity *18*, 141-154.

Banchereau,J. and Steinman,R.M. (1998). Dendritic cells and the control of immunity. Nature *392*, 245-252.

Banerjee,P.P., Pandey,R., Zheng,R., Suhoski,M.M., Monaco-Shawver,L., and Orange,J.S. (2007). Cdc42-interacting protein 4 functionally links actin and microtubule networks at the cytolytic NK cell immunological synapse. J. Exp. Med. *204*, 2305-2320.

Banin,S., Truong,O., Katz,D.R., Waterfield,M.D., Brickell,P.M., and Gout,I. (1996). Wiskott-Aldrich syndrome protein (WASp) is a binding partner for c-Src family protein-tyrosine kinases. Curr. Biol. *6*, 981-988.

Behnia,R. and Munro,S. (2005). Organelle identity and the signposts for membrane traffic. Nature *438*, 597-604.

Beltzner,C.C. and Pollard,T.D. (2004). Identification of functionally important residues of Arp2/3 complex by analysis of homology models from diverse species. J. Mol. Biol. *336*, 551-565.

Benesch,S., Lommel,S., Steffen,A., Stradal,T.E., Scaplehorn,N., Way,M., Wehland,J., and Rottner,K. (2002). Phosphatidylinositol 4,5-biphosphate (PIP2)-induced vesicle movement depends on N-WASP and involves Nck, WIP, and Grb2. J. Biol. Chem. *277*, 37771-37776.

Bernards,A. (2006). Ras superfamily and interacting proteins database. Methods Enzymol. *407*, 1-9.

Bimboim,H.C. and Doly,J. (1979). A rapid alkaline extraction procedure for screening recombinant plasmid DNA. Nucl. Acids Res. *7*, 1513-1523.

Binks,M., Jones,G.E., Brickell,P.M., Kinnon,C., Katz,D.R., and Thrasher,A.J. (1998). Intrinsic dendritic cell abnormalities in Wiskott-Aldrich syndrome. Eur. J. Immunol. *28*, 3259-3267.

Blanchoin,L., Amann,K.J., Higgs,H.N., Marchand,J.B., Kaiser,D.A., and Pollard,T.D. (2000a). Direct observation of dendritic actin filament networks nucleated by Arp2/3 complex and WASP/Scar proteins. Nature *404*, 1007-1011.

Blanchoin,L. and Pollard,T.D. (1999). Mechanism of interaction of Acanthamoeba actophorin (ADF/Cofilin) with actin filaments. J. Biol. Chem. *274*, 15538-15546.

Blanchoin,L., Pollard,T.D., and Mullins,R.D. (2000b). Interactions of ADF/cofilin, Arp2/3 complex, capping protein and profilin in remodeling of branched actin filament networks. Curr. Biol. *10*, 1273-1282.

Blundell,M.P., Bouma,G., Metelo,J., Worth,A., Calle,Y., Cowell,L.A., Westerberg,L.S., Moulding,D.A., Mirando,S., Kinnon,C., Cory,G.O., Jones,G.E., Snapper,S.B., Burns,S.O., and Thrasher,A.J. (2009). Phosphorylation of WASp is a key regulator of activity and stability in vivo. Proc. Natl. Acad. Sci. U. S. A 106, 15738-15743.

Bokoch,G.M., Wang,Y., Bohl,B.P., Sells,M.A., Quilliam,L.A., and Knaus,U.G. (1996). Interaction of the Nck Adapter Protein with p21-activated Kinase (PAK1). Journal of Biological Chemistry *271*, 25746-25749.

Bos,J.L., Rehmann,H., and Wittinghofer,A. (2007). GEFs and GAPs: Critical Elements in the Control of Small G Proteins. Cell *129*, 865-877.

Bouma,G., Burns,S., and Thrasher,A.J. (2007). Impaired T-cell priming in vivo resulting from dysfunction of WASp-deficient dendritic cells. Blood *110*, 4278-4284.

Bryce,N.S., Clark,E.S., Leysath,J.L., Currie,J.D., Webb,D.J., and Weaver,A.M. (2005). Cortactin promotes cell motility by enhancing lamellipodial persistence. Curr. Biol. *15*, 1276-1285.

Bu,W., Chou,A.M., Lim,K.B., Sudhaharan,T., and Ahmed,S. (2009). The Toca-1-N-WASP complex links filopodia formation to endocytosis. Journal of Biological Chemistry M805940200.

Buck,M., Xu,W., and Rosen,M.K. (2001). Global disruption of the WASP autoinhibited structure on Cdc42 binding. Ligand displacement as a novel method for monitoring amide hydrogen exchange. Biochemistry *40*, 14115-14122.

Burbelo,P.D., Drechsel,D., and Hall,A. (1995). A conserved binding motif defines numerous candidate target proteins for both Cdc42 and Rac GTPases. J. Biol. Chem. *270*, 29071-29074.

Burns,S., Hardy,S.J., Buddle,J., Yong,K.L., Jones,G.E., and Thrasher,A.J. (2004). Maturation of DC is associated with changes in motile characteristics and adherence. Cell Motil. Cytoskeleton *57*, 118-132.

Burns,S., Thrasher,A.J., Blundell,M.P., Machesky,L., and Jones,G.E. (2001).

Configuration of human dendritic cell cytoskeleton by Rho GTPases, the WAS protein, and differentiation. Blood *98*, 1142-1149.

Calle,Y., Burns,S., Thrasher,A.J., and Jones,G.E. (2006a). The leukocyte podosome. Eur. J Cell Biol. *85*, 151-157.

Calle,Y., Carragher,N.O., Thrasher,A.J., and Jones,G.E. (2006b). Inhibition of calpain stabilises podosomes and impairs dendritic cell motility. J. Cell Sci. *119*, 2375-2385.

Calle,Y., Chou,H.C., Thrasher,A.J., and Jones,G.E. (2004). Wiskott-Aldrich syndrome protein and the cytoskeletal dynamics of dendritic cells. J. Pathol. *204*, 460-469.

Canales,M.L. and Mauer,A.M. (1967). Sex-linked hereditary thrombocytopenia as a variant of Wiskott-Aldrich syndrome. N. Engl. J. Med. *277*, 899-901.

Cannon,J.L. and Burkhardt,J.K. (2004). Differential roles for Wiskott-Aldrich syndrome protein in immune synapse formation and IL-2 production. J Immunol *173*, 1658-1662.

Cannon,J.L., Labno,C.M., Bosco,G., Seth,A., McGavin,M.H., Siminovitch,K.A., Rosen,M.K., and Burkhardt,J.K. (2001). Wasp recruitment to the T cell:APC contact site occurs independently of Cdc42 activation. Immunity. *15*, 249-259.

Cantley,L.C. (2002). The phosphoinositide 3-kinase pathway. Science *296*, 1655-1657.

Carlier,M.F., Valentin-Ranc,C., Combeau,C., Fievez,S., and Pantoloni,D. (1994). Actin polymerization: regulation by divalent metal ion and nucleotide binding, ATP hydrolysis and binding of myosin. Adv. Exp. Med. Biol. 358, 71-81.

Carlier,M.F., Laurent,V., Santolini,J., Melki,R., Didry,D., Xia,G.X., Hong,Y., Chua,N.H., and Pantaloni,D. (1997). Actin depolymerizing factor (ADF/cofilin) enhances the rate of filament turnover: implication in actin-based motility. J. Cell Biol. *136*, 1307-1322.

Carlier,M.F., Nioche,P., Broutin-L'Hermite,I., Boujemaa,R., Le Clainche,C., Egile,C., Garbay,C., Ducruix,A., Sansonetti,P., and Pantaloni,D. (2000). GRB2 links signaling to actin assembly by enhancing interaction of neural Wiskott-Aldrich syndrome protein (N-WASp) with actin-related protein (ARP2/3) complex. J. Biol. Chem. *275*, 21946-21952.

Castellano,F., Le,C.C., Patin,D., Carlier,M.F., and Chavrier,P. (2001). A WASp-VASP complex regulates actin polymerization at the plasma membrane. EMBO J *20*, 5603-5614.

Chen,M., She,H., Davis,E.M., Spicer,C.M., Kim,L., Ren,R., Le Beau,M.M., and Li,W. (1998). Identification of Nck family genes, chromosomal localization, expression, and signaling specificity. J Biol. Chem. *273*, 25171-25178.

Chou,H.C., Anton,I.M., Holt,M.R., Curcio,C., Lanzardo,S., Worth,A., Burns,S., Thrasher,A.J., Jones,G.E., and Calle,Y. (2006). WIP regulates the stability and localization of WASP to podosomes in migrating dendritic cells. Curr. Biol. *16*, 2337-2344.

Coers,J., Ranft,C., and Skoda,R.C. (2004). A Truncated Isoform of c-Mpl with an Essential C-terminal Peptide Targets the Full-length Receptor for Degradation. J. Biol. Chem. *279*, 36397-36404.

Cooper,J.A. (1987). Effects of cytochalasin and phalloidin on actin. J. Cell Biol. *105*, 1473-1478.

Cooper,M.D., Chae,H.P., Lowman,J.T., Krivit,W., and Good,R.A. (1968). Wiskott-Aldrich syndrome. An immunologic deficiency disease involving the afferent limb of immunity. Am. J Med. *44*, 499-513.

Coppolino,M.G., Krause,M., Hagendorff,P., Monner,D.A., Trimble,W., Grinstein,S., Wehland,J., and Sechi,A.S. (2001). Evidence for a molecular complex consisting of Fyb/SLAP, SLP-76, Nck, VASP and WASP that links the actin cytoskeleton to Fcgamma receptor signalling during phagocytosis. J. Cell Sci. *114*, 4307-4318.

Cory,G.O., Cramer,R., Blanchoin,L., and Ridley,A.J. (2003). Phosphorylation of the WASP-VCA domain increases its affinity for the Arp2/3 complex and enhances actin polymerization by WASP. Mol. Cell *11*, 1229-1239.

Cory,G.O., Garg,R., Cramer,R., and Ridley,A.J. (2002). Phosphorylation of tyrosine 291 enhances the ability of WASp to stimulate actin polymerization and filopodium formation. Wiskott-Aldrich Syndrome protein. J. Biol. Chem. *277*, 45115-45121.

Cote,J.F., Chung,P.L., Theberge,J.F., Halle,M., Spencer,S., Lasky,L.A., and Tremblay,M.L. (2002). PSTPIP Is a Substrate of PTP-PEST and Serves as a Scaffold Guiding PTP-PEST Toward a Specific Dephosphorylation of WASP. Journal of Biological Chemistry *277*, 2973-2986.

Curcio,C., Pannellini,T., Lanzardo,S., Forni,G., Musiani,P., and Anton,I.M. (2007). WIP null mice display a progressive immunological disorder that resembles Wiskott-Aldrich syndrome. J Pathol. *211*, 67-75.

Dayel,M.J., Holleran,E.A., and Mullins,R.D. (2001). Arp2/3 complex requires hydrolyzable ATP for nucleation of new actin filaments. Proc. Natl. Acad. Sci. U. S. A *98*, 14871-14876.

Dayel,M.J. and Mullins,R.D. (2004). Activation of Arp2/3 complex: addition of the first subunit of the new filament by a WASP protein triggers rapid ATP hydrolysis on Arp2. PLoS. Biol. *2*, E91.

de la Fuente,M.A., Sasahara,Y., Calamito,M., Anton,I.M., Elkhal,A., Gallego,M.D., Suresh,K., Siminovitch,K., Ochs,H.D., Anderson,K.C.,

Rosen,F.S., Geha,R.S., and Ramesh,N. (2007). WIP is a chaperone for Wiskott-Aldrich syndrome protein (WASP). PNAS *104*, 926-931.

De Saint-Basile,G., Schlegel,N., Caniglia,M., Le,D.F., Kaplan,C., Lecompte,T., Piller,F., Fischer,A., and Griscelli,C. (1991). X-linked thrombocytopenia and Wiskott-Aldrich syndrome: similar regional assignment but distinct X-inactivation pattern in carriers. Ann. Hematol. *63*, 107-110.

de,N.S., Hardy,S., Sinclair,J., Blundell,M.P., Strid,J., Schulz,O., Zwirner,J., Jones,G.E., Katz,D.R., Kinnon,C., and Thrasher,A.J. (2005). Impaired dendritic-cell homing in vivo in the absence of Wiskott-Aldrich syndrome protein. Blood *105*, 1590-1597.

Derry,J.M., Kerns,J.A., Weinberg,K.I., Ochs,H.D., Volpini,V., Estivill,X., Walker,A.P., and Francke,U. (1995). WASP gene mutations in Wiskott-Aldrich syndrome and X-linked thrombocytopenia. Hum. Mol. Genet. *4*, 1127-1135.

Derry,J.M., Ochs,H.D., and Francke,U. (1994). Isolation of a novel gene mutated in Wiskott-Aldrich syndrome. Cell *78*, 635-644.

Devriendt,K., Kim,A.S., Mathijs,G., Frints,S.G., Schwartz,M., Van Den Oord,J.J., Verhoef,G.E., Boogaerts,M.A., Fryns,J.P., You,D., Rosen,M.K., and Vandenberghe,P. (2001). Constitutively activating mutation in WASP causes X-linked severe congenital neutropenia. Nat. Genet. *27*, 313-317.

Dewey,R.A., Diez,I.A., Ballmaier,M., Filipovich,A., Greil,J., Gungor,T., Happel,C., Maschan,A., Noyan,F., Pannicke,U., Schwarz,K., Snapper,S., Welte,K., and Klein,C. (2006). Retroviral WASP gene transfer into human hematopoietic stem cells reconstitutes the actin cytoskeleton in myeloid progeny cells differentiated in vitro. Experimental Hematology *34*, 1161-1169.

Dong,X., Patino-Lopez,G., Candotti,F., and Shaw,S. (2007). Structure-function analysis of WIP role in TCR-stimulated NFAT activation: Evidence that WIP/WASP dissociation is not required and that the WIP N-terminus is inhibitory. Journal of Biological Chemistry M704972200.

Donnelly,S.F., Pocklington,M.J., Pallotta,D., and Orr,E. (1993). A proline-rich protein, verprolin, involved in cytoskeletal organization and cellular growth in the yeast Saccharomyces cerevisiae. Mol. Microbiol. *10*, 585-596.

Donner,M., Schwartz,M., Carlsson,K.U., and Holmberg,L. (1988). Hereditary X-linked thrombocytopenia maps to the same chromosomal region as the Wiskott-Aldrich syndrome. Blood *72*, 1849-1853.

Dransart,E., Olofsson,B., and Cherfils,J. (2005). RhoGDIs revisited: novel roles in Rho regulation. Traffic. *6*, 957-966.

Dubinsky,W.P., Mayorga-Wark,O., and Schultz,S.G. (1999). Volume regulatory responses of basolateral membrane vesicles from Necturus enterocytes: role of the cytoskeleton. Proc. Natl. Acad. Sci. U. S. A *96*, 9421-9426.

Dupre,L., Trifari,S., Follenzi,A., Marangoni,F., Lain de,L.T., Bernad,A., Martino,S., Tsuchiya,S., Bordignon,C., Naldini,L., Aiuti,A., and Roncarolo,M.G. (2004). Lentiviral vector-mediated gene transfer in T cells from Wiskott-Aldrich syndrome patients leads to functional correction. Mol. Ther. *10*, 903-915.

Dupuis-Girod,S., Medioni,J., Haddad,E., Quartier,P., Cavazzana-Calvo,M., Le,D.F., de Saint,B.G., Delaunay,J., Schwarz,K., Casanova,J.L., Blanche,S., and Fischer,A. (2003). Autoimmunity in Wiskott-Aldrich syndrome: risk factors, clinical features, and outcome in a single-center cohort of 55 patients. Pediatrics *111*, e622-e627.

Egile,C., Rouiller,I., Xu,X.P., Volkmann,N., Li,R., and Hanein,D. (2005). Mechanism of filament nucleation and branch stability revealed by the structure of the Arp2/3 complex at actin branch junctions. PLoS. Biol. *3*, e383.

Egile,C., Loisel,T.P., Laurent,V., Li,R., Pantaloni,D., Sansonetti,P.J., and Carlier,M.F. (1999). Activation of the CDC42 Effector N-WASP by the Shigella flexneri IcsA Protein Promotes Actin Nucleation by Arp2/3 Complex and Bacterial Actin-based Motility. The Journal of Cell Biology *146*, 1319-1332.

Erickson,J.W., Cerione,R.A., and Hart,M.J. (1997). Identification of an Actin Cytoskeletal Complex That Includes IQGAP and the Cdc42 GTPase. Journal of Biological Chemistry *272*, 24443-24447.

Esslinger,C., Romero,P., and MacDonald,H.R. (2002). Efficient transduction of dendritic cells and induction of a T-cell response by third-generation lentivectors. Hum. Gene Ther. *13*, 1091-1100.

Facchetti,F., Blanzuoli,L., Vermi,W., Notarangelo,L.D., Giliani,S., Fiorini,M., Fasth,A., Stewart,D.M., and Nelson,D.L. (1998). Defective actin polymerization in EBV-transformed B-cell lines from patients with the Wiskott-Aldrich syndrome. J. Pathol. *185*, 99-107.

Faix,J. and Grosse,R. (2006). Staying in shape with formins. Dev. Cell *10*, 693-706.

Falet,H., Hoffmeister,K.M., Neujahr,R., Italiano,J.E., Jr., Stossel,T.P., Southwick,F.S., and Hartwig,J.H. (2002). Importance of free actin filament barbed ends for Arp2/3 complex function in platelets and fibroblasts. Proc. Natl. Acad. Sci. U. S. A *99*, 16782-16787.

Follenzi,A., Ailles,L.E., Bakovic,S., Geuna,M., and Naldini,L. (2000). Gene transfer by lentiviral vectors is limited by nuclear translocation and rescued by HIV-1 pol sequences. Nat. Genet. *25*, 217-222.

Fradelizi,J., Noireaux,V., Plastino,J., Menichi,B., Louvard,D., Sykes,C., Golsteyn,R.M., and Friederich,E. (2001). ActA and human zyxin harbour Arp2/3-independent actin-polymerization activity. Nat. Cell Biol. *3*, 699-707.

Fukuoka,M., Miki,H., and Takenawa,T. (1997). Identification of N-WASP

homologs in human and rat brain. Gene *196*, 43-48.

Fukuoka,M., Suetsugu,S., Miki,H., Fukami,K., Endo,T., and Takenawa,T. (2001). A novel neural Wiskott-Aldrich syndrome protein (N-WASP) binding protein, WISH, induces Arp2/3 complex activation independent of Cdc42. J. Cell Biol. *152*, 471-482.

Gallego,M.D., de la Fuente,M.A., Anton,I.M., Snapper,S., Fuhlbrigge,R., and Geha,R.S. (2006). WIP and WASP play complementary roles in T cell homing and chemotaxis to SDF-1alpha. Int. Immunol. *18*, 221-232.

Gallego,M.D., Santamaria,M., Pena,J., and Molina,I.J. (1997). Defective actin reorganization and polymerization of Wiskott-Aldrich T cells in response to CD3-mediated stimulation. Blood *90*, 3089-3097.

Gasperi,C., Rescigno,M., Granucci,F., Citterio,S., Matyszak,M.K., Sciurpi,M.T., Lanfrancone,L., and Ricciardi-Gastagnoli,P. (1999). Retroviral gene transfer, rapid selection, and maintenance of the immature phenotype in mouse dendritic cells. J Leukoc. Biol. *66*, 263-267.

Gil,D., Schamel,W.W., Montoya,M., Sanchez-Madrid,F., and Alarcon,B. (2002). Recruitment of Nck by CD3 epsilon reveals a ligand-induced conformational change essential for T cell receptor signaling and synapse formation. Cell *109*, 901-912.

Gimona,M., Buccione,R., Courtneidge,S.A., and Linder,S. (2008). Assembly and biological role of podosomes and invadopodia. Current Opinion in Cell Biology *20*, 235-241.

Gismondi,A., Cifaldi,L., Mazza,C., Giliani,S., Parolini,S., Morrone,S., Jacobelli,J., Bandiera,E., Notarangelo,L., and Santoni,A. (2004). Impaired natural and CD16-mediated NK cell cytotoxicity in patients with WAS and XLT: ability of IL-2 to correct NK cell functional defect. Blood *104*, 436-443.

Goley,E.D., Rodenbusch,S.E., Martin,A.C., and Welch,M.D. (2004). Critical conformational changes in the Arp2/3 complex are induced by nucleotide and nucleation promoting factor. Mol. Cell *16*, 269-279.

Goley,E.D. and Welch,M.D. (2006). The ARP2/3 complex: an actin nucleator comes of age. Nat. Rev. Mol. Cell Biol. *7*, 713-726.

Gournier,H., Goley,E.D., Niederstrasser,H., Trinh,T., and Welch,M.D. (2001). Reconstitution of human Arp2/3 complex reveals critical roles of individual subunits in complex structure and activity. Mol. Cell *8*, 1041-1052.

Greer,W.L., Shehabeldin,A., Schulman,J., Junker,A., and Siminovitch,K.A. (1996). Identification of WASP mutations, mutation hotspots and genotype-phenotype disparities in 24 patients with the Wiskott-Aldrich syndrome. Hum. Genet. *98*, 685-690.

Greg,J.T. (1999). One step screening of retroviral producer clones by real time

quantitative PCR. The Journal of Gene Medicine *1*, 352-359.

Gruber,A., Kan-Mitchell,J., Kuhen,K.L., Mukai,T., and Wong-Staal,F. (2000). Dendritic cells transduced by multiply deleted HIV-1 vectors exhibit normal phenotypes and functions and elicit an HIV-specific cytotoxic T-lymphocyte response in vitro. Blood *96*, 1327-1333.

Guinamard,R., Aspenstrom,P., Fougereau,M., Chavrier,P., and Guillemot,J.C. (1998). Tyrosine phosphorylation of the Wiskott-Aldrich syndrome protein by Lyn and Btk is regulated by CDC42. FEBS Lett. *434*, 431-436.

Haddad,E., Zugaza,J.L., Louache,F., Debili,N., Crouin,C., Schwarz,K., Fischer,A., Vainchenker,W., and Bertoglio,J. (2001). The interaction between Cdc42 and WASP is required for SDF-1-induced T-lymphocyte chemotaxis. Blood *97*, 33-38.

Hannigan,M., Zhan,L., Li,Z., Ai,Y., Wu,D., and Huang,C.K. (2002). Neutrophils lacking phosphoinositide 3-kinase gamma show loss of directionality during N-formyl-Met-Leu-Phe-induced chemotaxis. Proc. Natl. Acad. Sci. U. S. A *99*, 3603-3608.

Haugh,J.M. and Meyer,T. (2002). Active EGF receptors have limited access to PtdIns(4,5)P(2) in endosomes: implications for phospholipase C and PI 3-kinase signaling. J. Cell Sci. *115*, 303-310.

Heasman,S.J. and Ridley,A.J. (2008). Mammalian Rho GTPases: new insights into their functions from in vivo studies. Nat Rev Mol Cell Biol *9*, 690-701.

Hemsath,L., Dvorsky,R., Fiegen,D., Carlier,M.F., and Ahmadian,M.R. (2005). An electrostatic steering mechanism of Cdc42 recognition by Wiskott-Aldrich syndrome proteins. Mol Cell *20*, 313-324.

Higgs,H.N., Blanchoin,L., and Pollard,T.D. (1999). Influence of the C terminus of Wiskott-Aldrich syndrome protein (WASp) and the Arp2/3 complex on actin polymerization. Biochemistry *38*, 15212-15222.

Higgs,H.N. and Pollard,T.D. (2000). Activation by Cdc42 and PIP2 of Wiskott-Aldrich syndrome protein (WASp) stimulates actin nucleation by Arp2/3 complex. Journal of Cell Biology *150*, 1311-1320.

Hill,T.L. and Kirschner,M.W. (1982). Subunit treadmilling of microtubules or actin in the presence of cellular barriers: possible conversion of chemical free energy into mechanical work. Proc. Natl. Acad. Sci. U. S. A 79, 490-494.

Ho,H.Y., Rohatgi,R., Lebensohn,A.M., Le,M., Li,J., Gygi,S.P., and Kirschner,M.W. (2004). Toca-1 mediates Cdc42-dependent actin nucleation by activating the N-WASP-WIP complex. Cell *118*, 203-216.

Ho,H.Y.H., Rohatgi,R., Ma,L., and Kirschner,M.W. (2001). CR16 forms a complex with N-WASP in brain and is a novel member of a conserved proline-rich actin-binding protein family. Proceedings of the National Academy of

Sciences of the United States of America *98*, 11306-11311.

Holmes,K.C., Popp,D., Gebhard,W., and Kabsch,W. (1990). Atomic model of the actin filament. Nature 347, 44-49.

Hu,V.W. and Heikka,D.S. (2000). Radiolabeling revisited: metabolic labeling with (35)S-methionine inhibits cell cycle progression, proliferation, and survival. FASEB J. *14*, 448-454.

Hufner,K., Higgs,H.N., Pollard,T.D., Jacobi,C., Aepfelbacher,M., and Linder,S. (2001). The verprolin-like central (vc) region of Wiskott-Aldrich syndrome protein induces Arp2/3 complex-dependent actin nucleation. J. Biol. Chem. *276*, 35761-35767.

Hug,C., Jay,P.Y., Reddy,I., McNally,J.G., Bridgman,P.C., Elson,E.L., and Cooper,J.A. (1995). Capping protein levels influence actin assembly and cell motility in dictyostelium. Cell *81*, 591-600.

Humblet-Baron,S., Sather,B., Anover,S., Becker-Herman,S., Kasprowicz,D.J., Khim,S., Nguyen,T., Hudkins-Loya,K., Alpers,C.E., Ziegler,S.F., Ochs,H., Torgerson,T., Campbell,D.J., and Rawlings,D.J. (2007). Wiskott-Aldrich syndrome protein is required for regulatory T cell homeostasis. J. Clin. Invest. *117*, 407-418.

HUNTLEY,C.C. and DEES,S.C. (1957). Eczema associated with thrombocytopenic purpura and purulent otitis media; report of five fatal cases. Pediatrics *19*, 351-361.

Imai,K., Morio,T., Zhu,Y., Jin,Y., Itoh,S., Kajiwara,M., Yata,J., Mizutani,S., Ochs,H.D., and Nonoyama,S. (2004). Clinical course of patients with WASP gene mutations. Blood *103*, 456-464.

Imai,K., Nonoyama,S., and Ochs,H.D. (2003). WASP (Wiskott-Aldrich syndrome protein) gene mutations and phenotype. Curr. Opin. Allergy Clin Immunol. *3*, 427-436.

Imai,K., Nonoyama,S., Miki,H., Morio,T., Fukami,K., Zhu,Q., Aruffo,A., Ochs,H.D., Yata,J.i., and Takenawa,T. (1999). The Pleckstrin Homology Domain of the Wiskott-Aldrich Syndrome Protein Is Involved in the Organization of Actin Cytoskeleton. Clinical Immunology *92*, 128-137.

Insall,R., Muller-Taubenberger,A., Machesky,L., Kohler,J., Simmeth,E., Atkinson,S.J., Weber,I., and Gerisch,G. (2001). Dynamics of the Dictyostelium Arp2/3 complex in endocytosis, cytokinesis, and chemotaxis. Cell Motil. Cytoskeleton *50*, 115-128.

Insall,R.H. and Machesky,L.M. (2004). Regulation of WASP: PIP2 Pipped by Toca-1? Cell *118*, 140-141.

Iwasa,J.H. and Mullins,R.D. (2007). Spatial and temporal relationships between actin-filament nucleation, capping, and disassembly. Curr. Biol. *17*, 395-406.

Jaffe,A.B. and Hall,A. (2005). Rho GTPases: biochemistry and biology. Annu. Rev. Cell Dev. Biol. *21*, 247-269.

Jenne,L., Schuler,G., and Steinkasserer,A. (2001). Viral vectors for dendritic cell-based immunotherapy. Trends Immunol. *22*, 102-107.

Jin,Y., Mazza,C., Christie,J.R., Giliani,S., Fiorini,M., Mella,P., Gandellini,F., Stewart,D.M., Zhu,Q., Nelson,D.L., Notarangelo,L.D., and Ochs,H.D. (2004). Mutations of the Wiskott-Aldrich Syndrome Protein (WASP): hotspots, effect on transcription, and translation and phenotype/genotype correlation. Blood *104*, 4010-4019.

Joberty,G., Petersen,C., Gao,L., and Macara,I.G. (2000). The cell-polarity protein Par6 links Par3 and atypical protein kinase C to Cdc42. Nat. Cell Biol. *2*, 531-539.

Jones,G.E., Prigmore,E., Calvez,R., Hogan,C., Dunn,G.A., Hirsch,E., Wymann,M.P., and Ridley,A.J. (2003). Requirement for PI 3-kinase gamma in macrophage migration to MCP-1 and CSF-1. Exp. Cell Res. *290*, 120-131.

Jones,G.E., Zicha,D., Dunn,G.A., Blundell,M., and Thrasher,A. (2002). Restoration of podosomes and chemotaxis in Wiskott-Aldrich syndrome macrophages following induced expression of WASp. Int. J Biochem. Cell Biol. *34*, 806-815.

Kaksonen,M., Peng,H.B., and Rauvala,H. (2000). Association of cortactin with dynamic actin in lamellipodia and on endosomal vesicles. J Cell Sci. *113 Pt 24*, 4421-4426.

Kasai,M., Sakura,S., and Oosawa,F. (1962a). The G-F equilibrium in actin solutions under various conditions. Biochim. Biophys. Acta 57, 13-21.

Kato,M., Miki,H., Imai,K., Nonoyama,S., Suzuki,T., Sasakawa,C., and Takenawa,T. (1999). Wiskott-Aldrich syndrome protein induces actin clustering without direct binding to Cdc42. J Biol. Chem. *274*, 27225-27230.

Kato,M., Miki,H., Kurita,S., Endo,T., Nakagawa,H., Miyamoto,S., and Takenawa,T. (2002). WICH, a Novel Verprolin Homology Domain-Containing Protein That Functions Cooperatively with N-WASP in Actin-Microspike Formation. Biochemical and Biophysical Research Communications *291*, 41-47.

Kelleher,J.F., Atkinson,S.J., and Pollard,T.D. (1995). Sequences, structural models, and cellular localization of the actin-related proteins Arp2 and Arp3 from Acanthamoeba. J. Cell Biol. *131*, 385-397.

Kempiak,S.J., Yip,S.C., Backer,J.M., and Segall,J.E. (2003). Local signaling by the EGF receptor. J Cell Biol. *162*, 781-787.

Kempiak,S.J., Yamaguchi,H., Sarmiento,C., Sidani,M., Ghosh,M., Eddy,R.J., DesMarais,V., Way,M., Condeelis,J., and Segall,J.E. (2005). A Neural Wiskott-Aldrich Syndrome Protein-mediated Pathway for Localized Activation of Actin

Polymerization That Is Regulated by Cortactin. Journal of Biological Chemistry *280*, 5836-5842.

Kettner,A., Kumar,L., Anton,I.M., Sasahara,Y., de la,F.M., Pivniouk,V.I., Falet,H., Hartwig,J.H., and Geha,R.S. (2004). WIP regulates signaling via the high affinity receptor for immunoglobulin E in mast cells. J. Exp. Med. *199*, 357-368.

Kim,A.S., Kakalis,L.T., Abdul-Manan,N., Liu,G.A., and Rosen,M.K. (2000). Autoinhibition and activation mechanisms of the Wiskott-Aldrich syndrome protein. Nature *404*, 151-158.

Kim,M.K., Kim,E.S., Kim,D.S., Choi,I.H., Moon,T., Yoon,C.N., and Shin,J.S. (2004). Two novel mutations of Wiskott-Aldrich syndrome: the molecular prediction of interaction between the mutated WASP L101P with WASP-interacting protein by molecular modeling. Biochim. Biophys. Acta *1690*, 134-140.

Kinley,A.W., Weed,S.A., Weaver,A.M., Karginov,A.V., Bissonette,E., Cooper,J.A., and Parsons,J.T. (2003). Cortactin interacts with WIP in regulating Arp2/3 activation and membrane protrusion. Curr. Biol. *13*, 384-393.

Kirschner,M.W. (1980). Implications of treadmilling for the stability and polarity of actin and tubulin polymers in vivo. J Cell Biol. 86, 330-334.

Kiselar,J.G., Mahaffy,R., Pollard,T.D., Almo,S.C., and Chance,M.R. (2007). Visualizing Arp2/3 complex activation mediated by binding of ATP and WASp using structural mass spectrometry. Proc. Natl. Acad. Sci. U. S. A *104*, 1552-1557.

Kolluri,R., Tolias,K.F., Carpenter,C.L., Rosen,F.S., and Kirchhausen,T. (1996). Direct interaction of the Wiskott-Aldrich syndrome protein with the GTPase Cdc42. Proc. Natl. Acad. Sci. U. S. A *93*, 5615-5618.

Konno,A., Kirby,M., Anderson,S.A., Schwartzberg,P.L., and Candotti,F. (2007). The expression of Wiskott-Aldrich syndrome protein (WASP) is dependent on WASP-interacting protein (WIP). Int. Immunol. *19*, 185-192.

Korn,E.D., Carlier,M.F., and Pantaloni,D. (1987). Actin polymerization and ATP hydrolysis. Science *238*, 638-644.

Kozma,R., Ahmed,S., Best,A., and Lim,L. (1995). The Ras-related protein Cdc42Hs and bradykinin promote formation of peripheral actin microspikes and filopodia in Swiss 3T3 fibroblasts. Mol. Cell Biol. *15*, 1942-1952.

Krause,M., Sechi,A.S., Konradt,M., Monner,D., Gertler,F.B., and Wehland,J. (2000). Fyn-binding protein (Fyb)/SLP-76-associated protein (SLAP), Ena/vasodilator-stimulated phosphoprotein (VASP) proteins and the Arp2/3 complex link T cell receptor (TCR) signaling to the actin cytoskeleton. J Cell Biol. *149*, 181-194.

Kreishman-Deitrick,M., Goley,E.D., Burdine,L., Denison,C., Egile,C., Li,R.,

Murali,N., Kodadek,T.J., Welch,M.D., and Rosen,M.K. (2005). NMR analyses of the activation of the Arp2/3 complex by neuronal Wiskott-Aldrich syndrome protein. Biochemistry *44*, 15247-15256.

Krucker,T., Siggins,G.R., and Halpain,S. (2000). Dynamic actin filaments are required for stable long-term potentiation (LTP) in area CA1 of the hippocampus. Proc. Natl. Acad. Sci. U. S. A *97*, 6856-6861.

Kwan,S.P., Lehner,T., Hagemann,T., Lu,B., Blaese,M., Ochs,H., Wedgwood,R., Ott,J., Craig,I.W., and Rosen,F.S. (1991). Localization of the gene for the Wiskott-Aldrich syndrome between two flanking markers, TIMP and DXS255, on Xp11.22-Xp11.3. Genomics *10*, 29-33.

Lanzardo,S., Curcio,C., Forni,G., and Anton,I.M. (2007). A role for WASP Interacting Protein, WIP, in fibroblast adhesion, spreading and migration. The International Journal of Biochemistry & Cell Biology *39*, 262-274.

Le Clainche,C. and Carlier,M.F. (2008). Regulation of Actin Assembly Associated With Protrusion and Adhesion in Cell Migration. Physiol. Rev. *88*, 489-513.

Le,C.C., Didry,D., Carlier,M.F., and Pantaloni,D. (2001). Activation of Arp2/3 complex by Wiskott-Aldrich Syndrome protein is linked to enhanced binding of ATP to Arp2. J. Biol. Chem. *276*, 46689-46692.

Le,C.C., Pantaloni,D., and Carlier,M.F. (2003). ATP hydrolysis on actin-related protein 2/3 complex causes debranching of dendritic actin arrays. Proc. Natl. Acad. Sci. U. S. A *100*, 6337-6342.

LeClaire,L.L., III, Baumgartner,M., Iwasa,J.H., Mullins,R.D., and Barber,D.L. (2008). Phosphorylation of the Arp2/3 complex is necessary to nucleate actin filaments. J. Cell Biol. *182*, 647-654.

Lemahieu,V., Gastier,J.M., and Francke,U. (1999). Novel mutations in the Wiskott-Aldrich syndrome protein gene and their effects on transcriptional, translational, and clinical phenotypes. Hum. Mutat. *14*, 54-66.

Lemmon,M.A. (2003). Phosphoinositide recognition domains. Traffic. *4*, 201-213.

Leung,D.W. and Rosen,M.K. (2005). The nucleotide switch in Cdc42 modulates coupling between the GTPase-binding and allosteric equilibria of Wiskott-Aldrich syndrome protein. Proc. Natl. Acad. Sci. U. S. A *102*, 5685-5690.

Leverrier,Y., Lorenzi,R., Blundell,M.P., Brickell,P., Kinnon,C., Ridley,A.J., and Thrasher,A.J. (2001). Cutting Edge: The Wiskott-Aldrich Syndrome Protein Is Required for Efficient Phagocytosis of Apoptotic Cells. J Immunol *166*, 4831-4834.

Lewis,P.F. and Emerman,M. (1994). Passage through mitosis is required for oncoretroviruses but not for the human immunodeficiency virus. J. Virol. *68*,

510-516.

Lim,R.P., Misra,A., Wu,Z., and Thanabalu,T. (2007). Analysis of conformational changes in WASP using a split YFP. Biochem. Biophys. Res. Commun. *362*, 1085-1089.

Linder,S., Higgs,H., Hufner,K., Schwarz,K., Pannicke,U., and Aepfelbacher,M. (2000a). The polarization defect of Wiskott-Aldrich syndrome macrophages is linked to dislocalization of the Arp2/3 complex. J Immunol. *165*, 221-225.

Linder,S., Hufner,K., Wintergerst,U., and Aepfelbacher,M. (2000b). Microtubule-dependent formation of podosomal adhesion structures in primary human macrophages. J. Cell Sci. *113 Pt 23*, 4165-4176.

Linder,S. and Kopp,P. (2005). Podosomes at a glance. J. Cell Sci. *118*, 2079-2082.

Linder,S., Wintergerst,U., der-Gotze,C., Schwarz,K., Pannicke,U., and Aepfelbacher,M. (2003). Macrophages of patients with X-linked thrombocytopenia display an attenuated Wiskott-Aldrich syndrome phenotype. Immunol. Cell Biol. *81*, 130-136.

Liu,S.K., Fang,N., Koretzky,G.A., and McGlade,C.J. (1999). The hematopoietic-specific adaptor protein gads functions in T-cell signaling via interactions with the SLP-76 and LAT adaptors. Curr. Biol. *9*, 67-75.

Loisel,T.P., Boujemaa,R., Pantaloni,D., and Carlier,M.F. (1999). Reconstitution of actin-based motility of Listeria and Shigella using pure proteins. Nature *401*, 613-616.

Lommel,S., Benesch,S., Rottner,K., Franz,T., Wehland,J., and Kuhn,R. (2001). Actin pedestal formation by enteropathogenic Escherichia coli and intracellular motility of Shigella flexneri are abolished in N-WASP-defective cells. EMBO Rep. *2*, 850-857.

Lorenz,M., Popp,D., and Holmes,K.C. (1993). Refinement of the F-actin model against X-ray fiber diffraction data by the use of a directed mutation algorithm. J. Mol. Biol. *234*, 826-836.

Lorenz, Mike, Yamaguchi, Hideki, Wang, Yarong, Singer, Robert H., and Condeelis, John. Imaging Sites of N-WASP Activity in Lamellipodia and Invadopodia of Carcinoma Cells. 14[8], 697-703. 20-4-2004.
Ref Type: Abstract

Lorenzi,R., Brickell,P.M., Katz,D.R., Kinnon,C., and Thrasher,A.J. (2000). Wiskott-Aldrich syndrome protein is necessary for efficient IgG-mediated phagocytosis. Blood *95*, 2943-2946.

Luthi,J.N., Gandhi,M.J., and Drachman,J.G. (2003). X-linked thrombocytopenia caused by a mutation in the Wiskott-Aldrich syndrome (WAS) gene that disrupts interaction with the WAS protein (WASP)-interacting protein (WIP). Exp.

Hematol. *31*, 150-158.

Lutskiy,M.I., Rosen,F.S., and Remold-O'Donnell,E. (2005). Genotype-proteotype linkage in the Wiskott-Aldrich syndrome. J. Immunol. *175*, 1329-1336.

Ma,L., Cantley,L.C., Janmey,P.A., and Kirschner,M.W. (1998a). Corequirement of specific phosphoinositides and small GTP-binding protein Cdc42 in inducing actin assembly in Xenopus egg extracts. J. Cell Biol. *140*, 1125-1136.

Ma,L., Rohatgi,R., and Kirschner,M.W. (1998b). The Arp2/3 complex mediates actin polymerization induced by the small GTP-binding protein Cdc42. Proc. Natl. Acad. Sci. U. S. A *95*, 15362-15367.

Machesky,L.M., Atkinson,S.J., Ampe,C., Vandekerckhove,J., and Pollard,T.D. (1994). Purification of a cortical complex containing two unconventional actins from Acanthamoeba by affinity chromatography on profilin-agarose. J. Cell Biol. *127*, 107-115.

Machesky,L.M. and Insall,R.H. (1998). Scar1 and the related Wiskott-Aldrich syndrome protein, WASP, regulate the actin cytoskeleton through the Arp2/3 complex. Curr. Biol. *8*, 1347-1356.

Machesky,L.M., Mullins,R.D., Higgs,H.N., Kaiser,D.A., Blanchoin,L., May,R.C., Hall,M.E., and Pollard,T.D. (1999). Scar, a WASp-related protein, activates nucleation of actin filaments by the Arp2/3 complex. Proc. Natl. Acad. Sci. U. S. A *96*, 3739-3744.

Maciver,S.K., Zot,H.G., and Pollard,T.D. (1991). Characterization of actin filament severing by actophorin from Acanthamoeba castellanii. J. Cell Biol. *115*, 1611-1620.

Magdalena,J., Millard,T.H., Etienne-Manneville,S., Launay,S., Warwick,H.K., and Machesky,L.M. (2003). Involvement of the Arp2/3 complex and Scar2 in Golgi polarity in scratch wound models. Mol. Biol. Cell *14*, 670-684.

Maillard,M.H., Cotta-de-Almeida,V., Takeshima,F., Nguyen,D.D., Michetti,P., Nagler,C., Bhan,A.K., and Snapper,S.B. (2007). The Wiskott-Aldrich syndrome protein is required for the function of CD4+CD25+Foxp3+ regulatory T cells. J. Exp. Med. *204*, 381-391.

Manchanda,N., Lyubimova,A., Ho,H.Y., James,M.F., Gusella,J.F., Ramesh,N., Snapper,S.B., and Ramesh,V. (2005). The NF2 tumor suppressor Merlin and the ERM proteins interact with N-WASP and regulate its actin polymerization function. J Biol. Chem. *280*, 12517-12522.

Manes,S., Gomez-Mouton,C., Lacalle,R.A., Jimenez-Baranda,S., Mira,E., and Martinez,A. (2005). Mastering time and space: immune cell polarization and chemotaxis. Semin. Immunol. *17*, 77-86.

Manser,E., Leung,T., Salihuddin,H., Tan,L., and Lim,L. (1993). A non-receptor tyrosine kinase that inhibits the GTPase activity of p21cdc42. Nature *363*, 364-

367.

Manser,E., Leung,T., Salihuddin,H., Zhao,Z.s., and Lim,L. (1994). A brain serine/threonine protein kinase activated by Cdc42 and Rac1. Nature *367*, 40-46.

Marangoni,F., Trifari,S., Scaramuzza,S., Panaroni,C., Martino,S., Notarangelo,L.D., Baz,Z., Metin,A., Cattaneo,F., Villa,A., Aiuti,A., Battaglia,M., Roncarolo,M.G., and Dupre,L. (2007). WASP regulates suppressor activity of human and murine CD4+CD25+FOXP3+ natural regulatory T cells. J. Exp. Med. *204*, 369-380.

Marchand,J.B., Kaiser,D.A., Pollard,T.D., and Higgs,H.N. (2001). Interaction of WASP/Scar proteins with actin and vertebrate Arp2/3 complex. Nat. Cell Biol. *3*, 76-82.

Marchisio,P.C., Bergui,L., Corbascio,G.C., Cremona,O., D'Urso,N., Schena,M., Tesio,L., and Caligaris-Cappio,F. (1988). Vinculin, talin, and integrins are localized at specific adhesion sites of malignant B lymphocytes. Blood *72*, 830-833.

Marchisio,P.C., Cirillo,D., Teti,A., Zambonin-Zallone,A., and Tarone,G. (1987). Rous sarcoma virus-transformed fibroblasts and cells of monocytic origin display a peculiar dot-like organization of cytoskeletal proteins involved in microfilament-membrane interactions. Exp. Cell Res. *169*, 202-214.

Martin,A.C., Welch,M.D., and Drubin,D.G. (2006). Arp2/3 ATP hydrolysis-catalysed branch dissociation is critical for endocytic force generation. Nat. Cell Biol. *8*, 826-833.

Martin,F., Toscano,M.G., Blundell,M., Frecha,C., Srivastava,G.K., Santamaria,M., Thrasher,A.J., and Molina,I.J. (2005). Lentiviral vectors transcriptionally targeted to hematopoietic cells by WASP gene proximal promoter sequences. Gene Ther. *12*, 715-723.

Martinez-Quiles,N., Rohatgi,R., Anton,I.M., Medina,M., Saville,S.P., Miki,H., Yamaguchi,H., Takenawa,T., Hartwig,J.H., Geha,R.S., and Ramesh,N. (2001). WIP regulates N-WASP-mediated actin polymerization and filopodium formation. Nat. Cell Biol. *3*, 484-491.

May,R.C., Hall,M.E., Higgs,H.N., Pollard,T.D., Chakraborty,T., Wehland,J., Machesky,L.M., and Sechi,A.S. (1999). The Arp2/3 complex is essential for the actin-based motility of Listeria monocytogenes. Curr. Biol. *9*, 759-762.

McGavin,M.K., Badour,K., Hardy,L.A., Kubiseski,T.J., Zhang,J., and Siminovitch,K.A. (2001). The intersectin 2 adaptor links Wiskott Aldrich Syndrome protein (WASp)-mediated actin polymerization to T cell antigen receptor endocytosis. J. Exp. Med. *194*, 1777-1787.

Melloni,E., Michetti,M., Salamino,F., and Pontremoli,S. (1998). Molecular and Functional Properties of a Calpain Activator Protein Specific for ¦-Isoforms. J.

Biol. Chem. *273*, 12827-12831.

Miki,H., Miura,K., and Takenawa,T. (1996). N-WASP, a novel actin-depolymerizing protein, regulates the cortical cytoskeletal rearrangement in a PIP2-dependent manner downstream of tyrosine kinases. EMBO J. *15*, 5326-5335.

Miki,H., Sasaki,T., Takai,Y., and Takenawa,T. (1998a). Induction of filopodium formation by a WASP-related actin-depolymerizing protein N-WASP. Nature *391*, 93-96.

Miki,H., Suetsugu,S., and Takenawa,T. (1998b). WAVE, a novel WASP-family protein involved in actin reorganization induced by Rac. EMBO J. *17*, 6932-6941.

Miki,H. and Takenawa,T. (1998). Direct binding of the verprolin-homology domain in N-WASP to actin is essential for cytoskeletal reorganization. Biochem. Biophys. Res. Commun. *243*, 73-78.

Molina,I.J., Kenney,D.M., Rosen,F.S., and Remold-O'Donnell,E. (1992). T cell lines characterize events in the pathogenesis of the Wiskott-Aldrich syndrome. J Exp. Med. *176*, 867-874.

Molina,I.J., Sancho,J., Terhorst,C., Rosen,F.S., and Remold-O'Donnell,E. (1993). T cells of patients with the Wiskott-Aldrich syndrome have a restricted defect in proliferative responses. J Immunol. *151*, 4383-4390.

Moreau,V., Frischknecht,F., Reckmann,I., Vincentelli,R., Rabut,G., Stewart,D., and Way,M. (2000). A complex of N-WASP and WIP integrates signalling cascades that lead to actin polymerization. Nat. Cell Biol. *2*, 441-448.

Moreau,V., Tatin,F., Varon,C., and Genot,E. (2003). Actin can reorganize into podosomes in aortic endothelial cells, a process controlled by Cdc42 and RhoA. Mol. Cell Biol. *23*, 6809-6822.

Moulding,D.A., Blundell,M.P., Spiller,D.G., White,M.R., Cory,G.O., Calle,Y., Kempski,H., Sinclair,J., Ancliff,P.J., Kinnon,C., Jones,G.E., and Thrasher,A.J. (2007). Unregulated actin polymerization by WASp causes defects of mitosis and cytokinesis in X-linked neutropenia. J Exp. Med. *204*, 2213-2224.

Mullins,R.D., Heuser,J.A., and Pollard,T.D. (1998). The interaction of Arp2/3 complex with actin: nucleation, high affinity pointed end capping, and formation of branching networks of filaments. Proc. Natl. Acad. Sci. U. S. A *95*, 6181-6186.

Mullins,R.D. and Pollard,T.D. (1999). Rho-family GTPases require the Arp2/3 complex to stimulate actin polymerization in Acanthamoeba extracts. Curr. Biol. *9*, 405-415.

Mullins,R.D., Stafford,W.F., and Pollard,T.D. (1997). Structure, subunit topology, and actin-binding activity of the Arp2/3 complex from Acanthamoeba. J. Cell Biol. *136*, 331-343.

Myers,S.A., Leeper,L.R., and Chung,C.Y. (2006). WASP-interacting protein is important for actin filament elongation and prompt pseudopod formation in response to a dynamic chemoattractant gradient. Mol. Biol. Cell *17*, 4564-4575.

Naldini,L., Blomer,U., Gallay,P., Ory,D., Mulligan,R., Gage,F.H., Verma,I.M., and Trono,D. (1996). In vivo gene delivery and stable transduction of nondividing cells by a lentiviral vector. Science *272*, 263-267.

Neudauer,C.L., Joberty,G., Tatsis,N., and Macara,I.G. (1998). Distinct cellular effects and interactions of the Rho-family GTPase TC10. Curr. Biol. *8*, 1151-1160.

Neugebauer,J.M. (1990). [18] Detergents: An overview. In Methods in Enzymology
Guide to Protein Purification, P.D.Murray, ed. Academic Press), pp. 239-253.

Nicola,C., Timoshenko,A.V., Dixon,S.J., Lala,P.K., and Chakraborty,C. (2005). EP1 Receptor-Mediated Migration of the First Trimester Human Extravillous Trophoblast: The Role of Intracellular Calcium and Calpain. J Clin Endocrinol Metab *90*, 4736-4746.

Nobes,C. and Hall,A. (1994). Regulation and function of the Rho subfamily of small GTPases. Curr. Opin. Genet. Dev. *4*, 77-81.

Nobes,C.D. and Hall,A. (1995). Rho, rac, and cdc42 GTPases regulate the assembly of multimolecular focal complexes associated with actin stress fibers, lamellipodia, and filopodia. Cell *81*, 53-62.

Noguchi,M., Sarin,A., Aman,M.J., Nakajima,H., Shores,E.W., Henkart,P.A., and Leonard,W.J. (1997). Functional cleavage of the common cytokine receptor gamma chain (gammac) by calpain. Proc. Natl. Acad. Sci. U. S. A *94*, 11534-11539.

Nolen,B.J., Littlefield,R.S., and Pollard,T.D. (2004). Crystal structures of actin-related protein 2/3 complex with bound ATP or ADP. Proc. Natl. Acad. Sci. U. S. A *101*, 15627-15632.

Notarangelo,L.D., Mazza,C., Giliani,S., D'Aria,C., Gandellini,F., Ravelli,C., Locatelli,M.G., Nelson,D.L., Ochs,H.D., and Notarangelo,L.D. (2002). Missense mutations of the WASP gene cause intermittent X-linked thrombocytopenia. Blood *99*, 2268-2269.

Ochs, H. D personal communication. 2008.
Ref Type: Generic

Ochs, H. D. and Rosen, F. S. The Wiskott Aldrich Syndrome. Edited Ochs, H. D., Smith, C. I. E, and Puck, J. M. Primary Immunodeficiency Diseases, A molecular and Gnetic approach.2nd Ed , 454-470. 2007.
Ref Type: Generic

Ochs,H.D., Slichter,S.J., Harker,L.A., Von Behrens,W.E., Clark,R.A., and

Wedgwood,R.J. (1980). The Wiskott-Aldrich syndrome: studies of lymphocytes, granulocytes, and platelets. Blood *55*, 243-252.

Ochs,H.D. and Thrasher,A.J. (2006). The Wiskott-Aldrich syndrome. J. Allergy Clin. Immunol. *117*, 725-738.

Oda,A., Ochs,H.D., Druker,B.J., Ozaki,K., Watanabe,C., Handa,M., Miyakawa,Y., and Ikeda,Y. (1998). Collagen induces tyrosine phosphorylation of Wiskott-Aldrich syndrome protein in human platelets. Blood *92*, 1852-1858.

Oikawa,T., Yamaguchi,H., Itoh,T., Kato,M., Ijuin,T., Yamazaki,D., Suetsugu,S., and Takenawa,T. (2004). PtdIns(3,4,5)P3 binding is necessary for WAVE2-induced formation of lamellipodia. Nat. Cell Biol. *6*, 420-426.

Oosawa, F. & Asakura S. “Thermodynamics of the Polymerization of Protein.” 1975. New York, Academic.

Orange,J.S., Ramesh,N., Remold-O’Donnell,E., Sasahara,Y., Koopman,L., Byrne,M., Bonilla,F.A., Rosen,F.S., Geha,R.S., and Strominger,J.L. (2002). Wiskott-Aldrich syndrome protein is required for NK cell cytotoxicity and colocalizes with actin to NK cell-activating immunologic synapses. Proc. Natl. Acad. Sci. U. S. A *99*, 11351-11356.

Otsuki,M., Itoh,T., and Takenawa,T. (2003). Neural Wiskott-Aldrich syndrome protein is recruited to rafts and associates with endophilin A in response to epidermal growth factor. J. Biol. Chem. *278*, 6461-6469.

Otterbein,L.R., Graceffa,P., and Dominguez,R. (2001). The crystal structure of uncomplexed actin in the ADP state. Science *293*, 708-711.

Panchal,S.C., Kaiser,D.A., Torres,E., Pollard,T.D., and Rosen,M.K. (2003). A conserved amphipathic helix in WASP/Scar proteins is essential for activation of Arp2/3 complex. Nat. Struct. Biol. *10*, 591-598.

Pantaloni,D., Boujemaa,R., Didry,D., Gounon,P., and Carlier,M.F. (2000). The Arp2/3 complex branches filament barbed ends: functional antagonism with capping proteins. Nat. Cell Biol. *2*, 385-391.

Pantaloni,D. and Carlier,M.F. (1993). How profilin promotes actin filament assembly in the presence of thymosin beta 4. Cell *75*, 1007-1014.

Pantaloni,D., Le,C.C., and Carlier,M.F. (2001). Mechanism of actin-based motility. Science 292, 1502-1506.

Papayannopoulos,V., Co,C., Prehoda,K.E., Snapper,S., Taunton,J., and Lim,W.A. (2005). A polybasic motif allows N-WASP to act as a sensor of PIP(2) density. Mol. Cell *17*, 181-191.

Park,J.Y., Kob,M., Prodeus,A.P., Rosen,F.S., Shcherbina,A., and Remold-O’Donnell,E. (2004). Early deficit of lymphocytes in Wiskott-Aldrich syndrome: possible role of WASP in human lymphocyte maturation. Clin. Exp. Immunol.

136, 104-110.

Park,J.Y., Shcherbina,A., Rosen,F.S., Prodeus,A.P., and Remold-O'Donnell,E. (2005). Phenotypic perturbation of B cells in the Wiskott-Aldrich syndrome. Clin. Exp. Immunol. *139*, 297-305.

Pawson,T. (1994). Regulation of the Ras signalling pathway by protein-tyrosine kinases. Biochem. Soc. Trans. *22*, 455-460.

Penna,D., Muller,S., Martinon,F., Demotz,S., Iwashima,M., and Valitutti,S. (1999). Degradation of ZAP-70 following antigenic stimulation in human T lymphocytes: role of calpain proteolytic pathway. J Immunol *163*, 50-56.

Perry,G.S., III, Spector,B.D., Schuman,L.M., Mandel,J.S., Anderson,V.E., McHugh,R.B., Hanson,M.R., Fahlstrom,S.M., Krivit,W., and Kersey,J.H. (1980). The Wiskott-Aldrich syndrome in the United States and Canada (1892-1979). J. Pediatr. *97*, 72-78.

Peterson,F.C., Deng,Q., Zettl,M., Prehoda,K.E., Lim,W.A., Way,M., and Volkman,B.F. (2007). Multiple WASP-interacting protein recognition motifs are required for a functional interaction with N-WASP. J. Biol. Chem. *282*, 8446-8453.

Pinder,J.C., Ohanian,V., and Gratzer,W.B. (1984). Spectrin and protein 4.1 as an actin filament capping complex. FEBS Lett. 169, 161-164.

Ponti,A., Machacek,M., Gupton,S.L., Waterman-Storer,C.M., and Danuser,G. (2004). Two distinct actin networks drive the protrusion of migrating cells. Science *305*, 1782-1786.

Prehoda,K.E., Scott,J.A., Mullins,R.D., and Lim,W.A. (2000). Integration of multiple signals through cooperative regulation of the N-WASP-Arp2/3 complex. Science *290*, 801-806.

Prehoda, Kenneth E., Lee, Do J., and Lim, Wendell A. Structure of the Enabled/VASP Homology 1 DomainPeptide Complex: A Key Component in the Spatial Control of Actin Assembly. 97[4], 471-480. 14-5-1999.
Ref Type: Abstract

Pulecio,J., Tagliani,E., Scholer,A., Prete,F., Fetler,L., Burrone,O.R., and Benvenuti,F. (2008). Expression of Wiskott-Aldrich syndrome protein in dendritic cells regulates synapse formation and activation of naive CD8+ T cells. J. Immunol. *181*, 1135-1142.

Qiu,R.G., Abo,A., and Steven,M.G. (2000). A human homolog of the C. elegans polarity determinant Par-6 links Rac and Cdc42 to PKCzeta signaling and cell transformation. Curr. Biol. *10*, 697-707.

Ramesh,N., Anton,I.M., Hartwig,J.H., and Geha,R.S. (1997). WIP, a protein associated with wiskott-aldrich syndrome protein, induces actin polymerization and redistribution in lymphoid cells. Proc. Natl. Acad. Sci. U. S. A *94*, 14671-

14676.

Randolph,G.J., Angeli,V., and Swartz,M.A. (2005). Dendritic-cell trafficking to lymph nodes through lymphatic vessels. Nat. Rev. Immunol. *5*, 617-628.

Ravid,T., Doolman,R., Avner,R., Harats,D., and Roitelman,J. (2000). The Ubiquitin-Proteasome Pathway Mediates the Regulated Degradation of Mammalian 3-Hydroxy-3-methylglutaryl-coenzyme A Reductase. J. Biol. Chem. *275*, 35840-35847.

Rawlings,S.L., Crooks,G.M., Bockstoce,D., Barsky,L.W., Parkman,R., and Weinberg,K.I. (1999). Spontaneous Apoptosis in Lymphocytes From Patients With Wiskott-Aldrich Syndrome: Correlation of Accelerated Cell Death and Attenuated Bcl-2 Expression. Blood *94*, 3872-3882.

Remold-O'Donnell,E., Cooley,J., Shcherbina,A., Hagemann,T.L., Kwan,S.P., Kenney,D.M., and Rosen,F.S. (1997). Variable expression of WASP in B cell lines of Wiskott-Aldrich syndrome patients. J Immunol. *158*, 4021-4025.

Ridley,A.J. and Hall,A. (1992). The small GTP-binding protein rho regulates the assembly of focal adhesions and actin stress fibers in response to growth factors. Cell *70*, 389-399.

Ridley,A.J., Schwartz,M.A., Burridge,K., Firtel,R.A., Ginsberg,M.H., Borisy,G., Parsons,J.T., and Horwitz,A.R. (2003). Cell migration: integrating signals from front to back. Science *302*, 1704-1709.

Rivero-Lezcano,O.M., Marcilla,A., Sameshima,J.H., and Robbins,K.C. (1995). Wiskott-Aldrich syndrome protein physically associates with Nck through Src homology 3 domains. Mol. Cell. Biol. *15*, 5725-5731.

Robinson,R.C., Turbedsky,K., Kaiser,D.A., Marchand,J.B., Higgs,H.N., Choe,S., and Pollard,T.D. (2001). Crystal structure of Arp2/3 complex. Science *294*, 1679-1684.

Rodal,A.A., Sokolova,O., Robins,D.B., Daugherty,K.M., Hippenmeyer,S., Riezman,H., Grigorieff,N., and Goode,B.L. (2005). Conformational changes in the Arp2/3 complex leading to actin nucleation. Nat. Struct. Mol. Biol. *12*, 26-31.

Rogers,S.L., Wiedemann,U., Stuurman,N., and Vale,R.D. (2003). Molecular requirements for actin-based lamella formation in Drosophila S2 cells. J. Cell Biol. *162*, 1079-1088.

Rohatgi,R., Ho,H.Y., and Kirschner,M.W. (2000). Mechanism of N-WASP activation by CDC42 and phosphatidylinositol 4, 5-bisphosphate. J. Cell Biol. *150*, 1299-1310.

Rohatgi,R., Ma,L., Miki,H., Lopez,M., Kirchhausen,T., Takenawa,T., and Kirschner,M.W. (1999). The interaction between N-WASP and the Arp2/3 complex links Cdc42-dependent signals to actin assembly. Cell *97*, 221-231.

Rohatgi,R., Nollau,P., Ho,H.Y., Kirschner,M.W., and Mayer,B.J. (2001). Nck and phosphatidylinositol 4,5-bisphosphate synergistically activate actin polymerization through the N-WASP-Arp2/3 pathway. J. Biol. Chem. *276*, 26448-26452.

Rong,S.B. and Vihinen,M. (2000). Structural basis of Wiskott-Aldrich syndrome causing mutations in the WH1 domain. J Mol. Med. *78*, 530-537.

Root,A.W. and Speicher,C.E. (1963). The triad of thrombocytopenia, eczema, and recurrent infections (Wiskott-Aldrich syndrome) associated with milk antibodies, giant-cell pneumonia, and cytomegalic inclusion disease. Pediatrics *31*, 444-454.

Rudolph,M.G., Bayer,P., Abo,A., Kuhlmann,J., Vetter,I.R., and Wittinghofer,A. (1998). The Cdc42/Rac interactive binding region motif of the Wiskott Aldrich syndrome protein (WASP) is necessary but not sufficient for tight binding to Cdc42 and structure formation. J. Biol. Chem. *273*, 18067-18076.

Ryser,O., Morell,A., and Hitzig,W.H. (1988). Primary immunodeficiencies in Switzerland: first report of the national registry in adults and children. J. Clin. Immunol. *8*, 479-485.

Sarin,A., Adams,D.H., and Henkart,P.A. (1993). Protease inhibitors selectively block T cell receptor-triggered programmed cell death in a murine T cell hybridoma and activated peripheral T cells. J Exp. Med. *178*, 1693-1700.

Sasahara,Y., Rachid,R., Byrne,M.J., de la Fuente,M.A., Abraham,R.T., Ramesh,N., and Geha,R.S. (2002). Mechanism of recruitment of WASP to the immunological synapse and of its activation following TCR ligation. Mol. Cell *10*, 1269-1281.

Sato,K. and Kawashima,S. (2001). Calpain function in the modulation of signal transduction molecules. Biol. Chem. *382*, 743-751.

Schafer,D.A., Jennings,P.B., and Cooper,J.A. (1996). Dynamics of capping protein and actin assembly in vitro: uncapping barbed ends by polyphosphoinositides. J. Cell Biol. *135*, 169-179.

Schambach,A., Wodrich,H., Hildinger,M., Bohne,J., Krausslich,H.G., and Baum,C. (2000). Context dependence of different modules for posttranscriptional enhancement of gene expression from retroviral vectors. Mol. Ther. *2*, 435-445.

Schindelhauer,D., Weiss,M., Hellebrand,H., Golla,A., Hergersberg,M., Seger,R., Belohradsky,B.H., and Meindl,A. (1996). Wiskott-Aldrich syndrome: no strict genotype-phenotype correlations but clustering of missense mutations in the amino-terminal part of the WASP gene product. Hum. Genet. *98*, 68-76.

Schlessinger,J. (1994). SH2/SH3 signaling proteins. Curr. Opin. Genet. Dev. *4*, 25-30.

Schulte,R.J. and Sefton,B.M. (2003). Inhibition of the Activity of Src and Abl Tyrosine Protein Kinases by the Binding of the WiskottΓêÆAldrich Syndrome ProteinΓÇá. Biochemistry *42*, 9424-9430.

Scott,M.P., Zappacosta,F., Kim,E.Y., Annan,R.S., and Miller,W.T. (2002). Identification of novel SH3 domain ligands for the Src family kinase Hck. Wiskott-Aldrich syndrome protein (WASP), WASP-interacting protein (WIP), and ELMO1. J. Biol. Chem. *277*, 28238-28246.

Selliah,N., Brooks,W.H., and Roszman,T.L. (1996). Proteolytic cleavage of alpha-actinin by calpain in T cells stimulated with anti-CD3 monoclonal antibody. J Immunol *156*, 3215-3221.

Shcherbina,A., Miki,H., Kenney,D.M., Rosen,F.S., Takenawa,T., and Remold-O'Donnell,E. (2001). WASP and N-WASP in human platelets differ in sensitivity to protease calpain. Blood *98*, 2988-2991.

She,H.Y., Rockow,S., Tang,J., Nishimura,R., Skolnik,E.Y., Chen,M., Margolis,B., and Li,W. (1997). Wiskott-Aldrich syndrome protein is associated with the adapter protein Grb2 and the epidermal growth factor receptor in living cells. Mol. Biol. Cell *8*, 1709-1721.

Small,J.V., Herzog,M., and Anderson,K. (1995). Actin filament organization in the fish keratocyte lamellipodium. J. Cell Biol. *129*, 1275-1286.

Snapper,S.B., Meelu,P., Nguyen,D., Stockton,B.M., Bozza,P., Alt,F.W., Rosen,F.S., von Andrian,U.H., and Klein,C. (2005). WASP deficiency leads to global defects of directed leukocyte migration in vitro and in vivo. J. Leukoc. Biol. *77*, 993-998.

Snapper,S.B., Rosen,F.S., Mizoguchi,E., Cohen,P., Khan,W., Liu,C.H., Hagemann,T.L., Kwan,S.P., Ferrini,R., Davidson,L., Bhan,A.K., and Alt,F.W. (1998). Wiskott-Aldrich syndrome protein-deficient mice reveal a role for WASP in T but not B cell activation. Immunity. *9*, 81-91.

Snapper,S.B., Takeshima,F., Anton,I., Liu,C.H., Thomas,S.M., Nguyen,D., Dudley,D., Fraser,H., Purich,D., Lopez-Ilasaca,M., Klein,C., Davidson,L., Bronson,R., Mulligan,R.C., Southwick,F., Geha,R., Goldberg,M.B., Rosen,F.S., Hartwig,J.H., and Alt,F.W. (2001). N-WASP deficiency reveals distinct pathways for cell surface projections and microbial actin-based motility. Nat. Cell Biol. *3*, 897-904.

Snover,D.C., Frizzera,G., Spector,B.D., Perry,G.S., III, and Kersey,J.H. (1981). Wiskott-Aldrich syndrome: histopathologic findings in the lymph nodes and spleens of 15 patients. Hum. Pathol. *12*, 821-831.

Springer,T.A. (1994). Traffic signals for lymphocyte recirculation and leukocyte emigration: the multistep paradigm. Cell *76*, 301-314.

Steinhilb,M.L., Turner,R.S., and Gaut,J.R. (2001). The Protease Inhibitor,

MG132, Blocks Maturation of the Amyloid Precursor Protein Swedish Mutant Preventing Cleavage by beta -Secretase. J. Biol. Chem. *276*, 4476-4484.

Stewart,D.M., Tian,L., and Nelson,D.L. (1999). Mutations that cause the Wiskott-Aldrich syndrome impair the interaction of Wiskott-Aldrich syndrome protein (WASP) with WASP interacting protein. J. Immunol. *162*, 5019-5024.

Stray-Pedersen,A., Abrahamsen,T.G., and Froland,S.S. (2000). Primary immunodeficiency diseases in Norway. J. Clin. Immunol. *20*, 477-485.

Straub,F.B. (1989). Note on the work of F. Bruno Straub concerning 'Adenosine Triphosphate. The Functional Group of Actin'. Biochim. Biophys. Acta 1000, 179.

Strom,T.S., Turner,S.J., Andreansky,S., Liu,H., Doherty,P.C., Srivastava,D.K., Cunningham,J.M., and Nienhuis,A.W. (2003). Defects in T-cell-mediated immunity to influenza virus in murine Wiskott-Aldrich syndrome are corrected by oncoretroviral vector-mediated gene transfer into repopulating hematopoietic cells. Blood *102*, 3108-3116.

Suetsugu,S., Hattori,M., Miki,H., Tezuka,T., Yamamoto,T., Mikoshiba,K., and Takenawa,T. (2002). Sustained activation of N-WASP through phosphorylation is essential for neurite extension. Dev. Cell *3*, 645-658.

Suetsugu,S., Miki,H., and Takenawa,T. (1998). The essential role of profilin in the assembly of actin for microspike formation. EMBO J. *17*, 6516-6526.

Suetsugu,S., Miki,H., and Takenawa,T. (1999). Identification of two human WAVE/SCAR homologues as general actin regulatory molecules which associate with the Arp2/3 complex. Biochem. Biophys. Res. Commun. *260*, 296-302.

Suetsugu,S., Miki,H., and Takenawa,T. (2001a). Identification of another actin-related protein (Arp) 2/3 complex binding site in neural Wiskott-Aldrich syndrome protein (N-WASP) that complements actin polymerization induced by the Arp2/3 complex activating (VCA) domain of N-WASP. J. Biol. Chem. *276*, 33175-33180.

Suetsugu,S., Miki,H., Yamaguchi,H., and Takenawa,T. (2001b). Requirement of the basic region of N-WASP/WAVE2 for actin-based motility. Biochem. Biophys. Res. Commun. *282*, 739-744.

Sullivan,K.E., Mullen,C.A., Blaese,R.M., and Winkelstein,J.A. (1994). A multiinstitutional survey of the Wiskott-Aldrich syndrome. J. Pediatr. *125*, 876-885.

Svitkina,T.M. and Borisy,G.G. (1999). Arp2/3 complex and actin depolymerizing factor/cofilin in dendritic organization and treadmilling of actin filament array in lamellipodia. J. Cell Biol *145*, 1009-1026.

Svitkina,T.M., Verkhovsky,A.B., McQuade,K.M., and Borisy,G.G. (1997).

Analysis of the actin-myosin II system in fish epidermal keratocytes: mechanism of cell body translocation. J. Cell Biol. *139*, 397-415.

Symons,M., Derry,J.M., Karlak,B., Jiang,S., Lemahieu,V., Mccormick,F., Francke,U., and Abo,A. (1996). Wiskott-Aldrich syndrome protein, a novel effector for the GTPase CDC42Hs, is implicated in actin polymerization. Cell *84*, 723-734.

T.J.Cole (2000). Sympercents: symmetric percentage differences on the 100 log_{<FONT SIZE='-1'>e</FONT>} scale simplify the presentation of log transformed data. Statistics in Medicine *19*, 3109-3125.

Tarone,G., Cirillo,D., Giancotti,F.G., Comoglio,P.M., and Marchisio,P.C. (1985). Rous sarcoma virus-transformed fibroblasts adhere primarily at discrete protrusions of the ventral membrane called podosomes. Exp. Cell Res. *159*, 141-157.

Thrasher,A.J., Jones,G.E., Kinnon,C., Brickell,P.M., and Katz,D.R. (1998). Is Wiskott--Aldrich syndrome a cell trafficking disorder? Immunol. Today *19*, 537-539.

Tian,L., Nelson,D.L., and Stewart,D.M. (2000). Cdc42-interacting protein 4 mediates binding of the Wiskott-Aldrich syndrome protein to microtubules. J Biol. Chem. *275*, 7854-7861.

Tompa,P., Buzder-Lantos,P., Tantos,A., Farkas,A., Szilagyi,A., Banoczi,Z., Hudecz,F., and Friedrich,P. (2004). On the sequential determinants of calpain cleavage. J Biol. Chem. *279*, 20775-20785.

Torres,E. and Rosen,M.K. (2003). Contingent phosphorylation/ dephosphorylation provides a mechanism of molecular memory in WASP. Mol. Cell *11*, 1215-1227.

Torres,E. and Rosen,M.K. (2006). Protein-tyrosine kinase and GTPase signals cooperate to phosphorylate and activate Wiskott-Aldrich syndrome protein (WASP)/neuronal WASP. J. Biol. Chem. *281*, 3513-3520.

Tsuboi,S. (2006). A complex of Wiskott-Aldrich syndrome protein with mammalian verprolins plays an important role in monocyte chemotaxis. J. Immunol. *176*, 6576-6585.

Tsuboi,S. and Meerloo,J. (2007). Wiskott-Aldrich syndrome protein is a key regulator of the phagocytic cup formation in macrophages. J. Biol. Chem. *282*, 34194-34203.

Tsuboi,S. (2007). Requirement for a Complex of Wiskott-Aldrich Syndrome Protein (WASP) with WASP Interacting Protein in Podosome Formation in Macrophages. J Immunol *178*, 2987-2995.

Tsuboi,S., Takada,H., Hara,T., Mochizuki,N., Funyu,T., Saitoh,H., Terayama,Y., Yamaya,K., Ohyama,C., Nonoyama,S., and Ochs,H.D. (2009). FBP17 mediates

a common molecular step in the formation of podosomes and phagocytic cups in macrophages. Journal of Biological Chemistry M805638200.

Uruno,T., Liu,J., Li,Y., Smith,N., and Zhan,X. (2003). Sequential interaction of actin-related proteins 2 and 3 (Arp2/3) complex with neural Wiscott-Aldrich syndrome protein (N-WASP) and cortactin during branched actin filament network formation. J. Biol. Chem. *278*, 26086-26093.

Vaduva,G., Martinez-Quiles,N., Anton,I.M., Martin,N.C., Geha,R.S., Hopper,A.K., and Ramesh,N. (1999). The human WASP-interacting protein, WIP, activates the cell polarity pathway in yeast. J Biol. Chem. *274*, 17103-17108.

Vanhaesebroeck,B., Jones,G.E., Allen,W.E., Zicha,D., Hooshmand-Rad,R., Sawyer,C., Wells,C., Waterfield,M.D., and Ridley,A.J. (1999). Distinct PI(3)Ks mediate mitogenic signalling and cell migration in macrophages. Nat. Cell Biol. *1*, 69-71.

Verkhovsky,A.B., Chaga,O.Y., Schaub,S., Svitkina,T.M., Meister,J.J., and Borisy,G.G. (2003). Orientational order of the lamellipodial actin network as demonstrated in living motile cells. Mol. Biol. Cell *14*, 4667-4675.

Vermi,W., Blanzuoli,L., Kraus,M.D., Grigolato,P., Donato,F., Loffredo,G., Marino,C.E., Alberti,D., Notarangelo,L.D., and Facchetti,F. (1999). The spleen in the Wiskott-Aldrich syndrome: histopathologic abnormalities of the white pulp correlate with the clinical phenotype of the disease. Am. J Surg. Pathol. *23*, 182-191.

Vetter,I.R. and Wittinghofer,A. (2001). The guanine nucleotide-binding switch in three dimensions. Science *294*, 1299-1304.

Vetterkind,S., Miki,H., Takenawa,T., Klawitz,I., Scheidtmann,K.H., and Preuss,U. (2002). The rat homologue of Wiskott-Aldrich syndrome protein (WASP)-interacting protein (WIP) associates with actin filaments, recruits N-WASP from the nucleus, and mediates mobilization of actin from stress fibers in favor of filopodia formation. J Biol. Chem. *277*, 87-95.

Vicente-Manzanares,M. and Sanchez-Madrid,F. (2004). Role of the cytoskeleton during leukocyte responses. Nat. Rev. Immunol. *4*, 110-122.

Vignal,E., De Toledo,M., Comunale,F., Ladopoulou,A., Gauthier-Rouviere,C., Blangy,A., and Fort,P. (2000). Characterization of TCL, a New GTPase of the Rho Family related to TC10 and Cdc42. Journal of Biological Chemistry *275*, 36457-36464.

Villa,A., Notarangelo,L., Macchi,P., Mantuano,E., Cavagni,G., Brugnoni,D., Strina,D., Patrosso,M.C., Ramenghi,U., Sacco,M.G., and . (1995). X-linked thrombocytopenia and Wiskott-Aldrich syndrome are allelic diseases with mutations in the WASP gene. Nat. Genet. *9*, 414-417.

Volkman,B.F., Prehoda,K.E., Scott,J.A., Peterson,F.C., and Lim,W.A. (2002). Structure of the N-WASP EVH1 domain-WIP complex: insight into the molecular basis of Wiskott-Aldrich Syndrome. Cell *111*, 565-576.

Volkmann,N., Amann,K.J., Stoilova-McPhie,S., Egile,C., Winter,D.C., Hazelwood,L., Heuser,J.E., Li,R., Pollard,T.D., and Hanein,D. (2001). Structure of Arp2/3 complex in its activated state and in actin filament branch junctions. Science *293*, 2456-2459.

von Andrian,U.H. and Mempel,T.R. (2003). Homing and cellular traffic in lymph nodes. Nat. Rev. Immunol. *3*, 867-878.

Weaver,A.M., Karginov,A.V., Kinley,A.W., Weed,S.A., Li,Y., Parsons,J.T., and Cooper,J.A. (2001). Cortactin promotes and stabilizes Arp2/3-induced actin filament network formation. Curr. Biol. *11*, 370-374.

Weaver,A.M., Heuser,J.E., Karginov,A.V., Lee,W.L., Parsons,J.T., and Cooper,J.A. (2002). Interaction of cortactin and N-WASp with Arp2/3 complex. Curr. Biol. *12*, 1270-1278.

Weed,S.A., Du,Y., and Parsons,J.T. (1998). Translocation of cortactin to the cell periphery is mediated by the small GTPase Rac1. J Cell Sci. *111 (Pt 16)*, 2433-2443.

Weed,S.A., Karginov,A.V., Schafer,D.A., Weaver,A.M., Kinley,A.W., Cooper,J.A., and Parsons,J.T. (2000). Cortactin localization to sites of actin assembly in lamellipodia requires interactions with F-actin and the Arp2/3 complex. J Cell Biol. *151*, 29-40.

Weed,S.A. and Parsons,J.T. (2001). Cortactin: coupling membrane dynamics to cortical actin assembly. Oncogene *20*, 6418-6434.

Wegner,A. (1976). Head to tail polymerization of actin. J Mol. Biol. 108, 139-150.

Wegner,A. (1977). The mechanism of ATP hydrolysis by polymer actin. Biophys. Chem. 7, 51-58.

Wegner,A. (1982). Treadmilling of actin at physiological salt concentrations. An analysis of the critical concentrations of actin filaments. J Mol. Biol. 161, 607-615.

Welch,M.D., Iwamatsu,A., and Mitchison,T.J. (1997). Actin polymerization is induced by Arp2/3 protein complex at the surface of Listeria monocytogenes. Nature *385*, 265-269.

Wenk,M.R. and De,C.P. (2004). Protein-lipid interactions and phosphoinositide metabolism in membrane traffic: insights from vesicle recycling in nerve terminals. Proc. Natl. Acad. Sci. U. S. A *101*, 8262-8269.

Westerberg,L., Greicius,G., Snapper,S.B., Aspenstrom,P., and Severinson,E.

(2001). Cdc42, Rac1, and the Wiskott-Aldrich syndrome protein are involved in the cytoskeletal regulation of B lymphocytes. Blood *98*, 1086-1094.

Westerberg,L., Larsson,M., Hardy,S.J., Fernandez,C., Thrasher,A.J., and Severinson,E. (2005). Wiskott-Aldrich syndrome protein deficiency leads to reduced B-cell adhesion, migration, and homing, and a delayed humoral immune response. Blood *105*, 1144-1152.

Westerberg,L., Wallin,R.P., Greicius,G., Ljunggren,H.G., and Severinson,E. (2003). Efficient antigen presentation of soluble, but not particulate, antigen in the absence of Wiskott-Aldrich syndrome protein. Immunology *109*, 384-391.

Westerberg,L.S., de la Fuente,M.A., Wermeling,F., Ochs,H.D., Karlsson,M.C.I., Snapper,S.B., and Notarangelo,L.D. (2008). WASP confers selective advantage for specific hematopoietic cell populations and serves a unique role in marginal zone B-cell homeostasis and function. Blood *112*, 4139-4147.

Wiesner,S., Helfer,E., Didry,D., Ducouret,G., Lafuma,F., Carlier,M.F., and Pantaloni,D. (2003). A biomimetic motility assay provides insight into the mechanism of actin-based motility. J. Cell Biol. *160*, 387-398.

Wiskott,A. (1937). Familiarer,angeobren Morbus Werhofi? Monatschrift Kinderheil *68*, 212-216.

Wu,Y., Spencer,S.D., and Lasky,L.A. (1998). Tyrosine phosphorylation regulates the SH3-mediated binding of the Wiskott-Aldrich syndrome protein to PSTPIP, a cytoskeletal-associated protein. J. Biol. Chem. *273*, 5765-5770.

Wunderlich,L., Farago,A., Downward,J., and Buday,L. (1999). Association of Nck with tyrosine-phosphorylated SLP-76 in activated T lymphocytes. Eur. J Immunol *29*, 1068-1075.

Yamada,M., Ohtsu,M., Kobayashi,I., Kawamura,N., Kobayashi,K., Ariga,T., Sakiyama,Y., Nelson,D.L., Tsuruta,S., Anakura,M., and Ishikawa,N. (1999). Flow cytometric analysis of Wiskott-Aldrich syndrome (WAS) protein in lymphocytes from WAS patients and their familial carriers. Blood *93*, 756-757.

Yamaguchi,H., Lorenz,M., Kempiak,S., Sarmiento,C., Coniglio,S., Symons,M., Segall,J., Eddy,R., Miki,H., Takenawa,T., and Condeelis,J. (2005). Molecular mechanisms of invadopodium formation: the role of the N-WASP-Arp2/3 complex pathway and cofilin. J. Cell Biol. *168*, 441-452.

Yang,C., Huang,M., DeBiasio,J., Pring,M., Joyce,M., Miki,H., Takenawa,T., and Zigmond,S.H. (2000). Profilin enhances Cdc42-induced nucleation of actin polymerization. J Cell Biol. *150*, 1001-1012.

Yarar,D., D'Alessio,J.A., Jeng,R.L., and Welch,M.D. (2002). Motility determinants in WASP family proteins. Mol. Biol. Cell *13*, 4045-4059.

Yarar,D., To,W., Abo,A., and Welch,M.D. (1999). The Wiskott-Aldrich syndrome

protein directs actin-based motility by stimulating actin nucleation with the Arp2/3 complex. Curr. Biol. *9*, 555-558.

Yin,H.L. and Janmey,P.A. (2003). Phosphoinositide regulation of the actin cytoskeleton. Annu. Rev. Physiol *65*, 761-789.

Yokoyama,N., Lougheed,J., and Miller,W.T. (2005). Phosphorylation of WASP by the Cdc42-associated kinase ACK1: dual hydroxyamino acid specificity in a tyrosine kinase. J. Biol. Chem. *280*, 42219-42226.

Zalevsky,J., Lempert,L., Kranitz,H., and Mullins,R.D. (2001). Different WASP family proteins stimulate different Arp2/3 complex-dependent actin-nucleating activities. Curr. Biol. *11*, 1903-1913.

Zeng,R., Cannon,J.L., Abraham,R.T., Way,M., Billadeau,D.D., Bubeck-Wardenberg,J., and Burkhardt,J.K. (2003). SLP-76 coordinates Nck-dependent Wiskott-Aldrich syndrome protein recruitment with Vav-1/Cdc42-dependent Wiskott-Aldrich syndrome protein activation at the T cell-APC contact site. J. Immunol. *171*, 1360-1368.

Zettl,M. and Way,M. (2002). The WH1 and EVH1 domains of WASP and Ena/VASP family members bind distinct sequence motifs. Curr. Biol. *12*, 1617-1622.

Zhang,H., Schaff,U.Y., Green,C.E., Chen,H., Sarantos,M.R., Hu,Y., Wara,D., Simon,S.I., and Lowell,C.A. (2006). Impaired Integrin-Dependent Function in Wiskott-Aldrich Syndrome Protein-Deficient Murine and Human Neutrophils. Immunity *25*, 285-295.

Zhang,J., Shehabeldin,A., da Cruz,L.A., Butler,J., Somani,A.K., McGavin,M., Kozieradzki,I., dos Santos,A.O., Nagy,A., Grinstein,S., Penninger,J.M., and Siminovitch,K.A. (1999). Antigen receptor-induced activation and cytoskeletal rearrangement are impaired in Wiskott-Aldrich syndrome protein-deficient lymphocytes. J. Exp. Med. *190*, 1329-1342.

Zhang,J., Shi,F., Badour,K., Deng,Y., McGavin,M.K., and Siminovitch,K.A. (2002). WASp verprolin homology, cofilin homology, and acidic region domain-mediated actin polymerization is required for T cell development. Proc. Natl. Acad. Sci. U. S. A *99*, 2240-2245.

Zhong,L., Granelli-Piperno,A., Choi,Y., and Steinman,R.M. (1999). Recombinant adenovirus is an efficient and non-perturbing genetic vector for human dendritic cells. Eur. J Immunol. *29*, 964-972.

Zhu,Q., Watanabe,C., Liu,T., Hollenbaugh,D., Blaese,R.M., Kanner,S.B., Aruffo,A., and Ochs,H.D. (1997). Wiskott-Aldrich syndrome/X-linked thrombocytopenia: WASP gene mutations, protein expression, and phenotype. Blood *90*, 2680-2689.

Zhu,Q., Zhang,M., Blaese,R.M., Derry,J.M., Junker,A., Francke,U., Chen,S.H., and Ochs,H.D. (1995). The Wiskott-Aldrich syndrome and X-linked congenital

thrombocytopenia are caused by mutations of the same gene. Blood *86*, 3797-3804.

Zicha,D., Allen,W.E., Brickell,P.M., Kinnon,C., Dunn,G.A., Jones,G.E., and Thrasher,A.J. (1998). Chemotaxis of macrophages is abolished in the Wiskott-Aldrich syndrome. Br. J. Haematol. *101*, 659-665.

Zigmond,S.H., Joyce,M., Borleis,J., Bokoch,G.M., and Devreotes,P.N. (1997). Regulation of actin polymerization in cell-free systems by GTPgammaS and Cdc42. J. Cell Biol. *138*, 363-374.

Zufferey,R., Donello,J.E., Trono,D., and Hope,T.J. (1999). Woodchuck hepatitis virus posttranscriptional regulatory element enhances expression of transgenes delivered by retroviral vectors. J. Virol. *73*, 2886-2892.

Zufferey,R., Dull,T., Mandel,R.J., Bukovsky,A., Quiroz,D., Naldini,L., and Trono,D. (1998). Self-Inactivating Lentivirus Vector for Safe and Efficient In Vivo Gene Delivery. The Journal of Virology *72*, 9873-9880.